

NUREG/CR-3235  
SAND82-1557  
WH

TECHNICAL ASSISTANCE FOR REGULATORY DEVELOPMENT:  
REVIEW AND EVALUATION OF THE EPA STANDARD 40CFR191  
FOR DISPOSAL OF HIGH-LEVEL WASTE

VOLUME 1

EXECUTIVE SUMMARY

N. R. Ortiz  
K. K. Wahi\*

Manuscript Completed: April 1983  
Date Published: April 1983

Sandia National Laboratories  
Albuquerque, New Mexico 87185  
operated by  
Sandia Corporation  
for the  
U. S. Department of Energy

Prepared for  
Division of Waste Management  
Office of Nuclear Material Safety and Safeguards  
Washington, D.C. 20555

NRC FIN No. A-1165

\* Science Applications, Inc.

OTHER VOLUMES OF  
SAND82-1557  
NUREG/CR-3235

Main Title:

Technical Assistance for Regulatory Development: Review and Evaluation of the EPA Standard 40CFR191 for Disposal of High-Level Waste.

- Volume 1            Executive Summary  
                      N. R. Ortiz, K. Wahi
- Volume 2            A Simplified Analysis of a Hypothetical High-Level Waste Repository in a Basalt Formation  
                      R. E. Pepping, M. S. Chu, M. D. Siegel
- Volume 3            A Simplified Analysis of a Hypothetical High-Level Waste Repository in a Tuff Formation  
                      M. D. Siegel, M. S. Chu
- Volume 4            A Simplified Analysis of a Hypothetical High-Level Waste Repository in a Bedded Salt Formation  
                      R. E. Pepping, M. S. Chu, M. D. Siegel
- Volume 5            Health Effects Associated with Unit Radio-nuclide Releases to the Environment  
                      J. C. Helton
- Volume 6            Calculation of Health Effects Per Curie Release for Comparison with the EPA Standard  
                      G. E. Runkle

## ABSTRACT

The Environmental Protection Agency (EPA) has prepared a draft Standard (40CFR191, Draft 19)[1] which, when finalized, will provide the overall system requirements for the geologic disposal of radioactive waste. This document (Vol. 1) provides an "Executive Summary" of the work performed at Sandia National Laboratories, Albuquerque, NM. (SNLA) under contract to the US Nuclear Regulatory Commission (NRC) to analyze certain aspects of the draft Standard. The issues of radionuclide release limits, interpretation, uncertainty, achievability, and assessment of compliance with respect to the requirements of the draft Standard are addressed based on the detailed analyses presented in five companion volumes to this report.

Xerox D125 Copier-Printer  
Banner Sheet

freeflow1

Date & Time : 02/26/2020 9:11 AM

User Name :

freeflow1

---

Job Name : 3235v1-CR.pdf

Start Page

---

## Introduction

The Environmental Protection Agency (EPA) has prepared a draft Standard (40CFR191, Draft 19)[1] which, when finalized will provide the overall system requirements for the geologic disposal of radioactive waste. Volume 1 of this series of reports provides an "Executive Summary" of the work performed at Sandia National Laboratories, Albuquerque, NM (SNLA) under contract to the US Nuclear Regulatory Commission to analyze certain aspects of the draft Standard. There are five companion volumes to this report that describe, in detail, the analyses carried out. Analyses of hypothetical repositories in three candidate media (Vols. 2, 3, 4) were performed to address the issues of interpretation, achievability, uncertainty, and compliance with respect to the requirements of the draft Standard. An analysis investigating the health effects associated with unit radionuclide releases (Vol. 5) was performed to ascertain the release limits of the draft Standard and their relationship to the assumed health effects. Calculations of health effects per curie of release, similar to those in Volume 5, were carried out for the purpose of showing the effects of uncertainty (Vol. 6) in defining the release limits.

## Radionuclide Release Limits

The objective of the draft Standard is to set forth requirements that will ensure public health and safety by minimizing the risks associated with the permanent disposal of nuclear wastes. In an attempt to establish release limits for various radionuclides, the EPA selected a limit on long-term risks of 1,000 health effects (i.e., latent cancer fatalities) over 10,000 years for a 100,000 metric ton of heavy metal (MTHM) repository (for reasonably foreseeable releases). This is equivalent to ten health effects per 1,000 MTHM. The EPA determined the release limit for a given radionuclide by calculating the number of curies that, if released to the accessible environment, will not cause more than ten health effects per 1,000 MTHM over 10,000 years. Using the same health effects constraint, SNLA calculated independently the number of curies for each radionuclide as described in Volume 5 of this report. The results are compared with the EPA release limits in Table 1. The two sets of release limits are seen to be very similar, with the exception of  $^{99}\text{Tc}$ .

The release limits shown in Table 1 are derived, both by EPA and SNLA, by using single point values for the input parameters or variables that are known to have uncertainties. The effect of these uncertainties was scoped in the present study by performing calculations in which ranges and distributions were assigned to the distribution coefficients ( $R_d$ ), river discharge, regional erosion rates, and exchange factor between the

TABLE 1  
 A Comparison of Cumulative Release Limits  
 to the Accessible Environment  
 for 10,000 Years After Disposal

Radionuclide	Half-Life (years) <sup>a</sup>	Proposed Release Limit <sup>b</sup> (curies per 1000 MTHM)	Release Limit From Table 1-1 <sup>c</sup> (curies per 1000 MTHM)
Am241	458	10	14
Am243	7370	4	4
C14	5730	200	218
Cs135	3.E6	2000	2625
Cs137	30.2	500	505
Np237	2.14E6	20	17
Pu238	86	400	437
Pu239	2.44E4	100	145
Pu240	6580	100	153
Pu242	3.79E5	100	148
Ra226	1600	3	NE
Sr90	28.1	80	83
Tc99	2.12E5	2000	35,088
Sn126	1.E5	80	83
Any other alpha-emitting radionuclide		10	
Any other radionuclide which does not emit alpha particles		500	

a From Ref. 2  
 b From Ref. 1  
 c From Volume 5  
 NE no estimate

surface water and soil compartments. A sample comparison with the EPA calculation is presented in Figure 1, which shows the health effects associated with one curie of a given radionuclide when the ingestion pathways are considered.

The results of this analysis suggest that the release limits for  $^{241}\text{Am}$ ,  $^{243}\text{Am}$  and  $^{237}\text{Np}$  may be overly conservative and may warrant a re-examination by the EPA. Also, the EPA release limit for  $^{135}\text{Cs}$  would appear not to be restrictive enough and may also warrant some reconsideration.

Although the results in Volume 6 generally suggest that the EPA made assumptions conservative enough to cover the uncertainties expected in the input variables considered by SNLA, they do not establish that the EPA release limits proposed in the Standard are overly conservative. However, SNLA did not address all the uncertainties in the input parameters. A more complete comparison and discussion is included in Volume 6.

#### Interpretation of the Requirements

The draft Standard requires high-level waste repositories to be designed to provide a reasonable expectation that for 10,000 years after disposal: (1) reasonably foreseeable releases of waste to the accessible environment are projected to be less than the quantities in Table 1, and (2) very unlikely releases of waste to the accessible environment are projected to be less than ten times the quantities in Table 1. The draft Standard defines: (1) "reasonably foreseeable releases" as releases of radioactive wastes to the accessible environment that are estimated to have more than one chance in 100 of occurring within 10,000 years, and (2) "very unlikely releases" as releases of radioactive wastes to the accessible environment that are estimated to have between one chance in 100 and one chance in 10,000 of occurring within 10,000 years.

The draft Standard uses, but does not define, the word "release." The interpretation of this word affects the manner in which compliance is assessed. Two possible interpretations are:

Interpretation 1: The word "release" defines a unique scenario\* leading to radionuclide release. The draft Standard is applied independently to the probability of release for each scenario.

---

\* Scenarios are events, features, and processes, both natural and human induced, that could conceivably alter the natural state of the disposal site and result in human exposure to radionuclides released from the underground facility.

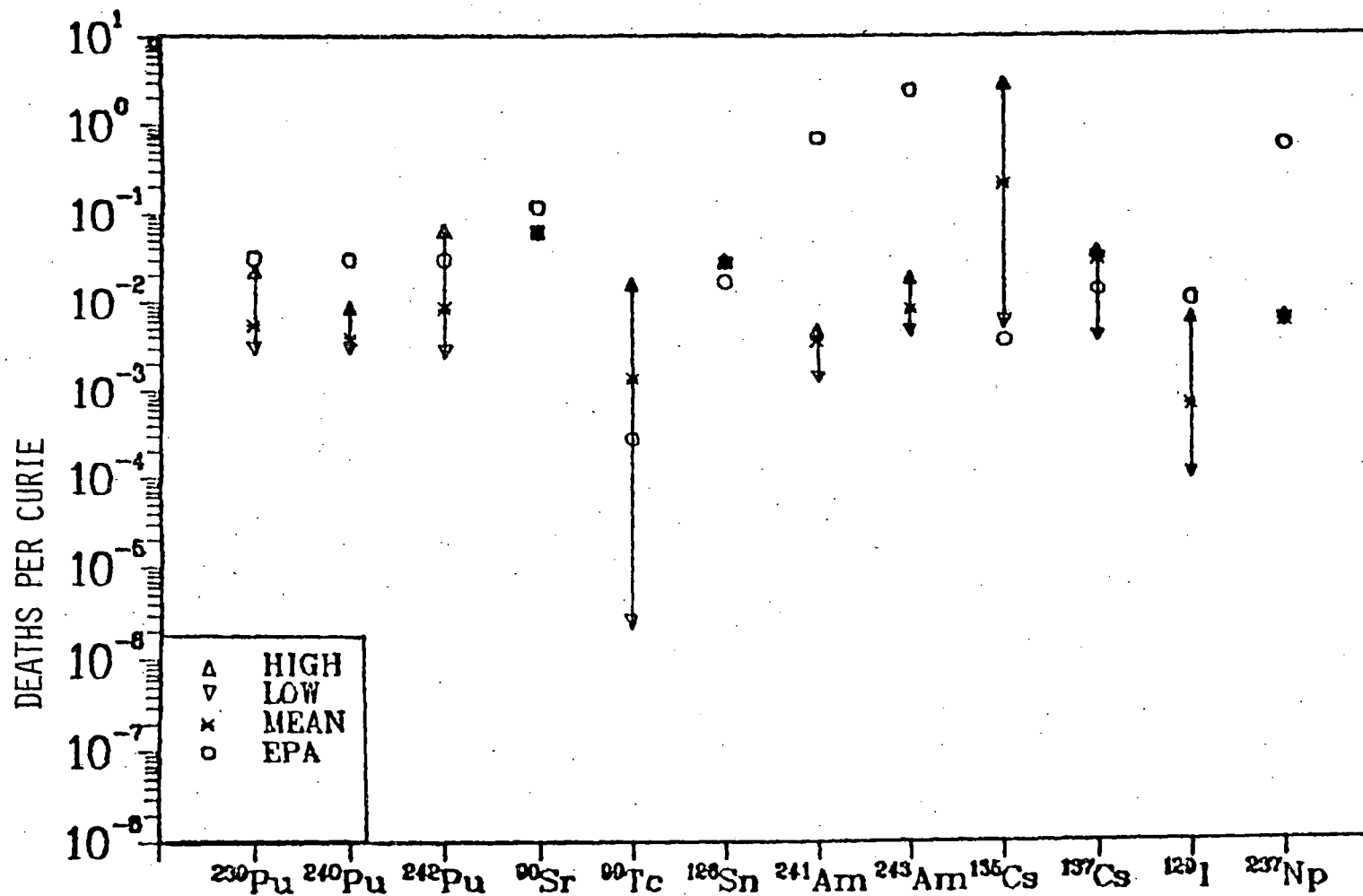


Figure 1: Health effects associated with one curie release for the ingestion pathways.

Interpretation 2: A "release" involves all scenarios that may result in discharges to the environment during the regulatory period. The magnitude of the discharge is given by its corresponding EPA Release Ratio.\* Estimation of the probability of exceeding a given value of the EPA Release Ratio includes contributions from all scenarios.

Analyses were performed based on the above interpretations. In the analyses of the hypothetical basalt repository (Vol. 2), compliance assessment was investigated in terms of Interpretation 1 and 2. In the analysis of the hypothetical tuff repository (Vol. 3), compliance assessments were made using a modified version of Interpretation 1 such that the scenario probability (and not release probability) determined the allowable release limit. In the analysis of a hypothetical bedded salt repository (Vol. 4), the results of the direct-hit scenarios are presented individually in conformance with Interpretation 1; the results of the four ground-water transport scenarios are combined as suggested by Interpretation 2. The results discussed in Volume 2 indicate that the number of predicted violations to the draft Standard will vary depending on the selected interpretation. As discussed in Volume 2, we feel that Interpretation 2 is more in the spirit of the risk-based requirements of the draft Standard, since it considers all sources producing a release greater or equal to the specified release limits. EPA should clarify the intended interpretation.

#### Achievability of the Requirements

Simplified analyses of hypothetical repositories in basalt, tuff, and bedded salt formations have been performed with the intent of predicting integrated releases to the accessible environment and comparing them to the release limits of the draft Standard. Each of the interpretations stated above has been used in expressing the results of these analyses in terms of the release limits of the draft Standard. An appropriate set of scenarios has been chosen for analysis in each of the three media; i.e., the scenarios chosen for a given medium are, in general, different from the ones chosen for the other two media. Table 2 summarizes the postulated scenarios for hypothetical repositories in basalt, tuff, and bedded salt. A

\* Obtained by summing over all radionuclides the ratio of the integrated discharge to the release limit. For a given radionuclide, the release limit is the value given in Table 1 or ten times that, depending on the probability of release.

TABLE 2

Scenarios Analyzed for Hypothetical Repositories in  
Basalt, Tuff, and Bedded Salt

Host Medium	Scenario Number and Description					
Basalt	<u>Scenario 1</u> Routine release with no disruption	<u>Scenario 2</u> Fractures in dense basalt	<u>Scenario 3A</u> Borehole connection to upper aquifer; mixing cell source model	<u>Scenario 3B</u> Borehole connection to upper aquifer; leach limited: $10^{-4}$ - $10^{-7}$ per year	<u>Scenario 3C</u> Borehole connection to upper aquifer; leach limited: $10^{-5}$ - $10^{-7}$ per year	
Tuff	<u>Scenarios 1 &amp; 1B</u> 1. No retardation in any fractured layers 1B. Rock matrix diffusion in fractured layers	<u>Scenarios 2 &amp; 2B</u> Both use rock matrix diffusion and the vertical gradient is unaffected by thermal pulse in each. 2B uses the mixing cell source model	<u>Scenario 3</u> Retardation in some fractured layers due to zeolites	<u>Scenario 4</u> Retardation in porous vitric or devitrified tuff in some fractured layers	<u>Scenarios 5 &amp; 5B</u> Both experience 300 ft. rise in water table 5. Retardation as in Scenario 1  5B. Retardation as in Scenario 1B	<u>Scenario 6</u> Retardation as in Scenario 1; accessible environment 8 miles from repository
Bedded Salt	<u>Scenario 1</u> U-tube formed by a failed shaft seal and one or more boreholes; water originates from and returns to primary aquifer	<u>Scenario 2</u> U-tube formed by two or more boreholes; water originates from and returns to primary aquifer	<u>Scenario 3</u> U-tube formed by a failed shaft seal and one or more boreholes; water originates from and returns to secondary aquifer	<u>Scenario 4</u> U-tube formed by two or more boreholes; water originates from and returns to secondary aquifer	<u>Scenario 5</u> Canister direct hit; rapid and direct movement of radionuclides to surface	<u>Scenario 6</u> Brine pocket penetration

leach-limited source model is implied unless stated otherwise in Table 2. The discharge location (accessible environment) is at a distance of one mile in all cases, except for Scenario 6 in tuff where this distance is eight miles.

The above analyses were performed using the SNLA Risk Assessment Methodology [3,4,5]. The methodology also incorporates uncertainty and sensitivity techniques to calculate consequences (integrated discharges) and the associated release probabilities. Ranges and distributions are assigned to those input variables, from the set of variables needed to define ground-water and radionuclide transport, that are known to have significant uncertainties. A Latin Hypercube Sampling (LHS) technique [5] is then used to sample input values to be used in the calculation of ground-water and radionuclide transport.

A quantitative description of the degradation of the waste form and its release at the boundary of the engineered barrier is provided by a "source model." Three different source models were utilized in the present work:

- Source #1      This is a leach-limited source model. A different leach-rate range is chosen for each medium. A range of  $10^{-3}$  to  $10^{-7}$ /yr is used for tuff, and a maximum range of  $10^{-4}$  to  $10^{-7}$ /yr is used for basalt and bedded salt. The complete inventory of waste is assumed to be available for leaching.
- Source #2      This leach-limited source has the same range as Source #1 in terms of release rate, but the amount of waste available for transport is reduced. Each borehole allows only the penetrated waste in the particular backfilled storage room to be available for transport.
- Source #3      This source resembles Source #2 but allows the backfilled rooms to be modeled as a mixing cell where wastefoms are leached uniformly. Solubility limits are allowed to apply to radionuclide concentrations in the mixing cell.

Only the repository in bedded salt was analyzed with all three source models.

Although the draft Standard has defined a regulatory period of 10,000 years, the present analysis was carried out to a total of 50,000 years, and the results are presented in increments of 10,000 years. This was done in order to assess the adequacy of the 10,000-yr period of regulation.

An examination of the results from the basalt analyses indicates that Scenario 1 does not violate the EPA release limits

when using Interpretation 1, during the first 50,000 years. Slight violations do occur for Scenario 2 in each of the five 10,000-yr increments. The Scenario 3 results show a strong dependence on the type of source model used. In Scenario 3A, no violations occurred during the first, second, and fifth 10,000-yr period. In Scenarios 3B and 3C, large to very large violations occurred in each of the five 10,000-yr periods considered.

In the tuff analysis, it was assumed that all the scenarios considered were reasonably foreseeable. During the first 10,000-yr period, Scenarios 1, 1B, 3, 4 and 5 show very slight to slight violation of the draft Standard limits; Scenarios 5B and 6 show no violation and Scenarios 2 and 2B show large violations. In general, the number of vectors\* or the extent of violation, or both, tend(s) to increase in each of the subsequent 10,000-yr periods analyzed. This increase, however, is gradual and typically within an order of magnitude.

As with the basalt results, the bedded salt results were evaluated using Interpretations 1 and/or 2. The ground-water transport scenarios (Scenarios 1-4) were repeated using three different source models, and the results are evaluated using Interpretation 2. Substantial variations in the results occur when different source models are used. Gross violations occur when Source #1 is used. No violation occurs during the first 10,000 years for Source #2; violations during the subsequent 10,000-yr period are extremely minor. No violations occur during any of the five 10,000-yr periods when Source #3 is used. Interpretation 1 was used in presenting the results of Scenarios 5 and 6. The direct hit scenario, Scenario 5, indicates a slight violation during the first 10,000-yr period. The brine-pocket penetration scenario, Scenario 6, indicates a relatively large violation of the EPA limit.

The results for all three media for the first 10,000 years are summarized in Table 3. Sample plots of probability of exceeding release ratio on the abscissa are shown in Figure 2 for basalt, Figure 3 for tuff, and Figures 4 and 5 for bedded salt. A direct comparison among the three different media is not recommended due mainly to the fact that the scenarios analyzed are different.

#### Conclusions and Recommendations

Based on the results of the analyses performed by SNLA, the following conclusions and recommendations are presented.

\* A vector, in the present context, represents a complete set of input values selected by the sampling program to carry out a transport calculation. Different vectors represent different combinations of input parameter values.

**TABLE 3**  
**Summary of Results of Simplified Analysis for**  
**Hypothetical Repositories in Basalt, Tuff, and Bedded Salt**  
**(10,000-yr period)**

Host Medium	Scenario Number and Description								
<u>Interpretation #1</u>									
BASALT	<u>Scenario 1</u>	<u>Scenario 2</u>		<u>Scenario 3A</u>	<u>Scenario 3B</u>	<u>Scenario 3C</u>			
percent violations	No violations	3%		No violations	~20%	~10%			
maximum release ratio		1.3			~1,000.	~100.			
contrib. radio-nuclides		C14			Several	Several			
<u>Interpretation #2</u>									
BASALT	No violations (Using Scenarios 1, 2 & 3A)								
percent violations									
<u>Modified Interpretation #1</u>									
TUFF	<u>Scenarios 1 and 1B</u>		<u>Scenarios 2 and 2B</u>		<u>Scenario 3</u>	<u>Scenario 4</u>	<u>Scenarios 5 and 5B</u>	<u>Scenario 6</u>	
percent violations	1%	1%	10%	8%	1%	1%	3%	none	none
maximum release ratio	2.4	1.7	207	22	.9	1.9	7.9		
contrib. radio-nuclides	Tc99	Tc99	U234 Np237 U238 U236	U234 U236 Np237	Tc99	Tc99	C14		
<u>Interpretation #1</u>									
BEDDED SALT	<u>Source #</u>	<u>Scenario 1</u>		<u>Scenario 2</u>		<u>Scenario 3</u>		<u>Scenario 4</u>	
percent violations	1 2 3	61% no violation no violation		59% 1% no violation		27% <1% no violation		28% no violation no violation	
maximum release ratio	1 2	44 -		43 1.6		25 1.2		25 -	
contrib. radio-nuclides	1 2	U234 Am243 U236 U238		U234 Am243 U236 U238		U234 U236 U238		U234 U236 U238	
		-		Am243+ U234+		U234+		-	
<u>Interpretation #1</u>					<u>Interpretation #2</u>				
BEDDED SALT	<u>Scenario 5</u>		<u>Scenario 6</u>		<u>Scenarios 1, 2, 3 &amp; 4</u>				
percent violations	Very slight violation		Some violations		Source 1: large violations Source 2: no violations Source 3: no violations				

\*The individual radionuclide gives release ratio  $< 1$ .

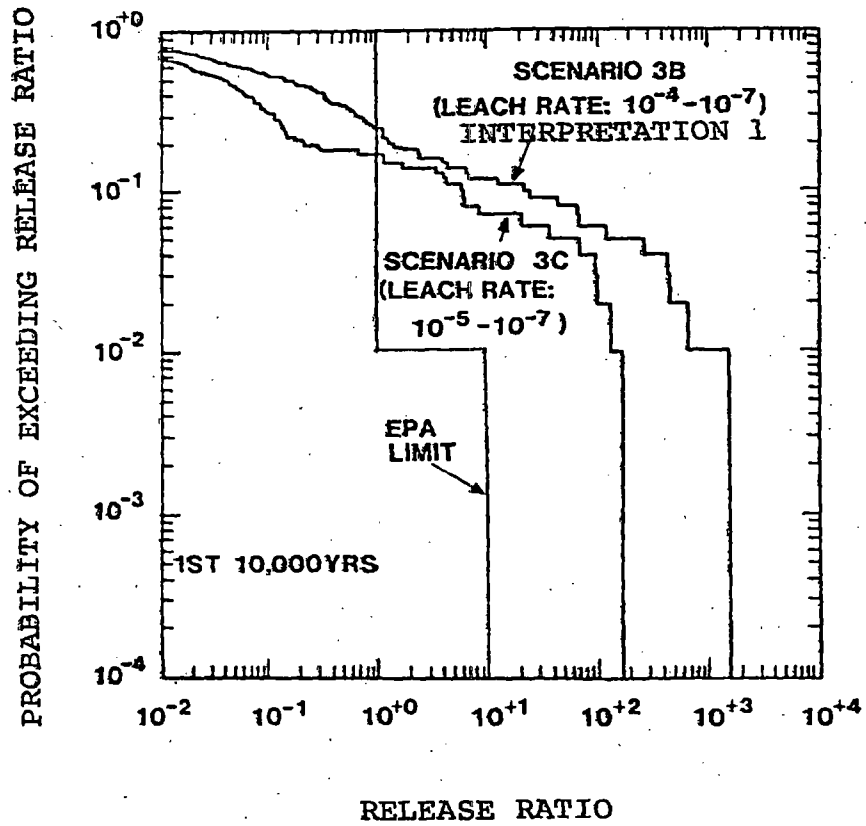


Figure 2(a). Probability of Exceeding Release Ratio, Scenarios 3B and 3C, Basalt Repository.

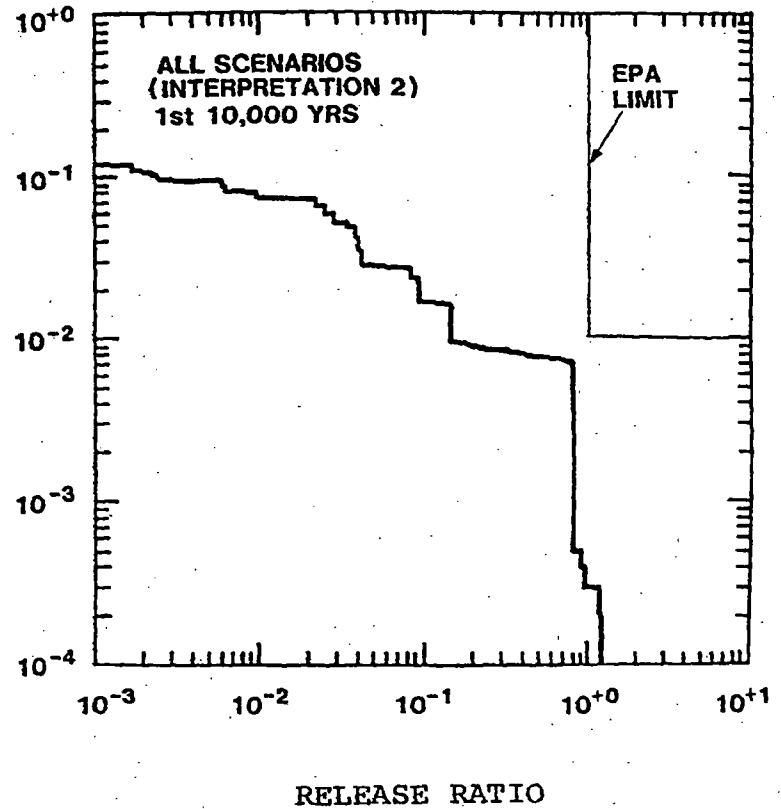


Figure 2(b). Probability of Exceeding Release Ratio, Scenarios 1, 2, 3A, Basalt Repository.

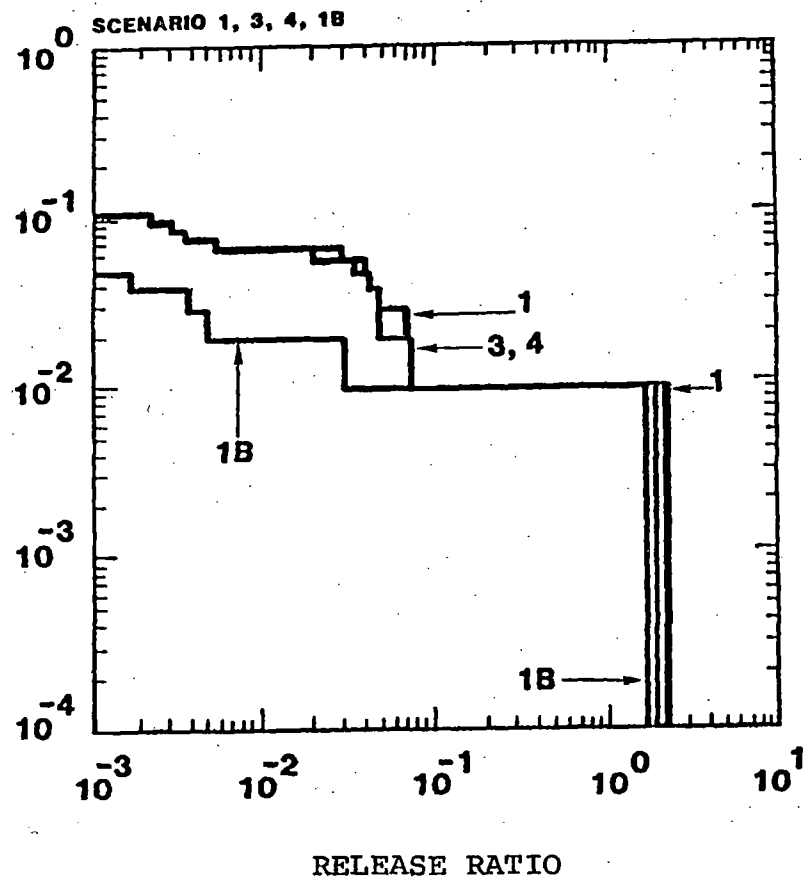
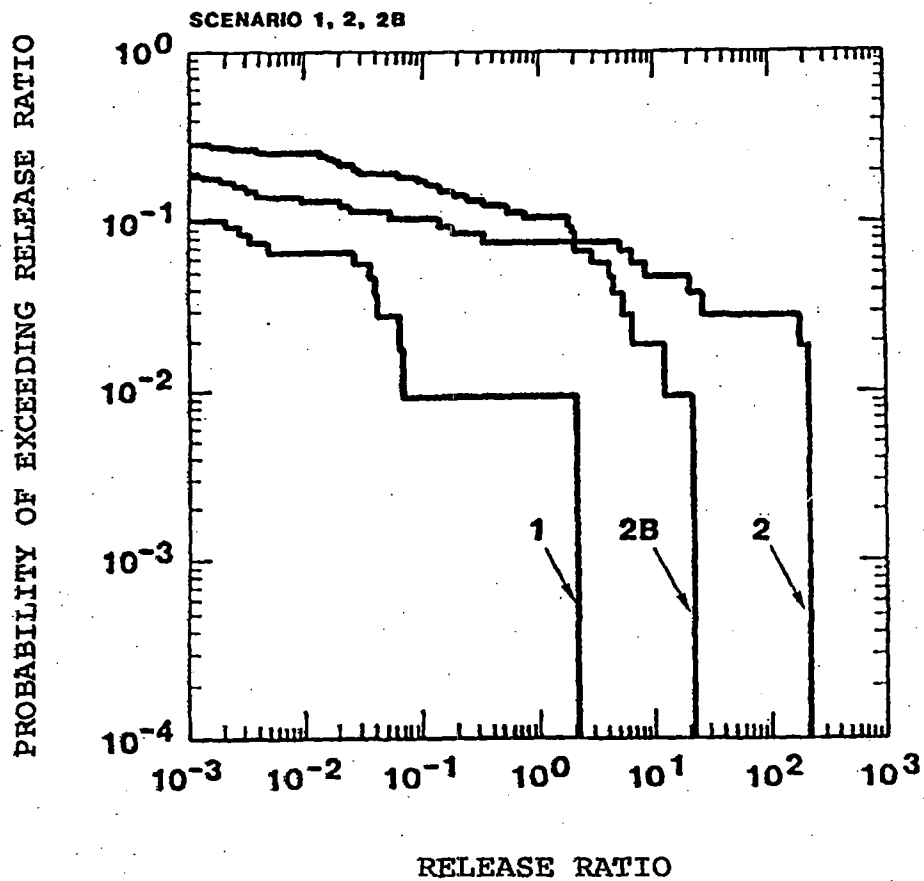


Figure 3. Probability of Exceeding Release Ratio During First 10,000 Years, Tuff Repository.

PROBABILITY OF EXCEEDING RELEASE RATIO

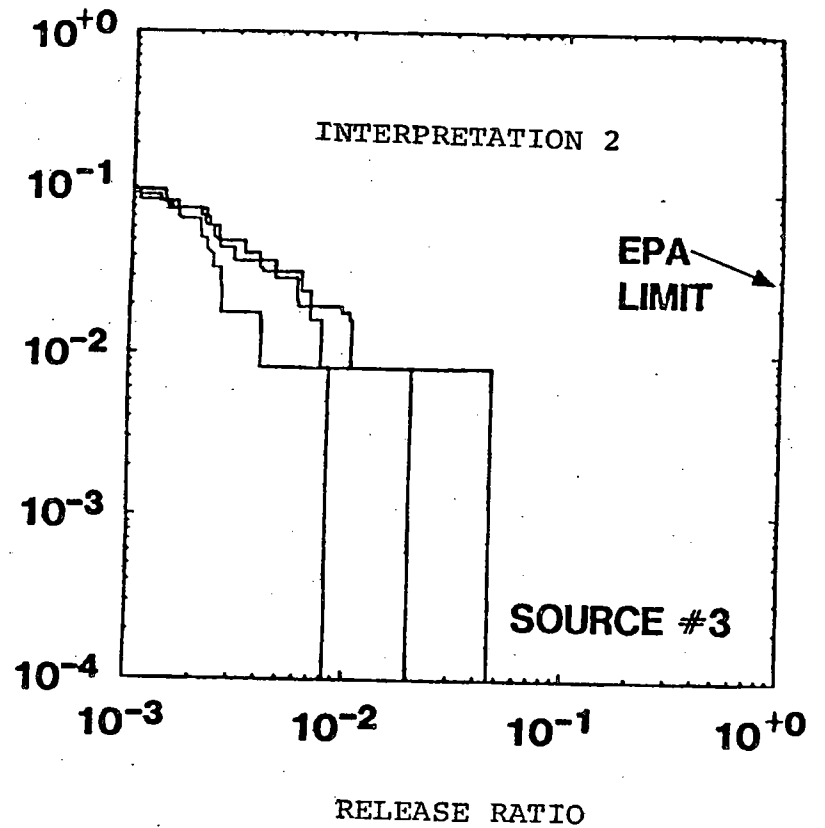
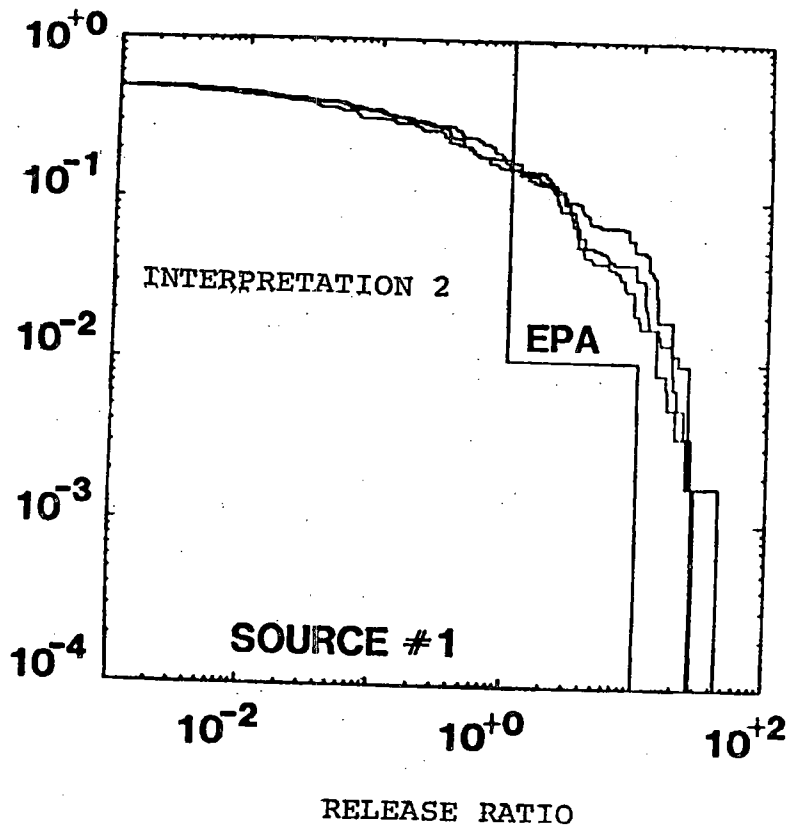


Figure 4. Probability of Exceeding Release Ratio During First 10,000 Years, Groundwater Transport Scenarios, Source #1 and Source #3, Bedded Salt Repository.

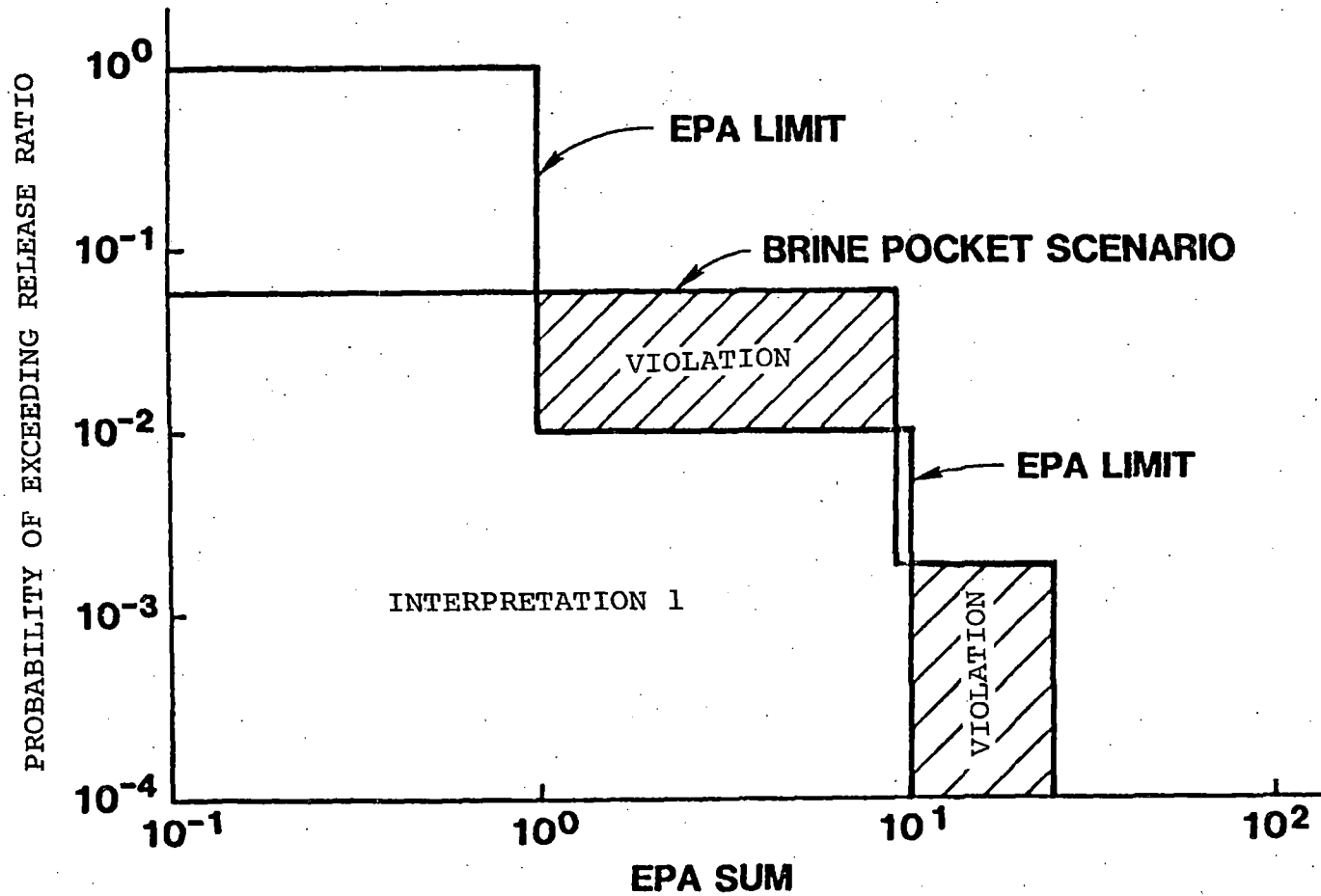


Figure 5. Probability of Exceeding Release Ratio, Scenario 6, First 10,000 Years, Bedded Salt Repository.

- The radionuclide release limits in the draft Standard are in agreement with the values calculated by SNLA with the exception of  $^{99}\text{Tc}$ . The draft Standard allows a lower release limit for  $^{99}\text{Tc}$ .
- In general, the health effects (per curie) calculated by EPA for the ingestion pathways are higher than the ranges calculated by SNLA. The exceptions are  $^{126}\text{Sn}$  and  $^{135}\text{Cs}$ . The results of this analysis for  $^{241}\text{Am}$ ,  $^{243}\text{Am}$  and  $^{237}\text{Np}$  indicate that the release limits for these radionuclides may be overly conservative and may warrant a re-examination by the EPA. Also, the EPA release limit for  $^{135}\text{Cs}$  would appear not to be restrictive enough according to the results of this analysis and, again, may warrant some reconsideration.
- The results suggest that higher release limits could be tolerated if the health effects per curie calculated in the present analysis were to be the basis for such a decision. However, the results do not establish that the release limits in the draft Standard are overly conservative.
- It is necessary to clearly state the intended interpretation in the draft Standard as to how the terms "reasonably foreseeable" and "very unlikely" releases should actually be applied. In other words, is it the scenario probability or the probability of release? Further, should the release probabilities be considered for individual scenarios (conditional) or all pertinent scenarios with a composite release probability?
- The results of the analyses for the reference basalt site performed under Interpretation 1 showed a small probability of violating the draft EPA Standard for Scenarios 2 and 3A. Under Interpretation 2, the same analyses indicate total compliance with the draft Standard, underscoring the need for a clear interpretation.
- Sorption of radionuclides by several thousand feet of zeolitized tuff may limit the release of actinides below the EPA release limits even in the absence of solubility constraints.
- Violations of the draft Standard for Scenarios 1, 1B, 3, 4, and 5 in tuff are due to discharges of  $^{99}\text{Tc}$  and  $^{14}\text{C}$ . Retardation due to matrix diffusion, however, could significantly reduce the discharge of these nuclides under realistic ground-water flow rates.

- If the radionuclides do not flow through thick sequences of zeolitized tuff, discharges of U and Np under oxidizing conditions may be much larger than the EPA limits.
- Drilling-related, direct-hit scenarios in sedimentary basins indicate slight violations of the draft Standard.
- Brine pockets in bedded salt may pose a significant problem in complying with the draft Standard. Therefore, site characterization should directly address the question of identifying any brine pockets that may be present.
- Analyses performed with different source models show the importance of the source-term assumption on compliance estimates. In general, the mixing-cell source model gives significantly lower releases, and hence discharges, to the accessible environment.
- A majority of the vectors examined in all scenarios produced radionuclide releases below the limits set by the draft Standard. In general, violations of the Standard occurred only when the most conservative assumptions were used or when combinations of input data produced groundwater flow rates that were unrealistically high.
- A practical difficulty in implementing the draft Standard is the lack of our ability to assign reliable numerical values to the scenario probabilities. The methodology to assess compliance with the Standard is, nevertheless, available as has been demonstrated by this and other similar studies.
- The predicted radionuclide releases over 10,000-yr intervals, from 10,000 to 50,000 years, are not significantly higher than for the first 10,000 years. The maximum release ratio over the 50,000 years increases by a factor of two to three.
- SNLA strongly recommends that detailed performance analyses be carried out for repositories in basalt and tuff (similar to the one performed for bedded salt in [3,4]) to assure that important variables, processes, or events have not been overlooked in the simplified analyses.

## REFERENCES

1. "Environmental Radiation Protection Standards for Management and Disposal of Spent Nuclear Fuel, High-Level and Transuranic Radioactive Wastes," 40CFR191. (Working Draft #19), Federal Register, March 19, 1981.
2. Weast, W. E., 1974, Handbook of Chemistry and Physics (55th edition), CRC Press, Cleveland, OH.
3. Cranwell, R. M., J. E. Campbell, and others, "Risk Methodology for Geologic Disposal of Radioactive Waste: Final Report," Sandia National Laboratories, SAND-81-2573, NUREG/CR-2452, 1982.
4. Cranwell, R. M., R. V. Guzowski, J. E. Campbell, and N. R. Ortiz, "Risk Methodology for Geologic Disposal of Radioactive Waste: Scenario Selection Procedure," Sandia National Laboratories, SAND80-1429, NUREG/CR-1667, 1982.
5. Iman, R. L., J. M. Davenport, and D. K. Zeigler, "Latin-Hypercube Sampling: Program User's Guide," Sandia National Laboratories, SAND79-1473, 1980.

NRC FORM 335 (11 81)		U.S. NUCLEAR REGULATORY COMMISSION BIBLIOGRAPHIC DATA SHEET		1 REPORT NUMBER (Assigned by DDC) NUREG/CR-3235, Vol. 1 SAND82-1557	
4 TITLE AND SUBTITLE (Add Volume No., if appropriate) Technical Assistance for Regulatory Development: Review and Evaluation of the Draft EPA Standard 40CFR191 For Disposal of High-Level Waste				2 (Leave blank)	
7 AUTHOR(S) Executive Summary Fuel Cycle Risk Analysis Division				3 RECIPIENT'S ACCESSION NO	
9 PERFORMING ORGANIZATION NAME AND MAILING ADDRESS (Include Zip Code) Sandia National Laboratories Fuel Cycle Risk Analysis Division 9413 Albuquerque, NM 87185				5 DATE REPORT COMPLETED MONTH April YEAR 1983	
12 SPONSORING ORGANIZATION NAME AND MAILING ADDRESS (Include Zip Code) Division of Waste Management Office of Nuclear Material Safety and Safeguards U.S. Nuclear Regulatory Commission Washington, DC 20555				DATE REPORT ISSUED MONTH April YEAR 1983	
13 TYPE OF REPORT Formal Report				PERIOD COVERED (Inclusive dates) July 1981 - April 1983	
15 SUPPLEMENTARY NOTES				6 (Leave blank)	
16 ABSTRACT (200 words or less) The Environmental Protection Agency (EPA) has prepared a draft Standard (40CFR191, Draft 19) which, when finalized, will govern the geologic disposal of radioactive waste. This document (Vol. 1) provides an "Executive Summary" of the work performed at Sandia National Laboratories, Albuquerque, N.M. (SNLA) under a contract to the U.S. Nuclear Regulatory Commission (NRC) to analyze certain aspects of the draft Standard. The issues of radionuclide release limits, interpretation, uncertainty, achievability, and assessment of compliance with respect to the requirements of the draft Standard are addressed based on the detailed analyses presented in five companion volumes to this report.				8 (Leave blank)	
17 KEY WORDS AND DOCUMENT ANALYSIS				10 PROJECT/TASK/WORK UNIT NO	
17b IDENTIFIERS, OPEN ENDED TERMS				11 FIN NO NRC FIN A 1165 Task 3	
18 AVAILABILITY STATEMENT Unlimited		19 SECURITY CLASS (This report) Unclassified		21 NO OF PAGES	
		20 SECURITY CLASS (This page) Unclassified		22 PRICE \$	

Xerox D125 Copier-Printer  
Banner Sheet

freeflow1

Date & Time : 02/26/2020 9:11 AM

User Name :

freeflow1

---

Job Name : 3235v2-4-CR.pdf

Start Page

---

NUREG/CR-3235  
SAND82-1557  
Vols. 2, 3, and 4

---

---

# Technical Assistance for Regulatory Development: Review and Evaluation of the Draft EPA Standard 40CFR191 for Disposal of High-Level Waste

- A Simplified Analysis of a Hypothetical Repository in a Basalt Formation
- A Simplified Analysis of a Hypothetical Repository in a Tuff Formation
- A Simplified Analysis of a Hypothetical Repository in a Bedded Salt Formation

---

---

Prepared by Fuel Cycle Risk Analysis Division

Sandia National Laboratories

April 1983

Prepared for  
U S Nuclear Regulatory  
Commission

OTHER VOLUMES OF  
SAND82-1557  
NUREG/CR-3235

Main Title:

Technical Assistance for Regulatory Development: Review and Evaluation of the EPA Standard 40CFR191 for Disposal of High-Level Waste.

- Volume 1            Executive Summary  
                     N. R. Ortiz, K. Wahi
- Volume 2            A Simplified Analysis of a Hypothetical High-Level Waste Repository in a Basalt Formation  
                     R. E. Pepping, M. S. Chu, M. D. Siegel
- Volume 3            A Simplified Analysis of a Hypothetical High-Level Waste Repository in a Tuff Formation  
                     M. D. Siegel, M. S. Chu
- Volume 4            A Simplified Analysis of a Hypothetical High-Level Waste Repository in a Bedded Salt Formation  
                     R. E. Pepping, M. S. Chu, M. D. Siegel
- Volume 5            Health Effects Associated with Unit Radio-nuclide Releases to the Environment  
                     J. C. Helton
- Volume 6            Calculation of Health Effects Per Curie Release for Comparison with the EPA Standard  
                     G. E. Runkle

**Volume 2**

**A Simplified Analysis of a Hypothetical Repository  
in a Basalt Formation**

NUREG/CR-3235  
SAND82-1557  
WH

TECHNICAL ASSISTANCE FOR REGULATORY DEVELOPMENT:  
REVIEW AND EVALUATION OF THE DRAFT EPA STANDARD 40CFR191  
FOR DISPOSAL OF HIGH-LEVEL WASTE

VOL. 2

A SIMPLIFIED ANALYSIS OF A HYPOTHETICAL REPOSITORY  
IN A BASALT FORMATION

R. E. Pepping  
M. S. Chu  
M. D. Siegel

Manuscript Completed: April 1983  
Date Published: April 1983

with contributions from:  
R. V. Guzowski\*

Sandia National Laboratories  
Albuquerque, New Mexico 87185  
operated by  
Sandia Corporation  
for the  
U. S. Department of Energy

Prepared for  
Division of Waste Management  
Office of Nuclear Material Safety and Safeguards  
Washington, D.C. 20555

NRC FIN. No. A-1165

\*Energy Management and Technology

## ABSTRACT

An analysis of a hypothetical nuclear waste repository in a basalt formation has been performed to demonstrate the application of existing analytical tools to the assessment of compliance of the repository with the draft EPA Standard, 40CFR191 (Draft #19). The tools have been developed by Sandia National Laboratories for use by NRC in such analyses. The hypothetical site is based on descriptive and quantitative data for a candidate basalt repository in the early stages of site characterization. The effects of uncertainty in the input data on the assessment of compliance are demonstrated. Other sources of uncertainty resulting from interpretation of the standard and its probabilistic nature are discussed. The results of the calculations presented indicate that compliance with the draft standard may be achieved depending on how the term "release" is interpreted; namely, is the release due to a unique (single) event or does it involve all probable scenarios.

## TABLE OF CONTENTS

<u>Chapter</u>	<u>Page</u>
1. INTRODUCTION .....	1
2. THE DRAFT EPA STANDARD, 40CFR191 .....	4
2.1 Interpretations of the Draft Standard.....	4
2.2 Implementation of Different Interpretations.....	6
2.3 Estimation of Probabilities of Scenarios..	9
3. THE REFERENCE BASALT SITE .....	11
4. WASTE AND REPOSITORY DESCRIPTION .....	16
4.1 Waste .....	16
4.2 Subsurface Facility .....	16
5. GEOCHEMISTRY .....	18
5.1 Retardation Factors .....	18
5.2 Solubility .....	23
5.3 Matrix Diffusion .....	23
6. GROUNDWATER TRANSPORT MODEL .....	25
7. SCENARIOS ANALYZED .....	27
7.1 Scenario 1 -- Routine Release .....	28
7.2 Scenario 2 -- Fractures in Dense Basalt ..	32
7.3 Scenario 3 -- Borehole .....	34
8. RESULTS OF DEMONSTRATION ANALYSES.....	44
9. CONCLUSIONS .....	71
REFERENCES .....	R-1

## APPENDICES

	<u>Page</u>
APPENDIX A -- RADIONUCLIDE RETARDATION .....	A-1
1. Calculation of the Retardation Factor ....	A-1
2. Estimation of Utilization Factor .....	A-3
APPENDIX B -- REDOX CONDITIONS IN THE REFERENCE REPOSITORY AND APPROPRIATE VALUES OF $R_d$ .....	B-1
1. Redox Conditions .....	B-1
2. Available Data for Values of $R_d$ .....	B-2
APPENDIX C -- AN APPROXIMATE TREATMENT OF MATRIX DIFFUSION AS A RETARDATION MECHANISM .	C-1
APPENDIX D -- CALCULATION OF THERMAL BUOYANCY GRADIENT .....	D-1
APPENDIX E -- THE MIXING CELL SOURCE MODEL .....	E-1
APPENDIX F -- RATIONALE FOR THE SELECTION OF SCENARIOS ANALYZED IN BASALT.....	F-1
APPENDIX G -- GEOCHEMICAL AND HYDRAULIC PARAMETER DATA.....	G-1

LIST OF FIGURES

<u>Figure</u>		<u>Page</u>
1.	General Geologic Features of the Reference Basalt Repository Site .....	12
2.	Stratigraphic Cross-Section of Hypothetical Repository in Basalt .....	13
3.	Routine Release Scenario (Scenario 1) .....	31
4.	Fractured Dense Basalt Scenario (Scenario 2) ..	33
5.	Borehole Scenario (Scenario 3) .....	37
6.	Scenario 1 CCDF - 1st 10,000 Years .....	45
7.	Scenario 1 CCDF - 2nd 10,000 Years .....	46
8.	Scenario 1 CCDF - 3rd 10,000 Years .....	47
9.	Scenario 1 CCDF - 4th 10,000 Years .....	48
10.	Scenario 1 CCDF - 5th 10,000 Years .....	49
11.	Scenario 2 CCDF - 1st 10,000 Years .....	50
12.	Scenario 2 CCDF - 2nd 10,000 Years .....	51
13.	Scenario 2 CCDF - 3rd 10,000 Years .....	52
14.	Scenario 2 CCDF - 4th 10,000 Years .....	53
15.	Scenario 2 CCDF - 5th 10,000 Years .....	54
16.	Scenario 3A CCDF - 1st 10,000 Years .....	55
17.	Scenario 3A CCDF - 2nd 10,000 Years .....	56
18.	Scenario 3A CCDF - 3rd 10,000 Years .....	57
19.	Scenario 3A CCDF - 4th 10,000 Years .....	58
20.	Scenario 3A CCDF - 5th 10,000 Years .....	59
21.	All Scenario CCDF - 1st 10,000 Years .....	60
22.	All Scenario CCDF - 2nd 10,000 Years .....	61

LIST OF FIGURES (continued)

<u>Figure</u>		<u>Page</u>
23.	All Scenario CCDF - 3rd 10,000 Years .....	62
24.	All Scenario CCDF - 4th 10,000 Years .....	63
25.	All Scenario CCDF - 5th 10,000 Years .....	64
26.	Scenarios 3B and 3C (leach limited) CCDFs - 1st 10,000 Years .....	65
27.	Scenarios 3B and 3C (leach limited) CCDFs - 2nd 10,000 Years .....	66
28.	Scenarios 3B and 3C (leach limited) CCDFs - 3rd 10,000 Years .....	67
29.	Scenarios 3B and 3C (leach limited) CCDFs - 4th 10,000 Years .....	68
30.	Scenarios 3B and 3C (leach limited) CCDFs - 5th 10,000 Years .....	69
B-1	$R_d$ Data .....	B-3
C-1	Idealized Fracture Geometry .....	C-2
C-2	Breakthrough Curve Depicting Behavior of Equation C1; $C(t)=C_0 \operatorname{erfc}(\eta)$ .....	C-5
D-1	Water Column Assumed for Thermal Buoyancy Calculation .....	D-1
D-2	Isotherms Used in Calculating Thermal Buoyancy ..	D-3
E-1	Implementation of the Mixing Cell Source Model for NWFT/DVM .....	E-3
E-2	Effects of the Mixing Cell Assumptuion on Integrated Discharge Relative to the Leach- Limited Source Model .....	E-5

TABLES

<u>Table</u>	<u>Page</u>
1. Cumulative Releases to the Accessible Environment for 10,000 Years After Disposal .....	5
2. Reference Hydraulic Properties .....	14
3. Inventory of Reference Repository .....	17
4. Geochemical Environment of Stratigraphic Layers in Basalt Repository .....	21
5. $R_d$ Ranges .....	22
6. Ranges of Solubilities of Selected Elements Used for Basalt Reference Repository Conditions.	24
7. Data Ranges and Distributions for Additional Variables .....	29
8. Scenario 2: EPA Ratios of Radionuclide Discharges into Aquifer I-M .....	35
9. Scenario 3: EPA Ratios of Radionuclides .....	40
10. Scenario 3A: EPA Ratios Summed Over All Radionuclides .....	41
11. Mean Values of Contributions to the EPA Sum (100 Vectors) for Scenario 3B with Leach-Limited Source .....	42
C-1 Scenario 2 Discharges Without Rock Matrix Retardation .....	C-8
C-2 Summary of Effects of Diffusion Into Rock Matrix on TID .....	C-9
C-3 Vector 15 Data Used to Estimate Retardation Due to Diffusion into the Rock Matrix .....	C-10
C-4 Vector 24 Data Used to Estimate Retardation Due to Diffusion into the Rock Matrix .....	C-11
C-5 Vector 62 Data Used to Estimate Retardation Due to Diffusion into the Rock Matrix .....	C-12

LIST OF TABLES (continued)

<u>Table</u>		<u>Page</u>
D-1	Hydraulic Gradients Produced by Thermal Effects .....	D-2
G-1	Ranges of $R_d$ Values for Basalt Host Rock .	G-1
G-2	$R_d$ Values for Basalt .....	G-2
G-3	$R_d$ Ranges in Basalt Aquifer .....	G-3
G-4	Basalt Hydraulic Parameters .....	G-4

## 1. INTRODUCTION

In the near future, the EPA is expected to issue a proposed standard (40CFR191) governing the geologic disposal of radioactive wastes. A 180 day period is expected for public comment on the standard. Other government agencies, such as the NRC, are also expected to comment on the standard. Sandia is funded by the NRC to provide information and insight useful in preparing these comments. The objective of this effort is to perform calculations similar to those performed by EPA in developing their standard<sup>1</sup> (Draft #19). We have calculated integrated discharges of radionuclides in plausible scenarios. A number of media have been proposed as candidate hosts for nuclear waste repositories; bedded salt, domed salt, basalt, tuff and granite. This report documents analyses of a hypothetical repository in basalt.

In order to assess compliance with the draft standard, it is necessary to normalize the predicted integrated discharges to the release limits prescribed in the standard. Two different interpretations of the standard, along with their respective methods of implementation are presented in Chapter 2. Also presented is a short discussion on the estimation of scenario probabilities.

The characteristics of the reference basalt site in this study were chosen to be consistent with our current understanding of the proposed candidate repository site in order to determine the realism of the assumed EPA repositories. Chapter 3 describes the reference site in this study. First, the general characteristics of the site and surrounding region are described; then, the stratigraphy and lithology of the reference site are presented.

Chapter 4 describes the reference repository and the radioactive wastes stored. This includes the waste inventory, the waste form, the waste canisters and the leaching behavior.

Chapter 5 presents the geochemical parameters used in the analysis. The geochemical environment of each subsurface layer has been described. Special emphasis has been placed on the calculation of retardation factors of radionuclides in basalt. We assumed that the transport of radionuclides in basalt takes place exclusively in partially filled fractures. Retardation factors were calculated using distribution coefficients for radionuclides in secondary minerals in the fractures.

Chapter 6 describes the groundwater transport model used in these analyses. The flow is represented by a quasi-two-dimensional Darcian model. Sandia's distributed velocity method (DVM)<sup>2</sup> was used to calculate radionuclide transport.

Chapter 7 describes the scenarios analyzed in calculating the integrated releases of radionuclides for times up to 50,000 years. A base case routine-release scenario and two disruptive scenarios were analyzed.

Chapter 8 presents results of numerical calculations, and compares them to the requirements of the EPA Standard.

Chapter 9 states the conclusion based on the results of our study.

It would be misleading to claim that the results of these model calculations can provide a detailed description of the performance of a real repository. A large amount of uncertainty in the results is introduced by the paucity of geochemical and hydrological data (experimental and field) relevant to the design of a waste repository in basalt formations. In addition, it was impossible to provide exact mathematical descriptions of fluid flow and radionuclide migration due to the complexity of this system and the time and budgetary constraints. However, with better in-situ measurements or site characterization, and additional resources, the realism and accuracy of these calculations could be greatly improved.

It should be noted that the results presented here represent a first attempt at the type of analyses that real repositories will require. The motivation for performing a demonstration analysis at this time is twofold. First, we gain experience in identifying necessary assumptions, areas of sparse data or weak models, and potential problems with implementing the draft standard. Secondly, the numerical predictions indicate the likelihood that the hypothetical repository complies with the draft standard. It therefore indicates the importance of validating assumptions and improving data for any real candidate repository that is similar.

Appendices A through G describe several assumptions and mathematical approximations that we have developed in order to estimate radionuclide discharges from the repository. Appendix A outlines and derives a new method for approximation of the retardation factor for radionuclide

migration in fractured media. Appendix B describes our conception of the geochemical environments along possible nuclide migration paths and discusses the uncertainty related to choices of relevant values of radionuclide distribution coefficient ( $R_d$ ). In Appendix C, a method to approximate the radionuclide retardation caused by matrix diffusion is discussed. In Appendix D, vertical hydraulic gradients induced by thermal effects are calculated. Appendix E describes an optional source model, the mixing cell, used in some of the analyses. Appendix F discusses the rationale for scenario selection. Appendix G summarizes the data ranges for  $R_d$  and hydraulic parameters in basalt, with appropriate references noted.

## 2. THE DRAFT EPA STANDARD, 40CFR191

The Environmental Protection Agency (EPA) has prepared a working draft of its proposed generally applicable standard for the protection of public health from the geologic disposal of radioactive wastes.<sup>1</sup> The standard is expressed in terms of the total integrated discharge of the radionuclides comprising the wastes to the accessible environment. In Table 1 a list is given of radionuclides expected in the radioactive waste inventory and the corresponding EPA release limits. Since events and processes leading to radionuclide release will generally result in the release of mixtures of radionuclides, a sum rule is imposed on mixtures of radionuclide discharges:

$$\text{EPA Sum} = \sum_i \frac{Q_i}{\text{EPA}_i} \leq 1. \text{ for reasonably foreseeable releases}$$
$$\leq 10. \text{ for very unlikely releases}$$

where  $Q_i$  is the integrated discharge over 10,000 years of radionuclide  $i$  and  $\text{EPA}_i$  is the release limit of radionuclide  $i$  in the draft standard.  $Q_i$  and  $\text{EPA}_i$  are scaled for the amount of waste in the geologic repository according to the assumed 1000 metric tons of heavy metal (MTHM).

In the draft EPA Standard, a "reasonably foreseeable" release is defined as any release expected to occur with a probability of greater than 0.01 in the 10,000 year period addressed by the standard. A "very unlikely release" is defined as any release expected to occur with a probability of less than 0.01 but greater than 0.0001 in the 10,000 year period. Any release with a probability of occurrence of less than 0.0001 in the 10,000 year period need not be considered in the analyses.<sup>3</sup>

### 2.1 Interpretations of the Draft Standard

In attempting to assess compliance with the draft standard, one is faced with the difficult task of how best to formulate the test for compliance. The intended interpretation of the standard is also subject to debate.

Table 1

Cumulative Releases to the Accessible Environment for 10,000 Years After Disposal<sup>1</sup>

<u>Radionuclide</u>	<u>EPA Release Limit (Curies per 1000 MTHM*)</u>
Americium-241	10
Americium-243	4
Carbon-14	200
Cesium-135	2000
Cesium-137	500
Iodine-129	500
Neptunium-237	20
Plutonium-238	400
Plutonium-239	100
Plutonium-240	100
Plutonium-242	100
Radium-226	3
Strontium-90	80
Technetium-99	2000
Tin-126	80
Any other alpha-emitting radionuclide	10
Any other radionuclide which does not emit alpha particles	500

\*MTHM denotes metric tons of heavy metal.

As a result of the uncertainties in input data, computer models, and the ability of models to represent the physical system, there exist inherent uncertainties in the calculations required to assess compliance. It will be shown in later sections that a fraction of the input vectors\* lead to violations of the standard. Typically, the parameter values constituting the vectors that apparently "violate" the standard are at the conservative extreme of the ranges assigned to those parameters. Clarification from EPA may be necessary as to how uncertainty in compliance assessment should be treated.

For example, the standard uses, but does not define, the word "release". The interpretation of this word affects the manner in which compliance is assessed. We offer two interpretations below.

Interpretation 1: The word "release" defines a unique event or scenario leading to radionuclide release. The draft EPA Standard is applied independently to each scenario.

Interpretation 2: A "release" involves all events or processes that may result in discharges to the environment during the regulatory period. The magnitude of the discharge is given by its corresponding EPA Sum. The standard could be rephrased as saying, for example, "Values of EPA Sum greater than 1 shall occur with a probability of less than 0.01 in 10,000 years". Estimation of the probability of exceeding a given value of EPA Sum includes contributions from all scenarios.

We have performed analyses based on both interpretations.

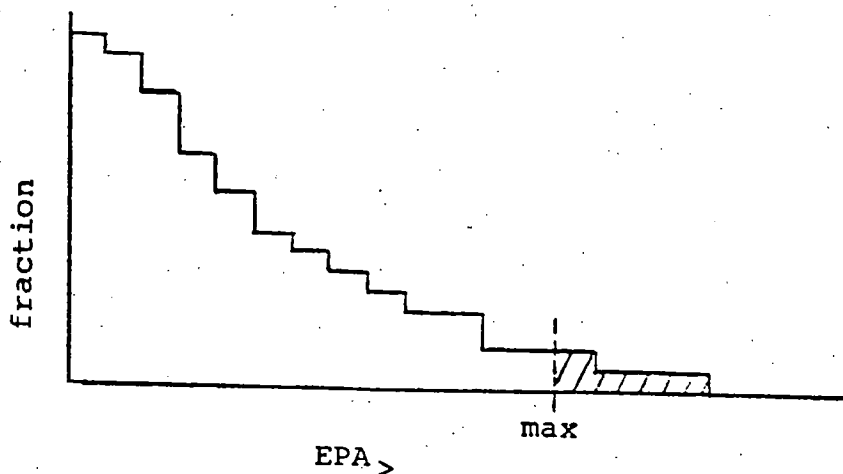
## 2.2 Implementation of Different Interpretations

### Interpretation 1:

The probability assigned to the scenario indicates whether values of the EPA Sum will be compared to 1 or 10. Different values of the EPA Sum result from different combinations of input data chosen by the sampling procedure.<sup>4</sup> Thus, there is a sampling error in the assessment of compliance.

\*See page 27 for a definition of "vector".

The results of calculations are presented in the form of a Complimentary Cumulative Distribution Function (CCDF) as suggested by EPA<sup>3</sup>. Such a CCDF is illustrated in the following diagram.



For N input vectors sampled for the scenario, the plotted curve enables one to see what fraction (if any) of the N vectors produce a value of the EPA Sum greater than some value denoted by EPA >. In this example, the shaded area indicates that a fraction of the vectors do violate the standard.

#### Interpretation 2

According to this interpretation, the analyst is presumed to have the same set of scenarios and probabilities as in Interpretation 1. Each scenario is again analyzed to estimate the EPA Sum as in Interpretation 1. However,

with this interpretation, compliance is estimated by constructing a CCDF from all scenarios. The construction of this CCDF is aided by first constructing a plot of probability versus the EPA Sum for each scenario. An important point should be made regarding the probabilities used in the construction of the CCDF; namely, that the probability used is that of the scenario's occurrence and the particular combination of the input data used in the calculation of the EPA Sum.

Construction of the CCDF then includes contributions from all scenarios analyzed and expected to produce an EPA Sum greater than a given value,  $EPA_{>}$ . The probability,  $p_{>}$ , associated with  $EPA_{>}$  is given by

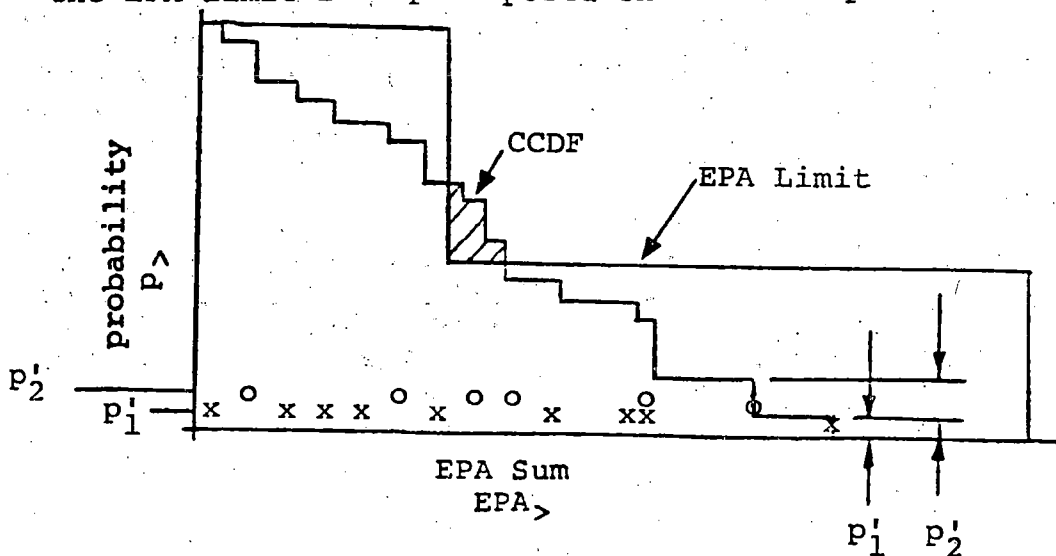
$$p_{>} = \sum_s p_s \cdot p_c (EPA \text{ Sum} > EPA_{>} | s)$$

$$= \sum_s \frac{p_s}{N} \cdot \text{Number of vectors with EPA Sum} > EPA_{>} \text{ for scenario, } s.$$

where  $p_s$  is the probability of scenario  $s$ , and  $p_c$  is the conditional probability of the state of the repository, given scenario  $s$ . The last step, substitution for  $p_c$ , follows from the fact that the LHS method selects  $N$  input vectors with equal probability. For simplicity, we write

$$p_s' = \frac{p_s}{N}$$

Construction of the CCDF is illustrated<sup>3</sup> in the following diagram for the case of two scenarios where, for clarity, the EPA limit is superimposed on the CCDF plot.



Compliance with the draft EPA Standard is then determined by comparison of the constructed CCDF with an "envelope" defined by the standard and illustrated in the diagram. The shaded area in the diagram defines the part of the constructed CCDF outside of the EPA limit and indicates non-compliance with the standard.

### 2.3 Estimation of Probabilities of Scenarios

Although the methods developed at Sandia may be used with ranges and distributions for  $p_s$ , the scenario probability, we have used fixed values in this analysis. The site we have assumed for this analysis has not been characterized sufficiently to allow estimation of the probabilities. Since the draft EPA Standard requires this information and, since it may introduce further uncertainty into estimates of compliance, it is appropriate in this work to discuss the likely sources of the probabilities.

- Source 1. Of the scenarios to be analyzed, the analyst may have reason to believe that the processes involved are stochastic in nature. In such a case, methods may exist to estimate this probability with the final uncertainty in the estimate resulting from uncertainty in input data and the accuracy of models used to perform the estimate. At least one attempt has been made to address faulting in this manner with input data describing existing fault density and stress states required.<sup>5</sup>
- Source 2. Historical data may be available that could be extrapolated into the future to estimate probabilities of some scenarios. An example of use of such data is the estimation of exploratory drilling for petroleum resources. In the reference site analysis of a hypothetical nuclear waste repository in bedded salt, drilling records for similar sites were used to estimate the probability of future exploratory drilling into the repository.<sup>6</sup>

Source 3. In the absence of historical records and detailed understanding of the processes involved, expert judgement may be used to estimate scenario probabilities. The Delphi method is one example of the many ways in which expert judgement can be used.

The use of expert judgement is implicit in Source 1 and Source 2, since unquantifiable judgements must be made as to the applicability of the data and models.

### 3. THE REFERENCE BASALT SITE

The reference basalt repository is located in the center of a drainage basin within a region of flood basalts. This reference site is shown schematically in Figure 1. Mountains along the northern, northwestern and southwestern edges of the site are zones of recharge to the groundwater system. A major river, River C, flows through the site from the northwest to the southeast. The deeper ground water near the repository site discharges to the upper unconfined aquifers west of mountain M1.

This region is underlain by a sequence of basaltic lava flows. The sequence of flows contains sedimentary beds of regional extent. Overlying the volcanic rocks is an unconfined aquifer consisting of alluvial sand and gravel. The geologic cross-section at the Reference Site (A-A' cut) is shown schematically in Figure 2. The repository is located in the middle of a dense basalt formation. Overlying this horizon is a sequence of four layers of alternating interflows and dense basalts. Above these four layers lies a water-bearing interbed (Layer I-V) consisting mainly of sandstone and clay. Above interbed I-V is a basalt formation consisting of three members with distinct chemical signatures. This basalt formation is overlain by a major confined aquifer system (Layer I-M) predominantly composed of tuffaceous siltstones and sandstone. Above aquifer I-M lies a basalt formation (J) which, in turn, is overlain by an unconfined aquifer (UA).

Ranges of horizontal and vertical hydraulic conductivity ( $K_h, K_v$ ) and effective porosity for each layer are presented in Table 2. These ranges are also summarized in Table 4 of Appendix G along with the appropriate references. To be consistent with a real basalt site, a normal distribution was assigned to each range of porosity. A lognormal distribution was assigned to the  $K_h$  data range. The sample population for  $K_v$  that was used in this work was determined by the following method. A lognormal distribution was assigned to the  $K_v$  data range in Table 2. Then using the Latin Hypercube Sampling Technique<sup>4</sup> (LHS),  $K_v$  values were sampled. The sampled values were then subtracted from  $K_v(\text{max})$ . The resulting sample population is skewed toward the high end of the range. For this system, this procedure produces more conservative estimates of discharge than those of the standard lognormal distribution.

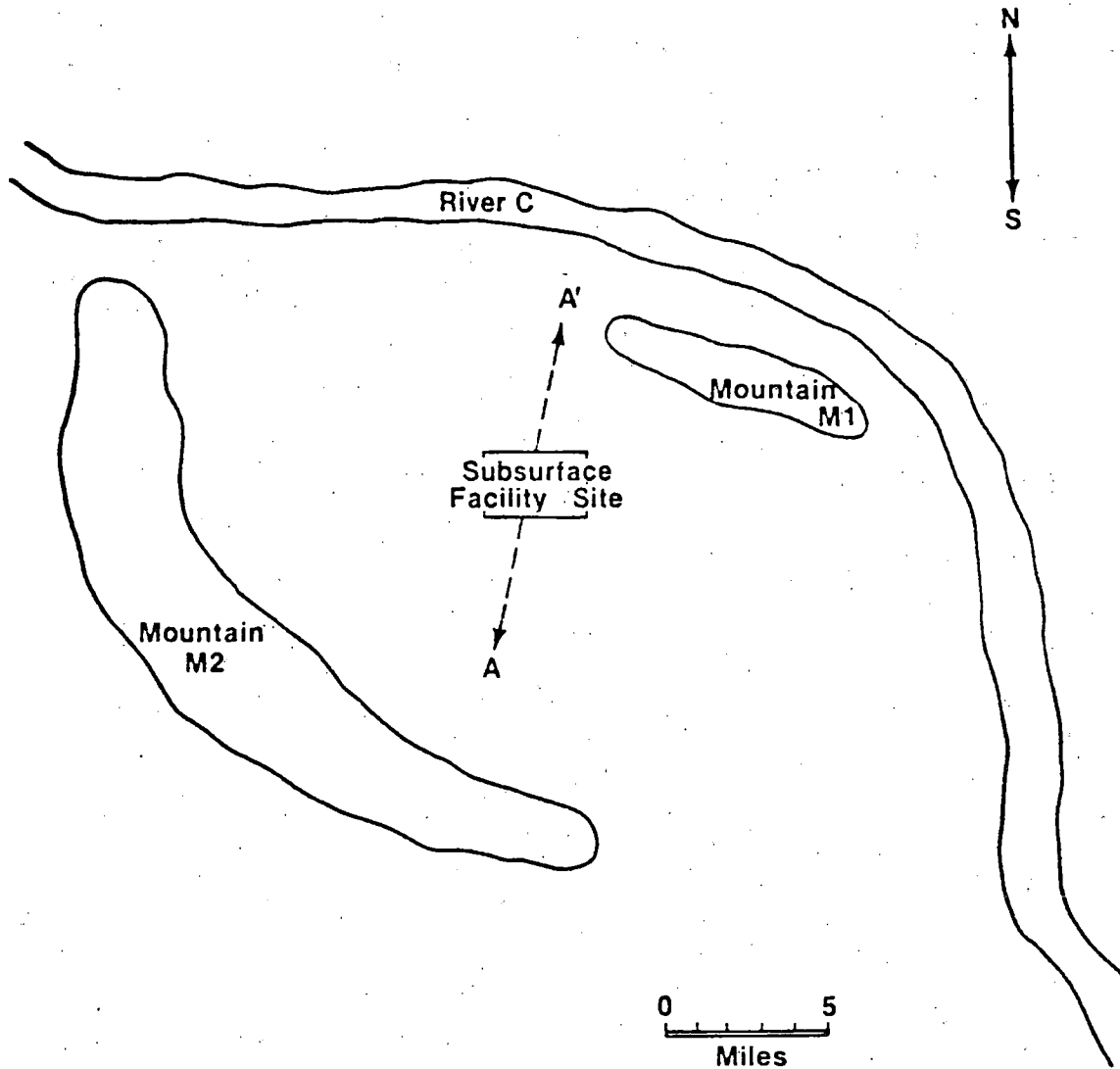


Figure 1. General Geologic Features of the Reference Basalt Repository Site

SYMBOL OF LAYER	THICKNESS (ft)	
UA	200	UNCONFINED AQUIFER
J	850	BASALT FLOWS
I-M	150	INTERBED
H	150	BASALT FLOWS
G	200	BASALT FLOWS
F	690	BASALT FLOWS
I-V	10	INTERBED
E	690	BASALT FLOWS
D	60	INTERFLOW
C	50	COL/ENT
B	150	INTERFLOW
A	300	DENSE BASALT
		 UNDERGROUND FACILITY

Figure 2. Stratigraphic Cross-Section of Hypothetical Repository in Basalt

Table 2

## Reference Hydraulic Properties\*

<u>Layer</u>	<u>Horizontal Hydraulic Conductivity (ft/d)</u>	<u>Vertical Hydraulic Conductivity (ft/d)</u>	<u>Effective Porosity</u>
A	( $10^{-8}$ - $10^{-5}$ )	( $10^{-7}$ - $10^{-4}$ )	( $10^{-3}$ - 0.025)
B	( $10^{-3}$ - $10^{-1}$ )	( $10^{-3}$ - $10^{-1}$ )	( $10^{-2}$ - 0.120)
C	( $10^{-8}$ - $10^{-3}$ )	( $10^{-7}$ - $10^{-2}$ )	( $10^{-3}$ - 0.025)
D	( $10^{-3}$ - $10^{-1}$ )	( $10^{-3}$ - $10^{-1}$ )	( $10^{-2}$ - 0.120)
E	( $10^{-8}$ - $10^{-3}$ )	( $10^{-7}$ - $10^{-2}$ )	( $10^{-3}$ - 0.120)
I-V	( $10^{-1}$ - 10)	( $10^{-2}$ - 1)	(0.1 - 0.2)
F	( $10^{-6}$ - $10^{-2}$ )	( $10^{-6}$ - $10^{-2}$ )	( $10^{-3}$ - 0.120)
G	( $10^{-4}$ - 10)	( $10^{-4}$ - 10)	( $10^{-3}$ - 0.120)
H	( $10^{-4}$ - $10^2$ )	( $10^{-4}$ - $10^2$ )	( $10^{-3}$ - 0.120)
I-M	(1 - 150)	( $10^{-1}$ - 15)	(0.1 - 0.2)
J	( $10^{-4}$ - 2000)	( $10^{-4}$ - 2000)	( $10^{-3}$ - 0.120)
UA	(1 - $10^4$ )		(0.1 - 0.3)

\* The references for the data in this table are included in Table 4 of Appendix G. Also, the ranges of the vertical conductivity of all the layers, except Layer UA, have been combined into a single range to represent a "uniform" vertical conductivity for the host rock system.

A 70 percent rank correlation<sup>4</sup> is assumed to exist between porosity and hydraulic conductivity. This minimizes the occurrence of physically unreasonable combinations of these variables.

The horizontal hydraulic gradients in I-V, I-M and UA are assumed to have a range of  $10^{-4}$  to  $10^{-2}$ . The vertical gradient is assumed to be upward and small in magnitude.

## 4. WASTE AND REPOSITORY DESCRIPTION

### 4.1 Waste

The inventory (Table 3) assumed in this work is equal to half the projected accumulation of 10-year-old spent fuel in the United States by the year 2010. This would contain a total of 103,250 BWR and 60,500 PWR assemblies; a total of 46,800 metric tons of heavy metal (MTHM). The criteria for selection of key radionuclides are described in detail elsewhere<sup>7</sup>. In addition to these criteria, all radionuclides specified in the Release Limit Table of the EPA Standard are included in this inventory list.

All canisters containing the wastes are assumed to have a life of 1,000 years after emplacement. At year 1,000, all canisters fail simultaneously and radionuclide release begins. Radionuclide release is assumed to be determined by a constant leach rate of the waste form. The waste matrix is assumed to dissolve at an annual rate of  $10^{-4}$  to  $10^{-7}$  of the original mass. Radionuclides are assumed to be uniformly distributed throughout the matrix so that their release rate is directly proportional to the matrix dissolution rate; this is also known as congruent dissolution.

### 4.2 Subsurface Facility

The reference subsurface facility is a mined facility at a depth of 3,000 feet below the surface. A description of the facility is summarized in the following data.

Areal dimensions -- 9,840 feet x 7,870 feet

Number of storage rooms -- 120

Storage room dimensions -- length = 3,560 feet

width = 100 feet

height = 40 feet

Porosity of backfilled region -- 18 percent

Table 3

Inventory of Reference Repository  
(Spent fuel from 46,800 MTHM)

<u>Radionuclide</u>	<u>Half Life</u>	<u>Curies</u> (at time=0)
Pu240	6.76E3	2.1E7
U236	2.39E7	1.0E4
Th232	1.41E10	1.7E-5
Ra228	6.7	4.7E-6
Cm245	8.27E3	8.4E3
Pu241	14.6	3.2E9
Am241	433.	7.5E7
Np237	2.14E6	1.5E4
U233	1.62E5	1.8
Th229	7300.	1.3E-3
Cm246	4710.	1.6E3
Pu242	3.79E5	7.5E4
U238	4.51E9	1.5E4
Pu238	89.	9.4E7
U234	2.47E5	3.5E3
Th230	8.E4	0.19
Ra226	1600.	3.5E-4
Pb210	21.	3.3E-5
Am243	7650.	6.6E5
Pu239	2.44E4	1.4E7
U235	7.1E8	7.5E2
Pa231	3.25E4	0.25
Ac227	21.6	5.2E-2
Tc99	2.14E5	6.1E5
I129	1.6E7	1.5E3
Sn126	1.0E5	2.2E4
Sr90	28.9	2.4E9
Cl4	5730.	3.5E4
Cs135	2.0E6	1.3E4
Cs137	30.	3.5E9

## 5. GEOCHEMISTRY

### 5.1 Retardation Factors

One of the most important barriers to the movement of dissolved radionuclides in ground water is retardation due to the interaction between radionuclides and the geologic medium. The retardation factor is defined as the ratio of the velocity of the fluid to the velocity of the retarded radionuclide. A radionuclide with a retardation factor of 10 would travel at one-tenth the velocity of the ground water. A general expression for the retardation factor is given by:<sup>8</sup>

$$R = 1 + R_d \rho \psi (1 - \phi_{\text{eff}}) / \phi_{\text{eff}} \quad (5.1)$$

where

$\psi$  = utilization factor

$R_d$  = sorption ratio of radionuclide  
in ml/g

$\rho$  = grain density of rock in g/cm<sup>3</sup>

$\phi_{\text{eff}}$  = effective porosity of rock matrix

The utilization factor ( $\psi$ ) is the fractional volume of the rock matrix that interacts with the fluid. For flow in porous media,  $\psi$  approaches unity. In fractured media such as basalt, ground water travels almost exclusively in fractures. Most of the bulk rock matrix does not interact with the fluid; under these conditions,  $\psi$  may be much less than unity. It will be shown that a simpler expression than Equation (5.1) can be used to calculate the retardation factor if we make certain assumptions about  $\psi$ .

At the reference site, nearly all of the fractures in the basalts are assumed to be lined with secondary mineralization. We have assumed that the ground water comes in contact only with the secondary minerals. Therefore, the volume of the rock matrix that interacts with the fluid is equal to the volume of the secondary mineralization. The utilization factor can be calculated as

$$\psi = \frac{\text{volume of secondary mineralization}}{\text{total rock volume}}$$

The volume of secondary mineralization is equal to a fraction or multiple (f) of the volume of open space remaining in the fractures (fracture porosity). For a unit volume of rock matrix, the utilization factor can be calculated as

$$\psi = \frac{f \cdot \text{fracture porosity}}{1 - \text{total porosity}}$$

If we assume

$$\phi_{\text{total}} \sim \phi_{\text{eff}} \sim \phi_{\text{fracture}}$$

then

$$\psi = f \cdot \phi_{\text{eff}} / (1 - \phi_{\text{eff}})$$

Therefore Equation (5.1) becomes

$$R = 1 + f R_d \rho \quad (5.3)$$

In our calculations, we have assumed that the original fractures have been on the average one-half filled with secondary minerals. Therefore,  $f = 1$  and

$$R = 1 + R_d \rho \quad (5.4)$$

In this study, Equation (5.4) rather than the more general Equation (5.1), has been used to calculate R for fractured media. Note that the values of  $R_d$  and  $\rho$  for the secondary minerals must be used in the equation. A more detailed derivation of Equation (5.3) is given in Appendix A.

The sorption ratio  $R_d$  for radionuclides in rock-water systems is defined as,

$$R_d = \frac{\text{mass on solid phase per unit mass of solid}}{\text{mass in solution per unit volume of solution}} \quad (5.5)$$

Calculations of radionuclide discharge from a repository are sensitive to values of  $R_d$ . The magnitude of  $R_d$  is influenced by many factors including solution composition, pH, Eh and temperature. Laboratory measurements of  $R_d$  have been made under a variety of physico-chemical conditions. The geochemical environment along postulated groundwater flow paths must be characterized in order to choose the  $R_d$  values that were obtained under the most relevant laboratory conditions.

The geochemical environment that was postulated for each stratigraphic layer shown in Figure 2 is described in Table 4. Equation (5.1), with a utilization factor of unity, was used to calculate the retardation factors for layers which are assumed to be porous. Equation (5.4) was used for layers in which ground water flows predominantly through fractures. The redox potential along the flow path and the nature of the minerals which interact with the fluid are also described in Table 4.

Table 5 shows the ranges and distributions of  $R_d$  used in this study. For basalt and secondary minerals it was assumed that data ranges obtained from experimental measurements mark the 95 percent confidence level interval. From these limits, new ranges for the 99.9 percent confidence level were generated and are shown in Table 5. The last column of the table shows the ranges of  $R_d$  in sandstone/siltstone for use in the unconfined aquifer layer. Appendices B and G contain a description of the data set from which the  $R_d$  values were selected and a discussion of the Eh-pH conditions in each stratum.

Table 4

Geochemical Environment of Stratigraphic  
Layers in Basalt Repository

<u>Layer</u>	<u>Type of Medium</u>	<u>Redox Conditions</u>	<u>Mineralogy</u>
A	Fractured	Reducing	Secondary minerals
B	Fractured	Reducing	Secondary minerals
C	Fractured	Reducing	Secondary minerals
D	Fractured	Reducing	Secondary minerals
E	Fractured	Reducing	Secondary minerals
I-V	Porous	Oxidizing	Secondary minerals
F	Fractured	Reducing	Secondary minerals
G	Fractured	Reducing	Secondary minerals
H	Fractured	Reducing	Secondary minerals
I-M	Porous	Oxidizing	Secondary minerals
J	Fractured	Reducing	Secondary minerals
UA	Porous	Oxidizing	Sandstone/silt

Density of secondary minerals =  $2.3 \text{ g/cm}^3$

Density of rock in layer I-V and I-M =  $3.3 \text{ g/cm}^3$

Table 5

 $R_d$  Ranges\* (ml/g)

Element	Reducing SM**	Oxidizing SM**	Reducing Basalt	Oxidizing Sandstone/Siltstone
Cm, Am	(25., 2.0E6)	(25., 2.0E6)	(33., 300.)	(1.0E-2, 1.0E5)
Pu	(45., 5.2E3)	(37., 1.5E4)	(0.35, 4.24E4)	(1.0E-2, 1.0E4)
Np	(1.5, 2.8E4)	(4.0, 430.)	(1.7, 1.56E3)	(1.0E-2, 50.)
U	(4.0, 1.3E3)	(2.4, 1.5E4)	(34., 57.)	(1.0E-2, 1.0E4)
Th	(25., 2.0E6)	(25., 2.0E6)	(33., 300.)	(1.0E-2, 1.0E4)
Pa	(25., 2.0E6)	(25., 2.0E6)	(33., 300.)	(1.0E-2, 1.0E4)
Ac	(25., 2.0E6)	(25., 2.0E6)	(33., 300.)	(1.0E-2, 1.0E4)
Pb	(17., 5.8E3)	(17., 5.8E3)	(68., 320.)	(1.0E-2, 1.0E4)
Ra	(17., 5.8E3)	(17., 5.8E3)	(68., 320.)	(1.0E-2, 500.)
Sn	(17., 5.8E3)	(17., 5.8E3)	(68., 320.)	(1.0E-2, 500.)
Tc	(0.2, 750.)	(0.6, 10:0)	(0.2, 4.16E4)	(1.0E-2, 1.0E3)
I	(0.7, 6.0)	(0.7, 6.0)	0	(1.0E-2, 100.)
Sr	(0.8, 1.38E3)	(185., 590.)	(67., 600.)	(1.0E-2, 500.)
Cs	(97., 1.3E6)	(97., 1.3E6)	(51., 2.0E3)	(1.0E-2, 1.0E4)
C	0.	0.	0.	0.

Distribution of  $R_d$ : Lognormal

\*More complete data ranges and their appropriate references are compiled in Tables 1, 2, and 3 of Appendix G.

\*\*SM = Secondary Minerals

## 5.2 Solubility

The determination of solubilities of radionuclides in ground water associated with a repository in basalt requires a detailed knowledge of the aqueous geochemistry of these radionuclides. Until detailed calculations can be made, the solubility ranges employed to characterize the bedded salt reference site environment<sup>9</sup> have been used in this study (Table 6). The upper limits of these ranges are probably too high. The solubilities of these elements in waters from the basalt repository would be lower than those in the salt brines due to the lower ionic strength and higher pH of the water in the basalt.

## 5.3 Matrix Diffusion

In our calculations, we have assumed that the radionuclide retardation caused by diffusion into the basalt matrix is negligible. This assumption leads to conservative (high) estimates of integrated discharge. It will be shown later that for several calculations this conservative estimate contributed to an apparent violation of the draft EPA Standard.<sup>1</sup> In Appendix C, a method to approximate the retardation due to matrix diffusion is outlined. It is shown that the retardation calculated in this manner has the potential to reduce all discharges to levels below the EPA standard.

Table 6

Ranges of Solubilities of Selected Elements  
Used for Basalt Reference Repository Conditions\*

<u>Element</u>	<u>Mass Fraction (g/g)</u>
Tc	1.1E-9 - 9.4E-5
I	No Limit
Sn	6.6E-17 - 1.5E-4
Cs	No Limit
Ra	8.1E-12 - 1.2E-5
Th	1.1E-9 - 5.7E-6
U	1.6E-8 - 2.0E-2
Np	1.3E-25 - 4.7E-7
Pu	1.7E-16 - 3.8E-4
Am	No Limit
Cm	No Limit
Pb	2.6E-11 - 3.9E-5
Pa	1.4E-7 - 7.1E-4
C	No Limit
Sn	2.2E-6 - 2.8E-3
Ac	No Limit

\*Data are calculated from the solubility data used in a bedded salt repository analysis.<sup>9</sup> Values are confidence intervals for an assumed lognormal distribution.

## 6. GROUNDWATER TRANSPORT MODEL

In the calculations of radionuclide transport it is assumed that ground water flows upward from the vicinity of the repository to an aquifer, whereupon it moves horizontally toward the biosphere. This flow is modelled as being quasi-two-dimensional and described by Darcy's Law:

$$q = Q/A = KI \quad (6.1)$$

where  $Q$  is the volumetric flow rate through an area  $A$ , normal to the flow direction,  $I$  is the hydraulic gradient,  $K$  is the hydraulic conductivity, and  $q$  is the Darcy velocity. When the flow passes through a series of layers with different hydraulic properties, an "effective" hydraulic conductivity may be calculated by

$$K = \frac{\sum_i L_i}{\sum_i \frac{L_i}{K_i}} \quad (6.2)$$

with

$L_i$  = thickness of layer  $i$

$K_i$  = hydraulic conductivity of layer  $i$

The total groundwater travel time is given by

$$\text{Time} = \sum_{i=1} \frac{L_i}{V_i} \quad (6.3)$$

where  $V_i$  is the interstitial groundwater velocity in layer  $i$  and is equal to  $q/\phi_i$ , with  $\phi_i$  being the effective porosity of layer  $i$ .

When a radionuclide (RN) is transported by ground water, the radionuclide travel time ( $T_{RN}$ ) is increased by its retardation factor. This is given by

$$T_{RN} = \sum_i \frac{L_i R_i^{RN}}{V_i} \quad (6.4)$$

where  $R_i^{RN}$  is the retardation factor of radionuclide RN in layer  $i$ .

The Distributed Velocity Method (DVM) has been developed by Sandia<sup>2</sup> to simulate long chains of radionuclides transported by ground water. In this study we calculated the average velocity of radionuclides using Equation (6.4). Then the DVM code was used to calculate the discharges of radionuclides.

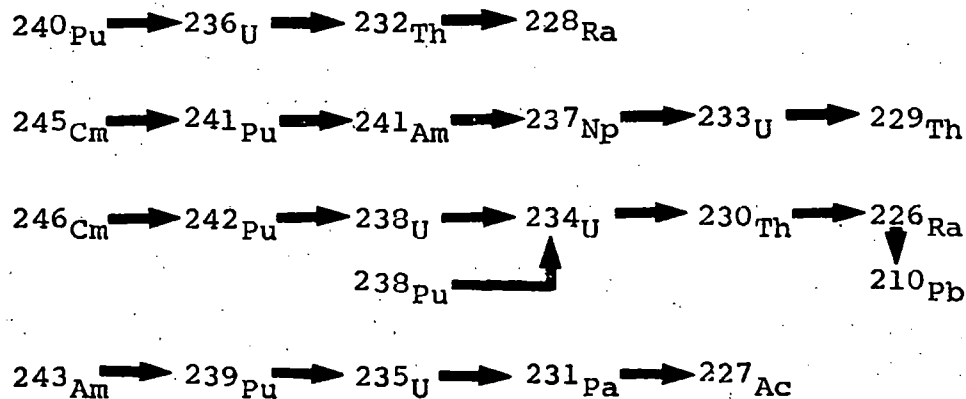
## 7. SCENARIOS ANALYZED

Large uncertainties were associated with many of the input variables in the model. These variables were assumed to be distributed according to user-specified probability distributions and ranges, rather than point values. The Latin Hypercube Sampling (LHS) technique<sup>4</sup> was used to select the input variables. A sample of 100 vectors was generated with this technique. Each vector consists of a particular combination of input variable values where the *i*th component of the vector corresponds to the sampled value of the *i*th variable.

Radionuclide discharge rates for each vector were calculated at some specified location. Discharge rates were integrated for 10,000 year periods from 0 to 50,000 years. The integrated discharge for each radionuclide was then divided by its EPA release limit<sup>1</sup> to assess compliance of that vector with the draft EPA Standard.

Three scenarios were analyzed for the basalt reference repository. A "no-disruption" base case scenario and two scenarios involving disruption of the repository were considered. Both of the latter two scenarios are consistent with the geological setting described in Chapter 3. The disruptions involve the introduction of a zone of high hydraulic conductivity and could be caused by either natural or artificial processes.

Based on the inventory and toxicity of each radionuclide, the following chains of radionuclides were considered:



The fission and activation product radionuclides Tc99, I129, Sn126, Sr90, Cl4, Cs135, and Cs137 were also considered in this work.

Table 7 shows the data ranges and distributions for some additional variables used in the calculations of these scenarios.

Two source model descriptions were used in this analysis. The first source model assumes that the solid matrix containing the waste radionuclides (e.g., spent fuel elements or borosilicate glass) breaks down at a constant rate. This is the so called "leach-limited source model". Radionuclide release then occurs at a rate determined by the inventory in each differential mass increment that is released. Solubility limits are not used at all with this source model. For simplicity, radionuclides are assumed to be homogeneously distributed throughout the solid matrix. The leach-limited source model is most easily compared with the requirements of 10CFR60. Simply stated, 10CFR60 requires that release rates not exceed a specified rate of  $10^{-5}$ /year. The release rate is equal to the reciprocal of the leach period.

The second source model assumes that the backfilled regions can be modeled as a mixing cell. The waste matrix still is assumed to decompose at a constant rate. However, the radionuclides are assumed to instantaneously mix with water in the mixing cell. Radionuclide release from the backfilled regions is sensitive to the radionuclide concentration in the mixing cell. This model is discussed further in Appendix E. Note that even when the mixing cell model is chosen, it is possible that for certain radionuclides (if their solubility limits are sufficiently high) the transport is effectively leach limited.

NWFT/DVM allows user-selection of the source model. It also has an algorithm for automatic source model selection. In the scenarios to be described, only Scenario 3 had the necessary conditions to select the mixing cell model. For comparison, this scenario was also analyzed with the leach-limited source model imposed.

### 7.1 Scenario 1 -- Routine Release

In this scenario, it was assumed that ground water migrates into the repository and saturates the pore volume of the repository. When the waste canisters fail at 1,000 years, this column of water, having the cross-sectional area

Table 7

## Data Ranges and Distributions for Additional Variables

	<u>Range</u>	<u>Distribution</u>
Leach Period (year)	$10^4 - 10^7$	Log Uniform
Horizontal gradient in aquifer	$10^{-4} - 10^{-2}$	Uniform
Conductivity of borehole	0.05 - 50	Log Uniform
Porosity of borehole	0.05 - 0.5	Normal
Vertical upward gradient in Scenarios 1 and 2	$5 \times 10^{-3} - 3 \times 10^{-2}$	Uniform
Vertical upward gradient in Scenario 3	$3 \times 10^{-3} - 2 \times 10^{-2}$	Uniform
Dispersivity (ft)	50	

of the repository, slowly transports leached and dissolved radionuclides vertically through the basalt layers to the aquifer system I-M and then horizontally through the aquifer to a discharge point 1 mile down gradient. In our base case and in the other scenarios, it was assumed that there existed little or no natural vertical gradient. A temperature field in the vicinity of the repository, due to the heat generated from the decaying wastes, produces an upward hydraulic gradient due to thermal buoyancy of the ground water. For our base case, we estimated that this thermal buoyancy effect generated a hydraulic gradient ranging from  $5 \times 10^{-3}$  to  $3 \times 10^{-2}$ . This gradient is assumed to be constant along a vertical column which has the hydraulic conductivity given by Equation (6.2). The derivation of this calculation is presented in more detail in Appendix D. It was also assumed that the upward flow of ground water into aquifer I-M does not alter the natural hydraulic gradient in that aquifer. Figure 3 schematically shows the transport route in this scenario.

Integrated discharges for each vector were calculated at a distance of 1 mile down gradient in aquifer I-M. The results of these calculations are as follows. The integrated discharges for each actinide radionuclide were all zero for all vectors. For the fission product radionuclides, there were some small discharges but they were all below the EPA release limits. This was true for all five of the 10,000-yr. increments of the 50,000-yr. total period of analysis.

In this scenario, all 100 vectors resulted in a leach-limited source as determined by the automatic source selection algorithm of NWFT/DVM. The algorithm selects the source model based largely on the anticipated residence time of the ground water in the near field.

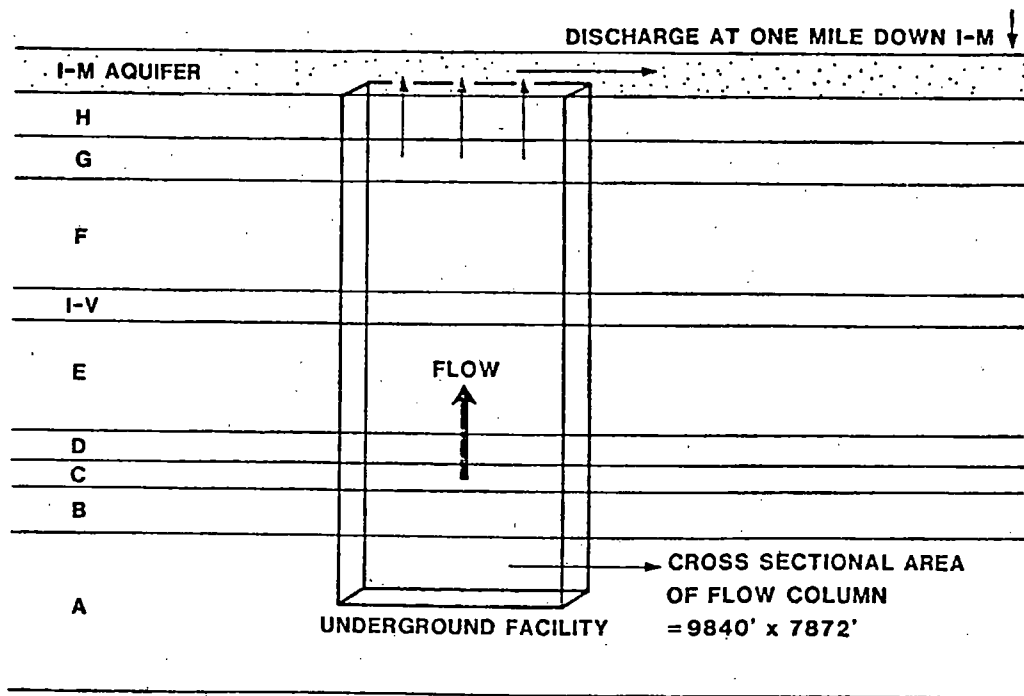


Figure 3. Routine Release Scenario (Scenario 1)

## 7.2 Scenario 2 -- Fractures in Dense Basalt

This scenario is based on the assumption that the hydrologic properties of the dense basalt unit (Layer A) containing the subsurface facility have been altered. Specifically, this scenario assumes that the hydraulic conductivity and porosity have been increased due to the repository-induced fracturing of the rock strata. The generation of these new fractures could be caused by one or more of several processes: thermal stress from waste heat, mechanical stress from the construction of the repository, or the occurrence of an earthquake swarm. The potential increase in conductivity and porosity can enhance the upward migration of radionuclides released from the subsurface facility.

In the calculations of radionuclide releases, the following assumptions were made (Figure 4):

1. The fractured zone is located above the subsurface facility in the dense basalt unit (Layer A).
2. The fractures in the dense basalt layer occur immediately after closure of the subsurface facility.
3. The fractured zone has the same cross-sectional area as that of the subsurface facility, i.e., 9840' x 7872', and it extends upward through all of Layer A.
4. The hydraulic conductivity of the fractured zone is arbitrarily increased by two orders of magnitude and the porosity is increased by a factor of four. That is,

$$K_{\text{fractured basalt}} = 100 \cdot K_{\text{dense basalt}}$$

$$\phi_{\text{fractured basalt}} = 4 \cdot \phi_{\text{dense basalt}}$$

5. The vertical hydraulic gradient is the same as that used in Scenario 1, i.e.,  $5 \times 10^{-3}$  to  $3 \times 10^{-2}$ .

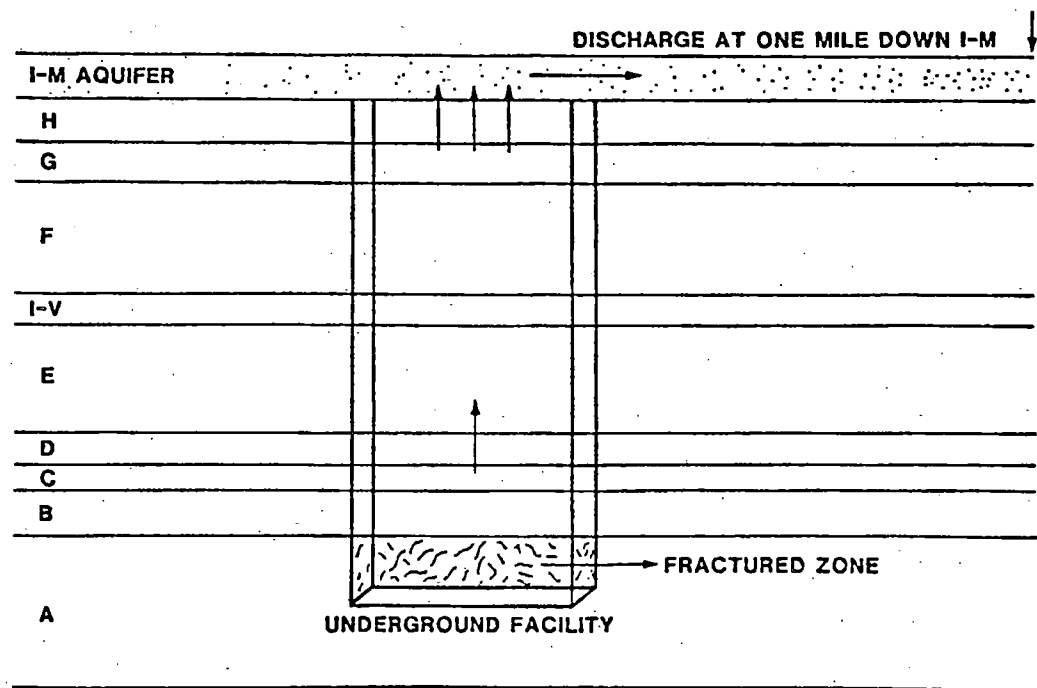


Figure 4. Fractured Dense Basalt Scenario (Scenario 2)

The same 100 vectors as those used in the routine-release scenario were used in the calculations of integrated discharges of radionuclides in this scenario. Two calculations were performed. The discharges were calculated at a location 1 mile down gradient in Aquifer I-M. Table 8 lists the radionuclides and the vectors that showed violation of the draft EPA Standard.

Table 8 also shows that few of the sampled input vectors violate the draft EPA Standard during the first 10,000 years. In these calculations, however, the effective retardation due to diffusion into the rock matrix was ignored. A method for estimating the magnitude of this effect is described in Appendix C. When the retardation, due to rock matrix diffusion calculated by this method, is taken into account, it is possible that no vectors violate the draft EPA Standard.

For readers familiar with the technical criteria of 10CFR60, it is worth mentioning that of all the "violating" vectors listed in Table 8, all except one (vector #24) have leach rates greater than  $10^{-5}$ /year. Also, all vectors except two (#4 and #71) have a groundwater travel time from the repository to the discharge location greater than 1,000 years.

For Scenario 2, all 100 vectors used the leach-limited source model as determined by the automatic source selection algorithm of NWFT/DVM.

### 7.3 Scenario 3 -- Borehole

This scenario assumes that there exists a borehole or a zone of high conductivity that connects the repository to the unconfined upper aquifer (Layer UA). This zone is of very small areal extent (Figure 5). The high conductivity zone could be related to one of the following:

- borehole
- degraded shaft seal
- disturbed rock zone around a borehole or shaft.

This last mode can occur during relaxation of emplacement stresses or as a result of an earthquake.

Table 8

Scenario 2

EPA Ratios\* of Radionuclide Discharges Into Aquifer I-M

0-10,000 years:

<u>Vector #</u>	<u><sup>14</sup>C</u>
5	1.34
71	1.15
77	1.22

10,000-20,000 years:

<u>Vector #</u>	<u><sup>99</sup>Tc</u>
62	1.18
65	1.68

20,000-30,000 years:

<u>Vector #</u>	<u><sup>99</sup>Tc</u>
5	1.29
25	1.08
62	3.43
65	2.00
87	2.04

30,000-40,000 years:

<u>Vector #</u>	<u><sup>99</sup>Tc</u>	<u><sup>234</sup>U</u>	<u><sup>236</sup>U</u>	<u><sup>238</sup>U</u>
5	4.21			
15	1.27			
20	2.27			
25	4.09			
62	1.42			
65	1.99			
87	2.22			

Table 8 (Continued)

40,000-50,000 years:

<u>Vector #</u>	<u><sup>99</sup>Tc</u>	<u><sup>234</sup>U</u>	<u><sup>236</sup>U</u>	<u><sup>238</sup>U</u>
4	1.22			
15	2.54			
20	2.88			
24		3.61	1.43	1.61
87	1.42			

\*EPA Ratio is the ratio of integrated discharge of radionuclide (over 10,000 years) to the allowed EPA Release Limit.

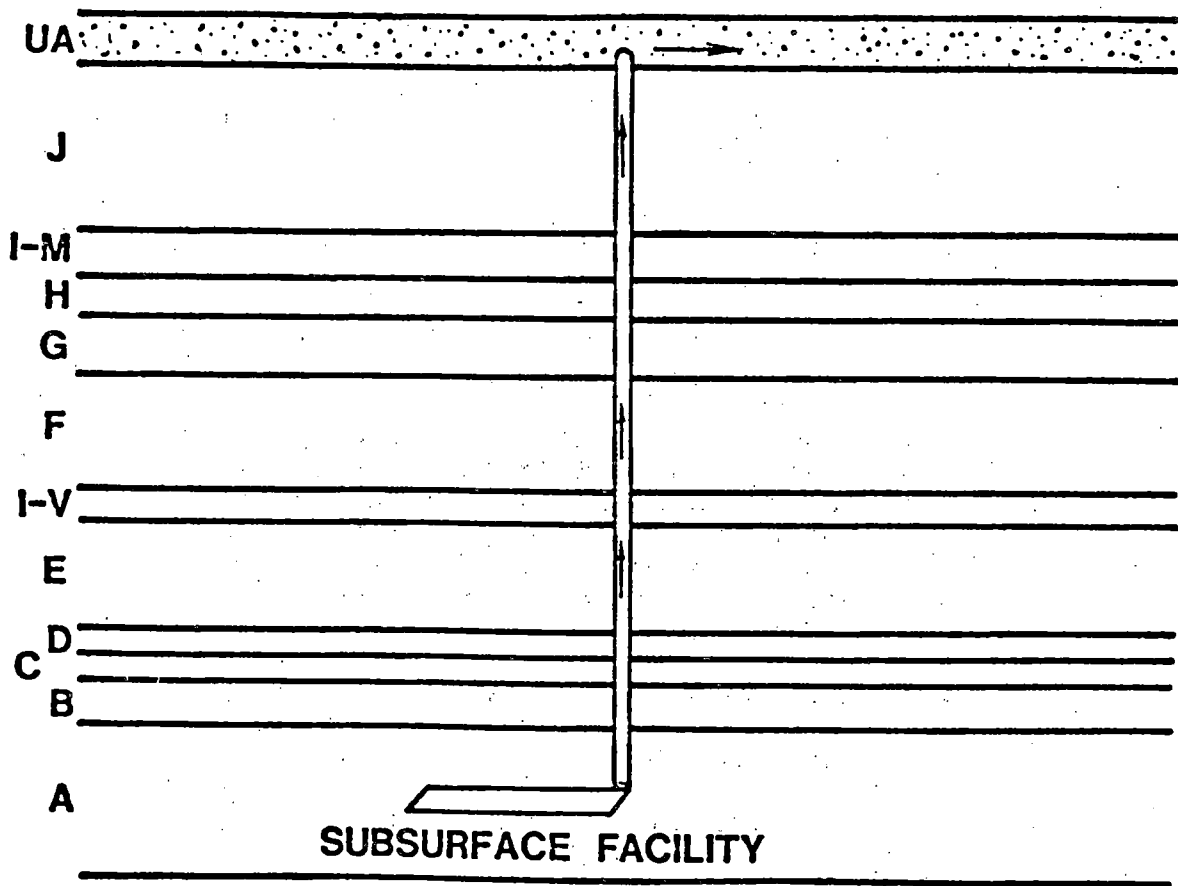


Figure 5. Borehole Scenario (Scenario 3)

The following assumptions were used in the calculations of this scenario:

1. Cross-sectional area of this disruptive zone is 2 square feet.
2. Hydraulic conductivity of this zone has a range of 0.05 ft/day to 50 ft/day. A lognormal distribution is assigned to this range.
3. Porosity of this zone has a range of 0.05 to 0.5. A normal distribution is assigned to this range.
4. The hydraulic gradient in UA is unperturbed due to the smallness of this zone.
5. The same head difference typical of thermal buoyancy as calculated in Appendix C, is assumed here. However, due to the extra 1,000 foot path length between I-M and UA the vertical upward gradient between the repository and aquifer UA is reduced to the range  $3 \times 10^{-3}$  -  $2 \times 10^{-2}$ .
6. Layer UA is composed mainly of sandstone/siltstone and is characterized by an oxidizing environment.
7. The redox potential in the small disruptive zone is reducing and the rock type is fresh basalt.
8. The discharge location is 1 mile down gradient in aquifer UA.
9. The entire radionuclide inventory in the repository is available for leaching and transport.

Three variations of this scenario were analyzed. In Scenario 3A, all 100 vectors chose the mixing cell source model as determined by the automatic source selection algorithm of NWFT/DVM.

Integrated discharges of each radionuclide were calculated for each vector and divided by the EPA Release Limit to produce the "EPA Ratio". Table 9 shows those radionuclides and vectors that produce EPA Ratios of magnitude exceeding one. For each vector, the EPA Ratios were then summed over all radionuclides, and the results are shown in Table 10.

For comparison, Scenario 3B was also analyzed with the leach-limited source model imposed. The range of leach rate was  $10^{-4}$  to  $10^{-7}$  per year. With this source model, too many vectors gave large discharges to list each violating vector as in Tables 9 and 10. In Table 11, we show the mean values for the 100 vectors for each radionuclide that had a significant discharge. From this table, the main contributing radionuclides appear to be 243Am, 240Pu, 239Pu, and 234U. The third variation, Scenario 3C, was also analyzed with the leach-limited source model; but the range of leach rate was  $10^{-5}$  to  $10^{-7}$  per year.

Table 9

Scenario 3A  
EPA Ratios of Radionuclides

<sup>243</sup>Am:

<u>Vector #</u>	<u>10<sup>4</sup>-2x10<sup>4</sup> Years</u>	<u>2x10<sup>4</sup>-3x10<sup>4</sup> Years</u>	<u>3x10<sup>4</sup>-4x10<sup>4</sup> Years</u>
13		1.30	1.15
36	2.34	1.93	

Table 10

Scenario 3A  
 EPA Ratios Summed Over All Radionuclides

<u>Vector #</u>	<u>10<sup>4</sup>-2x10<sup>4</sup> years</u>	<u>2x10<sup>4</sup>-3x10<sup>4</sup> years</u>	<u>3x10<sup>4</sup>-4x10<sup>4</sup> years</u>	<u>4x10<sup>4</sup>-5x10<sup>4</sup> years</u>
13		1.4	1.20	
36	2.49	2.25	1.73	1.55

Table 11

Mean Values of Contributions to the EPA Sum (100 Vectors)  
for Scenario 3B With Leach-Limited Source\*

Radionuclide	10,000 year period				
	1	2	3	4	5
240 Pu	8.56	9.75	3.23	1.87	.69
236 U	.12	.34	.46	.64	.56
245 Cm	.01	.02	.02	.01	.01
241 Am	.05	.02	.02	.01	.01
237 Np	.31	.78	.97	.81	.99
233 U	.01	.07	.13	.25	.31
229 Th	.01	.08	.21	.49	.78
242 Pu	.06	.14	.12	.18	.16
238 U	.15	.35	.49	.66	.54
234 U	.34	.82	1.15	1.52	1.22
230 Th	.01	.05	.10	.22	.30
226 Ra	.02	.20	.48	.91	1.24
210 Pb	0.	.03	.06	.13	.19
243 Am	1.35	3.83	2.60	1.84	1.16
239 Pu	9.02	17.95	12.38	13.91	10.19
235 U	.01	.02	.03	.04	.04
231 Pa	0.	0.	.01	.01	.02
227 Ac	0.	.01	.03	.05	.08
99 Tc	.05	.07	.06	.06	.06
126 Sn	0.	.04	.06	.04	.03
14 C	.13	.04	.01	0.	0.

\* The Range of leach rate is  $10^{-4}$  to  $10^{-7}$  per year

This page intentionally left blank.

## 8. RESULTS OF DEMONSTRATION ANALYSES

For this demonstration, three basic scenarios and several variations on them have been analyzed in detail. A detailed analysis of scenario probabilities has not been performed due to constraints on the allowed effort and the fact that site characterization is in its early stages. The three scenarios analyzed are assumed to form a complete set of mutually exclusive scenarios describing the repository over the 0-10,000 year interval.

$$\sum_s p_s = 1$$

The three scenarios analyzed have been discussed previously. We assume the following probabilities:

<u>Scenario, s</u>	<u>Description</u>	<u>P<sub>s</sub></u>
1	The undisturbed site	0.33
2	The large areal extent, high conductivity zone, e.g., fractures	0.01
3	The small areal extent, high conductivity zone, e.g., a borehole	0.66

Calculations have been performed for the three scenarios to estimate values of the EPA Sum during each 10,000 year interval from zero to 50,000 years following closure. Thus, for Interpretation 1, five CCDFs have been constructed for each of the three scenarios (Scenarios 1, 2, and 3A). For Interpretation 2, a total of five CCDFs have been constructed. The CCDFs based on Interpretation 1 appear in Figures 6 through 20. CCDFs based on Interpretation 2 appear in Figures 21 through 25.

For Scenarios 1 and 2, the automatic source selection algorithm of NWFT/DVM selected leach-limited sources for all 100 vectors. For Scenario 3A, the algorithm selected the mixing cell source model for all 100 vectors. Scenarios 3B and 3C were evaluated with the leach-limited source model imposed. These results are shown in Figures 26 through 30.

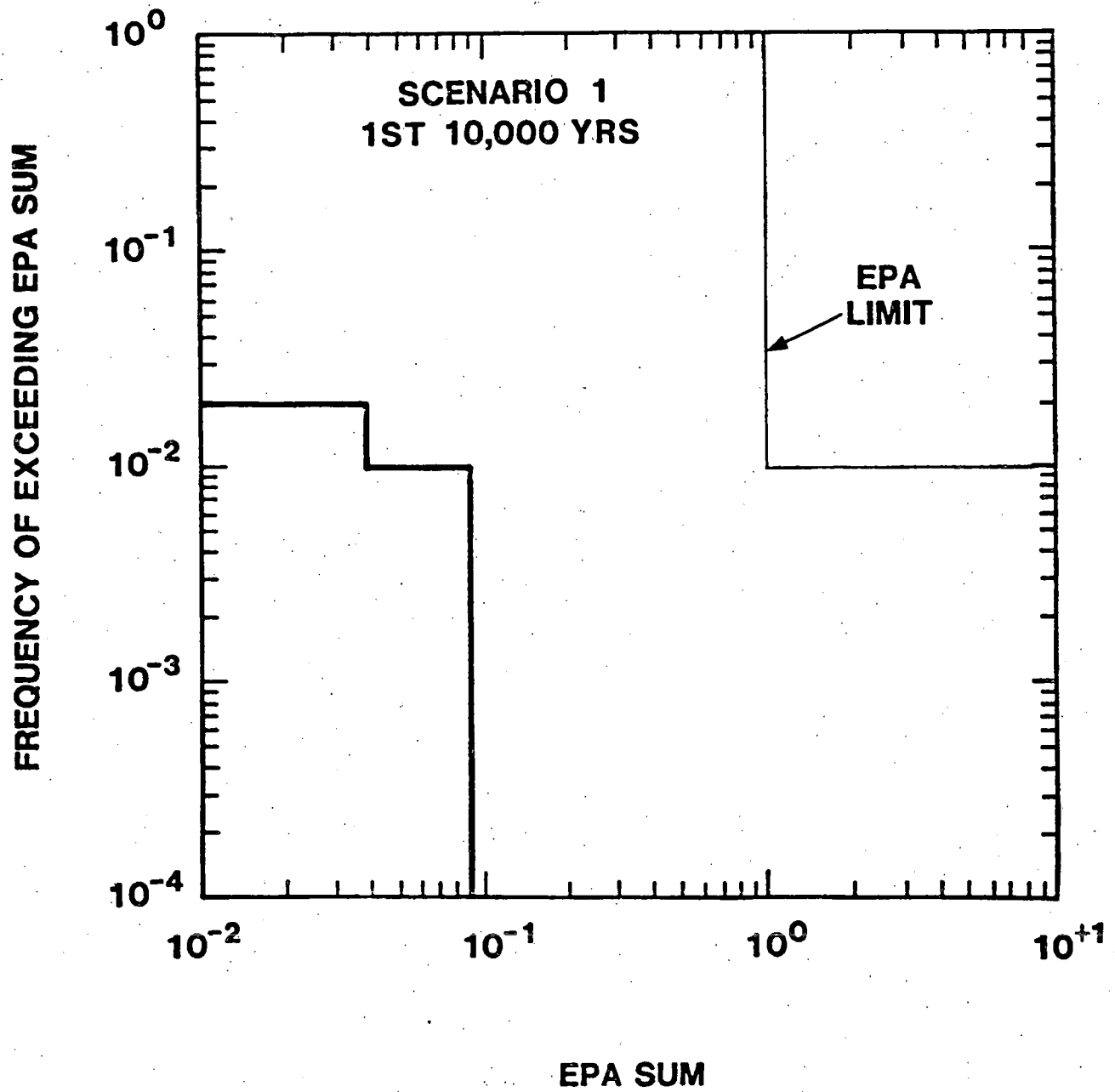


Figure 6. Scenario 1 CCDF - 1st 10,000 Years

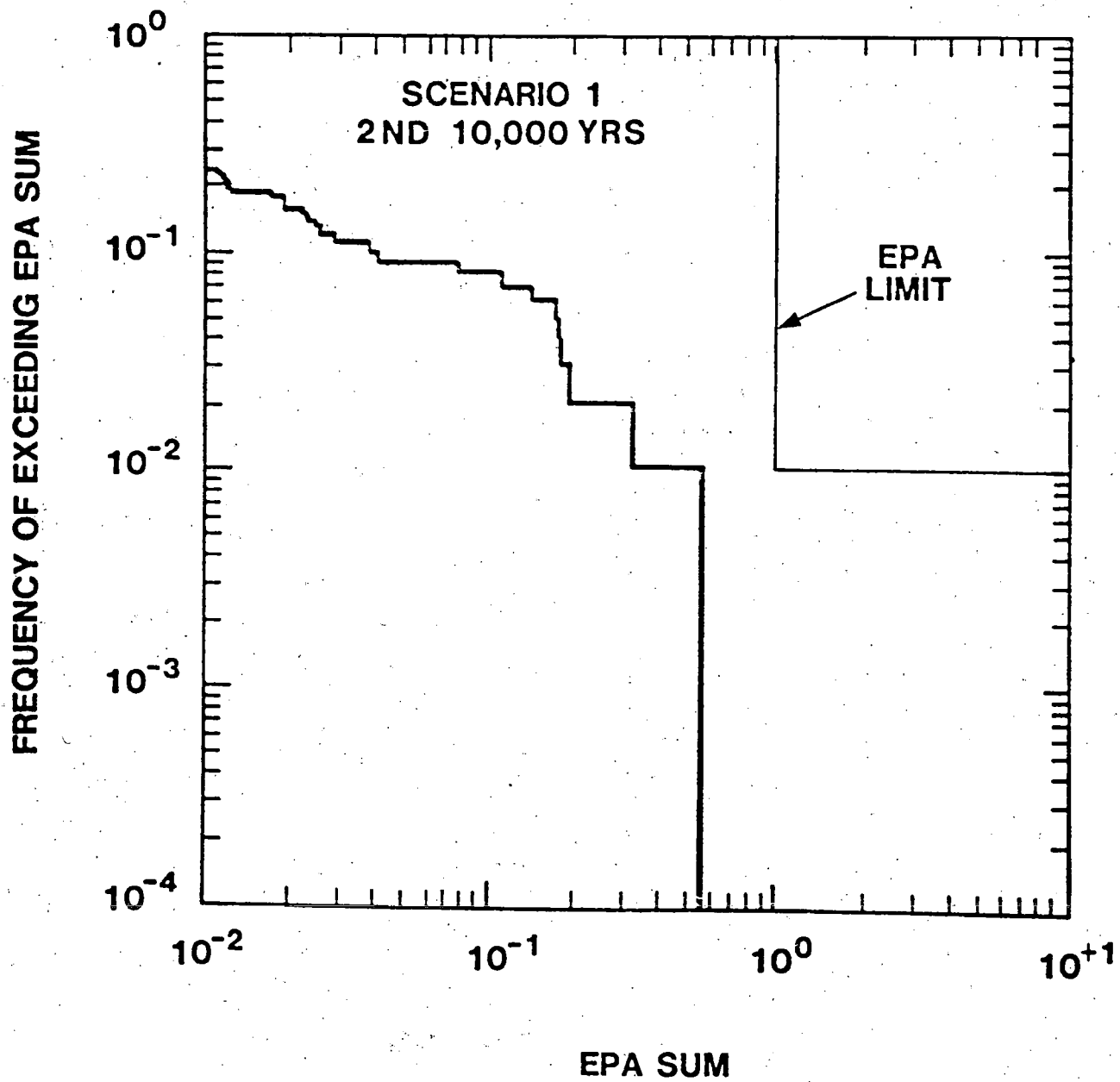


Figure 7. Scenario 1 CCDF - 2nd 10,000 Years

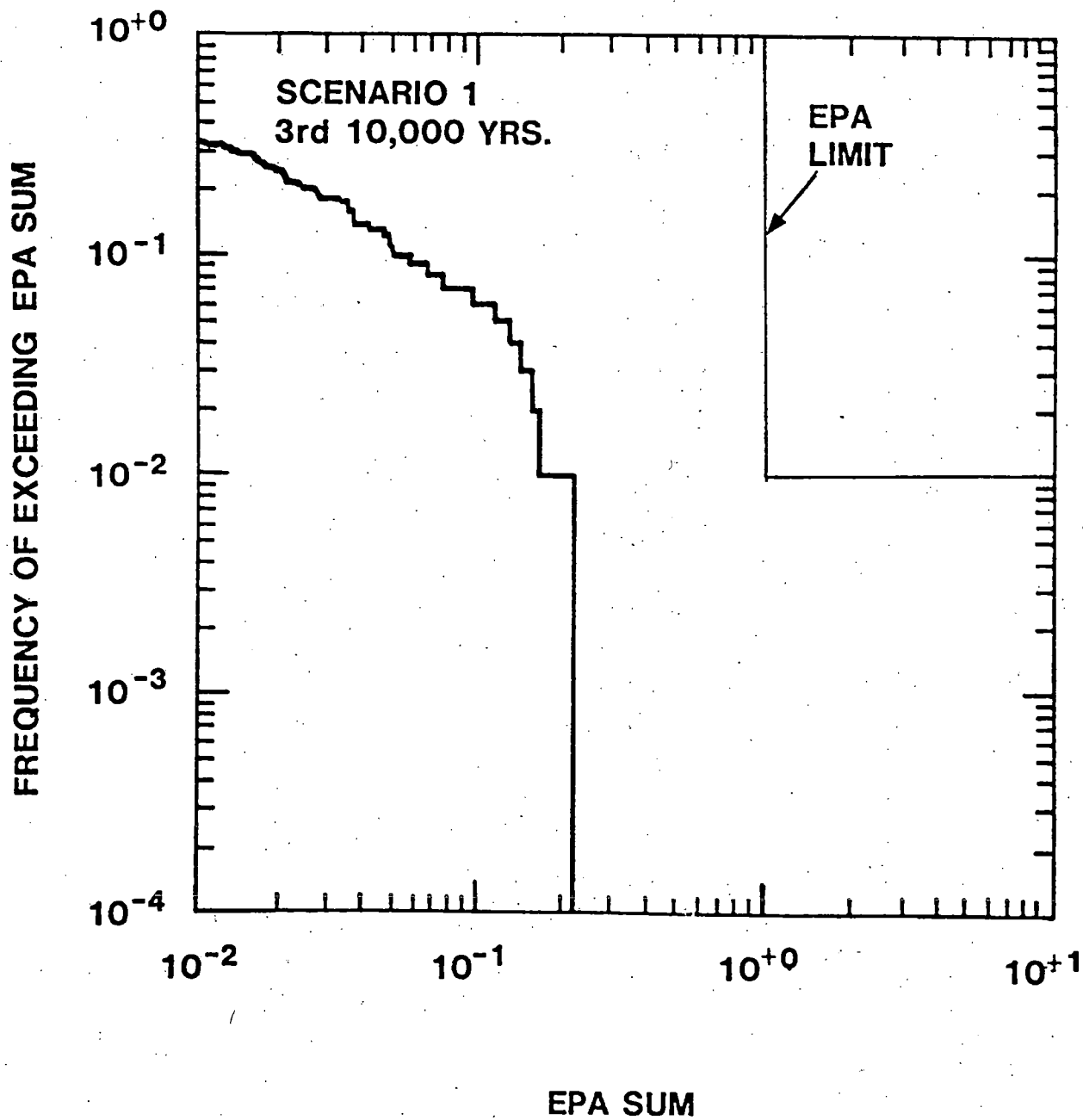


Figure 8. Scenario 1 CCDF - 3rd 10,000 Years

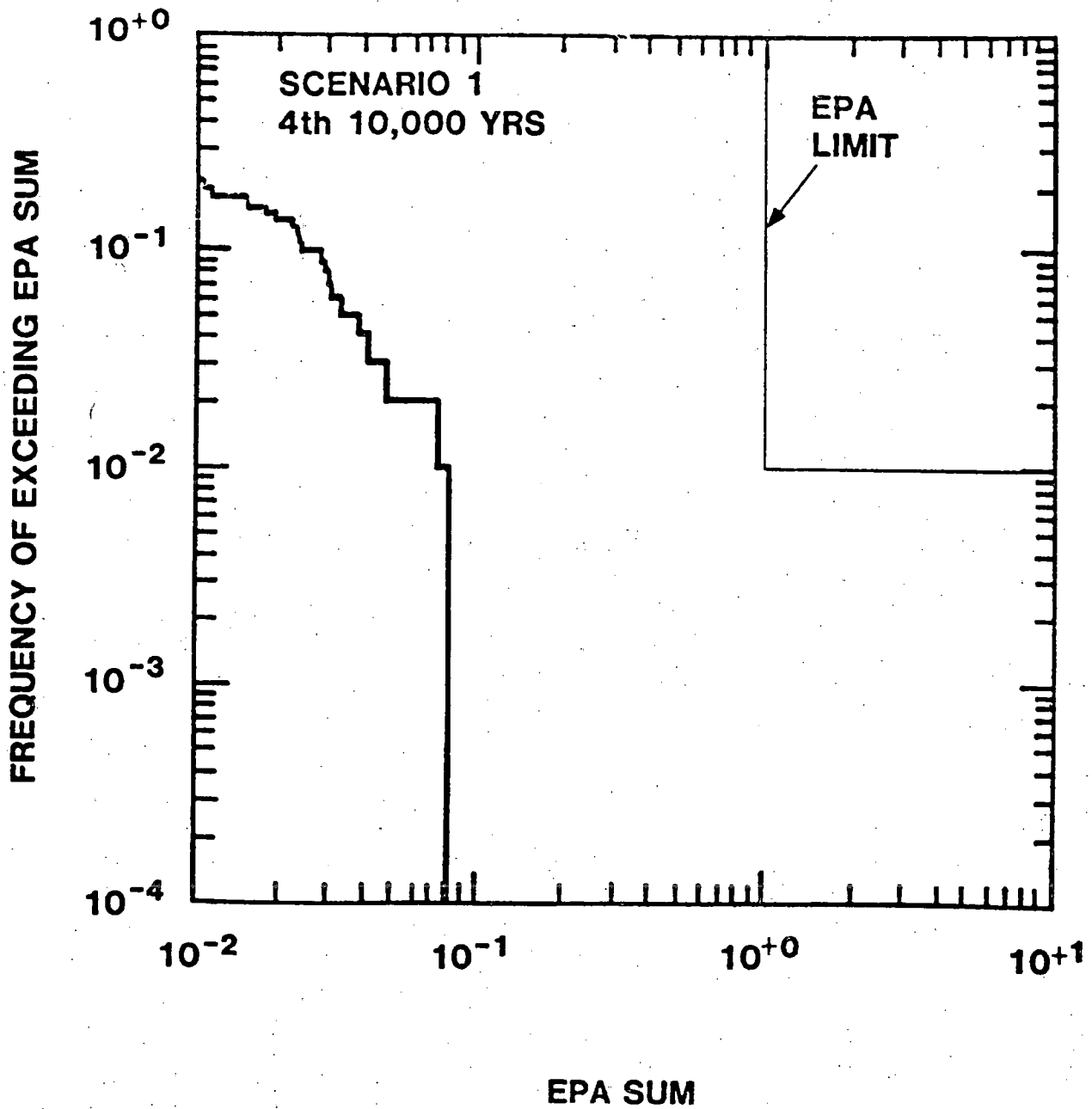


Figure 9. Scenario 1 CCDF - 4th 10,000 Years

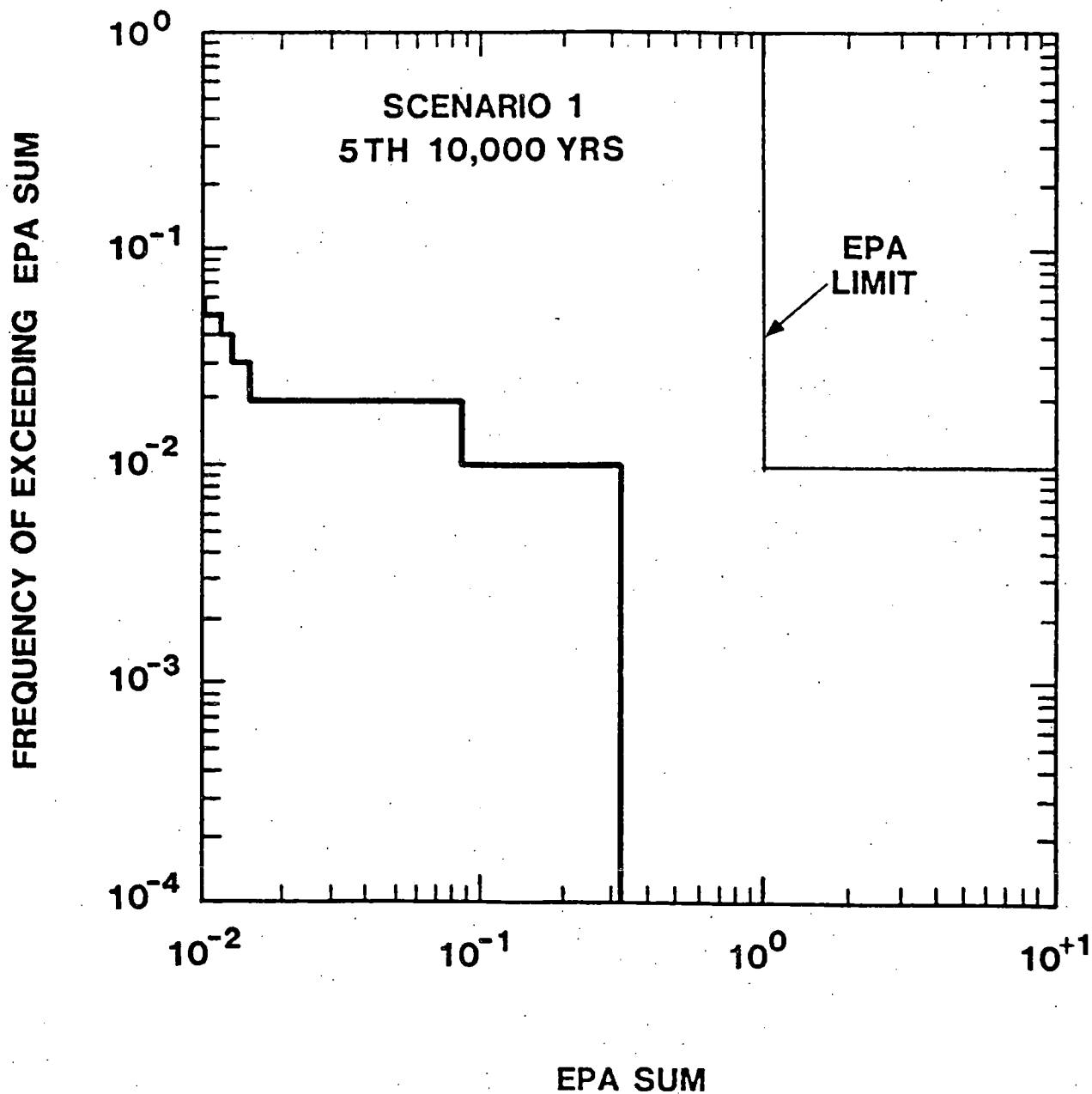


Figure 10. Scenario 1 CCDF - 5th 10,000 Years

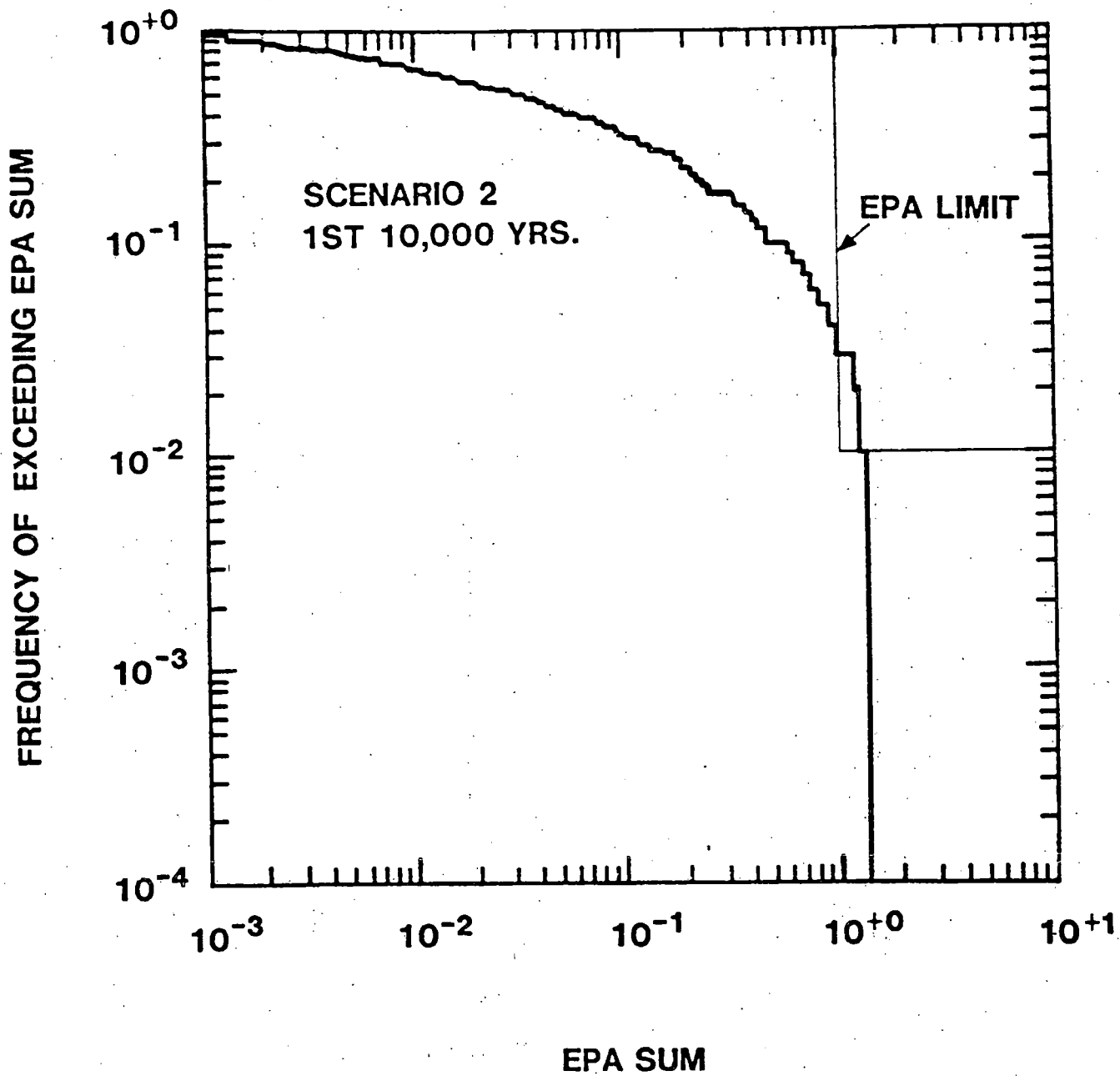


Figure 11. Scenario 2 CCDF - 1st 10,000 Years

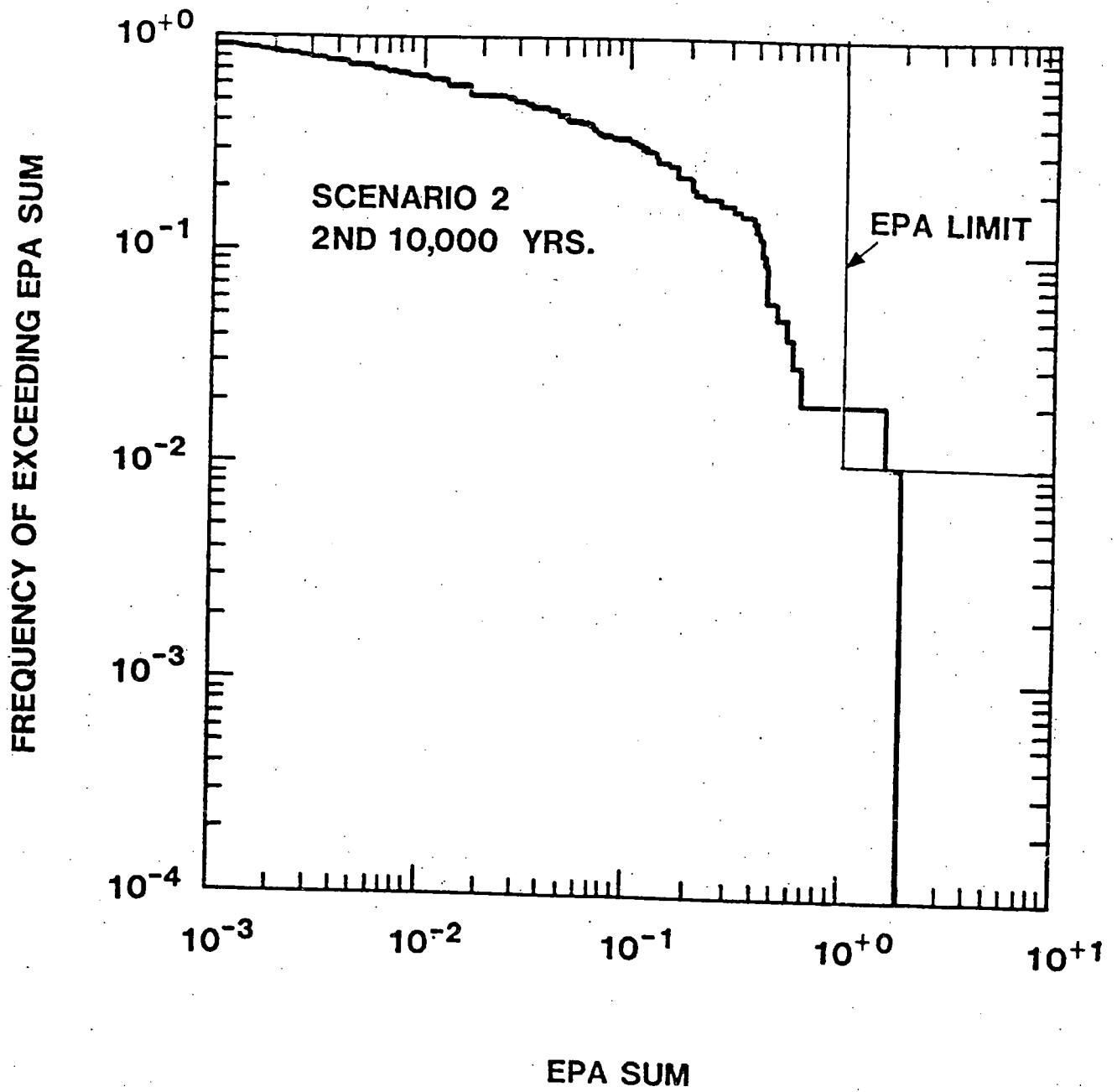


Figure 12. Scenario 2 CCDF - 2nd 10,000 Years

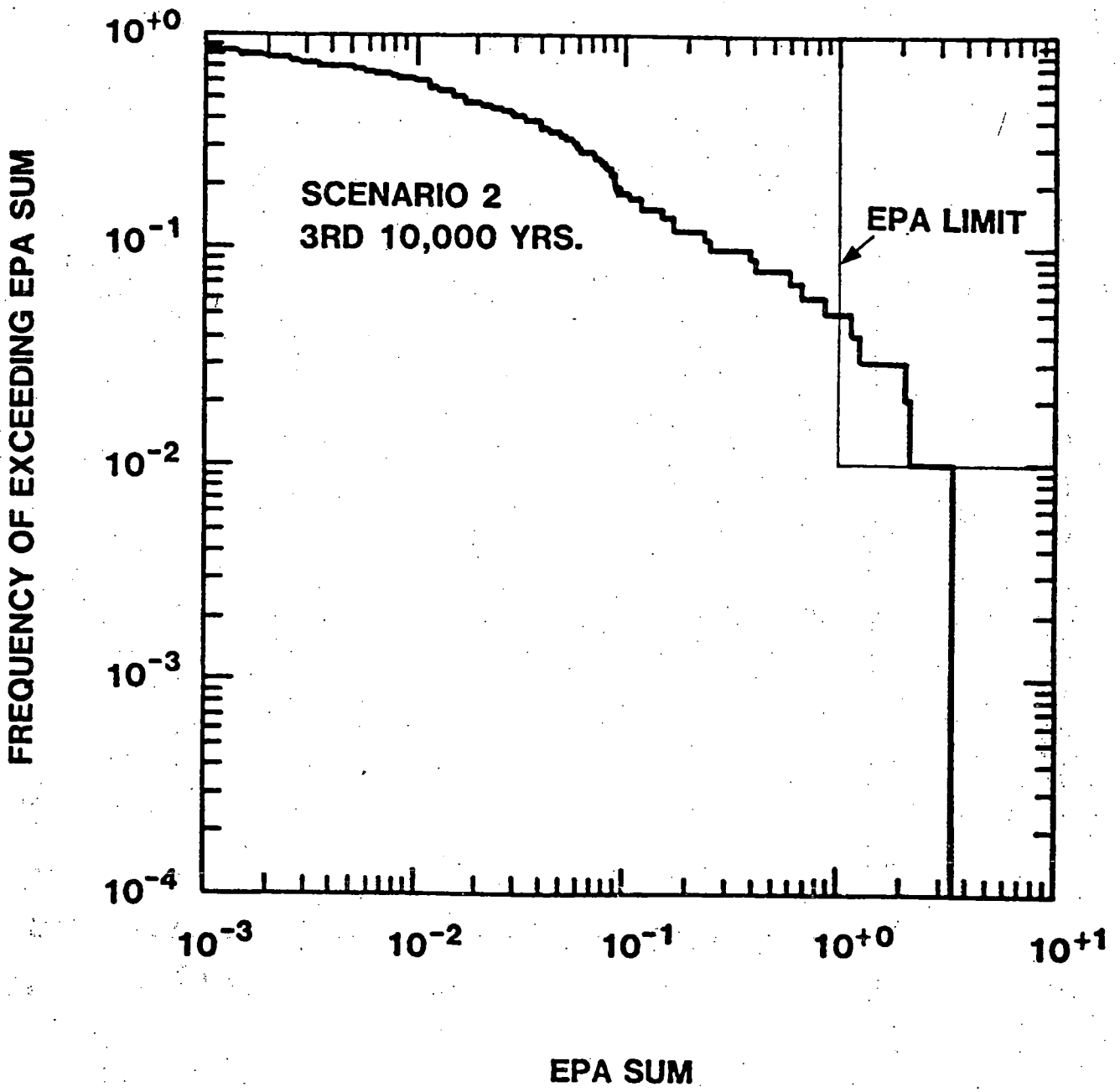


Figure 13. Scenario 2 CCDF - 3rd 10,000 Years

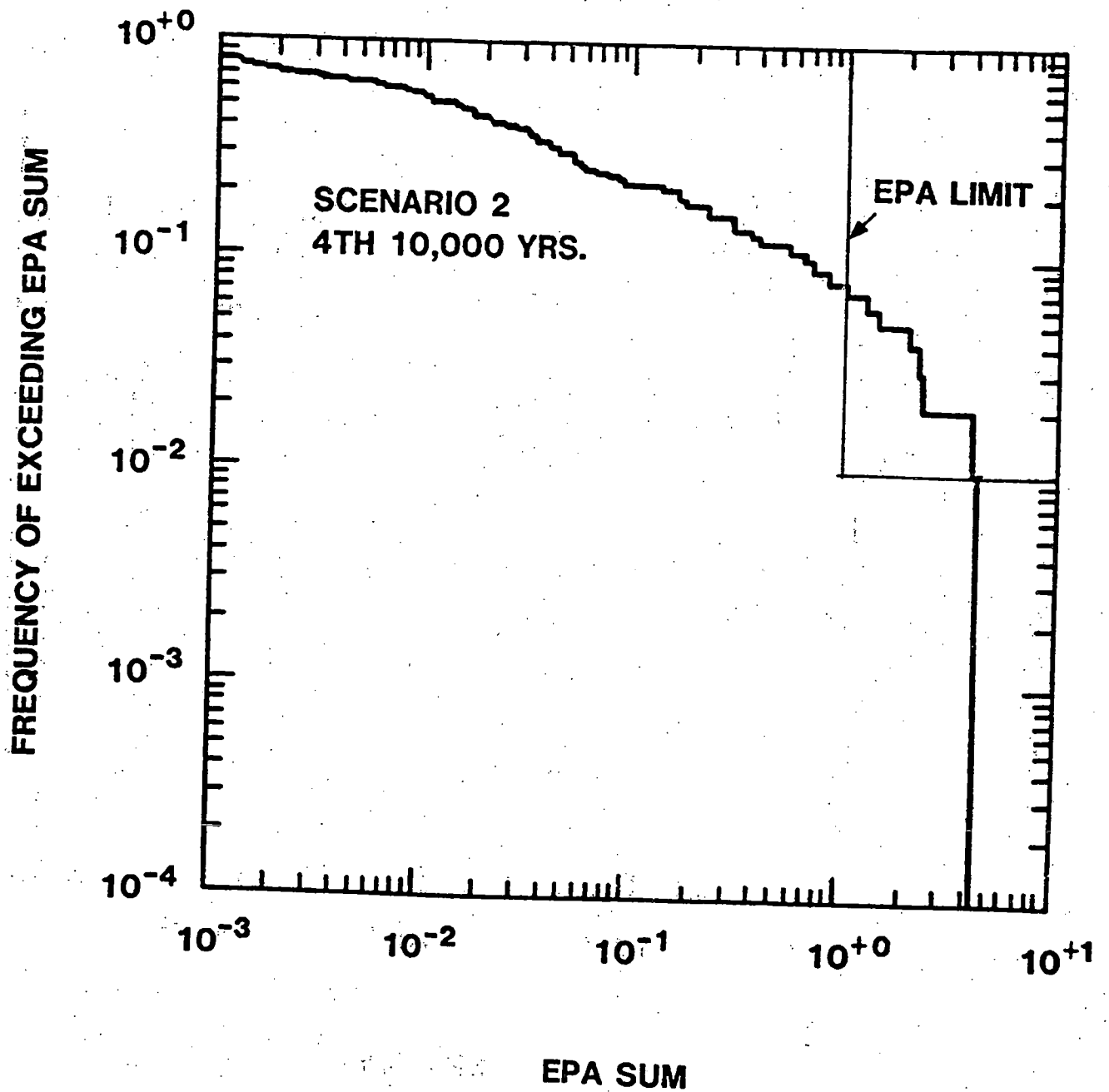


Figure 14. Scenario 2 CCDF - 4th. 10,000 Years

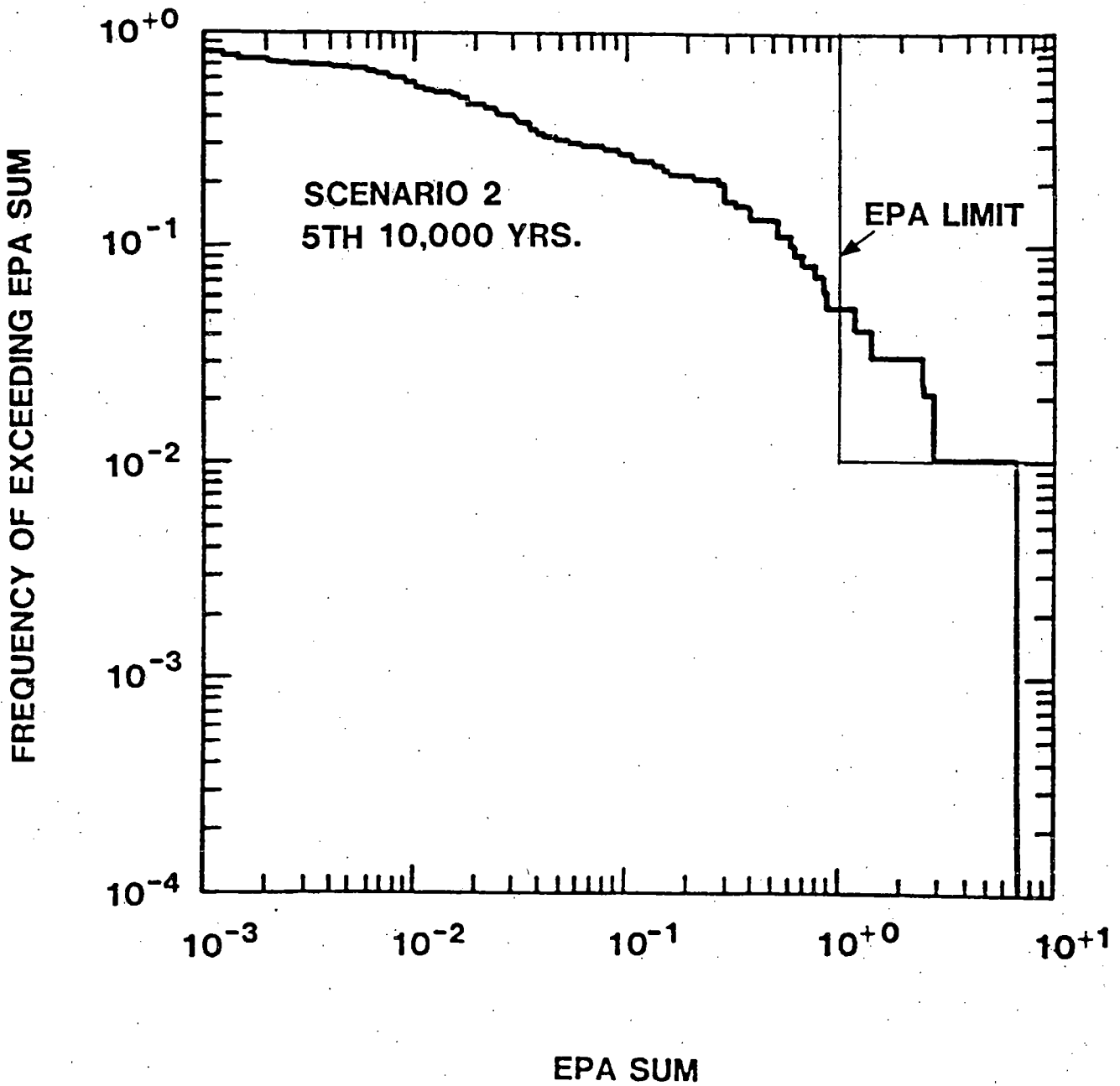


Figure 15. Scenario 2 CCDF - 5th 10,000 Years

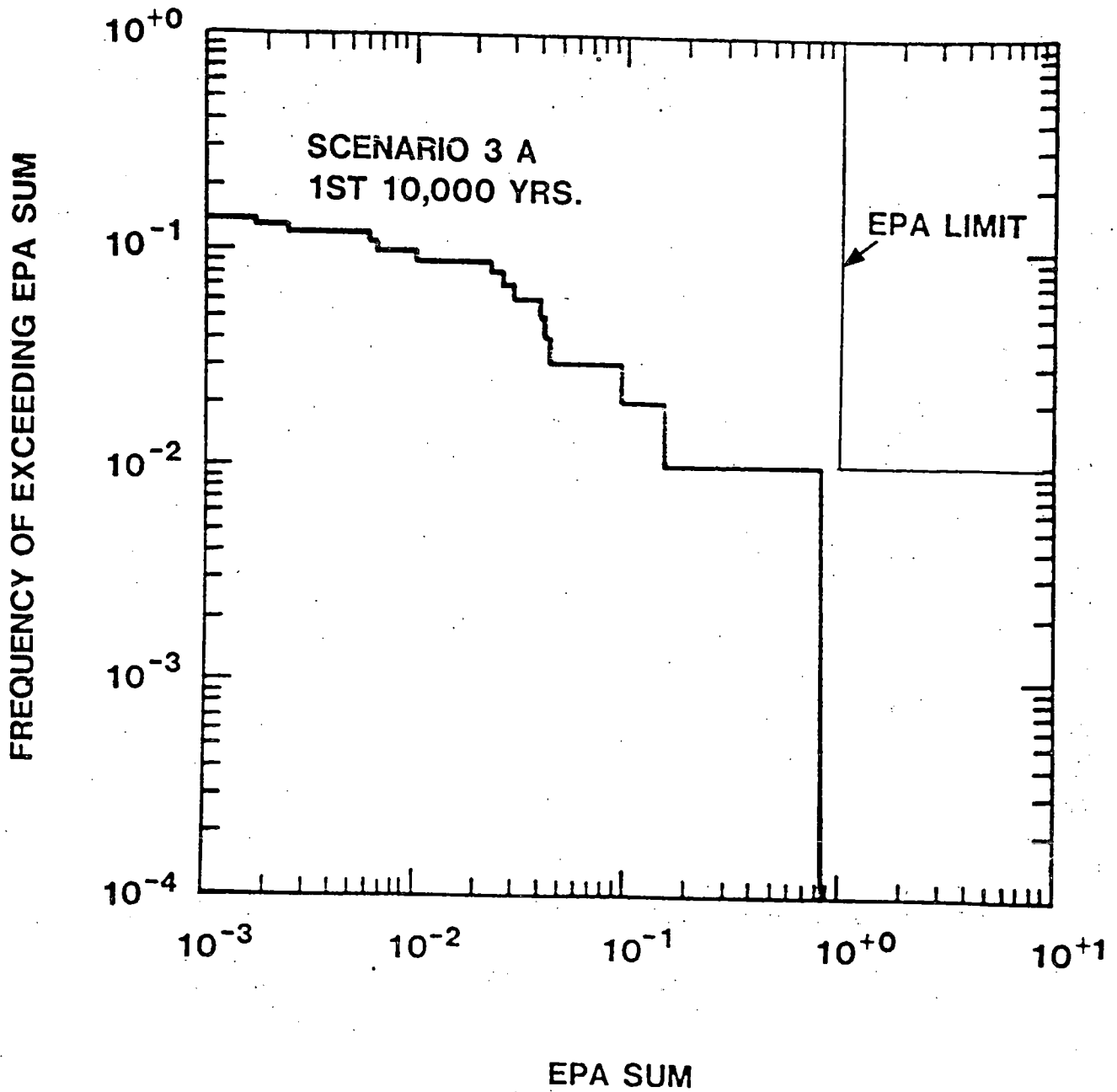


Figure 16. Scenario 3A CCDF - 1st 10,000 Years

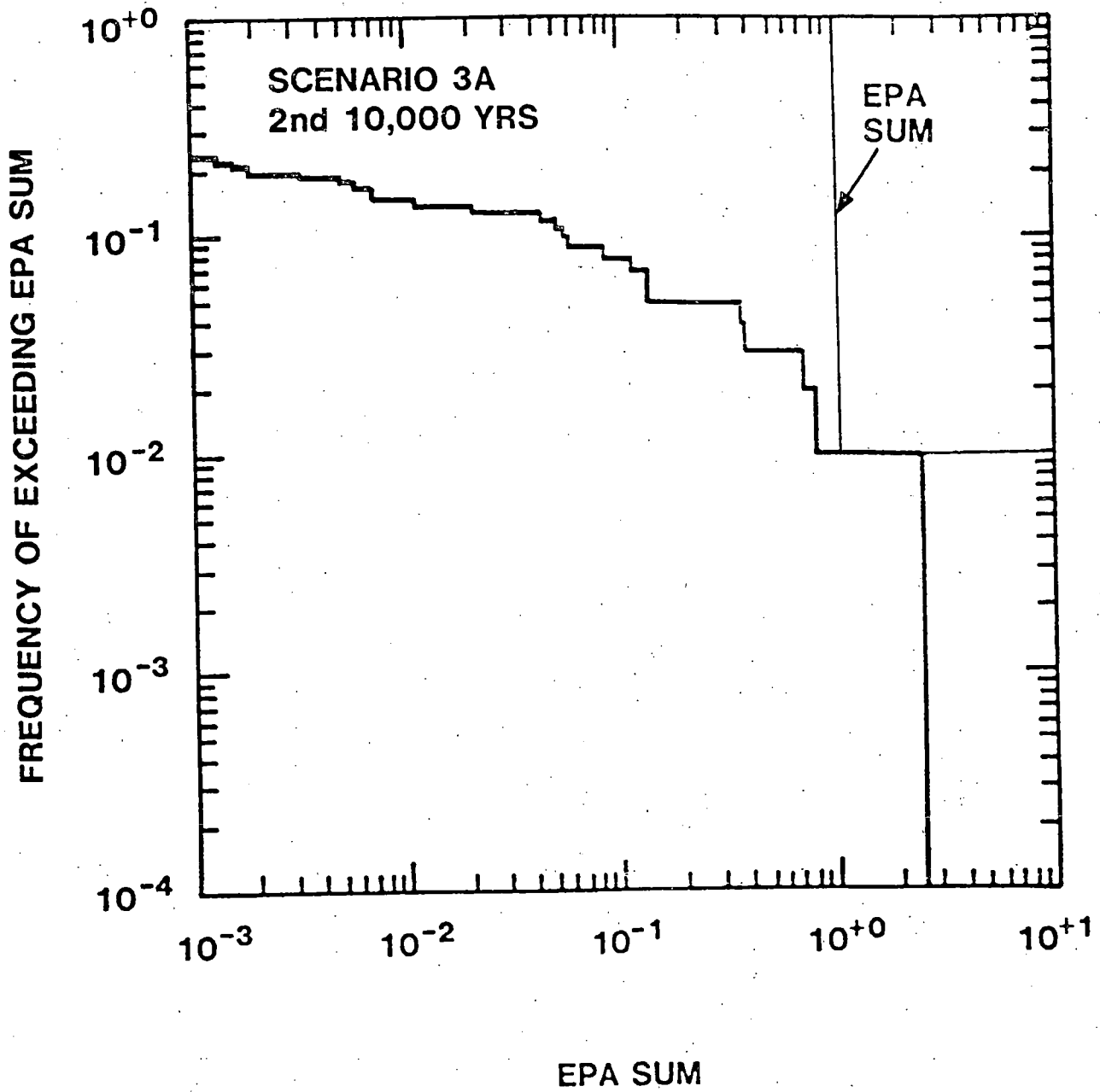


Figure 17. Scenario 3A CCDF - 2nd 10,000 Years

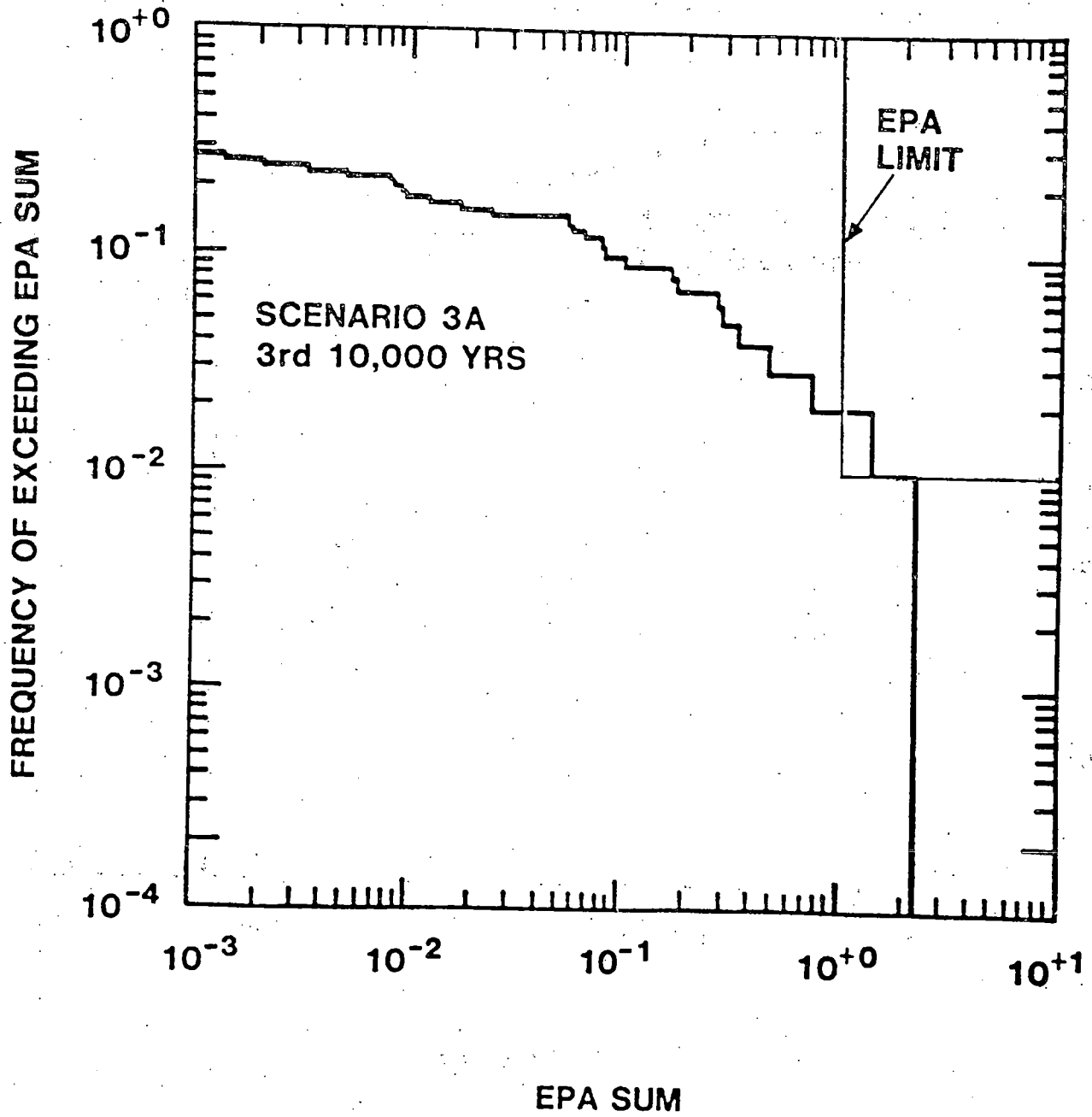


Figure 18. Scenario 3A CCDF - 3rd 10,000 Years

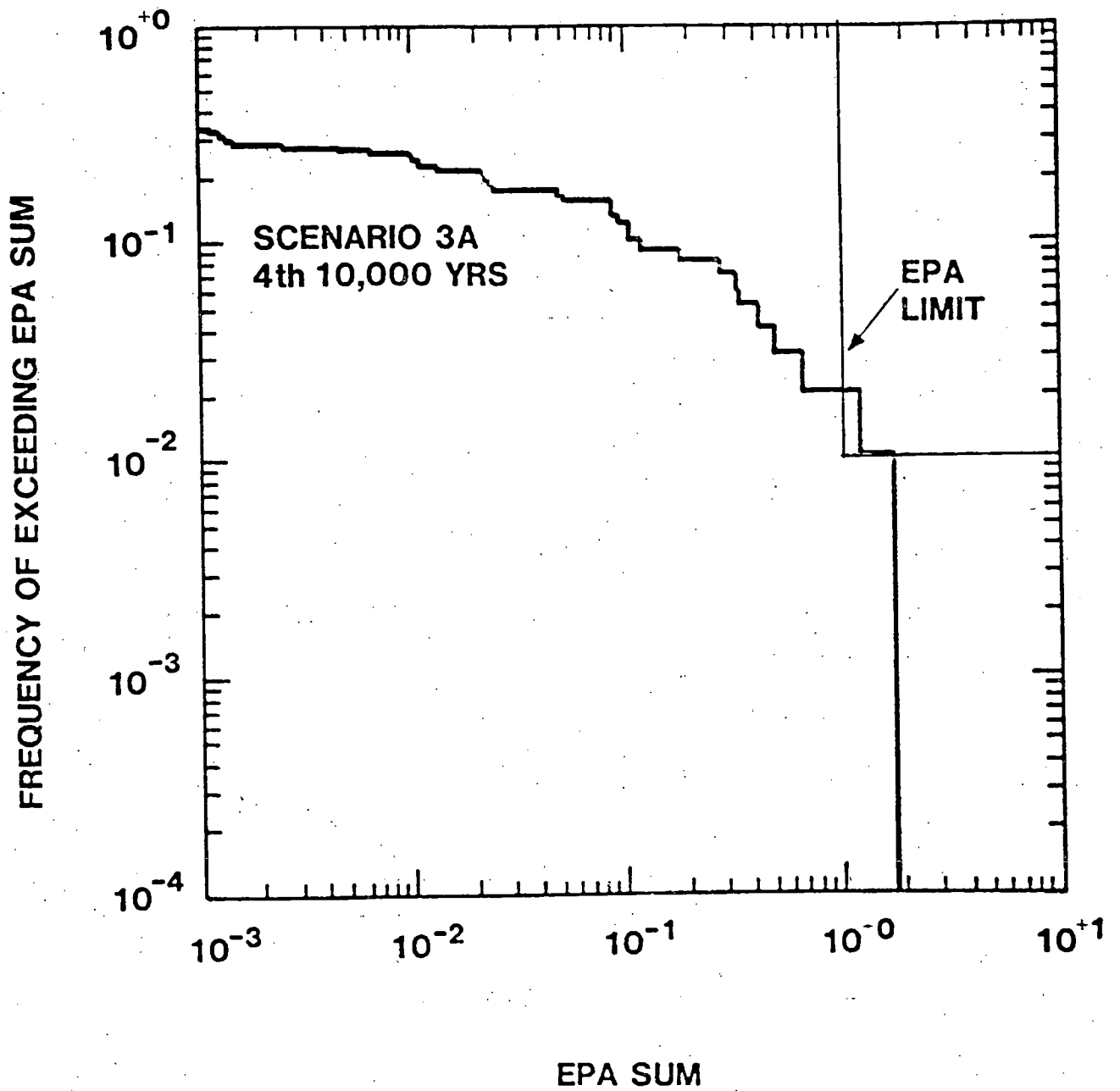


Figure 19. Scenario 3A CCDF - 4th 10,000 Years

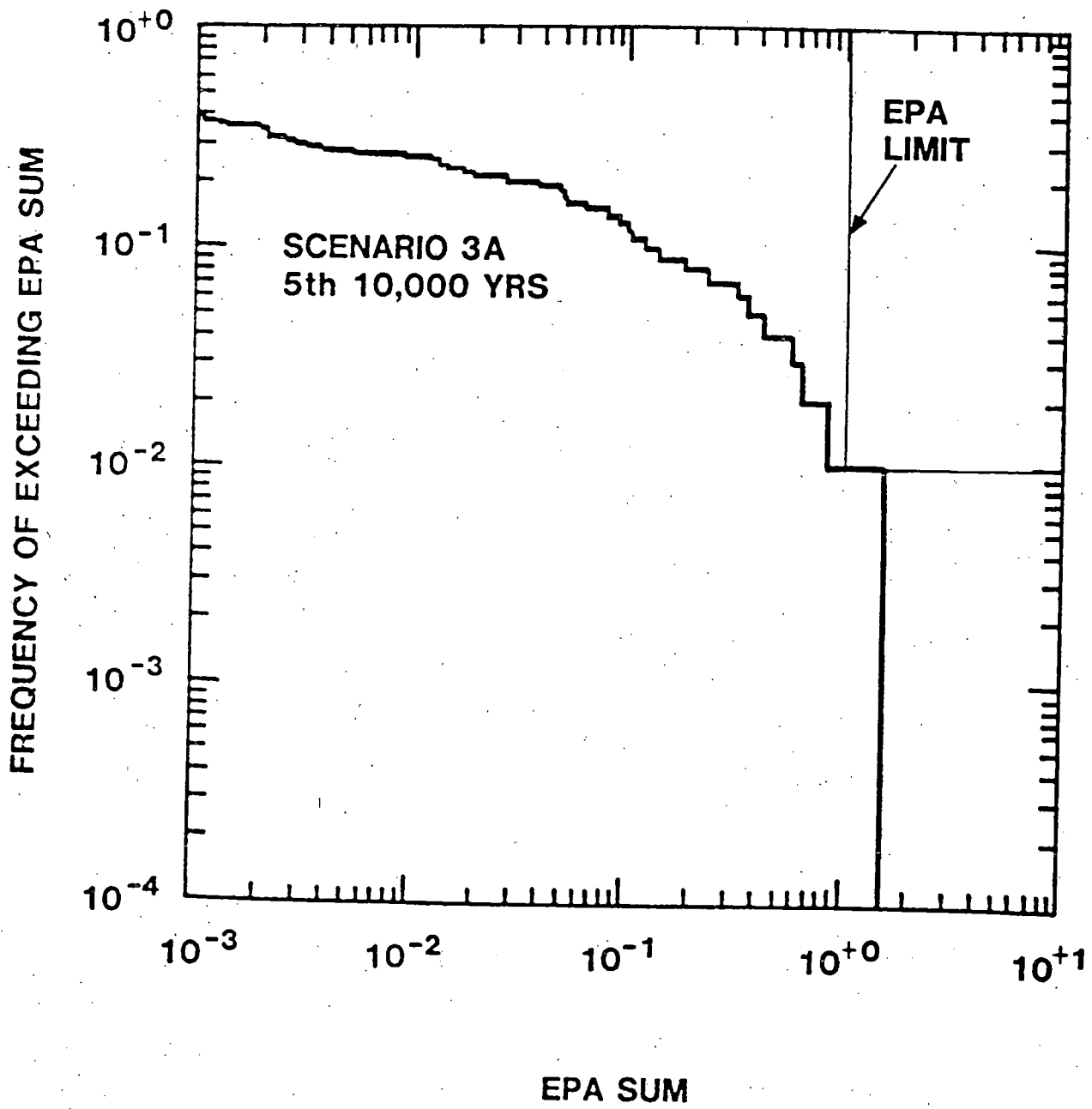


Figure 20. Scenario 3A CCDF - 5th 10,000 Years

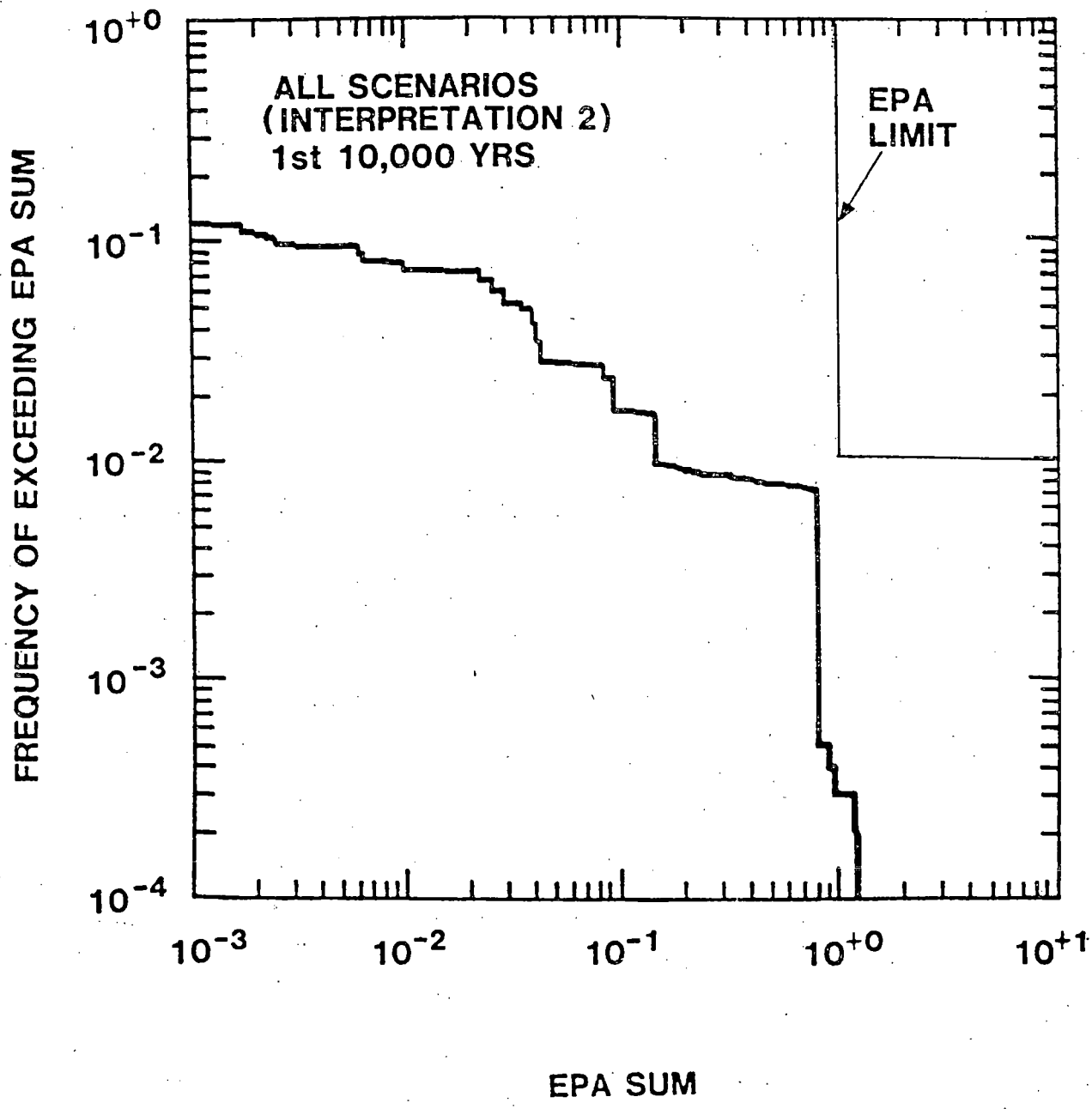


Figure 21. All Scenario CCDF - 1st 10,000 Years

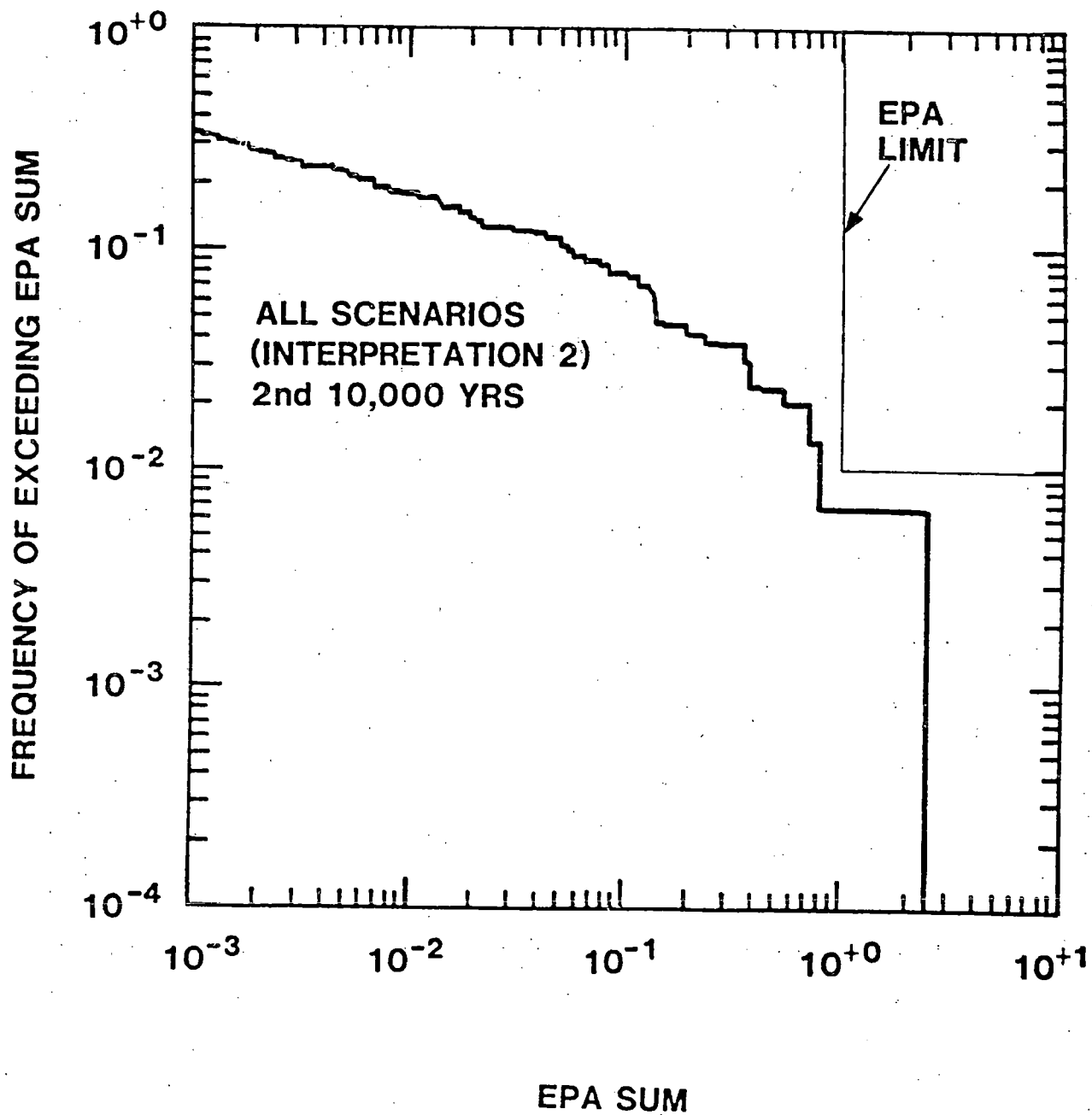


Figure 22. All Scenario CCDF - 2nd 10,000 Years

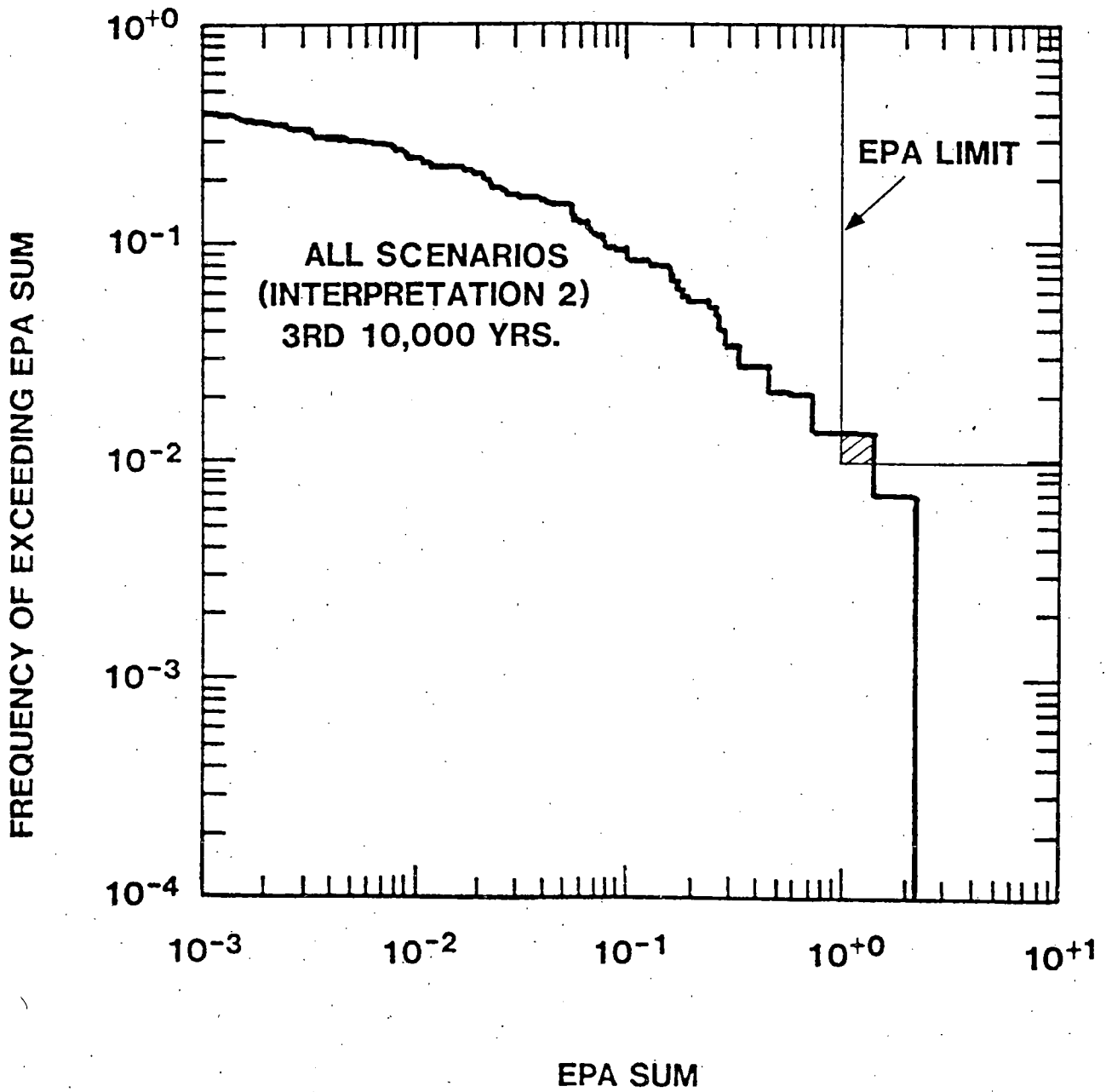


Figure 23. All Scenario CCDF - 3rd 10,000 Years

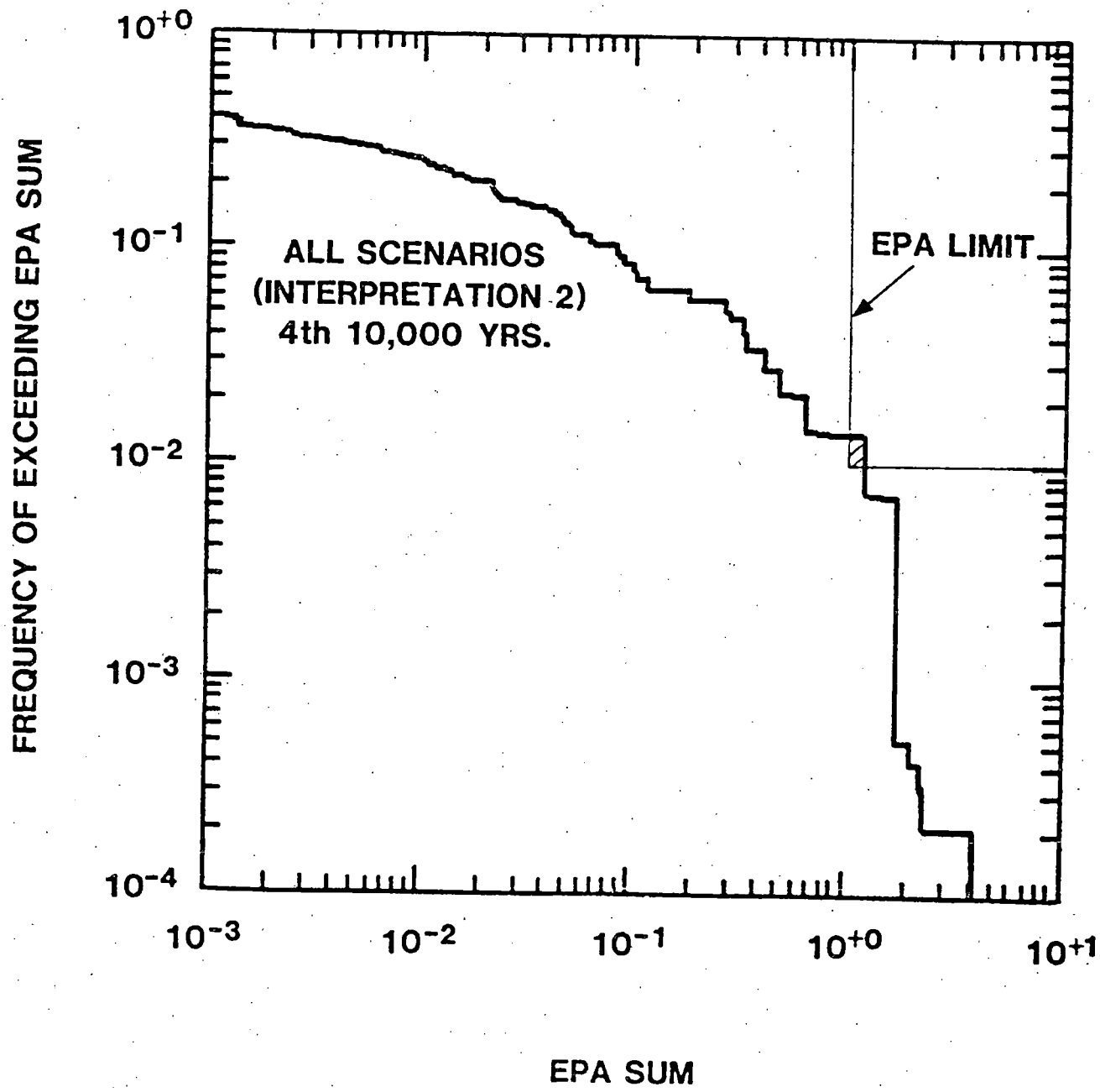


Figure 24. All Scenario CCDF - 4th 10,000 Years

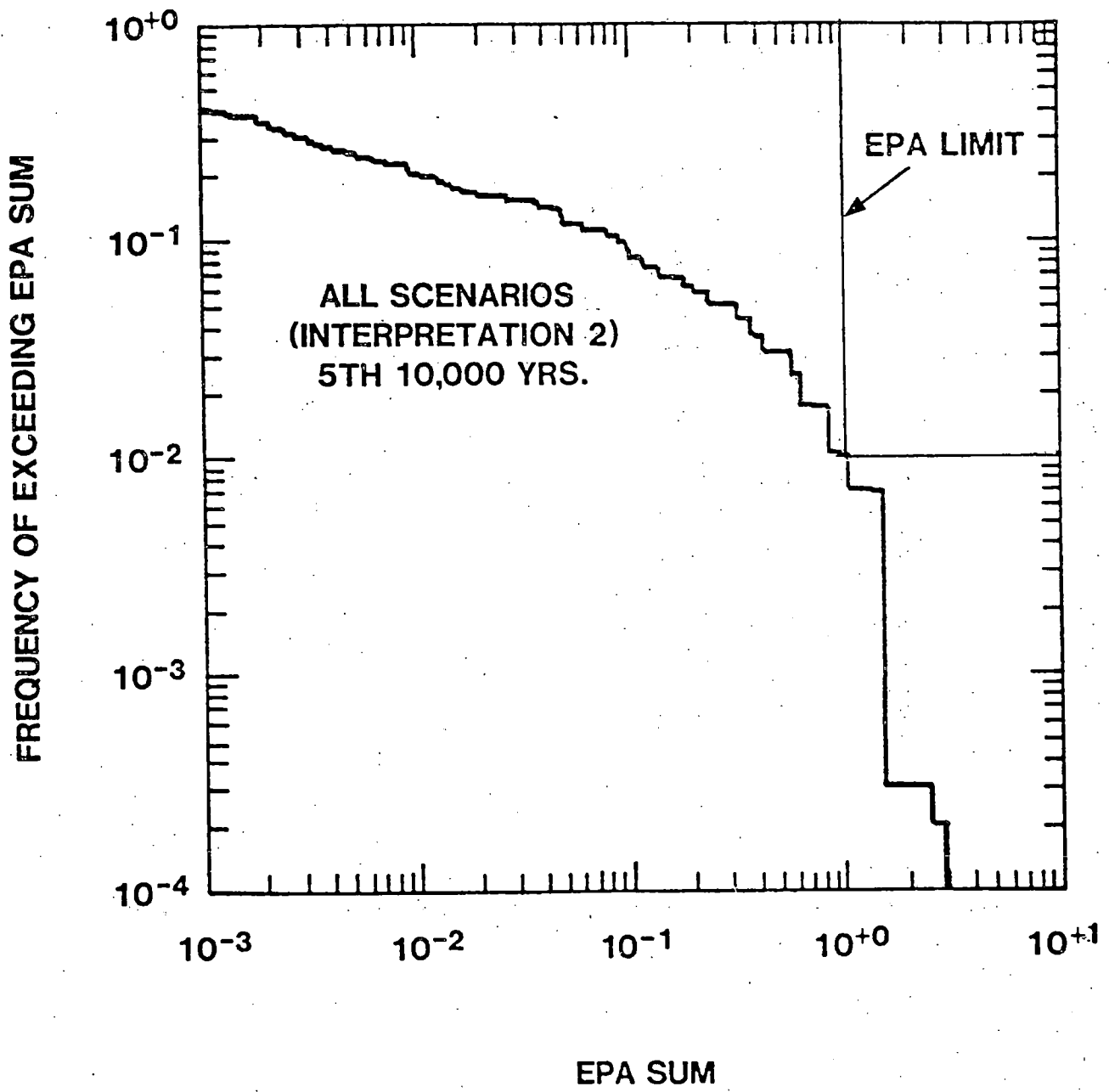


Figure 25. All Scenario CCDF - 5th 10,000 Years

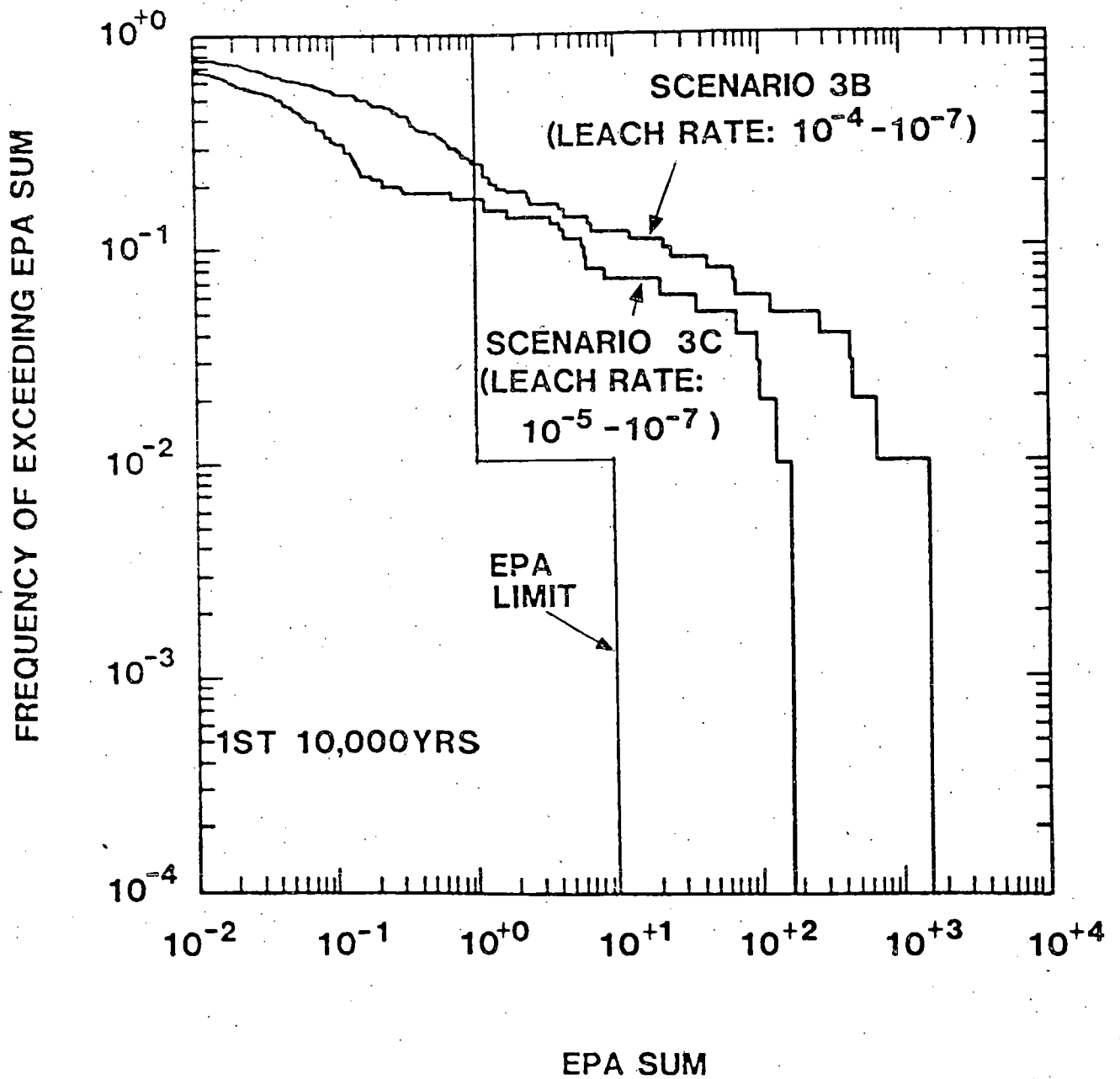


Figure 26. Scenarios 3B and 3C (Leach Limited)  
CCDF - 1st 10,000 Years

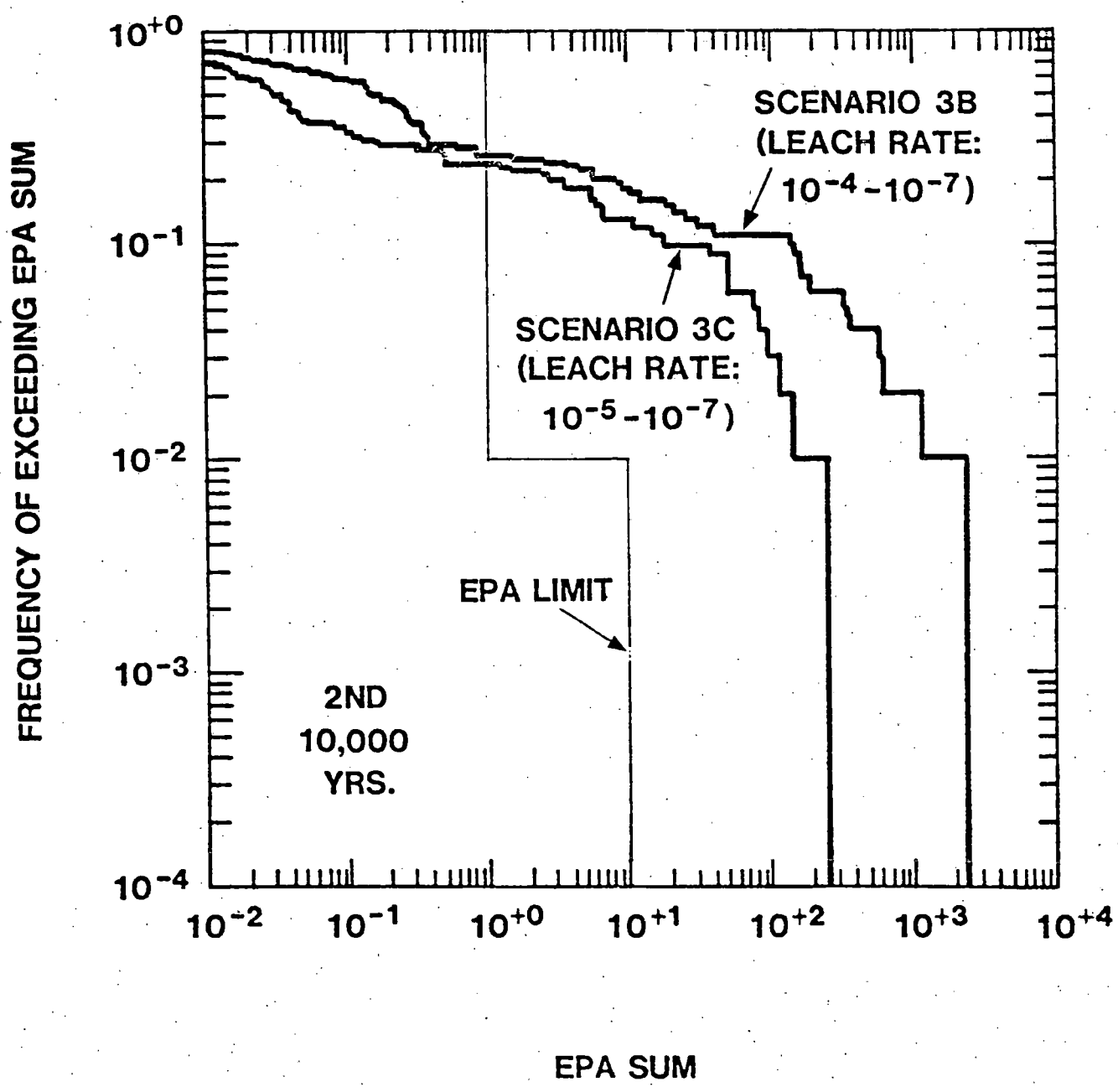


Figure 27. Scenarios 3B and 3C (Leach Limited)  
 CCDF - 2nd 10,000 Years

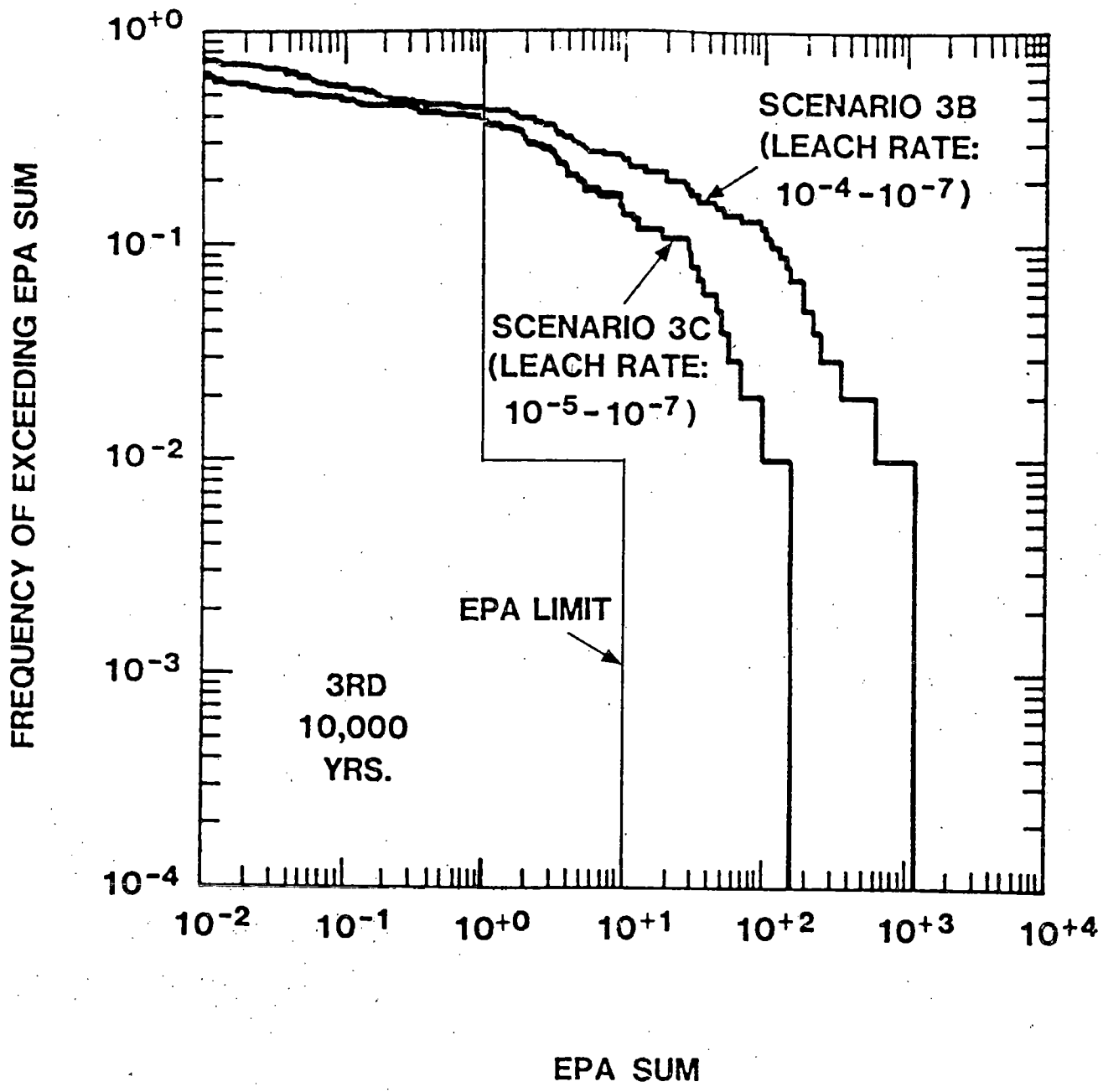


Figure 28. Scenarios 3B and 3C (Leach Limited)  
 CCDF - 3rd 10,000 Years

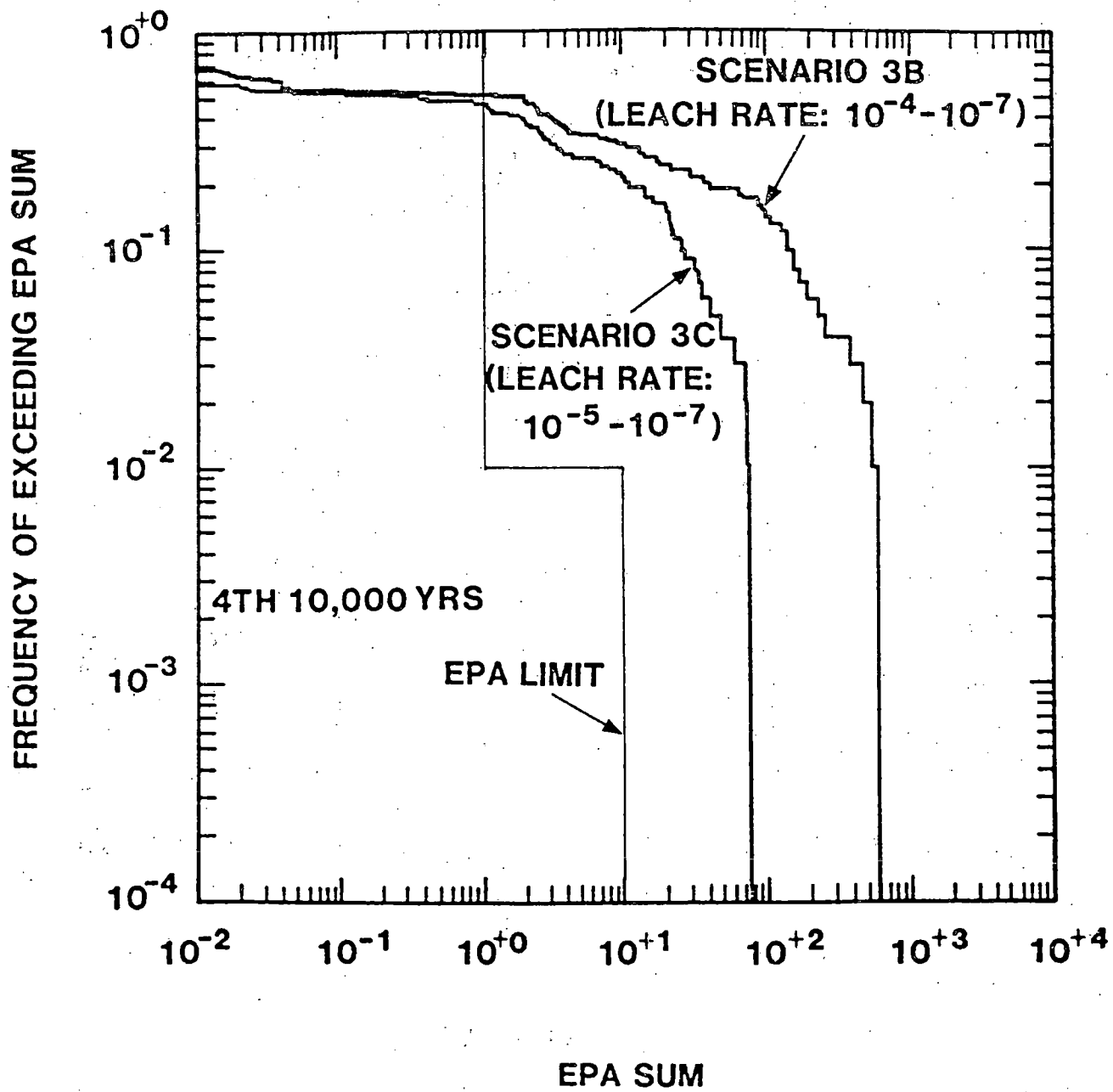


Figure 29. Scenarios 3B and 3C (Leach Limited)  
CCDF - 4th 10,000 Years

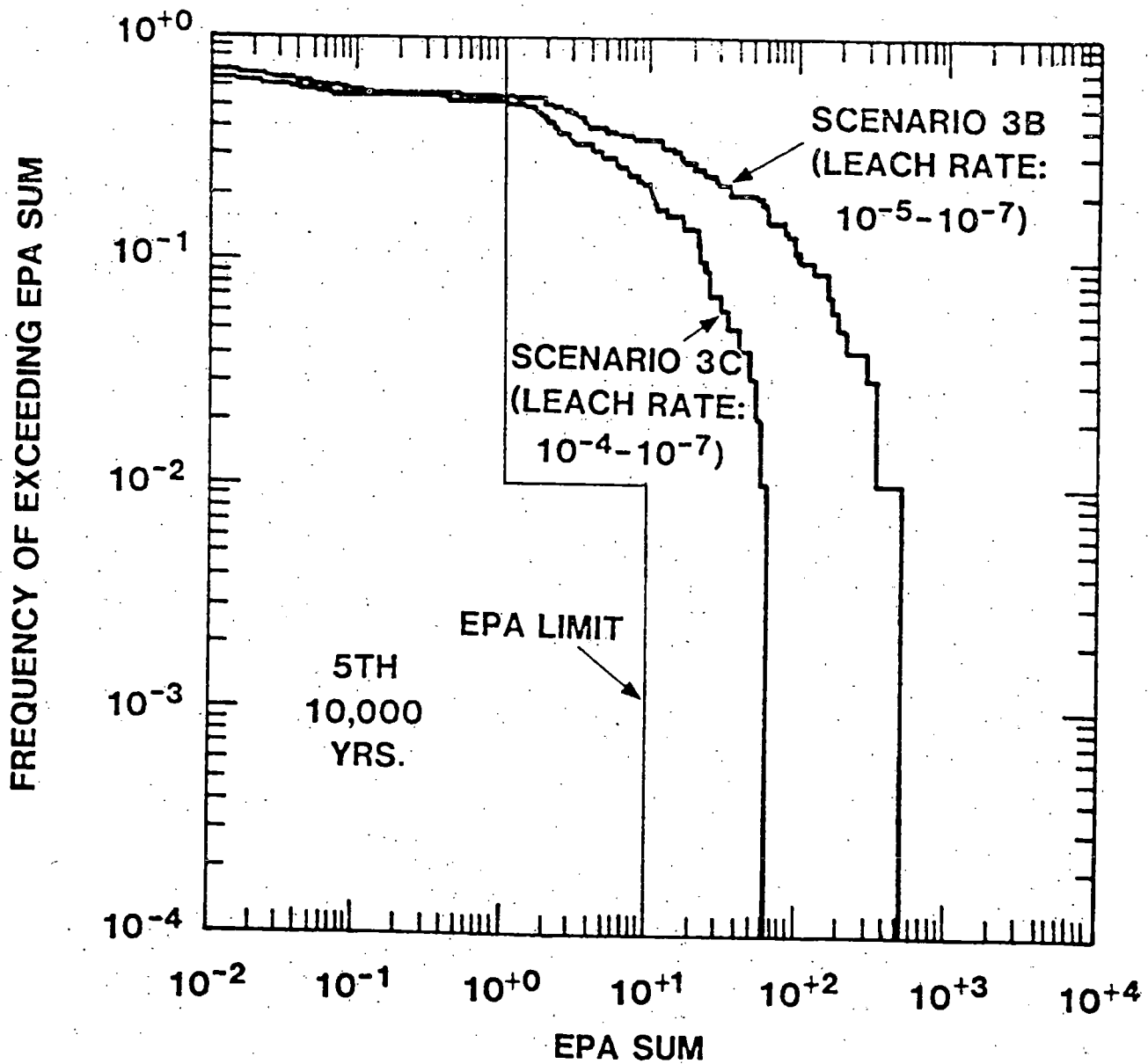


Figure 30. Scenarios 3B and 3C (leach Limited)  
CCDF - 5th 10,000 Years

All five CCDFs for Scenario 1 (Figures 6 through 10) show compliance with the EPA limit. Note that Interpretation 1 is implicit when the CCDF is for a single scenario. The CCDF results for Scenario 2 (fractures in dense basalt) are presented in Figures 11 through 15. All five of these figures indicate a violation of the EPA limit, with each successive 10,000-yr. period showing a greater degree of violation. As in Scenario 1, the leach-limited source model had been chosen by the computer model in Scenario 2. The dominating radionuclides, in terms of their contribution to the EPA Sum, appear to be  $^{14}\text{C}$  and  $^{99}\text{Tc}$ .

In the first of the three variations of the borehole scenario, Scenario 3A, the automatic source selection algorithm chose the mixing cell model. The CCDF plots for Scenario 3A are given in Figures 16 through 20. Although some violations are apparent in the 20,000 to 50,000-yr. period, none of the vectors exceed the EPA limit during the first 10,000-yr. period, which is the period of primary concern.

In an attempt to apply Interpretation 2 to the analysis, Scenarios 1, 2, and 3A were assigned probabilities such that their sum was equal to 1. Composite CCDFs were then constructed and compared to the EPA limit "envelope". Recall that when scenario probabilities are inherent in predicting the probability of a given release, two different EPA limits (EPA Sums of 1 or 10) are in effect, depending on the range of release probability. The composite CCDFs are shown in Figures 21 through 25, and it is seen that the frequency of violation is extremely small. This re-emphasizes the importance of the manner in which the standard could be interpreted.

The final set of CCDF results, Figures 26 through 30, are included to demonstrate the effect of meeting the release rate limit criterion of the proposed Rule (10CFR60).

The release rate and the leach rate are considered to be synonymous for demonstration purposes of this study. A leach-limited source model was imposed to obtain Scenario 3B (leach rate:  $10^{-4}$  -  $10^{-7}$  per year) and Scenario 3C (leach rate:  $10^{-5}$  -  $10^{-7}$  per year) responses. The EPA Sums associated with certain vectors of Scenario 3B are consistently higher than the corresponding vectors of Scenario 3C, as expected. Nevertheless, considerable violations of the EPA limit are indicated by each of the two leach-limited variations of Scenario 3. By contrast, the violations in Scenario 3A are not nearly as large or as frequent. This too is to be expected, since the mixing cell permits the solubility limit to be the controlling parameter instead of leach rate.

## 9. CONCLUSIONS

The analyses presented demonstrate how the existing analytical tools could be used to assess compliance with the draft EPA Standard. A detailed development of probabilities of scenarios will be needed in order to perform a more realistic assessment. As site characterization proceeds, one may expect improvements in the input data over that assumed in this analysis.

Ambiguities in the draft standard and assumptions necessary to assess compliance have been identified. These will need to be clarified, justified, or further developed before a reliable assessment of compliance can be made.

Two interpretations of the draft standard have been presented which should be discussed further, especially in light of the uncertainties in both the scenario probability and the estimated EPA Sum. Interpretation 1 is computationally the simpler, since scenarios may be analyzed one at a time as they are postulated. It is also easier to comprehend intuitively. Due to the uncertainty in scenario probability, arguments as to whether or not compliance is achieved are reduced to two basic issues,

1. Assurance that the scenario probability is: greater than  $10^{-2}$  (the conservative assumption), between  $10^{-4}$  and  $10^{-2}$  (arguable if uncertainty in the probability is large), or less than  $10^{-4}$  (negligible).
2. Confidence that the consequences are substantially less than the allowed maximum.

Computationally, Interpretation 2 is more difficult to utilize but seems to be more in the spirit of risk assessment as it has been applied to nuclear reactors in that it considers all sources of a given consequence (EPA Sum). Another difficulty in implementing this interpretation is the estimation of scenario probabilities. Uncertainty in scenario probability could be accommodated in this interpretation, at least in principle, by performing a sampling of a probability distribution assumed to describe each scenario. It would appear that the quantity of interest, as far as the standard is concerned, is the probability of release (regardless of what scenarios or events contribute to it). Therefore, in our opinion, Interpretation 2 is preferable in spite of some difficulties that have not been totally resolved.

The results of analyses for this reference basalt site performed under Interpretation 1 showed a small probability (a few percent) of violating the draft EPA Standard for Scenarios 2 and 3A without imposition of the 10CFR60 requirements on the release rate. Under Interpretation 2, the same analyses indicate nearly total compliance with the draft EPA Standard. Of course, both of these results are subject to sampling error. Future analyses should explicitly address the sampling error.

Analyses performed with different source models show the importance of the source term assumption on compliance estimates.

## APPENDIX A

### RADIONUCLIDE RETARDATION

#### 1. Calculation of the Retardation Factor

The retardation factor R for an aqueous species or a radionuclide traveling in a porous medium is usually defined as:

$$R = \frac{\text{velocity of ground water}}{\text{velocity of radionuclide}} \quad (1)$$

The value of R can be calculated by:

$$R = 1 + R_d \cdot \rho \cdot \frac{(1 - \phi_{\text{eff}})}{\phi_{\text{eff}}} \quad (2)$$

where

$R_d$  = the radionuclide sorption ratio  
in ml/gm

$\rho$  = grain density of rock in gm/cm<sup>3</sup>

$\phi_{\text{eff}}$  = effective porosity that contributes to the flow path; in porous media,  $\phi_{\text{eff}} = \phi_{\text{total}}$ .

A more general expression that is valid for porous as well as fractured media for a unit volume of rock, may be defined as follows:

$$R = \frac{M_T}{M_X} = \frac{\text{total mass of radionuclide in rock-water system}}{\text{mass of radionuclide in water}} \quad (3)$$

For porous media, it is shown below that this expression is equivalent to Equation (2).

Let:

$C_X$  = concentration of radionuclide in solution in gm/ml

$C_{MX}$  = concentration of radionuclide adsorbed by the rock in gm/gm

$M_R$  = mass of nuclide in rock in grams

Then for a unit volume of porous rock,

$$M_X = C_X \cdot \phi_{eff} \quad (4)$$

$$M_R = C_{MX} \cdot (1 - \phi_{eff}) \rho \quad (5)$$

$$M_T = M_X + M_R \quad (6)$$

From Equation (3),

$$R = \frac{M_R + M_X}{M_X} \quad (7)$$

substituting terms yields:

$$R = \frac{C_X \cdot \phi_{eff} + C_{MX} (1 - \phi_{eff}) \cdot \rho}{C_X \cdot \phi_{eff}} \quad (8)$$

$$R = 1 + \frac{C_{MX}}{C_X} \cdot \rho \cdot \frac{1 - \phi_{eff}}{\phi_{eff}} \quad (9)$$

but

$$R_d = \frac{C_{MX}}{C_X} \quad (\text{see Equation 5.5})$$

therefore,

$$R = 1 + R_d \cdot \rho \cdot \frac{(1 - \phi_{\text{eff}})}{\phi_{\text{eff}}}$$

In general however, the fluid is not in contact with the entire rock mass. We introduce the utilization factor,  $\psi$  in Equations (2) and (8), to correct R for this effect.

$$R = \frac{C_X \phi_{\text{eff}} + \psi C_{MX} (1 - \phi_{\text{eff}}) \cdot \rho}{C_X \phi_{\text{eff}}} \quad (10)$$

$$R = 1 + \psi R_d \cdot \rho \cdot (1 - \phi_{\text{eff}}) / \phi_{\text{eff}} \quad (11)$$

where  $\psi$  is the volume fraction of the rock that interacts with the fluid.

## 2. Estimation of Utilization Factor

In the reference repository we have assumed that most of the fractures are lined with secondary minerals.<sup>10</sup> Under these conditions, we can derive an expression for  $\psi$  and also simplify the expression for R. If we assume that the fluid in the fractures interacts only with secondary minerals, then

$$M_R = C_{SMX} \cdot V_{SM} \cdot \rho_{SM}$$

where  $\rho_{SM}$  and  $V_{SM}$  are the density and volume of secondary minerals in the unit volume of rock, respectively.  $C_{SMX}$  is the concentration of radionuclide adsorbed by the secondary minerals in gm/gm.

$$R_{dSM} \equiv \frac{C_{SMX}}{C_X}$$

Let

$$V_{SM} = \left( \frac{\text{volume of solid rock in unit}}{\text{volume of rock}} \right) \times \left( \frac{\text{fraction of rock composed of secondary minerals}}{\text{secondary minerals}} \right)$$

$$V_{SM} = (1 - \phi_T) \cdot \psi \cdot \text{unit volume}$$

where

$$\phi_T = \text{total porosity.}$$

If we assume that  $\phi_T \approx \phi_{eff}$ , then Equation (10) becomes,

$$R \approx \frac{C_X \cdot \phi_{eff} + \psi \cdot C_{SMX} \cdot (1 - \phi_{eff}) \cdot \rho_{SM}}{C_X \cdot \phi_{eff}} \quad (12)$$

Let  $R_{dSM} = C_{SMX}/C_X$ , which gives,

$$R \approx 1 + \psi \cdot R_{dSM} \cdot \rho_{SM} \cdot \frac{(1 - \phi_{eff})}{\phi_{eff}} \quad (13)$$

Note that in this scenario,  $R_{dSM}$  and  $\rho_{SM}$  refer to the sorption ratio and density of secondary minerals, and that  $\phi_{eff}$  refers to the basalt matrix. The utilization factor  $\psi$  is the volume fraction of the rock matrix occupied by secondary minerals.

Intuitively, we would expect that the amount of secondary mineralization in the basalt can be related to the volume of the fractures. At Hanford, for example, Long<sup>10</sup> examined 3 flows in the Grande Ronde. He found that nearly all the fractures contained some filling and that more than 75 percent of the fractures were filled completely. If we assume that the fractures that contribute to the effective porosity are, on the average, one-half filled, i.e.,

$$\text{"original" unfilled fracture porosity} = 2 \cdot \text{residual porosity}$$

Then

$$V_{SM} = \text{residual porosity} \cdot \phi_{eff}$$

and

$$\psi = \frac{V_{SM}}{V_{\text{solid rock}}} \approx \frac{\phi_{eff}}{(1 - \phi_{eff})} \quad (14)$$

This expression can be used to simplify Equation (13) as follows:

$$R = 1 + K_{dSM} \cdot \rho_{SM} \cdot \frac{\phi_{eff}}{(1 - \phi_{eff})} \cdot \frac{(1 - \phi_{eff})}{\phi_{eff}}$$

or,

$$R = 1 + K_{dSM} \cdot \rho_{SM} \quad (15)$$

In the more general case, we can assume that the volume of secondary mineralization is a multiple ( $f$ ) of the volume of residual connected pore space. Equations (14) and (15) become,

$$\psi = \frac{f \cdot \phi_{eff}}{(1 - \phi_{eff})} \quad (14a)$$

$$R = 1 + f K_{dSM} \cdot \rho_{SM} \quad (15a)$$

## APPENDIX B

### REDOX CONDITIONS IN THE REFERENCE REPOSITORY AND APPROPRIATE VALUES OF $R_d$

A large amount of uncertainty in our estimates of radionuclide discharge is introduced by a lack of knowledge about the geochemical environment that may be encountered by the migrating nuclides and by the paucity of reliable values of radionuclide sorption ratios ( $R_d$ s) relevant to this study. In this section we will describe the assumptions we have made in characterizing the geochemical environment and in choosing appropriate values of  $R_d$ s for our calculations.

#### 1. Redox Conditions

The difficulties encountered in attempting to predict the Eh-pH environment of natural systems from either theoretical considerations, or from direct measurements, have been discussed in detail by several authors.<sup>11,12,13</sup> Discussions of the probable nature of the geochemical environment within the Hanford Site and subsurface mines are given by Sato<sup>11</sup>, Smith<sup>14</sup>, and Guzowski, et al.<sup>15</sup> Field measurements and theoretical calculations based on observed mineral assemblages in basaltic environments suggest that ground water, in contact with basalt, will have a low Eh (-0.40 to -0.55), a high pH (9.4 - 10), and moderate temperatures (30 - 50°C). These Eh-pH conditions may be expected near the repository in part of Layer A in Figure 2 and along fresh basalt fractures exposed by faulting or drilling in other layers as described in the hypothetical disruption scenarios. In our characterization of the repository, we have not considered the oxidation potential of air and foreign materials introduced into the basalt during operation and construction of the repository. The two interbeds I-V and I-M are assumed to be relatively active aquifer systems, and are, therefore, assumed to be oxidizing and slightly alkaline.

In the "base" (no disruption) case, we have assumed that in all basalt layers, ground water flows through fractures lined with secondary minerals. The observed fracture-fill consists of amorphous silica, zeolites, calcite, and nontronite.<sup>10</sup> None of these

minerals have appreciable oxidizing power. Although nontronite contains  $\text{Fe}^{+3}$ , it forms under reducing conditions.<sup>16</sup> At low pH, the dissolution of iron-bearing minerals in basalt and precipitation of ferric oxyhydroxides will proceed under reducing conditions.<sup>11</sup> For these reasons, we have assumed that the geochemical environment of partially filled fractures in basalt is reducing.

## 2. Available Data for Values of $R_d$

The large amount of experimental error reported for determinations of  $R_d$ s and the questionable utility of this parameter for accurate calculations of radionuclide retardation have been discussed by several authors.<sup>15-22</sup>

The values for the ranges of radionuclide,  $R_d$ s, that were used in this report are presented in Table 5 (main text). The data were supplied by several researchers and are reviewed in Guzowski, et al.<sup>15</sup> Histograms of the number of determinations of  $R_d$ s for each radionuclide for the substrates under several geochemical environments considered are shown in Figure B-1. It is clear that there are relatively few reliable determinations of  $R_d$ s for the geochemical conditions relevant to this study. The large majority of data has been obtained for basalt under an oxidizing atmosphere, a condition that we do not feel is relevant to the geological system under consideration.

In most cases, the ranges of  $R_d$  values reported for reducing conditions overlap those reported for oxidizing conditions. For this reason, we have used the more limited number of data obtained under oxygen-free conditions to estimate the ranges of  $R_d$  for reducing environments and we have supplemented these data with values obtained under oxidizing conditions where necessary. No data are available for several elements: Cm, Pa, Ac, Th, and Pb. Based on similarities in solubility, valence and ionic radii, the following chemical homologs have been assumed: (Am = Cm, Pa, Ac, Th) and (Pb = Ra).<sup>15</sup> No values of the  $R_d$ s of Cs, I, Ra, or Am in contact with basalt under reducing conditions are available. The  $R_d$ s of these elements are assumed to be insensitive to redox conditions; values under oxidizing conditions were used for our calculations.

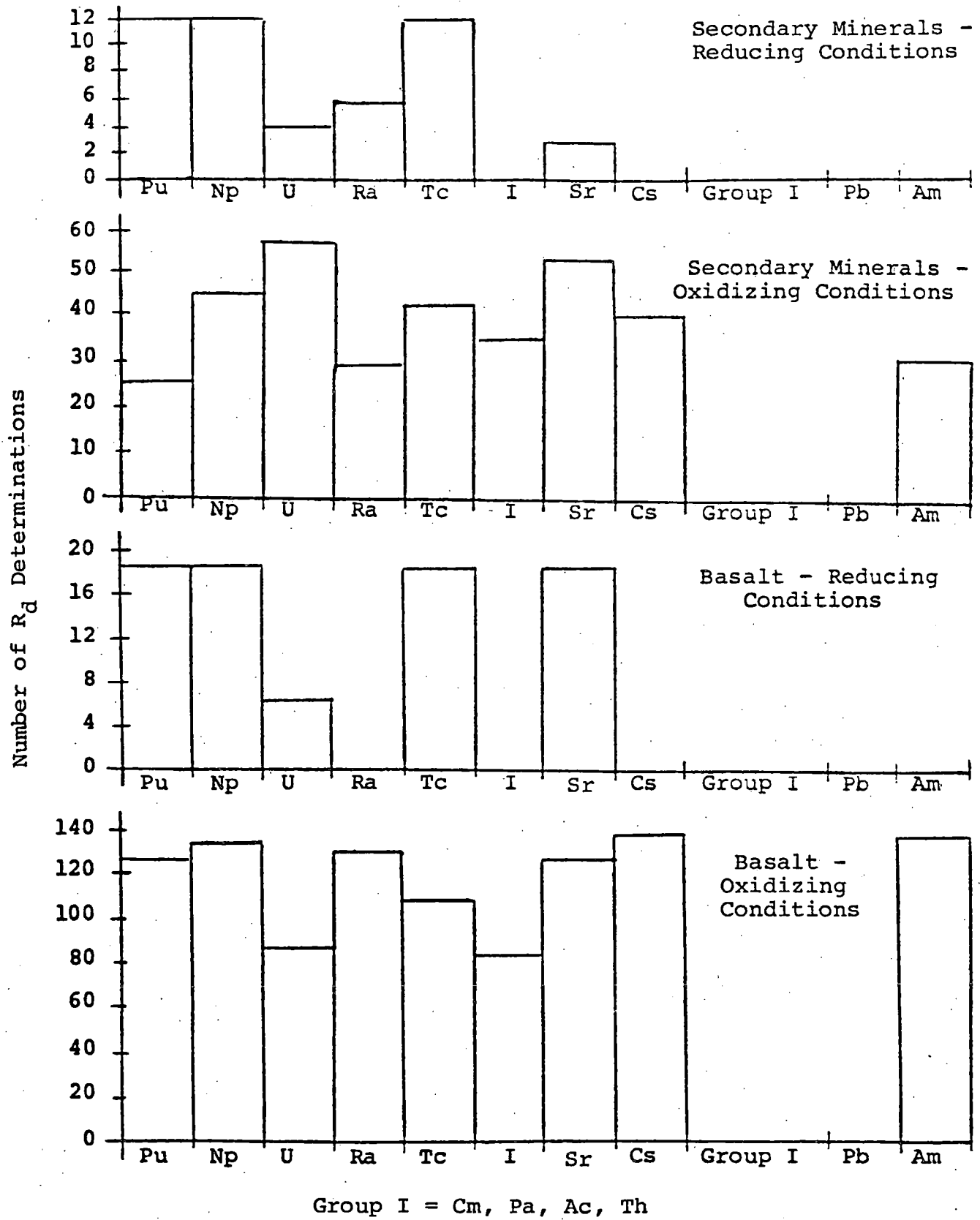


Figure B-1.  $R_d$  Data

## APPENDIX C

### AN APPROXIMATE TREATMENT OF MATRIX DIFFUSION AS A RETARDATION MECHANISM

We have assumed that groundwater flow and radionuclide migration occur predominantly through numerous narrow vertical features in the basalt. We have also attempted to show the effect of such a flow assumption on the chemical sorption processes expected to retard radionuclide migration and enhance the containment capability of the repository. In doing so, we have given up the traditional porous medium expression for the retardation factor of the form

$$R \approx \frac{\rho R_d}{\phi} (1 - \phi)$$

in favor of the form

$$R \approx \rho R_d$$

as discussed in Appendix A.

A few radionuclides are essentially unretarded by chemical sorption, i.e.,  $R_d \approx 0$ . Specifically,  $^{14}\text{C}$  and  $^{99}\text{Tc}$  dominate the EPA Sum for most vectors producing large values of the EPA Sum. For scenarios involving major hydraulic connections between the subsurface facility and overlying aquifers, e.g., boreholes, these radionuclides may be of most concern in licensing considerations. In scenarios resulting in enhancement of the repository hydraulic properties, e.g., fractures in dense basalt, transport may still be dominated by flow through narrow fractures. For these cases, we may have overestimated the releases by neglecting a potential retardation mechanism.

A number of authors have discussed the diffusion of contaminants into the rock matrix for cases similar to that which we have assumed, namely transport through narrow fractures in relatively impermeable rock.<sup>23,24,25</sup> The treatment presented here is essentially that of Erickson and Fortney<sup>26</sup> who have used this effect in the design of radionuclide migration experiments in non-welded tuffs. We would like to estimate the potential importance of this mechanism in radionuclide retardation. The validity of the method, as derived and implemented here, rests on a number of assump-

tions which will be made. Nevertheless, the results will demonstrate the potential importance of this retardation mechanism and the importance of understanding it better.

Consider the idealized fracture geometry depicted in Figure C-1 below:

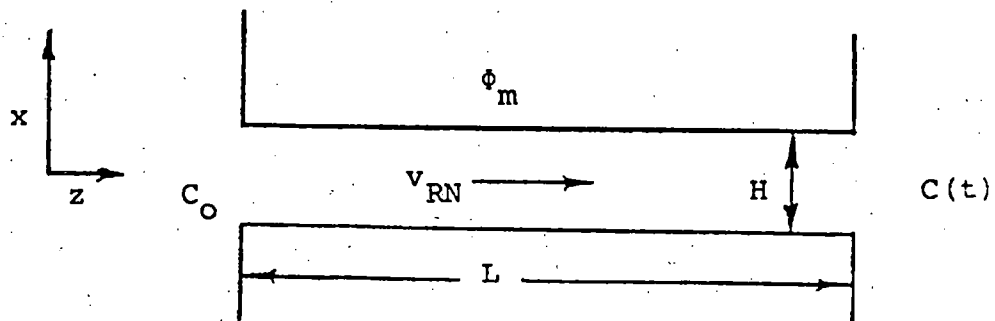


Figure C-1. Idealized Fracture Geometry

A fracture of width  $H$  and length  $L$  is assumed to exist in a rock matrix with a porosity,  $\phi_m$ . At time  $t = 0$  a constant radionuclide concentration,  $C_0$ , is introduced at the fracture inlet. An expression for the time dependent concentration,  $C(t)$ , at the outlet is desired. The rock is assumed to be infinite in the  $x$ -direction with the contaminant concentration in the rock,  $C_R(x, z)$ , maintained at zero at  $x = +\infty$ . In the fracture, radionuclide transport is assumed to be purely advective with the contaminant transported at a speed,  $v_{RN}$ , with no variation of the concentration in the  $x$ -direction within the fracture. Dispersion in the  $z$ -direction in the fracture is neglected. In the rock, transport is assumed to be purely diffusive and in the  $x$ -direction. For this situation, transport in the fracture is assumed to be described by

$$\frac{\partial C}{\partial t} + v \frac{\partial C}{\partial z} + \frac{2}{H} \frac{\partial Q}{\partial t} = 0$$

where

$$Q = \int_0^{\infty} q(x, z, t) dx$$

and  $q$  is the contaminant concentration in the rock matrix described by

$$\frac{\partial q}{\partial t} = \frac{D_{eff}}{R_R} \cdot \frac{\partial^2 q}{\partial x^2}$$

where

$D_{eff}$  is the effective diffusion coefficient in the rock and  $R_R$  is the standard porous medium retardation factor for the rock. Matching the contaminant flux in the x-direction at the fracture-rock interface gives the concentration of contaminant at the fracture exit ( $z = L$ ),

$$C(t) = C_0 \operatorname{erfc}(\eta) \quad (C1)$$

where

$$\eta = \frac{\phi_m R_R L \sqrt{D_{eff}/R_R}}{H v_{RN} \sqrt{t - z/v_{RN}}}$$

A "breakthrough time",  $t_B$ , may be defined as that value of  $\eta$ , where  $C(t_B)/C_0 = 1/2$ . The effect of the early tail of the erfc function will be addressed below. This value of  $\eta$  will be denoted by  $\eta_0$ , which has a numerical value of

approximately

$$\eta_0 = 0.48$$

The expression for  $\eta$  may be solved for  $t$ , giving

$$t_B = \frac{L}{v_{RN}} + \left( \frac{\phi_m R_R L}{H v_{RN} \eta_0} \right)^2 \left( \frac{D_{eff}}{R_R} \right)$$

In the absence of diffusion into the rock matrix ( $D_{eff} = 0$ ), radionuclides would be expected to appear at the exit in high concentration at time  $L/v_{RN}$ . Thus, we may define a retardation for this mechanism,  $R_{MD}$

$$R_{MD} = t_B / \left( \frac{L}{v_{RN}} \right) = 1 + \frac{R_R L D_{eff}}{v_{RN}} \left( \frac{\phi_m}{H \eta_0} \right)^2$$

If there is some chemical retardation in the fracture, then  $v_{RN}$  is retarded relative to the fluid velocity,  $v_{fl}$ , by the chemical retardation factor,  $R_{ch}$ , so that

$$R_{MD} = 1 + \frac{R_R R_{ch} L D_{eff}}{v_{fl}} \left( \frac{\phi_m}{H \eta_0} \right)^2$$

As will be shown, retardation factors resulting from use of this form can be very large. Transport calculations have not been performed for times long enough to demonstrate this effect. Thus, we do not have the results of numerical calculations of the total discharge to be compared to the EPA limits. It is not clear that the current version of the DVM transport model could be used for such a calculation due to the skewed shape of the breakthrough curve. We can, however, make a bounding estimate of the total integrated discharge based on simple considerations which should be applicable to one-member radionuclide decay chains such as  $^{14}C$  and  $^{99}Tc$ .

Consider the following breakthrough curve (Figure C-2) depicting the behavior of Equation C1,

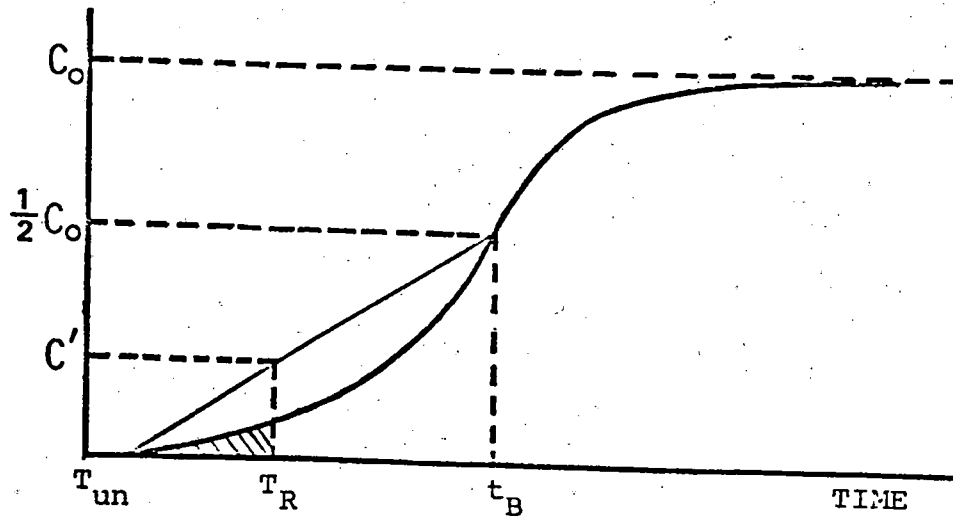


Figure C-2. Breakthrough Curve Depicting Behavior of Equation C1:  $C(t) = C_0 \operatorname{erfc}(\eta)$

- $C_0$  = maximum discharge rate
- $C'$  = estimated bound of the discharge rate for times less than  $T_R$  in the absence of matrix diffusion
- $T_{un}$  = time of transport in the absence of matrix diffusion  $L/v_{RN}$
- $T_R$  = regulatory time limit, e.g.,  $10^4$  years
- $t_B$  = estimated breakthrough time with matrix diffusion as a retardation mechanism

The shaded area represents the total integrated discharge, TID, that we seek to bound. The only assumption necessary is that the shape of the discharge curve be curved upward, as depicted, for times less than  $t_B$ . This assumption has not been investigated, but seems reasonable.

The shaded area is bounded by the area of the triangle of base  $(T_R - T_{un})$  and height,  $C'$ ,

$$TID \leq \frac{1}{2} C' (T_R - T_{un}) = \frac{1}{4} C_0 \frac{(T_R - T_{un})^2}{(t_B - T_{un})}$$

where the last step follows from similar triangles. The maximum discharge rate is given from the transport calculation performed without matrix diffusion.

No decay corrections have been considered. In fact, the correction terms already introduced are sufficient to significantly reduce the calculated discharges.

To implement these results for the multi-layered reference basalt system, we will assume the radionuclide migration path to be made up of a series of idealized fractures through each of the layers of the reference repository (except the thin sandstone layer). The subsurface facility is treated as an extended source releasing radionuclides through these idealized fractures. Discharges from the last set of fractures are collected by the overlying aquifers. Lateral variations in properties are neglected. We seek an equivalent single fracture representation of the actual multi-layered system.

The fluid transport time is given by

$$T_{fl} = \sum_{\substack{i \\ \text{layers}}} \frac{L_i}{v_{fl,i}} = \frac{1}{q} \sum_i L_i \phi_{h,i}$$

where  $q$  is the Darcy velocity which is the same in each layer,  $i$ , and  $L_i$  is the thickness of the  $i^{\text{th}}$  layer.  $\phi_{h,i}$  is the effective porosity assumed to be dominated by fractures. The transport time for the migrating contaminant,  $t_B$ , is given by

$$\begin{aligned} t_B &= \sum_i \frac{L_i}{v_i^{(md)}} = \sum_i \frac{L_i R_i^{(md)}}{v_{RN,i}} = \sum_i \frac{L_i R_i^{(md)} R_i^{(ch)}}{v_{fl,i}} \\ &= \frac{1}{q} \sum_i L_i R_i^{(md)} R_i^{(ch)} \phi_{h,i} \end{aligned}$$

So that

$$R_{\text{eff}} = \frac{t_B}{T_{\text{fl}}} = \frac{\sum_i L_i \phi_{h,i} R_i^{(\text{ch})} R_i^{(\text{md})}}{\sum_i L_i \phi_{h,i}}$$

Here, we have assumed the Darcy velocity and fluid velocity to be related by

$$v_{\text{fl},i} = \frac{q}{\phi_i}$$

Finally, to implement these results, we will make the following assumptions.

1.  $\phi_{m,i} = \phi_{h,i}$  an approximate relationship consistent with data on basalt<sup>15</sup>
2.  $R_{\text{ch}} = 1 + R_d \rho$  as in Appendix A
3.  $D_{\text{eff}} = 2 \times 10^{-7} \text{ cm}^2/\text{sec}$
4.  $H = .05 \text{ cm}$

To demonstrate the effect of diffusion into the rock matrix on estimates of the integrated discharge, three vectors of Scenario 2 have been chosen which led to violations of the EPA draft standard. The integrated discharges for these vectors are summarized in Table C-1. Applying the approximate treatment discussed above yields results presented in Table C-2. Data used in these calculations are presented in Tables C-3, 4, and 5.

It should be noted from this summary of results that the estimated contribution to the EPA Sum is the estimated integrated discharge from time zero to  $T_p$ . Thus, for Vector 15, for example, we estimate the total discharges, integrated to 50,000 years, divided by their EPA limits, and summed over all radionuclides to give a value of less than 0.140. Similarly, for Vector 62, the 50,000 year upper bound estimated for the EPA Sum is 0.2. The results for Vector 24 must be qualified. The method developed for this estimation is based on the treatment of a single-membered radioactive decay chain. All of the dominant contributors to the EPA Sum in Vector 24 are members of longer

Table C-1

SCENARIO 2 Discharges Without Rock Matrix RetardationVector 15

<u>Period</u> <u>(years)</u>	<u>0-10<sup>4</sup></u>	<u>10-20,000</u>	<u>20-30,000</u>	<u>30-40,000</u>	<u>40-50,000</u>
EPA Sum	.68	.34	.079	1.27	2.55
Tc99	-	-	-	1.27	2.55
C14	.68	.32	.05	-	-

Vector 24

EPA Sum	.093	.044	.015	1.02	6.97
236U				.19	1.42
238U				.25	1.61
234U				.55	3.61

Vector 62

EPA Sum	.81	1.57	3.46	1.42	-
Tc99	0	1.18	3.43	1.42	-
C14	.81	.39	-	-	-

Table C-2

Summary of Effects of Diffusion Into Rock Matrix on TID\*. Contributions to the EPA Sum less than .001 are omitted. No corrections for decay have been included.

SCENARIO 2

	Vector 15		Vector 24			Vector 62	
	Tc99	C14	234U	236U	238U	Tc99	C14
R <sub>eff</sub>	6.4E11	2.1E4	2.3E9	2.3E9	2.3E9	2.0E9	1.8E4
T <sub>fl</sub> (yr)	1.2E3	1.2E3	1.1E3	1.1E3	1.1E3	1.1E3	1.1E3
T <sub>B</sub> (yr)	7.4E14	2.5E7	2.4E12	2.4E12	2.4E12	2.3E12	2.1E7
C <sub>o</sub> (Ci/yr)	22.3	1.15	.22	.10	.093	33.2	1.4
Contributions to EPA Sum							
TR = 1.E4		.005					.007
2.E4		.021					.030
3.E4		.049					.070
4.E4		.088					.127
5.E4		.40					.200

\*Total integrated discharge

Table C-3

SCENARIO 2

Vector 15 Data Used to Estimate Retardation  
Due to Diffusion Into the Rock Matrix

i	$L_i$	$\phi_i$	$v_i^{fl}$	$R_{host}$	$R_{fracture}$	$R_{md}$
<u>Tc99</u>						
1	150.	.0537	2.449	.5859E+05	28.36	.3216E+10
2	150.	.0750	1.754	.4100E+05	28.36	.6132E+10
3	50.	.0129	10.23	.2552E+06	28.36	.6411E+08
4	60.	.0967	1.360	.3106E+05	28.36	.3981E+10
5	690.	.0887	1.483	.3416E+05	28.36	.3887E+11
6*	10.	.1639	.8026	33.91	33.91	1.000
7	690.	.625	2.105	.4988E+05	28.36	.1984E+11
8	200.	.0587	2.240	.5329E+05	28.36	.5101E+10
9	150.	.0600	2.193	.5212E+05	28.36	.3984E+10
<u>C14</u>						
1	150.	.0537	2.449	1.000	1.000	1936.
2	150.	.0750	1.754	1.000	1.000	5273.
3	50.	.0129	10.23	1.000	1.000	9.855
4	60.	.0967	1.360	1.000	1.000	4520.
5	690.	.0887	1.483	1.000	1.000	.4012E+05
6*	10.	.1639	.8026	1.000	1.000	1.000
7	690.	.0625	2.105	1.000	1.000	.1402E+05
8	200.	.0587	2.240	1.000	1.000	3375.
9	150.	.0600	2.193	1.000	1.000	2696.

\*No matrix diffusion assumed in Layer 6.

C-10

SCENARIO 2

Table C-4

Vector 24 Data Used to Estimate Retardation Due to Diffusion Into the Rock Matrix. (Caveats in the text on p. C-7 with regard to longer decay chains should be noted.)

i	$L_i$ (ft)	$\phi_i$	$\frac{f_i}{v_i}$	$\frac{ch}{R_{host}}$	$\frac{ch}{R_{fracture}}$	$R_{md}$
<u>U234, U236, U238</u>						
1	150.	.0484	2.619	2455.	10.20	.3678E+08
2	150.	.0440	2.878	2711.	10.20	.3058E+08
3	50.	.0125	10.09	9817.	10.20	.8559E+06
4	60.	.1017	1.246	1103.	10.20	.6139E+08
5	690.	.0675	1.876	1724.	10.20	.3231E+09
6*	10.	.1438	.8808	1317.	1317.	1.000
7	690.	.0639	1.981	1827.	10.20	.2907E+09
8	200.	.0552	2.297	2138.	10.20	.6329E+08
9	150.	.0708	1.790	1639.	10.20	.7687E+08

\*No matrix diffusion assumed in Layer 6.

C-11

Table C-5

Vector 62 Data Used to Estimate Retardation  
Due to Diffusion Into the Rock Matrix

<u>i</u>	<u>L<sub>i</sub></u>	<u>φ<sub>i</sub></u>	<u>f<sub>l</sub></u> <u>v<sub>i</sub></u>	<u>ch</u> <u>R<sub>host</sub></u>	<u>ch</u> <u>R<sub>fracture</sub></u>	<u>R<sub>md</sub></u>
<u>Tc99</u>						
1	150.	.0422	3.326	7215.	5.348	.3391E+08
2	150.	.0931	1.506	3095.	5.348	.1565E+09
3	50.	.0140	10.04	.2242E+05	5.348	.1277E+07
4	60.	.0694	2.021	4260.	5.348	.3570E+08
5	690.	.0786	1.784	3725.	5.348	.5213E+09
6	10.	.1694	.8276	76.98	76.98	1.000
7	690.	.0753	1.861	3899.	5.348	.4808E+09
8	200.	.0735	1.907	4002.	5.348	.1330E+09
9	150.	.0742	1.890	3964.	5.348	.1015E+09
<u>C14</u>						
1	150.	.0422	3.326	1.000	1.000	879.8
2	150.	.0931	1.506	1.000	1.000	9460.
3	50.	.0140	10.04	1.000	1.000	11.65
4	60.	.0694	2.021	1.000	1.000	1568.
5	690.	.0786	1.784	1.000	1.000	.2617E+05
6	10.	.1694	.8276	1.000	1.000	1.000
7	690.	.0753	1.861	1.000	1.000	.2306E+05
8	200.	.0735	1.907	1.000	1.000	6216.
9	150.	.0742	1.890	1.000	1.000	4789.

decay chains. The effect of other chain members on these estimates has not been investigated quantitatively.

Other violating vectors for this scenario have been investigated with this method and similar improvement observed. The accuracy of the estimates would be improved by estimating discharges at times earlier than  $t_B$  and correspondingly larger values of  $\eta_0$ . However, the treatment given is sufficient to demonstrate the potential importance of diffusion into the rock matrix as a retardation mechanism.

APPENDIX D

CALCULATION OF THERMAL BUOYANCY GRADIENT

Consider a cylindrical volume of fluid with length  $L$  and average temperature  $T$  immersed in a medium of average temperature  $T_0$  ( $T > T_0$ ), (Figure D-1). The difference in temperature produces an upward force on the volume of fluid. The velocity of the fluid in the cylindrical volume can be described by:

$$v \sim \alpha \Delta T K \quad (D-1)$$

with

- $v$  = Darcy velocity of fluid
- $\alpha$  = average linear coefficient of thermal expansion of fluid
- $\Delta T$  =  $T - T_0$
- $K$  = Hydraulic conductivity of medium

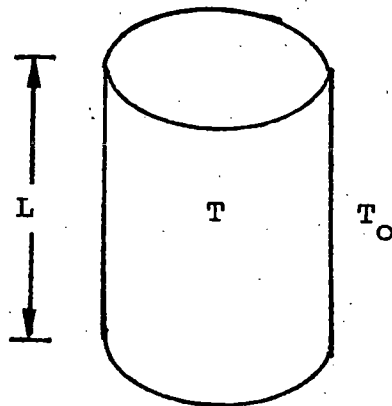


Figure D-1. Water Column Assumed for Thermal Buoyancy Calculation

Since Darcy velocity is equal to the product of hydraulic gradient (I) and conductivity, the upward gradient is given by

$$I = \alpha \Delta T \quad (D-2)$$

The temperature field around a repository at the Hanford Site (46,800 MTHM spent fuel) has been calculated for various times after closure. Figure D-2 presents the results of these calculations at 1,000, 4,000, and 30,000 years after repository closure.<sup>28</sup> The upward gradient for each time period is calculated as follows: the "disturbed zone" is assumed to be 4 km wide and has a height of 400 meters above the repository. The average temperature  $\bar{T}$  of this disturbed zone is calculated by

$$\bar{T} = \frac{1}{L} \int T dL.$$

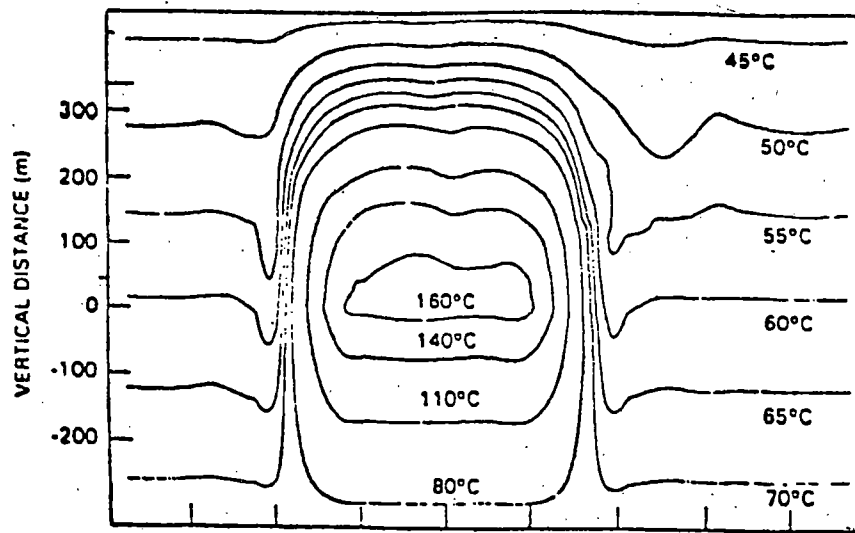
$\bar{T}_0$  is the average background temperature of the disturbed zone calculated from the natural geothermal field. The hydraulic gradient is then obtained by using Equation (D-2), i.e.,  $I = \alpha(\bar{T} - \bar{T}_0)$ .

The results of the calculations are shown in Table D-1.

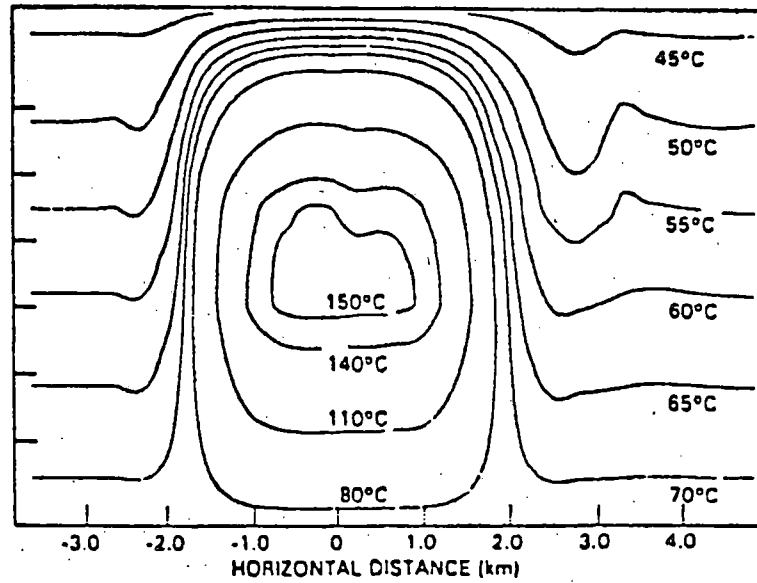
Table D-1

Hydraulic Gradients Produced by Thermal Effects

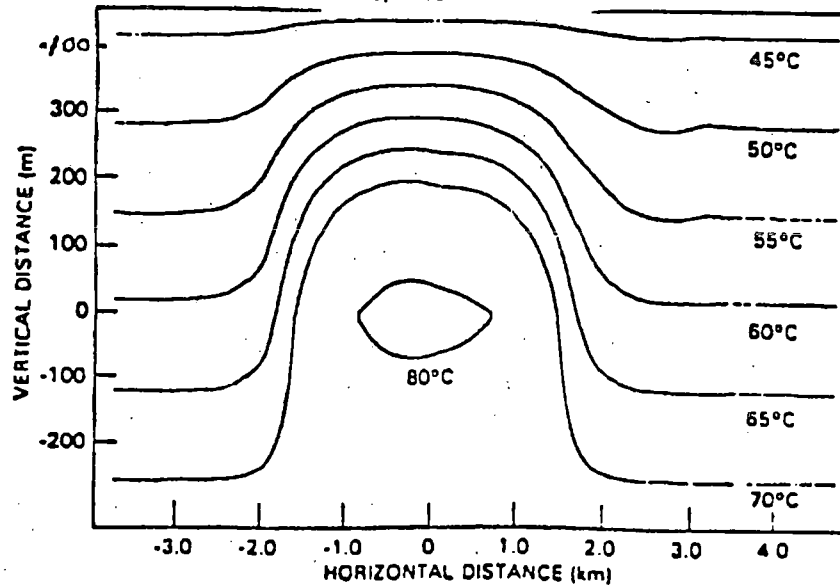
	$\bar{T} (^{\circ}\text{C})$	$\bar{T}_0 (^{\circ}\text{C})$	$\alpha(\bar{T})^{\circ}\text{C}^{-1}$	Gradient
1,000 year	98.2 <sup>o</sup>	53.2 <sup>o</sup>	608x10 <sup>-6</sup>	0.027
4,000 year	101.8 <sup>o</sup>	53.2 <sup>o</sup>	608x10 <sup>-6</sup>	0.030
10,000 year	64.3 <sup>o</sup>	53.2 <sup>o</sup>	513x10 <sup>-6</sup>	0.006



d) 1000 YEARS



e) 4000 YEARS



f) 30000 YEARS

NOTE:  
REPOSITORY LOCATED  
AT (0, 0) COORDINATES

Figure D-2. Isotherms Used in Calculating Thermal Buoyancy, from Reference 28

## APPENDIX E

### THE MIXING CELL SOURCE MODEL

In Source #3 we allow the backfilled regions to be modeled as a mixing cell in which flowing ground water is assumed to mix with radionuclides in the volume of the mixing cell. The concentration of radionuclides released from the backfilled regions is then given by the uniform concentration in the mixing cell. This model can be calculated analytically for a single stable species.

Let

$V$  = mixing cell volume,

$C$  = radionuclide concentration in water in the mixing cell,

$L$  = rate of radionuclide input into  $V$  from waste-form leaching,

$Q$  = rate of water flow through  $V$ .

In the mixing cell model, we assume the leach rate,  $L$ , to be a constant fractional rate,  $\lambda_L$ , of the initial inventory in the waste form,  $N_0$ ,

$$L = \lambda_L N_0$$

The contaminant concentration in the mixing cell is described by

$$V \frac{dC}{dt} = L - QC \quad (E1)$$

If we let

$$\lambda_0 = Q/V$$

the solution of Equation (E1) is,

$$C(t) = \frac{L}{Q} (1 - e^{-\lambda_0 t}) \quad (E2)$$

For small  $t$ ,

$$C(t) = \frac{tL}{V}$$

Thus the concentration of the radionuclide increases linearly with time from zero.

The asymptotic release rate  $QC_\infty$  can be obtained from Equation (E2) with  $t \rightarrow \infty$  :

$$QC_\infty = L$$

Thus, at long times, the release rate approaches a value governed by the rate of waste-form leaching. The release rate from the mixing cell is then less than or equal to, the release rate given by consideration of the waste form leaching alone.

For decaying radionuclide chains, this model is implemented numerically in NWFT/DVM according to the compartment model shown in Figure E-1. Radionuclides remaining in the waste form are represented by Compartments, R. The waste-form breakdown rate governs transfer from Compartments R to Compartments U. The inventory in Compartments U is examined along with the water volume in the mixing cell and solubility limits to transfer all or part of that inventory into the mixing cell. The mixing cell inventory is denoted by Compartments N. The mixing cell is flushed constantly to give a release source (S) of

$$S_i = \lambda_0 N_i$$

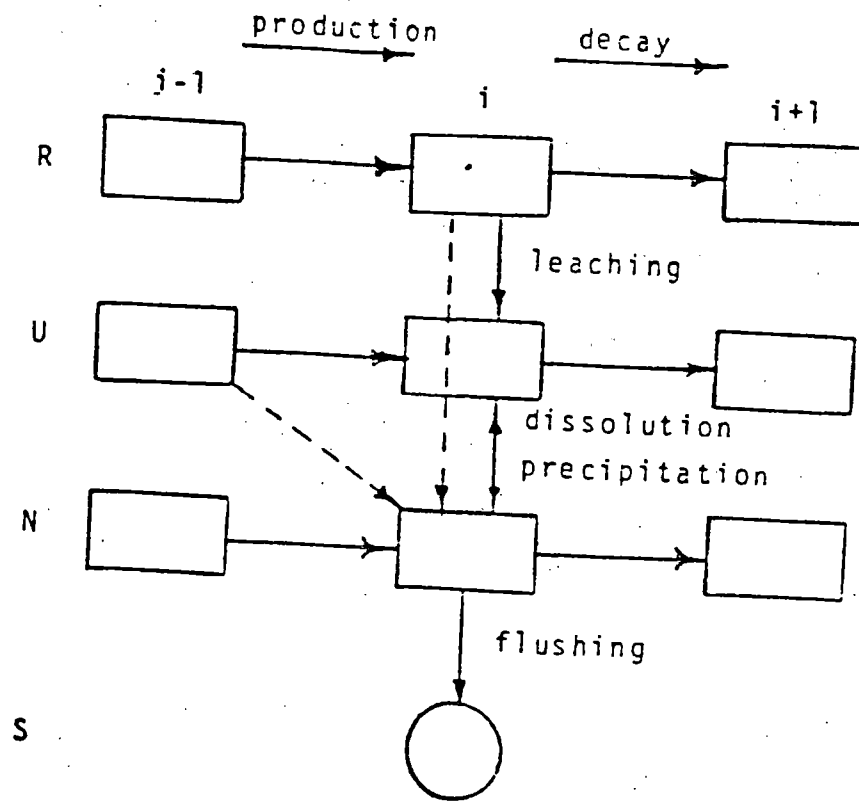


Figure E-1. Implementation of the Mixing Cell Source Model for NWFT/DVM.

where  $N_i$  is the inventory of radionuclide  $i$  in the mixing cell compartment.

When solubility limits are applied, radionuclides may be transferred from Compartments N to Compartments U, representing precipitation. For large solubility limits, Compartments U are emptied as quickly as they are filled.

Horizontal transfers between a compartment,  $i$ , and compartments  $i + 1$  or  $i - 1$  represent decay and/or production.

The effect of various source models can be illustrated by considering the total integrated discharge of the contaminant,  $D_i$

$$D_i = \int_0^t S_i dt$$

For a leach or solubility limited source,  $S_i$  is a constant. For the mixing cell,  $S_i$  is initially zero and approaches an asymptotic value determined by the leach or solubility limit. The discharge is illustrated in Figure E-2.

The integrated discharge is numerically equal to the area under the plot of  $S_i$  versus  $t$ . Due to its low initial value, the mixing cell always gives lower values of  $S_i$  and  $D_i$  at any finite time, than a leach or solubility limited model. It should be kept in mind that, the leach-limited source will be depleted at an earlier time, and the the total release will be the same for all models given sufficient time.

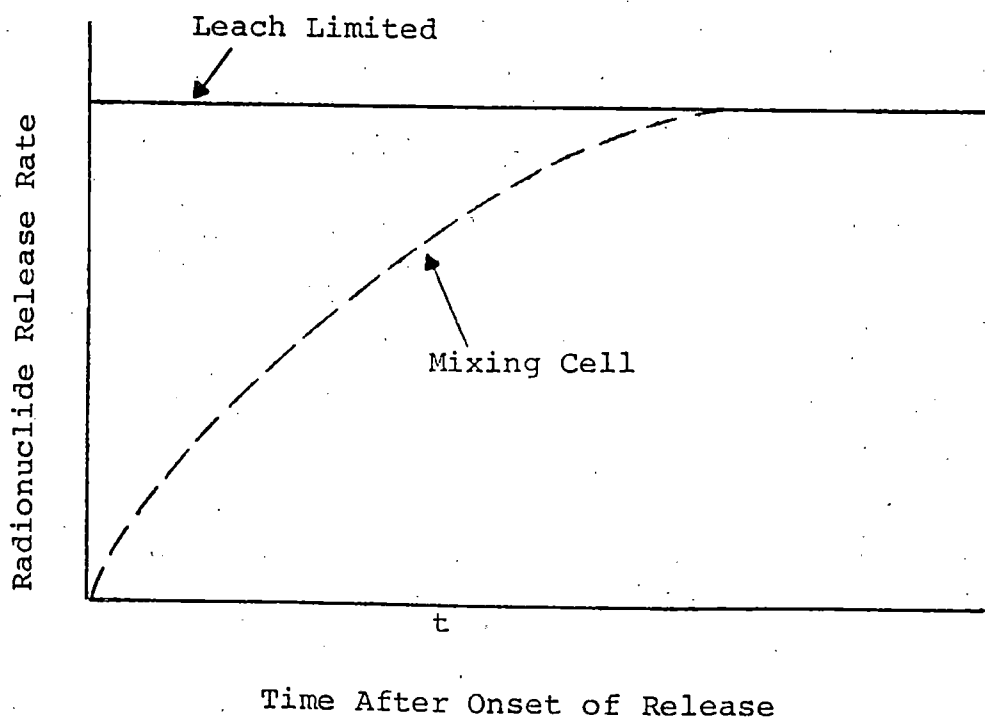


Figure E-2. Comparison of Radionuclide Releases in the Mixing Cell and the Leach-Limited Source Models

## APPENDIX F

### RATIONALE FOR THE SELECTION OF SCENARIOS ANALYZED IN BASALT

In these analyses, we have chosen scenarios which are both credible and consistent with the characteristics of a real basalt site currently being studied. It is felt that contaminant transport by ground water to an aquifer is the dominant transport mode. The first step, therefore, was to examine scenarios involving groundwater transport to an aquifer. The path of this transport from the underground facility could either be upward or downward, to an upper or lower aquifer, respectively. An upward path was chosen for our analyses for the following reasons:

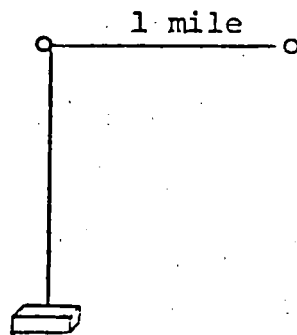
1. No indication exists that there is a downward gradient from the subsurface facility to the lower aquifer at the candidate site,
2. A lack of knowledge of the characteristics of the lower aquifer for the real site; that is, data involving flow direction, discharge location and hydraulic properties are very limited and inconsistent.
3. Based on expert judgement, the groundwater travel time from the underground facility to the accessible environment via a lower aquifer is likely to be much longer than via an upper aquifer. In other words, the lower aquifer path would probably be of much less radiological consequence than the upper case.

#### No Disruption Scenario

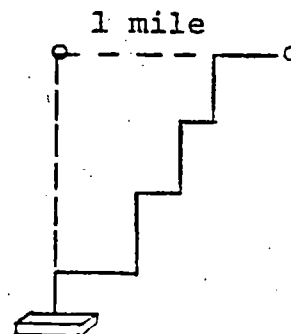
With an upward path chosen, a base case (no disruption) Scenario 1, was selected with the following rationale:

1. The cross-sectional area of the whole underground facility was used as the cross-sectional area of the upward flow column. This is the largest areal extent that can carry the wastes from the underground facility. This is a conservative approach.

2. Little or no natural upward gradient is indicated by the data from the real site. Therefore, an upward gradient that could be produced by the thermal buoyancy resulting from waste heat was used in the analyses.
3. The "shortest" path to the accessible environment was selected. First a location one mile down gradient in the first aquifer above the underground facility was chosen as the "accessible environment". Then a "vertical" path, rather than a "zig-zag" path, to the upper aquifer was used (see figures below).



Vertical Path



Zig-Zag Path

Each horizontal segment in the zig-zag path is a high conductivity zone in an interflow or an interbed layer. It was felt that the vertical segments in this path could be represented by one vertical segment as in the "vertical path" case. Available data on interflow and interbed zones of the real site suggest that the total travel time of ground water in the horizontal segments would most probably be longer than that in the 1-mile distance within the aquifer in the "vertical path" case. Therefore, a "vertical path" to the upper aquifer was chosen for our analyses.

### Disruption Scenarios

The disruption scenarios we chose involved the introduction of a high conductivity zone between the underground facility and the upper aquifer. One scenario (Scenario 2) involves a high conductivity zone of a large areal extent and another scenario (Scenario 3) a zone of small areal extent. For Scenario 2, the dense basalt layer containing the underground facility was assumed to be fractured by either earthquakes or stresses (mechanical or thermal) related to the proximity of the underground facility. The same rationales as (1), (2), and (3) in the "no disruption" scenario were applied here. Scenario 3 involves a small area of high conductivity. This could be a borehole, a degraded shaft, or fractured rock around a borehole or a shaft. We feel that the two scenarios selected represent events of high or credible probability and possibly of high consequences for the time period of interest.

No massive disruption scenario, e.g., faulting, was considered in our analyses. Due to the time constraint of this work, no detailed analysis of the probability of occurrence of massive disruption could be performed. We feel, however, that the probability of having a massive disruption through or near the underground facility at a site with these characteristics during the time period of interest, should be very small.

APPENDIX G  
GEOCHEMICAL AND HYDRAULIC PARAMETER DATA

Table G-1  
Ranges of  $R_d$  Values for Basalt Host Rock  
(Secondary Minerals)

Element	Ranges <sup>1</sup> in Table 5	Ranges From Literature <sup>2</sup>
Am	2.5E1, 2.0E6	1.9E2, 2.51E5
Pu	4.5E1, 5.2E3	1.1E2, 2.20E3
U	4.0E0, 1.3E3	1.2E1, 4.50E2
Np	1.5E0, 2.8E4	9.0E0, 4.60E3
Ra, Sn, Pb	1.7E1, 5.8E3	5.0E1, 2.00E3

<sup>1</sup> Ranges expanded to represent .001-.999 quantiles

<sup>2</sup> Values from literature review (see Table G-2), assumed to represent .5-0.95 quantiles

Table G-2

R<sub>d</sub> Values for Basalt  
 (Secondary Minerals, 0.05-0.95 quantiles)

Element	Value	Ref	Comment <sup>1</sup>
Am	1.9E2	29	normal pO <sub>2</sub> , GR-1, interbed/altered basalt, 23-60° C, ave. value
	2.51E5	29	
Pu	1.1E2	29	normal pO <sub>2</sub> , GR-1, interbed/altered low pO <sub>2</sub> , GR-1, fracture mineralization, ave. value + s.d.
	2.2E3	29	
U	1.2E1	29	normal pO <sub>2</sub> , GR-1, interbed/altered normal pO <sub>2</sub> , GR-1, fracture mineralization, 60°C, median value + s.d. for several temp., contact times, etc.
	4.5E2	29	
Np	9.0E0	29	normal pO <sub>2</sub> , GR-1, interbed/altered hydrazine reducing agent, altered basalt, GR-2
	4.65E3	30	
Ra, Sn,	5.0E1	29	normal pO <sub>2</sub> , GR-1, interbed/altered
Pb	2.0E3	29	normal pO <sub>2</sub> , GR-1, interbed/altered

<sup>1</sup> Experimental conditions are described including redox or atmospheric conditions, water used (see Ref. 31), type of rock and nature of the value quoted: average or absolute value + standard deviation (s.d.).

Table G-3

 $R_d$  Ranges in Basalt Aquifer (ml/g)

Radionuclide	$R_d$ Ranges in Table 5 of Rationale	$R_d$ Ranges in Ref.	Ref.	Comment
Am	(10 <sup>-2</sup> - 10 <sup>5</sup> )	300-134,000	32	Aquifer of Salt dome, pH6-8
		8-11	35	Sandstone, pH6
Pu	(10 <sup>-2</sup> - 10 <sup>4</sup> )	1,100-33,000	32	" Sandstone, pH6.8
		20-64	34	
U	(10 <sup>-2</sup> - 10 <sup>4</sup> )	2.89-10,900	32	Aquifer of salt dome, pH6-8
		7.45 - 65.3	33	Alluvium, pH8
Np	(10 <sup>-2</sup> - 50)	27	34	Argillite
		44	35	Argillite, pH8.2
Sr	(10 <sup>-2</sup> - 500)	7-500	32	Aquifer of salt dome, pH6-8
		109-569	33	Alluvium, pH8.5

Table G-4

## Basalt Hydraulic Parameters

Parameter	Range in Table 2	Range of Data in Available Ref.	Reference
Conductivity in Aquifer (ft/day)	1.0E0 - 1.0E4	9.9 1 - 2E4	36, Table 14 37
Porosity in Aquifer	0.1 - 0.3	0.1 - 0.15 0.2	36, Table 13 37
Conductivity in Host Rock(ft/day)	1.0E-7 - 1.0E0	2.8E-8 - 0.28	36, Table 11
Porosity in Host Rock	1.1E-3 - 2.0E-1	1.0E-3 - 1.0E-2 1.0E-3	37, Table 3 36, Table 13

## REFERENCES

1. "Environmental Radiation Protection Standards for Management and Disposal of Spent Nuclear Fuel, High-Level and Transuranic Radioactive Wastes," 40CFR191, (Working Draft #19), 1981.
2. Campbell, J. E., D. E. Longsine, and M. Reeves, Sandia National Laboratories, "Risk Methodology for Geologic Disposal of Radioactive Waste: The Distributed Velocity Method of Solving the Convective-Dispersion Equation," Report SAND80-0717, NUREG/CR-1376, 1980.
3. Egan, D. J., Environmental Protection Agency, Public Presentation at the Symposium on Uncertainties Associated With the Regulation of the Geologic Disposal of High-Level Radioactive Wastes, Gatlingburg, TN, March 9-13, 1981.
4. Iman, R. L., J. M. Davenport, and D. K. Zeigler, Sandia National Laboratories, "Latin-Hypercube Sampling: Program User's Guide," Report SAND79-1473, 1980.
5. Donath, F. A., and R. M. Cranwell, "Probabilistic Treatment of Faulting," in Geologic Media, Amer. Geophysical Union Monograph, 1981.
6. Cranwell, R. M., J. E. Campbell, and others, Sandia National Laboratories, "Risk Methodology for Geologic Disposal of Radioactive Waste: Final Report," SAND-81-2573, NUREG/CR-2452, 1982.
7. Pepping, R. E., and G. E. Runkle, Sandia National Laboratories, "Risk Methodology for Geologic Disposal of Radioactive Wastes: Decay Chain Representation for Geologic Transport of Radioactive Wastes," Report SAND81-0065, NUREG/CR-2376, 1981.
8. Fontes, J. C., I. Neretnieks, and others, IAEA, Vienna, "The Application of Isotope Techniques in the Assessment of Potential Sites for the Disposal of High-level Radioactive Wastes," in preparation, 1982.
9. Muller, A. B., N. C. Finley, and F. Pearson, Jr., Sandia National Laboratories, "Geochemical Parameters Used in the Bedded Salt Reference Repository Risk Assessment Methodology," Report SAND81-0557, NUREG/CR-1996, 1981.

10. Long, P. E., Rockwell Hanford Operations, Richland, Washington, "Characterization and Recognition of Intra Flow Structures, Grande Ronde Basalt," Report RHO-BWI-LD-10, 1978.
11. Sato, M., "Geochemical Environments in Terms of Eh and pH," in Econ. Geol., vol. 55, p. 928-961, 1960.
12. Garrels, R. M., and C. L. Christ, Solutions, Minerals and Equilibria, Harper and Row, New York.
13. Stumm, W., and J. J. Morgan, Aquatic Chemistry, Wiley, New York, 1970.
14. Smith, M. J., G. J. Anttonen, and other, Rockwell Hanford Operations, Richland, Washington, "Engineered Barrier Development for a Nuclear Waste Repository in Basalt," Report RHO-BWI-ST-7, 1980.
15. Guzowski, R. V., F. B. Nimick, and A. B. Muller, Sandia National Laboratories, "Repository Site Definition in Basalt: Pasco Basin, Washington," Report SAND81-2088, NUREG/CR-2352, 1982.
16. Harder, H., "Synthesis of Iron Layer Silicate Minerals Under Natural Conditions," in Clay and Clay Minerals, vol. 26, p. 65-72, 1978.
17. Erdal, B. R., B. P. Bayhurst, and others, "Parameters Affecting Radionuclide Migration in Geologic Media," in Scientific Basis for Nuclear Waste Management, vol. 2, C. J. M. Northrup, Jr., Ed., Plenum, N.Y., p. 609-616, 1980.
18. Wolfsberg, K., B. P. Bayhurst, and others, Los Alamos National Laboratory, "Sorption-Desorption Studies on Tuff, I: Initial Studies with Samples from the J-13 Drill Site, Jackass Flats, Nevada," Report LA-7480-MS, 1979.
19. Relyea, J. F., D. Rai, and R. J. Serne, "Interaction of Waste Radionuclides with Geomedia Program Approach and Progress," in Scientific Basis for Nuclear Waste Management, vol. 1, G. J. McCarthy, Ed., Plenum, N.Y., 1979.
20. Relyea, J. F., R. J. Serne, and D. Rai, Battelle Pacific Northwest Laboratories, Richland, Washington, "Methods for Determining Radionuclide Retardation Factors: Status Report," Report PNL-3349, 1980.

21. Hostetler, D. D., R. J. Serne, and A. Brandstetter, Battelle Pacific Northwest Laboratories, "Status of Sorption Information Retrieval System," Report PNL-3139, 1979.
22. Reardon, E. J., " $K_d$ 's -- Can They be Used to Describe Reversible Ion Sorption Reactions in Contaminant Migration?" in Ground Water, vol. 19, p. 279-286, 1981.
23. Neretnieks, I., Diffusion in the Rock Matrix: An Important Factor in Radionuclide Retardation?, in Journ. Geophysical Research, vol. 85, B8, p. 4379-4397, 1980.
24. Grisak, G. E., and J. F. Pickens, An Analytical Solution for Solute Transport Through Fractured Media with Matrix Diffusion, in Journ. Hydrology, vol. 52, p. 47-57, 1981.
25. Tang, D. H., E. O. Frind, and E. A. Sudicky, "Contaminant Transport in Fractured Porous Media: Analytical Solution for a Single Fracture," in Water Resource Research, vol. 17, 3, p. 555-564, 1981.
26. Erickson, K. L., and D. R. Fortney, Sandia National Laboratories, "Preliminary Transport Analyses for Design of the Tuff Radionuclide Migration Field Experiment," Report SAND81-1253, 1981.
27. Merkin, J. H., Free Convection Boundary Layers on Axi-Symmetric and Two-Dimensional Bodies of Arbitrary Shape in a Saturated Porous Medium, in International Journal of Heat and Mass Transfer, vol. 22, p. 1461-1462, 1979.
28. King, I. P., D. B. McLaughlin, W. R. Norton, R. G. Baca, and R. C. Arnett, Rockwell-International, "Parametric and Sensitivity Analysis of Waste Isolation in a Basalt Medium," Report RHO-BWI-C-94, 1981.
29. Serne, J., Pacific Northwest Laboratories, memorandum to A. B. Muller (SNLA), This report summarized data from the following reports: PNL-2817, PNL-3146, PNL-2797 and RHO-BWI quarterly reports for 1979 and 1980, May 13, 1981.
30. Deju, R. A., Ed., Rockwell Hanford Operations, "Basalt Water Isolation Project, Quarterly Report, October 1, 1980-December 31, 1980," Report RHO-BWI-81-100-IQ, 86 p., 1981.

31. Guzowski, R. V., F. B. Nimick, and A. B. Muller, Sandia National Laboratories, "Repository Site Definition in Basalt: Pasco Basin, Washington," Report SAND81-2088, NUREG/CR-2352, 1982.
32. Erdal, B. R., Los Alamos Laboratories, "Laboratory Studies of Radionuclide Distributions Between Selected Groundwaters and Geologic Media: Annual Report, October 1, 1978-September 20, 1979," Report LA-8088-PR, 1979.
33. Erdal, B. R., Los Alamos Laboratories, "Laboratory Measurements of Radionuclide Distribution Between Selected Groundwater and Geologic Media," Report LA-6877-MS, 1979.
34. Seitz, M. G., P. G. Rickert, S. M. Fried, A. M. Friedman, and M. J. Steindler, Argonne National Laboratory, "Studies of Nuclear Waste Migration in Geologic Media: Annual Report, November 1976-October 1977," Report ANL-78-8, 1978.
35. Barney, G. S., and P. D. Anderson, Pacific Northwest Laboratory, "The Kinetics and Reversibility of Radionuclide Sorption Reactions with Rocks: Progress Report for 1978, in Task 4 Second Contractor Information Meeting, vol. II, R. J. Serne, Ed., Report PNL-SA-7352, p. 161-218, 1979.
36. Rockwell International, Rockwell Hanford Operations, "Basalt Waste Isolation Project Reference Conditions for Long-Term Risk Assessment Calculations," Informal Report RHO-BWI-LD-36, January 1981.
37. Veatch, M. D., Pacific Northwest Laboratory, "Assessment of Effectiveness of Geologic Isolation Systems," Report PNL-2859, April 1980.

**Volume 3**

**A Simplified Analysis of a Hypothetical Repository  
in a Tuff Formation**



NUREG/CR-3235  
SAND82-1557  
WH

TECHNICAL ASSISTANCE FOR REGULATORY DEVELOPMENT:  
REVIEW AND EVALUATION OF THE EPA STANDARD 40CFR191  
FOR DISPOSAL OF HIGH-LEVEL WASTE

VOL. 3

A SIMPLIFIED ANALYSIS OF A HYPOTHETICAL REPOSITORY  
IN A TUFF FORMATION

Malcolm D. Siegel  
Margaret S. Y. Chu

Manuscript Completed: April 1983  
Date Published: April 1983

Sandia National Laboratories  
Albuquerque, New Mexico 87185  
operated by  
Sandia Corporation  
for the  
U. S. Department of Energy

Prepared for  
Division of Waste Management  
Office of Nuclear Material Safety and Safeguards  
Washington, D.C. 20555

NRC FIN. No. A-1165

## ABSTRACT

Potential radionuclide releases from a hypothetical tuff repository have been calculated and compared to the limits set by the EPA Draft Standard 40CFR191. The importance of several parameters and model assumptions to the estimated discharges has been evaluated. The areas that were examined included the radionuclide solubilities and sorption, the description of the local hydrogeology and the simulation of containment transport in the presence of fracture flow and matrix diffusion. The uncertainties in geochemical and hydrogeological parameters were represented by assigning realistic ranges and probability distributions to these variables. The Latin Hypercube sampling technique was used to produce combinations (vectors) of values of the input variables. Ground-water flow was described by Darcy's Law and radionuclide travel time was adjusted using calculated retardation factors. Radionuclide discharges were calculated using the Distributed Velocity Method (DVM). The discharges were integrated over five successive 10,000 year periods. The degree of compliance of the repository with the standard in each scenario was illustrated by the use of Complementary Cumulative Distribution Functions (CCDF).

Our calculations suggest the following conclusions for the hypothetical tuff repository: (1) sorption of radionuclides by zeolitized tuff is an effective barrier to the migration of actinides even in the absence of solubility constraints; (2) violations of the EPA Draft standard can still occur due to discharge of  $^{99}\text{Tc}$  and  $^{14}\text{C}$ . Retardation due to matrix diffusion, however, may eliminate discharge of these nuclides for realistic ground-water flow rates; (3) in the absence of sorption by thick sequences of zeolitized tuff, discharges of U and Np under oxidizing conditions might exceed the EPA standard. Under reducing conditions, however, the low solubilities of these elements may effectively control radionuclide release.

TABLE OF CONTENTS

	<u>Page</u>
1. INTRODUCTION	1
2. GEOLOGY AND HYDROLOGY OF THE REPOSITORY SITE	2
2.1 Regional geology and hydrology	2
2.2 Local geology and hydrology	6
3. WASTE AND REPOSITORY DESCRIPTION	10
3.1 Waste	10
3.2 Subsurface facility	10
4. SITE GEOCHEMISTRY AND RADIONUCLIDE RETARDATION	13
4.1 Geochemical environment	13
4.2 Sorption ratios	13
4.3 Solubility limits of radionuclides	15
4.4 Radionuclide retardation	15
5. GROUND-WATER TRANSPORT MODEL	18
6. DESCRIPTION OF SCENARIOS AND CALCULATIONS	20
6.1 Introduction	20
6.2 Scenarios 1, 3, 4 and 1B: Alternate representa- tions of retardation in welded tuff layers	23
6.3 Scenario 5: Effects of changes in the water table	34
6.4 Scenario 6: Accessible environment at eight miles	42
6.5 Scenarios 2 and 2B: Importance of solubility limits to discharge	47
7. CONCLUSIONS AND RECOMMENDATIONS	53
Appendix A -- HYDROGEOLOGICAL MODEL OF THE HYPOTHETICAL TUFF REPOSITORY SITE AND ITS RELATIONSHIP TO DATA FROM THE NEVADA TEST SITE	55
A.1 Physical properties of welded tuff	55
A.2 Vertical hydraulic gradient	56
A.3 Horizontal hydraulic gradient	65
Appendix B -- GEOCHEMISTRY AND RADIONUCLIDE RETARDATION	67
B.1 Geochemical environment of the hypothetical tuff site	67
B.2 Radionuclide solubilities	68
B.3 Radionuclide sorption ratios	71

TABLE OF CONTENTS (continued)

	<u>Page</u>
Appendix C -- APPROXIMATIONS FOR ADAPTING ONE-DIMENSIONAL POROUS MEDIA RADIONUCLIDE TRANSPORT MODELS TO THE ANALYSIS OF TRANSPORT IN JOINTED POROUS ROCK	76
REFERENCES	95

## LIST OF FIGURES

<u>Figure</u>		<u>Page</u>
1.	Regional Topography of the Hypothetical Tuff Site	3
2.	Regional Cross Section of the Repository Site	4
3.	Local Cross Section of the Repository Site	5
4.	Scenario 1	25
5.	Scenario 3	26
6.	Scenario 4	27
7.	Scenario 1B	28
8.	Complementary Cumulative Distribution Functions for Scenarios 1, 1B, 3 and 4	29
9.	Scenario 5	35
10.	Scenario 5B	36
11.	Complementary Cumulative Distribution Functions for Scenarios 1, 5 and 5B	38
12.	Scenario 6	43
13.	Complementary Cumulative Distribution Functions for Scenarios 1 and 6	44
14.	Scenarios 2 and 2B	48
15.	Complementary Cumulative Distribution Functions for Scenarios 1, 2 and 2B	49
A-1	Ranges of Hydraulic Conductivity Determined by Different Methods	58
A-2	Calculation of Thermal Buoyancy Gradient	61
A-3	Far Field Temperature Profile Along the Vertical Centerline for Gross Thermal Loading of 75 kW/Acre	62

LIST OF FIGURES (continued)

<u>Figure</u>		<u>Page</u>
A-4	Temperature Increase Histories at 307 and 711 Meters Below the Surface of the Earth for Spent Fuel at 100 kW/Acre	64
C-1	Schematic Diagrams of Porous and Jointed Porous Rock	80

## LIST OF TABLES

<u>Table</u>	<u>Page</u>
1. Stratigraphy of Hypothetical Tuff Site	7
2. Ranges of Hydrogeologic Parameters	8
3. Inventory of Reference Repository	12
4. Ranges of $R_d$ Values Sampled by Latin Hypercube	14
5. Element Solubilities Used in Mixing Cell Calculations	16
6. Descriptions of Scenarios	22
7. Number of Violating Vectors, Maximum Release Ratios and Sum of Release Ratios Over All Vectors for Each 10,000 Year Period	32
8. Properties of Vectors Which Violate EPA Standard in Scenario 1B	33
9. Number of Violating Vectors, Maximum Release Ratios and Sum of Release Ratios Over All Vectors for Each 10,000 Year Period	37
10. Properties of Vectors Which Violate EPA Standard in Scenario 5B	41
A-1 Properties of Fractured Tuff	57
A-2 Sources of Data for Ranges of Hydrogeologic Parameter Values	59
A-3 Hydraulic Gradients Associated with Thermal Effects I	63
A-4 Hydraulic Gradients Associated with Thermal Effects II	63
B-1 Analyses of Waters from the Nevada Test Site	68
B-2 Conservatism of Laboratory Determinations of $R_d$	72

LIST OF TABLES (continued)

<u>Table</u>		<u>Page</u>
B-3	Sources of Data for Ranges of $R_d$ Values for Vitric Tuff	73
B-4	Sources of Data for Ranges of $R_d$ Values for Zeolitized Tuff	74
B-5	Sources of Data for Ranges of $R_d$ Values for Devitrified Tuff	75
C-1	Definition of Terms	77
C-2	Application of Equivalent Porous Medium Criteria	93

## ACKNOWLEDGEMENTS

Michael Reade of C.G.S., Inc. collected and synthesized much of the hydrogeologic data from the Nevada Test Site that was used in this report. The equivalent porous media approximation used in these calculations was derived by K. L. Erickson, Division 1843, Sandia National Laboratory. Appendix C was written from information and text contained in several articles and notes by Dr. Erickson. Paul Davis, Division 9413, Sandia National Laboratory, provided valuable criticisms of an earlier draft of this report.

## 1. INTRODUCTION

In the near future, the EPA is expected to issue 40CFR191, a draft standard for the geologic disposal of radioactive wastes. During a 180 day period, government agencies such as NRC are expected to comment on the standard. Sandia is funded by the NRC to provide information and insights useful in preparing these comments. The objective of this effort is to perform calculations similar to those performed by EPA in developing the draft standard. We have calculated integrated discharges of radionuclides in plausible scenarios. A number of media have been proposed as candidate hosts for nuclear waste repositories: bedded salt, domed salt, basalt, tuff and granite. This report documents analysis of a repository in the saturated zone of a volcanic tuff formation.

The conceptual model of the repository site is consistent with our current understanding of the characteristics of volcanic tuff environments currently being studied by the Department of Energy. It must be stressed that we have not attempted to accurately model any specific real site. At the present time the available data are not sufficient for this purpose. Large uncertainties exist in the characterization of the solubilities and sorption of radionuclides, in the description of the regional and local hydrogeology and in the mathematical treatment of contaminant transport due to fracture flow and matrix diffusion. We feel, however, that in this analysis, we have calculated reasonable upper limits of radionuclide discharge for a generic tuff repository under realistic conditions. In our calculations we have also attempted to evaluate the relative importance of the aforementioned areas of uncertainty to the estimated radionuclide release.

Appendices A through C describe in detail the assumptions and mathematical approximations that we used in our analysis. In Appendix A we discuss the data obtained from studies of Yucca Mountain at the Nevada Test Site which were used in setting realistic limits to hydrogeological parameters used in our calculations. The assumptions used to calculate hydraulic gradients for the hypothetical repository site are also discussed. In Appendix B, the geochemical environment at Yucca Mountain is described. The data which were used to estimate realistic values of radionuclide sorption ratios ( $R_d$ 's or  $K_d$ 's) and solubilities are also discussed. In some of our calculations we have used a retardation factor which includes the effects of matrix diffusion for  $^{99}\text{Tc}$ , and  $^{14}\text{C}$  and  $^{129}\text{I}$ . Appendix C contains a derivation of the approximations we have used to adapt our one-dimensional porous media transport model to the analysis of transport in jointed porous rock.

## 2. GEOLOGY AND HYDROLOGY OF THE REPOSITORY SITE

### 2.1 Regional Geology and Hydrology

A map of the topographic setting and a regional cross-section of the repository site are shown in Figures 1 and 2 respectively. The repository (point R) is located in Mountain A on the flanks of a large volcanic caldera. The repository horizon lies approximately 3000 feet below the surface within a Tertiary volcanic tuff aquitard (Unit 3) in the saturated zone. In Mountain A, the water table is 1500 feet below the surface and 1500 feet above the repository. The tuff aquitard is composed of layers of moderately welded to nonwelded tuff units and extends several thousands of feet below the repository horizon. On a regional scale, the tuff aquitard is underlain by a Paleozoic clastic aquitard (Unit 2) and a Paleozoic carbonate aquifer (Unit 1). The basal no-flow boundary of the regional ground-water system lies at the base of the carbonate aquifer.

Above the tuff aquitard lies a densely welded and highly fractured Tertiary tuff aquifer. This unit reaches a maximum thickness of about 1000 feet at Mountain A. In the washes adjacent to the mountain, the water table lies within the tuff aquifer. The piezometric surface approaches the land surface gradually along the A-D section in Figures 1 and 2; at point D water flows freely in wells at the surface.

The lateral boundaries of the regional ground-water system are approximately coincident with the edges of Figure 1. The areas north of Mesa A and Mesa B comprise the northern border of the system. The eastern and southeastern limits of the basin are marked by a series of mountains and ridges. A mountain range in the southwest marks another boundary of the system. The northwest border at the regional system is not well defined, however, the area to the west of Mesa A is known to belong to another hydrogeologic system.

Recharge to the ground-water system through precipitation occurs only above the 5000 foot contour marked in Figure 1. Due to the high evaporation potential in this region, only about 15 percent of 15 inches of rainfall infiltrates to the water table in areas above this elevation. The ground-water system is sluggish because of the small amount of recharge. The hydraulic gradients are low to moderate ( $10^{-4}$  to  $10^{-3}$ ) except in regions where the rocks in the saturated zone are relatively impermeable. The regional ground-water flow is south-southeast through the repository and south-southwest in the southern portions of Figure 1.

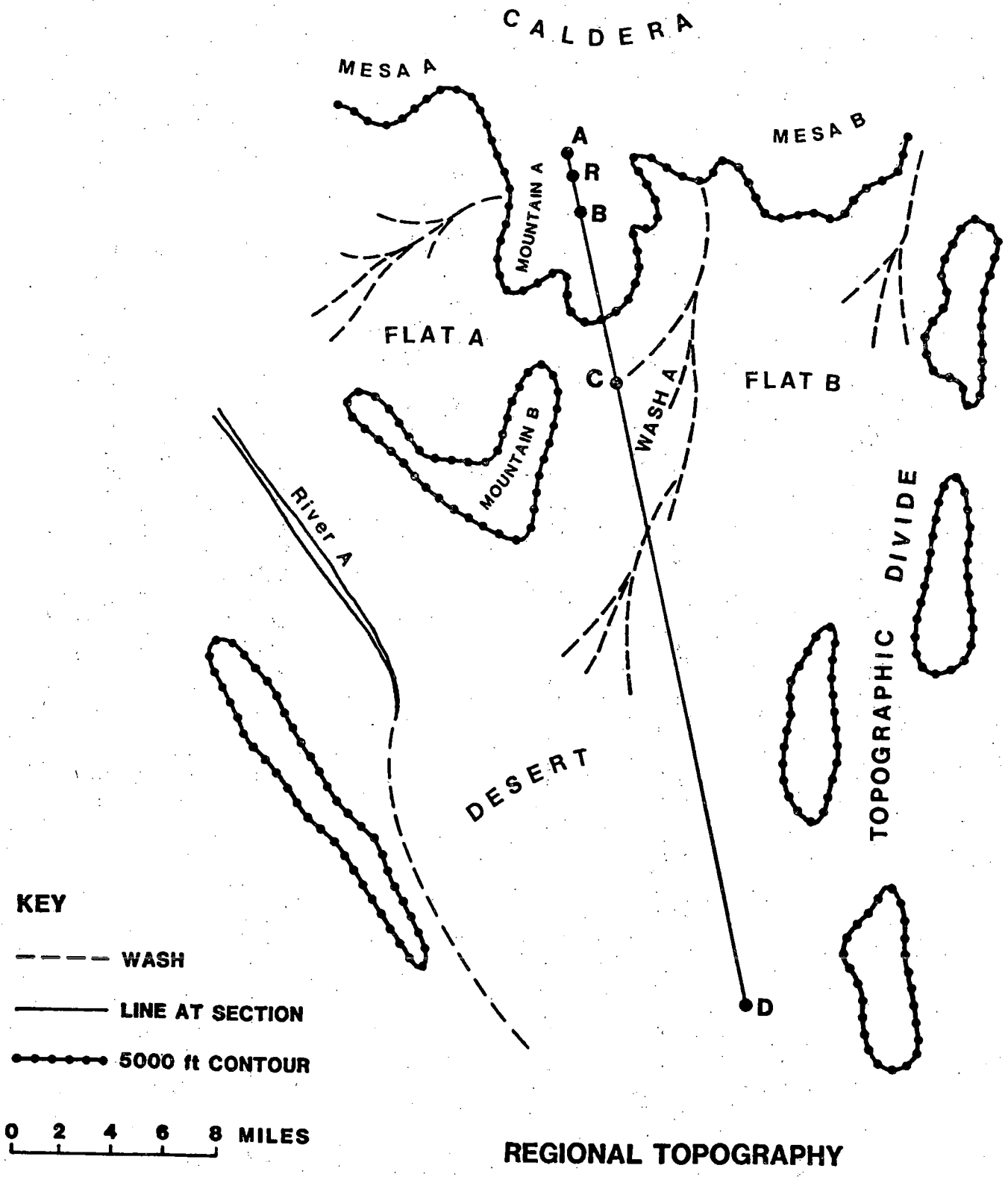


Figure 1. Regional Topography of the Hypothetical Tuff Repository Site.

## REGIONAL CROSS SECTION

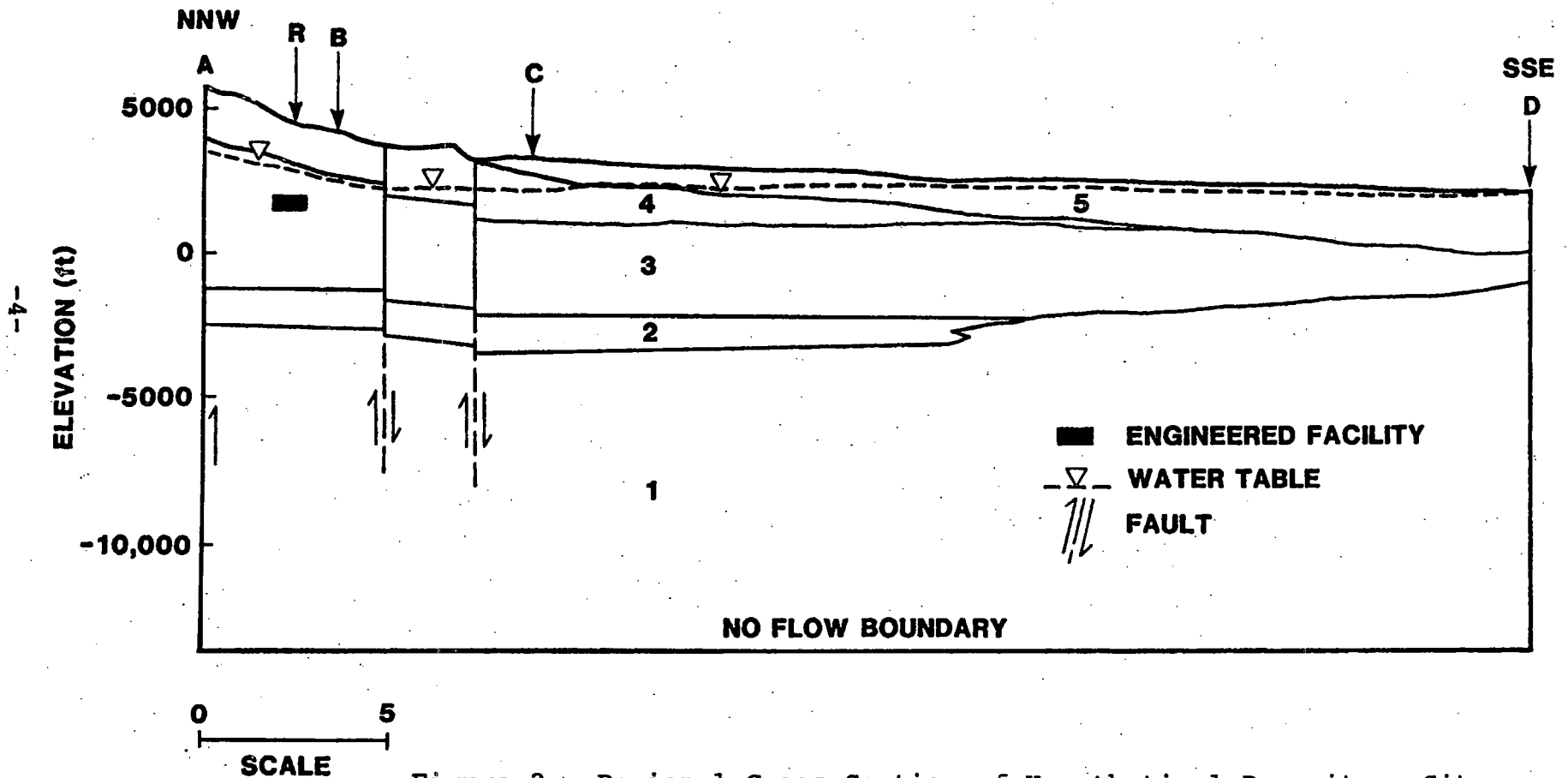


Figure 2. Regional Cross Section of Hypothetical Repository Site.  
Unit 1: Paleozoic carbonate aquifer; Unit 2: Paleozoic clastic aquitard; Unit 3: Tuff aquitard; Unit 4: Tuff aquifer.

### LOCAL CROSS SECTION

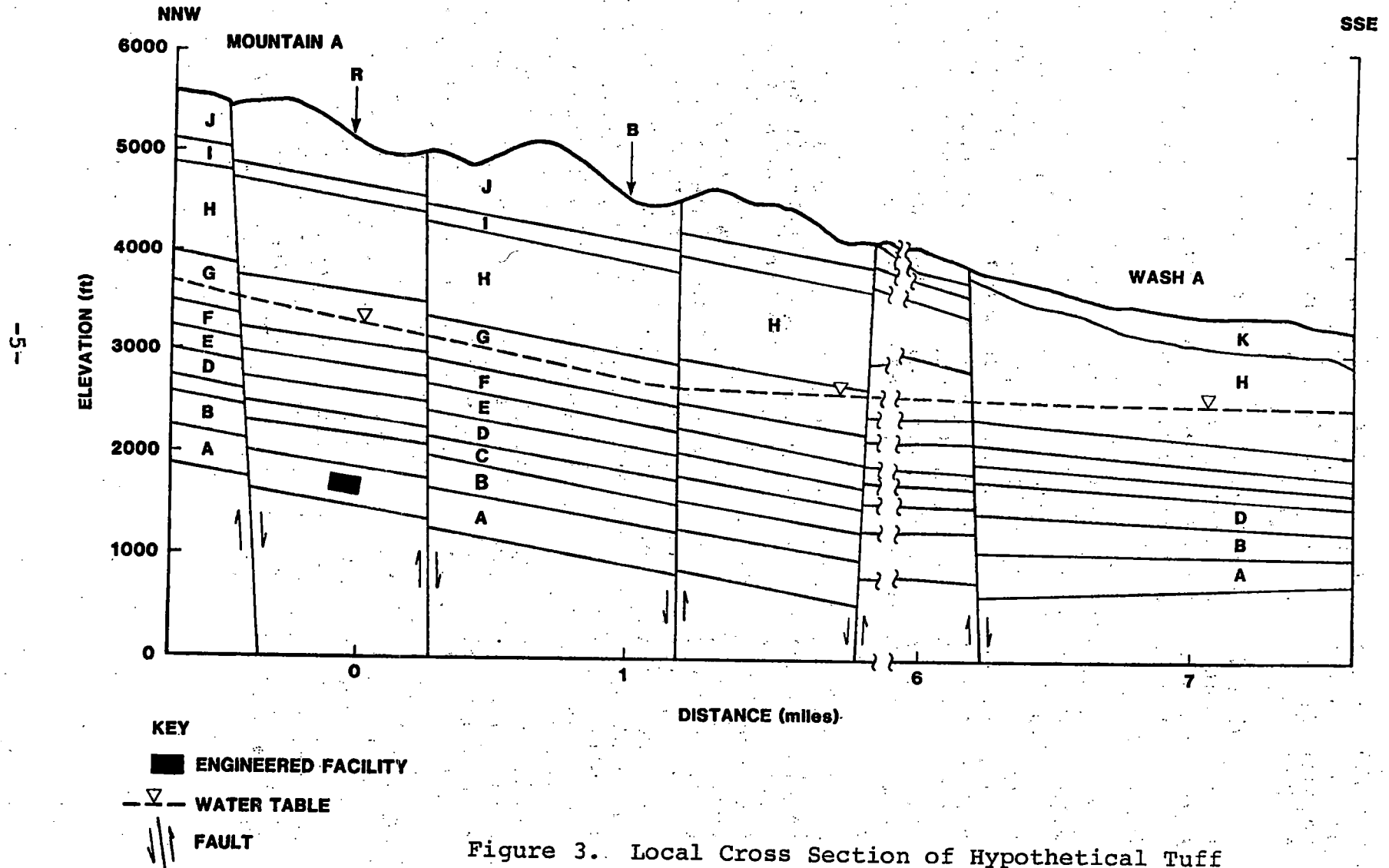


Figure 3. Local Cross Section of Hypothetical Tuff Repository Site.

## 2.2 Local Geology and Hydrology

A detailed cross section at the repository is shown in Figure 3. In Table 1, the stratigraphy for the site is described in more detail. An explanation of the petrological terms can be found in the section on Geochemistry.

In the vicinity of the volcanic caldera, the tuff layers are underlain only by granitic batholiths; all pre-existing rocks have been destroyed by volcanic eruptions. The tuff units thin with increasing distance from the volcanic centers as shown in Figure 2.

The engineered facility is located in the middle of Unit A, a densely welded member of the tuff aquitard. This unit is a devitrified tuff, composed primarily of alkali feldspar, tridymite and cristobalite. Layer B, directly above the repository horizon, is a nonwelded zeolitized tuff composed primarily of clinoptilolite. The water table lies in layer G which is similar in composition to Layer C. Layers E and I have not undergone devitrification. They have retained their original glassy nature and are designated as "vitric" in Table 1.

The geochemical and hydrological characteristics of these layers are determined primarily by the mineralogy and the degree of welding of the rocks. The local flow system and radionuclide retardation will in turn be strongly influenced by these characteristics. In Table 2, the ranges and types of distribution for several hydrogeologic parameters are described for the different types of tuff. Data from pump tests, laboratory measurements of matrix porosity of intact cores, and calculations based on fracture aperture and density were used to bound reasonable limits for hydraulic conductivity and porosity. Observations of the orientation of fractures in volcanic tuffs at the Nevada Test Site (1,2) suggest that two sets of vertical fractures dominate the joint system. In such systems, fluid flowing in the horizontal direction will effectively encounter only one set of fractures. Fluid flowing in the vertical direction will encounter both sets of fractures. In our calculations, therefore, we have assumed that values of hydraulic conductivity and effective porosity in the vertical direction are twice the values in the horizontal direction. The assumptions and methods used to delimit the ranges of hydraulic properties are discussed in more detail in Appendix A. The wide ranges of values for these parameters correspond to the limits of values of published data obtained from the different measurement techniques described above. It will be

Table 1

STRATIGRAPHY OF HYPOTHETICAL TUFF SITE

UNIT	DEGREE OF WELDING	ROCK TYPES	THICKNESS (FT)	COMMENT
(TUFF AQUIFER) K J I H	NA	ALLUVIUM	60-425	WATER TABLE AT DISTANCE=8 MILES
	DENSE	DEVITRIFIED	145	
	NONWELDED	VITRIC	150	
	DENSE	DEVITRIFIED	900	
(TUFF AQUITARD) G F E D C B A	NONWELDED	ZEOLITIZED	475	WATER TABLE AT DISTANCE=0 MILES
	MODERATE	DEVITRIFIED	270	
	MODERATE	VITRIC	180	
	NONWELDED	ZEOLITIZED	150	
	DENSE	DEVITRIFIED	250	
	NONWELDED	ZEOLITIZED	300	
DENSE	DEVITRIFIED	400	REPOSITORY HORIZON	

Table 2

## RANGES OF HYDROGEOLOGIC PARAMETERS

<u>Parameter</u>	<u>Densely Welded Tuff</u>	<u>Moderately Welded Tuff</u>	<u>Nonwelded Tuff</u>
Horizontal hydraulic conductivity (ft/day) <sup>''</sup>	$2 \times 10^{-5}$ -30 (LU) <sup>'</sup>	$3 \times 10^{-5}$ -5 (LN)	$10^{-5}$ -2 (LN)
Horizontal effective porosity (%) <sup>''</sup>	$4.4 \times 10^{-4}$ -0.32 (LN)	0.03-25 (LU)	20-48 (N)
Horizontal hydraulic gradient	$1 \times 10^{-3}$ - $1 \times 10^{-1}$ (LU)	$1 \times 10^{-3}$ -- $1 \times 10^{-1}$ (LU)	$1 \times 10^{-3}$ - $1 \times 10^{-1}$ (LU)
Vertical hydraulic gradient	$1 \times 10^{-2}$ - $4 \times 10^{-2}$ (U)	$1 \times 10^{-2}$ - $4 \times 10^{-2}$ (U)	$1 \times 10^{-2}$ - $4 \times 10^{-2}$ (U)
Grain density (g/cm <sup>3</sup> )	2.3	2.2	1.7
Horizontal fracture porosity <sup>''</sup> (%)	$4.4 \times 10^{-4}$ -0.32	0.0-0.06	---
Total Porosity (%)	3-10	10-38	20-50

<sup>'</sup> Type of distribution is indicated in parenthesis for variable sampled by Latin Hypercube Sample: (LU)-log uniform; (LN)-lognormal; (U)-uniform.

<sup>''</sup> Values of these properties in the vertical direction are 2x the values in the horizontal direction.

shown in Chapter 6 that this uncertainty in the input data can be related to the uncertainty in the results by the Latin Hypercube sampling technique (18) and the Complementary Cumulative Distribution Function (6).

The repository site is extensively block faulted, consequently, the water table lies in the tuff aquitard near Mountain A (an uplifted block) and in the tuff aquifer beneath the adjacent washes and flats (down-dropped blocks).

The water table in the vicinity of the repository is indicated in Figure 3. Near Mountain A, the piezometric surface lies within Unit H and parallels the top of this layer. The horizontal hydraulic gradient near the repository is within the range  $10^{-1}$  to  $10^{-3}$ . Approximately 2 miles from the repository, the water table enters the tuff aquifer (in Layer G) and the gradient decreases to a range of  $10^{-2}$  to  $10^{-4}$ . This change in gradient is due to the combined effects of stratigraphy, contrasts in hydraulic conductivity, and increased recharge at elevations above 5000 feet. In our calculations, however, we have sampled the horizontal gradient over a range of  $10^{-1}$  to  $10^{-3}$  for conservatism.

The block faulting can create local abrupt changes in head at vertical faults where relatively permeable water-bearing zones are abutted against impermeable layers. For the purpose of our calculations, however, we have ignored these local heterogeneities. The water lies more than 1000 feet below the surface at all points along section ARBC. Local changes in the water table will not substantially affect radionuclide transport on the scale of our model; the water table, therefore, is represented by straight lines in Figure 3.

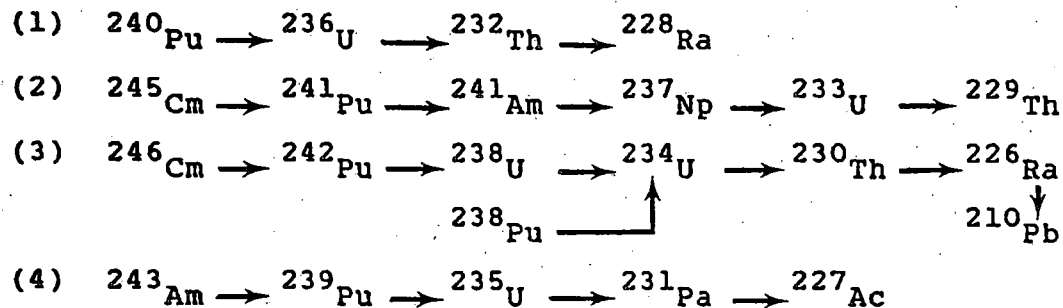
In all of the release scenarios (except scenarios 2 and 2B) we have assumed that radionuclides travel vertically from the engineered facility to the water table under the influence of thermal buoyancy related to the heat generated by the emplaced waste. We have also assumed that the volume of annual groundwater flow through the repository is not large enough to appreciably perturb the regional flow system. Supply of groundwater to the repository will be sufficient to saturate the repository at all times during the 50,000 year period of interest. This assumption adds another element of conservatism to our calculations and will be discussed further in Appendix A.

### 3. WASTE AND REPOSITORY DESCRIPTION

#### 3.1 Waste

The inventory (Table 3) assumed in this work is equal to half the projected accumulation of 10-year-old spent fuel in the United States by the year 2010. This would contain a total of 103,250 BWR and 60,500 PWR assemblies; a total of 46,800 metric tons of heavy metal (MTHM). All radionuclides specified in the Release Limit Table of the EPA Standard are included in this inventory list.

Based on the inventory and toxicity of each radionuclide the following chains of radionuclides were considered:



The fission and activation product radionuclides  $^{99}\text{Tc}$ ,  $^{129}\text{I}$ ,  $^{126}\text{Sn}$ ,  $^{90}\text{Sr}$ ,  $^{14}\text{C}$ ,  $^{135}\text{Cs}$ , and  $^{137}\text{Cs}$  were also considered in this work.

All canisters containing the wastes are assumed to have a life of 1,000 years after emplacement. At year 1,000, all canisters fail simultaneously and radionuclide release begins. Radionuclide release is assumed to be determined by a constant rate of breakdown of the waste form. The waste matrix is assumed to dissolve at an annual rate of  $10^{-3}$  to  $10^{-7}$  of the original mass. Radionuclides are assumed to be uniformly distributed throughout the matrix so that their release rate is directly proportional to the matrix dissolution rate.

#### 3.2 Subsurface Facility

The reference subsurface facility is a mined facility at a depth of 3,000 feet below the surface. A description of the facility is summarized as follows:

Areal dimensions -- 2,000 acres ( $8.71 \times 10^7 \text{ft}^2$ )  
(Reference 3, Table C1)

Height = 23 ft.

Rep. Volume =  $8.71 \times 10^7 \text{ft}^2 \times 23 \text{ft} = 2.0 \times 10^9 \text{ft}^3$

Extraction Ratio = 20% (Reference 3, p. 88)

Porosity of Backfill = 20%

Porosity volume of depository =  $8.0 \times 10^7 \text{ft}^3$

Table 3

INVENTORY OF REFERENCE REPOSITORY  
(SPENT FUEL FROM 46,800 MTHM)

<u>Radionuclide</u>	<u>Half Life</u>	<u>Curies</u>
Pu240	6.76E3	2.1E7
U236	2.39E7	1.0E4
Th232	1.41E10	1.7E-5
Ra228	6.7	4.7E-6
Cm245	8.27E3	8.4E3
Pu241	14.6	3.2E9
Am241	433.	7.5E7
Np237	2.14E6	1.5E4
U233	1.62E5	1.8
Th229	7300.	1.3E-3
Cm246	4710.	1.6E3
Pu242	3.79E5	7.5E4
U238	4.51E9	1.5E4
Pu238	89.	9.4E7
U234	2.47E5	3.5E3
Th230	8.E4	0.19
Ra226	1600.	3.5E-4
Pb210	21.	3.3E-5
Am243	7650.	6.6E5
Pu239	2.44E4	1.4E7
U235	7.1E8	7.5E2
Pa231	3.25E4	0.25
Ac227	21.6	5.2E-2
Tc99	2.14E5	6.1E5
I129	1.6E7	1.5E3
Sn126	1.0E5	2.2E4
Sr90	28.9	2.4E9
Cl4	5730.	3.5E4
Cs135	2.0E6	1.3E4
Cs137	30.	3.5E9

#### 4. SITE GEOCHEMISTRY AND RADIONUCLIDE RETARDATION

##### 4.1 Geochemical Environment of the Hypothetical Tuff Site

The migration rate of radionuclide in the tuff repository site will depend on the interactions between the dissolved species and the rock matrix and between the different aqueous species in the liquid phase. Important geochemical parameters which must be characterized include the major and minor element composition, pH, Eh, and temperature of the ground water and the mineralogy of tuff layers through which the radionuclides migrate.

The lithology of each tuff unit in our hypothetical tuff site is described in Table 1. They are classified as zeolitized, vitric or devitrified. A more detailed discussion of the mineralogy may be found in Appendix B. The ground water in the repository site is assumed to be a sodium-potassium-bicarbonate water similar to that described by Winograd and Thordarson (4) at the Nevada Test Site. The Eh is assumed to be mildly oxidizing and the pH is between 7.2 and 8.3. The chemical composition of water from the vicinity of Yucca Mountain and the justification for the above assumptions are described in detail in Appendix B. The temperature assumed in the transport legs in the far field of the repository site is between 30°C and 40°C. This range is based on the geothermal gradient at Yucca Mountain (3).

##### 4.2 Sorption Ratios

The sorption ratio ( $R_d$ ) is an experimentally determined ratio of the amount of radionuclide bound to a solid phase to the amount of nuclide in a volume of liquid in contact with the solid.

$$R_d \text{ (ml/g)} = \frac{\text{grams radionuclides per gram rock}}{\text{grams radionuclide per ml water}}$$

Values for ranges of  $R_d$  for the different types of tuff found at the reference repository site are given in Table 4. These ranges are based primarily on a review of the results of sorption ratio studies by scientists at Los Alamos Laboratories (5-10).

The degree of conservatism for these ranges is discussed in Appendix B. Elements for which no sorption data are published are enclosed in brackets in Table 4. They have been assigned to  $R_d$  values of chemical homologs for which data are available (11). To our knowledge, there are no acceptable data for

Table 4

RANGES OF  $R_d$  (ml/g) VALUES SAMPLED BY LATIN HYPERCUBE

<u>Element</u>	<u>Vitric Tuff</u>	<u>Devitrified Tuff</u>	<u>Zeolitized Tuff with Clinoptilolite</u>
Sr, [Ra, Pb, Sn]	117-300	50-450	290-213,000
Cs	429-8600	120-2000	615-33,000
Pu	70-450	80-1400	250-2000
Am, [Cm, Pa, Th, Ac]	85-360	190-4600	600-9500
Np	5-7	5-7	4.5-31
U	0-11	1-14	5-15
I, <sup>14</sup> c	0	0	0
Tc	0-2	0.3-1.2	0.2-2

Np sorption on vitric tuff; the sorption ratio range for devitrified tuff was assigned to this medium.

#### 4.3 Solubility Limits of Radionuclides

The solubility limits that were assigned to each element in this study are listed in Table 5. Based on data available at this time, the values in the table are approximate upper bounds for the solubilities of these elements in a volcanic tuff environment. The determination of solubilities of radionuclides in ground water associated with a repository in tuff requires experimental studies and calculations describing the possible interactions between nuclides and ligands over a range of temperatures, water compositions and redox conditions. The theoretical calculations are not within the scope of this contract and to our knowledge have not been carried out. Few experimental data describing radionuclide solubility in tuff are available at this time. Due to the time constraints of this contract, we have compiled this list of solubility values from a limited amount of experimental data and solubilities calculated from a limited review of thermochemical data (12-16). A discussion of the conservatism of these data may be found in Appendix B.

#### 4.4 Radionuclide Retardation

The following expression was used to describe radionuclide retardation in layers of zeolitized tuff in all scenarios.

$$R = 1 + R_d \cdot \rho \cdot \frac{(1 - \phi_{\text{eff}})}{\phi_{\text{eff}}} \quad (4.1)$$

Where  $\phi_{\text{eff}}$  is the effective porosity of the rock  
 $\rho$  is the grain density of the rock  
 $R_d$  is the radionuclide sorption ratio (ml/g)

The calculation of retardation in moderately and densely welded tuff layers was different in each scenario. In scenarios 3 and 4, expression 4.1 was used for moderately welded tuff layers. It was assumed that all radionuclides were unretarded in densely welded layers in scenarios 1, 3, 4, 5, and 6. In scenarios 1, 5, and 6 it was assumed that all radionuclides were unretarded in moderately welded tuff layers also. Detailed descriptions of the scenarios and rationales for these representations of retardation are found in the next section.

Table 5

ELEMENT SOLUBILITIES USED IN  
MIXING CELL CALCULATIONS

<u>Element</u>	<u>Solubility</u> <u>g/g</u>	<u>Reference</u>
Pu	$2.4 \times 10^{-4}$	*
U	$2.4 \times 10^{-5}$	15
Th	$2.3 \times 10^{-7}$	13
Ra	$2.3 \times 10^{-8}$	16
Cm	$2.5 \times 10^{-11}$	*
Am	$2.4 \times 10^{-12}$	15
Np	$2.4 \times 10^{-8}$	15
Pb	$2.1 \times 10^{-6}$	*
Pa	$2.3 \times 10^{-2}$	13
Ac	no limit	*
Tc	no limit	*
I	no limit	*
Sn	$1 \times 10^{-3}$	13
Sr	$2 \times 10^{-6}$	13, 16
Cs	no limit	*
C	$3 \times 10^{-5}$	*

\* See discussion in Appendix B

In scenarios 1B, 2, 2B, and 5B matrix diffusion for Tc,  $^{14}\text{C}$ , and I was included explicitly in the calculations of radionuclide retardation:

$$R = 1 + \phi_m \left( \frac{1 - \epsilon}{\epsilon} \right) \cdot \left( 1 + R_d \cdot \rho \cdot \left( \frac{1 - \phi_m}{\phi_m} \right) \right) \quad (4.2)$$

Where:  $\phi_m$  = matrix porosity  
 $\epsilon$  = fracture porosity  
 $\rho$  = grain density of rock matrix  
 $R_d$  = radionuclide sorption ratio (ml/g)

The derivation of this expression and constraints on its use are discussed in Appendix C.

## 5. GROUNDWATER TRANSPORT MODEL

In the calculations of radionuclide transport it is assumed that ground-water flow is described by Darcy's Law:

$$q = Q/A = KI \quad (5.1)$$

where  $Q$  is the volumetric flow rate through an area  $A$ , normal to the flow direction,  $I$  is the hydraulic gradient,  $K$  is the hydraulic conductivity, and  $q$  is the Darcy velocity. When the flow passes through a series of layers with different hydraulic properties, an "effective" hydraulic conductivity may be calculated by

$$K = \frac{\sum_i L_i}{\sum_i \frac{L_i}{K_i}} \quad (5.2)$$

with

$L_i$  = thickness of layer  $i$

$K_i$  = hydraulic conductivity of layer  $i$

The total ground-water travel time is given by

$$\text{Time} = \sum_{i=1} \frac{L_i}{V_i} \quad (5.3)$$

where  $V_i$  is the interstitial ground-water velocity in layer  $i$  and is equal to  $q/\phi_i$ , where  $\phi_i$  is the effective porosity of layer  $i$ . We have assumed that  $\phi_i$  and  $K_i$  are correlated and  $r^2 = 0.70$ . The geometry of the flow path is described for each scenario in Section 6.

When a radionuclide (RN) is transported by ground water, the radionuclide travel time ( $T_{RN}$ ) is increased by its retardation factor. This is given by

$$T_{RN} = \sum_i \frac{L_i \cdot R_i^{RN}}{V_i} \quad (5.4)$$

where  $R_i^{RN}$  is the retardation factor of radionuclide RN in layer i.

The Distributed Velocity Method (DVM) (17) has been developed by Sandia to simulate long chains of radionuclides transported by ground water. In this study we calculated the average velocity of radionuclides using Equation (5.4). The DVM code was then used to calculate the discharges of radionuclides.

## 6. DESCRIPTIONS OF SCENARIOS AND CALCULATIONS

### 6.1 Introduction

The conceptual model of our hypothetical repository site is consistent with our current understanding of the characteristics of volcanic tuff environments being studied by the Department of Energy. We have not attempted to accurately model any particular real site; at the present time the available data are not sufficient for this purpose. Large uncertainties exist in the characterization of the solubilities and sorption of radionuclides, in the description of the regional and local hydrogeology and in the mathematical treatment of contaminant transport in the presence of fracture flow and matrix diffusion. In our calculations, we have attempted to evaluate the relative importance of these areas of uncertainty to the estimated radionuclide discharge. We have calculated radionuclide release for several scenarios using different combinations of the following assumptions:

- A. Release rate of radionuclides from the engineered facility
  - 1. limited by leach rate
  - 2. solubility limited
  
- B. Representation of retardation of radionuclides in moderately welded units
  - 1. no retardation
  - 2. porous media approximations with zeolite  $R_d$ 's
  - 3. porous media approximations with  $R_d$ 's for vitric or devitrified tuff
  
- C. Matrix diffusion
  - 1. no credit given for retardation by matrix diffusion
  - 2. calculation of retardation of  $^{99}\text{Tc}$ ,  $^{129}\text{I}$ , and  $^{14}\text{C}$  in welded units
  
- D. Distance to accessible environment
  - 1. one mile
  - 2. eight miles
  
- E. Flow path
  - 1. vertical path and gradient controlled by thermal effect
  - 2. horizontal migration only
  
- F. Location of water table
  - 1. in zeolitized tuff
  - 2. in densely welded tuff (300 ft above present day level)

The characteristics of each scenario are summarized in Table 6. The release rate of radionuclides from the engineered facility was set equal to the leach rate ( $10^{-3}$  to  $10^{-7}$  of the original inventory) in all scenarios except scenario 2B.

The mixing cell option of NWFT/DVM was used in the scenario 2B and will be described in more detail in Section 6.5.

The uncertainties in geochemical and hydrogeological parameters were represented by assigning realistic ranges and probability distributions to these variables. The Latin Hypercube Sampling Technique (18) was used to produce 106 combinations (vectors) of values of the input variables. Integrated radionuclide discharges for five successive 10,000 year periods were calculated as described in Section 5. A release ratio was calculated for each vector by dividing the magnitude of the discharge of each radionuclide by the corresponding EPA release limit (19, 23) and then summing over all radionuclides.\* The results are presented as probability distributions of the release ratios for each scenario (Complementary Cumulative Distribution Functions) (20). The curve indicates the ability of the repository site to limit the release of radionuclides and to comply with the Draft EPA Standard. They also illustrate how our ability to assess the compliance of a repository with the EPA Draft Standard is affected by the uncertainty in the input data.

We have not made quantitative estimates of the probability of occurrence of any of the scenarios. We have assumed only that each of the scenarios is an "anticipated event" (corresponding to a "reasonably foreseeable release" in the EPA Draft Standard (19)). We feel that the scenarios have a reasonable probability of occurrence within the 10,000 year regulatory period.

The water table is at least 1,000 feet below the land surface at all points within the hypothetical repository site of our analyses. All of the scenarios require that a well be drilled at least to the depth of the water table and that the radionuclides are withdrawn continuously for 10,000 years or longer. We have based our subjective estimate of the probability of drilling at the hypothetical tuff site on estimates of the water, hydrocarbon and heavy metal ore potential of the Nevada Test Site. Our estimate of the probability of a pluvial period and subsequent rise in the water table at the repository site (scenario 5) is based on information concerning past climatic changes at NTS (22).

\*EPA release ratio =  $\sum Q_i / EPA_i$ , where  $Q_i$  is the integrated release of radionuclide  $i$  and  $EPA_i$  is the EPA release limit for radionuclide  $i$  for the 10,000 year interval. For "reasonably foreseeable releases" the EPA release ratio must be less than or equal to unity for compliance.

Table 6

## DESCRIPTIONS OF SCENARIOS

SCENARIO	DISTANCE BETWEEN DEPOSITORY AND POINT OF DISCHARGE		REPRESENTATION OF RETARDATION IN WELDED UNITS DENSELY AND MODERATELY WELDED      MODERATELY WELDED ONLY				VERTICAL GRADIENT CONTROLLED BY THERMAL PULSE		CLIMATIC CHANGE CAUSES 300 FT RISE IN WATER TABLE	
	1 MILE PUMP	8 MILE PUMP	MATRIX DIFFUSION MODEL	FRACTURED MEDIUM WITH NO RETARDATION	POROUS MEDIUM WITH ZEOLITES	POROUS MEDIUM WITH DEVITRIFIED TUFF OR VITRIC TUFF	YES	NO	YES	NO
#1	X			X			X			X
#1B	X		X				X			X
#2	X		X					X		X
#2B	X		X					X		X
#3	X				X		X			X
#4	X					X	X			X
#5	X			X			X		X	
#5B	X		X				X		X	
#6		X		X			X			X

\* Scenarios 2 and 2B differ from each other in their treatment of the source term. Scenario 2 was a leach limited source term with no solubility limits. In scenario 2B we used the mixing cell option of NWFT/DVM which allows solubility limits to constrain the rate of radionuclide release from the repository.

## 6.2 Scenarios 1, 3, 4, and 1B: Alternate representations of retardation in welded tuff layers

### Scenario 1 - The "Base Case"

Scenario 1 can be considered the base case scenario in our analyses of the hypothetical tuff site (Figure 4). The major geological barriers to radionuclide migration are the layers of zeolitized tuff above the repository. The magnitude of the vertical hydraulic gradient is determined by a buoyancy effect of water heated by the repository as described in Appendix A. Ground water and radionuclides from the repository will travel along the vertical gradient to the top of the water table and then migrate horizontally down the horizontal hydraulic gradient. The horizontal gradient is calculated as the sum of the regional gradient plus a component related to the upwelling heated water from the repository (see Appendix A.3).

At a distance of one mile from the repository, a well pumps water from this upper saturated unit. The major barrier to horizontal transport of the radionuclide is retardation in the zeolitized layer G. Layers of zeolitized tuff are treated as porous media in the fluid transport and retardation calculations. Layers of moderately or densely welded tuff are treated as porous media in the transport calculations but it is assumed that no retardation occurs in these layers. Since no credit is given to retardation in the welded units, the calculated discharge may be an upper bound for release associated with the fluid transport path described above.

### Scenarios 3 and 4 -Porous media approximations for moderately welded tuff layers

Scenarios 3 and 4 differ from scenario 1 only in the treatment of retardation in the moderately welded tuff layers (Figures 5 and 6). In both scenarios these layers are treated as porous media. Moderately welded tuffs are characterized by physical and chemical properties that are intermediate between densely welded devitrified tuffs and nonwelded zeolitized tuffs. In scenario 3,  $R_d$  values of zeolitized tuff (Table 4) are used to calculate retardation factors. These calculations may provide a lower bound to discharge from the site for scenarios 1, 3, and 4.  $R_d$  values for vitric tuffs and devitrified tuffs are used to calculate retardation in layers E and F respectively in scenario 4. Values of all other variables are the same as in corresponding vectors of scenario 1.

## Scenario 1B - Matrix diffusion in welded tuff layers

Scenario 1B (Figure 7) differs from scenario 1 only by the inclusion of matrix diffusion in calculations of radionuclide retardation in moderately and densely welded tuff layers. The calculation of a retardation factor which includes the effects of matrix diffusion has been described in Equation 4.2 and in Appendix C. At present, it can only be shown that this expression is valid for radionuclides with  $R_d = 0$  (K. Erickson, personal communication). For scenario 1B, therefore, retardation due to matrix diffusion was considered only for  $^{129}\text{I}$ ,  $^{99}\text{Tc}$  and  $^{14}\text{C}$  (see Table 4).

## Results

Radionuclide discharge rates for each vector were calculated. Discharge rates were integrated for 10,000 year periods from 0 to 50,000 years. The results of the calculations are presented as Complementary Cumulative Distribution Functions for each 10,000 year period in Figures 8A-8E. (20) The number of vectors that violate the EPA Standard, the maximum violation and the sum of the release ratio over all vectors are presented in Table 7. For these scenarios, all violations of the EPA Standard are due to discharges of  $^{99}\text{Tc}$  and  $^{14}\text{C}$ . The effect of retardation in the moderately welded units on the integrated discharge can be assessed by comparing the values for scenarios 3 and 4 to corresponding values for scenario 1. It can be seen that discharge is decreased for the first 40,000 years and increased in the period from 40,000 to 50,000 years relative to scenario 1. Comparison of the results for scenario 1B with those for scenario 1 shows that although discharge of the radionuclides is decreased significantly by matrix diffusion, violations of the EPA release limit still occur.

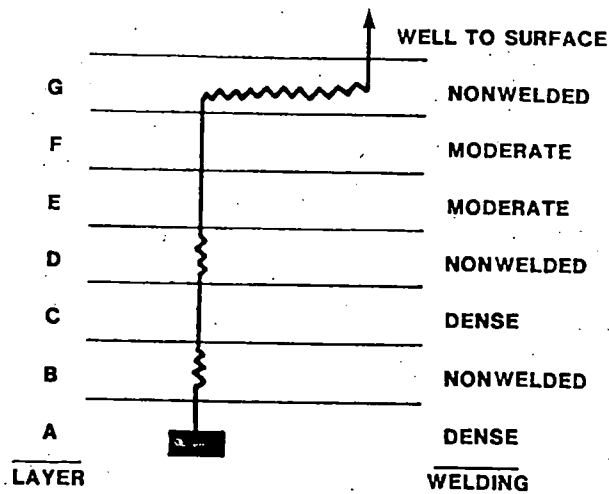
The characteristics of the three vectors whose radionuclide discharges violate the EPA Standard are shown in Table 8. When these values of hydraulic gradient and Darcy velocity are compared to the ranges of hydrogeologic parameters sampled by the LHS for input, it can be seen that the high radionuclide discharges are due primarily to large ground-water fluxes. These annual ground-water discharges range from 2 percent to 7 percent of the present day recharge of the Pahute Mesa ground-water system at the Nevada Test Site (21, 22). In Appendix A it is shown that this fraction is unrealistically high for Yucca Mountain. Therefore, we can conclude that violations of the EPA Standard for a ground-water flow path similar to scenario 1B is very unlikely.

SCENARIO 1

1 mile well; moderate = fractured; thermal buoyancy; no pluvial

LEG	LAYERS	WELDING - RETARDATION	LENGTH (ft)
1	A	dense - no retardation	200
2	B	nonwelded - porous - zeolites	300
3	C	dense - no retardation	250
4	D	nonwelded - porous - zeolites	150
5	E	moderate - no retardation	180
6	F	moderate - no retardation	270
7	G	nonwelded - porous - zeolites	5280

FLOW PATH



- KEY
-  DEPOSITORY
  -  LAYERS WITH NO RETARDATION
  -  LAYERS WITH RETARDATION

Figure 4

SCENARIO 3

1 mile well; moderate = porous zeolite; thermal buoyancy;  
no pluvial

LEG	LAYERS	WELDING - RETARDATION	LENGTH (ft)
1	A	dense - no retardation	200
2	B	nonwelded - porous - zeolites	300
3	C	dense - no retardation	250
4	D	nonwelded - porous - zeolites	150
5	E	moderate - porous - zeolites	180
6	F	moderate - porous - zeolites	270
7	G	nonwelded - porous - zeolites	5280

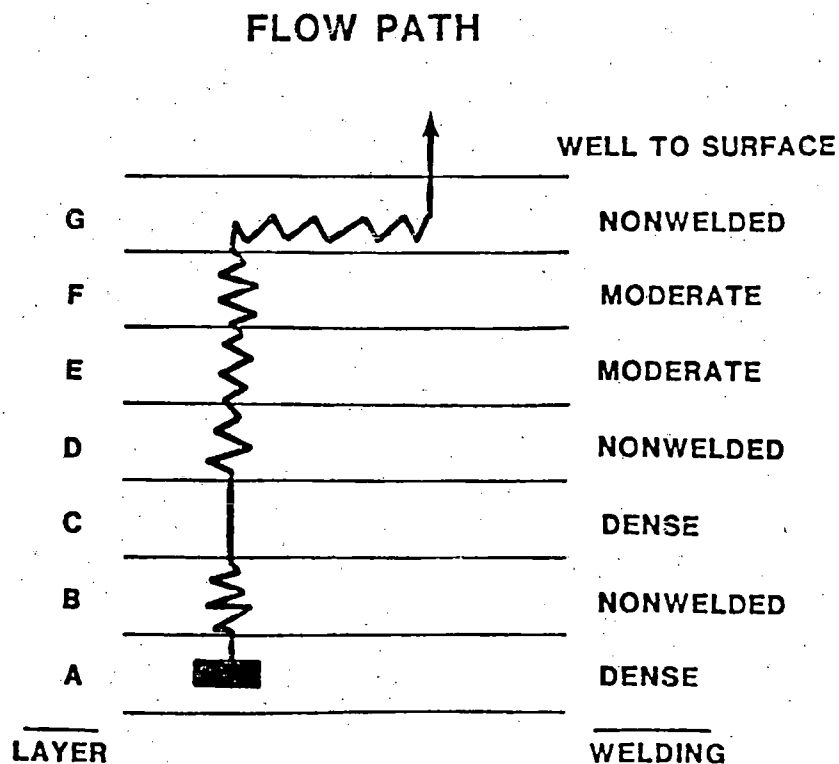


Figure 5

SCENARIO 4

1 mile well; moderate = porous, vitric or devitrified tuff,  
thermal buoyancy

LEG	LAYERS	WELDING - RETARDATION	LENGTH (ft)
1	A	dense - no retardation	200
2	B	nonwelded - porous - zeolites	300
3	C	dense - no retardation	250
4	D	nonwelded - porous - zeolites	150
5	E	moderate - porous - vitric	180
6	F	moderate - porous - devitrified	270
7	G	nonwelded - porous - zeolites	5280

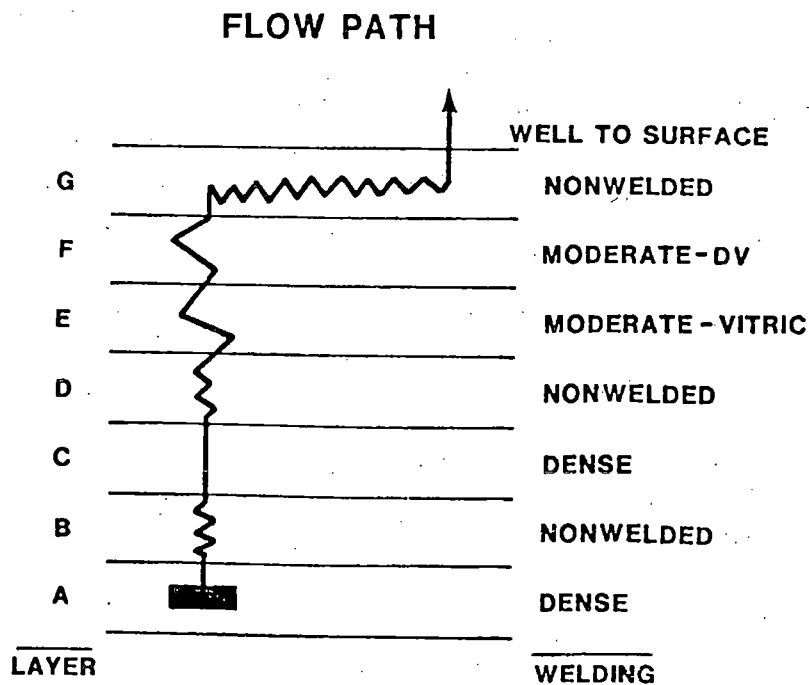


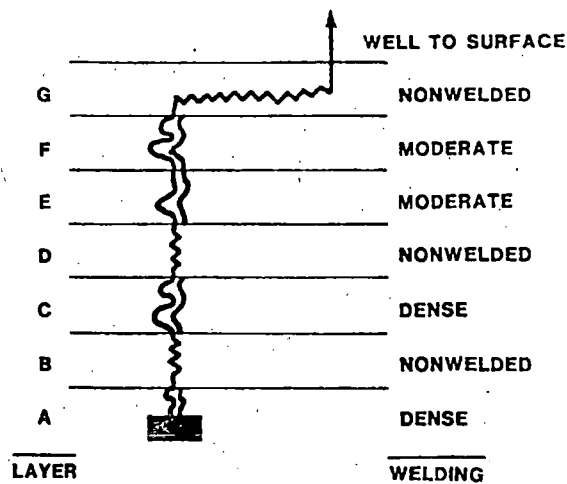
Figure 6

SCENARIO 1B

1 mile well; matrix diffusion, thermal buoyancy; no pluvial

LEG	LAYERS	WELDING - RETARDATION	LENGTH (ft)
1	A	dense - matrix diffusion	200
2	B	nonwelded - porous - zeolites	300
3	C	dense - matrix diffusion	250
4	D	nonwelded - porous - zeolites	150
5	E	moderate - matrix diffusion	180
6	F	moderate - matrix diffusion	270
7	G	nonwelded - porous - zeolites	5280

FLOW PATH



KEY

- DEPOSITORY
- LAYERS WITH MATRIX DIFFUSION
- LAYERS WITH RETARDATION (POROUS MEDIA)

Figure 7

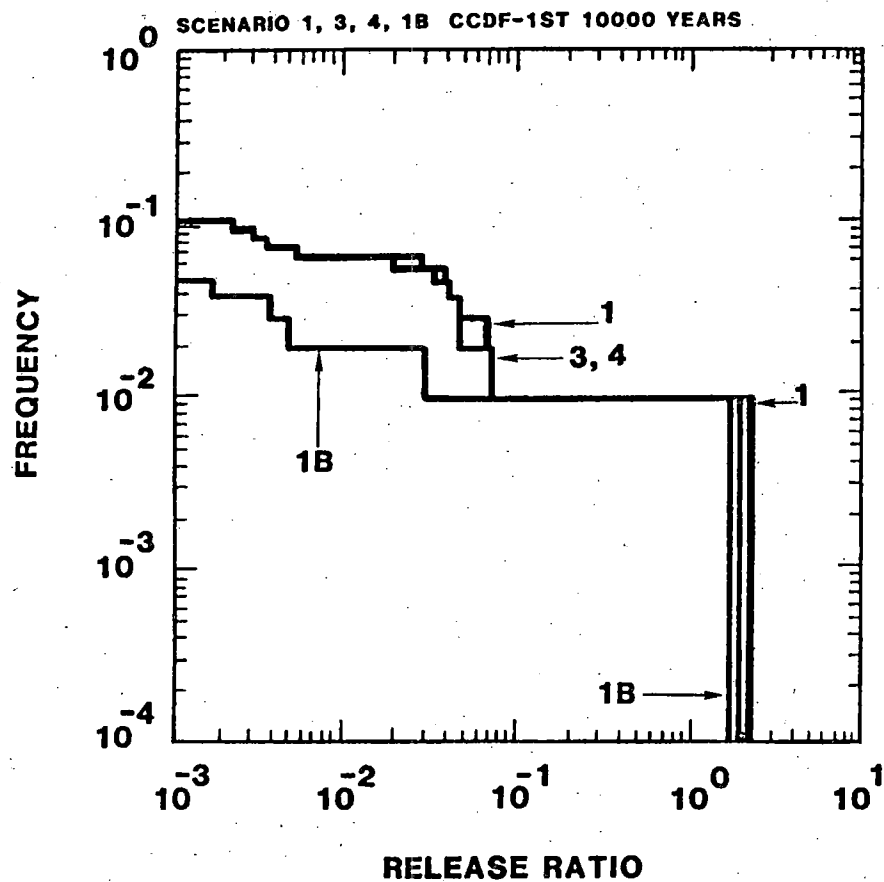


Figure 8.a

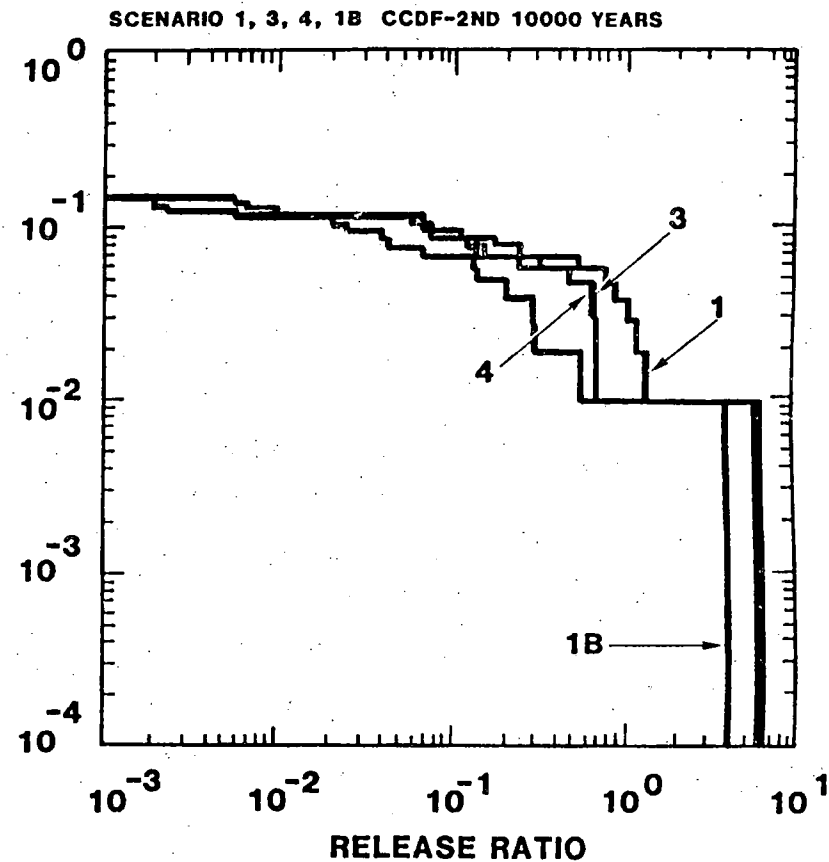


Figure 8.b

Figure 8. Complementary Cumulative Distribution Functions for Scenarios 1, 1B, 3, and 4: Alternate Representations of Retardation in Welded Tuff Units.

1 = base case; 1B = base case with matrix diffusion; 3 = zeolites;  
4 = vitric or devitrified

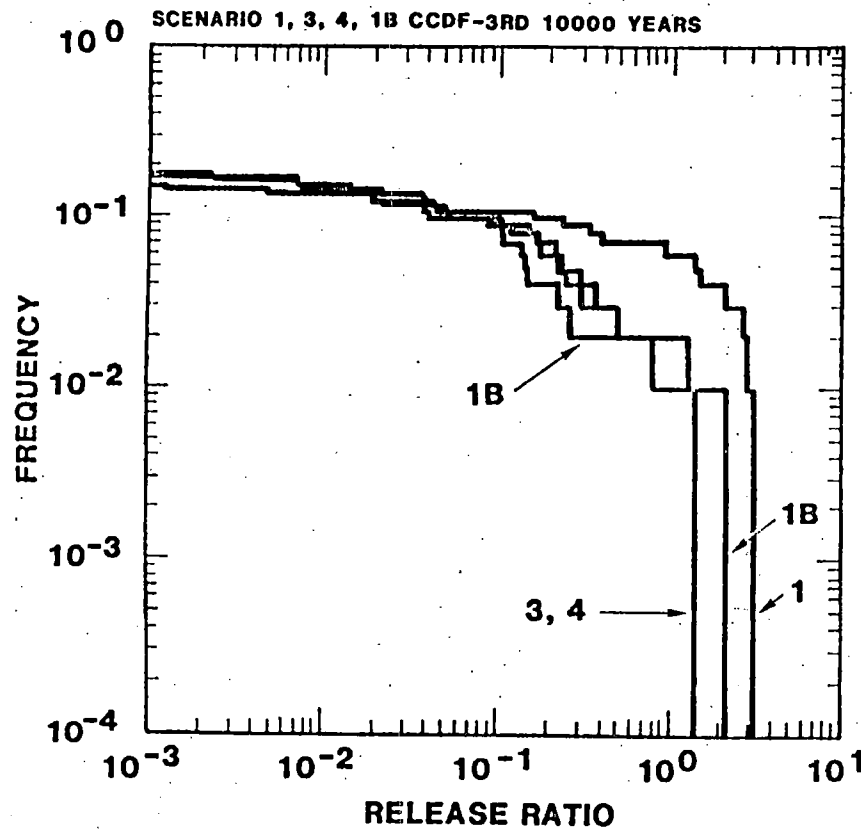


Figure 8.c

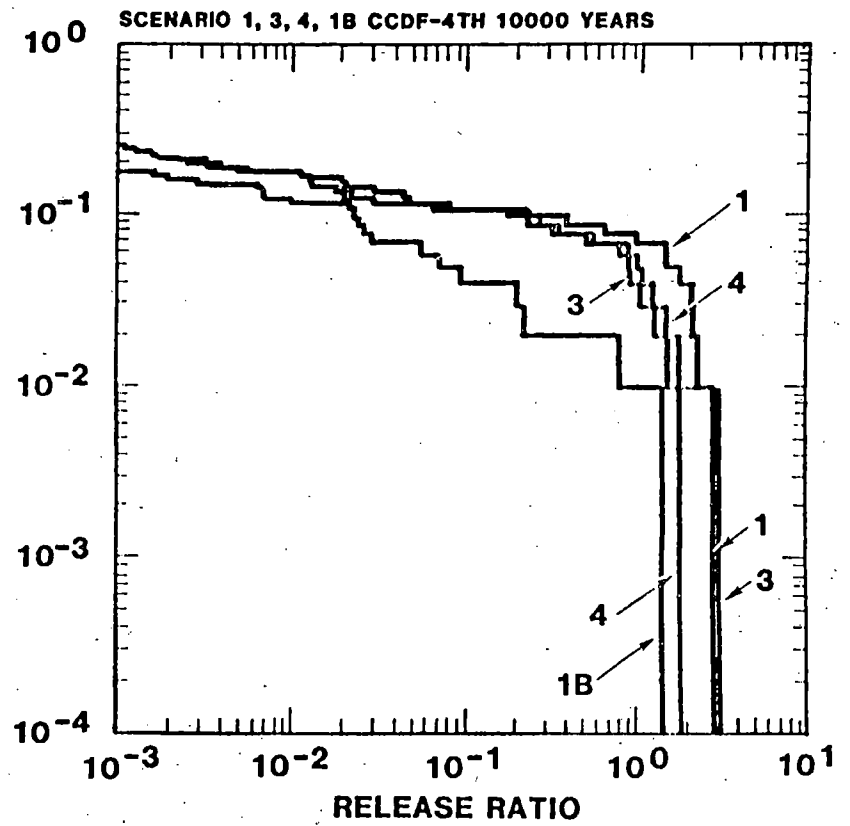


Figure 8.d

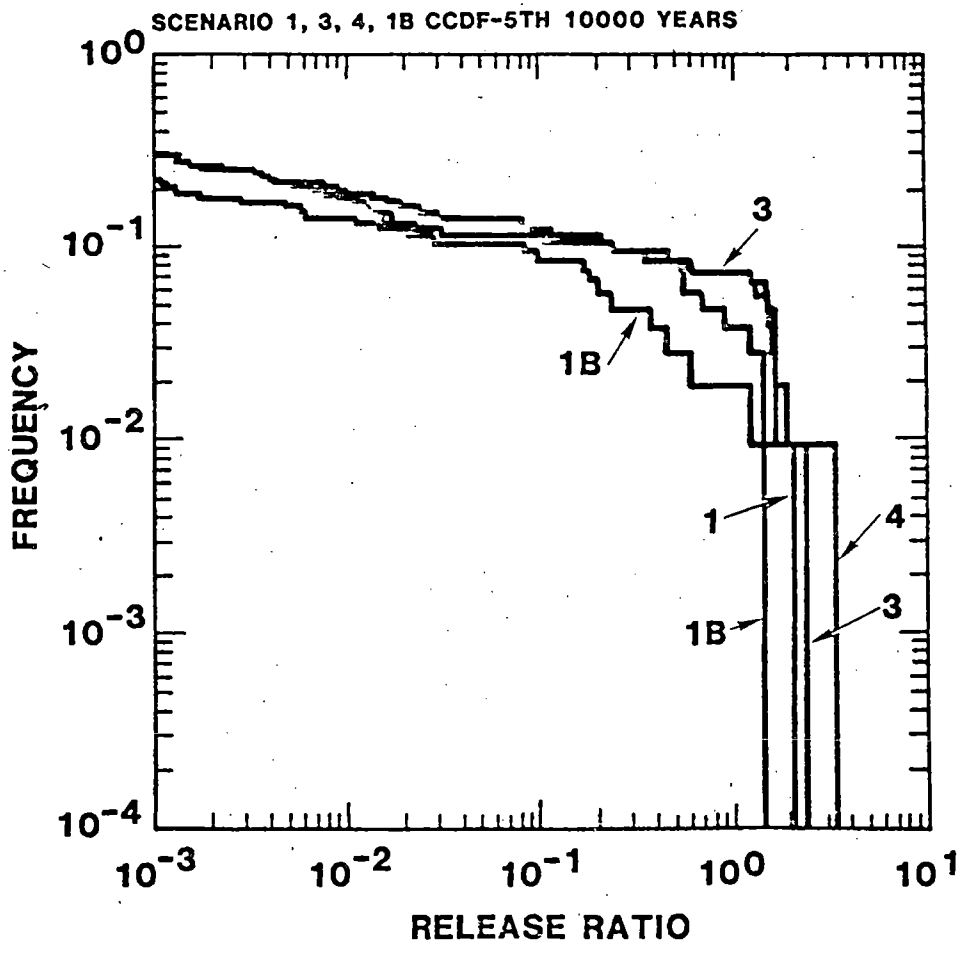


Figure 8.e

Table 7

NUMBER OF VIOLATING VECTORS, MAXIMUM OF RELEASE RATIOS AND SUM OF RELEASE RATIOS  
OVER ALL VECTORS FOR EACH 10,000 YEAR PERIOD

---

<u>Scenario</u>	<u>0-10,000yr</u>	<u>10,000-20,000yr</u>	<u>20,000-30,000yr</u>	<u>30,000-40,000yr</u>	<u>40,000-50,000yr</u>
1	1*	4	7	8	4
	2.4**	5.9	3.1	2.9	2.0
	2.5***	12.1	16.5	17.0	10.7
3	1	1	1	4	8
	1.9	6.2	1.4	3.1	2.3
	2.2	10.2	4.8	12.0	14.4
4	1	1	1	6	8
	1.9	6.1	1.4	1.5	3.4
	2.1	10.1	4.6	10.6	15.6
1B	1	1	2	1	2
	1.7	3.9	2.2	1.5	1.5
	1.8	5.7	5.0	3.1	5.2

---

\* number of violating vectors out of 106 vectors analyzed

\*\* maximum release ratio

\*\*\* sum of release ratios for all 106 vectors

Table 8  
 PROPERTIES OF VECTORS WHICH VIOLATE EPA STANDARD  
 IN SCENARIO 1B

VECTOR	3	24	51
<b>PARAMETER</b>			
Maximum R* for Tc	10827	7570	14364
Average vertical Darcy velocity (ft/yr)	0.32	0.13	0.41
Vertical hydraulic gradient	0.04	0.03	0.03
Average horizontal Darcy velocity (ft/yr)	0.17	0.88	0.36
Horizontal hydraulic gradient	0.02	0.08	0.02
Total ground-water travel time (yr)	10197	3781	6069
Discharge** (ft <sup>3</sup> /yr)	2.7x10 <sup>7</sup>	1.1x10 <sup>7</sup>	3.6x10 <sup>7</sup>
Maximum release ratio***	1.2	3.9	1.5

\*R = retardation factor

\*\*annual recharge of regional ground-water system is approximately 5x10<sup>8</sup> ft<sup>3</sup>/yr

\*\*\*maximum during 50,000 year period

### 6.3 Scenario 5: Effects of changes in the water table

In scenario 5, the water table has risen 300 feet during a pluvial period and is located in the densely welded tuff of layer H. Radionuclides migrate from the repository to this layer under the influence of the vertical hydraulic gradient (Figure 9). The zeolitized tuff of layer G is not a barrier to horizontal radionuclide migration in this scenario. In this calculation we have assumed that no retardation occurs in layer H. Ground water and dissolved radionuclides are pumped from the aquifer from a well located one mile from the repository. In all other respects, this scenario is equivalent to scenario 1.

Scenario 5B (Figure 10) differs from scenario 5 by the inclusion of matrix diffusion in calculations of radionuclide retardation in the moderately and densely welded layers A, C, E, F, and H. As in scenario 1B, retardation by matrix diffusion was considered only for  $^{129}\text{I}$ ,  $^{99}\text{Tc}$ , and  $^{14}\text{C}$ .

#### Results

The results of the calculations for scenario 5 are presented in Figures 11A-11E and in Table 9. It can be seen that the lack of retardation in the horizontal transport leg has resulted in discharges that are much larger than those calculated for scenario 1. Violation of the EPA Release limit results from discharges of  $^{236}\text{U}$ ,  $^{233}\text{U}$ ,  $^{238}\text{U}$ ,  $^{234}\text{U}$ ,  $^{237}\text{Np}$ ,  $^{99}\text{Tc}$ , and  $^{14}\text{C}$ . In the first 10,000 year period, violations are due primarily to releases of  $^{99}\text{Tc}$  and  $^{14}\text{C}$ . After 30,000 years, releases of other radionuclides comprise the major part of the discharge.

Results from scenario 5B are summarized in Figures 11A-11E and in Table 9. Matrix diffusion decreases the discharges of  $^{99}\text{Tc}$  and  $^{14}\text{C}$  to levels below the EPA release limit during the first 10,000 years. After 20,000 years, the release of  $^{236}\text{U}$ ,  $^{237}\text{Np}$ ,  $^{233}\text{U}$ ,  $^{238}\text{U}$ , and  $^{234}\text{U}$  may exceed the EPA Standard.

The properties of the vectors which violate the EPA Standard in scenario 5B are described in Table 10. The large radionuclide releases associated with vectors 3, 24, and 51 are due to their large ground-water discharge rates and short travel times. In vectors 72 and 85, the high horizontal Darcy velocity is indicative of the short travel time associated with the horizontal legs (0.03-0.6 yr). Although the retardation factors

SCENARIO 5

1 mile well; moderate = fractured; thermal buoyancy; pluvial

LEG	LAYERS	WELDING - RETARDATION	LENGTH (ft)
1	A	dense - no retardation	200
2	B	nonwelded - porous - zeolites	300
3	C	dense - no retardation	250
4	D	nonwelded - porous - zeolites	150
5	E	moderate - no retardation	180
6	F	moderate - no retardation	270
7	G	nonwelded - porous - zeolites	475
8	H	dense - no retardation	5280

FLOW PATH

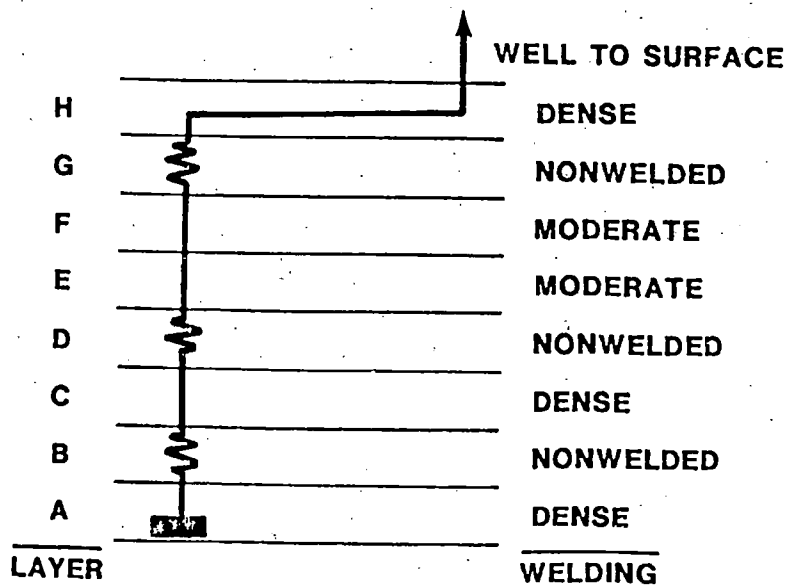


Figure 9

SCENARIO 5B

1 mile well; matrix diffusion, thermal buoyancy; pluvial

LEG	LAYERS	WELDING - RETARDATION	LENGTH (ft)
1	A	dense - matrix diffusion	200
2	B	nonwelded - porous - zeolites	300
3	C	dense - matrix diffusion	250
4	D	nonwelded - porous - zeolites	150
5	E	moderate - matrix diffusion	180
6	F	moderate - matrix diffusion	270
7	G	nonwelded - porous - zeolites	475
8	H	dense - matrix diffusion	5280

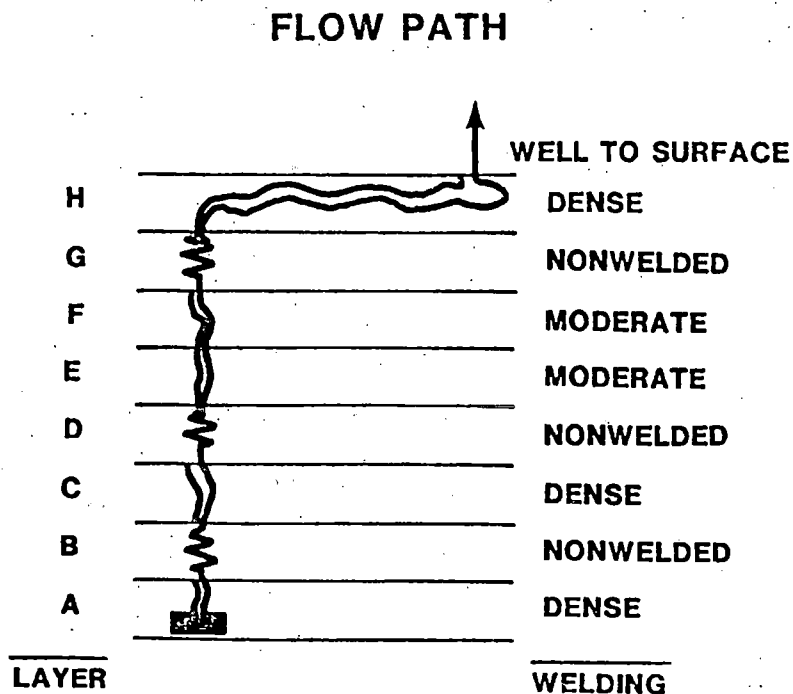


Figure 10

Table 9

NUMBER OF VIOLATING VECTORS, MAXIMUM OF RELEASE RATIOS AND SUM OF RELEASE RATIOS  
OVER ALL VECTORS FOR EACH 10,000 YEAR PERIOD

<u>Scenario</u>	<u>0-10,000yr</u>	<u>10,000-20,000yr</u>	<u>20,000-30,000yr</u>	<u>30,000-40,000yr</u>	<u>40,000-50,000yr</u>
5	3* 7.9** 13.4***	6 6.2 29.6	11 20.9 54.2	14 43.7 102.1	16 54.0 178.8
5B	0 0.90 1.1	1 2.1 5.9	3 19.3 28.8	4 42.1 75.9	4 53.4 153.0
6	0 0.1 0.1	1 1.5 2.5	1 1.6 3.7	4 4.4 12.5	3 2.2 7.6
2	11 207 667	14 85 392	19 87 461	20 57 424	19 55 434
2B	8 22 62	10 24 114	16 21 116	17 20 123	19 21 130

\* number of violating vectors out of 106 vectors analyzed  
 \*\* maximum release ratio  
 \*\*\* sum of release ratios for all 106 vectors

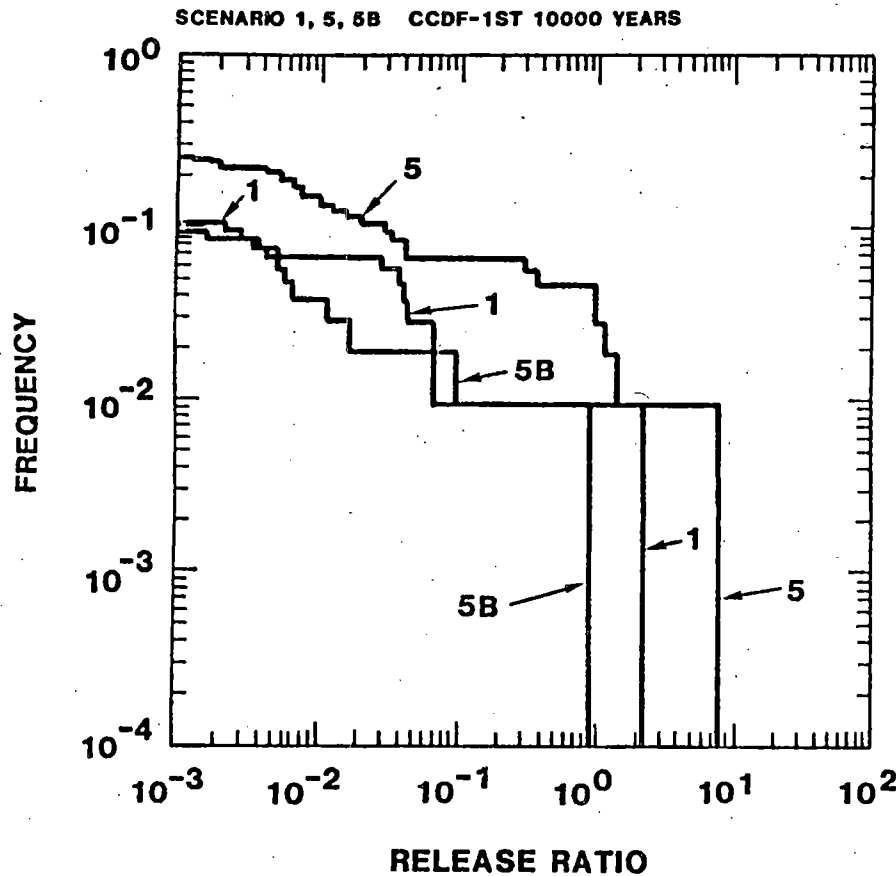


Figure 11.a

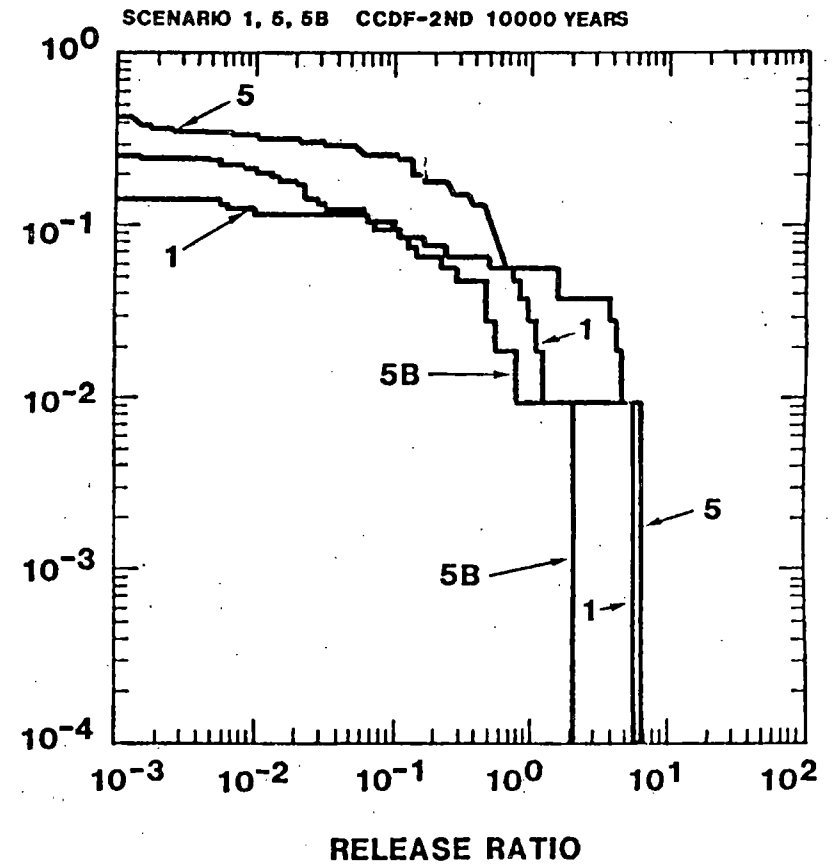


Figure 11.b

Figure 11. Complementary Cumulative Distribution Functions for Scenarios 1, 5 and 5B: Effects of Changes in the Water Table on Discharge.

1 = base case; 5 = water table rise; 5B = water table rise with matrix diffusion.

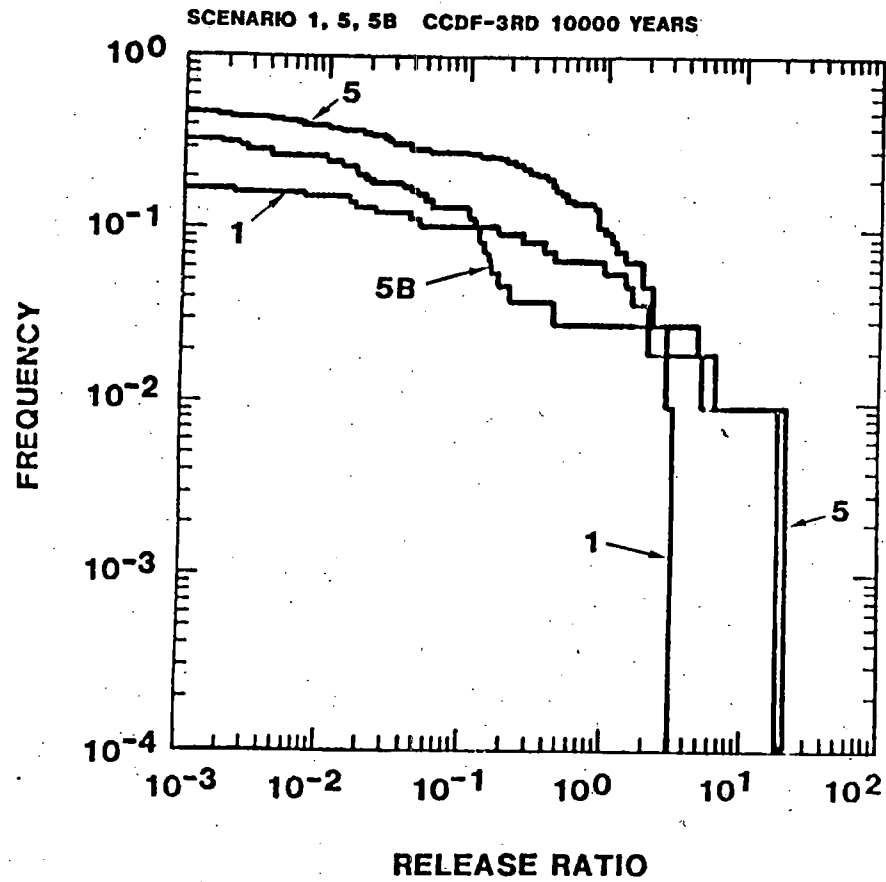


Figure 11.c

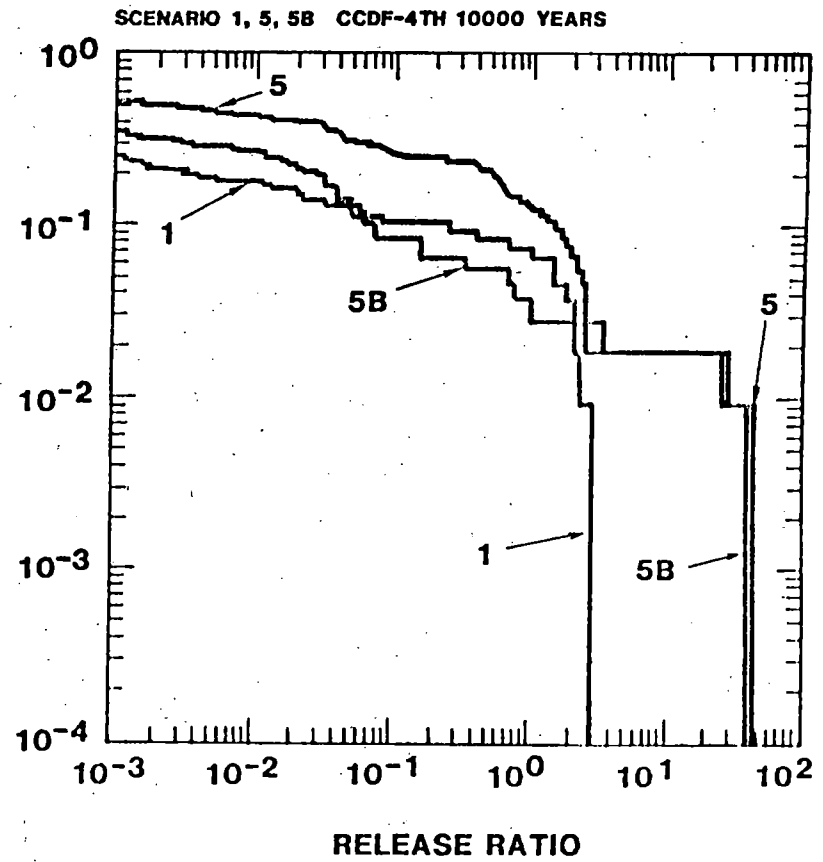


Figure 11.d

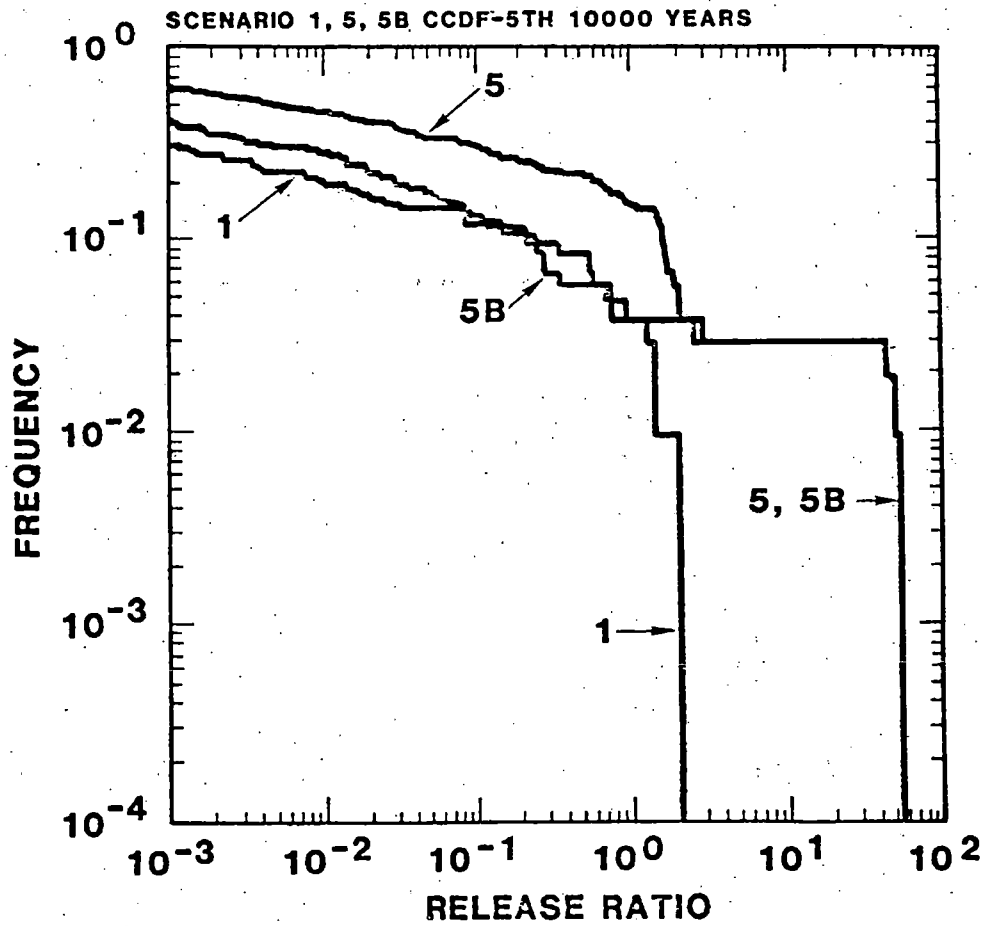


Figure 11.e

Table 10

PROPERTIES OF VECTORS WHICH VIOLATE EPA STANDARD  
IN SCENARIO 5B

VECTOR	3	24	51	72	85
<b>PARAMETER</b>					
Maximum R for U	32	27	23	47	35
Maximum R for Np	41	37	39	52	68
Maximum R for Tc	10827	20063	26659	13866	14888
Average vertical Darcy velocity (ft/yr)	0.3	0.16	0.43	0.04	0.07
Vertical gradient	0.04	0.03	0.03	0.03	0.04
Average horizontal Darcy velocity (ft/yr)	0.03	0.002	$2 \times 10^{-4}$	1.5	169
Horizontal gradient	0.02	0.08	0.02	0.02	0.03
Total ground-water travel time (yr)	1024	2585	2203	7877	4939
Discharge (ft <sup>3</sup> /yr)	$2.7 \times 10^7$	$1.4 \times 10^7$	$3.8 \times 10^7$	$3.5 \times 10^6$	$6.1 \times 10^7$
<b>Maximum release ratios</b>					
U234	16	26	19	0	0
Np237	8.7	$7 \times 10^{-5}$	12	0	0
Tc99	0	0	0	2.6	3.5
TOTAL	44.4	48.7	53.4	2.6	3.5

for Tc in leg 8 are high for these vectors (5076 and 2569 respectively), the high Darcy velocity indicates that this leg is not a barrier to migration of this radionuclide.

#### 6.4 Scenario 6: Accessible environment at eight miles

At the hypothetical repository site, the water table passes from the nonwelded zeolitized aquitard (layer G) into the overlying densely welded aquifer (layer H) at a distance of approximately two miles from the depository. In scenario 6, we have postulated that a well eight miles from the repository withdraws ground water and radionuclides from this aquifer. This scenario differs from scenario 1 by the additional one mile transport in the nonwelded unit and by six miles of transport in the densely welded tuff layer. No retardation occurs in the densely welded layer.

#### Results

The results of the calculation are presented in Figures 13A-13E and in Table 9. It can be seen that the additional seven miles of travel through layers G and H reduce the discharge during the first 10,000 years to levels below the EPA release limit. Discharges of the unretarded radionuclides  $^{99}\text{Tc}$  and  $^{14}\text{C}$  in vectors 12, 76, 77, and 105, however, exceed the EPA limit after 10,000 years. Due to time constraints, the effect of matrix diffusion on discharge was not calculated for the flow path of scenario 6. It was shown previously in scenario 1B that matrix diffusion in 900 feet of welded tuff decreased the discharge of  $^{99}\text{Tc}$  and  $^{14}\text{C}$  for the above vectors below the EPA Standard. It can be assumed, therefore, that matrix diffusion would eliminate all violations of the EPA Standard for a flow path similar to scenario 6.

SCENARIO 6

8 mile well; moderate = fractured; thermal buoyancy; no pluvial

LEG	LAYERS	WELDING - RETARDATION	LENGTH (ft)
1	A	dense - no retardation	200
2	B	nonwelded - porous - zeolites	300
3	C	dense - no retardation	250
4	D	nonwelded - porous - zeolites	150
5	E	moderate - no retardation	180
6	F	moderate - no retardation	270
7	G	nonwelded - porous - zeolites	11000
8	H	dense - no retardation	31000

FLOW PATH

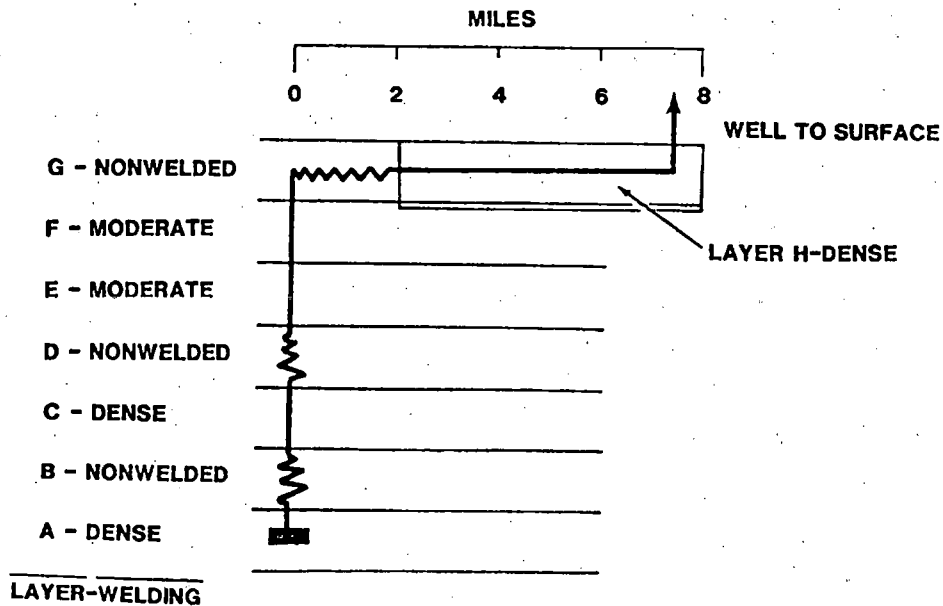


Figure 12

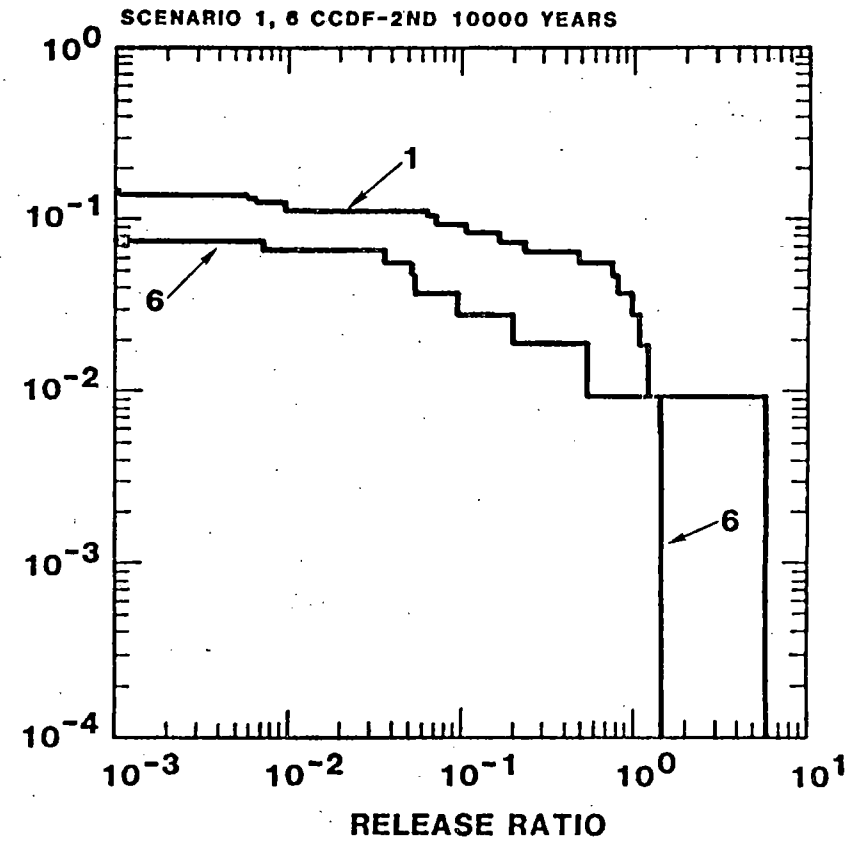
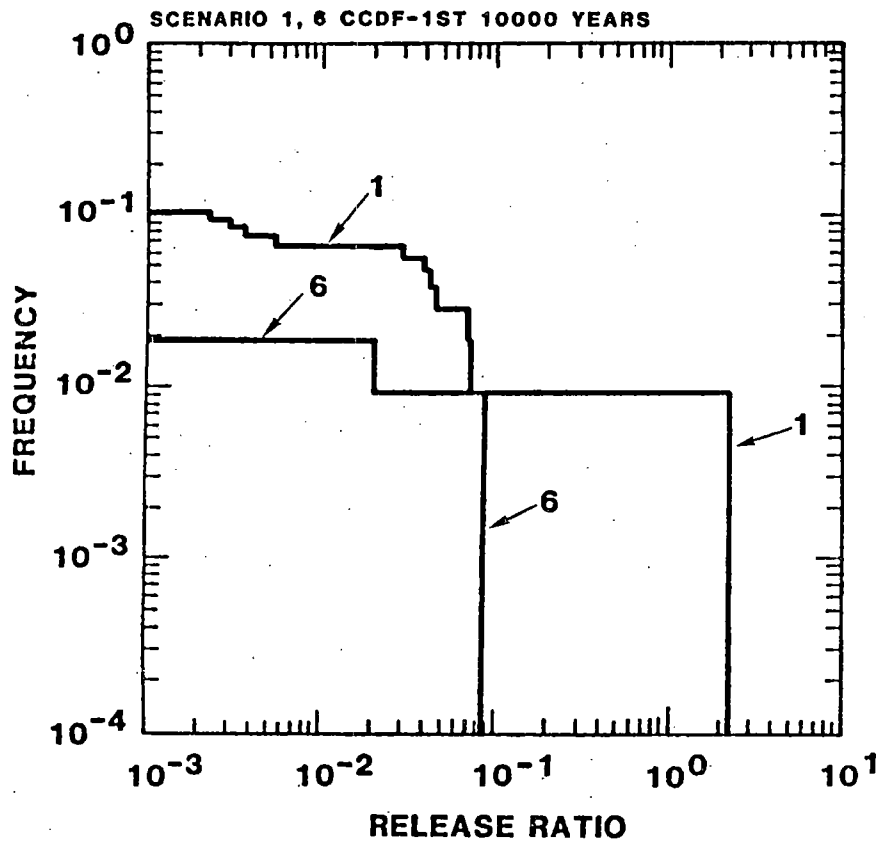


Figure 13.a

Figure 13.b

Figure 13. Complementary Cumulative Distribution Functions for Scenarios 1 and 6: Accessible environment at eight miles.

1 = base case; 6 = 8 miles

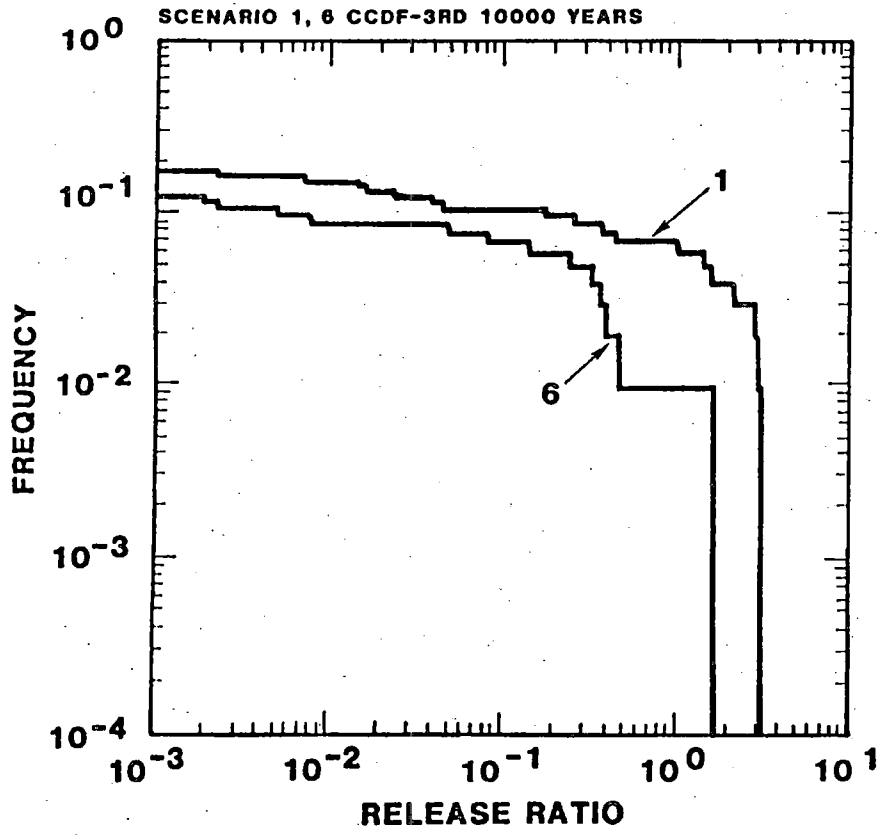


Figure 13.c

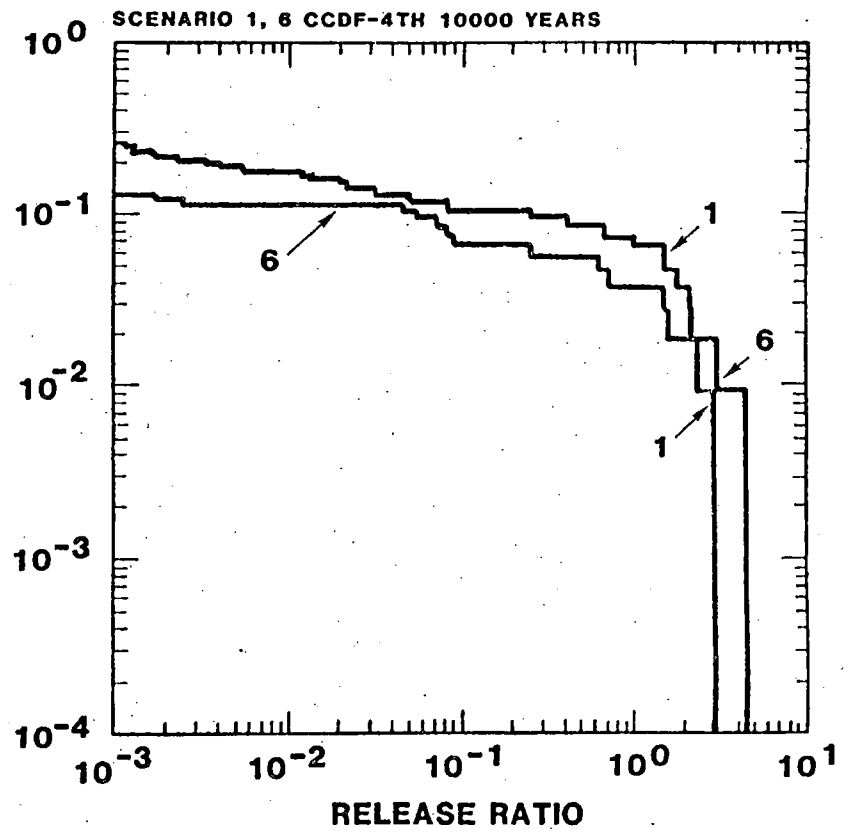


Figure 13.d

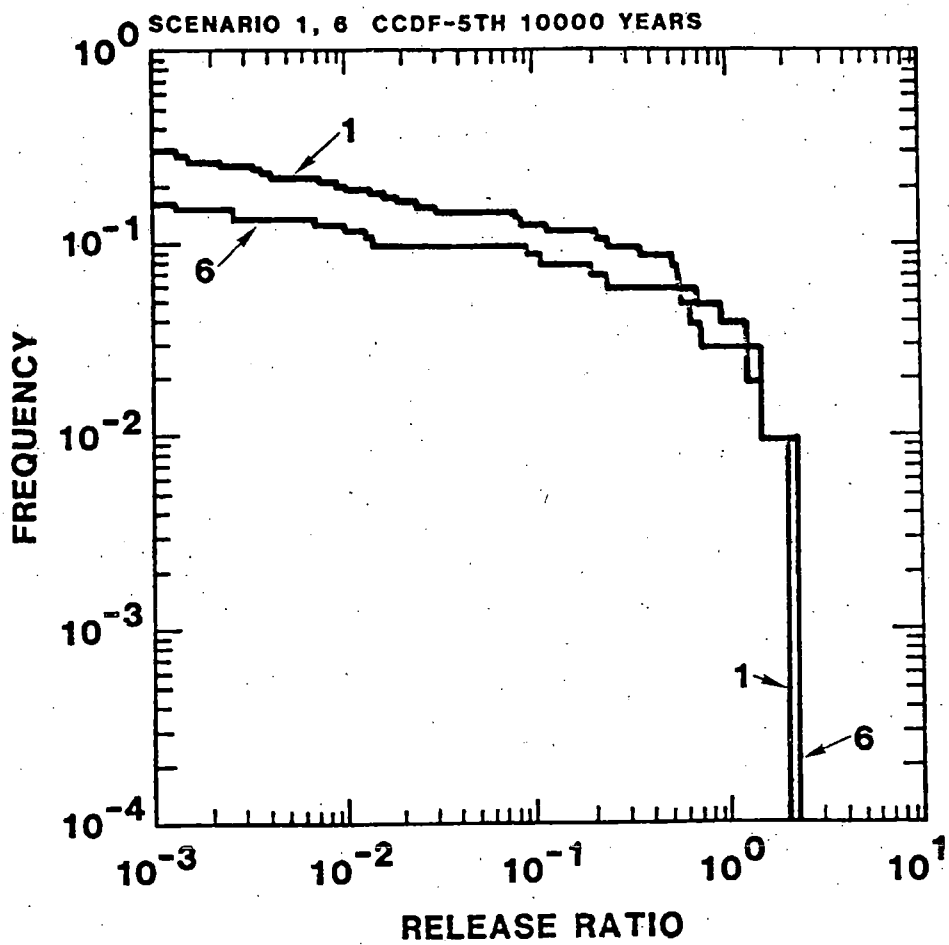


Figure 13.e

## 6.5 Scenarios 2 and 2B: Importance of solubility limits to discharge

We consider scenario 2 (Figure 14) our "worst case" scenario. The source term is entirely leach-limited; the solubility limits of radionuclides are not specified. Ground water migrates laterally from the depository. Due to the block faulting and dip of the tuff units in the repository site, the lateral fluid flow path cuts across several stratigraphic layers. At a distance of one mile from the repository, water and radionuclides are pumped by a well that extends to a depth of 3,000 feet. Technetium,  $^{129}\text{I}$  and  $^{14}\text{C}$  are retarded by matrix diffusion in the densely welded layers A and C. Layer B is highly sorbent zeolitic tuff which retards the movement of the other isotopes. This scenario has a shorter path length and thinner sequence of zeolitized tuff than the other scenarios.

Scenario 2B differs from scenario 2 only in the calculation of the source term. We have used the mixing-cell option of NWFT/DVM for this scenario (17,23). For each time step, the mass of a radionuclide that is assumed leached from the waste form is compared to the maximum amount that is consistent with a user-specified solubility limit. The solubility limits are listed in Table 5 and are discussed in detail in section 4.3 and in Appendix B. The smaller of these two amounts of radionuclide is transported in that time step.

### Results

Results of calculations for scenarios 2 and 2B are summarized in Figures 15A-15E and in Table 9. Discharges in scenario 2 are the highest calculated in this study and lead to large violations of the EPA Standard. During the first 10,000 years, releases of  $^{234}\text{U}$ ,  $^{237}\text{Np}$ ,  $^{238}\text{U}$  and  $^{236}\text{U}$  account for 94 percent of the sum of the EPA release ratios. During the fifth 10,000 year interval they continue to dominate discharge and account for 85 percent of the violation of the EPA Standard. The importance of solubility limits in controlling discharge in scenario 2B can be seen in the figures and table. The sum of the release ratios for all uranium species is reduced by an order of magnitude and Np discharge is decreased by a factor of 30 for the first 10,000 year interval. Discharges of these radionuclides, however, still are in excess of the EPA standard. The solubilities that were assumed for uranium and neptunium were based on experimental studies under oxic conditions. They are upper bounds for the solubilities; under reducing conditions the solubilities of U and Np are several orders of magnitude lower. We feel that the transport of

SCENARIOS 2 and 2B

1 mile borehole; matrix diffusion;  
no thermal buoyancy or pluvial

LEG	LAYERS	WELDING - RETARDATION	LENGTH (ft)
1	A	dense - matrix diffusion	2600
2	B	nonwelded - zeolitized	300
3	C	dense - matrix diffusion	2600

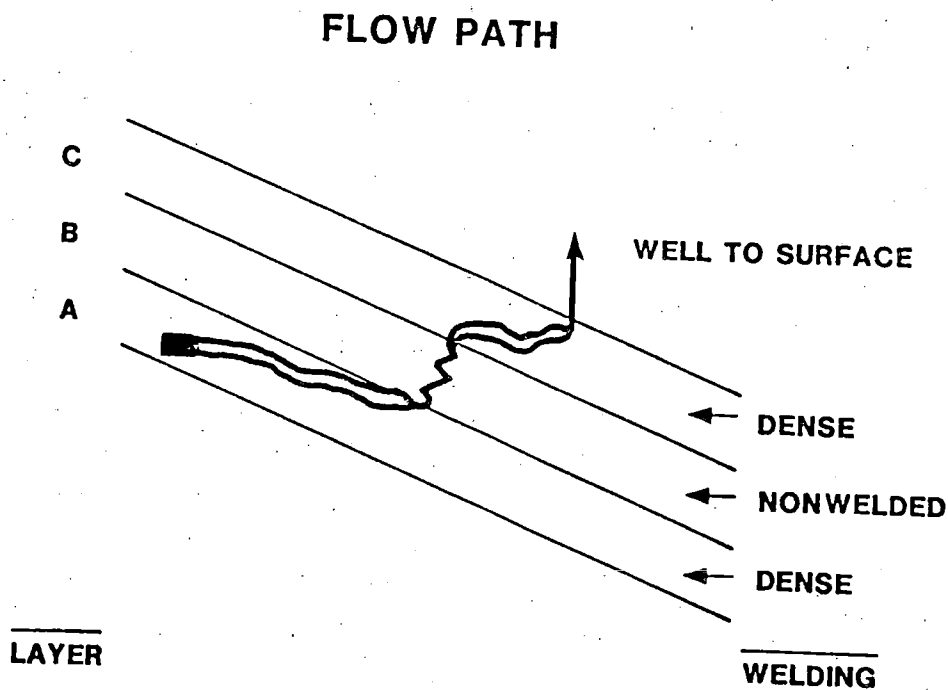


Figure 14

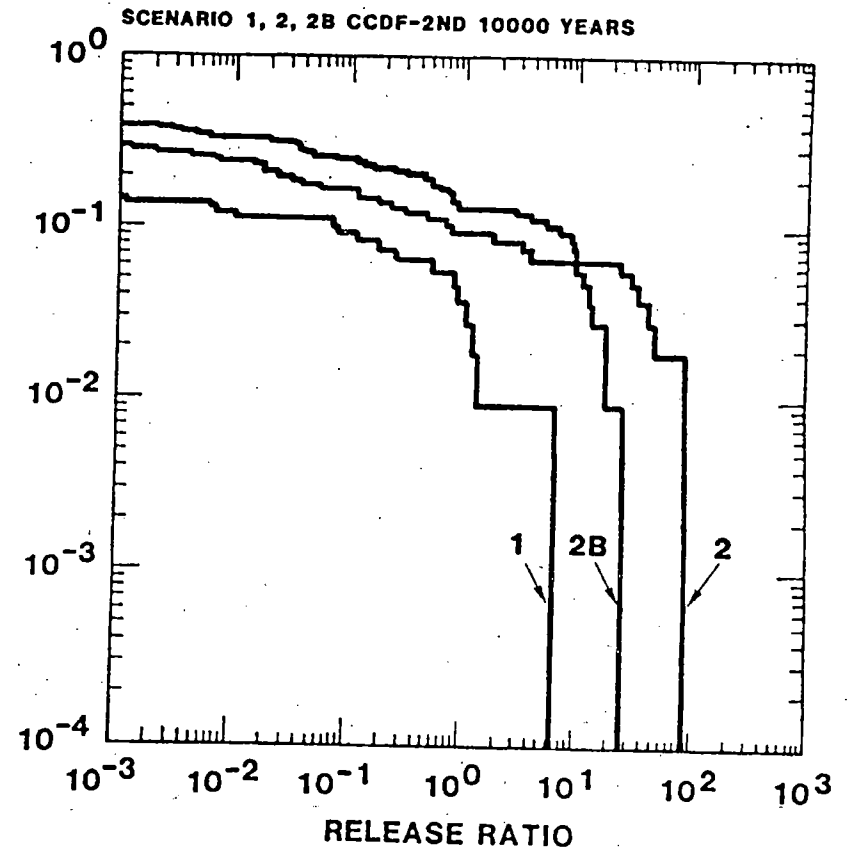
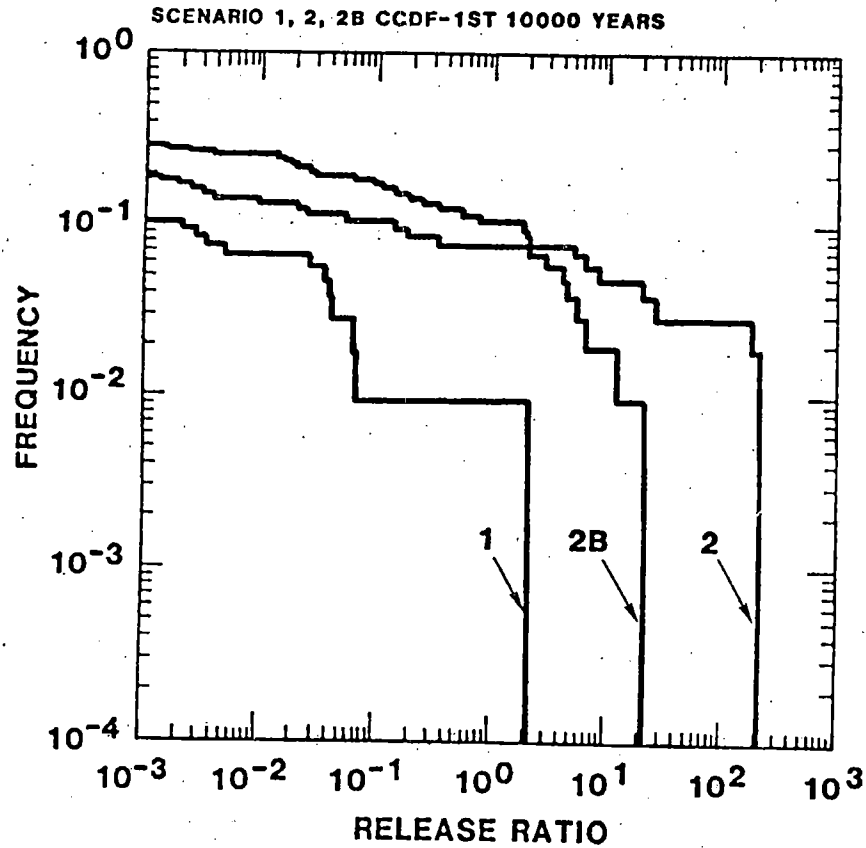


Figure 15.a

Figure 15.b

Figure 15. Cumulative Complementary Distribution Functions for Scenarios 1, 2 and 2B: Importance of Solubility Limits to Discharge.

1 = base case; 2 = leach-limited; 2B = solubility-limited

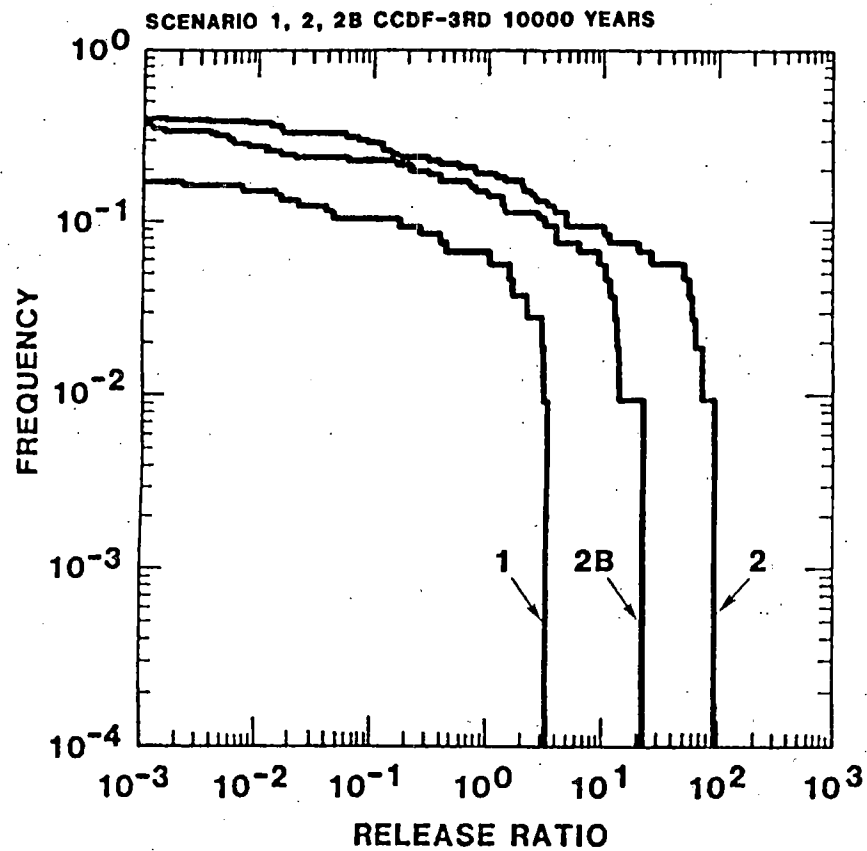


Figure 15.c

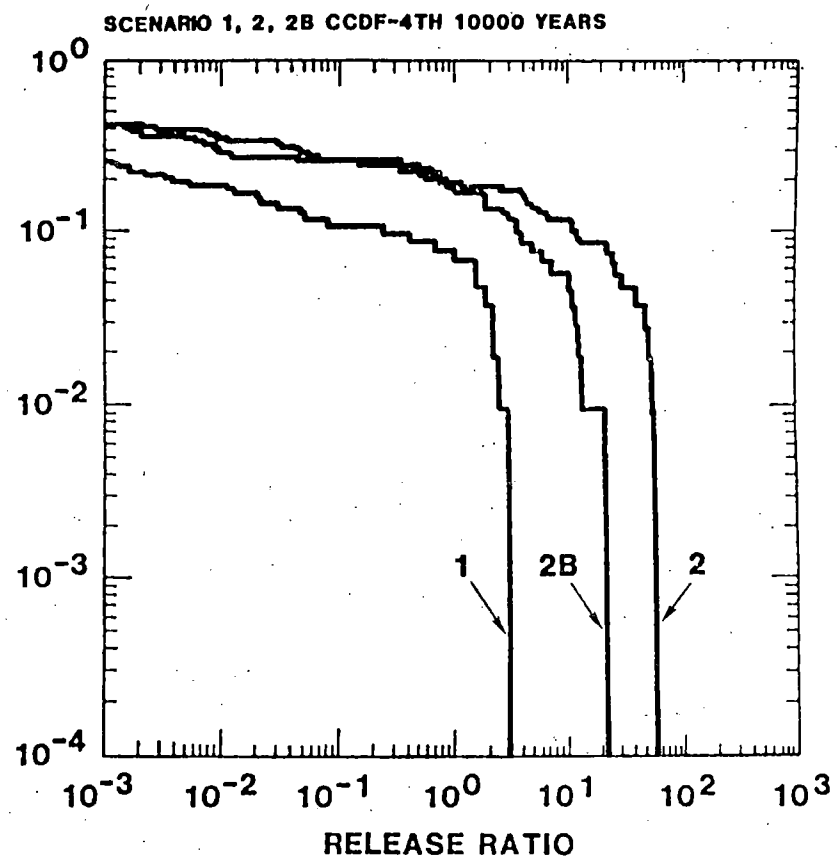


Figure 15.d

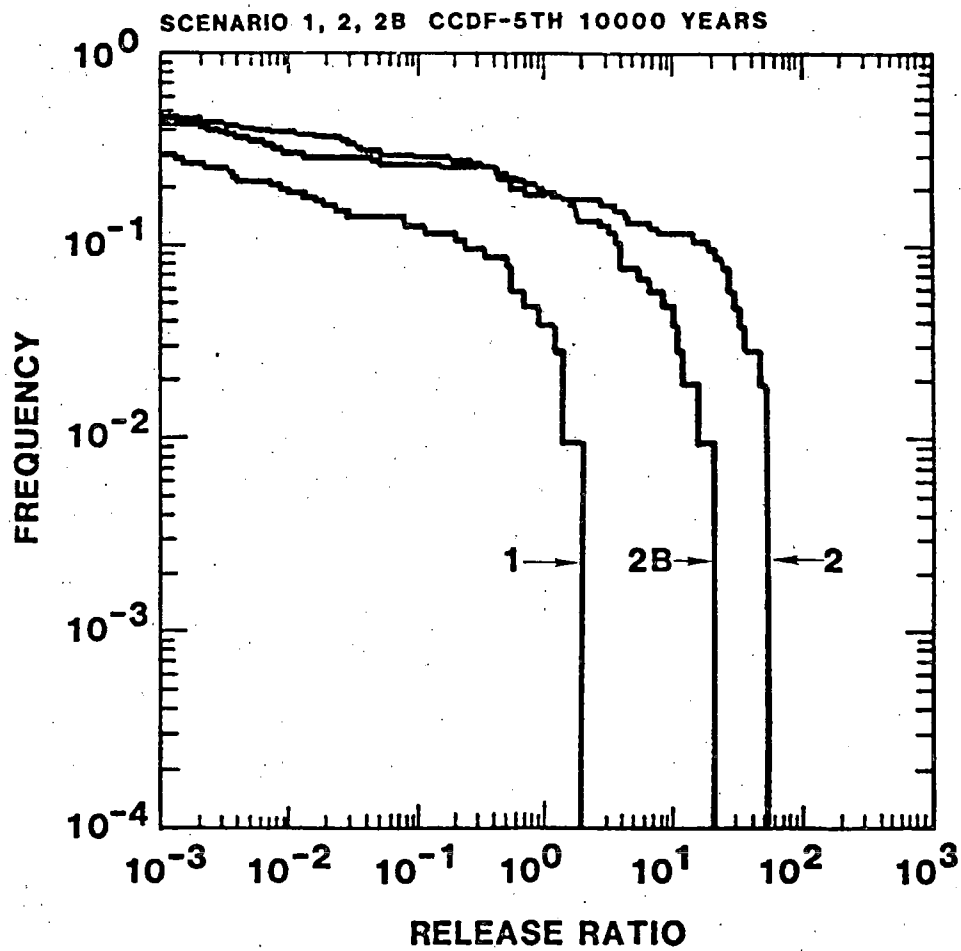


Figure 15.e

radionuclides along the flow path described in scenarios 2 and 2B is less likely than transport as described in the other scenarios. The calculated violations of the EPA Standard, therefore, should not be interpreted as an indication that releases from a repository in tuff are likely.

## 7. CONCLUSIONS AND RECOMMENDATIONS

Estimates of potential radionuclide releases from HLW storage facilities in geologic formations are an integral part of the technical basis for the regulation of nuclear waste disposal. At present, the available data is insufficient to accurately model any real repository sites. Large uncertainties exist in the characterization of the solubilities and sorption of radionuclides, in the description of the regional and local hydrogeology and in the mathematical treatment of contaminant transport in the presence of fracture flow and matrix diffusion. We feel, however, that it is possible to place realistic upper limits on radionuclide discharge for a generic hypothetical tuff repository. We have also attempted to assess the importance of the variation of several variables and model assumptions to the calculations of radionuclide release from a repository in the saturated zone of a volcanic tuff site.

Our calculations suggest the following conclusions for the hypothetical tuff repository described in this paper:

- 1) Sorption of radionuclides by several thousand feet of zeolitized tuff may limit the release of actinides below the EPA release limits even in the absence of solubility constraints.
- 2) All violations of the EPA Draft Standard in the "base case" are due to discharges of  $^{99}\text{Tc}$  and  $^{14}\text{C}$ . Retardation due to matrix diffusion, however, could eliminate discharge of these nuclides under realistic ground-water flow rates.
- 3) If the radionuclides do not flow through thick sequences of zeolitized tuff, discharges of U and Np under oxidizing conditions may be much larger than the EPA limits. Under reducing conditions, however, the low solubilities of these elements may reduce their discharges to levels below the EPA limit.
- 4) The radionuclide release limits set by Draft 19 of the EPA Standard are probably achievable for a repository site similar to the hypothetical site described in this report. The majority of the vectors examined in all scenarios produced radionuclide releases below the limits set by the draft standard. In general, violations of the standard occurred only when the most conservative assumptions were used or when combinations of input data produced ground-water flow rates that were unrealistically high.

We feel that the following topics merit further investigation by the NRC:

- 1) Detailed calculations of limiting solubilities of uranium, neptunium and radium under geochemical conditions expected at the tuff site.
- 2) Calculations of the potential retardation of actinides due to matrix diffusion in welded tuff.
- 3) Calculations of the sensitivity of radionuclide discharges to assumptions about radionuclide speciation.
- 4) A study of the frequency of oil and water drilling and mineral exploration in areas like Yucca Mountain. All of the scenarios examined in this involve human intrusion. A study of the probability of such activities in areas like Yucca Mountain would yield valuable insights about the safety of such a repository site.

## APPENDIX A

### HYDROGEOLOGICAL MODEL OF THE HYPOTHETICAL TUFF REPOSITORY SITE AND ITS RELATIONSHIP TO DATA FROM THE NEVADA TEST SITE

A major objective in the program of simplified repository analyses performed at Sandia is the definition of a hypothetical site which exhibits hydrogeological characteristics which might be found at real potential repository sites. We have defined our reference tuff site to be consistent with available hydrogeologic data from the Nevada Test Site. Where certain data are not available from the real site, we have postulated properties that are physically reasonable for the reference site. We have not attempted to accurately represent the Nevada Test Site in our analyses; instead we have modeled a hypothetical site which is internally self-consistent.

#### A.1 Physical properties of welded tuff

The tuff units at the reference tuff repository are described as densely welded, moderately welded or nonwelded. Densely welded tuff units are highly fractured; the blocks between fractures have low interstitial matrix porosity. Nonwelded tuff units have few fractures but have a high matrix porosity. This dual porosity of the rock must be considered when modeling fluid flow. We have used data from the UE25a-1 drill core log to obtain reasonable values of fracture density, aperture width and orientation in the tuff units (1,2). The maximum, minimum and median of the range of values of these parameters for different tuff lithologies are shown in Table A-1.

We have represented the fracture system as two sets of perpendicular vertical fractures. Values of horizontal fracture porosity ( $\epsilon_h$ ) are calculated by

$$\epsilon_h = N_a H / \sin (90^\circ - \theta)$$

where  $N_a$  is the observed fracture density in the core,  $\theta$  is an estimate of the average inclination of the fractures from the horizontal plane, and  $H$  is the fracture aperture width observed under a petrographic microscope. Horizontal hydraulic conductivity for a parallel array of planar fractures is given (24) by:

$$K_H = \left( \frac{\rho g}{\mu} \right) \cdot \left( \frac{N_a H^3}{12 \sin (90 - \theta)} \right)$$

where:

- $\rho$  = density of water = 1.0 gm/cm<sup>3</sup>  
 $g$  = 9.81x10<sup>2</sup> cm/sec<sup>2</sup>  
 $\mu$  = viscosity of water = 1.0 centipoise

In the assumed joint system, fluid flowing in the horizontal direction will effectively encounter only one set of fractures. Fluid flowing in the vertical direction will encounter both sets of fractures. For this reason, values of hydraulic conductivity and fracture porosity in the vertical direction are twice the horizontal values.

The hydraulic conductivity is very sensitive to changes in fracture aperture. In welded zones, the majority of fractures are 5-20 microns wide; the maximum observed width was 150 microns (1, 2). Fractures in nonwelded zones were generally filled with secondary minerals. For these units, aperture widths of 0-5 microns are probably realistic and were used to estimate the hydraulic properties in Table A-1. Results of calculations using a 150-micron aperture width are also shown in the table. Ranges of values presented for total porosity are taken from data in references 4 and 25.

In Figure A-1, the ranges of values of matrix hydraulic conductivity of unfractured cores of tuff measured in the laboratory are compared to the values calculated from fracture properties. The values are based on data compiled in references 4, 22, and 25. Values of the bulk hydraulic conductivity, as measured by actual pump tests at the Nevada Test Site, are also shown. Data obtained in these tests reflect contributions from fluid flow in both the fractures and the rock matrix between joints. It can be seen that flow in fractures may dominate the bulk hydraulic conductivity of densely welded tuffs, whereas fluid flow in the porous rock matrix dominates the properties of nonwelded units. Both fracture flow and porous flow are important for moderately welded tuffs. The insights gained from Figure A-1 were used to estimate reasonable ranges for effective porosity and hydraulic conductivity for the Latin Hypercube Sample Program (18). The data ranges and the shape of their distributions are tabulated in Table 2 of the main text. References for similar values in the literature are described in Table A-2. The shapes of the frequency distributions were estimated by comparing the median values to the upper and lower limits of the data ranges of the different types of hydraulic conductivity and porosity.

## A.2 Vertical Hydraulic Gradient

There are insufficient data in the open literature at present to estimate vertical hydraulic gradients at the Nevada Test

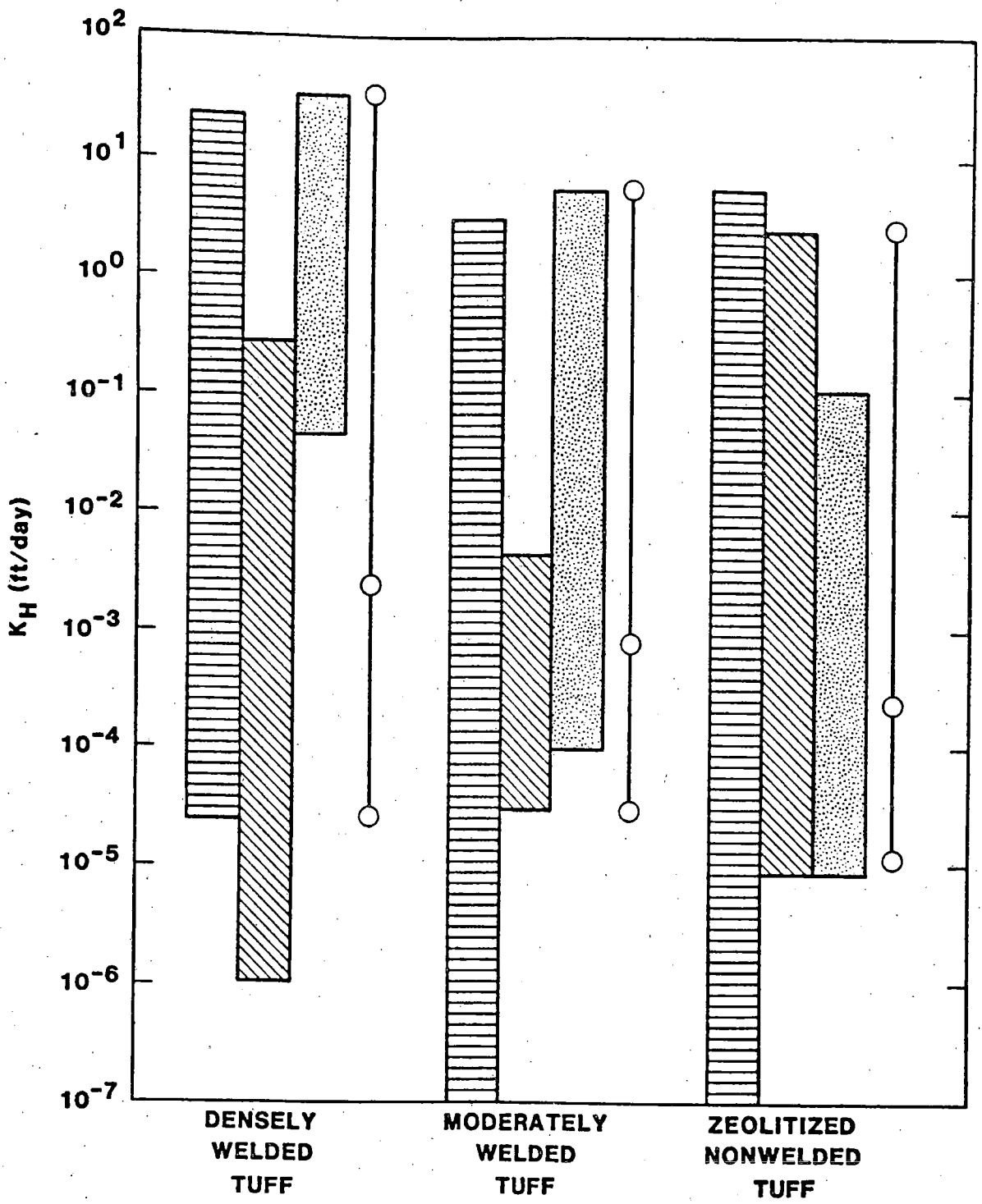
Table A-1

## PROPERTIES OF FRACTURED TUFF

	Densely Welded Tuff	Moderately Welded Tuff	Nonwelded Tuff
<b>*Fracture Aperture</b>			
H (microns)			
min	5	5	0
median	12	12	5
max	150	150	5 (150) <sup>+</sup>
<b>*Apparent Fracture</b>			
Density - $N_a$ ( $ft^{-1}$ )			
min	0.2	0	0
median	1.2	0.4	0.1
max	4.8	0.8	0.3
<b>*Inclination of Fractures</b>			
from Horizontal — $\theta$	42°	45°	80°
<b>Horizontal Fracture</b>			
Porosity - $\epsilon_h$ (%)			
min	$4.4 \times 10^{-4}$	0	0
median	$6.4 \times 10^{-3}$	$2.2 \times 10^{-3}$	$9.5 \times 10^{-4}$
max	0.32	0.06	$2.8 \times 10^{-3}$ (0.09) <sup>+</sup>
<b>Horizontal Fracture</b>			
Hydraulic Conductivity			
( $K_H$ ) - (ft/day)			
min	$2.6 \times 10^{-5}$	0	0
median	$2.1 \times 10^{-3}$	$7.5 \times 10^{-4}$	$5.5 \times 10^{-5}$
max	16.7	2.9	$1.7 \times 10^{-4}$ (4.5) <sup>+</sup>
Total Porosity (%)	3-10	10-38	20-50

\*References (1, 2)

+Values corresponding to aperture width of 150 microns.



RANGES OF VALUES OF HYDRAULIC CONDUCTIVITY DETERMINED BY DIFFERENT METHODS



Figure A-1

Table A-2

SOURCES OF DATA FOR RANGES\* OF  
HYDROGEOLOGIC PARAMETER VALUES

Parameter	Value	Similar Value From Literature	Reference	Comment
Hydraulic conductivity of densely welded tuff (ft/day)	$2 \times 10^{-5}$	--	--	Calculated from data in Table A-1 in this report. Table 3 (Tiva Canyon)
	30	19	22	
Hydraulic conductivity of moderately welded tuff (ft/day)	$3 \times 10^{-5}$	$3 \times 10^{-5}$	22	Table 3 (Topopah Springs) pp. 38 - 39
	5	$4.4 \times 10^{-5}$	10	
			2.9	--
		2.1	22	Table 3 (Topopah Springs)
Hydraulic conductivity of nonwelded tuff (ft/day)	$10^{-5}$	$1.7 \times 10^{-5}$	10	pp. 38 - 39 Table A-1
	2	2.3	25	
Effective porosity of densely welded tuff (%)	$4.4 \times 10^{-4}$	--	--	Calculated from data in Table A-1 in this report.
	0.32	--	--	Calculated from data in Table A-1 in this report.
Effective porosity of moderately welded tuff (%)	0.03	--	--	Maximum fracture porosity calculated from data in Table A-1 in this report for moderately welded tuff Table 3 (Tiva Canyon)
	25	25	22	

Table A-2 (Continued)

Effective porosity of nonwelded tuff (%)	20	19.8	4	Table 5, p. C45, minimum for zeolitized tuff
	48	48.3	4	Table 5, p. C45, maximum for zeolitized tuff
Total porosity of densely welded tuff (%)	3	5	4	p. C32
	10	10	4	p. C32
Total porosity of moderately welded tuff (%)	10	10	4	p. C32
	38	35	4	p. C32
Total porosity of nonwelded tuff (%)	20	35	4	p. C32
	50	50	4	p. C32

\*Ranges for Table 2. Values tabulated here are for hydraulic properties in the horizontal direction.

Site with an acceptable degree of certainty. In our reference site, we have assumed that the vertical gradient in the vicinity of the repository will be dominated by a thermal buoyancy gradient related to the heat generated by the decay of the radioactive waste. The calculation of the thermal buoyancy gradient is described below.

Consider a cylindrical volume of fluid with length  $L$  and average temperature  $\bar{T}$  immersed in a medium of average temperature  $\bar{T}_0$  ( $\bar{T} > \bar{T}_0$ ). (Figure A-2). The difference in temperature produces an upward force on the volume of fluid. The velocity of the fluid in the cylindrical volume can be described (26) by:

$$v \sim \alpha \Delta T K \quad (A-1)$$

with

$v$  = Darcy velocity of fluid

$\alpha$  = average coefficient of thermal expansion of fluid

$$\Delta T = \bar{T} - \bar{T}_0$$

$K$  = hydraulic conductivity of medium

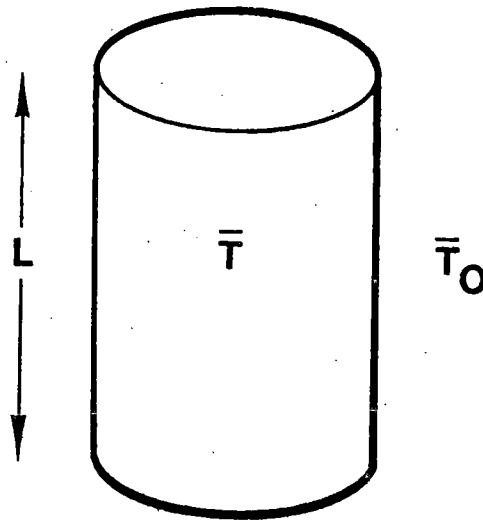


Figure (A-2)

Since Darcy velocity is equal to the product of hydraulic gradient ( $I$ ) and conductivity, the upward gradient is given by

$$I = \alpha \Delta T \quad (A-2)$$

The temperature field around a repository in tuff for spent fuel at 75 kW/Acre thermal loading has been calculated (3).

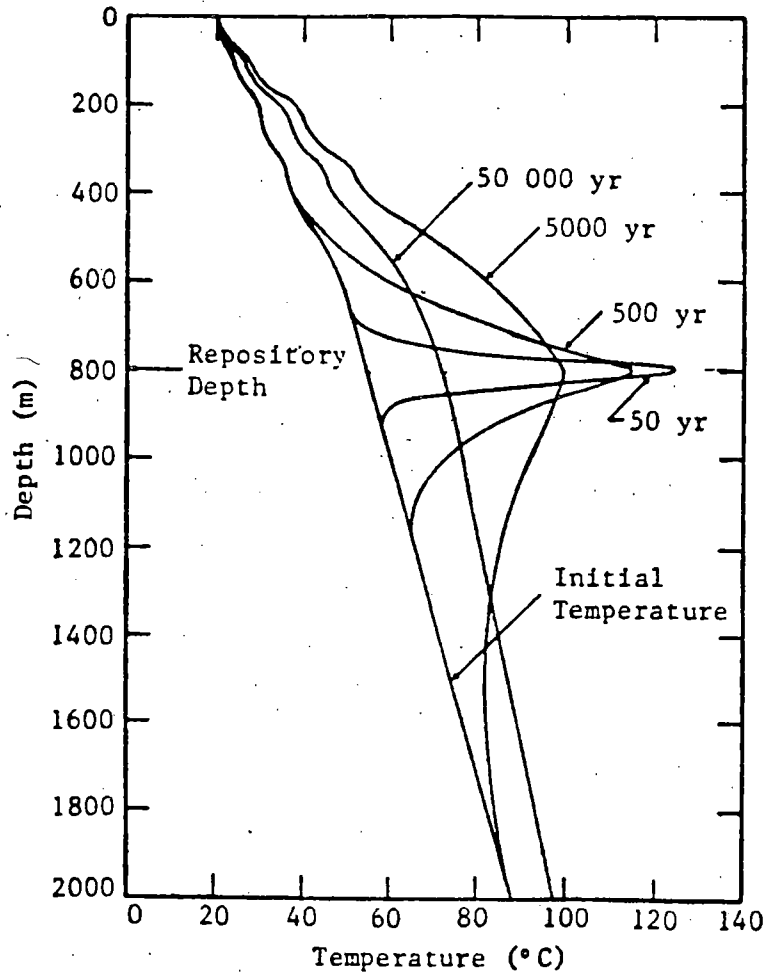


Figure (A-3) Far-Field Temperature Profile Along the Vertical Centerline for Gross Thermal Loading of 75 kW/Acre

Figure A-3 shows the temperature profile along the vertical centerline of the repository as a function of depth and time after closure. The "disturbed zone" is assumed to extend from the repository to 470 meters below surface where the water table lies. The average temperature of this disturbed zone is calculated by:

$$\bar{T} = \frac{1}{L} \int T \, dL$$

where L is the distance from the repository to the water table and is equal to 330 meters.  $\bar{T}_0$  is the average background temperature of the same zone as calculated from the natural geothermal field. The ambient temperature at the repository horizon is 50°C. Under these assumptions, the hydraulic gradients calculated are shown in Table A-3:

Table A-3

<u>Time After Closure (yr)</u>	<u><math>\bar{T}</math> (°C)</u>	<u><math>\bar{T}_0</math> (°C)</u>	<u><math>\alpha</math> (1/°C)</u>	<u>Gradient</u>
500	73	50	$6.01 \times 10^{-4}$	$1.4 \times 10^{-2}$
5,000	85	50	$6.68 \times 10^{-4}$	$2.3 \times 10^{-2}$
50,000	65.4	50	$5.54 \times 10^{-4}$	$8.5 \times 10^{-3}$

More recent field work indicates that the ambient rock temperature at the repository horizon will be 35°C (27). This temperature corresponds to an average ambient temperature of 30°C. Table A-4 shows the calculated upward gradient when this temperature is assumed.

Table A-4

<u>Time (yr)</u>	<u><math>\bar{T}</math> (°C)</u>	<u><math>\bar{T}_0</math> (°C)</u>	<u><math>\alpha</math> (1/°C)</u>	<u>Gradient</u>
500	73	30	$6.01 \times 10^{-4}$	$2.6 \times 10^{-2}$
5,000	85	30	$6.68 \times 10^{-4}$	$3.7 \times 10^{-2}$
50,000	65.4	30	$5.54 \times 10^{-4}$	$1.9 \times 10^{-2}$

Thermal histories at 307 and 711 meters below the surface for a repository with a 100 kW/Acre thermal loading have been calculated and are presented in Figure A-4 (27). From these curves, it is apparent that the peak temperature occurs before 10,000 years after closure of the facility. The hydraulic gradient at 500 years for an average ambient temperature of 50°C was selected as a lower bound for our calculations. The gradient at 5,000 years with the average ambient temperature of 30°C was used as the upper bound for the vertical hydraulic gradient. A range of vertical hydraulic gradients of  $1 \times 10^{-2}$  to  $4 \times 10^{-2}$  was sampled by the Latin Hypercube Sample technique for the transport calculations.

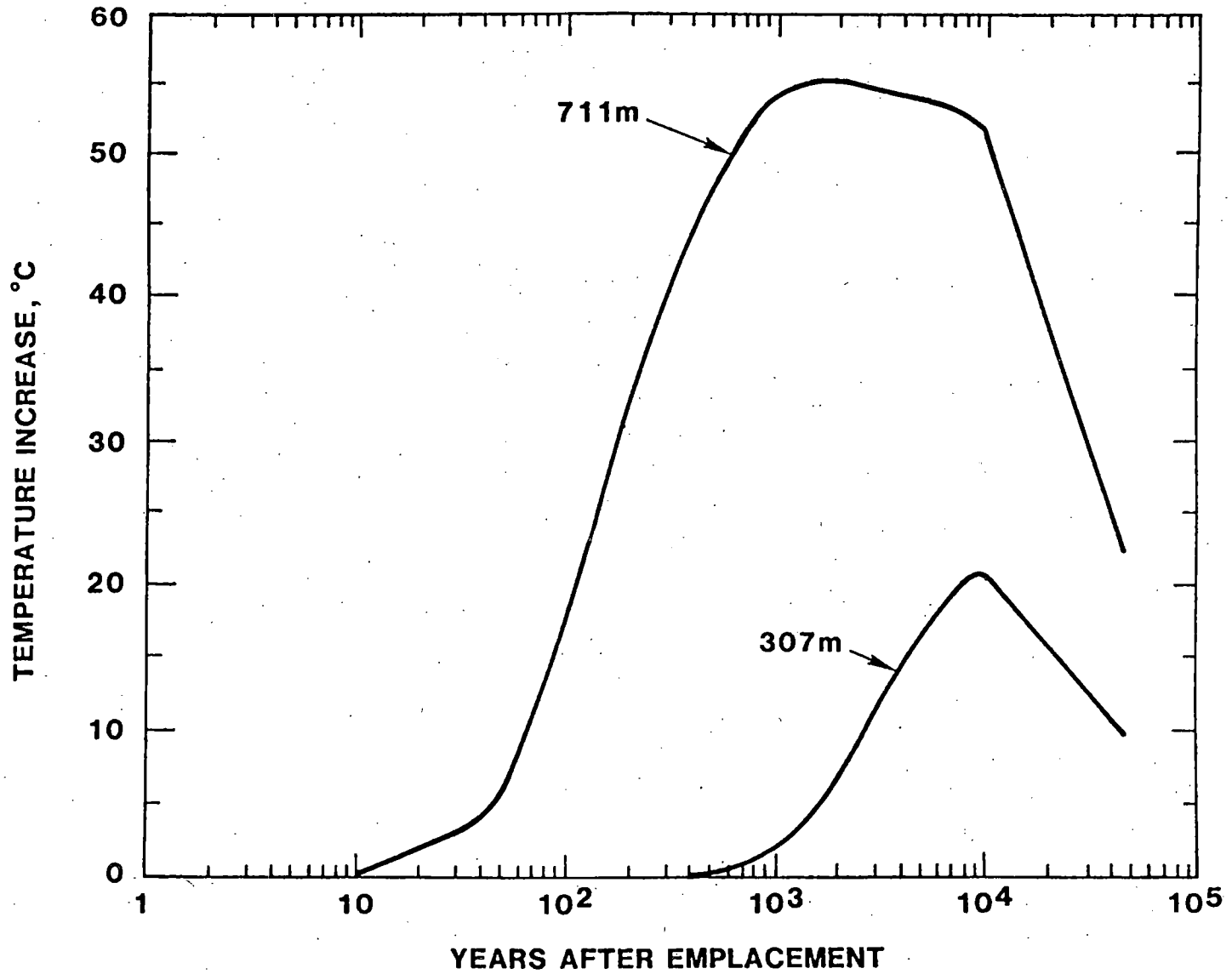


Figure A-4. Temperature Increase Histories at 307 and 711 Meters Below the Surface of the Earth for SF at 100 kW/acre.

The volume of annual recharge at the repository site places a constraint on the maximum flow through the repository under the influence of this thermal gradient. The maximum vertical discharge calculated from the vectors sampled by the LHS technique was  $3.6 \times 10^7$  ft<sup>3</sup>/yr (vector #51). This is approximately 7 percent of the volume of ground water moving through the Pahute Mesa ground-water system of the Nevada Test Site. The area of the repository comprises less than 0.1 percent of the area of this flow system. Although all of the recharge in this system is limited to areas above 5000-ft elevation, this volume of ground-water flow through the repository is probably unrealistically high. As discussed in Section 6 (Table 7), nearly all of the vectors whose radionuclide releases violated the EPA Standard in scenarios 1, 3, 4, 5, 6, 1B, and 5B were characterized by similarly unrealistic flows. Most of the other vectors considered in these calculations had ground-water discharges at least an order of magnitude smaller than vector #51.

### A.3 Horizontal Hydraulic Gradient

We have considered two contributions to the horizontal hydraulic gradient in our calculations. One component is the regional gradient of the undisturbed site. Static water levels from four wells near Yucca Mountain were used to estimate ranges of the regional horizontal gradient. Three of the wells have similar static water levels (~2400 ft) while the fourth and only well which is actually on Yucca Mountain has an anomalously high head (~3400 ft) (22). The range of regional hydraulic gradients was set to span the highest and lowest values that could be calculated from these data. The LHS routine, therefore, sampled a range of  $10^{-1}$  to  $10^{-3}$ .

The second component to the horizontal gradient is a local gradient related to the local rise in the water table above the repository due to the thermal buoyancy effect described previously. We can place an upper bound on this rise in water table ( $\Delta Z$ ) by assuming that the heated water in the cylinder described in Figure A-2 is constrained to expand only in the upward ( $Z$ ) direction. By applying Archimedes' Principle, we can show that the height of the heated cylinder can be related to the height of a cylinder of water of equal weight at the background temperature  $\bar{T}_0$ . Since the height of the cylinder of water at temperature  $\bar{T}_0$  equals the distance from the repository to the water table, we can calculate  $\Delta Z$  as follows:

$$w = \pi r^2 g \bar{\rho} (L + \Delta Z) = \pi r^2 g \rho L \quad (\text{Archimedes' Principle}) \quad (\text{A-3})$$

$$\Delta Z = L(\rho/\bar{\rho} - 1) \quad (\text{A-4})$$

where

- $\rho, \bar{\rho}$  = average density of water at  $\bar{T}_0$  and  $\bar{T}$ , respectively
- $L$  = height of cylinder of water at temperature  $\bar{T}_0$
- $r$  = radius of cylinder of water
- $\Delta Z$  = rise of water table
- $w$  = weight of water in both cylinders

If  $V$  equals the volume of the cylinder of water at temperature  $\bar{T}_0$ , then

$$w = \rho V = \bar{\rho} (V + \Delta V) \quad (A-5)$$

$$\Delta V = \alpha V \Delta T \quad (A-6)$$

$$\bar{\rho} = w/V(1 + \alpha \Delta T) = \rho/(1 + \alpha \Delta T) \quad (A-7)$$

where  $\Delta T$  and  $\Delta V$  refer to differences in temperature and volume between the two cylinders and  $\alpha$  is the average coefficient of thermal expansion of the fluid. Substituting (A-7) into (A-4) we obtain:

$$\Delta Z = L \alpha \Delta T \quad (A-8)$$

We have shown that  $\alpha \Delta T$  is equal to  $I_V$ , the vertical hydraulic gradient (equation A-2). We can therefore calculate  $\Delta Z$  for each input vector in our calculations by using the value of  $I_V$  sampled by the LHS technique. The horizontal hydraulic gradient ( $I_H$ ) used in our transport calculations is set equal to the sum of the regional gradient and the local gradient:

$$I_H = I_{HS} + I_V L/X \quad (A-9)$$

where:

$I_{HS}$  = value of regional horizontal hydraulic gradient sampled by the LHS

$I_V$  = value of vertical gradient sampled by LHS

$L$  = sum of vertical leg lengths in transport path

$X$  = sum of horizontal leg lengths in transport path

## APPENDIX B

### GEOCHEMISTRY AND RADIONUCLIDE RETARDATION

#### B.1 - Geochemical Environment of the Hypothetical Tuff Site

The mineralogy of each rock unit at the hypothetical tuff site is described in Table 1. The mineralogy and chemical composition of a tuff unit depend in part upon its cooling history and degree of post-depositional alteration. Vitric tuffs are porous tuffs which are composed of pumice or fragments of glass shards which have undergone a moderate to slight degree of welding. Their chemical composition is simple; the sum  $\text{SiO}_2 + \text{Al}_2\text{O}_3 + \text{K}_2\text{O} + \text{Na}_2\text{O}$  is greater than 95 weight percent. Minor elements include Ca, Mg, Cl, F and transition metals. Alteration of the glass to clay is ubiquitous in minor amounts and locally may be nearly complete. Devitrified tuffs are chemically very similar to vitric tuffs but are quite different in their mineralogy and physical properties. They are composed primarily of fine-grained aggregates of sanadine and cristobalite. They may contain phenocrysts of amphiboles, clinopyroxene and feldspar as well as lithic clasts. Low-temperature alteration of devitrified tuffs is not significant; access of ground water to the rocks is limited by the low interstitial porosity. Zeolitized tuffs are the products of low temperature alteration of nonwelded volcanic ash. They are composed primarily of the zeolites clinoptilolite, mordenite, and analcime.

An average chemical composition of the ground water (6) is shown in Table B-1. The water is classified as a sodium-potassium-bicarbonate water by Winograd et al. (4). Locally the composition of ground water is dependent upon lithology. Water associated with vitric tuffs is highest in silica, sodium, calcium and magnesium whereas ground water in zeolitic tuffs is depleted in the bivalent cations (28). The pH of these waters ranges from near-neutral to slightly alkaline (7.2-8.5). The Eh of the ground water in the repository horizon is unknown. Dissolved oxygen contents from several shallow wells at the Nevada Test Site are fairly high (~ 5 ppm) (29). The concentrations of several redox indicators and the alteration features of the mafic minerals in several units indicate that oxidizing conditions prevailed at one time below the water table (9). Negative redox potentials and low levels of dissolved oxygen, however, have been measured in sections of a drill hole in the Crater Flat Tuff (33). These observations are consistent with measured values of sulfide in the ground-water and the occurrence of pyrite ( $\text{FeS}_2$ ) in the rock matrix. The measurements are subject to a large amount of

TABLE B-1

## ANALYSES OF WATERS FROM THE NEVADA TEST SITE (mg/l)

<u>Well Species</u>	<u>J-13</u> <sup>1</sup>	<u>USW-H1</u> <sup>2</sup>	<u>USW-VH1</u> <sup>2</sup>
Na <sup>+</sup>	47.00	74.90	97.10
K <sup>+</sup>	4.70	5.10	4.30
Ca <sup>2+</sup>	13.00	7.20	10.30
Mg <sup>2+</sup>	2.00	0.40	1.90
Ba <sup>2+</sup>	0.20	0.01	0.04
Sr <sup>2+</sup>	0.06	0.02	0.08
HCO <sub>3</sub> <sup>-</sup> + CO <sub>3</sub> <sup>2-</sup>	130.00		
Cl <sup>-</sup>	7.70		
SO <sub>4</sub> <sup>2-</sup>	21.00		
NO <sub>3</sub> <sup>2-</sup>	5.60		
F <sup>-</sup>	1.70		
SiO <sub>2</sub>	61.00	11.00	53.40
pH	7.1-8.3	-	-
TDS	> 294.00		

<sup>1</sup> LA-7480-MS - reference 6

<sup>2</sup> LA-8847-PR - reference 8

uncertainty and must be confirmed by further investigations. In light of this uncertainty, we assumed that the ground waters at the hypothetical repository are oxidizing. The importance of redox to both the solubilities and  $R_d$  values for the radionuclides that were considered in our calculations will be discussed below.

## B.2 Radionuclide Solubilities

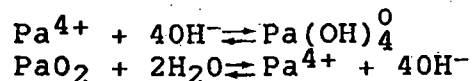
As discussed in Section 4.3, we have attempted to estimate upper bounds for the radionuclide solubilities at the tuff repository. These limits were set after a limited review of available experimental data and theoretical calculations. Most of the redox-sensitive elements are least soluble under reducing conditions. In light of the uncertainty concerning the redox conditions at Yucca Mountain and in order to ensure that our calculated releases are conservative, we have used the estimated radionuclide solubilities for oxic conditions in our calculations.

The estimated solubility limit for each element is discussed below. In this discussion, a pH = 8 and a ground-water composition similar to J-13 water (Table B-1) are assumed.

- Pu: Experimental studies reviewed by Wood and Rai (15) suggest that Pu solubility is relatively insensitive to redox conditions. They suggested a value of  $4 \times 10^{-10}$  M from their data. A more conservative value of  $10^{-3}$  M ( $2.4 \times 10^{-4}$  g/g) was used in order to account for the possible dominance of a Pu-carbonate complex (12).
- U: Uranium solubility could be very high if considerable ( $>10^{-2}$  M)  $\text{CO}_3^{2-}$  is present. However, the ground-water composition at NTS (6,8) does not support this possibility. We have used the experimental data presented in (15) to set the U solubility limit at  $2.4 \times 10^{-5}$  g/g. Under reducing conditions the solubility would be several orders of magnitude lower.
- Th: The dominant species at Th is probably  $\text{Th}(\text{OH})_4^0$  at pH values above 5 (13,31,32). We used the reaction:
- $$\text{Th}(\text{OH})_4^0 \rightleftharpoons \text{ThO}_2(\text{s}) + 2\text{H}_2\text{O}$$
- to estimate the solubility limit at  $2.3 \times 10^{-7}$  g/g at pH=8. The solubility is not sensitive to redox.
- Ra: Radium is another element whose solubility is relatively insensitive to redox. Its solubility is controlled primarily by  $\text{RaSO}_4(\text{s})$  or  $\text{RaCO}_3(\text{s})$ . The value from (16) is a very conservative upper bound for Ra solubility at the tuff site.
- Cm: Few data are available to estimate Cm solubility in natural waters. In a 0.1M NaCl solution at pH=3, the Cm solubility was  $10^{-11}$  M. The solubility decreases at lower pH (14). A conservative value of  $10^{-10}$  M ( $2.5 \times 10^{-11}$  g/g) was used in the calculations.
- Am: Am solubility has been studied by Wood and Rai (15). They suggest that a value of  $7 \times 10^{-12}$  M is reasonable over a wide range of redox conditions. Complexing by  $\text{Cl}^-$ ,  $\text{SO}_4^{2-}$ , or  $\text{NO}_3^-$  will not be significant.
- Np: Neptunium is least soluble under reducing conditions ( $10^{-10}$  M) (15). At an Eh = +0.26 and pH=7 the solubility of  $\text{NpO}_2(\text{c})$  is approximately  $2.4 \times 10^{-8}$  g/g.

Pb:  $\text{PbCO}_3$  or  $\text{PbSO}_4$  will limit the solubility of lead in an oxic tuff environment to less than  $10^{-6}$  M. If any sulfide is present,  $\text{PbS}$  will precipitate and further decrease the solubility.

Pa: Little data are available for protactinium solubility in natural waters. We use the reactions:



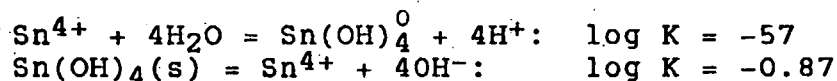
to set the solubility limit at  $2.3 \times 10^{-2}$  M.

Ac: We had no data to estimate the solubility of actinium; we therefore assumed that it had no solubility limit in our calculations.

Tc: Tc is least soluble under reducing conditions and precipitates as  $\text{TcO}_2$ . Under oxidizing conditions it is probably present as  $\text{TcO}_4^-$  and is very soluble. We have assumed that it has no solubility limit in our calculations (13, 16).

I, Cs: These elements probably have no limiting solubilities under repository conditions (13, 16).

Sn: We have assumed that these redox-insensitive reactions determine the solubility of tin (13, 16):



Sr: The solubility of Sr is probably set by strontianite  $\text{SrCO}_3$  (13, 16). At pH=8, the reported 130 ppm of  $\text{HCO}_3^- + \text{CO}_3^{2-}$  (Table B-1) is dominantly bicarbonate and  $[\text{CO}_3^{2-}]$  is about  $10^{-5}$  M.  $\log K_{\text{sp}}$  of  $\text{SrCO}_3$  is -9.6 which means the solubility of Sr is about  $2 \times 10^{-6}$  g/g.

C: We set the solubility limit of C at a level consistent with the concentration of  $\text{HCO}_3^-$  in J-13 water (~26 ppm carbon in a solution of 130 ppm  $\text{HCO}_3^-$ ).

### B.3 Radionuclide Sorption Ratios

The ranges of radionuclide distribution coefficients ( $R_d$ ) used in our calculations are listed in Table 4. The values were chosen after a review of the published experimental studies that were conducted at Los Alamos National Laboratory (LANL) through June, 1981, (5-10).

$R_d$  values from batch experiments obtained under the following conditions were included in the ranges shown in Table 4.

temperature = 22°C  
solid: solution ratio = 1:20  
atmosphere = oxidizing  
particle size = 106-500 microns  
water = J-13 water pre-equilibrated with the  
rock sample  
rocks = samples from UE25a-1, G-1 and J-13  
drill holes

Parametric studies by LANL scientists (5-10) suggest that the measured  $R_d$  values are dependent upon all of the parameters listed above. The conservatism of the data collected under these experimental conditions with respect to natural conditions expected at the tuff repository site is described in Table B-2.

For several elements,  $R_d$  values obtained under these experimental conditions can vary up to 3 orders of magnitude between samples of the same bulk mineralogy. The measured  $R_d$  value are strongly dependent upon the abundance of minor minerals such as montmorillonite, the duration of the experiment and upon the method used to measure the concentration of the sorbed radionuclide. Values obtained from desorption experiments are almost always significantly higher than those obtained from sorption experiments. The data ranges in Table 4 bracket the highest average  $R_d$  values obtained from desorption experiments and the lowest average sorption  $R_d$  value. The references for similar values in the literature are described in Tables B-3 to B-5.

TABLE B-2

CONSERVATISM<sup>1</sup> OF LABORATORY  
DETERMINATIONS OF R<sub>d</sub> (LANL)

PARAMETER	ELEMENT								
	Pu	Am	U	Sr	Cs	Ba	Ce	Eu	Tc
Radionuclide Concentration	*O	ND	ND	-	-	-	ND	O	ND
Solid/Solution Ratio	ND	ND	ND	-O	-O	-	-	-	ND
Ionic Strength	ND	ND	ND	-*	-*	-*	-*	-*	ND
Temperature	ND	O	+	+	+	+	*	*	ND
Particle Size	-O	+O	+O	+O*	+O*	+O*	O	O	ND
TYPE EXPERIMENT:									
Batch vs. Column	ND	ND	-*	-	-	-	-*	ND	ND
Eh (Atmosphere)	+	O	+	O	O	O	O	O	+

**KEY:** + Conservative  
 - Not conservative  
 O Little effect  
 \* Inconclusive or interaction effects  
 ND Not determined

1. Assuming the following experimental conditions:

T = 22°C	Atmospheric conditions (in air)
Solid : Solution = 1:20	106-500 micron particle size range
Batch experiment	Element-specific concentration
J-13 water	

Table B-3

SOURCES OF DATA FOR RANGES<sup>1</sup> OF R<sub>d</sub>  
VALUES FOR VITRIC TUFF

Element	Value	Reference <sup>2</sup>	Comment <sup>3</sup>
Am	85	6(27)	JA-18, minimum sorption value
	360	6(27)	JA-18, maximum sorption value
Pu	70	6(27)	JA-18, minimum sorption value
	450	6(27)	JA-18, maximum sorption value
U	0.01	-	conservative lower limit
	11	9(8)	YM-54, YM-22 (devitrified) max. or ave. desorption value
Np	5	10(12)	YM-49, G1-1883 (devitrified), (ave. sorption value - s.d.)
	7	10(12)	G1-1883 (devitrified), (ave. sorption value + s.d.)
Sr	117	8(10)	G1-1292, sorption average
	300	9(1)	YM-5, desorption average
Cs	429	8(10)	G1-1292, sorption average
	8600	9(1)	YM-5, Cs desorption average
Tc	0.01	-	conservative lower limit
	2	7(16)	YM-48, desorption average (glass + zeolites)
I	0	6(25)	conservative value

<sup>1</sup>Ranges in Table 4.

<sup>2</sup>References are numbered in bibliography; number in parantheses is table number in the reference.

<sup>3</sup>Information given includes: rock sample number, mineralogy if different from that stated at top of table, type of value (s.d. = standard deviation of average value). Averages include contribution from several particle size fractions and contact times.

Table B-4

SOURCES OF DATA FOR RANGES OF  $R_d$  VALUES  
FOR ZEOLITIZED TUFF

Element	Value	Reference <sup>2</sup>	Comment <sup>3</sup>
Am	600	6(32)	JA-37, sorption average
	9500	9(6)	YM-38, desorption average
Pu	250	9(6)	YM-38, sorption average
	2000	9(6)	YM-38, desorption average
U	5	9(8)	YM-38, sorption average
	15	9(8)	YM-38, desorption average
Np	4.5	10(12)	YM-49, (average sorption value - s.d.)
	31	10(12)	U12G-RNM9, single sorption value for 3 wk. contact time
Sr	290	6(21)	JA-37, sorption average
	213,000	8(10)	G1-2698, desorption average
Cs	615	6(21)	JA-37, sorption average
	33,000	3(A1)	YM-49, desorption average
Tc	0.2	3(A1)	YM-49, sorption average
	2	3(A1)	YM-49, desorption average
I	0	6(25)	conservative value

<sup>1</sup>Ranges in Table 4.

<sup>2</sup>See note 2, Table B-3.

<sup>3</sup>See note 3, Table B-3.

Table B-5

SOURCES OF DATA FOR RANGES<sup>1</sup> OF R<sub>d</sub> VALUES  
FOR DEVITRIFIED TUFF

Element	Value	Reference <sup>2</sup>	Comment <sup>3</sup>
Am	180	9(4)	YM-54, minimum sorption value
	4600	9(6)	YM-22, desorption average
Pu	84	9(6)	YM-54, sorption average
	1400	9(6)	YM-22, desorption average
U	1.2	9(7)	YM-22, sorption average (106-500 μm)
	14.3	9(7)	YM-54, desorption average (<106 μm)
Np	5	10(12)	YM-49, G1-1883 (devitrified), (ave. sorption value - s.d.)
	7	10(12)	G1-1883 (devitrified), (ave. sorption value + s.d.)
Sr	53	6(19)	JA-32, desorption average
	450	8(10)	G1-1982, maximum sorption value
Cs	123	6(19)	JA-32, sorption average
	2020	8(10)	G1-1982, desorption average
Tc	0.3	3(A1)	sorption average
	1.2	3(A1)	desorption average
I	0	6(25)	conservative value

<sup>1</sup>Ranges in Table 4.

<sup>2</sup>See note 2, Table B-3.

<sup>3</sup>Information includes: rock sample number, type of value, particle size fraction if not all fractions were considered in average. Maximum values are maxima for several size fractions, samples or contact times.

## APPENDIX C

### APPROXIMATIONS FOR ADAPTING POROUS MEDIA RADIONUCLIDE TRANSPORT MODELS TO ANALYSIS OF TRANSPORT IN JOINTED POROUS ROCK

#### C.1 Introduction

This attachment summarizes results of initial analyses (34, 35, 36) to develop equivalent porous media models for analysis of transport in jointed porous rock. Much of the text and approach are taken from (36). First, the equations and underlying assumptions used to describe radionuclide transport in both porous and jointed porous media are summarized. General conditions are then defined for which transport in jointed porous rock can be approximated as occurring in equivalent porous media having effective porosities defined by joint aperture, orientation and spacing. An expression for the retardation factor in the equivalent porous media transport equations is derived. Next numerical criteria for use of the porous media transport equations are derived. Then numerical criteria for use of the porous media approximation are derived for a specific flow system. The equations describing flow through a system of joints which form plate-like regions of jointed rock are presented. It is shown that the criteria for the use of a porous media approximation can be derived from solution of these equations. The specific criteria for this system are shown to be equivalent to those defined for the general case. Definitions of the symbols used in this discussion are summarized in Table C-1 and described in Figure C-1.

#### C.2. Radionuclide Transport in Porous and in Jointed Porous Media

##### Porous Media

Consider a reasonably homogeneous porous medium, shown schematically in Fig. C-1, which has average effective porosity  $\phi$  and grain density  $\rho_s$ . Assume that the physical and chemical properties of the rock can be considered uniform and continuous. Let the pore space be fully saturated, and assume that flow is relatively uniform throughout that pore space. Also, let sorption of radionuclides by the rock result from only reversible processes such as adsorption or ion

Table C-1  
DEFINITION OF TERMS

<u>Symbol</u>	<u>Definition</u>
$\phi$	matrix porosity (*)
$\rho_s$	grain density (g/cc)
C	radionuclide concentration in flowing fluid (g/ml)
$q'$	radionuclide concentration on solid phase (g/g)
$K_d$	sorption equilibrium distribution coefficient, = $q'/C$ (ml/g)
$q_s$	radionuclide concentration on surface of solid phase (g/cc)
$q_i$	local radionuclide concentration in solid phase (g/cc)
q	bulk radionuclide concentration in porous matrix (g/cc)
$\vec{v}$	bulk-mass average velocity of fluid (cm/sec), (interstitial or joint fluid velocity)
v	average velocity of fluid in x direction (cm/sec)
x	direction of fluid flow (cm)
x/v	mean residence time of fluid (sec)
R	retardation factor for radionuclide transport in porous media (*)
$\epsilon$	porosity of rock associated with joints (*)
m	void volume (associated with joints) per unit volume of porous matrix = $\epsilon/(1-\epsilon)$ (*)
$V_p$	volume of plate-like regions of porous matrix (cm <sup>3</sup> )
H	joint aperture (cm)
2b	joint spacing or width of plate-like regions of porous matrix, (cm)

Table C-1 (continued)

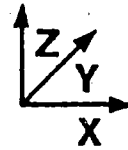
<u>Symbol</u>	<u>Definition</u>
$\bar{K}$	bulk sorption distribution coefficient: $= q/c = R\phi$ (*)
D	molecular diffusion coefficient of radionuclide (cm <sup>2</sup> /sec)
$\alpha$	tortuosity (*)
D <sub>e</sub>	effective diffusion coefficient of radionuclide in porous matrix = $D\phi/\alpha^2\bar{K}$ (cm <sup>2</sup> /sec)
R <sub>f</sub>	effective interfacial resistance to mass transfer (sec <sup>-1</sup> )
R <sub>j</sub>	retardation factor for equivalent porous media approximation = $1+\bar{K}/m$ (*)
z	direction of diffusion, perpendicular to rock-fluid interface (cm)
M <sub>m</sub>	mass of radionuclide on rock matrix per unit control volume (g)
M <sub>p</sub>	mass of radionuclide in pore water per unit control volume (g)
M <sub>f</sub>	mass of radionuclide in flowing fluid in joint per unit control volume (g)
$\lambda$	radionuclide decay constant (sec <sup>-1</sup> )
$\hat{C}$	solution to transport equations for $\lambda = 0$
a	interfacial area per unit volume of bulk rock = $1/b = 2m/H$ (cm <sup>-1</sup> )
t <sub>0.5</sub>	elapsed time required for $\hat{C}/C_0$ to reach a value of 0.5
$\sigma$	$D_e/b^2$ (sec <sup>-1</sup> )

Table C-1 (continued)

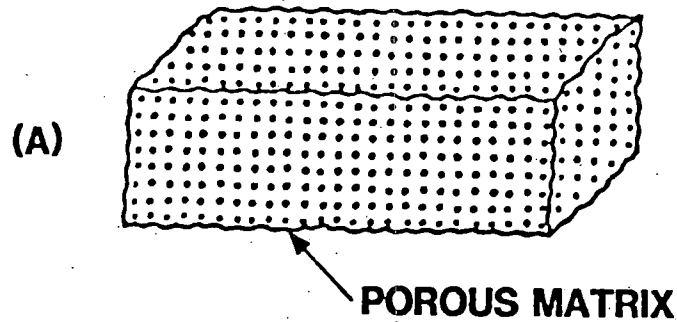
<u>Symbol</u>	<u>Definition</u>
$\theta$	$t-x/v$ (sec)
$\gamma$	$D_e \bar{K}/b^2$ (sec <sup>-1</sup> )
$w$	$x/mv$ (sec)
$\gamma w$	effective bed length (cm)
$g$	$\gamma R_f$ (cm)

\* = dimensionless variables

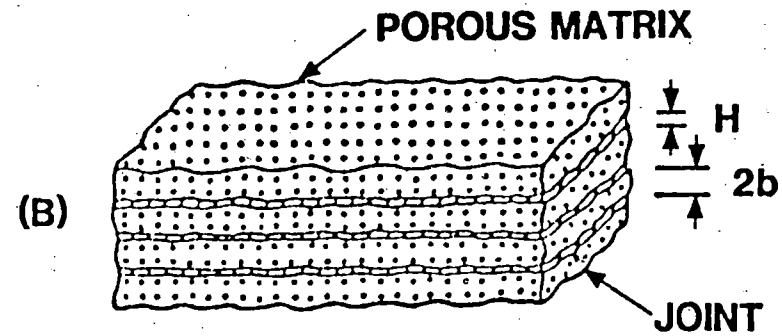
(A) POROUS ROCK



(B) JOINTED POROUS ROCK



Matrix porosity =  $\phi$   
Grain Density =  $\rho_s$



Matrix porosity =  $\phi$   
Fracture porosity =  $\epsilon$   
Grain density =  $\rho_s$   
Volume of plate-like regions of porous matrix =  $V_p$   
Plate thickness =  $2b$   
Joint aperture =  $H$

Figure C-1. Schematic Diagrams of Porous (A) and Jointed Porous Rock (B). Coordinate system is same for both diagrams. Origin for z coordinate is at center of block.

exchange, and let fluid-phase concentrations be sufficiently dilute so that sorption can be represented by linear isotherms of the form  $q' = K_d C$ , where  $C$ ,  $K_d$ , and  $q'$  are the radionuclide concentration in the flowing fluid, the sorption equilibrium distribution coefficient, and the radionuclide concentration associated with the solid phases, respectively. Furthermore, assume that the radionuclide concentration  $C$  is due only to dissolved species. For such media, the following assumptions are generally made:

- Assumption A: The interstitial fluid velocity profile can be approximated by the bulk mass-average pore fluid velocity  $\bar{v}$ .
- Assumption B: The cross section of the pores is sufficiently small so that the radionuclide concentration in the pores can be considered cross-sectionally uniform.
- Assumption C: Local sorption equilibrium exists between pore water and mineral phases.

When these conditions obtain, then for constant-valued parameters, the basic equation describing radionuclide transport is the material balance for the flowing fluid

$$\frac{\partial C}{\partial t} = \frac{\bar{v}}{R} \cdot \nabla C = \text{terms for } \begin{cases} \text{decay} \\ \text{reaction} \\ \text{dispersion} \end{cases} \quad (\text{C-1})$$

where  $R$  is the retardation factor given by  $R = 1 + (1 - \phi) \rho_s K_d / \phi$ , and it is assumed that essentially all pore space is available to fluid flow.

#### Jointed media

Now consider a jointed, but otherwise reasonably homogeneous, porous medium which has porosity  $\phi$  and grain density  $\rho_s$  associated with the bulk porous matrix and has porosity  $\epsilon$  associated with the joints, as determined from joint aperture  $H$ , orientation, and spacing  $2b$  (Figure C-1b). Let fluid flow occur primarily in the joints, and convective

radionuclide transport in the bulk porous rock be negligible. Let the joints be linear, have rectangular cross-sections of approximately uniform dimensions, and have constant and continuous physical and chemical properties. Furthermore, assume that the joints and porous matrix are fully saturated, and let the regions of porous rock bounded by the joints have approximately uniform, plate-like shape and volume  $V_p$ . Again assume that the radionuclide concentration  $C$  only results from dissolved species. Also assume that radionuclide retardation, relative to convective transport in the joints, is due to molecular diffusion in the pore water and simultaneous sorption by the solid phases of the bulk rock. Again let sorption of radionuclides by the rock result from only reversible processes, and let the concentration  $C$  be sufficiently small so that sorption can be represented by linear isotherms, and radionuclide diffusion through the pore water by Fick's law. Assume that the plate thickness  $2b$  is sufficiently small so that radionuclide concentrations resulting from diffusion are non-trivial over the entire thickness of the plate.

Three other assumptions, analogous to Assumptions A-C for porous media need to be made for jointed porous media. In modeling radionuclide transport in jointed media, it is generally assumed that the velocity profiles in the joints also can be approximated by the bulk mass-average fluid velocity  $\bar{v}$  in the joints, again obtained from an appropriate hydrologic model. However, it cannot be assumed that concentration in the fluid in the joints generally will be cross-sectionally uniform or that local sorption equilibrium generally exists between bulk phases. Instead the following assumptions are usually made:

Assumption B1: Joint apertures are sufficiently small so that in the joints, diffusion of radionuclides in the fluid phase can be approximated as a quasi-steady state process which is represented by a linear driving force expression.

Assumption C1: Local sorption equilibria exist at the interface between flowing fluid and bulk rock and between pore water and solid phases of the porous matrix.

When these conditions obtain, then for constant-valued parameters, radionuclide transport can be described by the following equations:

(material balance for the fluid in the joint)

$$\frac{\partial C}{\partial t} + \vec{v} \cdot \vec{\nabla} C + \frac{1}{m} \frac{\partial q}{\partial t} = \text{terms for } \begin{cases} \text{decay} \\ \text{reaction} \\ \text{dispersion} \end{cases} \quad (\text{C-2})$$

(flux expression at the interface between flowing fluid and bulk rock)

$$\frac{\partial q}{\partial t} - \frac{1}{R_f} (C - q_s / \bar{K}) = \text{terms for } \begin{cases} \text{decay} \\ \text{reaction} \end{cases} \quad (\text{C-3})$$

(material balance for the bulk rock)

$$\frac{\partial q_i}{\partial t} - D_e \nabla^2 q_i = \text{terms for } \begin{cases} \text{decay} \\ \text{reaction} \end{cases} \quad (\text{C-4})$$

where

$$q = \frac{1}{V_p} \int_{V_p} q_i dV_p \quad (\text{C-5})$$

The terms in these expressions are defined in Table C-1 and Figure C-1.  $D_e$  is the effective radionuclide diffusion coefficient for the bulk porous rock;  $\bar{K}$  is the bulk sorption distribution coefficient between porous matrix and external solution;  $m$  is the void volume (based on joint aperture, orientation, and spacing per unit volume of porous matrix;  $R_f$  is an effective interfacial resistance to mass transfer;  $q_i$  is the local concentration in the porous rock;  $q_s$  is the value of  $q_i$  at the interface between matrix and flowing fluid, and the Laplacian  $\nabla^2$  is defined in a coordinate system convenient for describing diffusion in porous rock.

### C.3 Equivalent Porous Media Approximation

Qualitatively, it should be evident from the preceding discussion that radionuclide transport in the jointed porous rock described above could be approximated as occurring in an equivalent porous media if the joint aperture  $H$ , joint spacing  $2b$ , and the physical and chemical properties of the radionuclides and bulk rock were such that the conditions described by Assumptions B1 and C1 reduced to the conditions described in Assumptions B and C respectively. These equivalent porous media assumptions can be stated as

Assumption B2: Radionuclide concentrations in the flowing fluid can be considered approximately cross-sectionally uniform.

Assumption C2: The bulk rock can be considered approximately to be in local sorption equilibrium with fluid flowing in the joints.

In the paragraphs below, quantitative criteria, which determine when the above two conditions are valid, are developed in terms of the joint aperture  $H$ , spacing  $2b$ , and the fundamental parameters describing the physical and chemical properties of the bulk rock. The expression for the retardation factor  $R_j$  to be used in the equivalent porous media equation is also developed.

#### Criteria for equivalent porous media approximation

##### Flowing fluid

Let  $x$  denote a spatial coordinate in the direction of bulk fluid motion, and let  $D$  be the radionuclide diffusion coefficient (assumed constant) for dilute aqueous solutions of the nuclide. A criterion for approximately uniform radionuclide concentrations in the flowing fluid is that the average residence time  $x/v$  for the flowing fluid is much greater than the relaxation time for a concentration gradient. The equilibration time for a plane sheet which has thickness  $H/2$  and one face maintained at a constant concentration is approximately  $H^2/4D$  (37) and should be a reasonably general estimate of the relaxation time for a concentration gradient. The desired criterion is then  $x/v \gg H^2/4D$  or  $x/v \geq A_1 H^2/4D$ , where  $A_1$  is an appropriate constant, on the order of 10 to 100. In previous analyses (34, 35) of specific cases in jointed porous rock, the preceding criterion was derived using the solutions to the transport equations for porous rock.

The value of the constant  $A_1$  so obtained varied between 23 and 24. Therefore, a reasonable criterion for approximately cross-sectionally uniform radionuclide concentrations in the flowing fluid should be

$$x/v \geq 6H^2/D \quad (C-6)$$

Bulk rock.

For the bulk rock to be approximately in local sorption equilibrium with the fluid flowing in the joints, radionuclide concentrations in the plate-like regions must be nearly cross-sectionally uniform. Again a criterion for such approximately uniform concentrations is that the mean residence time  $x/v$  of the flowing fluid is much greater than the relaxation time for a concentration gradient. Following the preceding arguments, that criterion would be  $x/v \gg b^2/D_e$ . However, diffusion of radionuclides into the porous matrix will retard the convective transport of radionuclides relative to bulk fluid motion. The mean residence time of the radionuclides would be greater than the fluid residence time  $x/v$ . In particular, if radionuclide concentrations in the bulk rock are indeed nearly uniform, then the radionuclide residence time would be greater than the fluid residence time by a factor of  $R_j$ , the retardation factor defined below for jointed media. Then the preceding criterion can be stated in less restrictive form as

$$R_j \cdot x/v \gg b^2/D_e \text{ or } x/v \gg A_2 b^2/R_j D_e.$$

where  $A_2$  again is an appropriate constant, on the order of 10 to 100. It is shown later that

$$R_j D_e \approx \bar{K} D_e / m = \phi D / \alpha^2 m = \phi D (1 - \epsilon) / \alpha^2 \epsilon.$$

and that a typical value for  $A_2$  would be about 50. Therefore, a reasonable criterion for approximate local sorption equilibrium should be

$$\frac{x}{v} \geq 50 \frac{mb^2}{\bar{K} D_e} = 50 \frac{\alpha^2}{\phi} \cdot \left( \frac{\epsilon}{1 - \epsilon} \right) \cdot \frac{b^2}{D} \quad (C-7)$$

### Retardation factor for equivalent porous media approximation

By definition, the interfacial resistance  $R_f$  to mass transfer (Eq. C-3) is proportional to the fluid phase concentration gradient perpendicular to the interface between bulk rock and flowing fluid. As that concentration gradient decreases, the resistance  $R_f$  decreases correspondingly, and for sufficiently small gradients, that is, nearly cross-sectionally uniform concentrations in the joints, Eq. C-3 reduces to  $q_s = \bar{K}C$ . Furthermore, for approximately cross-sectionally uniform radionuclide concentrations in the bulk rock, Eq. C-4 reduces to  $q_i \approx$  a constant, which implies  $q_s \approx q_i$ , and Eq. C-5 reduces to  $q \approx q_i$ , which implies  $q \approx \bar{K}C$ . Then, Eqs. C-2 to C-5 reduce to

$$\frac{\partial C}{\partial t} + \frac{\vec{v}}{R_j} \cdot \vec{\nabla} C = \text{terms for } \begin{cases} \text{decay} \\ \text{reaction} \\ \text{dispersion} \end{cases} \quad (\text{C-8})$$

Eq. C-8 is analogous to Eq. C-1 for porous media.

An expression for the retardation factor  $R_j$  for jointed porous media can now be derived in terms of measurable fundamental parameters. In general, a retardation factor can be defined as the ratio of the mass of solute in the rock-water system to the mass of solute in the fluid in a unit control volume. In a jointed porous media this definition can be expressed as:

$$R_j = \frac{M_m + M_f}{M_f} = \frac{M_r + M_p + M_f}{M_f} \quad (\text{C-9})$$

where:

- $M_f$  = mass of radionuclide in water in fractures in a unit control volume
- $M_m$  = mass of radionuclide in the porous matrix bound by fractures in a unit control volume
- $M_r$  = mass of radionuclide sorbed onto solid phases of porous matrix in unit volume
- $M_p$  = mass of radionuclide in pore water of porous matrix in unit volume

When the local equilibrium assumptions defined above obtain, then:

$$M_f = \epsilon C \cdot \text{unit volume}$$

$$M_p = \phi C \cdot (1 - \epsilon) \cdot \text{unit volume}$$

$$M_r = (1 - \phi) \rho_s K_d C \cdot (1 - \epsilon) \cdot \text{unit volume}$$

therefore:

$$R_j = \frac{\epsilon C + [(1 - \phi) \rho_s K_d C + \phi C] (1 - \epsilon)}{\epsilon C}$$

$$R_j = 1 + \left( \frac{1 - \epsilon}{\epsilon} \right) \cdot \left[ \phi \left( 1 + \rho_s \frac{(1 - \phi)}{\phi} K_d \right) \right] \quad (\text{C-10})$$

which is the desired expression.

The criterion in Equation C-7 can now be derived.

By definition:

$$\bar{K} = \phi R = \phi + (1 - \phi) \rho_s K_d$$

$$m = \epsilon / (1 - \epsilon)$$

$$\text{therefore, } R_j = 1 + \bar{K}/m \quad (\text{C-11})$$

Now, if most of the porosity of the bulk rock is available to radionuclide diffusion, and if surface diffusion at the mineral surfaces is negligible, the effective diffusion coefficient  $D_e$  for porous rock often is defined by  $D_e = D/\alpha^2 R$  or  $D_e = D/\alpha^2 [1 + (1 - \phi) \rho_s K_d / \phi]$ , where  $\alpha^2$  is a tortuosity factor for the porous matrix. Furthermore, for most jointed media, the porosity  $\epsilon$  associated with the joints will be relatively small and much less than  $\phi$ . Since  $m = \epsilon / (1 - \epsilon)$ ,  $\bar{K}/m \gg 1$ , and  $R_j \approx \bar{K}/m$ . From the definitions of  $\bar{K}$  and  $D$ , it then follows that  $R_j D_e \approx \phi D (1 - \epsilon) / \epsilon \alpha^2$ , as mentioned in the preceding section. Since  $x/v > 50b^2 / R_j D_e$ , Equation C-7 can be easily derived by substitution.

#### C.4. Criteria and Retardation Factor Derived from Solution of the Transport Equations

In this section the preceding principles are illustrated using the transport equations for a specific flow system. Consider transport of a radionuclide through a uniform, jointed porous medium illustrated in Figure C-1b. Let the nuclide be initially present in the inventory but not subsequently generated as a daughter product. Let flow in the joints and diffusion into the bulk rock be one-dimensional. Assume that no competing chemical reactions occur and that radionuclide transport resulting from dispersion in the direction of flow is small relative to convective transport. Let  $x$ ,  $y$ , and  $z$  be rectangular Cartesian coordinates where  $x$  is again parallel to flow and  $z$  is perpendicular to the interface between flowing fluid and bulk rock. For relatively uniform joint spacing, Eqs. C-2 to C-4 then become

$$\frac{\partial C}{\partial t} + v \frac{\partial C}{\partial x} + \frac{1}{m} \frac{\partial q}{\partial t} = -\lambda C - \frac{\lambda}{m} q \quad (\text{C-12})$$

$$\frac{\partial q}{\partial t} - \frac{1}{R_f} (C - q_s/\bar{K}) = -\lambda q \quad (\text{C-13})$$

$$\frac{\partial q_i}{\partial t} - D_e \frac{\partial^2 q_i}{\partial z^2} = -\lambda q_i \quad (\text{C-14})$$

where  $q = 1/b \int_0^b q_i dz$ ;  $\lambda$  is the radionuclide decay constant, and appropriate initial and boundary conditions are as follows:  $C(z, 0) = 0$  for  $z \geq 0$ ;  $C(0, t) = 0$  for  $t \leq 0$ , and  $C(0, t) = C_0 e^{-\lambda t}$  for  $t > 0$ ;  $q_i(x, z, 0) = 0$  for  $0 \leq z \leq b$  and  $x \geq 0$ ;  $\partial q_i(x, 0, t)/\partial z = 0$  for  $x \geq 0$  and  $t \geq 0$ .

#### Solution of transport equations

If, for the above initial and boundary conditions,  $\hat{C}$ ,  $\hat{q}$ , and  $\hat{q}_i$  are the solutions to Eqs. C-12 to C-14 for  $\lambda = 0$ , it can be verified by direct substitution that for  $\lambda > 0$ , the solutions to Eqs. C-12 to C-14 using the above initial and boundary conditions are given by  $C = \hat{C} e^{-\lambda t}$ ,  $q = \hat{q} e^{-\lambda t}$ , and  $q_i = \hat{q}_i e^{-\lambda t}$ . For  $\lambda = 0$ , details of the method of solution are given by Rosen (38, 39) for the analogous equations for flow around spherical rather than plate-like regions. A similar solution is given by Erickson (34, 35) for a fluid flowing through a single fracture between two parallel

plates in which radionuclide diffusion perpendicular to the fracture was limited to a finite penetration depth. By substituting the appropriate expression for  $m$ , that is  $\epsilon/(1 - \epsilon)$ , in the single fracture result, the solution can be obtained for flow through a system of joints which form several plate-like regions of porous rock, such as shown on Fig. C-1b. The resulting solution is in the form of an infinite integral which requires numerical evaluation. However, for sufficiently large values of  $x/v$ , the integral approaches a relatively simple asymptotic expression. In particular, if  $x/v \geq 50 mb^2/\bar{K}D_e$ , then

$$\hat{C}/C_0 \approx \frac{1}{2} + \frac{1}{2} \operatorname{erf} \left[ \frac{\frac{2\sigma\theta}{\gamma w} - 1}{2 \left( \frac{1 + 3g}{3\gamma w} \right)^{1/2}} \right] \quad (\text{C-15})$$

where  $\sigma = D_e/2b^2$ ;  $\theta = t - x/v$ ;  $\gamma = D_e\bar{K}/b^2$ ;  $w = x/mv$ ;  $g = \gamma R_f$ . It should be noted that the expression  $x/v \geq 50mb^2/\bar{K}D_e$  is equivalent to  $\gamma w \geq 50$ .

#### Derivation of numerical criteria for assumption B2

For  $g/\gamma w =$  a constant  $>0$  and sufficiently large  $\gamma w$ , the argument of the error function in Eq. C-15 becomes  $[(2\sigma\theta/\gamma w) - 1]/2(g/\gamma w)^{1/2}$ , and at a given value of  $g/\gamma w$ ,  $\hat{C}$  depends only on the ratio  $\sigma\theta/\gamma w$ . It then can be seen by analogy with Rosen's discussion (39) that for  $\gamma w \geq 50$ , the shape of the breakthrough curve  $\hat{C}(\theta, w)$  is relatively unaffected by values of  $g/\gamma w \leq 0.01$ . This implies that a criterion for approximately cross-sectionally uniform concentrations in the flowing fluid would be  $g/\gamma w = R_f/w \leq 0.01$ , or  $x/v \geq 100 mR_f$ .

We can now obtain the criterion in terms of fundamental properties of the bulk rock from Equation (C-13). In general, at the interface between flowing fluid and bulk rock,  $\partial q/\partial t = -aD\partial C_i/\partial z$ . The term  $a$  is the interfacial area per unit volume of bulk rock;  $C_i$  the local radionuclide concentration, and  $C$  in Eqs. C-2 and C-3 should be defined more precisely here as the average value of  $C_i$  for the cross section of the joints. The term  $\partial C_i/\partial z$  generally monotonically decreases nonlinearly from its value at the fluid-rock interface to a value of zero at distance  $H/2$  from the interface. The value of  $\partial C_i/\partial z$  at the interface then would be at least twice the average value. We can obtain expressions for  $m$  and  $a$  in terms of  $b$  and  $H$  by referring to

Figure C-1b. For the bulk rock:

$$m = \frac{\epsilon}{1 - \epsilon} \cong \frac{H \cdot (2b)^2}{(2b)^3} = \frac{H}{2b} \quad (C-16)$$

$$a = \frac{\text{interfacial area}}{\text{unit volume}} \cong \frac{2 \cdot (2b)^2}{(2b)^3} = \frac{1}{b} = \frac{2m}{H} \quad (C-17)$$

If the average of  $-\partial C_i / \partial z$  is approximated by  $(C - q_s / \bar{K}) / (H/4)$ , then at the interface:

$$\partial C_i / \partial z \geq 2(C - q_s / \bar{K}) / (H/4) \quad (C-18)$$

$$\partial q / \partial t \geq 8aD(C - q_s / \bar{K}) / H = 16mD(C - q_s / \bar{K}) / H^2 \quad (C-19)$$

From Eq. C-13, if  $\lambda = 0$

$$\partial q / \partial t = (1/R_f)(C - q_s / \bar{K}) \geq 16mD(C - q_s / \bar{K}) / H^2 \quad (C-20)$$

therefore

$$mR_f \leq H^2 / 16D. \quad (C-21)$$

The criterion for approximately cross-sectionally uniform concentration in the flowing fluid can now be written as  $x/v \geq 100H^2/16D$  or  $x/v \geq 6H^2/D$ , which is identical to Eq. C-6.

Derivation of retardation factor for equivalent porous media and numerical criterion for assumption C2

The right side of Eq. C-15 is symmetrical about the value of  $\hat{C}/C_0 = 0.5$ . For a given value of  $t$ ,  $t_{0.01}$  is defined as the elapsed time required for  $\hat{C}/C_0$  to reach a value of 0.01, and  $t_{0.5}$ ,  $t_{0.99}$ , and  $\theta_{0.5}$  are defined analogously. For sufficiently small radionuclide concentrations gradients in the joints (i.e. Assumption C2),  $R_f \rightarrow 0$  and  $g = \gamma R_f \approx 0$ . From Eq. C-15 and appropriate values of the error function, therefore

$$\frac{t_{0.99} - t_{0.01}}{\theta_{0.5}} = \frac{6.6}{(3\gamma w)^{1/2}} \quad (\text{C-22})$$

and for  $\gamma w > 50$

$$\frac{t_{0.99} - t_{0.01}}{\theta_{0.5}} < 0.54$$

This implies that as  $\gamma w$  becomes large, the spread in the breakthrough curve becomes small relative to the distance its midpoint has traveled. This is because the time interval by which the value of  $\hat{C}/C_0 = 0.01$  precedes the value of  $\hat{C}/C_0 = 0.5$ , and the interval by which the value of  $\hat{C}/C_0 = 0.99$  trails, become small relative to  $\theta_{0.5}$  or  $(t_{0.5} - x/v)$ . For example, when  $\gamma w > 50$ , the intervals are about twenty-five percent or less of  $\theta_{0.5}$ . Furthermore, from Eq. C-15 when  $\hat{C}/C_0 = 0.5$ , the argument of the error function is equal to zero and  $2\theta_{0.5}/\gamma w = 1$ . Using the definitions in Table C-1 we obtain:

$$t_{0.5} = (1 + \bar{K}/m)x/v \quad (\text{C-23})$$

and if  $v_{0.5} = x/t_{0.5}$ , then:

$$v_{0.5} = v/(1 + \bar{K}/m). \quad (\text{C-24})$$

and

$$R_j = \frac{v}{v_{0.5}} = 1 + \bar{K}/m \quad (\text{C-25})$$

which is equivalent to Eq. C-11. Therefore, as  $\gamma w$  becomes large,  $\hat{C}(x,t)$  approaches  $\hat{C}(0,t - R_j x/v)$  and  $C(z,t)$  approaches  $e^{-\lambda t} \hat{C}(0,t - R_j x/v)$ , which is the solution to the corresponding form of Eq. C-1.

$$\frac{\partial C}{\partial t} + \frac{v}{R_j} \frac{\partial C}{\partial x} = - \frac{\lambda}{R_j} C \quad (C-26)$$

Due to the inherent uncertainties associated with analyses of radionuclide transport in geologic media, a 27% spread in the value of  $C$  about  $t_{0.5}$  probably is not serious, and values of  $\gamma w \geq 50$  should be sufficiently large for Eqs. C-12 to C-14 to be approximated by Eq. C-26. Furthermore, the criterion  $\gamma w \geq 50$ , or  $x/v \geq 50 \text{mb}^2 / \overline{KD}_e$ , is the same as that given by Eq. C-7 for approximate local sorption equilibrium between bulk phases.

#### C.5. Discussion

##### Application of equivalent porous medium criteria to the hypothetical tuff site.

The criteria described for Assumptions B2 and C1 (Equations C-6 and C-7 respectively) were evaluated for the welded tuff units of the hypothetical repository site. Equation C-7 can be written in terms of the parameters listed in Tables 2 and A-1 as

$$x/v > 50 \cdot (1/N^2 D) \cdot (\alpha^2 / \phi) \cdot (\epsilon / 1 - \epsilon) = A_3 \quad (C-27)$$

where:

- D = ionic diffusion constant
- $\alpha$  = tortuosity
- x = path length in fractured media
- v = Darcy velocity  $\div$  fracture porosity
- $\phi$  = matrix porosity of unfractured blocks
- $\rho$  = grain density of rock
- $\epsilon$  = fracture porosity =  $2NH$  for our system where  
N = fracture density; H = fracture aperture

The criterion was evaluated for densely and moderately welded tuff units, for individual beds as well as for the entire welded tuff thickness. The maximum, median and minimum values of the ranges used for the LHS input variables were used to evaluate the term ( $A_3$ ). The results are presented in Table C-2.

Table C-2

	<u><math>A_3</math> max</u>	<u><math>A_3</math> min</u>	<u><math>A_3</math> median</u>
x	200 ft	200 ft	100 ft
$\epsilon$	$6.4 \times 10^{-3}$	$8.8 \times 10^{-6}$	$1.3 \times 10^{-4}$
$\phi$	0.03	0.10	0.06
N	6.5 ft <sup>-1</sup>	0.27 ft. <sup>-1</sup>	1.6 ft. <sup>-1</sup>
K	60 ft/day	$4 \times 10^{-5}$ ft/day	4.2 ft/day
i	$4 \times 10^{-2}$	$1 \times 10^{-2}$	$2 \times 10^{-2}$
v	375 ft/day	0.045 ft/day	0.646 ft/day
x/v	0.533 day	$4.4 \times 10^3$ day	155 day
$A_3$	0.19 day	0.045 day	0.031 day

where:

i = vertical hydraulic gradient

D =  $10^{-5}$  cm<sup>2</sup>/sec =  $3.39 \times 10^{-1}$  ft<sup>2</sup>/yr

$\alpha$  = 1.0

K = hydraulic conductivity in LHS range for densely welded units

v =  $iK/\epsilon$

It can be seen from these calculations that the criterion  $x/v \geq A_3$  holds for the conditions encountered at the tuff site.

The criterion in equation C-6 can also be evaluated from the above data. The condition  $x/v \geq 6H^2/D$  is equivalent to  $x/v \geq 0.6$  sec. when an average aperture with H of 10 microns and  $D=10^{-5}$  cm<sup>2</sup>/sec are assumed. The values of fluid residence time  $x/v$  listed in Table C-2 all exceed this value. Therefore both of the criteria required for the equivalent porous media are met for the hypothetical tuff site.

### SUMMARY

If the criteria given by Eqs. C-6 and C-7, for approximately cross-sectionally uniform radionuclide concentrations in the flowing fluid and bulk rock are satisfied, then radionuclide transport in jointed porous rock can be approximated as occurring in equivalent porous media. Flow can be described by the appropriate form of Eq. C-1, where the retardation factor is given by Eq. C-10 to C-11. The criteria and retardation factor are given in terms of fundamental physical and chemical parameters. Those which can be evaluated in the laboratory include the radionuclide diffusion coefficient D for dilute aqueous solution, the distribution coefficient  $K_d$  for sorption equilibrium between pore water and mineral phases, the tortuosity factor  $\alpha$ , grain density  $\rho_s$ , and porosity  $\phi$  of the bulk rock. Parameters which must be evaluated from field data include the joint spacing  $2b$  and aperture H, average fluid velocity  $\bar{v}$ , and porosity  $\epsilon$  associated with the joints. The last parameter is determined from joint aperture, orientation, and spacing.

In terms of parameters evaluated from laboratory data, the distribution coefficient  $K_d$  and the ratio  $D/\alpha^2$  generally dominate Eqs. C-7 and C-10 and also involve the greatest uncertainties. For very porous rock and for chemically-simple radionuclides, evaluation of  $K_d$  and  $D/\alpha^2$  is not difficult. However, for rock having very "tight" porosity and (or) for chemically-complicated radionuclides, much laboratory and analytical work is required to determine appropriate "effective" values. In terms of parameters obtained from field data, Eqs. C-6, C-7, and C-10 are most sensitive to joint aperture H, joint spacing  $2b$ , and porosity  $\epsilon$ . Evaluation of H inherently involves considerable uncertainty, which correspondingly affects evaluation of  $\epsilon$ . Evaluation of the average fluid velocity  $\bar{v}$  involves many uncertainties which can substantially affect use of Eqs. C-6 and C-7.

## REFERENCES

1. Spengler, R. W., Muller, D. C., and Livermore, R. B., Preliminary Report on the Geology and Geophysics at Drill Hole UE25a-1 Yucca Mountain, Nevada Test Site. U. S. G. S. Open File Report 79-1244, 1979.
2. Sykes, M. L., Heiken, G. H., and Smyth, J. R., Mineralogy and Petrology of Tuff Units from the UE25a-1 Drill Site, Yucca Mountain, Nevada, Los Alamos National Laboratory Report LA-8139-MS, 1979.
3. Johnstone, J. K., and Wolfsberg, K. eds., Evaluation of Tuff as a Medium for a Nuclear Waste Repository: an Interim Status Report on the Properties of Tuff, Sandia National Laboratories Report SAND80-1464, 1980.
4. Winograd, I. J. and Thordarson, W., Hydrogeologic and Hydrochemical Framework, South-Central Great Basin, Nevada-California, with Special Reference to the Nevada Test Site, U. S. G. S. Prof. Pap. 712-C, 1975.
5. Wolfsberg, K., Sorption-Desorption Studies of Nevada Test Site Alluvium and Leaching Studies of Nuclear Test Debris, Los Alamos Scientific Laboratory Report LA-7216-MS, 1978.
6. Wolfsberg, K., Bayhurst, B. P. and others, Sorption-Desorption Studies on Tuff I. Initial studies with samples from the J-13 Drill Site, Jackass Flats, Nevada, Los Alamos Scientific Laboratory Report LA-7480-MS, 1979.
7. Vine, E. N., Aguilar, R. D. and others, Sorption-Desorption Studies on Tuff II. A continuation of studies with samples from Jackass Flats, Nevada, and initial studies with samples from Yucca Mountain, Nevada, Los Alamos Scientific Laboratory Report LA-8110-MS, 1980.
8. Erdal, B. R., Daniels, W. R. and Wolfsberg, K., eds., Research and Development related to Nevada Nuclear Waste Storage Investigations, January 1 - March 31, 1981, Los Alamos Scientific Laboratory Report LA-8847-PR, 1981.

9. Wolfsberg, K., Aguilar, R. D. and others, Sorption-Desorption Studies on Tuff III. A continuation of studies with samples from Jackass Flats and Yucca Mountain, Nevada, Los Alamos National Laboratory Report LA-8747-MS, 1981.
10. Erdal, B. R., Daniels, W. R., Vaniman, D. T. and Wolfsberg, K., Research and Development related to the Nevada Nuclear Waste Storage Investigations, April 1 - June 30, 1981, Los Alamos National Laboratory Report LA-8959-PR, 1981.
11. Guzowski, R. V., Nimick, F. B. and Muller, A. B., Repository Site Definition in Basalt: Pasco Basin, Washington, Sandia National Laboratories Report, SAND81-2088, NUREG/CR-2352, 1982.
12. Wolfsberg, K., Daniels, W. R., Erdal, B. R. and Vaniman, D. T., Research and Development Related to the Nevada Nuclear Waste Storage Investigations, April 1 - June 30, 1982, Los Alamos National Laboratory Report LA-9484-PR, 1982.
13. Letter From F. Nimick, Sandia National Laboratories, to L. Rossbach, NRC, Subject: Preliminary calculations of solubilities of radionuclides in basalt groundwaters, dated April 27, 1982. Available in NRC PDR for inspection and copying for a fee.
14. Rai, D and Serne, R. J., Solid Phases and Solution Species of Different Elements in Geologic Environments, Battelle, Pacific Northwest Laboratories Report PNL-2651, 1978.
15. Wood, B. J. and Rai, Dhanpat, Nuclear Waste Disposal: Actinide Migration from Geologic Repositories, Battelle, Pacific Northwest Laboratories Report PNL-SA-9549, 1981.
16. Muller, A. B., Finley, N. C. and Pearson, F. J., Geochemical Parameters used in the Bedded Salt Reference Repository Risk Assessments Methodology, Sandia National Laboratories Report, SAND81-0557, NUREG/CR-1996, 1981.

17. Campbell, J. E., Longsine, D. E. and Cranwell, R. M., Risk Methodology for Geologic Disposal of Radioactive Waste: The NWFT/DVM Computer Code Users Manual, Sandia National Laboratories Report SAND81-0886, November 1981.
18. Iman, R. L., Davenport, J. M. and Zeigler, D. M., Latin Hypercube Sampling (Program Users Guide), Sandia National Laboratories Report SAND79-1475, January, 1980.
19. Environmental Protection Agency. "Environmental Radiation Protection Standards for Management and Disposal of Spent Nuclear Fuel, High-Level and Transuranic Radioactive Wastes," Working Draft #19 40CFR191. Available in NRC PDR for inspection and from the EPA.
20. Cranwell, R. M., and others, Risk Methodology for Geologic Disposal of Radioactive Waste: Final Report, Sandia National Laboratories Report SAND81-2573, NUREG/CR-2452, December 1982.
21. Rush, F. E., Regional Ground-Water Systems in the Nevada Test Site area, Nye, Lincoln, and Clark Counties, Nevada: Nevada Department of Conservation and Natural Resources, Water Resources - Reconnaissance Series Report 54, 1970.
22. Reade, M. T. and McKay, E. D. Geology and Hydrology of Yucca Mountain and Vicinity, Nevada Test Site, CGS/8116R028, C.G.S., Inc., Urbana, Illinois 61801, 1982.
23. Pepping, R. E., Chu, M. S. and Siegel, M. D., A Simplified Analysis of a Hypothetical High-Level Waste Repository in a Basalt Formation, Sandia National Laboratories Report, SAND82-1557, NUREG/CR-3235, v. 2, 1982.
24. Freeze, R. A. and Cherry, J. A., Groundwater, Prentice-Hall Inc., Englewood Cliffs, N.J., 1979.
25. Guzowski, R. V., Nimick, F. B., Siegel, M. D. and Finley, N. C., Repository Site Definition in Tuff: Yucca Mountain, Nevada, Sandia National Laboratories Report SAND82-2105, NUREG/CR-2937, to be published.

26. Merkin, J. H., Free Convection Boundary Layers on Axi-Symmetric and Two-Dimensional Bodies of Arbitrary Shape in a Saturated Porous Medium, *Int. J. Heat Mass Transfer*, v. 22, pp. 1461-1462, 1979.
27. Interim Reference Repository Conditions for Spent Fuel and Commercial High Level Nuclear Waste Repositories in Tuff. Battelle Project Management Division (ONW1) NWTS-12, September 1981.
28. White, A. F., Claassen, H. C. and Benson, L. V., The Effect of Dissolution of Volcanic Glass on the Water Chemistry in a Tuffaceous Aquifer, Rainier Mesa, Nevada, Geological Survey Water-Supply Paper 1535-Q, 1980.
29. Winograd, I. J. and Robertson, F. N., Deep Oxygenated Ground Water Anomaly or Common Occurrence?, *Science*, v. 216, pp. 1227-1230, 1982.
30. Allard, B., Solubilities of Actinides in Neutral or Basic Solutions, in *Proceedings of the Actinides 1981 Conference*: Oxford, Pergamon Press, 1982.
31. Letter from J. Serne, Battelle Pacific Northwest Laboratories, to A. Muller, Sandia National Laboratories, Subject: Sorption Data for Radionuclides in Basalt Ground-Water Systems, dated May 13, 1981. Available in NRC PDR for inspection and copying for a fee.
32. Baes, C. F. and Mesmer, R. E. *The Hydrolysis of Cations*, Wiley Interscience, John Wiley and Sons, New York, N. Y., 1976.
33. Daniels, W. R., Erdal, B. R., Vaniman, D. T., Wolfsberg, K., Research and Development Related to the Nevada Nuclear Waste Storage Investigations, January 1 - March 31, 1982, Los Alamos National Laboratory Report LA-9327, 1982.
34. Erickson, K. L., Preliminary Rate Expressions for Analysis of Radionuclide Migration Resulting from Fluid Flow Through Jointed Media, *Scientific Basis for Nuclear Waste Management, Volume 2*: New York, Plenum Press, p. 729-738, 1980.

35. Erickson, K. L., Fundamental Approach to the Analysis of Radionuclide Transport Resulting from Fluid Flow Through Jointed Media, Sandia National Laboratories Report SAND80-0457, 1981.
36. Erickson, K. L., Approximations for Adapting Porous Media Radionuclides Transport Models to Analysis of Transport in Jointed Porous Rock, Scientific Basis for Nuclear Waste Management, Volume 6: in press.
37. Crank, J., The Mathematics of Diffusion (2nd ed.). Oxford, Clarendon Press, pp. 49-53, 1975.
38. Rosen, J. B., Kinetics of a Fixed Bed System for Solid Diffusion into Spherical Particles: Jour. Chem. Phys., v. 20, no. 3, pp. 387-393, 1952.
39. Rosen, J. B., General Numerical Solution for Solid Diffusion in Fixed Beds: Ind. Eng. Chem., v. 46, pp. 1590, 1954.

**Volume 4**

**A Simplified Analysis of a Hypothetical Repository  
in a Bedded Salt Formation**



NUREG/CR-3235  
SAND82-1557  
WH

TECHNICAL ASSISTANCE FOR REGULATORY DEVELOPMENT:  
REVIEW AND EVALUATION OF THE DRAFT EPA STANDARD 40CFR191  
FOR DISPOSAL OF HIGH-LEVEL WASTE

VOL. 4

A SIMPLIFIED ANALYSIS OF A HYPOTHETICAL REPOSITORY  
IN A BEDDED SALT FORMATION

R. E. Pepping  
M. S. Chu  
M. D. Siegel

Manuscript Completed: April 1983  
Date Published: April 1983

with contributions from:  
Pei-Lin Tien\*  
Adel A. Bakr\*

Sandia National Laboratories  
Albuquerque, New Mexico 87185  
operated by  
Sandia Corporation  
for the  
U. S. Department of Energy

Prepared for  
Division of Waste Management  
Office of Nuclear Material Safety and Safeguards  
Washington, D. C. 20555

NRC FIN. No. A-1165

\*Science Applications, Inc.

## ABSTRACT

An analysis of a hypothetical nuclear waste repository in a bedded salt formation has been performed to demonstrate the application of existing analytical tools to the assessment of compliance of the repository with the draft EPA Standard, 40CFR191 (Draft #19). The tools have been developed by Sandia National Laboratories for use by NRC in such analyses. The hypothetical site is based on data that are representative of bedded salt geologies in the continental U.S. The effects of uncertainty in the input data on the assessment of compliance are demonstrated. Other sources of uncertainty resulting from interpretation of the standard and its probabilistic nature are discussed. The results of the calculations presented indicate that compliance with the draft standard may be achieved for the groundwater transport scenarios depending on which source model is used. The penetration scenarios (direct canister hit or brine pocket hit) indicate potentially serious consequences; however, these could be mitigated by proper site selection and institutional controls.

## Table of Contents

	Page
I. Introduction .....	1
II. The Draft EPA Standard .....	2
III. Sequence of Discussion .....	4
IV. The Hypothetical Repository .....	5
V. Radionuclide Release Scenarios and Probabilities .....	16
VI. Computer Models (NWFT/DVM) Used for Groundwater Transport Scenarios .....	28
A. The GroundWater Transport Scenarios (NWFT/DVM) .....	28
B. Penetration Scenarios .....	38
C. Construction of the CCDFs .....	40
D. Sensitivity Analysis Results .....	56
VII. Conclusions .....	58
Appendix A. The Mixing Cell Source Model (Source #3) .....	A-1
Appendix B. Geohydrologic Data for Bedded Salt...	B-1
References .....	R-1

## Figures

	Page
1. General Setting of the Bedded Salt Reference Site (Plan View) .....	6
2. Schematic Cross-Sections Across the Subbasin .....	8
3. Floor Plan of the Reference Underground Facility .....	13
4. The U-Tube Flow and Migration Pattern for the Groundwater Transport Scenario .....	18
5. Scenario 2 Geometry .....	22
6. Reference Area, $A_m$ , Containing M Spherical Brine Pockets.....	27
7. Flow and Transport Network Assumed by NWFT/DVM .....	29
8. CCDF for Scenario 5, Direct Hit Scenario .....	42
9. CCDF for the Brine Pocket Penetration Scenario .....	45
10. CCDFs for the Groundwater Transport Scenario With Source #1 .....	46-48
11. CCDFs for the Groundwater Transport Scenario With Source #2 .....	49-51
12. CCDFs for the Groundwater Transport Scenario With Source #3 .....	52-54
A-1 Implementation of the Mixing Cell Source Model for NWFT/DVM .....	A-3

Tables

	Page
1. Release Limits in the Draft EPA Standard .....	3
2. Stratigraphic Units, Lithology, and Thickness of Hypothetical Bedded Salt Repository Site .....	9-10
3. Hydraulic Properties of Geologic Units, Bedded Salt Site .....	12
4. Radionuclide Inventories (Ci) at Time of Closure (t=0) .....	15
5. Lengths and Elevations Corresponding to Figure 7 for the Groundwater Transport Scenarios .....	30
6. Hydraulic Properties and Sampled Distributions .....	31
7. NWFT/DVM Source Models .....	34
8. Sorption Data, Bedded Salt Site .....	35
9. Solubility Limits of Various Radionuclides ...	37
10. Repository Hazard Index .....	38
11. Probabilities (per 10,000 yr) and Consequences for the "Direct Hit" Scenario .....	41
12. Probabilities (per 10,000 yr) and Consequences for the Brine Pocket Scenario .....	44
B-1 $R_d$ Ranges in Aquifer (Bedded Salt) .....	B-1
B-2 Bedded Salt Hydraulic Parameters .....	B-2

## Tables

	Page
1. Release Limits in the Draft EPA Standard .....	3
2. Stratigraphic Units, Lithology, and Thickness of Hypothetical Bedded Salt Repository Site .....	9-10
3. Hydraulic Properties of Geologic Units, Bedded Salt Site .....	12
4. Radionuclide Inventories (Ci) at Time of Closure ( $t=0$ ) .....	15
5. Lengths and Elevations Corresponding to Figure 7 for the Groundwater Transport Scenarios .....	30
6. Hydraulic Properties and Sampled Distributions .....	31
7. NWF/DVM Source Models .....	34
8. Sorption Data, Bedded Salt Site .....	35
9. Solubility Limits of Various Radionuclides ...	37
10. Repository Hazard Index .....	38
11. Probabilities (per 10,000 yr) and Consequences for the "Direct Hit" Scenario .....	41
12. Probabilities (per 10,000 yr) and Consequences for the Brine Pocket Scenario .....	44

## I. Introduction

### Background

The Environmental Protection Agency (EPA) has drafted a standard for protection against highly radioactive wastes to be stored underground. The standard, which will apply to all geologic repositories, is still being developed and an internal working draft is available [1]. The Nuclear Regulatory Commission (NRC) will enforce the standard, and is developing appropriate Federal regulations [2].

To assign quantitative, that is, numerical values to such factors as release of radionuclides from a geologic repository, the EPA used simple computer models [3]. The agency expects the NRC to use computer modeling to assess compliance with the EPA Standard. To support NRC, Sandia National Laboratories (SNL) is developing computer models that may be used in such a compliance assessment [4]. We expect that NRC will use the models to evaluate applications for license to construct actual repositories.

The Department of Energy (DOE) is also involved in that it selects actual sites for geologic repositories and submits applications to construct them. To determine their suitability for waste disposal, the DOE is investigating basalt and tuff flows, bedded salt and granite formations, and salt domes. Some of these geologic formations are being characterized, but no specific sites have yet been selected. Neither are they modeled in enough detail to evaluate any given site to the rigorous compliance requirements set down by the draft EPA Standard. However, whatever information does exist can be supplemented with general information taken from such sources as similar formations or host-rock descriptions, hydraulic properties, and geochemical characteristics. We can then apply the models thus developed to evaluate a similar but hypothetical repository. Using the capability of SNL models as a base, we then determine how well the hypothetical site meets the draft EPA Standard: does it comply?

### Scenarios

To select scenarios for detailed analysis, we used the results of risk analysis methods development programs at SNL [5]. In that work a number of scenarios were identified that may be important in understanding risks from real repositories. Most of those scenarios involved flowing groundwater intruding into the backfilled regions of the repository. Various water-bearing geologic strata were

the sources of groundwater as well as potential paths for migrating radionuclides.

After considering the previous scenario development efforts and the details of the repository (discussed below), we chose two types of scenarios: groundwater transport and penetration. In the first type of scenario, radionuclides are presumed to be released at low rates over an extended period. Radionuclides are transported to the accessible environment by the natural, or slightly perturbed, groundwater flow system. In penetration scenarios, radionuclides are transported rapidly to the accessible environment over a short period.

## II. The Draft EPA Standard

The EPA assumes that natural or man-induced disruptions will cause the repository to release some radionuclides and that they will find their way to the accessible environment.\* In Draft #19 of its standard, the EPA sets the limits for total integrated discharges that may be expected from such disruptions (Equation (1)):

$$\text{EPA Sum} = \sum_i \frac{Q_i}{\text{EPA}_i} \quad (1)$$

where:  $Q_i$  = total integrated release of radionuclide  $i$   
 $\text{EPA}_i$  = release limit for radionuclide  $i$ .

The sum over  $i$  includes all radionuclides present in the waste. The proposed release limits are listed in Table 1.

A more detailed discussion of the draft EPA Standard, its interpretations and implementation in assessing compliance are presented elsewhere [6,7].

\*The accessible environment is "any location on the surface where radionuclides may be released or any aquifer that may be contaminated by radionuclides at a distance of 1 mile from the perimeter of the underground facility."

Table 1

Release Limits in the Draft EPA Standard

Radionuclide	Release Limit
Americium-241 - - - - -	10
Americium-243 - - - - -	4
Carbon-14 - - - - -	200
Cesium-135 - - - - -	2000
Cesium-137 - - - - -	500
Neptunium-237 - - - - -	20
Plutonium-238 - - - - -	400
Plutonium-239 - - - - -	100
Plutonium-240 - - - - -	100
Plutonium-242 - - - - -	100
Radium-226 - - - - -	3
Strontium-90 - - - - -	80
Technetium-99 - - - - -	2000
Tin-126 - - - - -	80
Any other alpha-emitting radionuclide - - - - -	10
Any other radionuclide which does not emit alpha particles - - - - -	500

### III. Sequence of Discussion

Below we will discuss our findings as follows:

1. Description of the hypothetical repository --
  - rock types found at the site
  - hydraulic properties of the rock formations
  - properties of any aquifers
  - sizes of various formations,
2. Scenarios -- such situations or potential states of the repository that may lead to release of radionuclides -- and their probabilities of occurrence,
3. Models -- description and details of their application to this analysis,
4. Required geochemical data,
5. Quantitative data -- numerical results from this analysis: how much, when, how long?

As we discuss our findings, we are assuming that the reader is familiar with the problems of disposal of radioactive wastes and the methods developed at SNL to address them.

#### IV. The Hypothetical Repository

If we are to use the SNL models to verify compliance with the draft EPA Standard, we need a description of the repository to be licensed. The description should include the geologic, hydrologic, and geochemical properties of the site; the shape, size, and layout of the engineered underground facility; and the nature of the nuclear waste.

##### Bedded Salt Site

The bedded salt repository site is located in a subsidiary basin within a major sedimentary basin. The crust of the region sank, allowing sediments to accumulate. Beginning 300 million years ago, within this depressed region, small blocks of the crust were displaced along deep-seated faults, creating a system of subbasins separated by basement uplifts. The subbasin where the site is located (Figure 1) is bounded on the north by Uplift A and on the south by Arch M. River C, approximately 40 to 50 miles to the north, flows eastward. A small river, River R, about 25 miles to the east, flows northwest to southeast. The uplift and the arch are bounded by high-angle reverse faults that steepen with depth, indicating that the subbasin is a block of crust that was uplifted with respect to surrounding regions. The subbasin is situated within a tectonically stable region that is associated with a shield area to the north. Several faults strike northwest just south of the uplift, but the rest of the subbasin lacks evidence of faulting or volcanism.

Current seismicity in the region is localized along the uplift, which is the dominant structural feature and the focus of any seismic energy release; most earthquakes in the area have foci in the basement. In the past, only a few earthquakes with intensities between V and VI on the Modified Mercalli Intensity Scale have been registered, and none with destructive intensities of VII and above. Accordingly, this region is in Zone 1 on a seismic-risk map, which means that minor earthquake damage may be expected in the next 100 years. However, the level of shaking hazards is expected to be less than  $0.04g$ , where  $g$  is the acceleration due to gravity.

Active subsurface dissolution is evident along the northern and eastern margins of the subbasin; collapse features such as sinkholes, depressions, small faults, and fractures are common within the salt dissolution zone, which is at least 10 miles from the site. The mean rates of salt dissolution range from 19 feet (6 m) to 1150 feet

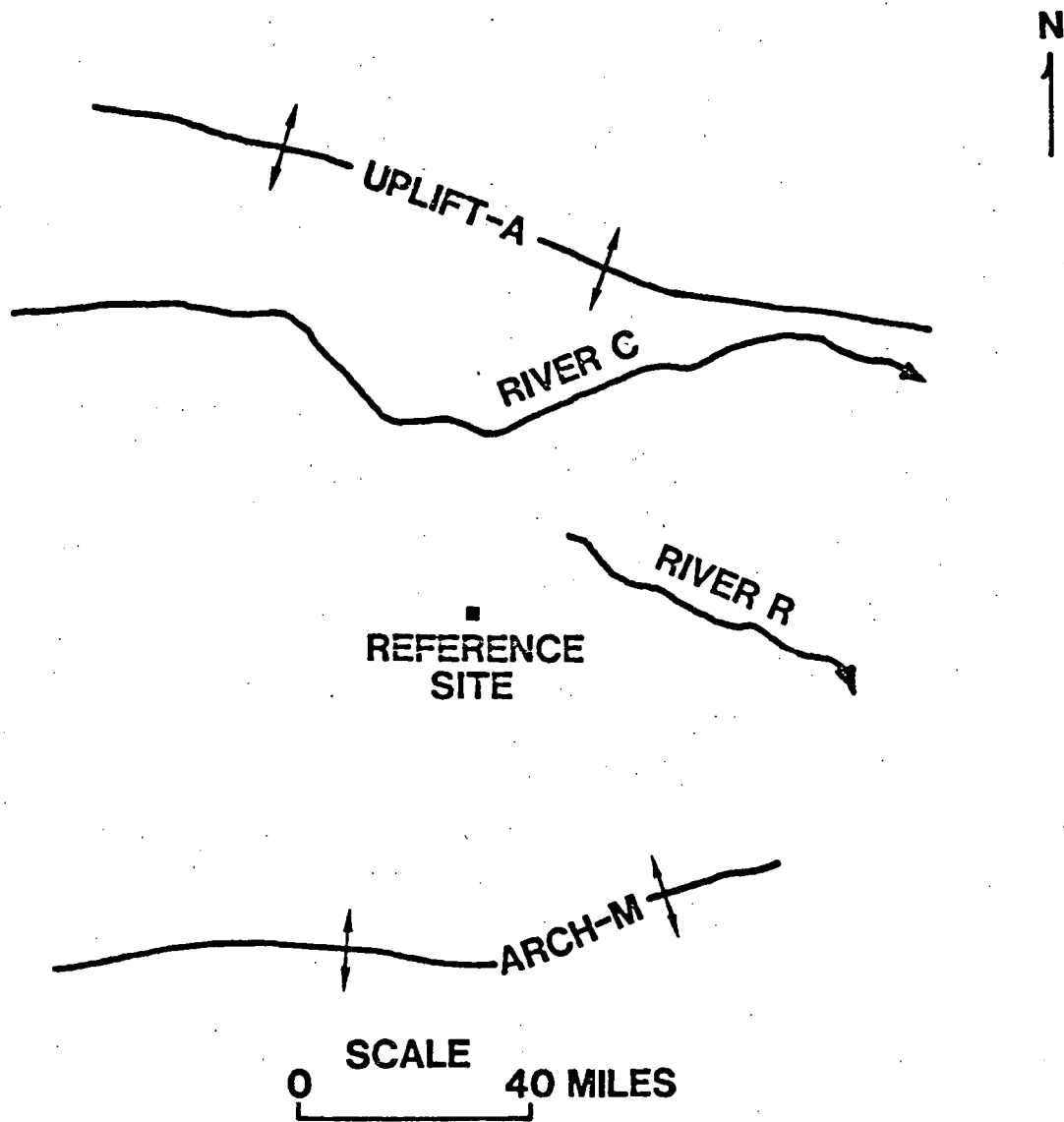


Figure 1. General Setting of the Bedded Salt Reference Site (Plan View).

(350 m) per 10,000 years. Salt dissolution along the north side is slower than along the east side of the subbasin.

The subbasin is a relatively shallow, continental-interior basin. The Precambrian basement is at most, 10,000 feet below the surface. The repository is located in the center of Unit SA (Figure 2), which consists of 1,000 to 1,200 feet of evaporites, mainly halite with small amounts of anhydrite and dolomite (Table 2). Unit SA is overlain by Unit PSA, which ranges in thickness from 550 to 850 feet and consists of siltstone, sandstone, salt and anhydrite. Unit PSA is an aquitard slowing the downward movement of groundwater. Overlaying the PSA unit is 300 to 900 foot-thick Unit D, which consists of sand and clay, and is a minor aquifer. Unit O, which overlays Unit D, is between 50 to 300 feet thick and is the major unconfined aquifer in the area. The major constituents of Unit O are sand and clay, with small amounts of gravel and some caliche that thinly covers the surface.

Below Unit SA is Unit CF, which ranges from 1,750 to 2,050 feet in thickness and is composed predominantly of halite, anhydrite, and clay. CF is also an aquitard. Below Unit CF is Unit WP, which is from 2,300 to 4,200 feet thick and consists mainly of shale, limestone, and sandstone. This unit, which is brine-saturated, is considered an aquifer but with such low conductivity that no pumping at all takes place.

Geochemical analyses of shale samples from Unit WP show an average total organic carbon content of 2.4 percent. The sediments of the layers deposited after Unit WP show a total organic carbon content of up to 5.38 percent. Kerogen color, which indicates thermal maturity when plotted against kerogen type, shows that samples from this unit are in transition between maturity and immaturity, and that those of post Unit WP never reached temperatures high enough to generate hydrocarbons. This means that, since the site is away from any potential hydrocarbon reservoir, intensive exploration and drilling will not likely take place within the area.

About 50 miles west of the site, the shallow aquifers (Units O and D), are recharged at a rate of between 0.2 and 1.0 inch/year, but discharge along the eastern margin of the subbasin. In these aquifers, the groundwater flows slowly from west to east, several inches to a few feet per year. Flow in the overlying aquifers is driven by gravity. The aquifer Units O and D dip over a range of 10 to 50 feet

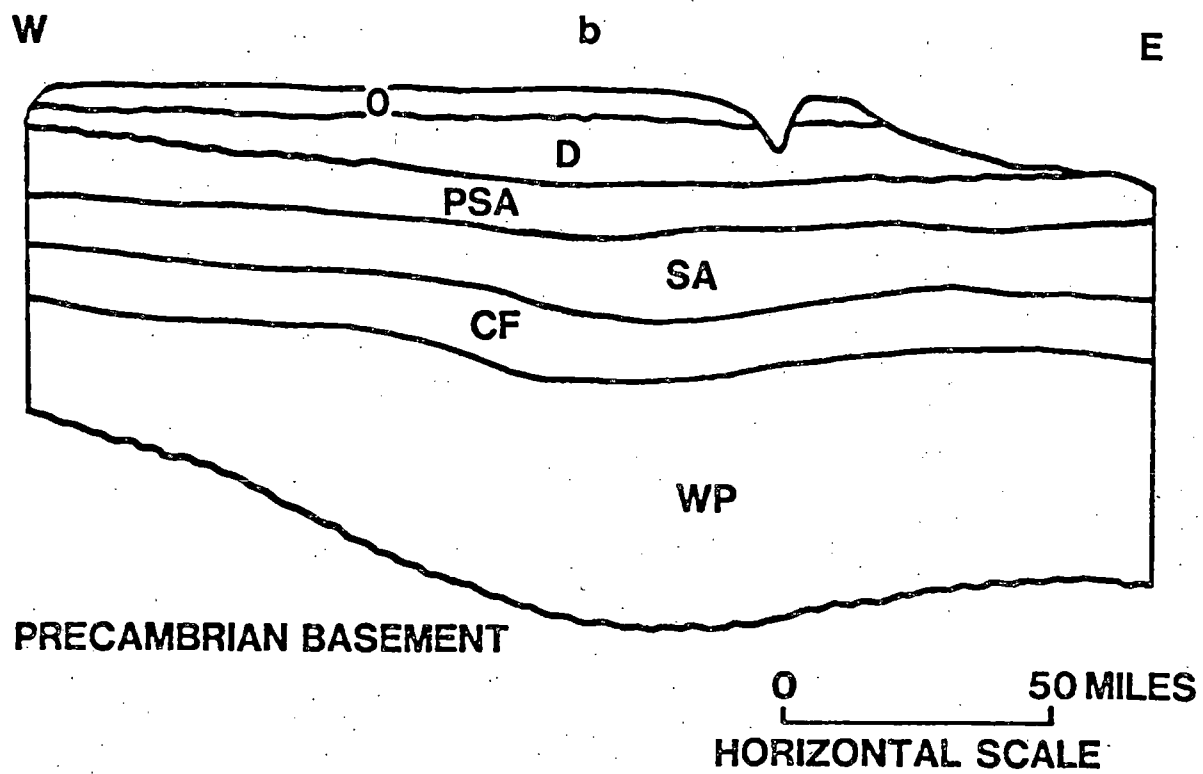
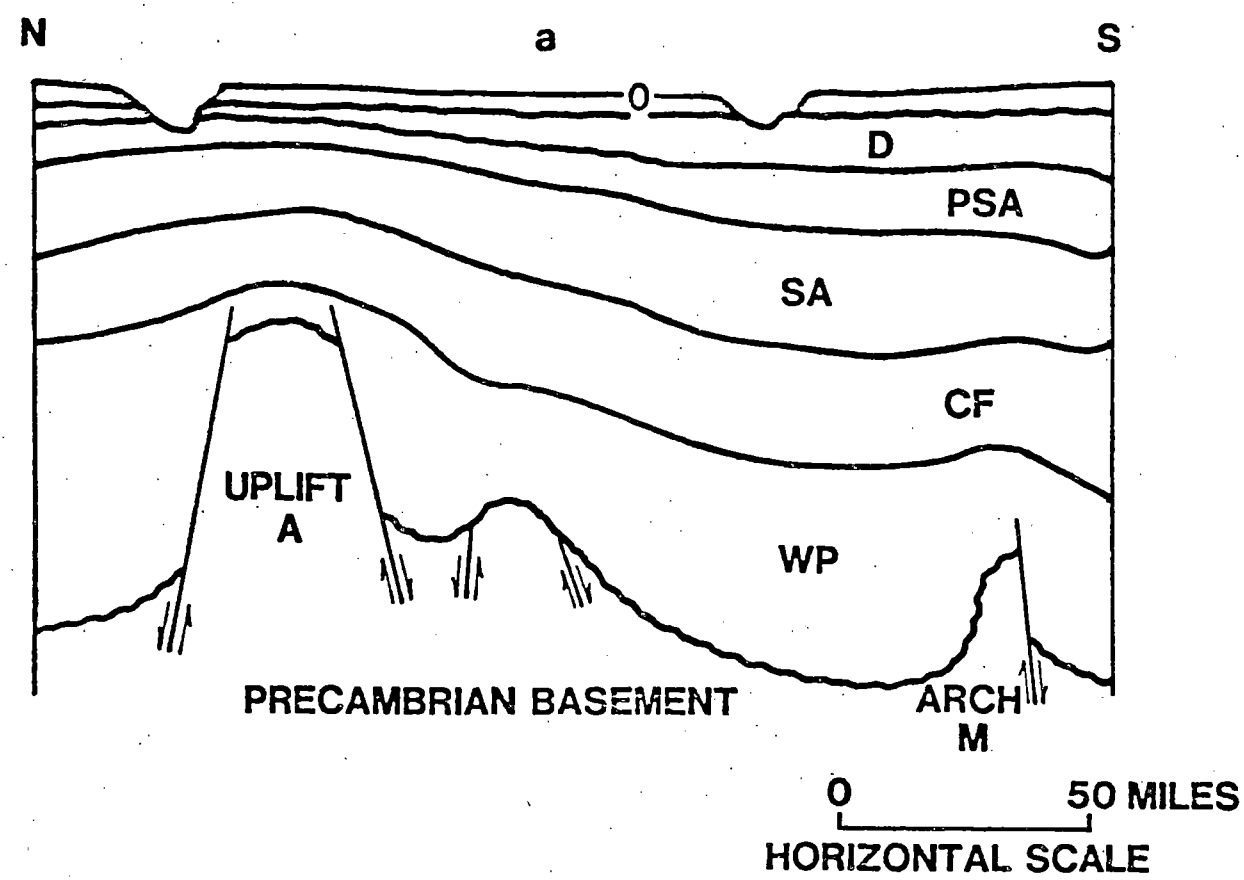


Figure 2. Schematic Cross-Sections Across the Subbasin.

Table 2

Stratigraphic Units, Lithology, and Thickness of  
Hypothetical Bedded Salt Repository Site

Unit	Thickness (Ft)	Lithology	% Thickness
O	50 - 300	silt clay	45
		sand gravel	50
		caliche	< 5
D	300 - 900	shale clay	30
		siltstone	7
		sandstone conglomerate	60
		limestone	< 3
PSA	550 - 850	anhydrite	7
		claystone	8
		salt	23
		mudstone	22
		siltstone	28
		sandstone	12

(cont'd)

Table 2 (Cont'd)

Stratigraphic Units, Lithology, and Thickness of  
Hypothetical Bedded Salt Repository Site

Unit	Thickness (Ft)	Lithology	% Thickness	
SA	1000 - 1200	dolomite	13	
		anhydrite	22	
		claystone	5	
		salt	59	
		mudstone	}	< 1
		siltstone		
		sandstone		
CF	1750 - 2050	dolomite	< 5	
		anhydrite	20	
		claystone	15	
		salt	50	
		mudstone	5	
		siltstone	5	
		sandstone	< 1	
WP	2300 - 4200	limestone	55	
		sandstone	9	
		claystone shale	}	36

per mile. This results in a head gradient of 2 to  $10 \times 10^{-3}$  driving horizontal flow within Units O and D. Vertical gradients in Units O and D are downward and small in magnitude. The dispersivity of Units O and D is small, less than 100 feet, and typically tens of feet.

Unit WP recharges very slowly -- much slower than the shallow aquifers -- a few hundred miles west of the site and discharges several hundred miles southeast of the subbasin. The briny groundwater in this unit flows slowly, mostly from west to east, at a rate of a few inches per year. Its hydraulic gradient varies between 10 and 30 feet/mile, i.e., from 2 to  $6 \times 10^{-3}$ . The vertical hydraulic gradient in this unit, however, is steep (about 1), and is directed upward.

Table 3 lists ranges of horizontal and vertical hydraulic conductivities and porosities for each unit. Values of conductivities for the O and D units mean that approximately 50 percent of conductivity measurements made in these units would fall in the given range. For the remaining units, the values indicate that 85 percent of the measurements would fall in the given range.

#### Engineered Underground Facility

The DOE has conceived a design for a subsurface facility where nuclear wastes can be emplaced [8-10]. We will use this facility for our analyses. Since the facility has already been described elsewhere [11], we will present only the few gross features that are important to our analyses. The reader is cautioned that the repository being modeled is hypothetical.

Dimensions -- The mined repository, which is located at a depth of 2,300 feet, has a storage area that extends over a 3,000-acre rectangular area (15,370 ft by 8,600 ft). A shaft pillar area extends 2,000 feet horizontally away from the waste storage area, the "panhandle" area shown in Figure 3.

Each storage room in the design is 4,000 feet (long) by 17.5 feet (wide) by 19 feet (high). For our calculations, we will assume the height to be 15 feet to account for creep closure that takes place over the operational life of the repository. The central corridors, which are 18.5 feet (wide) by 19 feet (high), will also be calculated as being 15 feet (high).

Table 3

Hydraulic Properties of Geologic Units,  
Bedded Salt Site\*

Unit	Horizontal Hydraulic Conductivity (ft/d)	Vertical Hydraulic Conductivity (ft/d)	Porosity (dimensionless)
O	4 - 25	0.4 - 3	0.1 - 0.2
D	0.4 - 2.5	0.04 - 0.25	0.05 - 0.1
PSA	$10^{-5}$ - $10^{-2}$	$10^{-6}$ - $10^{-3}$	0.01 - 0.05
SA	$10^{-7}$ - $10^{-3}$	$10^{-8}$ - $10^{-4}$	0.001 - 0.01
CF	$10^{-6}$ - $10^{-3}$	$10^{-7}$ - $10^{-4}$	0.005 - 0.05
WP	$10^{-5}$ - $10^{-2}$	$10^{-6}$ - $10^{-3}$	0.01 - 0.05

\* Please refer to Table B-2 in Appendix B for original source and reference.

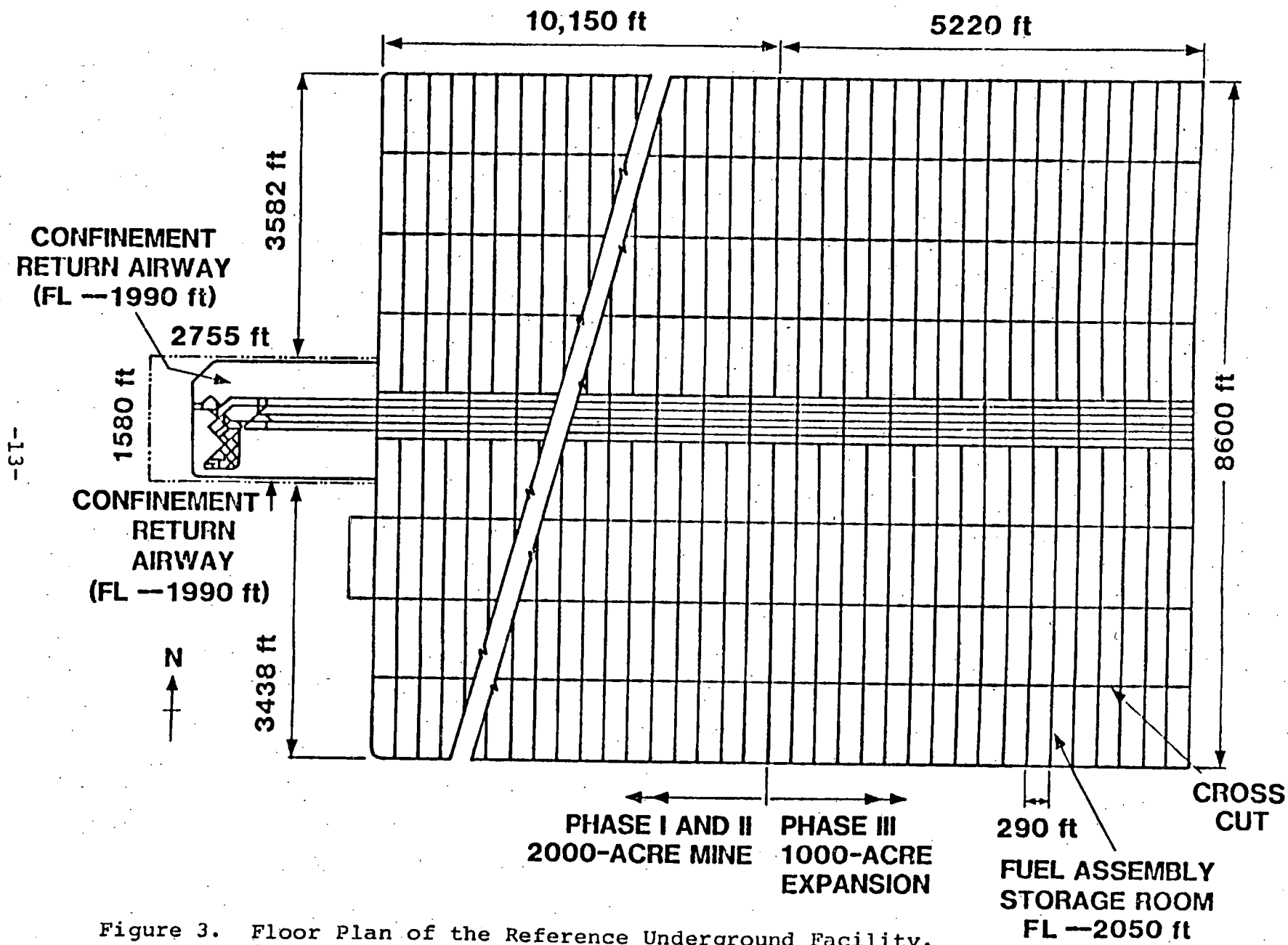


Figure 3. Floor Plan of the Reference Underground Facility.  
 (Shafts are located in the panhandle section)

-13-

Capacity -- The mine can accept unprocessed spent fuel assemblies from approximately 86,000 metric tons of heavy metal (MTHM). This translates to about 204,000 canisters containing either one assembly from a pressurized water reactor (PWR) or two from a boiling water reactor (BWR). The cylindrical canisters, which are 14 inches in diameter and 15 feet long, are to be placed in vertical holes drilled into the floor of the storage rooms. Total volume of excavated salt is  $1.56 \times 10^8$  cubic feet.

Backfill -- After waste emplacement is completed, the mine is backfilled with crushed salt, leaving a residual porosity of 20 percent.

### Waste Inventory

The draft EPA Standard requires that all radionuclides in the waste inventory (Table 1) be considered. However, we have found through experience that a subset of the inventory (Table 4) dominates the response and is sufficiently representative of the total inventory to estimate compliance. Therefore, we will use that subset in this study.

The inventory listed in Table 4 is that of the full repository at the time it is sealed closed ( $t = 0$ ). Although the inventory varies from canister to canister because of reactor type (BWR/PWR), we will assume that each canister contains a uniform fraction of the entire inventory:  $1/204,000$ , that is,  $4.9 \times 10^{-6}$ .

Table 4

Radionuclide Inventories\* (Ci) at Time of Closure (t = 0)

<u>Radioisotope</u>	<u>Half-Life (years)</u>	<u>Ci at t=0</u>
Pu240	6.76E3	4.6E7
U236	2,39E7	3.2E4
Th232	1.41E10	3.2E-5
Ra228	6.7	9.0E-6
Cm245	8.27E3	3.3E4
Pu241	14.6	4.4E9
Am241	433.	2.0E8
Np237	2.14E6	4.0E4
U233	1.62E5	8.0
Th229	7300.	1.2E-2
Cm246	4710.	6.6E3
Pu242	3.79E5	1.3E5
U238	4.51E9	3.0E4
Pu238	89.	3.1E8
U234	2.47E5	1.0E5
Th230	8.E4	16.8
Ra226	1600.	8.1E-2
Pb210	21.	1.8E-2
Am243	7650.	1.7E6
Pu239	2.44E4	3.2E7
U235	7.1E8	1.6E3
Pa231	3.25E4	3.4
Ac227	21.6	1.4
Tc99	2.14E5	1.3E6
I129	1.6E7	3.0E3
Sn126	1.0E5	5.2E4
Sr90	28.9	4.8E9
Cl4	5730.	4.8E4
Cs135	2.0E6	3.3E4
Cs137	30.	6.7E9

---

\*Inventories correspond to 86,000 metric tons  
of heavy metal

## V. Radionuclide Release Scenarios and Probabilities

The three types of scenarios with radionuclide transport that we analyzed were groundwater transport, drilling into a canister, and brine pocket penetration.

In all cases, the sealed repository is violated either because mineshaft seals fail or because exploratory drill holes penetrate the underground engineered facility. The draft EPA Standard requires that each radionuclide release have an associated probability assigned to it. Since all scenarios that we considered were caused by either the shaft seal failing or by drilling, we had to determine the likelihood that either would happen.

Since Unit WP has low hydraulic conductivity and groundwater flows through it extremely slowly -- a few inches per year -- we will ignore it as a source of groundwater or a migration path.

Wells sunk into Unit WP could shorten the path of radionuclides to the accessible environment. However, because of its tightness, salinity, and overlying units of greater transmissivity, we do not feel that wells are likely to be drilled into the lower units for the extraction of water. Also, the natural discharge location for the unit is more than 100 miles away. With the groundwater moving at 1 mile/1,000 years (5.28 inches/year) it would take over 100,000 years for the radionuclides to escape. This time is much greater than the 10,000-year limit set by the draft EPA Standard.

We should note that the objective of this study is to choose and analyze a set of representative scenarios. As will be shown, the scenarios chosen will indeed be important scenarios in the compliance assessment of the assumed repository. This is not to say that they are the only scenarios. A full scenario development, characterization, and analysis is beyond the scope of this work.

### Probability of Seal Failure

Without a detailed study of the properties of sealing materials, we can only assume a non-mechanistic probability of their failure. Thus, we assume that:

$$\left. \begin{array}{l} \text{Probability of} \\ \text{shaft seal failure} \\ \text{at 1000 years} \end{array} \right\} = 0.001$$

For our calculations, we also assume that the shaft seal remains defective throughout the calculation, that is, it is not resealed.

#### Groundwater Transport Scenarios

In order that the Units (O and D) overlying the back-filled repository be able to transport radionuclides, two hydraulic conduits are required between them. One allows water to enter and contact the canisters. The other carries contaminated water back to the geologic units. The two conduits and the repository would thus form a U-shaped path, called a U-tube (Figure 4).

The vertical conduits could be formed along former mine shafts leading to the repository whose seals had failed. Another possibility would be an inadvertent penetration by exploratory drill holes made by future generations seeking petrochemicals or evaporite minerals.

In Figure 4, the conduit to the left is either a mine shaft whose seal has failed, or a borehole. The one to the right is a borehole. Water is driven through the U-tube by the head difference between the vertical conduits and the units overlying the repository. The difference is caused by the water flowing horizontally through Units O and D.

Below, we analyze two variations of the characteristics of the overlying aquifer. In one we assume that Unit O is nearly saturated and that the vertical legs of Figure 4 connect with it. Water and radionuclides flow from the backfilled regions back into Unit O. Once there, the radionuclides are transported through the unit.

In the other variation, we assume that Unit O has been depleted, say for irrigation. Unit D is then the migration path for radionuclides, although slower because of its lower conductivity.

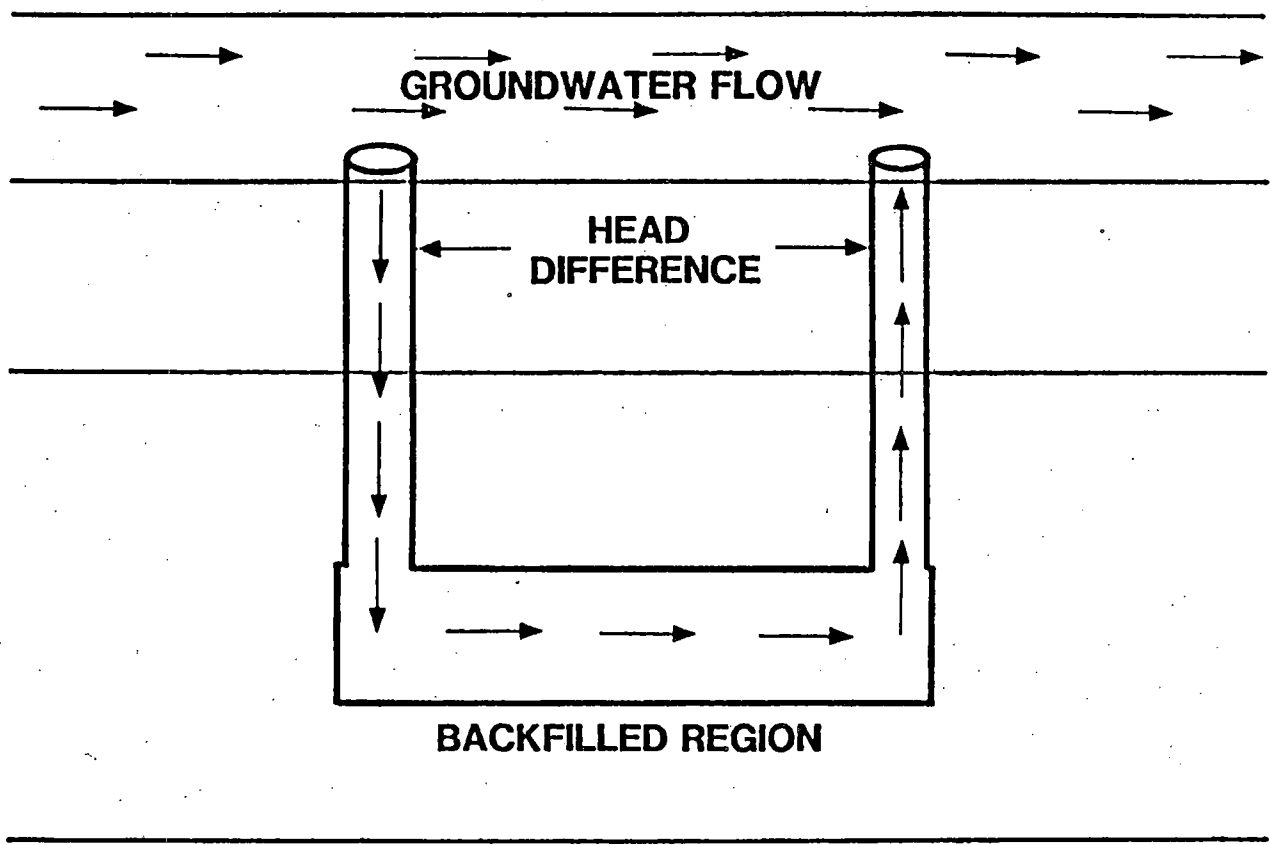
Probability of U-Tube Formation -- To determine the likelihood that a borehole will intrude into the repository, we first assume that the drilling rate into the 3,000-acre tract is  $1.9 \times 10^{-3}$ /year. This rate is relatively low for drilling into strata containing bedded salt [4]. However, it is a reasonable value considering the thermal maturity of the strata, discussed previously in the description of the report. The floor space of the engineered facility covers a smaller area than that of its gross extent, typically

UNIT

O OR D

PSA

SA



-18-

Figure 4. The U-Tube Flow and Migration Pattern for the Groundwater Transport Scenario.

25 percent or less extraction ratio. In the assumed design, this fraction is less than 10 percent [8-10]. For the calculations presented in this report, we assumed this fraction to be about 15 percent. Thus, the number of boreholes expected to penetrate the back-filled regions in 10,000 years is:

$$19 \times 0.15 = 3$$

We can thus assume that three boreholes are expected to penetrate the backfilled regions during the 10,000-year period.

However, other factors enter the picture. If water is to flow through a U-tube, there must be enough driving head. For example, in the case where water originates in Unit O and returns loaded with radionuclides, there is a minimum distance that must separate the vertical legs of the U-tube. This distance is determined by applying the DNET Model [12]. The water in the U-tube's entry leg is fresh until it comes into contact with the salt. Therefore, the exit leg contains saturated brine, which is heavier. Given the hydraulic gradient of Unit O, the minimum downdip separation calculates as 11,500 feet.

In the case where water originates from and returns to Unit D, both vertical legs are filled with brine. Therefore, there is no difference in their weights and two or more holes, regardless of separation, may form a successful U-tube, as long as both penetrate the back-filled regions.

To implement all our assumptions, we further assume that exploratory drilling is a Poisson process with a distribution on the number of boreholes into the 450-acre (15 percent of 3,000) target area given by

$$P(n) = \frac{(\lambda T)^n e^{-\lambda T}}{n!}, \quad (5)$$

where:  $\lambda T = 3.$

In the Unit O case, where we require a minimum distance of 11,500 feet, we must adjust the value of  $\lambda T$ . The adjustment needed is a scaling of the value of  $\lambda T$  by the ratio of the target area to 3,000 acres.

We will consider four variations of the U-tube scenario. In two of the variations, Unit O will be assumed to transport the radionuclides. In the other two, Unit D will be assumed to transport the radionuclides. For each of the assumed major transporting units, two types of vertical conduits (Figure 4) will be considered. In all the U-tube scenarios analyzed, the vertical conduit at the right in Figure 4 will be assumed to be formed by one or more boreholes. The conduit at the left of Figure 4 will be assumed to be one or more failed shaft seals in one case, and one or more boreholes in the other. In the discussion that follows, probabilities for these scenarios will be given. In order to describe the hydraulic properties of the vertical legs, conditional probabilities will also be needed to describe the number of boreholes that may occur. These will also be given in the following discussion.

Scenario 1 -- Water originates in and returns to Unit O. The entrance leg is a shaft whose seal has failed and the exit leg is one or more boreholes. Both legs are separated by at least 11,500 feet. The size of the target area (Figure 3) is approximated as:

$$\text{Area} = (17,000 - 11,500) \times 8,600 \text{ feet}^2 = 1,086 \text{ acres.}$$

Thus, we scale  $\lambda T$  appropriately to get  $(\lambda T)'$ :

$$(\lambda T)' = \lambda T \frac{1,086 \text{ Acres}}{3,000 \text{ Acres}} = 1.09 \quad (6)$$

Using Equation (5),  $P(0) = 0.34$  and the probability of one or more holes penetrating the target is

$$P_{\geq 1} = 1 - 0.34 = 0.66.$$

Therefore, the probability that Scenario 1 will occur is:

$$P_1 = P_{\text{shaft}} * P_{\geq 1} = 0.001 * 0.66 = 6.6 \times 10^{-4} \quad (7)$$

We can now use Equation (5) to generate a conditional probability,  $P_c(n)$  distribution on the number of boreholes in the 1,086 x 15 percent target area:

n	1	2	3	4	5	6	7	$\geq 8$
$P_c(n)$	0.56	0.30	0.11	0.03	0.01	0.0011	$1.7 \times 10^{-4}$	nil

Scenario 2 -- Water originates from and returns to Unit O. Both legs of the U-tube are two or more boreholes separated by at least 11,500 feet. Since any two boreholes separated by that distance can form a successful U-tube, we need a convolution of probabilities of boreholes in differential target areas at greater than minimum separation. To avoid this complicated computation, we present a simplified treatment to estimate the number of boreholes, ignoring the 2,000-ft long "panhandle" of the repository since no waste is stored there (Figure 5).

The two 2,700-ft sections at each end of the repository are targets for the boreholes forming a U-tube with those at the opposite end. The size of each target area is thus 2,700 feet x 8,600 feet = 533 acres. Therefore, adjusting  $\lambda T$  gives us,

$$(\lambda T)' = \lambda T \cdot \frac{533}{3000} = 0.53. \quad (8)$$

The probability that there will be no boreholes in a target area that is 15 percent of 533 acres is 0.59 [Equation (5)], so that the probability of one or more borehole at each end is

$$P_2 = (1 - .59)^2 = 0.17. \quad (9)$$

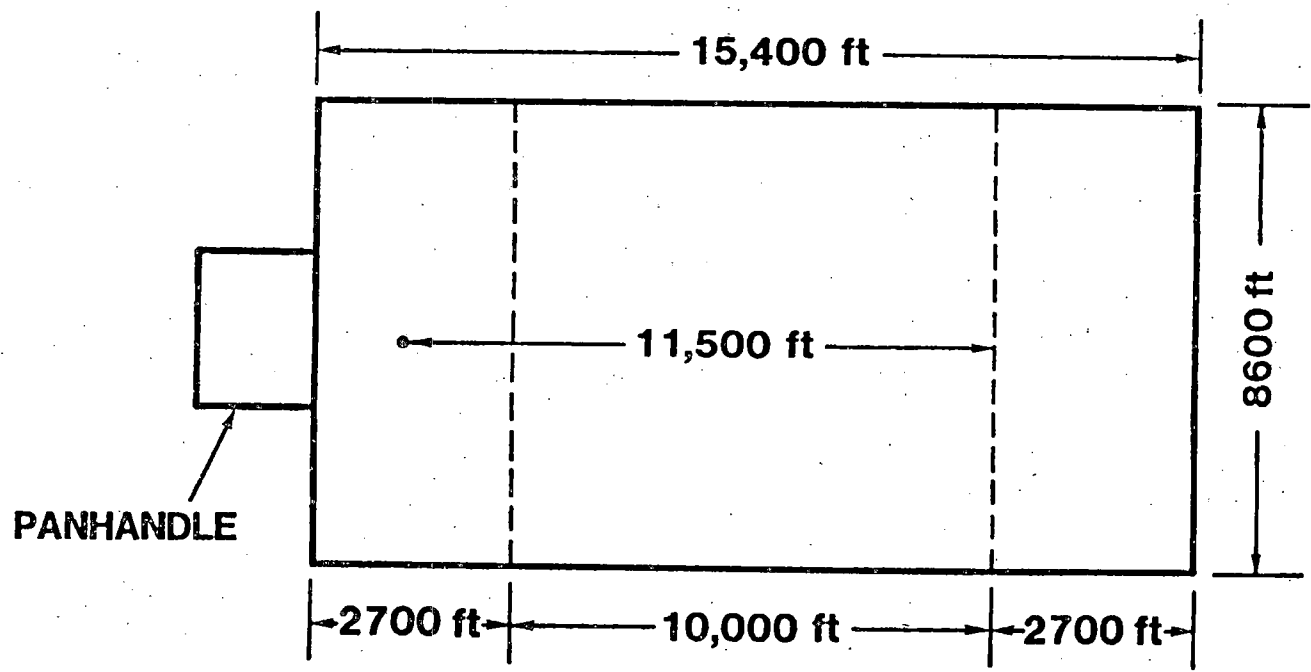


Figure 5. Scenario 2 Geometry

However, in order to perform our calculations, we need the distribution of the number of boreholes. This number can be generated from Equation (5) to give us a conditional probability distribution of boreholes in each target area:

n	1	2	3	4	5	6	≥ 7
P <sub>C</sub> (n)	.7549	.2031	.0364	.0049	.0005	.00005	nil.

Scenario 3 -- Water originates in and returns to Unit D. One leg of the U-tube is a shaft whose seal has failed and the other is one or more boreholes at any distance, not exceeding the size of the backfilled regions. We use the same calculations as for Scenarios 1 and 2. However, we do not adjust for target area and instead use  $\lambda T = 3$ . Using Equation (5), we calculate the probability of one or more boreholes penetrating the target area as  $P_{\geq 1} = 0.95$  so that the probability of this scenario occurring is:

$$P_3 = P_{\text{shaft}} * P_{\geq 1} = 0.001 * 0.95 = 9.5 \times 10^{-4} \quad (10)$$

Thus, the conditional probability distribution on the number of boreholes is:

<u>n</u>	<u>P<sub>C</sub>(n)</u>	<u>n</u>	<u>P<sub>C</sub>(n)</u>
1	0.16	6	0.05
2	0.24	7	0.02
3	0.24	8	0.01
4	0.18	9	0.003
5	0.11	10	0.001
		≥ 11	nil.

Scenario 4 -- Water originates in and returns to Unit D. Both legs of the U-tube are boreholes with no minimum separation. No adjustment of  $\lambda T$  is needed and we use  $\lambda T = 3$ . By using Equation (5), we calculate the probability of two or more boreholes penetrating the target area as  $P_{\geq 2} = 0.80 \equiv P_4$ . The conditional probability of distribution is

<u>n</u>	<u>P<sub>C</sub>(n)</u>	<u>n</u>	<u>P<sub>C</sub>(n)</u>
2	0.28	7	0.03
3	0.28	8	0.01
4	0.21	9	0.003
5	0.13	10	0.001
6	0.06	≥ 11	nil.

Since we cannot assume Unit O to be both saturated and depleted, we assume each of these possibilities to be equally probable. This translates to an additional factor of 1/2 on the probabilities above. Also, we treat only one scenario at a time. For example, we do not consider a U-tube formed by a failed shaft seal which, after subsequent drilling, becomes a U-tube with boreholes providing additional water conduits. Thus, the shaft seal failures compete with boreholes for U-tube formation. Including the factors of 1/2 for Unit O vs Unit D scenarios, we calculate probabilities for the mutually exclusive scenarios,  $P_i'$

$$P_1' = 1/2 P_1 (1 - 1/2 P_2)$$

$$P_2' = 1/2 P_2 (1 - 1/2 P_1)$$

$$P_3' = 1/2 P_3 (1 - 1/2 P_4)$$

$$P_4' = 1/2 P_4 (1 - 1/2 P_3)$$

In summary, the probability assigned to each scenario,  $P_i'$ , is:

<u>Scenario</u>	<u><math>P_i</math></u>	<u><math>P_i'</math></u>
1	.00066	.00030
2	.17	.0850
3	.00095	.00029
4	.80	.40

### Penetration Scenarios

#### Scenario 5: The canister "direct hit."

In this scenario, the radionuclides move to the surface directly and rapidly. While sinking a borehole, possibly while exploring for minerals, the drill bit strikes a waste canister and brings a fraction of the contents to the surface.

In the scenarios previously described, we determined that in 10,000 years, 19 boreholes could be expected over the 3,000 acre site. The same probability applies to

this penetration scenario. Each borehole will have a fixed probability of making a "direct hit" on a canister. The probability is determined by comparing the area of the waste canisters with that of the facility.

Since there are 204,000 canisters, each with an end area of 1.15 foot<sup>2</sup>, any drill bit penetrating the back-filled repository has a probability of hitting a canister of

$$P_{hit} = \frac{2.04 * 10^5 \text{ canisters} * 1.15 \text{ foot}^2/\text{canister}}{15,370 \text{ feet} * 8,600 \text{ feet}} \quad (11)$$

$$= 1.8 * 10^{-3} .$$

For n boreholes, the probability of N direct hits will be given by a binomial distribution,

$$P(N,n) = \frac{n!}{N! (n-N)!} P_{hit}^N (1-P_{hit})^{n-N} \quad 0 \leq N \leq n. \quad (12)$$

Thus, the probability of N hits is:

$$P(N) = \sum_{n=N}^{\infty} p(n) \cdot P(N,n) \quad (13)$$

$$= \sum_{n=N}^{\infty} \frac{(\lambda T)^n e^{-T}}{n!} \cdot \frac{n!}{N!(n-N)!} P_{hit}^N (1 - P_{hit})^{n-N}$$

where  $\lambda T = 19$

and  $P_{hit} = 1.8E-3$ .

A more detailed analysis of this scenario might include the spatial extent of the drill bit, the drilling direction, and the distribution of waste within the canister.

### Scenario 6: Brine pocket penetration

We have not had time during this study to analyze this scenario in detail. However, it has been suggested as a potentially important scenario to be considered when analyzing risks from nuclear waste disposal [13]. The suggestion is that for a specific repository site, approximately 1 borehole in 27 will hit a brine pocket [13]. Therefore, we use this number with some other assumptions to describe this scenario.

We use the probabilistic expression of Equation (13) because conceptually, the canister "direct hit" scenario is the same as that of the brine pocket penetration (Figure 6), the brine pocket now being the target, rather than the canister. Therefore, we have to develop an expression for  $P_{hit}$ .

As indicated in Figure 6, we assume that  $M$  brine pockets exist below the horizon of the subsurface facility, with an area,  $A_m$ . Each brine pocket is spherical with a cross-sectional area,  $a$ , projecting to the surface. We assume that the ratio of total brine pocket area,  $Ma$ , to  $A_m$  is a constant,  $\alpha$ , i.e.,

$$Ma = \alpha A_m.$$

The constant  $\alpha$  then gives the probability that a random drill bit will penetrate a brine pocket. A value of  $1/25$  was given for  $\alpha$  with no mention of the thickness of the salt layer [13]. However, since we are concerned only with the lower half of the salt layer, we will assume that

$$\alpha = 1/2 \cdot 1/25 = 0.02$$

This value will be used for  $P_{hit}$  in Equation (13) to evaluate this scenario.

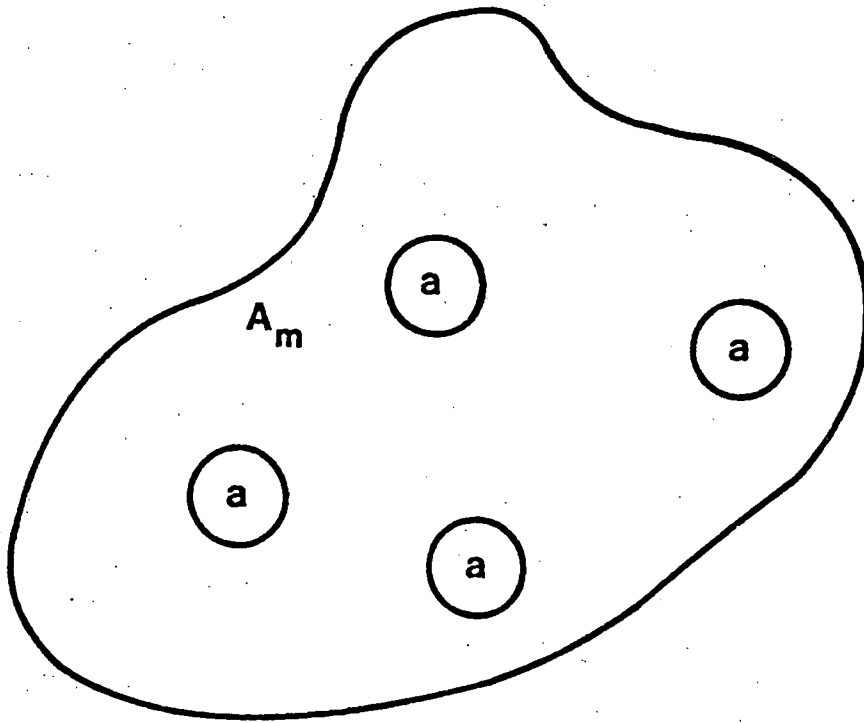


Figure 6. Reference Area,  $A_m$ , Containing  $M$  Spherical Brine Pockets. (Each brine pocket has a projected area,  $a$ , at the surface.)

## VI. Computer Models (NWFT/DVM) Used for Groundwater Transport Scenarios

We used different models to estimate discharges expected from the various scenarios. For groundwater transport (U-tube) scenarios, we used the NWFT/DVM model [14] developed at SNL for the NRC. For the penetration scenarios, we used more simplistic models.

### A. The Groundwater Transport Scenarios (NWFT/DVM)

This model is used to calculate time-dependent discharge rates of radionuclides into the accessible environment for the four groundwater transport scenarios. Figure 7 shows the simple network of points and distances used in the calculations. In the figure, " $l$ " indicates the length between junctions at elevations, " $d$ "; and " $p$ " is the hydraulic pressure of the aquifer. The numerical values assigned to the  $l$ 's and  $d$ 's vary from scenario to scenario. These values are presented in Table 5.

The upper horizontal legs represent the overlying aquifer, either Unit O or Unit D, the vertical legs represent the borehole(s) or failed shaft, and the lower horizontal leg,  $l_6$  represents the backfilled region.

We used the Latin Hypercube Sampling Method [15] to select input data for flow and transport calculations (Table 6). For example, to calculate discharges in each groundwater transport scenario, we chose 50 combinations of input data (vectors) from the distributions in the table. We repeated this procedure three times so as to observe the effects of sampling error on the calculated discharges.

In order to avoid physically unreasonable combinations of porosity and hydraulic conductivity, we assumed a rank correlation of 0.7 when sampling these parameters for any feature [15]. Leg 6 is the backfilled repository, which is a hydraulic "short circuit" between legs 4 and 5 and has an arbitrarily high hydraulic conductivity of  $10^6$  feet/day.

The NWFT/DVM Model also requires that we assign a value to the cross-sectional area of this "short circuit". Depending on the source model (see below), we assign an end-view, cross-sectional area of  $1.3 \times 10^5$  ft<sup>2</sup>, if the entire waste inventory is available to access by groundwater. If the available fraction is proportional to the

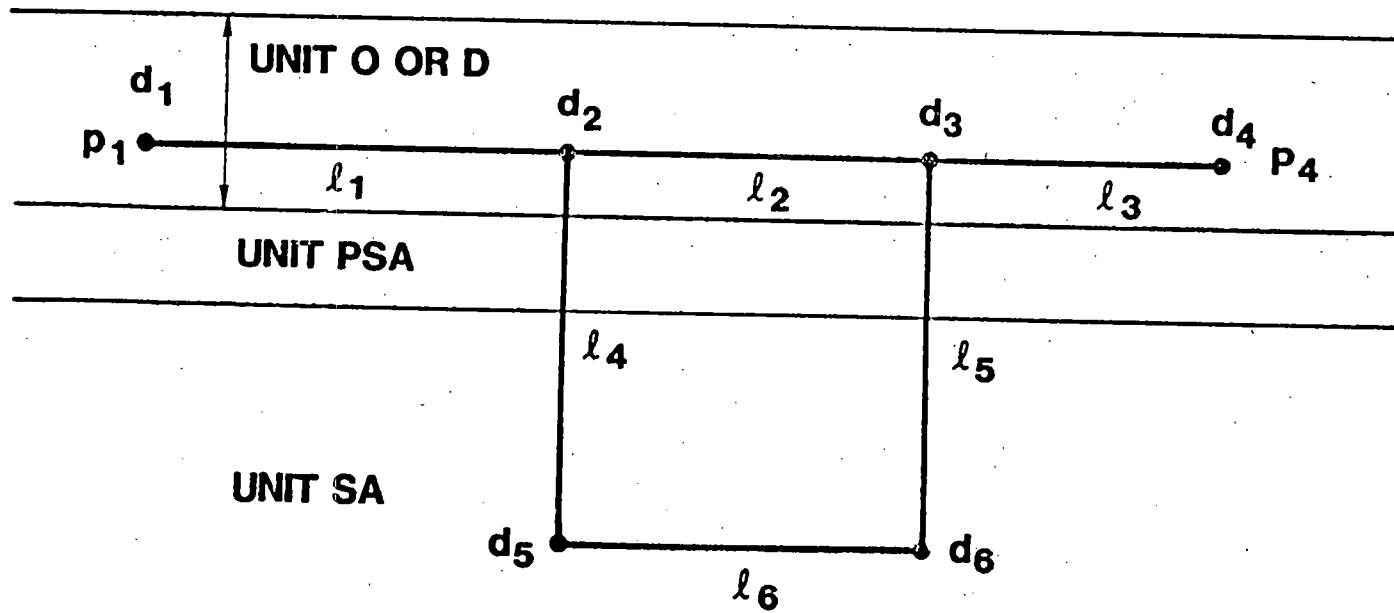


Figure 7. Flow and Transport Network Assumed by NWFT/DVM.

Table 5

Lengths and Elevations Corresponding to Figure 7  
for the Groundwater Transport Scenarios.

Index, i:	1	2	3	4	5	6	
lengths, $l_i$ (feet)							
Groundwater Transport Scenario	1	100,000	17,370	5,280	2,000	1,878	17,370
	2	102,000	15,370	5,280	1,986	1,878	15,370
	3	100,000	17,370	5,280	1,500	1,378	17,370
	4	102,000	15,370	5,280	1,486	1,378	15,370
Elevations, $d_i$ (feet)							
Groundwater Transport Scenario	1	859	159	37	0	-1,841	-1,841
	2	859	145	37	0	-1,841	-1,841
	3	359	-341	-463	-500	-1,841	-1,841
	4	359	-355	-463	-500	-1,841	-1,841

Table 6

## Hydraulic Properties and Sampled Distributions\*

Conductivities are assumed to be lognormally distributed. Porosities are assumed to be normally distributed. The given ranges specify the 0.001 and 0.999 quantiles of the assumed distributions.

<u>Property</u>	<u>0.001 Quantile</u>	<u>0.999 Quantile</u>
1. Hydraulic Conductivity (ft/day) of Unit O	0.15	680.
2. Porosity of Unit O	0.1	0.2
3. Hydraulic Conductivity (ft/day) of Unit D	0.015	68
4. Porosity of Unit D	0.05	0.1
5. Hydraulic Conductivity (ft/day) of Failed Shaft	0.05	50.0
6. Porosity of Failed Shaft	0.05	0.5
7. Hydraulic Conductivity (ft/day) of Boreholes	0.05	25.0
8. Porosity of Boreholes	0.05	0.5

\*The references and data ranges supporting the assumed values for the rock units in this table are given in Appendix B.

number of boreholes, the cross-sectional area can be deduced by the number of boreholes multiplied by the cross-sectional area of the penetrated storage room (262.5 ft<sup>2</sup>). Actually, since leg 6 is a "short-circuit" anyway, these assignments are of little practical value, but are assigned because the model requires them.

Note that we have consistently assumed the maximum lateral separation between the vertical legs for simplicity. Due to the density difference between fresh water and brine, a minimum distance of 11,500 ft between legs 4 and 5 is required to push the brine upward in leg 5 for Scenarios 1 and 2. Therefore, the assumption of maximum lateral separation is fairly representative for those scenarios. For the remaining two U-tube scenarios, the actual separation between legs 4 and 5 could be smaller. However, due to the assumption of a "short circuit" through leg 6, the separation defined in the computer model is immaterial.

The cross-sectional area of the U-tube legs ( $l_4, l_5$ ) depends on whether the legs are mineshafts (2,000 ft<sup>2</sup>) or boreholes (0.8 foot<sup>2</sup>/hole). We also assume that the inlet and outlet pressures ( $p_1$  and  $p_4$ ) are zero since the aquifers are unconfined.

We have neglected dispersivity in our NWFT/DVM calculations. We feel this is justified since the dispersivity is small for the assumed repository. More importantly, the effect of dispersivity is to make the leading edge of the discharge curve more diffuse. Since we are calculating time-integrated discharges, we expect little error from the neglect of dispersion. The error is largest when integration begins or ends during the diffuse part of the discharge. The effect is to assign a portion of the discharge to the adjacent 10,000-year period.

In our calculations, we have assumed three models for NWFT/DVM, each describing a different source of nuclide release (Table 7). We did not perform detailed modeling of each source; the sources are simply assumptions chosen to demonstrate their efficacy.

Source #1 -- This source complies with the release rate limit imposed by NRC [2], that is,  $10^{-5}$ /year of the entire radionuclide inventory at 1,000 years. We have assumed that the inventory is homogeneously dispersed throughout the wasteform so that if  $N_i(t)$  denotes the  $i$ th radionuclide in the inventory at time  $t$ , in the absence

of release, the release rate of that radionuclide is  $(10^{-5}$  to  $10^{-7}) \times N_i(t)$ . We assume that the entire waste inventory is available for transport.

Source #2 -- This source has the same range as Source #1 in terms of release rate, but the amount of waste available for transport is reduced. Each borehole allows only the amount of waste in the particular penetrated backfilled storage room to be available for transport. This model would be valid if we assumed the flow through the backfilled regions to be localized to the vicinity of the borehole (there are 106 storage rooms).

Source #3 -- This source resembles Source #2 but allows the backfilled rooms to be modeled as a mixing cell where wasteforms are leached uniformly (Appendix A). The range of leach rate has been changed to allow a more rapid rate in the breakdown of wasteforms. The calculated discharges thus show how a less stable wasteform can be compensated if mixing mechanisms can be assumed. We also allow solubility limits to apply to radionuclide concentrations in the mixing cell.

#### Geochemical Data

We assume that retardation of radionuclides occurs only in the aquifer units (O and D) of the transport path. The retardation factor,  $R$ , is thus given by

$$R = 1 + R_d \rho \frac{(1-\phi)}{\phi} \quad (14)$$

where

$\rho$  = the assumed rock density ( $2.7 \text{ g/cm}^3$ )

$\phi$  = the unit's porosity (see Table 6)

$R_d$  = the sorption ratio\* (Table 8)

---

\*We use the symbol  $R_d$  to signify an experimentally-determined radionuclide distribution coefficient where we do not assume that equilibrium has been achieved. Although they are called "sorption ratios," there is no assurance that sorption is the only chemical process occurring during the experiments. We use the term  $K_d$  in its classical sense, i.e., ideal ion exchange equilibrium involving trace constituents.

Table 7

## NWFT/DVM Source Models

Model Number	Source Type	Available Fraction of Inventory	Leach Rate (Release) Range (yr <sup>-1</sup> )	Leach Rate Distribution
1	Leach Limited	1.00	10 <sup>-5</sup> to 10 <sup>-7</sup>	Log Uniform
2	Leach Limited	$\frac{\# \text{ of boreholes}}{106^*}$	10 <sup>-5</sup> to 10 <sup>-7</sup>	Log Uniform
3	Mixing Cell	$\frac{\# \text{ of boreholes}}{106^*}$	10 <sup>-3</sup> to 10 <sup>-7</sup>	Log Uniform

\*106 denotes the number of storage rooms in the repository

Table 8  
 Sorption Data,  
 Bedded Salt Site\*

Element	Percentiles of assumed lognormal distribution	
	0.001	0.999
Cm	$10^2$	$10^5$
Am	50	$10^4$
Pu	30	$10^4$
Np	2	400
U	.01	270
Th	$10^3$	$10^5$
Ac	$10^2$	$10^5$
Pb	100	500
Ra	100	500
Pa	0.01	$10^4$
Sr	1.0	2000
Cs	0.01	3000
I	0.01	100
Sn	0.01	500
Tc	0.01	3

$^{14}\text{C}$  is assumed to be completed unretarded, i.e.,  $R_d=0$ .

\*Supporting data and references are summarized in Appendix B.

The LHS method is used to select values from the distributions for each input vector according to the distributions given in Table 8. Data appearing in Table 8 are taken from Reference [16] and the supplemental information from the open literature.

Solubility limits are needed for Source #3 to treat concentration limits on each radionuclide. These data are presented in Table 9. Elements not appearing in Table 9 are assumed to have unlimited solubility.

The sources for the data used in compiling the ranges for the hydrogeologic and geochemical variables are identified in Appendix B.

Table 9

## Solubility Limits of Various Radionuclides

The given ranges specify the 0.001 and 0.999 quantiles of an assumed lognormal distribution.

<u>Element</u>	<u>Range of Solubility Limit (gm/gm)</u>	
	<u>0.001 quantile</u>	<u>0.999 quantile</u>
Pu	1.6E-16	4.0E-4
U	1.6E-8	3.0E-2
Th	1.1E-9	5.8E-6
Ra	7.9E-12	1.3E-5
Np	1.3E-25	5.0E-7
Pb	2.5E-11	4.0E-5
Pa	1.4E-7	7.2E-4
Sn	6.3E-17	1.6E-4
Tc	1.9E-9	9.5E-5
Sr	2.2E-6	2.8E-3

## B. Penetration Scenarios

The penetration scenarios are quite different from our usual analyses; therefore, the manner in which we evaluated their consequences is discussed here. For each, the consequence of the scenario depends on the time of its occurrence and each consequence depends on the inventory at the time of penetration.

As a measure of the time-dependent consequence, Table 10 shows the hazard represented by the waste inventory in terms of EPA release limits. We obtained the table by evaluating Equation (1) for the entire inventory.

Table 10  
Repository Hazard Index

<u>Time (yr)</u>	<u>EPA Sum (Eq. (1))</u>
1,000	8.3E7
1,500	4.3E6
2,000	2.5E6
5,000	8.9E5
10,000	6.4E5

In the direct hit scenario, for example, to use Table 10 to find the hazard on a per-canister basis, divide its value in the second column by 204,000 (the number of canisters). The penetration scenarios have been described in terms of the number of boreholes expected to cause them, independent of when these boreholes occur. Since the consequences are time dependent, it is essential for consequence evaluation that a time of occurrence be assumed. The assumption made, is that the N hits considered, occur uniformly over the period of interest. For the "direct hit" scenario, the period is the 9900 years following loss of administrative control after 100 years. For the brine pocket scenario, the period is the 9000 years following containment lifetime (1000 years) when all waste packages are assumed to fail simultaneously and completely. Thus, for N hits causing the scenarios, each is assumed to occur at a time,  $t_j$ , where

$$t_j = \begin{cases} \frac{9900}{N} \left( j - \frac{1}{2} \right) + 100 & \text{"direct hit"} \\ \frac{9000}{N} \left( j - \frac{1}{2} \right) + 1000 & \text{brine pocket} \end{cases} \quad (15)$$

In the "direct hit" case, we assume that a fraction,  $f_0 = 1/4$  of the canister contents are removed.

Thus, a 1-borehole, direct hit occurs at 5050 years with a consequence (Table 10) of approximately,

$$C^{(1)}_{\text{direct hit}} = 1/4 \cdot \frac{8.9 \times 10^5}{204,000} = 1.1 \quad (16)$$

For the brine pocket scenario, we assume that the pressure in the pocket is relieved by expelling a fraction of its volume. This brine flows up the borehole into a back-filled room. We assume that the backfilled rooms have become resaturated before the waste packages fail at 1000 years. When a waste package fails, its contents are assumed to be released uniformly to the entire volume of water in the backfilled regions, at a constant rate over a period,  $\tau$ . Thus, at time  $t_j$ , the fraction of wastes that have been released is  $f_1$ :

$$f_1 = \frac{t_j - 1000}{\tau}$$

We assume that the brine flow will be of short duration and will remove only those radionuclides in the water volume in the immediate vicinity of the borehole. No modeling was used to test this assumption. We assumed that 1/40 of the water in the backfilled room is mixed with the flowing brine and released to the accessible environment. This choice corresponds to the water volume contained in a 100-foot length (50 feet either way from the borehole) of the 4,000-ft. long room.

The consequence from this scenario is obtained by evaluating Equation 1 (through interpolation of Table 10) with the assumptions made,

$$C(N)_{\text{brine pocket}} = \sum_{j=1}^N \left( \frac{1}{40} \right) \left( \frac{t_j - 1000}{\tau} \right) \left( \frac{\text{EPA Sum}(t_j)}{106} \right) \quad (17)$$

We will assume  $\tau = 100,000$  years. For example, a one brine-pocket scenario occurs at  $t_j = 5,500$  years and has a consequence of approximately,

$$C(1)_{\text{brine pocket}} = \left( \frac{1}{40} \right) \left( \frac{4500}{100,000} \right) \left( \frac{8.9 \times 10^5}{106} \right) = 9.45$$

Since both penetration scenarios involve a relatively small fraction of the waste inventory, we do not consider them as competing with the groundwater transport scenarios. The boreholes that cause them, however, may also contribute to the U-tube formation. We have neglected the small perturbation the penetration scenarios may have on the consequence of the groundwater transport scenarios.

### C. Construction of the CCDFs

As we discussed in volume 2, assessing compliance with the draft EPA Standard should probably combine all scenarios to produce a final CCDF. However, for the scenarios analyzed, it is more illuminating to examine them individually. We will first present the penetration scenarios followed by the groundwater transport scenarios. CCDFs for the groundwater transport scenarios have been constructed for each of the three source models described previously.

#### Scenario 5: The "Direct Hit" Penetration Scenario

Equation (13) was evaluated to give probability,  $P(N)$ , of the N-hit scenario. Equation (15) gives the time,  $t_j$ , for each of the N direct hits. Values from Table 10 were interpolated at  $t_j$  to give values of the EPA Sum, as illustrated in Equation (16). These results are presented in Table 11 and Figure 8. As can be seen in Figure 8, this scenario, when considered by itself, is in slight violation of the draft EPA Standard.

Table 11

Probabilities (per 10,000 yr) and Consequences  
for the "Direct Hit" Scenario\*

N	P(N)	Consequence (EPA Sum)
0	9.82E-1	0
1	3.33E-2	1.09
2	5.59E-4	3.65
3	6.26E-6	6.18
4	6.27E-8	40.40

\*Contributions with probabilities of less than  $10^{-4}$  need not be considered.

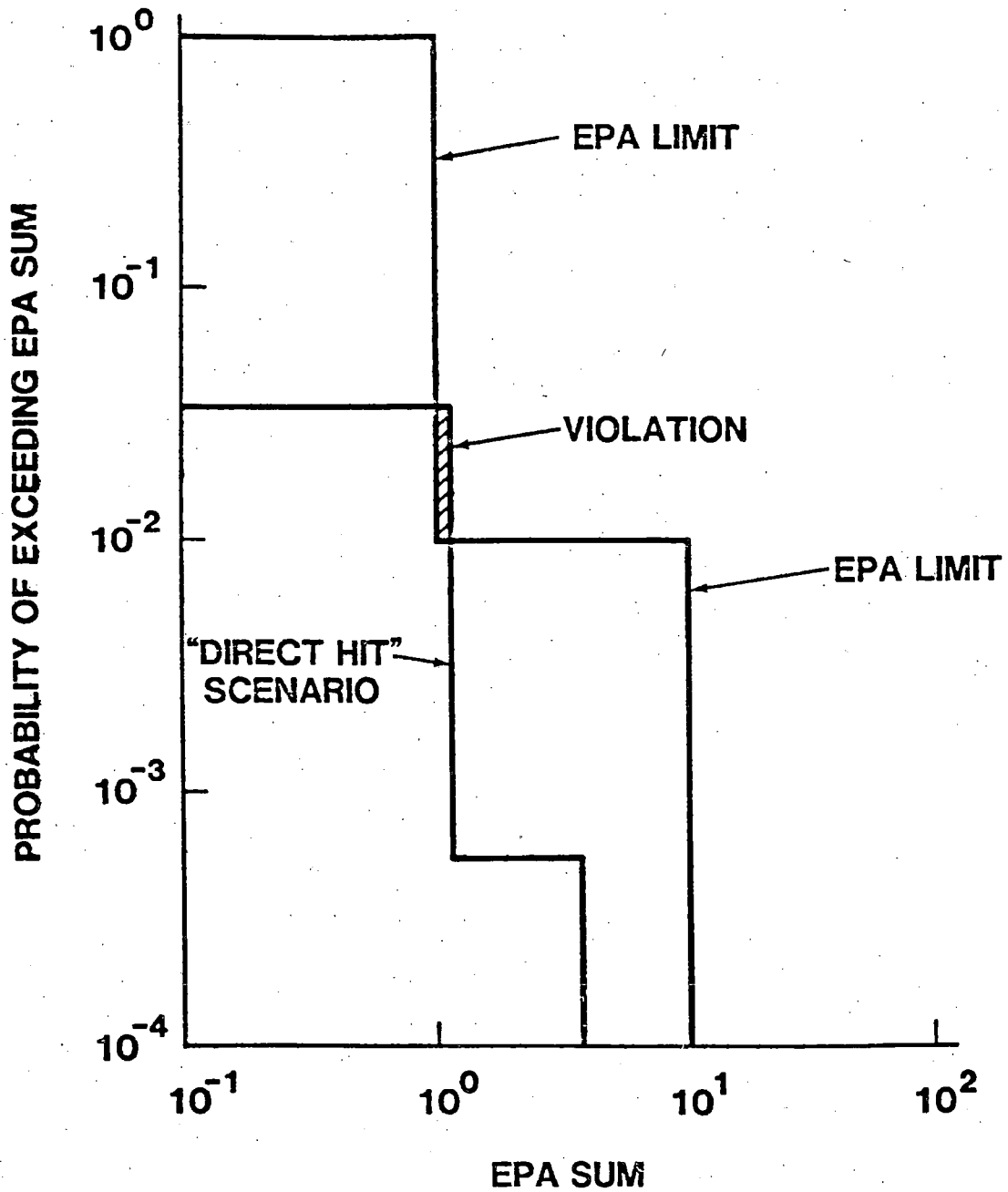


Figure 8. CCDF for Scenario 5, Direct Hit Scenario. (The Shaded Area Indicates Violation of the Draft EPA Standard.)

### Scenario 6: Brine Pocket Penetration Scenario

Equation (13) was used with  $P_{hit} = .02$  to evaluate probabilities,  $P(N)$ , of  $N$  brine pocket penetrations that release radionuclides. Equation (15) was used to evaluate  $t_j$  and the EPA Sum was evaluated according to Equation (17). Table 10 values were interpolated to give values at  $t_j$ . These results are tabulated in Table 12 and the resulting CCDF is presented in Figure 9. As can be seen from Figure 9, this scenario, when considered by itself, violates the draft EPA Standard.

### Scenarios 1-4: Groundwater Transport Scenarios

We evaluated the groundwater transport scenarios for three source-term assumptions discussed previously:

- Source #1: fractional release of  $10^{-5}$  to  $10^{-7}$ /year of entire inventory,
- Source #2: fractional release of  $10^{-5}$  to  $10^{-7}$ /year of a portion of the inventory, given by considering the number of boreholes and assigning one roomful of waste to each borehole,
- Source #3: fractional release rate from the waste form of  $10^{-3}$  to  $10^{-7}$  with the waste-fraction assumption of Source #2. In addition, we considered solubility limits and mixing assumed in the back-filled regions (Appendix A).

In addition, for these scenarios, we sampled the variables required for the analysis from the ranges given in Tables 6, 7, 8, and 9 by the LHS technique [15]. We chose 50 combinations of input and calculated an EPA Sum (Equation 1) for each. Also, we chose two additional independent samples of 50 vectors each to estimate the effects of sampling error.

We calculated radionuclide discharge rates for 50,000 years following waste emplacement. We integrated these discharge rates over each of the five 10,000-year periods and evaluated Equation (1). Thus, we calculated a CCDF for each of the five 10,000-year periods for each of the three independent samples and for each of the source term assumptions. When appropriate, room number and release rates were also sampled. Figures 10, 11, and 12 give the resulting CCDFs.

Table 12

Probabilities (per 10,000 yr) and Consequences  
for the Brine Pocket Scenario

<u>N</u>	<u>P(N)</u>	<u>Consequence (EPA Sum)</u>
0	.942	0
1	.0565	9.21
2	.0017	24.0
3	3.39E-5	38.0

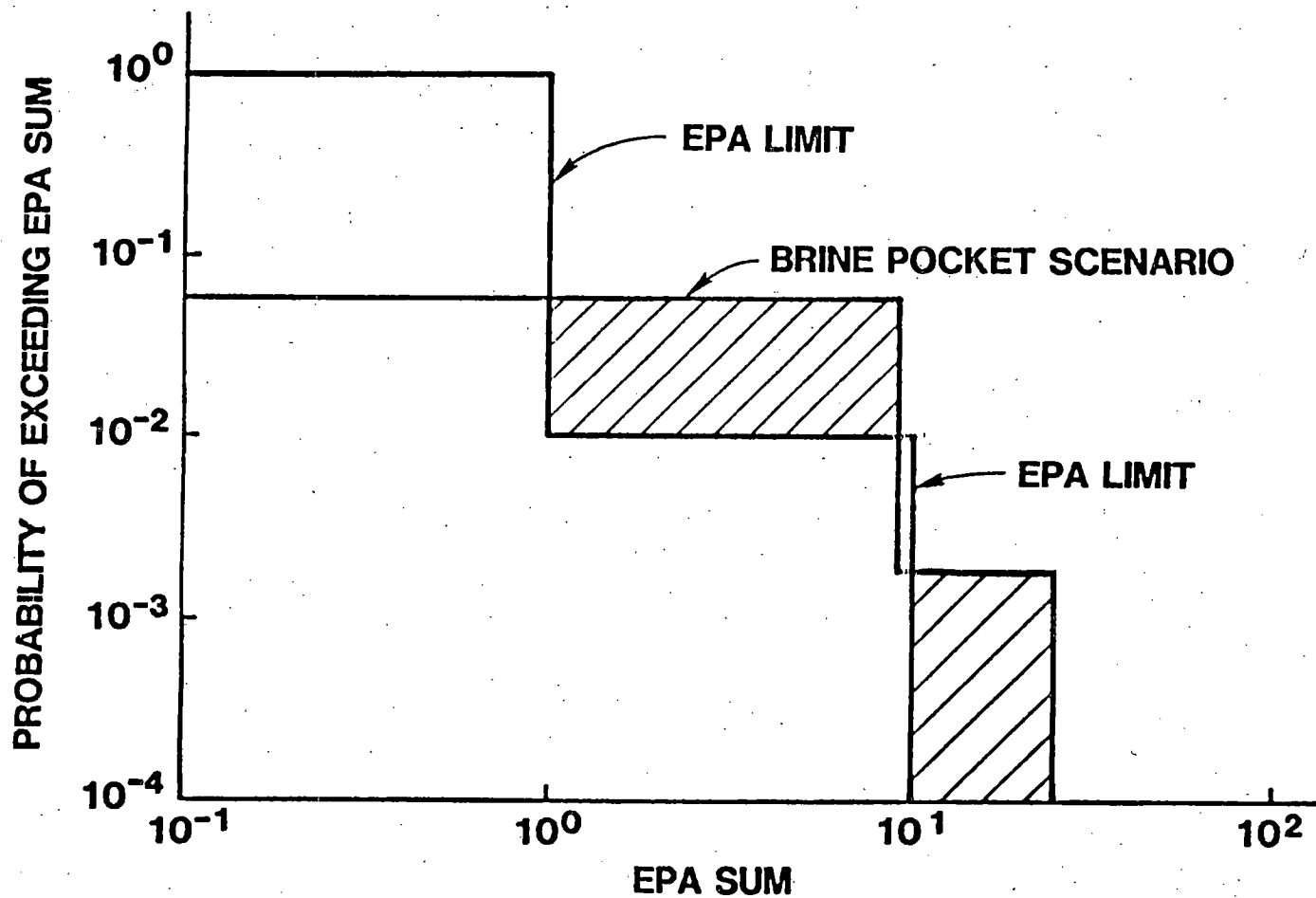


Figure 9. CCDF for the Brine Pocket Penetration Scenario. (The Shaded Areas Indicate Violation of the Draft EPA Standard.)

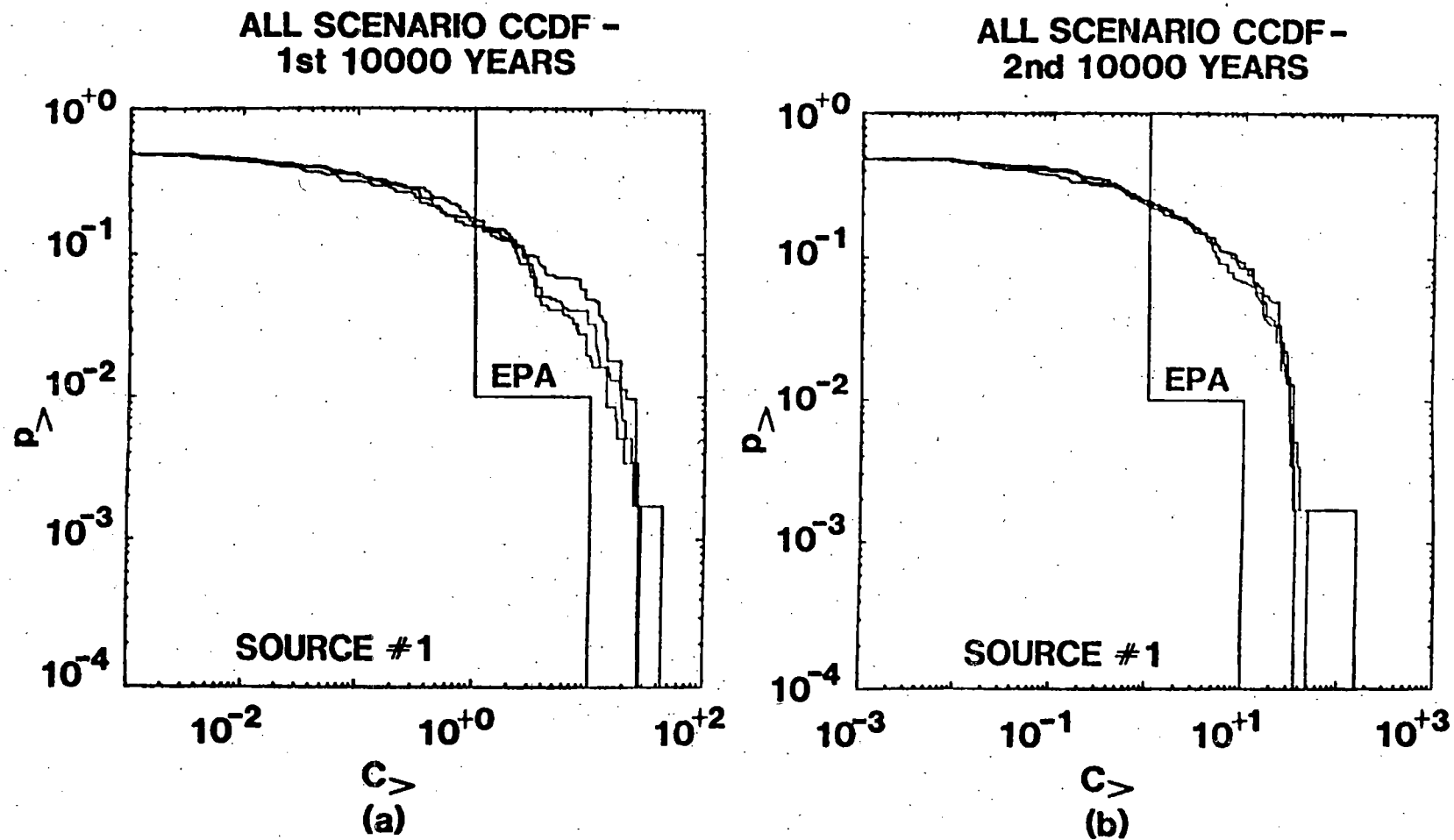
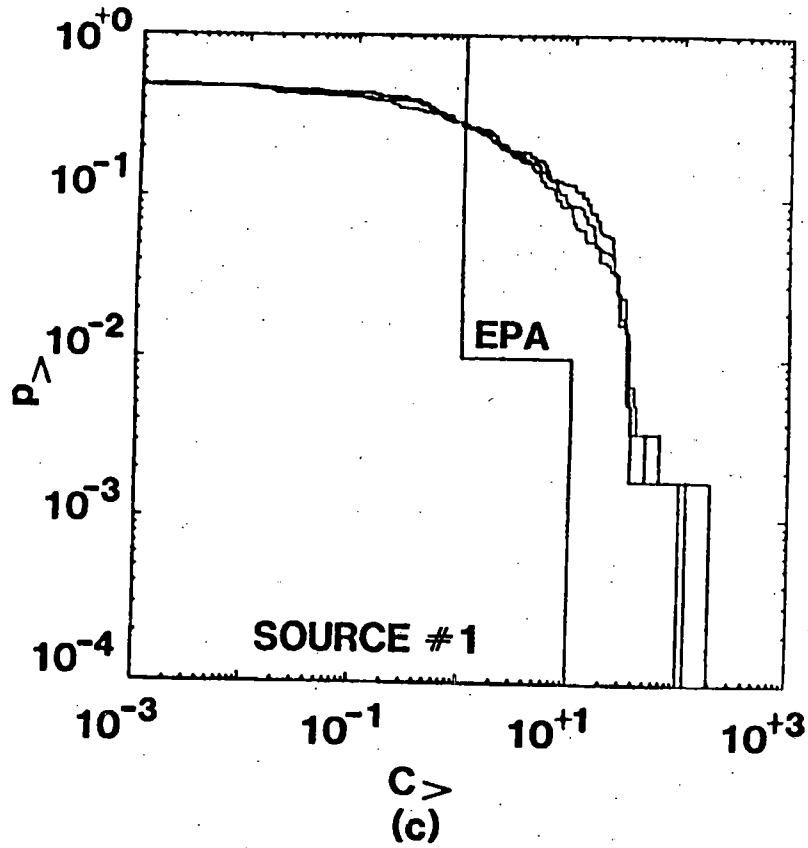


Figure 10. CCDFs for the Groundwater Transport Scenarios With Source #1.

ALL SCENARIO CCDF -  
3RD 10000 YEARS



ALL SCENARIO CCDF -  
4TH 10000 YEARS

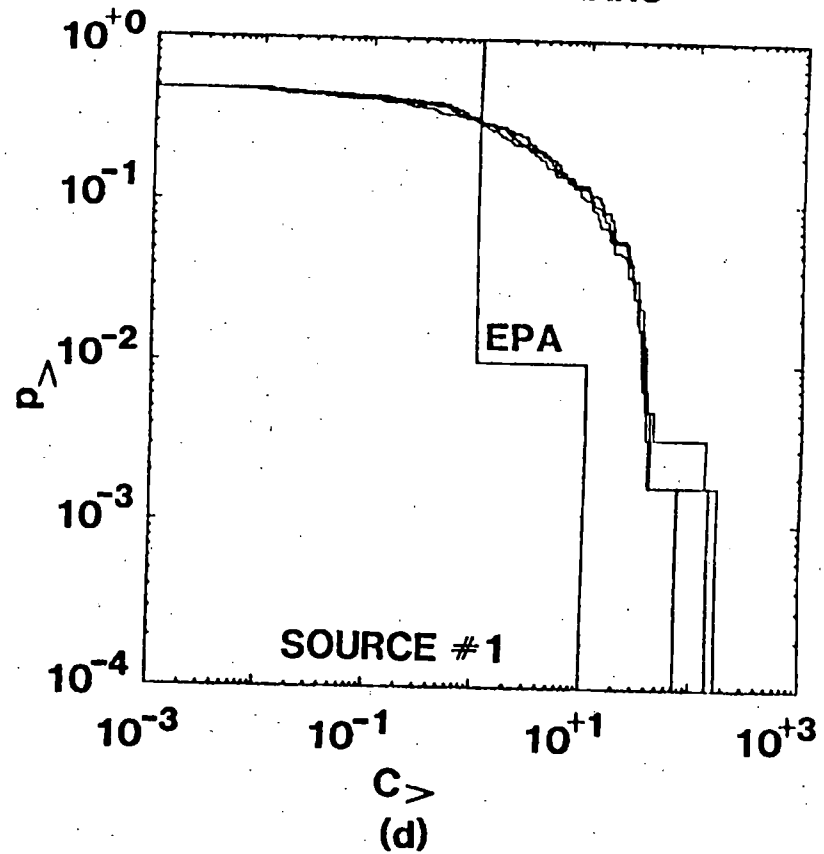


Figure 10. CCDFs for the Groundwater Transport Scenario With Source #1.

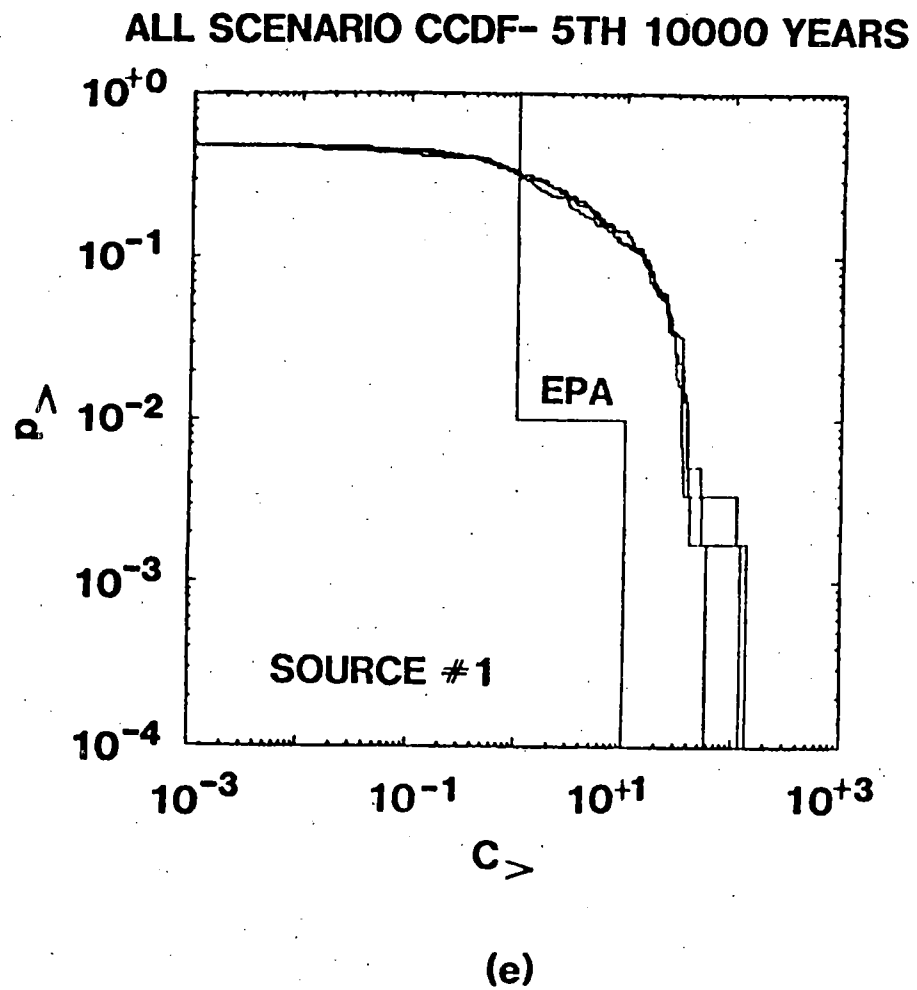
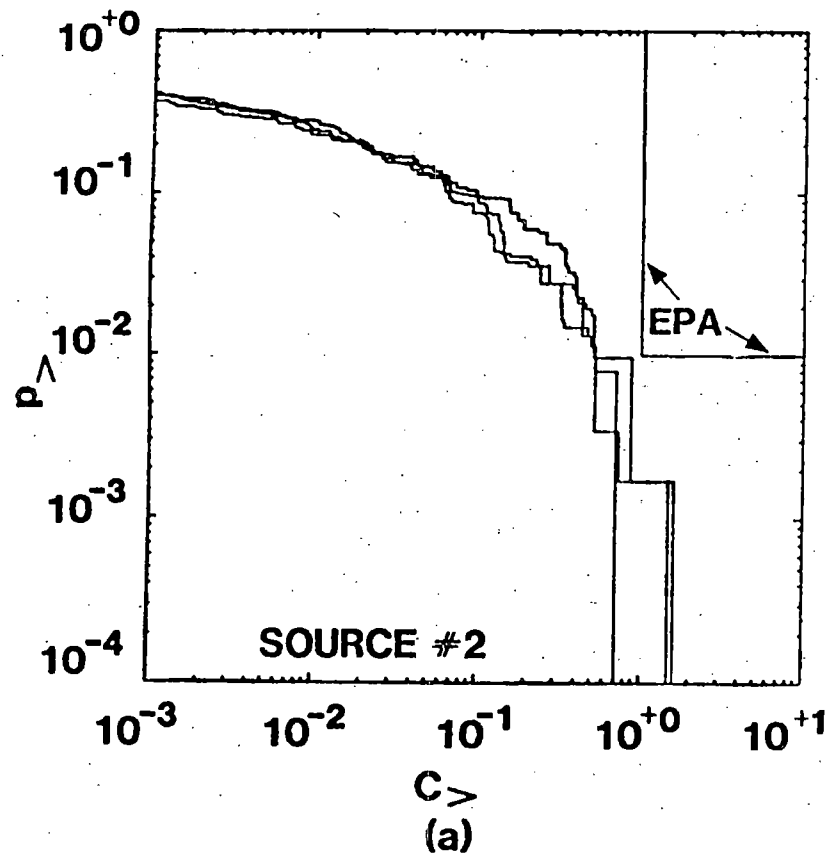


Figure 10. CCDFs for the Groundwater Transport Scenario With Source #1.

ALL SCENARIO CCDF -  
1ST 10000 YEARS



ALL SCENARIO CCDF -  
2ND 10000 YEARS

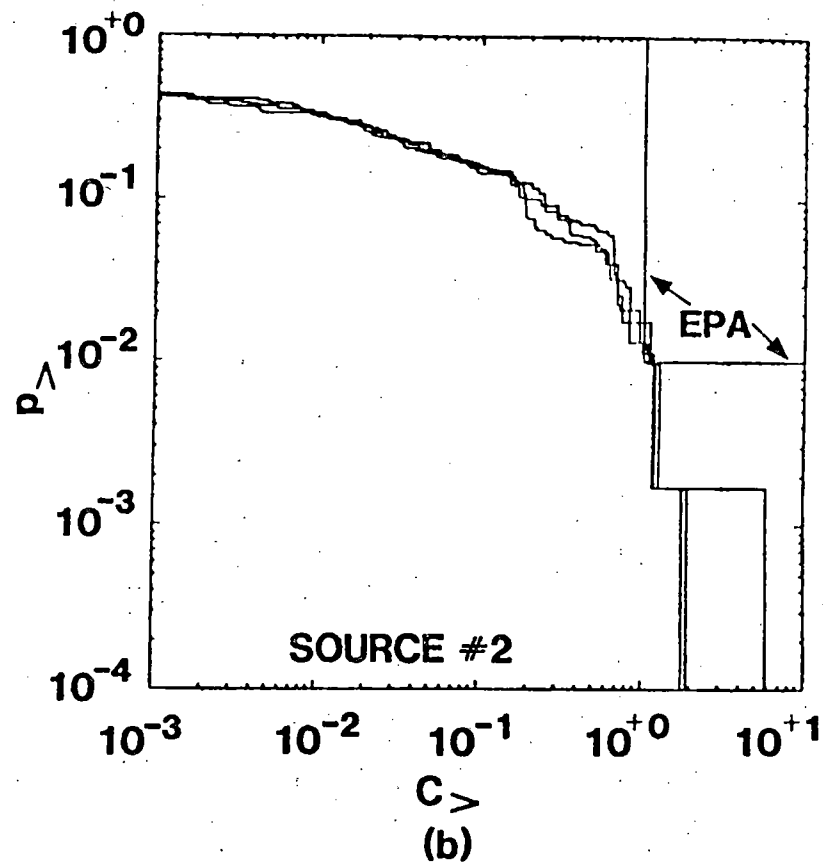
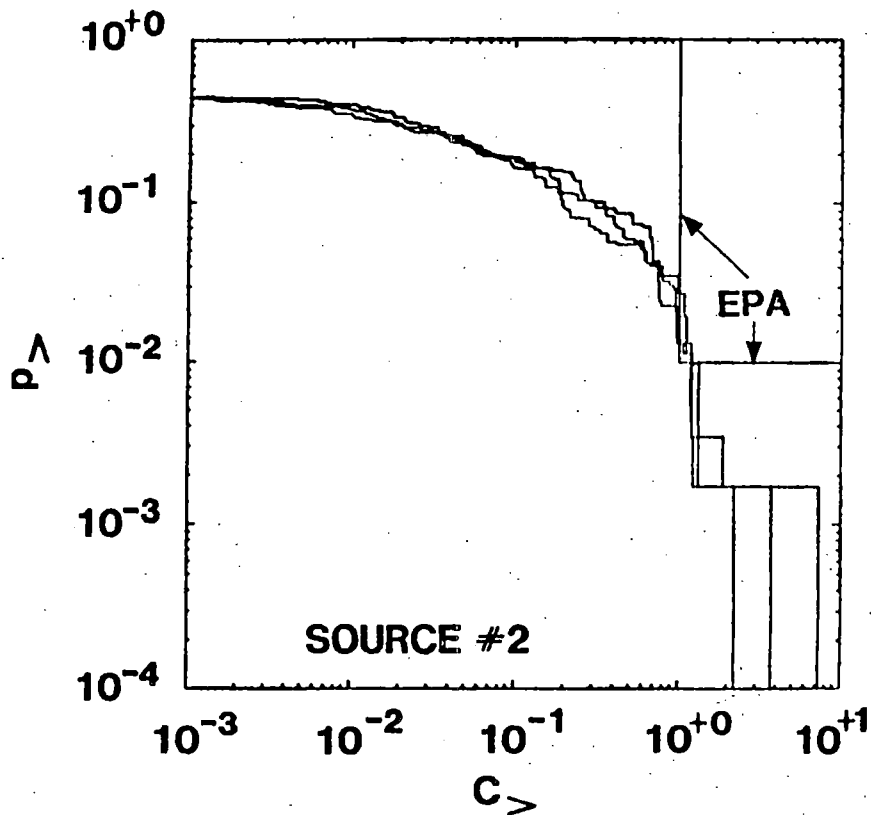


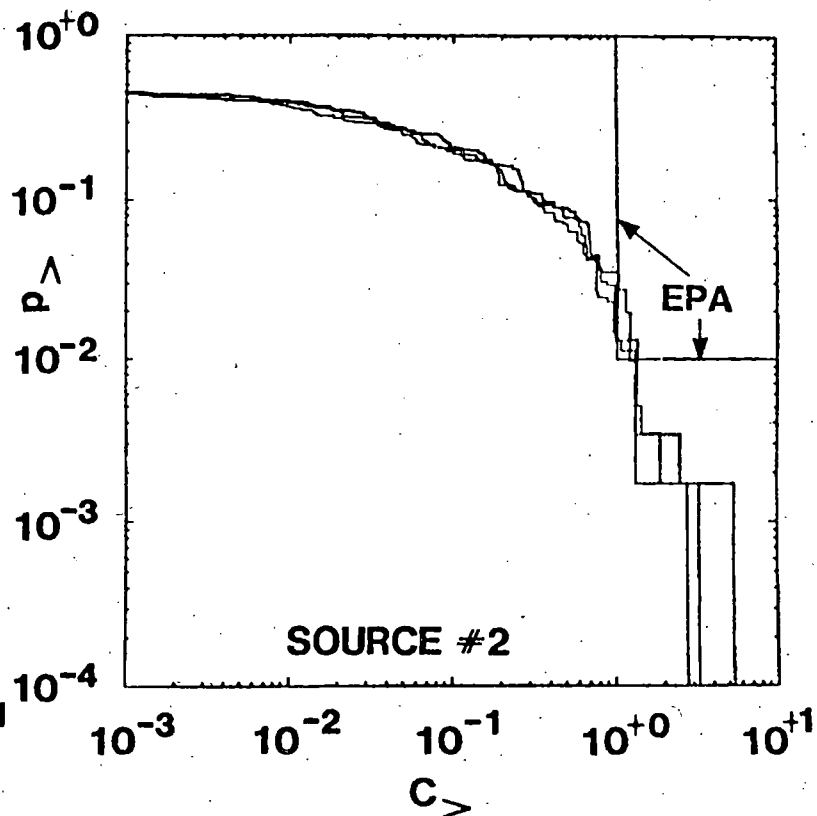
Figure 11. CCDFs for the Groundwater Transport Scenario  
With Source #2.

ALL SCENARIO CCDF-  
3RD 10000 YEARS



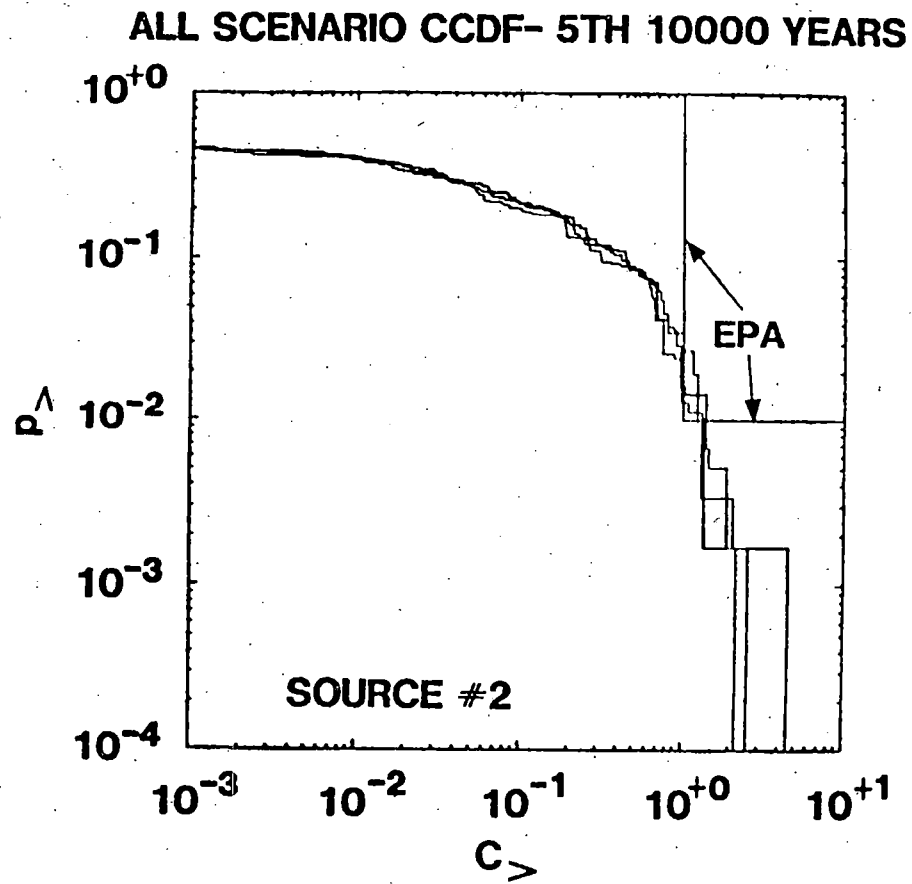
(c)

ALL SCENARIO CCDF-  
4TH 10000 YEARS



(d)

Figure 11. CCDFs for the Groundwater Transport Scenario With Source #2



(e)

Figure 11. CCDFs for the Groundwater Transport Scenario With Source #2

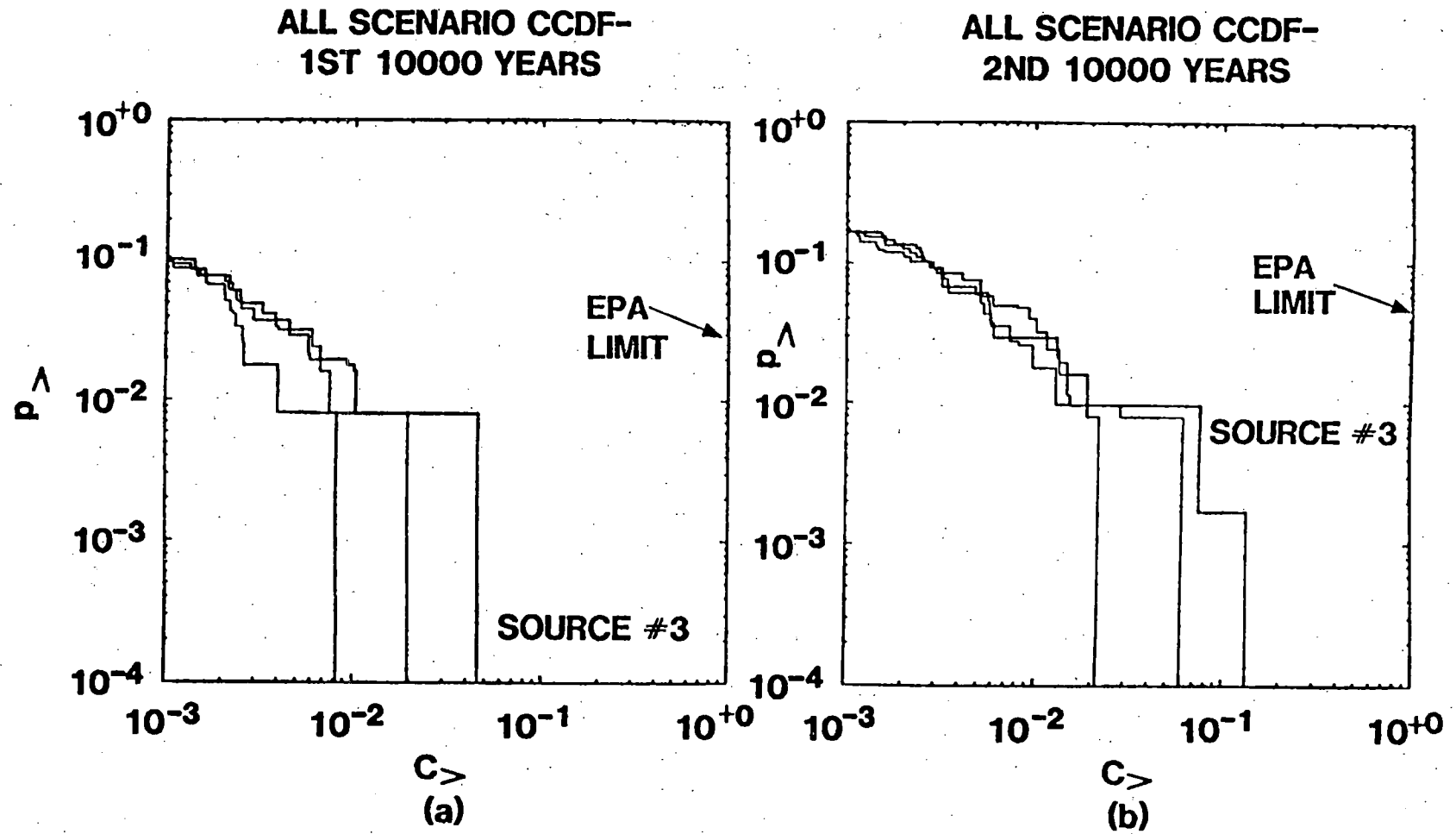


Figure 12. CCDFs for the Groundwater Transport Scenario With Source #3

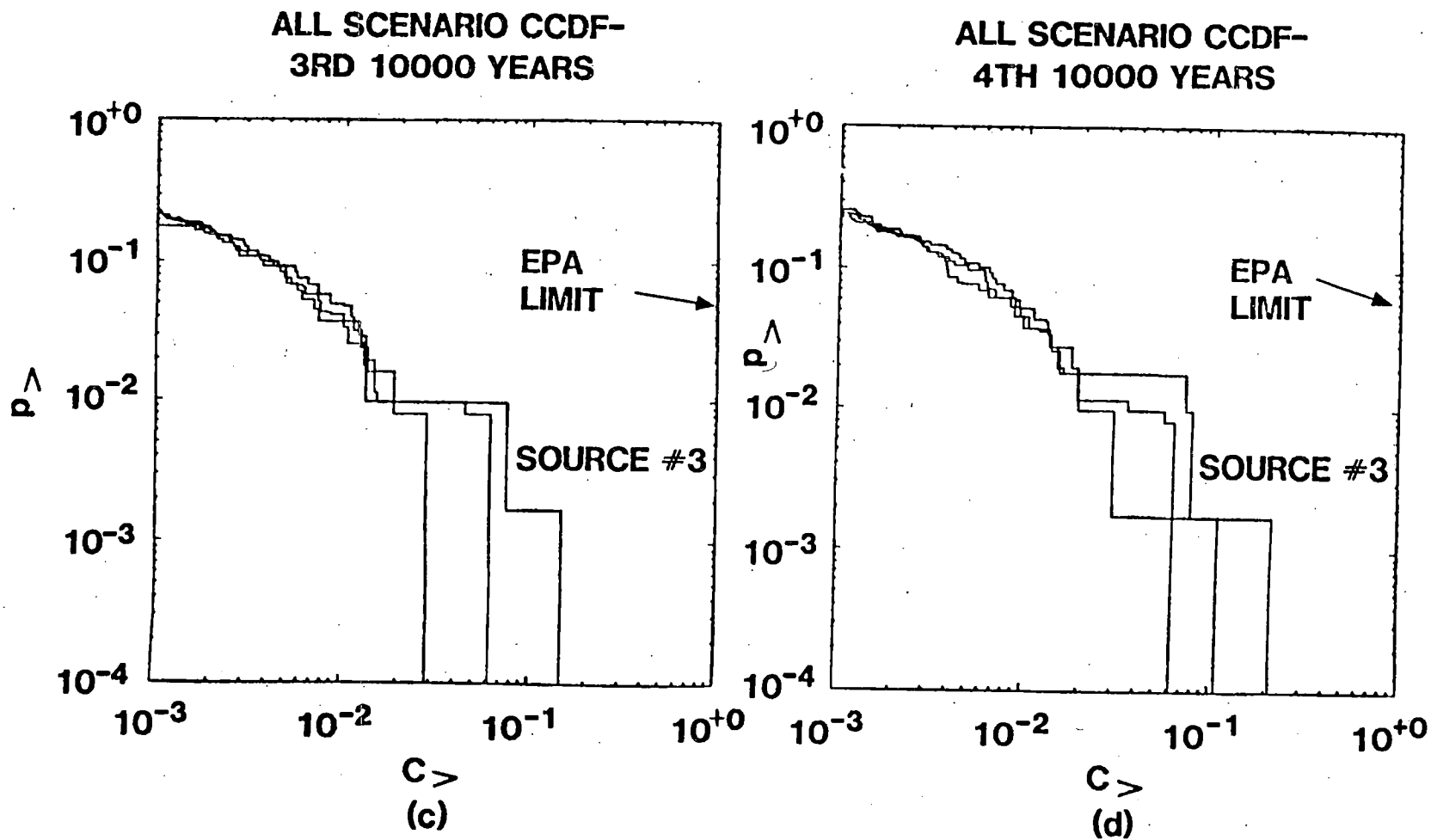
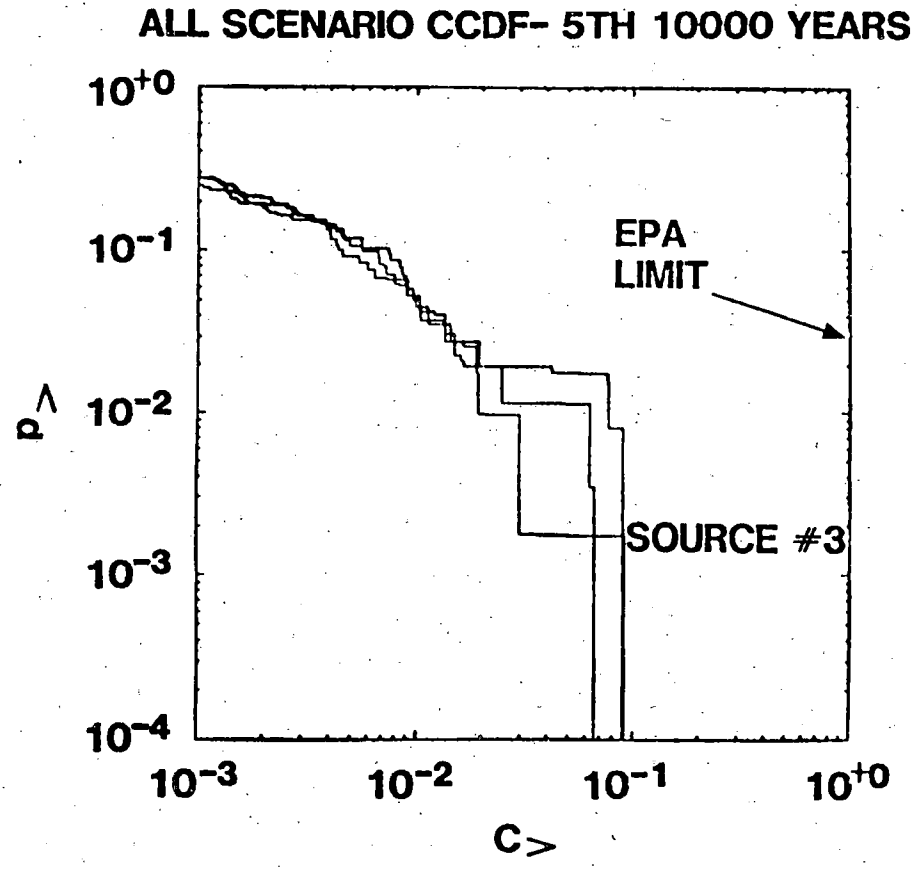


Figure 12. CCDFs for the Groundwater Transport Scenario With Source #3



(e)

Figure 12. CCDFs for the Groundwater Transport Scenario With Source #3

The three traces shown in each figure result from evaluations with the three independent samplings of 50 vectors each. The vertical spread in these plots represents an estimate of sampling error associated with the LHS method. As can be seen, the sampling error is small over most of the curve.

All scenarios evaluated with Source #1 (Figure 10) yield large discharges. The results indicate a violation of the draft EPA Standard in each of the five 10,000-year periods.

The scenarios evaluated with Source #2 (Figure 11) result in much lower discharges, and it appears that compliance is achieved during the first 10,000-year period. The results indicate that the magnitude of the violation is very small.

All scenarios, when evaluated with Source #3, indicate that compliance may be achieved, provided that the mixing cell assumption can be justified. As shown in Appendix A, the release rate with this type of source assumption should asymptotically approach that given by the waste-form description alone (Table 7). Since we assumed a less stable wasteform, in conjunction with the mixing cell model, we can infer that the time required to achieve that asymptotic release rate was long compared to the times for which discharges were calculated. The importance of the release rate assumption is indicated by comparing Figures 10, 11, and 12.

#### D. Sensitivity Analysis Results

For the groundwater transport scenarios we applied standard sensitivity analysis methods to the calculated discharges as measured by the EPA Sum (Equation 1) [17]. The results of this analysis indicate the relative importance of the various data used in the transport calculations (Tables 6 through 9). The important variables determined by this analysis are tabulated here:

Scenario	Source	
	#1 and #2	#3
1	$R_d(U), \tau$	$S(U), \tau$
2	$R_d(U), \tau$	$S(U), \tau$
3	$R_d(U), \tau, K_{ua}$	$S(U), \tau$
4	$R_d(U), \tau, K_{ua}$	$S(U), \tau$

In this table,

$R_d(U)$  = Uranium sorption ratio (Table 8),

$\tau$  = Leach period (reciprocal of Table 7),

$S(U)$  = Uranium solubility limit (Table 9),

$K_{ua}$  = Hydraulic conductivity of the upper aquifer, Unit O or D (Table 6).

The variables appearing in the table are those that control the time of onset of discharge (breakthrough) and the rate of discharge. For slowly varying discharge rates.

$$\left( \begin{array}{c} \text{Integrated} \\ \text{Discharge} \end{array} \right) \cong \left( \begin{array}{c} \text{Discharge} \\ \text{Rate} \end{array} \right) * \left( \begin{array}{c} \text{Breakthrough} \\ T - \\ \text{Time} \end{array} \right)$$

where T denotes the end of the period of interest, e.g., T = 10,000 years.

For Source #3 the variables controlling the breakthrough time do not appear to be as important as for Sources #1 and #2. This is likely due to the shape of the leading edge of the discharge pulse. As shown in Appendix A, the mixing cell model gives a release rate (source term for NWFT/DVM) that is initially proportional to the leach rate,  $\tau^{-1}$ , and increases linearly with time initially. For the leach limited sources, the discharge rate is nearly a step-function. Thus, we expect a larger sensitivity to variables controlling the time of breakthrough for sharply defined breakthroughs than for the slowly increasing breakthroughs typical of Source #3.

Of note is the importance of the sorption ratio and solubility limit values of Uranium. Since we calculated discharges for a mixture of radionuclides, the variables influencing all radionuclides may be expected to be most important e.g.,  $\tau$ ,  $K_{ua}$ . The appearance of element-specific variables indicates the dominance of the element(s) in the mixture.

## VII. Conclusions

From the analyses presented here, we can draw several conclusions and make recommendations:

- Drilling-related direct-hit scenarios in sedimentary basins indicate only slight violations of the draft EPA standard.
- Brine pockets in bedded salt may pose a significant problem in complying with the draft EPA Standard. Therefore, site characterization should directly address the question of identifying any brine pockets that may be present. If few brine pockets and low drilling rates can be expected, the probability of this scenario can be kept low. Our modeling of this scenario is admittedly simplistic. Impermeable backfills may be expected in actual designs serving to limit the amount of waste that may mix with the flowing brine. Refining the description of this scenario is clearly needed. For example, we assumed that  $(1/40) \times (1/106)$  of the entire waste inventory came into contact with the flowing brine. This fraction represents some 48 canisters distributed over a 100-foot length of the storage room. In fact, one may expect the brine to flow predominantly in the vicinity of the borehole, contacting a much smaller fraction of the waste and reducing the consequences of this scenario. The descriptions of flow along such a borehole and in the backfilled room, as well as the description of brine pocket characteristics require further analysis. One would expect a description in terms of the fraction of the waste contacted and the amount of flow expected; only such a description would be useful in analyzing such scenarios.
- The importance of the groundwater transport scenarios in contributing to estimates of releases may be great or small, depending on the source model chosen. Since they all result from drilling, steps should be taken to keep future drilling rates low. A reduction in the consequence may be achieved if the assumptions used in Sources #2 and #3 can be justified. Clearly, the fraction of waste available to flowing groundwater, solubilities, and mixing processes must be understood to estimate the importance of their contribution. Unfortunately, we have not analyzed any processes in the area adjacent to a repository. Such analyses would be needed to make definitive statements on these assumptions.

An important assumption that has been made throughout this analysis should be noted. We have assumed failed shafts and boreholes to remain open throughout the calculational period of 50,000 years. In fact, they are likely to close due to creep, unless the groundwater flowing through them dissolves enough salt to keep the conduit open. We have not investigated this assumption in detail. The capability to address it with the DNET Model [12] is currently being developed.

It should be noted that, in general, we have not addressed the entire set of scenarios developed in Reference [5]. We have addressed a subset of scenarios that we feel may be important. Judging from the results calculated, these scenarios are indeed important for any repository similar to the one we have assumed.

A practical difficulty in implementing the draft EPA Standard is the lack of our ability to assign reliable numerical values to the scenario probabilities. The methodology to assess compliance with the standard is, nevertheless, available as has been demonstrated by this and other similar studies.

## APPENDIX A

### The Mixing Cell Source Model (Source #3)

In Source #3 we allow the backfilled regions to be modeled as a mixing cell in which flowing groundwater is assumed to mix with radionuclides in the volume of the mixing cell. The concentration of radionuclides released from the backfilled regions is then given by the uniform concentration in the mixing cell. This model can be calculated analytically for a single stable species.

Let

$V$  = mixing cell volume,

$C$  = radionuclide concentration in water in the mixing cell,

$L$  = rate of radionuclide input into  $V$  from waste form leaching,

and,  $Q$  = rate of water flow through  $V$ .

In the mixing cell model we assume the leach rate,  $L$ , to be given as a constant fractional rate,  $\lambda_L$ , of the initial inventory in the waste form,  $N_0$ ,

$$L = \lambda_L N_0$$

The contaminant concentration in the mixing cell is described by

$$V \frac{dC}{dt} = L - QC \quad (A.1)$$

If we let

$$\lambda_0 = Q/V$$

the solution of A.1 is

$$C(t) = \frac{L}{Q} \left( 1 - e^{-\lambda_0 t} \right) \quad (\text{A.2})$$

For small  $t$ ,

$$C(t) = \frac{tL}{V} .$$

Thus the concentration of the radionuclide increases linearly from zero.

The asymptotic release rate  $QC_\infty$  can be obtained from Equation (A.2) with  $t \rightarrow \infty$ :

$$QC_\infty = L$$

Thus, for long times, the release rate approaches a value governed by the rate of waste-form leaching. The release rate from the mixing cell is then less than or equal to the prescribed waste-form leach rate.

For decaying radionuclide chains, this model is implemented numerically in NWFT/DVM according to the compartment model shown in Figure A-1.

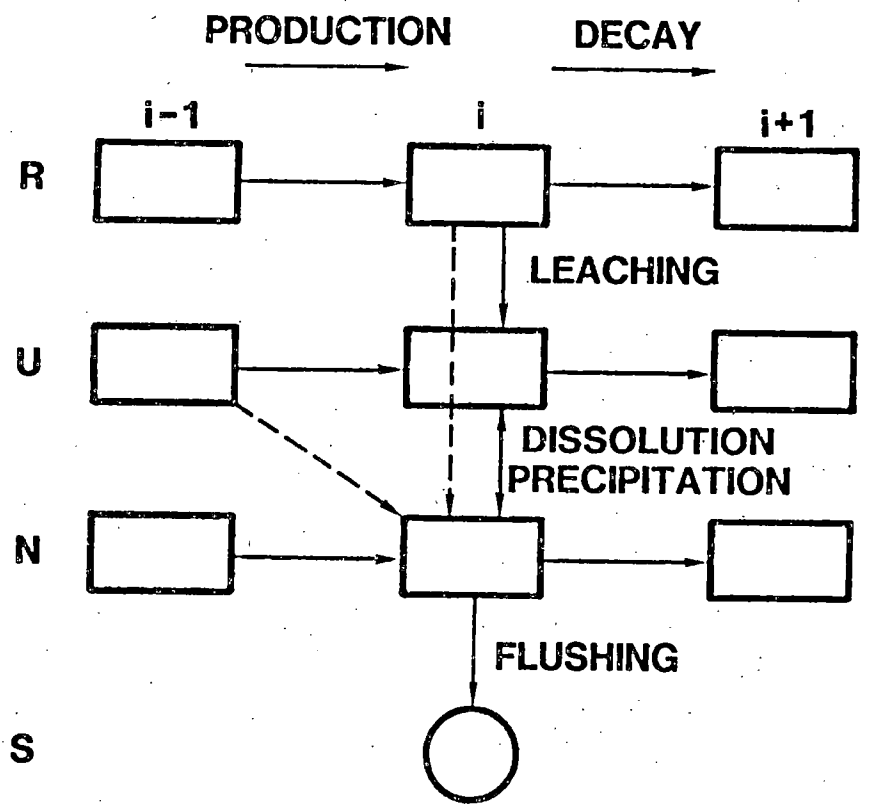


Figure A-1. Implementation of the Mixing Cell Source Model for NWFT/DVM

Radionuclides remaining in the waste form are represented by Compartments, R. The waste-form breakdown rate governs transfer from Compartments R to Compartments U. The inventory in Compartments U is examined along with the water volume in the mixing cell and solubility limits to transfer all or part of that inventory into the mixing cell. The mixing cell inventory is denoted by Compartments N. The mixing cell is flushed constantly to give a release source (S) of

$$S_i = \lambda_0 N_i$$

When solubility limits are applied, radionuclides may be transferred from Compartments N to Compartments U, representing precipitation. For large solubility limits, Compartments U may be empty. Then, transfer to Compartments N may occur directly along the dotted paths of Figure A-1.

Horizontal transfer between radionuclides compartment,  $i$ , and compartments  $i + 1$  or  $i - 1$  represents decay and production.

APPENDIX B

Geohydrologic Data for Bedded Salt

Table B-1

R<sub>d</sub> Ranges in Aquifer\* (Bedded Salt)

Radionuclide	Media**	R <sub>d</sub> Range (ml/g)	References
Am	a	50-1,000	40,41,59,60,74,77
	b	700-10 <sup>4</sup>	20,21,28,33,34,37, 40,41,53,69,74
Pu	a	300-3,000	24,40,48,55,56,58 60-63,76,77
	b	30-10 <sup>4</sup>	20,21,24,28-32,37 41,53,54,69,76,77
U	a	0	57
	b	1-270	26, 27, 33, 34, 41
Np	a	2-40	41,58,60,61,74
	b	2-400	20,21,41,59-61,74
Fission Products (Cs)	a	0-100	19,22,34,51,52,59,60, 64
	b	70-3,000	20,21,24,28,30,33,34, 41-43,45-47,51-53,65, 70,73,76,78,80.

\*These data are in oxidizing, relative fresh (potable) water  
(pH 6-8; salinity < 5,000 ppm)

\*\*a-Quartz and clean sediments;  
b-dirty and clayey sediments.

TABLE B-2

Bedded Salt Hydraulic Parameters

Parameter	Range in Table 6 and/or Main Text	Range of Data in Available Ref.	Reference	Explanation
Conductivity in Aquifer (ft/day)	0.15-680	9.4-37 8	81 82	A range of 4-25 (0.25-0.75 quantiles) was expanded to 0.15-680 to represent 0.001-0.999 quantiles
Porosity in Aquifer	0.1-0.2	0.1-0.2	83,84	NA
Gradient in Aquifer (ft/ft)	1.E-4 - 1.E-2	2.E-3	87	

B-2

## REFERENCES

1. Environmental Protection Agency, 40CFR191, Internal Working Draft 19, Federal Register, March 19, 1981.
2. Nuclear Regulatory Commission, 10CFR60 (Draft), Federal Register 46, No. 130, July 8, 1981.
3. Smith, C. B., D. J. Egan, Jr., and others, "Population Risks From Disposal of High Level Radioactive Wastes in Geologic Repositories" (Draft), EPA 520/3-80-006, Environmental Protection Agency, 1982.
4. Cranwell, R. M., J. E. Campbell, and others, "Risk Methodology for Geologic Disposal of Radioactive Waste: Final Report," SAND81-2573 (NUREG/CR-2452), Sandia National Laboratories, 1982.
5. Cranwell, R. M., R. V. Guzowski, J. E. Campbell, and N. R. Ortiz, "Risk Methodology for Geologic Disposal of Radioactive Waste: Scenario Selection Procedure," SAND80-1429, (NUREG/CR-1667), Sandia National Laboratories, 1982.
6. Pepping, R. E., M. S. Chu, and M. D. Siegel, "Technical Assistance for Regulatory Development: Review and Evaluation of the Draft EPA Standard 40CFR191 for Disposal of High-Level Waste. Volume 2, A Simplified Analysis of a Hypothetical Repository in a Basalt Formation," SAND82-1557, (NUREG/CR-3235), Sandia National Laboratories, 1983.
7. Egan, D. J., Environmental Protection Agency, Public Presentation at the Symposium of Uncertainties Associated With the Regulation of the Geologic Disposal of High-Level Radioactive Wastes, Gatlinburg, Tennessee, March 9-13, 1981.
8. Ritchie, J. S., "A National Waste Terminal Storage Repository in a Bedded Salt Formation for Spent Unreprocessed Fuel: Conceptual Design Description," Report 78-58-R, Oakland, California, Kaiser Engineers, December 1978.
9. Ritchie, J. S., "A National Waste Terminal Storage Repository in a Bedded Salt Formation for Spent Unreprocessed Fuel: Conceptual Design Report," Vols. 1 and 2, Report 78-57-RE, Oakland, California, Kaiser Engineers, December 1978.

REFERENCES (Continued)

10. Ritchie, J. S., "A National Waste Terminal Storage Repository in a Bedded Salt Formation for Spent Unreprocessed Fuel: Twenty-Five-Year Retrievability, Special Study," Report 78-60-RE, Oakland, California, Kaiser Engineers, December 1978.
11. Pepping, R. E., R. J. Campana, D. D. Jensen, and P. H. Raabe, "Risk Analysis Methodology for Spent Fuel Repositories in Bedded Salt: Reference Repository Definition and Contributions From Handling Activities," SAND81-0219, (NUREG/CR-1931), Sandia National Laboratories, July 1981.
12. Cranwell, R. M., J. E. Campbell, and S. E. Stuckwisch, "Risk Methodology for Geologic Disposal of Radioactive Waste: The DNET Computer Code User's Manual," SAND81-1663, (NUREG/CR-2343), Sandia National Laboratories, January 1982.
13. Channell, J. K., "Calculated Radiation Doses from Radionuclides Brought to the Surface if Future Drilling Intercepts the WIPP Repository and Pressurized Brine," EEG-11, Environmental Evaluation Group, Health and Environment Department, State of New Mexico, January 1982.
14. Campbell, J. E., D. E. Longsine, and M. Reeves, "Risk Methodology for Geologic Disposal of Radioactive Waste: The Distributed Velocity Method of Solving the Convective-Dispersion Equation," SAND80-0717 (NUREG/CR-1376), Sandia National Laboratories, 1980.
15. Iman, R. L., J. M. Davenport, and D. K. Zeigler, "Latin-Hypercube Sampling (Program User's Guide)," SAND79-1473, Sandia National Laboratories, 1980.
16. Muller, A. B., N. C. Finley, and F. Pearson, Jr., "Geochemical Parameters Used in the Bedded Salt Reference Repository Risk Assessment Methodology," SAND81-0557 (NUREG/CR-1996), Sandia National Laboratories, 1981.
17. Iman, R. L., J. C. Helton, and J. E. Campbell, "Risk Methodology for Geologic Disposal of Radioactive Waste: Sensitivity Analysis Techniques," SAND78-0912, (NUREG/CR-0390), Sandia National Laboratories, October 1978.

18. Baetsle, L. and P. Dejonghe, "Investigations on the Movement of Radioactive Substances in the Ground. Part III: Practical Aspects of the Program and Physicochemical Consideration," In: Ground Disposal of Radioactive Wastes, TID-7628, pp. 198-210, 1962.
19. Baetsle, L. H., P. Dejonghe, W. Maes, E. S. Simpson, J. Souffriau, and P. Staner, "Underground Radionuclide Movement," EURAEC-703, 1964.
20. Barney, G. S., and P. D. Anderson, "The Kinetics and Reversibility of Radionuclide Sorption Reactions with Rocks - Progress Report for 1978," in Task 4 Second Contractor Information Meeting, Vol. II, R. J. Serne editor, PNL-SA-7352 Vol. II, Pacific Northwest Laboratory, Richland, Washington, pp. 161-218, 1979.
21. Barney, G. S., and G. E. Brown, "The Kinetics and Reversibility of Radionuclide Sorption Reactions with Rocks," in Task 4 Third Contractor Information Meeting Vol. II, edited by J. F. Relyea, PNL-SA-8572, Pacific Northwest Laboratory, Richland, Washington, pp. 261-308, 1980.
22. Berak, L., "The Sorption of Microstrontium and Microcesium on the Silicate Minerals and Rocks," UJV-528-63, 1963.
23. Cerrai, E., M. G. Mezzadri and C. Triulzi, "Sorption Experiments of Strontium, Cesium, Promethium, and Europium on Marine Sediment Samples," Energia Nucleare, 16(6) p. 378-385, 1969.
24. Coles, D. G., H. C. Weed, and J. D. Tewhey, "Geochemical Studies of Sorption and Transport of Radionuclides in Rock Media," in Task 4 Third Contractor Information Meeting, Vol. I, edited by J. F. Relyea, PNL-SA-8572, Pacific Northwest Laboratory, Richland, Washington, pp. 357-434, 1980.
25. Dlouhy, A., "Movement of Radionuclides in the Aerated Zone," In: Disposal of Radioactive Wastes into the Ground, IAEA-SM-93/18, pp. 241-249, 1967.
26. Dosch, R. G., "Assessment of Potential Radionuclide Transport in Site-Specific Geologic Formations," SAND79-2468, Sandia National Laboratories, 1980.
27. Dosch, R. G., "Solubility and Sorption Characteristics of Uranium (VI) Associated with Rock Samples and Brines/ Groundwaters from WIPP and NTS," SAND80-1595, Sandia National Laboratories, 1981.

28. Dosch, R. G., and A. W. Lynch, "Interaction of Radionuclides with Geomedia Associated with the Waste Isolation Pilot Plant (WIPP) Site in New Mexico," SAND78-0297, Sandia National Laboratories, 1978.
29. Duursma, E. K. and C. J. Bosch, "Theoretical, Experimental, and Field Studies Concerning Diffusion of Radioisotopes in Sediments and Suspended Particles of the Sea. Part B: Methods and Experiments," Netherlands Journal of Sea Research, 4, p. 395-469, 1970.
30. Duursma, E. K., and M. G. Gross, "Marine Sediments and Radioactivity," In: Radioactivity in the Marine Environment, National Academy of Sciences, Washington, D.C., pp. 147-160, 1971.
31. Duursma, E. K., and P. Parsi, "Distribution Coefficients of Plutonium Between Sediment and Seawater," In: Activities of the International Laboratory of Marine Radioactivity, IAEA-163, pp. 94-96, 1974.
32. Duursma, E. K., P. Parsi, and G. Statham, "Fixation of Radionuclides with Time by Marine Sediments." IAEA-163, pp. 107-108, 1974.
33. Erdal, B. R., and others, "Laboratory Studies of Radionuclide Distributions Between Selected Ground Waters and Geologic Media," in Task 4 Second Contractor Information Meeting Vol. II, edited by R. J. Serne, PNL-SA-7352 Vol. II, Pacific Northwest Laboratory, Richland, Washington, pp. 4-160, 1979.
34. Erdal, B. R., and others, "Laboratory Studies of Radionuclide Distribution Between Selected Ground Waters and Geologic Media," in Task 4 Third Contractor Information Meeting Vol. I, edited by J. F. Relyea, PNL-SA-8571, Pacific Northwest Laboratory, Richland, Washington, pp. 435-525, 1980.
35. Francis, C. W., and E. A. Bondietti, "Sorpton of Long-Lived Radionuclide Species on Geologic Media FY79 Annual Report," in Task 4 Third Contractor Information Meeting, Vol II, edited by J. F. Relyea, PNL-SA-8572, Pacific Northwest Laboratory, Richland, Washington, pp. 81-133, 1980.
36. Fukai, R. and H. N. Lang, "Studies on the Chemical Behavior of Radionuclides in Seawater. I. General Considerations, and Study of Precipitation of Trace Amounts of Chromium, Maganese, Iron, Cobalt, Zinc and Cerium," IAEA. Radioactivity in the Sea, Publication No. 22, 1968.

37. Fukai, R., and C. N. Murray, "Adsorption and Desorption of Plutonium and Americium in Freshwater - Sediment and Seawater - Sediment Systems," In: Activities of the International Laboratory of Marine Radioactivity, IAEA-163, pp. 96-103, 1974.
38. Garder, K., and O. Skulberg, "Sorption Phenomena of Radionuclides to Clay Particles in River Water," Intern. J. Air Water Pollution, 8, p. 229-41, 1964.
39. Gast, R. G., "The Behavior of Technetium-99 in Soils and Plants," Progress Report, COO-2447-1, 1975.
40. Hamstra, J., and B. Verkerk, "Review of Netherlands Program for Geologic Disposal of Radioactive Waste," IAEA-CN-36/289, In: Nuclear Power and Its Fuel Cycle Proceedings of Salzberg Conference, IAEA, 1977.
41. Harwell, M. A., "Reference Site Initial Assessment for a Salt Dome Repository," PNL-2955, Vol. 1, Pacific Northwest Laboratory, Richland, Washington, 1980.
42. Janzer, V. J., M. C. Goldberg, C. G. Angelo, and W. A. Beetem, "Summary of Distribution Coefficients for Fission Products Between Ground Water and Rocks from Project Gnome," In: Hydrologic and Geologic Studies for Project Gnome. Part IV, U.S.G.S., 1962.
43. Kuznetsov, Y. V., and V. N. Schebetkovskii, "Distribution of Radioactive Isotopes Between Sea Waters and Sediments," Geokhimiya, No. 12, p. 1466-1472 (in Russian), 1971.
44. McHenry, J. R., "Adsorption and Retention of Cesium by Soils of the Hanford Project," HW-31011, 1954.
45. Meyer, R. E., S. Y. Shiao, P. Rafferty, J. S. Johnson, Jr., I. L. Thomas, and K. A. Kraus, "Systematic Study of Nuclide Sorption on Select Geologic Media," in Waste Isolation Safety Assessment Program Task 4 Contractor Information Meeting Proceedings, edited by R. J. Serne, PNL-SA-6957, Pacific Northwest Laboratory, Richland, Washington, pp. 343-369, 1978.
46. Meyer, R. E., "Systematic Study of Metal Ion Sorption on Selected Geologic Media," in Task 4 Second Contractor Information Meeting Vol. I, edited by R. J. Serne, PNL-SA-7352, Vol I, Pacific Northwest Laboratory, Richland, Washington, pp. 231-329, 1979.

47. Meyer, R. E., "Systematic Study on Nuclide Adsorption on Selected Geologic Media," In Task 4 Third Contractor Information Meeting Vol. II, edited by J. F. Relyea, PNL-SA-8571, Pacific Northwest Laboratory, Richland, Washington, pp. 1-79, 1980.
48. Nishita, H., B. W. Kowalewsky, A. J. Steen, and K. H. Larson, "Fixation and Extractability of Fission Products Contaminating Various Soils and Clays: I. Strontium-90, Ruthenium-106, Cesium-137, and Cesium-144," Soil Science, 81, p. 317-326, 1956.
49. Nishita, H., M. Hamilton, and A. J. Steen, "Extractability of  $^{238}\text{Pu}$  and  $^{242}\text{Cm}$  from a Contaminated Soil as a Function of pH and Certain Soil Components.  $\text{HNO}_3$  -  $\text{NaOH}$  System," Presented at Annual Meeting of Soil Science Society of America, Houston, Texas, 1976.
50. Nishiwaki, Y., Y. Honda, Y. Kimura, H. Morishima, T. Koga, Y. Miyaguchi, and H. Kawai, "Behavior and Distribution Of Radioactive Substances in Coastal and Estuarine Waters," In: Radioactive Contamination of the Marine Environment, IAEA-SM-158-11, pp. 177-193, 1972.
51. Nork, W. E., and P. R. Fenske, "Radioactivity in Water - Project Rulison," NVO-1229-131, 1970.
52. Nork, W. E., E. J. Forslow, and E. H. Essington, "Radioactivity in Water, Central Nevada Test Area," NVO-1229-175, 1971.
53. Nowak, E. J., "Radionuclide Sorption and Migration Studies of Getters for Backfill Barriers," SAND79-1110, Sandia National Laboratories, 1980.
54. Pillai, K. C., and E. Mathew, "Plutonium in Aquatic Environment -- Its Behavior, Distribution and Significance," IAEA-SM-199/27, 1975.
55. Prout, W. E., "Adsorption of Radioactive Wastes by Savannah River Plant Soil," Soil Science, 86, p. 13-17, 1958.
56. Prout, W. E., "Adsorption of Fission Products by Savannah River Plant Soil," DP-394, 1959.
57. Rancon, D., "The Behavior in Underground Environments of Uranium and Thorium Discharged by the Nuclear Industry," In: Environmental Behavior of Radionuclides Released in the Nuclear Industry, IAEA-SM-172/55, pp. 333-346 (in French), 1973.

58. Relyea, J. F., and D. A. Brown, "The Diffusion of Pu-238 in Aqueous and Soil Systems," Agronomy Abstracts, p. 124, 1975.
59. Relyea, J. F., R. J. Serne, D. Rai and M. J. Mason. "Batch Kd Experiments with Common Minerals and Representative Ground Waters," in Waste Isolation Safety Assessment Program Task 4 Contractor Information Meeting Proceedings, edited by R. J. Serne, PNL-SA-6957, Pacific Northwest Laboratory, Richland, Washington, pp. 125-150, 1978.
60. Relyea, J. F., and others, "Batch Kd Experiments with Common Minerals and Representative Ground Waters," in Task 4 Second Contractor Information Meeting Vol. II, edited by R. J. Serne, PNL-SA-7352, Vol. II, Pacific Northwest Laboratory, Richland, Washington, pp. 259-330, 1979.
61. Relyea, J. F., R. J. Serne, R. W. Fulton, C. D. Washburn, and W. J. Martin, "Laboratory Studies of Pu-237 Sorption on Selected Minerals Under Anoxic Conditions," in Task 4 Third Contractor Information Meeting Vol. II, edited by J. F. Relyea, PNL-SA-8571, Pacific Northwest Laboratory, Richland, Washington, pp. 135-158, 1980.
62. Rhodes, D. W., "Preliminary Studies of Plutonium Adsorption in Hanford Soil," HW-24548, 1952.
63. Rhodes, D. W., "The Adsorption of Plutonium by Soil," Soil Science, 84, pp. 465-471, 1957.
64. Rhodes, D. W., "The Effect of pH on the Uptake of Radioactive Isotopes from Solution by a Soil," Soil Science Society of America, Proceedings, 21, pp. 389-392, 1957.
65. Routson, R. C., "A Review of Studies on Soil-Waste Relationships on the Hanford Reservation from 1944 to 1967," BNWL-1464, Battelle Northwest Laboratory, 1973.
66. Routson, R. C., G. Jansen, and A. V. Robinson, "<sup>241</sup>Am, <sup>237</sup>Np, and <sup>99</sup>Tc Sorption on Two United States Subsoils from Differing Weathering Intensity Areas," BNWL-1889, Battelle Northwest Laboratory, 1976.
67. Schebetkovskii, V. N., and Y. V. Kuzketsov, "W73-04324 Behavior of Cs-137 and Ce-144 in the Sorption System Sea Water-Sediment." Trans. from Radiokhimiya, 13(6), pp. 911-913, 1971.

68. Schell, W. R., T. H. Sibley, A. Nevissi, and A. Sanchez, "Distribution Coefficients for Radionuclides in Aquatic Environments. II. Studies on Marine and Freshwater Sediment Systems Including the Radionuclides 106-Ru, 137-Cs and 241-Am," Second Annual Research Progress Report, NUREG/CR-0802, 1979.
69. Schell, W. R., T. H. Sibley, A. Sanchez and J. R. Clayton, Jr., "Distribution Coefficients for Radionuclides in Aquatic Environments, III. Adsorption and Desorption Studies of 106Ru, 137Cs, 241Am, 85Sr and 237Pu in Marine Freshwater Systems," NUREG/CR-0803, 1980.
70. Schmalz, B. L., "Radionuclide Distribution in Soil Mantle of the Lithosphere as a Consequence of Waste Disposal at the National Reactor Testing Station," IDO-10049, 1972.
71. Serne, R. J., "Ra Kd Values for Utah Soils," Subcontracted from Dames and Moore, Battelle-Northwest, Richland, Washington, 1974.
72. Serne, R. J., D. Rai, M. J. Mason, and M. A. Molecke, "Batch Kd Measurements of Nuclides to Estimate Migration Potential at the Proposed Waste Isolation Pilot Plant in New Mexico," PNL-2448, Pacific Northwest Laboratory, Richland, Washington, 1977.
73. Seymour, A. H., A. Nevissi, W. R. Schell and A. Sanchez, "Distribution Coefficients for Radionuclides in Aquatic Environments. I. Development of Methods and Results for Plutonium and Americium in Freshand Marine Water-Sediment Systems," First Annual Research Progress Report, NUREG/CR-0801, 1979.
74. Sheppard, J. C., J. A. Kittrick, and T. L. Hart, "Determination of Distribution Ratios and Diffusion Coefficients of Neptunium, Americium and Curium in Soil-Aquatic Environments," RLO-2221-T-12-2, 1976.
75. Sorathesn, A., G. Bruscia, T. Tamura, and E. G. Struxness, "Mineral and Sediment Affinity for Radionuclides," CF-60-6-93, 1960.
76. Tamura, T., "Sorption Phenomena Significant in Radioactive - Waste Disposal," In: Underground Waste Management and Environmental Implications, edited by T. D. Cook, Am. Assoc. Petrol. Geol. pp. 318-330, 1972.
77. Van Dalen, A., F. DeWitte, and J. Wiskstra, "Distribution Coefficients for Some Radionuclides Between Saline Water and Clays, Sandstones and Other Samples from the Dutch Subsoil," Reactor Centrum Nederland, pp. 75-109, 1975.

78. Wilding, M. W., and D. W. Rhodes, "Removal of Radioisotopes from Solution by Earth Materials from Eastern Idaho," IDO-14624, 1963.
79. Wildung, R. E., R. C. Routson, R. J. Serne, and T. R. Garland, "Pertechnetate, Iodide and Methyl Iodide Retention by Surface Soils," BNWL-1950, Pt. 2, Battelle Northwest Laboratory, pp. 37-40, 1975.
80. Winslow, C. D., "The Sorption of Cesium and Strontium from Concentrated Brines by Backfill Barrier Materials," SAND80-2046, Sandia National Laboratories, 1981.
81. Myers, B. N., "Compilation of Results of Aquifer Tests in Texas," Texas Water Devel. Board Rept. 98, 537 p., 1969.
82. Popkin, B. P., "Ground-water Resources of Conley County, Texas," Texas Water Devel. Board Rept. 64, 75 p., 1973.
83. Cronin, J. G., "A Summary of the Occurrence and Development of Ground Water in the Southern High Plains of Texas," Texas Board of Water Engineers Bull. 6107, 110 p., 1961.
84. Alexander, W. M., Jr., "Geology and Ground-water Resources of the Northern High Plains of Texas," Progress Report No. 1: Texas Board of Water Engineers Bull. 6109, 47 p., 1961.
85. Bassett, R. L., M. E. Bentley, and W. W. Simpkins, "Regional Ground-water Flow in the Panhandle of Texas, A Conceptual Model," Texas Bur. Econ. Geol., Geol. Circ. 81-3, pp. 102-107, 1981.
86. Touloukian, Y. S., W. R. Judd, and R. F. Roy, eds., Physical Properties of Rocks and Minerals: McGraw-Hill/CINDAS data series on material properties, v. II-2, 548 p., 1981.
87. Cronin, J. G., "Ground Water in Ogallala Formation in the Southern High Plains of Texas and New Mexico," U.S.G.S., Hydrologic Inv. Atlas HA-330, 1969.

<b>NRC FORM 335</b> (11-81)		<b>U.S. NUCLEAR REGULATORY COMMISSION</b> <b>BIBLIOGRAPHIC DATA SHEET</b>		1. REPORT NUMBER (Assigned by DDC) NUREG/GR-3235, Vols. 2,3 and 4 SAND82-1557	
4. TITLE AND SUBTITLE (Add Volume No., if appropriate) <b>Technical Assistance for Regulatory Development: Review and Evaluation of the Draft EPA Standard 40CFR191 for Disposal of High-Level Waste</b>				2. (Leave blank)	
7. AUTHOR(S) <b>Fuel Cycle Risk Analysis Division</b>				5. DATE REPORT COMPLETED MONTH: <b>April</b> YEAR: <b>1983</b>	
9. PERFORMING ORGANIZATION NAME AND MAILING ADDRESS (Include Zip Code) <b>Sandia National Laboratories          Fuel Cycle Risk Analysis          Division 9413          Albuquerque, New Mexico 87185</b>				DATE REPORT ISSUED MONTH: <b>April</b> YEAR: <b>1983</b>	
12. SPONSORING ORGANIZATION NAME AND MAILING ADDRESS (Include Zip Code) <b>Division of Waste Management          Office of Nuclear Material Safety and Safeguards          U.S. Nuclear Regulatory Commission          Washington, D.C. 20555</b>				6. (Leave blank)	
13. TYPE OF REPORT <b>Formal Report</b>				8. (Leave blank)	
15. SUPPLEMENTARY NOTES				10. PROJECT/TASK/WORK UNIT NO.	
16. ABSTRACT (200 words or less) <b>Analyses of a hypothetical nuclear waste repository in each of three geologic media (basalt, tuff and bedded salt) have been performed to assess compliance with the Draft (#19) EPA Standard 40CFR191. Hypothetical sites are based on representative data for geologies in the continental U.S. The effects of uncertainties in the input data and in the interpretation of the standard on the assessment of compliance are demonstrated. The results of the calculations indicate: 1) For basalt media, compliance with the draft standard may be achieved depending on how the term "release" is interpreted; namely, is the release due to a unique (single) event or does it involve all probable scenarios. 2) For tuff media, sorption of radionuclides is an effective barrier to actinide migration even in the absence of solubility constraints. Discharges of <sup>99</sup>Tc and <sup>14</sup>C may cause violations of the draft standard; however, retardation due to matrix diffusion may eliminate discharge of these radionuclides for realistic conditions. For short groundwater travel times to the accessible environment, discharges of uranium and neptunium could exceed the draft standard under oxidizing conditions if the radionuclides do not pass through thick sequences of sorbent zeolitized tuff. 3) For bedded salt media, compliance depends on the source model used. Penetration scenarios (direct canister hit or brine pocket hit) indicate potentially serious consequences. However, these could be mitigated by proper site selection and institutional controls.</b>				11. FIN NO. <b>NRC FIN A 1165</b>  <b>Task 3</b>	
17. KEY WORDS AND DOCUMENT ANALYSIS				PERIOD COVERED (Inclusive dates) <b>July 1981-April 1983</b>	
17b. IDENTIFIERS/OPEN-ENDED TERMS				14. (Leave blank)	
18. AVAILABILITY STATEMENT <b>Unlimited</b>		19. SECURITY CLASS (This report) <b>Unclassified</b>		21. NO. OF PAGES	
20. SECURITY CLASS (This page) <b>Unclassified</b>		22. PRICE <b>S</b>			

Xerox D125 Copier-Printer  
Banner Sheet

freeflow1

Date & Time : 02/26/2020 9:13 AM

User Name :

freeflow1

---

Job Name : 3235v5-6-CR.pdf

Start Page

---

---

---

# Technical Assistance for Regulatory Development: Review and Evaluation of the Draft EPA Standard 40CFR191 for Disposal of High-Level Waste

- Health Effects Associated with Unit Radionuclide Releases to the Environment
- Calculation of Health Effects per Curie Release for Comparison with the EPA Standard

---

---

Prepared by Fuel Cycle Risk Analysis Division

Sandia National Laboratories

April 1983

Prepared for  
U.S. Nuclear Regulatory  
Commission

OTHER VOLUMES OF  
SAND82-1557  
NUREG/CR-3235

Main Title:

Technical Assistance for Regulatory Development: Review and Evaluation of the EPA Standard 40CFR191 for Disposal of High-Level Waste.

- Volume 1            Executive Summary  
                     N. R. Ortiz, K. Wahi
- Volume 2            A Simplified Analysis of a Hypothetical High-  
                     Level Waste Repository in a Basalt Formation  
                     R. E. Pepping, M. S. Chu, M. D. Siegel
- Volume 3            A Simplified Analysis of a Hypothetical High-  
                     Level Waste Repository in a Tuff Formation  
                     M. D. Siegel, M. S. Chu
- Volume 4            A Simplified Analysis of a Hypothetical High-  
                     Level Waste Repository in a Bedded Salt  
                     Formation  
                     R. E. Pepping, M. S. Chu, M. D. Siegel
- Volume 5            Health Effects Associated with Unit Radio-  
                     nuclide Releases to the Environment  
                     J. C. Helton
- Volume 6            Calculation of Health Effects Per Curie  
                     Release for Comparison with the EPA Standard  
                     G. E. Runkle

**Volume 5**

**Health Effects Associated with Unit  
Radionuclide Releases to the Environment**

NUREG/CR-3235  
SAND82-1557  
WH

**TECHNICAL ASSISTANCE FOR REGULATORY DEVELOPMENT:  
REVIEW AND EVALUATION OF THE DRAFT EPA STANDARD 40CFR191  
FOR DISPOSAL OF HIGH-LEVEL WASTE**

VOL. 5

**HEALTH EFFECTS ASSOCIATED WITH UNIT  
RADIONUCLIDE RELEASES TO THE ENVIRONMENT**

J. C. Helton<sup>\*</sup>

Manuscript Completed: April 1983  
Date Published: April 1983

Sandia National Laboratories  
Albuquerque, New Mexico 87185  
Operated by  
Sandia Corporation  
for the  
U. S. Department of Energy

Prepared for  
Division of Waste Management  
Office of Nuclear Material Safety and Safeguards  
Washington, D.C. 20555

NRC FIN. No. A-1165

<sup>\*</sup>Arizona State University

## ABSTRACT

Simple models are presented for the estimation of individual and population health effects (i.e., latent cancer fatalities) for long-term radionuclide releases to the surface environment. These models were suggested by techniques employed by the Environmental Protection Agency in the development of a proposed standard for the disposal of high-level radioactive waste. The modeling approach is based on the use of asymptotic solutions to mixed-cell models in conjunction with appropriate usage rates, dose factors, risk factors, and population estimates. Although the models are simple, it is felt that they can be used in preliminary investigations of topics in high-level waste disposal such as potential importance of individual radionuclides, relative importance of different release patterns or exposure pathways, and relationships between individual and population exposures. The use of the models is illustrated by calculating the population health effects along various exposure pathways for the radionuclides considered in the proposed Environmental Protection Agency Standard. The results of these calculations are compared with the calculated population exposures on which the proposed Environmental Protection Agency Standard is based.

## TABLE OF CONTENTS

<u>CHAPTER</u>	<u>PAGE</u>
1. Overview	1-1
1.1 Preliminary Comments	1-1
1.2 Computational Approach	1-1
1.3 Computational Results	1-7
1.4 Comparison With Environmental Protection Agency Results	1-22
1.5 Discussion	1-32
2. Mixed-Cell Models	2-1
3. Release to Surface Water	3-1
3.1 Preliminary Comments	3-1
3.2 Exposure From Water Consumption	3-3
3.3 Exposure From Fish Consumption	3-4
3.4 Exposure From Inhalation of Suspended Sediment	3-6
3.5 Exposure From Water Immersion	3-8
3.6 Exposure from Shoreline Sediment	3-9
3.7 Exposure From Suspended Sediment	3-11
4. Release to Soil	4-1
4.1 Preliminary Comments	4-1
4.2 Exposure From Plant Consumption	4-5
4.3 Exposure From Milk Consumption	4-7
4.4 Exposure From Meat Consumption	4-9
4.5 Exposure From Inhalation of Suspended Soil	4-9
4.6 Exposure From Soil	4-11
4.7 Exposure From Suspended Soil	4-13
5. Irrigation After Release to Surface Water	5-1
5.1 Preliminary Comments	5-1
5.2 Exposure From Plant Consumption	5-4
5.3 Exposure From Milk Consumption	5-5
5.4 Exposure From Meat Consumption	5-9
REFERENCES	R-1

LIST OF FIGURES

<u>FIGURE</u>		<u>PAGE</u>
2-1	Flows Associated With a Single Uniformly-Mixed Cell With No Radionuclide Partitioning Between a Liquid and a Solid Phase	2-2
2-2	Flows Associated With a Single Uniformly-Mixed Cell With Radionuclide Partitioning Between a Liquid and a Solid Phase	2-5

## LIST OF TABLES

<u>TABLE</u>		<u>PAGE</u>
1-1	Health Effects per Curie Released for Different Release Modes	1-2
1-2	Cumulative Releases to the Accessible Environment for 10,000 Years After Disposal Proposed by the Environmental Protection Agency	1-3
1-3	Variables Appearing in Tables 1-4, 1-5 and 1-6	1-8
1-4	Exposure to Organ Associated With Cancer J Due to Radionuclide I for Releases to Surface Water	1-12
1-5	Exposure to Organ Associated With Cancer J Due to Radionuclide I for Releases to Soil	1-13
1-6	Exposure to Organ Associated With Cancer J Due to Radionuclide I for Releases to Surface Water With Subsequent Use of Surface Water for Livestock and Sprinkler Irrigation	1-15
1-7	Population Health Effects for 1. Curie Radionuclide Releases to Surface Water	1-16
1-8	Population Health Effects for 1. Curie Radionuclide Release to Soil	1-17
1-9	Population Health Effects for 1. Curie Radionuclide Release to Surface Water with Subsequent Use of Surface Water for Livestock and Sprinkler Irrigation	1-18
1-10	Organs and Risk Factors Considered	1-21
1-11	Variables Used in Calculation of Results Presented in Tables 1-7, 1-8 and 1-9	1-23
1-12	Health Effects per Curie Released for Releases to a River	1-24

## 1. Overview

### 1.1 Preliminary Comments

The Environmental Protection Agency has recently performed an analysis of the population health effects associated with a release to the surface environment of selected radionuclides contained in high-level waste (Sm81). Table 1-1 contains a synopsis of the population health effects calculated in the Environmental Protection Agency analysis due to a one curie release of each of the indicated radionuclides over an extended period of time. In turn, the values contained in this table were used in the derivation of the Environmental Protection Agency's draft standard for the geologic disposal of high-level radioactive waste (En80). Specifically, it was decided to allow 1000 health effects (i.e., latent cancer fatalities) over a 10,000 year period per 100,000 metric tons of heavy metal (MTHM) used as reactor fuel. For each radionuclide, the allowable release limit per 1000 MTHM over a 10,000 year period was obtained by dividing 10 health effects by the health effects per curie for a release to surface water given in Table 1-1. The proposed standard and the results of the indicated calculation are given in Table 1-2.

Releases to surface water are probably the most likely, tended to dominate health effects in the Environmental Protection Agency calculations shown in Table 1-1, and were used in the derivation of the proposed standard given in Table 1-2. For these reasons, it was decided to examine the calculations related to the surface-water exposure pathway. Specifically, it was decided to examine the Environmental Protection Agency calculations by developing simple models of the same type that they used and then using these models to predict individual and population exposures and health effects. In this development, the dose and risk factors presented in Runkle et al. (Ru81) are used.

### 1.2 Computational Approach

The computational results presented are obtained with the use of simple linear models to represent radionuclide movement. Specifically, the models considered are of the form

$$dx/dt = R - AX , \quad (1.1)$$

Table 1-1. Health Effects per Curie Released for Different Release Modes\*

Nuclide	Releases to a River	Releases to an Ocean	Releases to Land Surface	Releases to the Air
C- 14	4.58 E- 2	1.12 E- 7	2.58 E- 5	2.04 E- 4
Ni- 59				
Sr- 90	1.21 E- 1	1.91 E- 6	9.75 E- 4	1.63 E- 2
Zr- 93				
Tc- 99	2.85 E- 4	1.04 E- 6	6.03 E- 8	3.67 E- 5
Sn-126	1.20 E- 1	7.86 E- 6	4.13 E- 2	1.12 E- 1
I-129	1.08 E- 2	9.62 E- 5	2.31 E- 5	1.38 E- 3
Cs-135	3.81 E- 3	1.58 E- 5	4.01 E- 4	7.36 E- 4
Cs-137	1.98 E- 2	1.60 E- 5	5.62 E- 4	6.91 E- 3
Sm-151				
Ra-226				
U-234				
Np-237	5.96 E- 1	2.44 E- 3	3.22 E- 3	8.03 E- 2
Pu-238	2.29 E- 2	2.38 E- 5	3.21 E- 3	1.47 E- 2
Pu-239	6.92 E- 2	1.31 E- 4	5.55 E- 2	5.18 E- 2
Pu-240	6.53 E- 2	1.15 E- 4	4.94 E- 2	4.76 E- 2
Am-241	7.19 E- 1	1.19 E- 2	8.98 E- 2	1.59 E- 1
Pu-242	6.76 E- 2	1.30 E- 4	5.63 E- 2	5.13 E- 2
Am-243	2.68 E 0	8.81 E- 2	1.03 E 0	1.14 E 0

\*This table is a reprint of Table D-1 of (Sm81).

Table 1-2. Cumulative Releases to the Accessible Environment for 10,000 Years After Disposal Proposed by the Environmental Protection Agency

Radionuclide	Half-Life <sup>a</sup> (years)	Proposed Release Limit <sup>b</sup> (curies per 1000 MTHM)	Release Limit From Table 1-1 <sup>c</sup> (curies per 1000 MTHM)
Americium-241	458.	10	13.9*
Americium-243	7370.	4	3.73
Carbon-14	5730	200	218.3
Cesium-135	3.E6	2000	2624.7
Cesium-137	30.2	500	505.0
Iodine-129	1.7E7	900	925.9
Neptunium-237	2.14E6	20	16.8
Plutonium-238	86.	400	436.7
Plutonium-239	2.44E4	100	144.5
Plutonium-240	6580.	100	153.1
Plutonium-242	3.79E5	100	147.9
Radium-226	1600.	3	3.0
Strontium-90	28.1	80	82.6
Technetium-99	2.12E5	2000	35,087.7
Tin-126	1.E5	80	83.3
Any other alpha-emitting radionuclide		10	10
Any other radionuclide which does not emit alpha particles		500	500

a From (We74)

b From (En80)

c Derived from "Releases to a River" in Table 1-1.

where X is the amount of radionuclide in some region of interest (units: Ci), R is the rate of radionuclide input to this region (units: Ci/yr) and A is a rate constant for movement out of that region (units: yr<sup>-1</sup>). The solution of the preceding equation is given by

$$X(t) = e^{-At}X_0 + (R/A)(1. - e^{-At}), \quad (1.2)$$

where X(0) = X<sub>0</sub>. Further, when A is positive as is the case for situations considered in this presentation, the asymptotic or steady state solution to (1.1) is given by

$$SX = R/A . \quad (1.3)$$

It is this latter solution which will be used in the development of dose and risk results to be presented.

The equation appearing in (1.1) is used to represent three different situations. The first situation is a radionuclide release to a surface-water body. Here, for each radionuclide considered,

$$R = TD(I)/T \quad \text{and} \quad A = F/VW , \quad (1.4)$$

where TD(I) equals total release for radionuclide I (units: Ci) over a time period of length T (units: yrs), F equals the flow rate out of the water body under consideration (units: L/yr), and VW equals the volume of the water body (units: L). For completeness, the rate constant A appearing in (1.4) should also contain a term representing radioactive decay. However, as this term would be very small relative to F/VW for the radionuclides commonly considered in the geologic disposal of high-level waste, it is omitted. Radionuclide releases over relatively long time periods will be considered. In particular, dose factors which provide a 70. year dose commitment from a 70. year chronic exposure will be used. Therefore, T must be significantly greater than 70. years. The coefficient A is derived from the assumption that the surface-water body can be treated as a uniformly mixed cell such that a radionuclide can leave the cell only by outward movement.

of water. Additional discussion of R and A can be obtained in Chapter 3.

The second situation is a radionuclide release to soil. Here, for each radionuclide considered, R is defined as in (1.4) and A is defined by

$$A = \frac{S(I)*ER}{DP*(1. - PO)*DE} + \frac{(1. - S(I))*RO}{DP*PO*SA*1000.} + \frac{ALOG(2.)}{HLIFE(I)} , \quad (1.5)$$

where S(I) represents radionuclide partitioning between the liquid and solid phases of the soil and is defined in Table 1-5 (units: unitless), ER represents erosion rate per unit area (units: kg/m<sup>2</sup> per yr), DP represents depth of soil (units: m), PO represents porosity of soil (units: unitless), DE represents mean particle density of soil material (units: kg/m<sup>3</sup>), RO represents runoff rate per unit area (units: L/m<sup>2</sup> per yr), SA represents percent saturation of pore space in soil (units: unitless), ALOG(2.) is the natural logarithm of 2. and HLIFE(I) is the half-life of radionuclide I (units: yr). Due to the slower processes associated with radionuclide movement in soil, radioactive decay is incorporated into the expression appearing in (1.5). The coefficient A is derived from the assumptions that the soil can be treated as a uniformly mixed cell with a water phase and a solid phase such that (1) a radionuclide is partitioned between the water and solid phases on the basis of a distribution coefficient and (2) a radionuclide can leave the cell only by radioactive decay or movements of water and solids. Additional discussion of A can be obtained in Chapter 4.

The third situation is radionuclide deposition on crops due to sprinkler irrigation. In this case,

$$R = FRET*TD(I)*FRIV/T \quad (1.6)$$

and

$$A = ALOG(2.)/WHRHL , \quad (1.7)$$

where TD(I), T and ALOG(2.) are already defined, FRET is

the fraction of deposited radionuclides in sprinkler irrigation initially retained on plants (units: unitless), FRIV is the fraction of the river receiving the radionuclide release used for sprinkler irrigation (units: unitless) and WRRHL is the weathering half life for radionuclides deposited by sprinkler irrigation (units: yrs). The variables R and A are derived from the assumption that the radionuclides retained on plants due to sprinkler irrigation can be treated as being in a uniformly-mixed cell such that radionuclides can enter this cell only by deposition on plants and can leave the cell only by weathering. Due to the generally short weathering half lives which are considered, radioactive decay is omitted in the definition of A. Additional discussion on the derivation of R and A is provided in Chapter 5.

For each of the situations indicated in the three preceding paragraphs, radionuclide movement can be represented by a differential equation of the form given in (1.1). As indicated in (1.3), each of these equations will have an asymptotic solution of the form R/A which represents the amount of radionuclide in the system at steady state. From this solution, steady state concentrations can be obtained by dividing by the appropriate volume or mass. For radionuclide I and release to surface water, the steady state solution is

$$R/A = (TD(I)/T)/(F/VW) = TD(I)*VW/(F*T) \quad (1.8)$$

and so division by VW yields a steady-state concentration of

$$TD(I)/(F*T) \quad (1.9)$$

Similar calculations will yield steady-state concentrations for release to soil and deposition on plants due to sprinkler irrigation.

Once the concentrations indicated in the preceding paragraph are known, they can be used to calculate individual exposure rates. In turn, multiplication of these exposure rates by appropriate dose factors will yield individual dose rates. Then, multiplication by risk factors will yield individual cancer risk. Finally, multiplication of individual dose and risk by popula-

tion size will yield population dose and population risk. Tables 1-4, 1-5 and 1-6 contain selected formulas for individual dose (units: rem/ind) and associated population size (units: ind). Table 1-3 contains definitions for variables used in Tables 1-4, 1-5 and 1-6. Detailed derivations for all relations are given later in the presentation. However, all were derived as already indicated. That is, an asymptotic concentration was obtained in each substrate of interest. Next, these concentrations were used in conjunction with individual usage rates and dose factors to obtain individual dose. Then, multiplication by the appropriate risk factor yields individual risk, and multiplication by the indicated population size yields population dose and risk. Due to the assumed linearity of many of the relations, multiplication by population size often results in considerable simplification of the algebraic expressions for population dose and risk. The appearance of the factor 70 in many of the expressions results from the fact that dose factors for a 70-year dose commitment from a 70-year chronic exposure are being used for ingestion and inhalation. Multiplication of a one year chronic (i.e., assumed to be the same over an entire lifetime) exposure rate by these factors yields the indicated dose commitment.

### 1.3 Computational Results

This section presents population health effects obtained with the relations given in Tables 1-4, 1-5 and 1-6. These results are presented in Tables 1-7, 1-8 and 1-9 and were calculated for a total discharge of 1. curie per radionuclide (i.e.,  $TD(I) = 1.$ ). The dose factors used in these calculations are given in Tables 2.1, 2.2 and 2.3 of Runkle et al. (Ru81). The cancers and associated risk factors used are listed in Table 1-10. For each exposure mode, the indicated population health effect is the sum of the health effects for the individual cancers. All water treatment factors are assumed to be 1. (i.e.,  $WT(I) = 1.$ ), and concentration ratios (i.e.,  $CRDM(I)$ ,  $CRDMT(I)$ ,  $CRSP(I)$ ,  $CRWF(I)$ ) are taken from Tables A-8 and C-5 of Nuclear Regulatory Commission Guide 1.109 (Nu76). The distribution coefficients employed for surface water and soil are the same as those given in the Environmental Protection Agency analysis for sediment (Sm81, Table 5-5); however, all distribution coefficients indicated as being zero in the preceding table were assigned the value of 1. for our analysis. The Environmental Protection Agency may have used different distribution coefficients for soil calculations but their documentation does not make this clear

Table 1-3. Variables Appearing in Tables 1-4,  
1-5 and 1-6

Variable	Definition
AIRCON	Concentration of suspended solids in air (units: $\text{kg}/\text{m}^3$ )
ALOG(2.)	Natural logarithm of 2.
AR	Area of soil (units: $\text{m}^2$ )
CMLK	Individual milk consumption (units: L/yr)
CMF	Individual meat consumption (units: $\text{kg}/\text{yr}$ )
CPLT	Individual plant consumption (units: $\text{kg}/\text{yr}$ )
CRDM(I)	Concentration ratio for radionuclide I from diet to milk (units: Ci/L per Ci/day)
CRDMT(I)	Concentration ratio for radionuclide I from diet to meat (units: Ci/kg per Ci/day)
CRSP(I)	Concentration ratio for radionuclide I from soil to plant (units: unitless)
CRWF(I)	Concentration ratio for radionuclide I from water to fish (units: Ci/kg per Ci/L)
DOEF(I)	Distribution coefficient for radionuclide I (units: Ci/kg per Ci/L)
DE	Mean particle density of soil material (units: $\text{kg}/\text{m}^3$ )
DENSITY	Mean particle density for external exposure calculations (units: $\text{kg}/\text{m}^3$ )
DEPTH	Depth to which radionuclides are assumed to be concentrated on surface for external exposure calculations (units: m)
DFEXT(I,1,J)	Dose factor for ground exposure to organ J from radionuclide I (units: $\text{rem}/\text{hr}$ per $\text{Ci}/\text{m}^2$ )
DFEXT(I,2,J)	Same as DFEXT(I,1,J) but for water immersion (units: $\text{rem}/\text{hr}$ per $\text{Ci}/\text{m}^3$ )

Table 1-3. (continued)

Variable	Definition
DFEXT(I,3,J)	Same as DFEXT(I,1,J) but for air immersion (units: rem/hr per Ci/m <sup>3</sup> )
DFING(I,J)	Dose factor for exposure to organ J from ingestion of radionuclide I (units: rem per Ci/yr)
DFINH(I,J)	Same as DFING(I,J) but for inhalation
DFSH	Constant relating fish production to river flow (units: kg/yr per L/yr)
DMLK	Individuals supported by milk production (units: ind/m <sup>2</sup> )
DMT	Individuals supported by meat production (units: ind/m <sup>2</sup> )
DP	Depth of soil (units: m)
DPLT	Individuals supported by plant production (units: ind/m <sup>2</sup> )
DPOP	Constant relating population size to river flow (units: ind per L/yr)
DSL	Population density for inhalation and external exposure calculations (units: ind/m <sup>2</sup> )
ER	Erosion rate (units: kg/m <sup>2</sup> per yr)
F	River flow rate (units: L/yr)
FMLK	Fraction of land used for milk production (units: unitless)
FMT	Fraction of land used for meat production (units: unitless)
FPLT	Fraction of land used to grow plants for human consumption (units: unitless)

Table 1-3. (continued)

Variable	Definition
FRET	Fraction of radionuclides in sprinkler irrigation initially retained on plants (units: unitless)
FRIV	Fraction of river used for sprinkler irrigation (units: unitless)
HLIFE(I)	Half-life for radiouclide I (units: yr)
PDEN	Plant density (units: $\text{kg}/\text{m}^2$ )
PMLK	Plant consumption by dairy cattle (units: $\text{kg}/\text{day}$ )
PMF	Plant consumption by beef cattle (units: $\text{kg}/\text{day}$ )
PO	Porosity of soil (units: unitless)
POROSIT	Porosity for external exposure calculations (units: unitless)
REXARSD	Exposure to suspended sediment (units: $\text{hr}/\text{yr}$ )
REXARSL	Exposure to suspended soil (units: $\text{hr}/\text{yr}$ )
REXTSD	Exposure to sediment (units: $\text{hr}/\text{yr}$ )
REXTSL	Exposure to soil (units: $\text{hr}/\text{yr}$ )
REXTWAT	Exposure water (units: $\text{hr}/\text{yr}$ )
RINGWAT	Water ingestion rate (units: $\text{L}/\text{yr}$ )
RINHAIR	Inhalation rate (units: $\text{m}^3/\text{yr}$ )
RO	Runoff rate (units: $\text{L}/\text{m}^2$ per yr)
SA	Percent saturation of pore space in soil (units: unitless)
T	Length of radionuclide discharge (units: yr)
TD(I)	Total discharge of radionuclide I (units: Ci)

Table 1-3. (continued)

Variable	Definition
TMINSD	Fraction of year that individual is exposed to suspended sediment (units: unitless)
TMINSL	Fraction of year that individual is exposed to suspended soil (units: unitless)
WHRHL	Weathering half life for radionuclides deposited by sprinkler irrigation (units: yr)
WMLK	Water consumption by dairy cattle (units: L/day)
WMT	Water consumption by beef cattle (units: L/day)
WT(I)	Water treatment factor for radionuclide I (units: unitless)
70.	Average life expectancy (units: yr)

Table 1-4. Exposure to Organ Associated With Cancer J Due to Radionuclide I for Releases to Surface Water

Exposure From Water Consumption

Individual :  $RINGWAT * TD(I) * WT(I) * DFING(I, J) / (F * T)$   
(rem/ind)

Pop. Size :  $DPOP * F * T / 70.$   
(ind)

Exposure From Fish Consumption

Individual :  $TD(I) * CRWF(I) * DFSH * DFING(I, J) / (DPOP * F * T)$   
(rem/ind)

Pop. Size :  $DPOP * F * T / 70.$   
(ind)

Exposure From Inhalation of Suspended Sediment

Individual :  $DCOEF(I) * TD(I) * AIRCON * RINHAIR * TMINS * DFINH(I, J) / (F * T)$   
(rem/ind)

Pop. Size :  $DPOP * F * T / 70.$   
(ind)

Exposure From Water Immersion

Individual :  $TD(I) * REXTWAT * DF(I, 2, J) * 7.E4 / (F * T)$   
(rem/ind)

Pop. Size :  $DPOP * F * T / 70.$   
(ind)

Exposure From Shoreline Sediment

Individual :  $DCOEF(I) * TD(I) * DEPTH * DENSITY * (1. - POROSIT) * REXTSD$   
(rem/ind)  $* DFEXT(I, 1, J) * 70. / (F * T)$

Pop. Size :  $DPOP * F * T / 70.$   
(ind)

Exposure From Suspended Sediment

Individual :  $DCOEF(I) * TD(I) * AIRCON * REXARSD * DFEXT(I, 3, J) * 70. / (F * T)$   
(rem/ind)

Pop. Size :  $DPOP * F * T / 70.$   
(ind)

Table 1-5. Exposure to Organ Associated With Cancer J Due to Radionuclide I for Releases to Soil

Expressions Introduced to Simplify Notation

$$S(I) = \text{DCOEF}(I) * (1. - \text{PO}) * \text{DE} / (\text{DCOEF}(I) * (1. - \text{PO}) * \text{DE} + \text{PO} * 1000.)$$

(units: unitless)

$$A(I) = S(I) * \text{ER} / (\text{DP} * (1. - \text{PO}) * \text{DE}) + (1. - S(I)) * \text{RO} / (\text{DP} * \text{PO} * 1000.)$$

$$+ \text{ALOG}(2.) / \text{HLIFE}(I)$$

(units: yr<sup>-1</sup>)

$$\text{FAC}(I) = 1. / (A(I) * \text{DP} * (1. - \text{PO}) * \text{DE})$$

(units: m<sup>2</sup> yr/kg)

Exposure From Plant Consumption

Individual :  $\text{CPLT} * \text{TD}(I) * \text{FAC}(I) * \text{CRSP}(I) * \text{DFING}(I, J) / (\text{T} * \text{AR})$   
(rem/ind)

Pop. Size :  $\text{AR} * \text{FPLT} * \text{DPLT} * \text{T} / 70.$   
(ind)

Exposure From Milk Consumption

Individual :  $\text{TD}(I) * \text{FAC}(I) * \text{CRSP}(I) * \text{PMLK} * \text{CRDM}(I) * \text{CMLK} * \text{DFING}(I, J) / (\text{T} * \text{AR})$   
(rem/ind)

Pop. Size :  $\text{AR} * \text{FMLK} * \text{DMLK} * \text{T} / 70.$   
(ind)

Exposure From Meat Consumption

Individual :  $\text{TD}(I) * \text{FAC}(I) * \text{CRSP}(I) * \text{PMT} * \text{CRDMT}(I) * \text{CMT} * \text{DFING}(I, J) / (\text{T} * \text{AR})$   
(rem/ind)

Pop. Size :  $\text{AR} * \text{FMT} * \text{DMT} * \text{T} / 70.$   
(ind.)

Table 1-5. (continued)

Exposure From Inhalation of Suspended Soil

Individual :  $TD(I)*FAC(I)*(AIRCON*RINHAI*TMINSL*DFINH(I,J))/(T*AR)$   
(rem/ind)

Pop. Size :  $AR*DSL*T/70.$   
(ind)

Exposure From Soil

Individual :  $TD(I)*FAC(I)*DEPTH*DENSITY*(1. - POROSIT)*REXTSL$   
(rem/ind)

$*DFEXT(I,1,J)*70./(T*AR)$

Pop. Size :  $AR*DSL*T/70.$   
(ind)

Exposure From Suspended Soil

Individual :  $TD(I)*FAC(I)*AIRCON*REXARSL*DFEXT(I,3,J)*70./(T*AR)$   
(rem/ind)

Pop. Size :  $AR*DSL*T/70.$   
(ind.)

Table 1-6. Exposure to Organ Associated With Cancer J Due to Radionuclide I for Releases to Surface Water With Subsequent Use of Surface Water for Livestock and Sprinkler Irrigation

Exposure From Plant Consumption

Individual :  $FRET \cdot TD(I) \cdot FRIV \cdot WHRHL \cdot CPLT \cdot DFING(I, J) / (T \cdot AR \cdot PDEN \cdot ALOG(2.))$   
(rem/ind)

Pop. Size :  $AR \cdot FPLT \cdot DPLT \cdot T / 70.$   
(ind)

Exposure From Milk Consumption

Individual<sup>a</sup>:  $FRET \cdot TD(I) \cdot FRIV \cdot WHRHL \cdot PMLK \cdot CRDM(I) \cdot CMLK \cdot DFING(I, J)$   
(rem/ind)  
 $/(T \cdot AR \cdot PDEN \cdot ALOG(2.))$

Individual<sup>b</sup>:  $TD(I) \cdot WMLK \cdot CRDM(I) \cdot CMLK \cdot DFING(I, J) / (F \cdot T)$   
(rem/ind)

Pop. Size :  $AR \cdot FMLK \cdot DMLK \cdot T / 70.$   
(ind.)

Exposure From Meat Consumption

Individual<sup>a</sup>:  $FRET \cdot TD(I) \cdot FRIV \cdot WHRHL \cdot PMT \cdot CRDMT(I) \cdot CMT \cdot DFING(I, J)$   
(rem/ind)  
 $/(T \cdot AR \cdot PDEN \cdot ALOG(2.))$

Individual<sup>b</sup>:  $TD(I) \cdot WMT \cdot CRDMT(I) \cdot CMT \cdot DFING(I, J) / (F \cdot T)$   
(rem/ind)

Pop. Size :  $AR \cdot FMT \cdot DMT \cdot T / 70.$   
(ind)

<sup>a</sup>Exposure from radionuclides deposited by sprinkler irrigation on plants which are subsequently used as animal feed.

<sup>b</sup>Exposure from radionuclides in water used for livestock.

Table 1-7. Population Health Effects for 1. Curie Radionuclide Releases to Surface Water

NUCLIDE	WRHETOT <sup>a</sup>	FHHETOT <sup>b</sup>	INSDTOT <sup>c</sup>	EXWRTOT <sup>d</sup>	EXSDTOT <sup>e</sup>	EXARSDT <sup>f</sup>
C14	2.08E-05	2.58E-04	9.95E-16	0.	0.	1.98E-20
NI59	5.75E-05	1.55E-05	5.34E-14	0.	0.	0.
SR90	3.91E-02	3.17E-03	2.15E-11	2.18E-10	0.	6.78E-19
ZR93	5.89E-06	5.25E-08	7.24E-11	1.61E-11	3.42E-08	4.71E-17
TC99	2.00E-06	8.10E-08	2.22E-14	5.24E-11	0.	8.19E-20
SN126	4.68E-04	3.79E-03	3.55E-13	7.26E-09	1.27E-07	1.86E-14
I129	8.87E-05	3.60E-06	4.35E-15	6.86E-09	6.35E-09	2.54E-17
CS135	1.60E-04	8.65E-04	4.89E-13	2.66E-11	0.	7.91E-19
CS137	9.72E-04	5.25E-03	2.95E-12	4.03E-07	1.19E-06	1.33E-14
SM151	1.26E-05	8.53E-07	1.90E-11	1.05E-10	2.03E-07	1.14E-12
RA226	2.34E+00	3.17E-01	2.07E-09	1.31E-06	1.81E-06	2.13E-14
U234	4.39E-03	2.37E-05	5.36E-09	4.76E-10	3.10E-08	2.19E-16
NP237	5.04E-03	1.36E-04	7.90E-10	1.45E-07	1.98E-08	2.05E-16
PU238	1.73E-04	1.64E-06	7.69E-08	6.05E-11	3.67E-08	1.92E-16
PU239	2.87E-03	2.72E-05	3.04E-06	4.84E-11	2.23E-08	1.58E-16
PU240	2.87E-03	2.72E-05	3.04E-06	5.65E-11	3.67E-08	1.84E-16
AM241	3.21E-03	2.17E-04	5.14E-07	1.57E-08	2.54E-06	2.54E-14
PU242	2.68E-03	2.53E-05	2.83E-06	4.44E-11	3.11E-08	1.44E-16
AM243	3.22E-03	2.18E-04	5.11E-07	1.25E-07	1.84E-05	1.98E-13

<sup>a</sup>WRHETOT ~ Total health effects from drinking water

<sup>b</sup>FHHETOT ~ Total health effects from eating fish

<sup>c</sup>INSDTOT ~ Total health effects from inhalation of sediment

<sup>d</sup>EXWRTOT ~ Total health effects from water immersion

<sup>e</sup>EXSDTOT ~ Total health effects from external exposure to sediment

<sup>f</sup>EXARSDT ~ Total health effects from external exposure to suspended sediment

Table 1-8. Population Health Effects for 1. Curie Radionuclide Release to Soil

NUCLIDE	PLHETOT <sup>a</sup>	MKHETOT <sup>b</sup>	MTHETOT <sup>c</sup>	INSLTOT <sup>d</sup>	EXSLTOT <sup>e</sup>	EXARSLT <sup>f</sup>
C14	2.05E-04	5.35E-05	1.67E-05	4.89E-13	0.	9.74E-18
NI59	1.36E-05	1.97E-06	1.89E-07	2.27E-11	0.	0.
SR90	2.16E-03	3.75E-05	3.40E-06	9.56E-09	0.	3.02E-16
ZR93	1.29E-06	1.40E-10	1.15E-07	1.27E-08	6.02E-06	8.31E-15
TC99	8.97E-07	4.87E-07	9.42E-07	1.09E-11	0.	4.03E-17
SN126	2.10E-06	1.14E-07	4.41E-07	1.74E-10	6.26E-05	9.18E-12
I129	3.19E-06	4.15E-07	2.43E-08	2.14E-12	3.13E-06	1.25E-14
CS135	4.86E-05	1.27E-05	5.10E-07	2.03E-10	0.	3.29E-16
CS137	2.48E-04	6.47E-05	2.61E-06	1.03E-09	4.15E-04	4.65E-12
SM151	6.80E-06	7.38E-10	8.92E-08	3.72E-09	4.00E-05	2.25E-10
RA226	1.12E-02	1.94E-03	9.99E-04	8.71E-07	7.63E-04	9.00E-12
U234	4.17E-03	4.52E-05	3.72E-06	1.86E-06	1.08E-05	7.61E-14
NP237	2.26E-05	2.46E-09	1.19E-08	3.88E-07	9.74E-06	1.01E-13
PU238	1.47E-05	6.37E-10	5.39E-10	3.56E-06	1.70E-06	8.91E-15
PU239	9.15E-04	3.97E-08	3.36E-08	5.30E-04	3.89E-06	2.76E-14
PU240	8.91E-04	3.87E-08	3.28E-08	5.15E-04	6.24E-06	3.12E-14
AM241	5.30E-04	5.75E-08	2.78E-07	9.28E-05	4.60E-04	4.60E-12
PU242	8.60E-04	3.73E-08	3.16E-08	4.97E-04	5.47E-06	2.54E-14
AM243	7.13E-04	7.74E-08	3.74E-07	1.23E-04	4.45E-03	4.79E-11

<sup>a</sup>PLHETOT ~ Total health effects from plant ingestion due to radionuclide uptake by plants from soil

<sup>b</sup>MKHETOT ~ Total health effects from milk ingestion due to radionuclide uptake by plants from soil

<sup>c</sup>MTHETOT ~ Total health effects from meat ingestion due to radionuclide uptake by plants from soil

<sup>d</sup>INSLTOT ~ Total health effects from inhalation of suspended soil

<sup>e</sup>EXSLTOT ~ Total health effects from external exposure to soil

<sup>f</sup>EXARSLT ~ Total health effects from external exposure to suspended soil

Table 1-9. Population Health Effects for 1. Curie Radionuclide Release to Surface Water With Subsequent Use of Surface Water for Livestock and Sprinkler Irrigation

NUCLIDE	IPLRHET <sup>a</sup>	PLHETOT <sup>b</sup>	IRPLHET <sup>c</sup>
C14	1.12E-04	2.05E-04	3.17E-04
NI59	3.10E-04	1.36E-05	3.23E-04
SR90	2.10E-01	2.16E-03	2.13E-01
ZR93	3.17E-05	1.29E-06	3.30E-05
TC99	1.08E-05	8.97E-07	1.17E-05
SN126	2.52E-03	2.10E-06	2.52E-03
I129	4.78E-04	3.19E-06	4.81E-04
CS135	8.62E-04	4.86E-05	9.11E-04
CS137	5.24E-03	2.48E-04	5.48E-03
SM151	6.80E-05	6.80E-06	7.48E-05
RA226	1.26E+01	1.12E-02	1.26E+01
U234	2.36E-02	4.17E-03	2.78E-02
NP237	2.71E-02	2.26E-05	2.72E-02
PU238	9.34E-04	1.47E-05	9.48E-04
PU239	1.55E-02	9.15E-04	1.64E-02
PU240	1.55E-02	8.91E-04	1.64E-02
AM241	1.73E-02	5.30E-04	1.78E-02
PU242	1.44E-02	8.60E-04	1.53E-02
AM243	1.74E-02	7.13E-04	1.81E-02

<sup>a</sup>IPLRHET ~ Total health effects from plant ingestion due to foliar deposition

<sup>b</sup>PLHETOT ~ Total health effects from plant ingestion due to radionuclide uptake by plants from soil

<sup>c</sup>IRPLHET ~ IPLRHET + PLHETOT

Table 1-9. (continued)

NUCLIDE	IMKRHET <sup>d</sup>	IMKWHET <sup>e</sup>	MKHETOT <sup>f</sup>	IRMKHET <sup>g</sup>
C14	2.92E-05	1.69E-05	5.35E-05	9.95E-05
NI59	4.51E-05	2.60E-05	1.97E-06	7.30E-05
SR90	3.66E-03	2.11E-03	3.75E-05	5.81E-03
ZR93	3.44E-09	1.99E-09	1.40E-10	5.57E-09
TC99	5.84E-06	3.37E-06	4.87E-07	9.70E-06
SN126	1.37E-04	7.91E-05	1.14E-07	2.16E-04
I129	6.23E-05	3.60E-05	4.15E-07	9.86E-05
CS135	2.25E-04	1.30E-04	1.27E-05	3.67E-04
CS137	1.36E-03	7.88E-04	6.47E-05	2.22E-03
SM151	7.38E-09	4.27E-03	7.38E-10	1.24E-08
RA226	2.19E+00	1.27E-00	1.94E-03	3.46E+00
U234	2.57E-04	1.48E-04	4.52E-05	4.50E-04
NP237	2.94E-06	1.70E-06	2.46E-09	4.65E-06
PU238	4.05E-08	2.34E-08	6.37E-10	6.46E-08
PU239	6.73E-07	3.88E-07	3.97E-08	1.10E-06
PU240	6.72E-07	3.88E-07	3.87E-08	1.10E-06
AM241	1.88E-06	1.08E-06	5.75E-08	3.02E-06
PU242	6.26E-07	3.625E-07	3.73E-08	1.02E-06
AM243	1.88E-06	1.09E-08	7.74E-08	3/05E-06

<sup>d</sup>IMKRHET ~ Total health effects from foliar deposition and subsequent plant use in milk production

<sup>e</sup>IMKWHET ~ Total health effects from water used for milk cattle

<sup>f</sup>MKHETOT ~ Total health effects from milk ingestion due to radionuclide uptake by plants from soil

<sup>g</sup>IRMKHET ~ IMKRHET + IMKWHET + MKHETOT

Table 1-9. (Continued)

NUCLIDE	IMTRHET <sup>h</sup>	IMTWHET <sup>i</sup>	MTHETOT <sup>j</sup>	IRMTHET <sup>k</sup>
C14	9.11E-06	4.39E-06	1.67E-05	3.02E-05
N159	4.31E-06	2.07E-06	1.89E-07	6.57E-06
SR90	3.32E-04	1.60E-04	3.40E-06	4.94E-04
ZR93	2.83E-06	1.36E-06	1.15E-07	4.31E-06
TC99	1.13E-05	5.44E-06	9.42E-07	1.77E-05
SN126	5.30E-04	2.55E-04	4.41E-07	7.85E-04
I129	3.64E-06	1.75E-06	2.43E-08	5.41E-06
CS135	9.05E-06	4.36E-06	5.10E-07	1.39E-05
CS137	5.50E-05	2.65E-05	2.61E-06	8.41E-05
SM151	8.93E-07	4.30E-07	8.92E-08	1.41E-06
RA226	1.13E+00	5.43E-01	9.99E-04	1.67E+00
U234	2.11E-05	1.02E-05	3.72E-06	3.50E-05
NP237	1.42E-05	6.86E-06	1.19E-08	2.11E-05
PU238	3.43E-08	1.65E-08	5.39E-10	5.14E-08
PU239	5.69E-07	2.74E-07	3.36E-08	8.77E-07
PU240	5.69E-07	2.74E-07	3.28E-08	8.75E-07
AM241	9.07E-06	4.37E-06	2.78E-07	1.37E-05
PU242	5.30E-07	2.55E-07	3.16E-08	8.16E-07
AM243	9.12E-06	4.39E-06	3.74E-07	1.39E-05

<sup>h</sup>IMTRHET ~ To health effects from foliar deposition and subsequent plant use in meat production

<sup>i</sup>IMTWHET ~ Total health effects from water used for meat production

<sup>j</sup>MTHETOT ~ Total health effects from meat ingestion due to radionuclide uptake by plants from soil

<sup>k</sup>IRMTHET ~ IMTRHET + IMTWHET + MTHETOT

Table 1-10. Organs and Risk Factors Considered

Organ/Cancer	Risk Factor EPA <sup>a</sup> (cancer/ind-rem)	Risk Factor Sandia <sup>b</sup> (cancer/ind-rem)
Bone	1.00E-5	9.75E-6
Red Marrow/ Leukemia	4.00E-5	2.85E-5 <sup>c</sup>
Lung	4.00E-5	2.5E-5
Liver	1.00E-5	
GI-LLI	2.00E-5	
Stomach		1.15E-5 <sup>d</sup>
Pancreas		3.85E-6 <sup>d</sup>
Other GI		3.85E-6 <sup>d</sup>
Thyroid	1.00E-6	
Kidney	1.00E-5	
Breast		2.88E-5 <sup>e</sup>
Other	7.00E-5	3.60E-5 <sup>e</sup>

<sup>a</sup>From Table 4.3-1 of (Sm81)

<sup>b</sup>From Table 3.4 of (Ru81)

<sup>c</sup>Dose factor for bone used

<sup>d</sup>Dose factor for GI-LLI used

<sup>e</sup>Dose factor for total body used

(see Sm81, p. 93). The values used for all other variables are indicated in Table 1-11.

To generate the values for IMKWHET and IMTWHET in Table 1-9, it was necessary to know the area AR under consideration. This was obtained by assuming that an irrigation rate IRAT of 300 L/m<sup>2</sup> per yr was used. Then, AR can be expressed in terms of IRAT, F and FRIV.

#### 1.4 Comparison With Environmental Protection Agency Results

The Environmental Protection Agency results for a release to surface water are presented in Table 1-12. As already noted, it is the numbers appearing in the column labeled "TOTAL" of this table that were used in obtaining the Environmental Protection Agency draft standard for radionuclide releases in the context of geologic disposal for high-level waste; these numbers were obtained by summing the numbers in the other columns and represent total population health effects. The population health effects in columns labeled "p = 1" through "p = 8" are now compared with related results in Tables 1-7, 1-8 and 1-9.

The results for drinking water ingestion appearing in column p = 1 of Table 1-12 and column WRHETOT of Table 1-7 were calculated with models that are essentially identical. This similarity tends to be obscured by the differences in notation and derivation technique used in this report and in (Sm81). Therefore, the computational approach used in the two developments will be compared. Much of the apparent difference arises from the nature of the dose factors used. In this regard, the reader is reminded that the dose factors in (Sm81) for ingestion and inhalation yield a 50. year dose commitment from a 1. year exposure. In contrast, in our analysis the dose factors for ingestion and inhalation yield a 70. year dose commitment from a 70. year chronic exposure. For the former dose factors, multiplication of a 1. year ingestion or inhalation rate by the dose factor provides the 50. year commitment from the 1. year of exposure; for the latter dose factors, multiplication of the average annual ingestion or inhalation rate by the dose factor provides the dose commitment over 70. years which results from 70. years of exposure.

Table 1-11. Variables Used in Calculation of Results  
Presented in Tables 1-7, 1-8 and 1-9

Variable	Definition	Variable	Definition
AIRCON	3.5E-9 kg/m <sup>3</sup> (Bon73, Table 1.4-5)	PDEN	2. kg/m <sup>2</sup> (Nu76, p. 1.109-55)
CMLK	110. L/yr (Nu76, Table D-1)	PMLK	50. kg/day (Nu76, Table A-10)
CMT	95. kg/yr (Nu76, Table D-1)	PMT	50. kg/day (Nu76, Table A-10)
CPLT	190. kg/yr (Nu76, Table D-1)	PO	.5 (To70, Table 4-25)
DE	2800. kg/m <sup>3</sup> (Cu73, Table 34-20)	POROSIT	.5 (To70, Table 4-25)
DENSITY	2800. kg/m <sup>3</sup> (Cu73, Table 34-20)	REXARSD	8.3 hr/yr (Nu76, Table D-1)
DEPTH	.025 m	REXARSL	8760. hr/yr (Nu76, Table D-1)
DFSH	3.3E-7 kg/L (Sm81, p. 87)	REXTSD	8.3 hr/yr (Nu76, Table D-1)
DMLK	1.5E-3 ind/m <sup>2</sup> (Sm81, p. 91)	REXTSL	8760 hr/yr (Nu76, Table D-1)
DMT	2.1E-4 ind/m <sup>2</sup> (Sm81, p. 91)	REXTWAT	8.3 hr/yr (Nu76, Table D-1)
DP	.15m (Sm81, p. 85)	RINGWAT	370. L/yr (Nu76, Table D-1)
DPLT	1.0E-3 ind/m <sup>2</sup> (Sm81, p. 91)	RINHAIK	7300 m <sup>3</sup> /yr (Nu76, Table D-1)
DPOP	3.3E-7 ind-yr/L (Sm81, p. 86)	RO	510 L/m <sup>2</sup> -yr (To70, Table 2-22)
DSL	6.67E-5 ind/m <sup>2</sup> (Sm81, p. 91)	SA	.5 (To70, Figure 4-2)
ER	.35 kg-yr/m <sup>2</sup> (To70, Table 2-33)	TMINSD	9.5E-4 (Nu76, Table D-1)
FMLK	.25 (Sm81, p. 89)	TMINSL	1. (Nu76, Table D-1)
FMT	.25 (Sm81, p. 89)	WHRHL	.038 yr (Boo81)
FPLT	.5 (Sm81, p. 89)	WMLK	60 L/day (Nu76, Table A-10)
FRET	.25 (Boo81)	WMT	50 L/day (Nu76, Table A-10)
FRIV	1.		

Table 1-12. Health Effects per Curie Released  
for Releases to a River<sup>a</sup>

Nuclide	TOTAL	Drinking	Freshwater	Above	Milk	Beef	Inhalation	External	External
		Water	Fish	Surface					
		(p = 1)	(p = 2)	(p = 3)	(p = 4)	(p = 5)	(p = 6)	(p = 7)	(p = 8)
C-14	4.58 E- 2	7.40 E- 5	5.59 E- 4	2.99 E- 2	1.11 E- 2	4.10 E- 3	1.46 E-12	0.0	0.0
Mi-59									
Sr-90	1.21 E- 1	8.03 E- 3	6.66 E- 5	1.05 E- 1	7.79 E- 3	1.04 E- 4	7.87 E- 7	0.0	0.0
Zr-93									
Tc-99	2.85 E- 4	2.42 E- 5	6.02 E- 7	1.92 E- 4	6.25 E- 5	5.82 E- 6	4.92 E-10	0.0	0.0
Sn-126	1.20 E- 1	1.41 E- 3	7.01 E- 3	6.66 E- 3	2.95 E- 4	2.09 E- 3	3.71 E- 6	1.02 E- 1	5.61 E- 9
I-129	1.08 E- 2	1.63 E- 3	4.05 E- 5	6.43 E- 3	2.44 E- 3	1.84 E- 4	1.22 E- 8	9.19 E- 5	1.54 E-12
Cs-135	3.81 E- 3	2.55 E- 4	1.69 E- 4	2.13 E- 3	9.99 E- 4	2.65 E- 4	1.12 E- 7	0.0	0.0
Cs-137	1.98 E- 2	2.01 E- 3	1.33 E- 3	7.83 E- 3	2.08 E- 3	5.55 E- 4	7.51 E- 8	5.96 E- 3	3.35 E-10
Sr-151									
Ra-226									
U-234									
Np-237	5.96 E- 1	1.30 E- 1	2.15 E- 3	4.60 E- 1	9.21 E- 5	3.90 E- 4	1.03 E- 1	4.95 E- 1	2.22 E- 8
Pu-238	2.29 E- 2	3.92 E- 3	2.28 E- 3	1.42 E- 2	3.03 E- 8	1.16 E- 9	2.40 E- 3	5.16 E- 5	2.63 E-13
Pu-239	6.92 E- 2	4.32 E- 3	2.50 E- 3	2.51 E- 2	5.39 E- 8	2.06 E- 9	3.69 E- 2	3.24 E- 4	1.71 E-12
Pu-240	6.53 E- 2	4.32 E- 3	2.51 E- 3	2.37 E- 2	5.16 E- 8	1.97 E- 9	3.41 E- 2	5.86 E- 4	3.00 E-12
Am-241	7.19 E- 1	1.32 E- 1	5.47 E- 3	5.61 E- 1	8.32 E- 4	3.91 E- 6	1.14 E- 2	8.61 E- 3	1.64 E-10
Pu-242	6.76 E- 2	4.10 E- 3	2.38 E- 3	2.43 E- 2	4.44 E- 8	4.29 E- 8	3.62 E- 2	6.07 E- 4	3.10 E-12
Am-243	2.68 E 0	3.38 E- 1	1.40 E- 2	2.13 E 0	3.28 E- 3	1.55 E- 5	8.93 E- 2	1.13 E- 1	4.61 E- 9

<sup>a</sup>This table is a reprint of Table D-2 of (Sm81).

From (3.1.2-6) in (Sm81), the population exposure from a release to a river is given by

$$S_{nop} = P_R I_W D_{nop} Q_{np} / R, \quad (1.8)$$

where  $S_{nop}$  represents population exposure to organ o from radionuclide n for path p (in this case,  $p = 1$ ),  $P_R$  represents the size of the population exposed each year to drinking water,  $I_W$  represents individual water consumption per year,  $D_{nop}$  represents the dose factor to organ o from radionuclide n for path p,  $Q_{np}$  represents the total release of radionuclide n for path p, and R represents annual river discharge. From the relations in Table 1-4, the same population exposure is given by

$$RINGWAT * TD(I) * WT(I) * DFING(I, J) * DPOP / 70. \quad (1.9)$$

The expressions for population exposure in (1.8) and (1.9) are essentially the same as the following correspondences exist:

$$P_R / R = DPOP = 3.3E-7 \text{ ind-yr/L in both analyses}$$

$$I_W = RINGWAT = \begin{cases} 603 \text{ L/yr in EPA analysis} \\ 370 \text{ L/yr in present analysis} \end{cases}$$

$$Q_{np} = TD(I) = 1. \text{ Ci in both analyses}$$

$$WT(I) = 1. \text{ in both analyses.}$$

The difference between the expressions  $D_{nop}$  and  $DFING(I, J) / 70.$  arises from the nature of the dose factors; this is best seen by first calculating an individual dose commitment and then converting to a population dose commitment.

From (3.1.2-1) in (Sm81), the 50. year dose commitment to an individual from the radionuclides in water ingested during 1. year is given by

$$DI'_{nop} = Q'_{np} I_w D_{nop} / R. \quad (1.10)$$

For the preceding relation,  $DI_{nop}$  and  $Q_{np}$  are being considered functions of time  $DI_{nop}(t)$  and  $Q_{np}(t)$  such that  $DI_{nop}(t)$  is the total dose commitment to an individual from birth to time  $t$  and  $Q_{np}(t)$  is the total radionuclide release from time 0 to time  $t$ . Then,  $DI'_{nop}(t)$  and  $Q'_{np}(t)$  represent the derivatives of these functions with respect to time and thus correspond to annual individual dose commitment rate at time  $t$  and annual discharge rate at time  $t$ . Multiplication of the expression in (1.10) by population size  $P_R$  yields the population dose commitment rate

$$S'_{nop} = DI'_{nop} P_R = Q'_{np} I_w D_{nop} P_R / R. \quad (1.11)$$

Now, integration can be used to recover  $S_{nop}$  for a time period of length  $T$  in the following manner:

$$\begin{aligned} S_{nop}(T) &= \int_0^T S'_{nop}(t) dt \\ &= \int_0^T Q'_{np}(t) I_w D_{nop} P_R / R dt \\ &= Q_{np}(T) I_w D_{nop} P_R / R, \end{aligned} \quad (1.12)$$

which yields the relation in (1.8).

In comparison, Table 1-4 provides the following expression for a 70. year dose commitment to an individual from a chronic 70. year exposure:

$$RINGWAT * TD(I) * WT(I) * DFING(I, J) / (F * T). \quad (1.13)$$

The expression for total population size is derived from the assumptions that the size of the population exposed to drinking water each year is  $DPOP \cdot F$ , that the time period considered is of length  $T$ , and that the average life expectancy is 70. years. Thus, if  $T$  is significantly larger than 70., then the total number of individuals exposed is given by

$$DPOP \cdot F \cdot T / 70. \quad (1.14)$$

Now, multiplication of the expressions in (1.13) and (1.14) yields the relation in (1.9).

The use of derivatives and integrals in (1.10), (1.11), and (1.12) tends to obscure the relation between the expressions in (1.8) and (1.9). Therefore, the expression in (1.10) for individual dose commitment will be reconsidered with an average annual discharge rate rather than a time varying discharge rate obtained by differentiating  $Q_{np}(t)$ . Specifically, with the assumption that a total discharge of size  $Q_{np}$  takes place over a time period of length  $T$ , the expression for 50. year dose commitment to an individual from 1. year of exposure in (1.10) becomes

$$Q_{np} I_W D_{nop} / (R \cdot T), \quad (1.15)$$

and so the dose commitment to an individual from 50. years of exposure can be estimated as

$$Q_{np} I_W D_{nop} \cdot 50. / (R \cdot T). \quad (1.16)$$

The expression for lifetime dose commitment in (1.16) from the Environmental Protection Agency analysis is comparable to the similar expression in (1.13) for lifetime dose commitment. For both expressions, multiplication by total population size for the time period considered will yield population dose. The population for (1.16) is

$$P_R \cdot T / 50. = DPOP \cdot R \cdot T / 50. \quad (1.17)$$

while the population for (1.13) is given in (1.14). Now, multiplication of the expressions in (1.16) and (1.17) will yield (1.8). Similarly, multiplication of the expressions in (1.13) and (1.14) will yield (1.9).

Overall, the results appearing for drinking water ingestion in Tables 1-12 and 1-7 are quite similar. In most cases, the difference was less than one order of magnitude; however, in a few cases the difference was greater. As both approaches used the same technique to calculate surface water concentration, the differences are due to the water ingestion rates assumed, the cancers considered and the dose and risk factors used. The organs and risk factors used for ingestion and inhalation calculations are given in Table 1-10. Further, the differences in the dose factors considered has already been discussed.

The results for freshwater fish ingestion appearing in column  $p = 2$  of Table 1-13 and column FHETOT of Table 1-7 were calculated with models that are essentially identical. Again, the results are similar; in most cases, the results are within an order of magnitude. However, in some cases, the difference is closer to two orders of magnitude. As for water ingestion, differences are introduced by the cancers, dose factors and risk factors used. Although most of the concentration ratios from water to fish used in the two analyses are similar, some variation is also introduced here (see Table 5-2 of (Sm81) and Table A-8 of (Nu76)).

The results for plant ingestion appearing in column  $p = 3$  of Table 1-12 and column IRPLHET of Table 1-9 are calculated with similar models. Both models have a submodel for radionuclide build-up on plants due to sprinkler irrigation and a submodel for radionuclide build-up in soil. For IRPLHET, the population health effects associated with these two submodels are given in the columns labeled IPLRHET and PLHETOT, respectively, in Table 1-9; no such distinction is made in the results presented in (Sm81). For both analyses, a radionuclide release is assumed to take place to soil through sprinkler irrigation with 50 percent of the soil being used to grow plant material for direct human consumption. In the Environmental Protection Agency study (Sm81), it is assumed that a .5 curie release to the soil for each radionuclide takes place; for the calculations that generated Table 1-9, a 1. curie release is assumed to take place. Therefore, as the models are linear with respect to radionuclide input, the appropriate comparison between the ingestion rates should be made with the indicated values for IRPLHET divided by 2. Both models use the same exponential model for radionuclide build-up on plants due to sprinkler irrigation (i.e., the submodel

used in determining IPLRHET); however, some of the parameters used within the model were different (e.g., .20 for fraction of radionuclides initially retained in the Environmental Protection Agency analysis and .25 in our analysis). Both models also use similar exponential models to represent radionuclide build-up in the soil (i.e., the submodel used in determining PLHETOT). In the Environmental Protection Agency analysis, radionuclide removal is by water flow and radioactive decay. Our analysis includes those two removal mechanisms and also solid-material outflow. However, the models may differ in some details (e.g., the exact manner in which the rate constants for radionuclide outflow in water were determined) and in the actual parameters used in the analyses (e.g., water outflow rates, distribution coefficients). However, the final calculated health effects are generally within an order of magnitude of each other. The differences are probably due to the different cancers, dose factors and risk factors considered and to the different values used for the same or similar parameters. Also, the inclusion of soil removal (i.e., erosion) in the calculation of PLHETOT may have an effect.

The results for milk ingestion appearing in column p = 4 of Table 1-12 can be compared with the sum of the values appearing in columns IMKRHET and MKHETOT of Table 1-9. In both analyses, it is assumed that 25 percent of the available land is used to grow plant material for use in milk production. The values for IMKRHET result from the radionuclides retained on plants due to sprinkler irrigation and the values for MKHETOT result from the radionuclides in plants due to uptake from soil. As for direct plant ingestion, the results in Table 1-12 are the sum of these two paths. Also, as a 1. curie release was considered in the generation of the results contained in Table 1-9, the proper comparison is between the values in Table 1-12 and one-half of the sum of IMKRHET and MKHETOT. As radionuclide concentration in plants for animal feed was determined in the same manner as radionuclide concentration in plants for human consumption, the discussion in the preceding paragraph is also relevant to the present comparison. There is a considerable amount of difference between the milk ingestion results in the Environmental Protection Agency analysis and in our analysis. Although the results are similar for some radionuclides, for other radionuclides a difference of up to three orders of magnitude exists. These differences are probably caused by factors of the

type already indicated. However, to identify the major causes of these differences, it would be necessary to compare calculations for the same radionuclides on a parameter-by-parameter basis. The health effects that result from radionuclides in livestock water for dairy cattle are indicated in column IMKWHET of Table 1-9. This path is not included in the calculation of the results presented in Table 1.12.

The results for beef ingestion appearing in column p = 5 of Table 1-12 can be compared with the sum of values appearing in columns IMTRHET and MTHETOT of Table 1-9. As the calculations for beef ingestion are the same as those for milk ingestion except for the use of appropriate concentration ratios and ingestion rates, the discussion for milk ingestion also pertains to beef ingestion. Overall, the results for beef ingestion for the two analyses are more similar than those for milk ingestion. For most radionuclides, the results are within one order of magnitude. However, in some cases, this difference goes up to approximately two orders of magnitude. The health effects that result from radionuclides in livestock water for beef cattle are indicated in column IMTWHET of Table 1-9. As for milk consumption, this path is not included in the calculation of the results presented in Table 1-12.

Results in the Environmental Protection Agency analysis for health effects due to inhalation of suspended material, external exposure due to ground contamination and external exposure due to suspended material in air are presented in columns p = 6, p = 7, and p = 8, respectively, of Table 1-12. Similar results for our analysis are presented in columns INSLTOT, EXSLTOT, and EXARSLT, respectively, of Table 1-8. As our analysis was for a total release of 1. curie, the values in Table 1-12 should be compared with one-half the corresponding values in Table 1-8. Generally, the results in our analysis are one to two orders of magnitude below corresponding results in Table 1-12. In the Environmental Protection Agency analysis, it is assumed that all radionuclides in the soil are concentrated on the surface for the calculation of the exposure modes now under consideration (see Equations (3.1.5-9) and (3.1.5-10) in (Sm81)). This alone is sufficient to cause discernable differences between the results.

To determine inhalation exposure, the Environmental Protection Agency obtained suspended radionuclide concentration through multiplication of surface radionuclide concentration (units: Ci/m<sup>2</sup>) by a resuspension factor of 10<sup>-9</sup> m<sup>-1</sup> (Sm81, p. 92). In contrast, we obtained suspended radionuclide concentration by multiplication of soil radionuclide concentration (units: Ci/m<sup>3</sup>) by an assumed concentration of suspended material in air of 3.5E-9 kg/m<sup>3</sup>. For an assumed amount X of a particular radionuclide in a soil region of area AR, the Environmental Protection Agency approach yields a suspended concentration of

$$(X/AR)*10^{-9} = X*10^{-9}/AR \text{ Ci/m}^3 \quad (1.18)$$

while our approach yields a suspended radionuclide concentration of

$$\begin{aligned} & (X/(AR*.15*2800*.5))*3.5E-9 \\ & = (X/AR)*1.7E-11 \text{ Ci/m}^3. \end{aligned} \quad (1.19)$$

Thus, this difference alone will cause the results from Tables 1-12 and 1-8 for inhalation of radionuclides and external exposure to suspended radionuclides to differ by a factor of approximately 59. Similarly, for ground exposure, we assume that only the radionuclides in the top 2.5 cm of the soil are available for external exposure. Thus, as our soil was assumed to be 15. cm deep and the Environmental Protection Agency analysis assumed that all radionuclides in soil were on the surface, this difference alone will cause the results from Table 1-12 and 1-8 for ground exposure to differ by a factor of 6. Other differences are due to the cancers, dose factors and risk factors considered and to the individual parameters used in determining the amount of each radionuclide in soil.

In summary, the population health effects in our analysis were generally within one to two orders of magnitude of the results obtained in the Environmental Protection Agency analysis. However, in some cases, the differences were closer to three orders of magnitude. As the two analyses used similar models, these differences are due primarily to the cancers, dose factors,

and risk factors used and to the parameters actually used within the models. If desired, the exact cause of the differences can be determined for individual radionuclides and specific exposure pathways from a parameter by parameter comparison of the two calculations.

### 1.5 Discussion

Overall, it is felt that the computational relationships indicated in Tables 1-4, 1-5 and 1-6 will yield conservative results. For example, no radionuclide removal by sedimentation is considered in the results related to surface-water concentration in Table 1-4. However, the individual using these relationships has a great deal of control on the conservatism of the final calculated results through the selection of ingestion rates, concentration ratios, risk factors, constants used in the definition of population size, and other parameters.

The relationships presented in Tables 1-4, 1-5 and 1-6 provide a convenient way to observe the differences between exposures to individuals and populations. In particular, the exposure to individuals can vary dramatically while population exposure remains unchanged. This results from the assumed linearity of the processes considered. Thus, while length of release and size of river receiving the release will affect individual exposure, these properties will not affect population exposure obtained with the models in use.

Computational relationships of the form given in Tables 1-4, 1-5 and 1-6 provide a way of comparing hazards from different substances. They could be used to compare risks between artificially and naturally occurring radioactivity. Also, there is nothing in the models which is inherently tied to radioactive materials. Therefore, provided appropriate dose and risk factors were defined, they could be used to calculate the consequences associated with nonradioactive pollutants. In turn, such values could be used in the comparison of the risks associated with waste disposal and the risks associated with other activities. In making such comparisons, it is essential that the compared risks be calculated in the same manner and with the same degree of conservatism. Otherwise, the comparisons are meaningless. Hopefully, with relatively simple models such as those in Tables 1-4, 1-5 and 1-6, it would be possible to treat all the substances considered in the same manner.

The computational relationships in Tables 1-4, 1-5 and 1-6 provide a way to screen for the most appropriate radionuclides to consider in the regulation of geologic disposal of high-level waste. The consequences associated with a unit release of each radionuclide of possible interest can be calculated. These consequences can then be weighted by the inventory of the radionuclide present. Once this has been done for all radionuclides, consideration of the relative size of the weighted consequences provides one way to select the radionuclides for regulatory consideration.

Unfortunately, many of the variables used in Tables 1-4, 1-5 and 1-6 will be imprecisely known in any analysis. The relative simplicity of the relationships in these tables permits an easy inspection of the effects of uncertainty in individual variables. Quite often, this effect is linear. For example, a doubling of the water ingestion rate will double the associated consequences. Discernment of the effects of variation in several (possibly correlated) variables is more difficult. However, techniques exist which can be used in such analyses (Im78).

Tables 1-7, 1-8 and 1-9 present the population health effects for the various pathways considered in Tables 1-4, 1-5 and 1-6 with a release of 1. Ci. The individual parameters used in the associated calculations are indicated in Section 1.3. It is often possible to investigate the effects of other parameters without reproducing an entire calculation. For example, the health effects for a water ingestion rate of 603. L/yr (Sm81, p. 86) rather than 370. L/yr can be obtained by multiplying the results in column WRHETOT of Table 1-7 by 603./370. The combined effects of various release modes can be obtained by taking appropriate linear combinations of values in Tables 1-7, 1-8 and 1-9. For example, the population health effects for each radionuclide due to water and plant ingestion resulting from a release to a river with 10 percent of the river used for flood irrigation are given by

$$1.*WRHETOT + .1*PLHETOT. \quad (1.20)$$

Such relationships can be used to investigate different sites and different assumptions about a specific site.

This discussion ends with a caveat. The models presented are very simple and probably tend to overestimate health effects. They will certainly do so if one is sufficiently aggressive in seeking out conservative values for the individual parameters in the models. Therefore, care must be exercised in the interpretation and presentation of model predictions. In particular, care must be taken in comparing results obtained with these models with results obtained with other methods. However, there is also an advantage to this simplicity. It permits consideration of different hazards at an equivalent level of complexity.

## 2. Mixed-Cell Models

The exposure calculations presented in later chapters are based on radionuclide concentrations obtained by using one compartment mixed-cell models. For releases to surface water, no radionuclide partitioning within the cell is considered. However, for releases to soil, such partitioning is considered. To facilitate presentation of the later exposure calculations, derivations are presented in this chapter for the differential equations which underlie the models in use. This presentation is adapted from Sections B-2 and B-3 of Helton and Finley (He82).

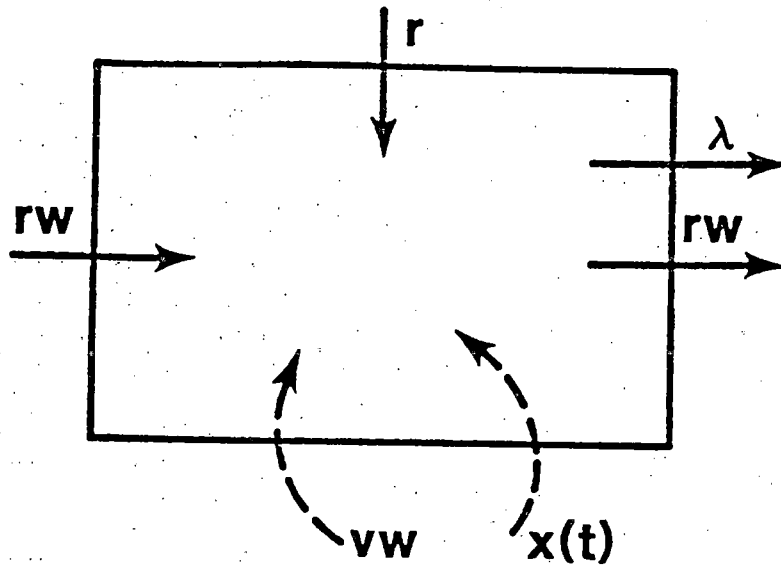
The differential equation for a single uniformly-mixed cell without radionuclide partitioning between a liquid and a solid phase is presented first. The situation under consideration is indicated in Figure 2-1. The cell is assumed to have a constant volume  $VW$  (units: L). Further, it is assumed that water enters and leaves the cell at a rate  $RW$  (units: L/yr) and that a radionuclide with decay constant  $\lambda$  (units:  $\text{yr}^{-1}$ ) enters the cell at a rate  $R$  (units: Ci/yr). It is desired to determine the amount  $X(t)$  (units: Ci) of the radionuclide present in the cell at time  $t$  (units: yrs). The basic assumption used in deriving  $X(t)$  is that the cell is uniformly-mixed; mathematically, this means that the radionuclide concentration  $C(t)$  (units: Ci/L) at any time  $t$  is given by

$$C(t) = X(t)/VW. \quad (2.1)$$

A differential equation representing the rate of change of  $X(t)$  is now derived. Then,  $X(t)$  can be obtained by solving this equation. The derivative  $dX(t)/dt$  (units: Ci/yr) is defined by the limit

$$\lim_{\Delta t \rightarrow 0} \frac{X(t + \Delta t) - X(t)}{\Delta t} \quad (2.2)$$

and represents the rate at which  $X(t)$  is changing. In turn, this rate is equal to the difference between the rate  $R_1$  (units: Ci/yr) at which the radionuclide is entering the cell and the rate  $R_2$  (units: Ci/yr) at which the radionuclide is leaving the cell. The rate



- R: rate at which radionuclide enters cell  
(units: Ci/yr)
- RW: rate at which water enters and leaves cell  
(units: L/yr)
- $\lambda$ : decay constant for radionuclide  
(units: yr<sup>-1</sup>)
- VW: volume of water in cell (units: L)
- X(t): amount of radionuclide in cell at time t  
(units: Ci)

Figure 2-1. Flows Associated With a Single Uniformly-Mixed Cell With no Radionuclide Partitioning Between a Liquid and a Solid Phase.

$R_1$  is given by  $R$ . The rate  $R_2$  is the sum of two components: a rate due to physical flow out of the cell, and a rate due to radioactive decay. The rate due to physical flow is equal to the product of the radionuclide concentration  $X(t)/VW$  in the cell and the rate of water flow  $RW$  out of the cell; the rate due to decay is equal to the product of the decay constant  $\lambda$  and the amount  $X(t)$  of radionuclide present. Thus,

$$R_1 = R \text{ and } R_2 = [(RW/VW) + \lambda] X(t), \quad (2.3)$$

and hence, the desired equation is given by

$$\begin{aligned} dX(t)/dt &= R_1 - R_2 \\ &= R - [(RW/VW) + \lambda] X(t). \end{aligned} \quad (2.4)$$

Also associated with the preceding equation is an initial value condition  $X(0) = X_0$ , which represents the amount of radionuclide present at time  $t = 0$ .

Thus, determination of  $X(t)$  reduces to the solution of an initial value problem of the form

$$dX(t)/dt = R - AX(t), \quad X(0) = X_0, \quad (2.5)$$

where

$$A = (RW/VW) + \lambda. \quad (2.6)$$

Such problems are relatively easy to solve and applicable solution techniques include separation of variables, introduction of integration factors, and application of Laplace transforms. The preceding techniques are discussed in introductory texts on differential equations and lead to the following unique solution for the initial value problem in (2.5):

$$X(t) = e^{-At} X_0 + (R/A)(1 - e^{-At}). \quad (2.7)$$

If the initial value condition is  $X(0) = 0$ , then the preceding solution becomes

$$X(t) = (R/A)(1 - e^{-At}). \quad (2.8)$$

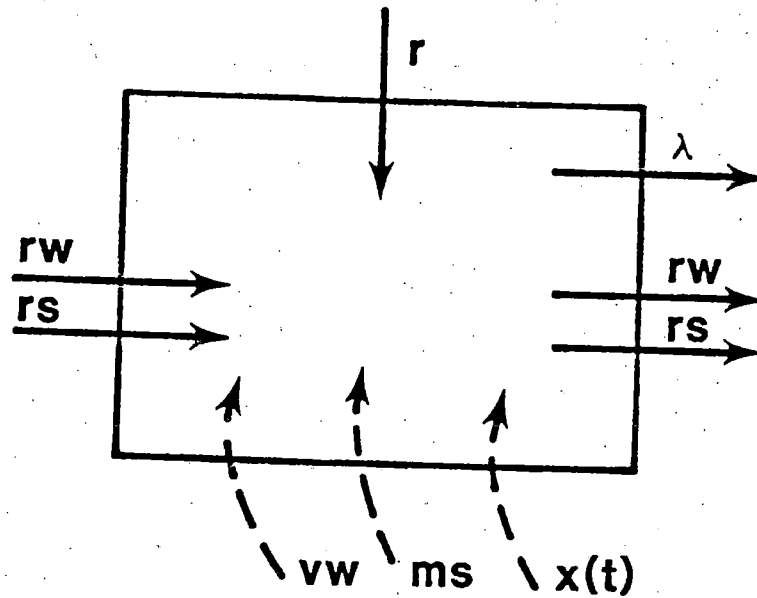
Further, regardless of the initial value condition, the steady state or asymptotic solution  $SX$  to which any solution of (2.5) converges is given by

$$\begin{aligned} SX &= \lim_{t \rightarrow \infty} X(t) \\ &= \lim_{t \rightarrow \infty} [e^{-At} X_0 + (R/A)(1 - e^{-At})] \\ &= R/A, \end{aligned} \quad (2.9)$$

provided  $A > 0$ .

The differential equation for a single uniformly-mixed cell with radionuclide partitioning between a liquid and a solid phase is presented next. The situation under consideration is indicated in Figure 2-2. The cell is assumed to have a constant volume  $VW$  (units: L) and to contain a constant mass  $MS$  of solid material (units: kg). Further, it is assumed that water enters and leaves the cell at a rate  $RW$  (units: L/yr), that solid material enters and leaves the cell at a rate  $RS$  (units: kg/yr), and that a radionuclide with decay constant  $\lambda$  (units:  $\text{yr}^{-1}$ ) enters the cell at a rate  $R$  (units: Ci/yr). The partitioning of the radionuclide between the liquid and solid phases of the system is assumed to be described by the ratio

$$KD = \frac{\text{conc. of radionuclide sorbed to solids}}{\text{conc. of radionuclide dissolved in water}} = \frac{AW/MS}{AW/VW}, \quad (2.10)$$



- R: rate at which radionuclide enters cell  
(units: Ci/yr)
- RW: rate at which water enters and leaves cell  
(units: L/yr)
- RS: rate at which solid material enters and  
leaves cell (units: kg/yr)
- $\lambda$ : decay constant for radionuclide  
(units: yr<sup>-1</sup>)
- VW: volume of water in cell (units: L)
- MS: mass of solids in cell (units: kg)
- X(t): amount of radionuclide in cell at time t  
(units: Ci)

Figure 2-2. Flows Associated With a Single Uniformly-Mixed Cell With Radionuclide Partitioning Between a Liquid and a Solid Phase.

where AS (units: Ci) is the amount of radionuclide in the system sorbed to solids and AW (units: Ci) is the amount of radionuclide in the system dissolved in water. The ratio in (2.10) is known as a KD-value or a distribution coefficient.

It is desired to determine the amount  $X(t)$  (units: Ci) of the radionuclide present in the cell at time  $t$  (units: yr). Three basic assumptions underlie the derivation of  $X(t)$ . First, it is assumed that the radionuclide is uniformly distributed through the cell and is partitioned between the liquid and solid phases on the basis of its distribution coefficient. A derivation for this partitioning is presented in the next paragraph. Second, it is assumed that the flow of water and solid material out of the cell is the only mechanism involved in the physical transport of the radionuclide. Third, it is assumed that all radionuclides associated with a phase, liquid or solid, remain with that phase in movements out of the cell. In essence, the cell is treated as a uniformly mixed "vessel" in which the radionuclides are partitioned between the liquid and solid phases on the basis of the distribution coefficient and such that radionuclides can be carried out of this "vessel" and out of the system only by movements of water or solid material.

A derivation for the partitioning of a radionuclide between the liquid and solid phases of a system is now presented. The following notation is used in the derivation:

- X = amount of radionuclide in system (units: Ci),
- XS = amount of radionuclide in system sorbed to solids (units: Ci),
- XW = amount of radionuclide in system dissolved in water (units: Ci),
- MS = mass of solid in system (units: kg),
- VW = volume of water in system (units: L).

Assume X, MS, VW, and KD are known for the system under consideration. Now, XS and XW are determined. Since

$$KD = (XS/MS)(XW/VW)^{-1} \text{ and } X = XS + XW, \quad (2.11)$$

we have that

$$(KD)(MS) = (XS)(VW)(XW)^{-1} \text{ and } XW = X - XS. \quad (2.12)$$

Thus,

$$(KD)(MS) = (XS)(VW)(X - XS)^{-1}. \quad (2.13)$$

Further, multiplication by  $(X - XS)$  gives

$$(KD)(MS)(X) - (KD)(MS)(XS) = (XS)(VW) \quad (2.14)$$

or

$$(KD)(MS)(X) = [(KD)(MS) + VW] XS, \quad (2.15)$$

and hence

$$XS = \left[ \frac{(KD)(MS)}{(KD)(MS) + VW} \right] X. \quad (2.16)$$

Further, since  $XW = X - XS$ ,

$$XW = \left[ 1 - \frac{(KD)(MS)}{(KD)(MS) + VW} \right] X. \quad (2.17)$$

The relations in (2.16) and (2.17) represent the desired partitioning.

A differential equation representing the rate of change of  $X(t)$  is now derived. Then,  $X(t)$  can be obtained by solving this equation. The following derivation is similar to that previously presented for a uniformly-mixed cell without partitioning. As for that case,  $dX(t)/dt$  is equal to the difference between the rate  $R_1$  at which the radionuclide is entering the cell and the rate  $R_2$  at which the radionuclide is leaving the cell. The rate  $R_1$  is given by  $R$ . The rate  $R_2$  is the sum of three components: a rate due to physical flow out of the cell with solid material, a rate due to physical flow out of the cell with water, and a rate due to radioactive decay. The two rates due to physical flow are equal to the products of the concentrations  $X_S(t)/MS$  and  $X_W(t)/VW$  with the flow rates  $RS$  and  $RW$ , where  $X_S(t)$  represents the amount of radionuclide in the cell sorbed to solid material and  $X_W(t)$  represents the amount of radionuclide in the cell dissolved in water. The functions  $X_S(t)$  and  $X_W(t)$  can be obtained from (2.16) and (2.17). The rate due to decay is equal to the product of the decay constant and the amount  $X(t)$  of radionuclide present. Thus,

$$R_1 = R \quad (2.18)$$

and

$$\begin{aligned} R_2 &= [X_S(t)/MS][RS] + [X_W(t)/VW][RW] + \lambda X(t) \\ &= \left[ \frac{(KD)(MS)}{(KD)(MS) + VW} \right] [X(t)] \left[ \frac{RS}{MS} \right] \\ &+ \left[ 1. - \frac{(KD)(MS)}{(KD)(MS) + VW} \right] [X(t)] \left[ \frac{RW}{VW} \right] + \lambda X(t) \end{aligned}$$

[From (2.16) and (2.17)]

$$= \left[ \frac{S(RS)}{MS} + \frac{(1. - S)(RW)}{VW} + \lambda \right] X(t) \quad (2.19)$$

where

$$S = \frac{(KD)(MS)}{(KD)(MS) + VW} \quad (2.20)$$

Hence, the desired equation is given by

$$\begin{aligned} dx(t)/dt &= R_1 - R_2 \\ &= R - \left[ \frac{S(RS)}{MS} + \frac{(1. - S)(RW)}{VW} + \lambda \right] X(t). \end{aligned} \quad (2.21)$$

Also associated with the preceding equation is an initial value condition  $X(0) = X_0$ .

Thus, determination of  $X(t)$  reduces to the solution of an initial value problem of the form

$$dX(t)/dt = R - AX(t), \quad X(0) = X_0, \quad (2.22)$$

where

$$A = \frac{S(RS)}{MS} + \frac{(1. - S)(RW)}{VW} + \lambda \quad (2.23)$$

with  $S$  defined as in (2.20). Various forms of the solution to the preceding initial value problem are given in (2.7), (2.8), and (2.9).

### 3. Release to Surface Water

#### 3.1 Preliminary Comments

Population exposures and resultant health effects are now calculated for radionuclide release to a surface-water body. In particular,  $WRDS(I,J)$ ,  $WRHE(I,J)$  and  $WRHETOT(I)$  are determined for exposure from water consumption, where

$WRDS(I,J)$  = population dose (units: rems) to organ associated with cancer J from radionuclide I,

$WRHE(I,J)$  = number of occurrences of cancer J in population due to radionuclide I,

$WRHETOT(I)$  = total number of cancers in population due to radionuclide I.

Similarly,  $FHDS(I,J)$ ,  $FHHE(I,J)$  and  $FHHETOT(I)$  are determined for fish ingestion;  $INSDDS(I,J)$ ,  $INSDHE(I,J)$  and  $INSDTOT(I)$  are determined for inhalation of suspended sediment;  $EXWRDS(I,J)$ ,  $EXWRHE(I,J)$  and  $EXWRTOT(I)$  are determined for water immersion;  $EXSDDS(I,J)$ ,  $EXSDHE(I,J)$  and  $EXSDTOT(I)$  are determined for external exposure from shoreline sediments; and  $EXARSDD(I,J)$ ,  $EXARSDDH(I,J)$  and  $EXARSDDT(I)$  are determined for external exposure from suspended sediments.

The quantities indicated in the preceding paragraph are obtained in the following manner. First, individual radionuclide exposure rates are determined. Then, these exposure rates are used in conjunction with appropriate dose and risk factors to yield individual dose and risk for selected organs and cancers. Next, these individual doses and risks are multiplied by population size to obtain population dose and risk for selected organs and cancers. Further, as many algebraic simplifications as possible are carried out; due to the nature of the models used, this results in relatively simple expressions for population dose and risk which are independent of the population size, river size, and time period considered. Finally, population risk from the various cancers is summed to give an overall population risk estimate.

It is assumed that the surface-water body under consideration can be represented as a single uniformly-mixed cell as described by the differential equation appearing in (2.5). For radionuclide I, it is assumed that a release of size TD(I) (units: Ci) takes place into the surface water over a time period of length T (units: yrs). Further, for use in (2.5), it is assumed that the annual discharge (units: Ci/yr) for radionuclide I is given by TD(I)/T. Thus, for each radionuclide, the asymptotic concentration (units: Ci/L) in the surface water is given by

$$CW(I) = TD(I)/F*T , \quad (3.1)$$

where F denotes the annual flow (units: L/yr) of the river which constitutes the surface water body under consideration.

As in the EPA analysis (Sm81), it is assumed that population size and fish production are linear, homogeneous functions of river flow F. That is, it is assumed that

$$POP = DPOP*F \quad (3.2)$$

and

$$FSH = DFSH*F , \quad (3.3)$$

where

POP = population (units: ind\*) supported by river

DPOP = constant (units: ind per L/yr)

FSH = fish production (units: kg/yr) supported by river

DFSH = constant (units: kg/yr per L/yr).

Further, with an assumed life expectancy of 70. yr, the total population TP (units: ind) supported by the river over a time period of length T is

---

\*individuals

$$TP = DPOP * F * T / 70. \quad (3.4)$$

### 3.2 Exposure From Water Consumption

The population exposures and resultant health effects are now calculated for water ingestion. It follows from (3.1) that the amount of radionuclide I ingested by an individual (units: Ci/yr) is given by

$$CW(I) * RINGWAT * WT(I) = RINGWAT * TD(I) * WT(I) / F * T, \quad (3.5)$$

where

RINGWAT = individual water ingestion rate (units: L/yr)

WT(I) = water treatment removal factor for radionuclide I (units: unitless).

Thus, the dose (units: rem/ind) to the organ associated with cancer J due to radionuclide I and the resultant cancer risk (units: cancer/ind) are given by

$$RINGWAT * TD(I) * WT(I) * DFING(I, J) / F * T \quad (3.6)$$

and

$$RINGWAT * TD(I) * WT(I) * DFING(I, J) * RISK(J) / F * T, \quad (3.7)$$

respectively.

Population exposure and risk now follow from the expressions in (3.6) and (3.7). Specifically, with use of the relation in (3.4),

$$\begin{aligned} WRDS(I, J) &= [RINGWAT * TD(I) * WT(I) * DFING(I, J) / F * T] \\ &\quad * [DPOP * F * T / 70.] \\ &= RINGWAT * TD(I) * WT(I) * DFING(I, J) * DPOP / 70. \end{aligned} \quad (3.8)$$

and

$$\begin{aligned} \text{WRHE}(I,J) &= [\text{RINGWAT} \cdot \text{TD}(I) \cdot \text{WT}(I) \cdot \text{DFING}(I,J) \cdot \text{RISK}(J) / \text{F} \cdot \text{T}] \\ &\quad \cdot [\text{DPOP} \cdot \text{F} \cdot \text{T} / 70.] \\ &= \text{RINGWAT} \cdot \text{TD}(I) \cdot \text{WT}(I) \cdot \text{DFING}(I,J) \cdot \text{RISK}(J) \\ &\quad \cdot \text{DPOP} / 70. \end{aligned} \quad (3.9)$$

Thus, the total cancers from radionuclide I are given by

$$\text{WRHETOT}(I) = \sum_J \text{WRHE}(I,J) \quad (3.10)$$

### 3.3 Exposure from Fish Consumption

The population exposures and resultant health effects are now calculated for fish ingestion. It follows from (3.2) and (3.3) that average individual fish consumption is

$$(\text{DFSH} \cdot \text{F}) / (\text{DPOP} \cdot \text{F}) = \text{DFSH} / \text{DPOP} \quad (3.11)$$

Thus, it follows from (3.1) that the amount of radionuclide I ingested by an individual from fish consumption (units: Ci/yr) is given by

$$\begin{aligned} &\text{CW}(I) \cdot \text{CRWF}(I) \cdot (\text{DFSH} / \text{DPOP}) \\ &= \text{TD}(I) \cdot \text{CRWF}(I) \cdot \text{DFSH} / (\text{DPOP} \cdot \text{F} \cdot \text{T}) \end{aligned} \quad (3.12)$$

where

$\text{CRWF}(I)$  = concentration ratio for radionuclide I from water to fish (units: Ci/kg per Ci/L).

Thus, the dose (units: rem/ind) to the organ associated with cancer J due to radionuclide I and the resultant cancer risk (units: cancer/ind) are given by

$$(TD(I)*CRWF(I)*DFSH*DFING(I,J))/(DPOP*F*T) \quad (3.13)$$

and

$$\begin{aligned} & (TD(I)*CRWF(I)*DFSH*DFING(I,J)*RISK(J)) \\ & / (DPOP*F*T) , \end{aligned} \quad (3.14)$$

respectively.

Population exposure and risk now follow from the expressions in (3.13) and (3.14). Specifically, with use of the relation in (3.4),

$$\begin{aligned} FHDS(I,J) &= \left\{ [TD(I)*CRWF(I)*DFSH*DFING(I,J)] \right. \\ & \quad \left. / [DPOP*F*T] \right\} * \left\{ DPOP*F*T/70. \right\} \\ &= TD(I)*CRWF(I)*DFSH*DFING(I,J)/70 \end{aligned} \quad (3.15)$$

and

$$\begin{aligned} FHHE(I,J) &= \left\{ [TD(I)*CRWF(I)*DFSH*DFING(I,J)*RISK(J)] \right. \\ & \quad \left. / [DPOP*F*T] \right\} * \left\{ DPOP*F*T/70. \right\} \\ &= TD(I)*CRWF(I)*DFSH*DFING(I,J)*RISK(J)/70. \end{aligned} \quad (3.16)$$

Thus, the total cancers from radionuclide I are given by

$$FHETOT(I) = \sum_J FHHE(I,J) . \quad (3.17)$$

### 3.4 Exposure From Inhalation of Suspended Sediment

The population exposures and resultant health effects are now calculated for inhalation of suspended sediment. For this calculation and for subsequent exposure calculations involving sediment, it is assumed that sediment concentration CSED(I) (units: Ci/kg) of the I<sup>th</sup> radionuclide is given by

$$\begin{aligned} CSED(I) &= DCOEF(I) * CW(I) \\ &= DCOEF(I) * TD(I) / F * T , \end{aligned} \quad (3.18)$$

[From (3.1)]

where

DCOEF(I) = distribution coefficient for radionuclide I (units: Ci/kg per Ci/L).

Hence, the amount of radionuclide I inhaled by an individual (units: Ci/yr) is given by

$$\begin{aligned} &CSED(I) * AIRCON * RINHAIR * TMINS D \\ &= DCOEF(I) * TD(I) * AIRCON * RINHAIR * TMINS D / F * T , \end{aligned} \quad (3.19)$$

where

AIRCON = concentration of suspended sediment in the air (units: kg/m<sup>3</sup>),

RINHAIR = rate of inhalation (units: m<sup>3</sup>/yr),

TMINS D = fraction of year that individual is exposed to suspended sediment (units: unitless).

Thus, the dose (units: rem/ind) to the organ associated with cancer J due to radionuclide I and the resultant cancer risk (units: cancer/ind) are given by

$$[\text{DCOEF}(I) * \text{TD}(I) * \text{AIRCON} * \text{RINHAIR} * \text{TMINS D} * \text{DFINH}(I, J)] / [F * T] \quad (3.20)$$

and

$$[\text{DCOEF}(I) * \text{TD}(I) * \text{AIRCON} * \text{RINHAIR} * \text{TMINS D} * \text{DFINH}(I, J) * \text{RISK}(J)] / [F * T] , \quad (3.21)$$

respectively.

Population exposure and risk now follow from the expressions in (3.20) and (3.21). Specifically, with the use of the relation in (3.4),

$$\begin{aligned} \text{INSDDS}(I, J) &= \left\{ [\text{DCOEF}(I) * \text{TD}(I) * \text{AIRCON} * \text{RINHAIR} * \text{TMINS D} * \text{DFINH}(I, J)] / [F * T] \right\} * \left\{ \text{DPOP} * F * T / 70. \right\} \\ &= [\text{DCOEF}(I) * \text{TD}(I) * \text{AIRCON} * \text{RINHAIR} * \text{TMINS D} * \text{DFINH}(I, J) * \text{DPOP}] / 70. \end{aligned} \quad (3.22)$$

and

$$\begin{aligned} \text{INS DHE}(I, J) &= \left\{ [\text{DCOEF}(I) * \text{TD}(I) * \text{AIRCON} * \text{RINHAIR} * \text{TMINS D} * \text{DFINH}(I, J) * \text{RISK}(J)] / [F * T] \right\} * \left\{ \text{DPOP} * F * T / 70. \right\} \\ &= [\text{DCOEF}(I) * \text{TD}(I) * \text{AIRCON} * \text{RINHAIR} * \text{TMINS D} * \text{DFINH}(I, J) * \text{RISK}(J) * \text{DPOP}] / 70. \end{aligned} \quad (3.23)$$

Thus, the total cancers from radionuclide I are given by

$$\text{INSDTOT}(I) = \sum_J \text{INSDHE}(I, J) . \quad (3.24)$$

### 3.5 Exposure From Water Immersion

The population exposures and resultant health effects are now calculated for water immersion. The external exposure (units: rem/ind) to the organ associated with cancer J due to radionuclide I and the resultant cancer risk (units: cancer/ind) are given by

$$\begin{aligned} & \text{CW}(I) * \text{REXTWAT} * \text{DFEXT}(I, 2, J) * 70. * 1000. \\ & = \text{TD}(I) * \text{REXTWAT} * \text{DFEXT}(I, 2, J) * 7.E4 / F * T \end{aligned} \quad (3.25)$$

[From (3.1)]

and

$$\text{TD}(I) * \text{REXTWAT} * \text{DFEXT}(I, 2, J) * 7.E4 * \text{RISK}(J) / F * T , \quad (3.26)$$

where

REXTWAT = exposure rate to contaminated water  
(units: hr/yr),

70. = average life expectancy (units: yr/ind)

1000. = liters per cubic meter (units: L/m<sup>3</sup>).

The factors 70. yr/ind and 1000. L/m<sup>3</sup> appear in (3.25) to produce necessary unit conversions.

Population exposure and risk now follow from the expressions in (3.25) and (3.26). Specifically, with use of the relation in (3.4),

$$\begin{aligned}
 \text{EXWRDS}(I,J) &= [\text{TD}(I) * \text{REXTWAT} * \text{DFEXT}(I,2,J) * 7.E4 / F * T] \\
 &\quad * [\text{DPOP} * F * T / 70.] \\
 &= \text{TD}(I) * \text{REXTWAT} * \text{DFEXT}(I,2,J) * \text{DPOP} * 1.E3 \quad (3.27)
 \end{aligned}$$

and

$$\begin{aligned}
 \text{EXWRHE}(I,J) &= [\text{TD}(I) * \text{REXTWAT} * \text{DFEXT}(I,2,J) * 7.E4 * \text{RISK}(J) \\
 &\quad / F * T] * [\text{DPOP} * F * T / 70.] \\
 &= \text{TD}(I) * \text{REXTWAT} * \text{DFEXT}(I,2,J) * \text{RISK}(J) \\
 &\quad * \text{DPOP} * 1.E3. \quad (3.28)
 \end{aligned}$$

Thus, the total cancers from radionuclide I are given by

$$\text{EXWRTOT}(I) = \sum_J \text{EXWRHE}(I,J) \quad (3.29)$$

### 3.6 Exposure From Shoreline Sediment

The population exposures and resultant health effects are now calculated for external exposure to shoreline sediment. For these calculations, it is first necessary to determine a surface radionuclide concentration. To do this, it is assumed that all radionuclides down to a certain depth in the sediment are concentrated on the sediment surface. Then, the surface concentration CSURF(I) (units: Ci/m<sup>2</sup>) for radionuclide I is given by

$$\begin{aligned}
 \text{CSURF}(I) &= \text{CSED}(I) * \text{DEPTH} * \text{DENSITY} * (1. - \text{POROSIT}) \\
 &= \text{DCOEF}(I) * \text{TD}(I) * \text{DEPTH} * \text{DENSITY} * (1. - \text{POROSIT}) \\
 &\quad / F * T, \quad (3.30)
 \end{aligned}$$

[From (3.18)]

where

DEPTH = depth to which radionuclides are assumed to be concentrated on surface (units: m),

DENSITY = mean particle density of sediment (units: kg/m<sup>3</sup>),

POROSIT = porosity of sediments (units: unitless).

Hence, the external exposure (units: rem/ind) to the organ associated with cancer J due to radionuclide I and the resultant cancer risk (units: cancer/ind) are given by

$$\begin{aligned} & \text{CSURF}(I) * \text{REXTSD} * \text{DFEXT}(I, 1, J) * 70. \\ & = [\text{DCOEF}(I) * \text{TD}(I) * \text{DEPTH} * \text{DENSITY} * (1. - \text{POROSIT}) / \text{F} * \text{T}] \\ & \quad * [\text{REXTSD} * \text{DFEXT}(I, 1, J) * 70.]. \end{aligned} \tag{3.31}$$

[From (3.30)]

and

$$\begin{aligned} & [\text{DCOEF}(I) * \text{TD}(I) * \text{DEPTH} * \text{DENSITY} * (1. - \text{POROSIT}) / \text{F} * \text{T}] \\ & * [\text{REXTSD} * \text{DFEXT}(I, 1, J) * 70.] * \text{RISK}(J), \end{aligned} \tag{3.32}$$

respectively, where

REXTSD = exposure rate to sediment (units: hr/yr),

70. = average life expectancy (units: yr/ind).

Population exposure and risk now follow from the expressions in (3.31) and (3.32). Specifically, with use of the relation in (3.4),

$$\begin{aligned}
\text{EXSDDS}(I,J) &= [\text{DCOEF}(I) * \text{TD}(I) * \text{DEPTH} * \text{DENSITY} \\
&\quad * (1. - \text{POROSIT}) / \text{F} * \text{T}] * [\text{REXTSD} * \text{DFEXT}(I,1,J) \\
&\quad * 70.] * [\text{DPOP} * \text{F} * \text{T} / 70.] \\
&= \text{DCOEF}(I) * \text{TD}(I) * \text{DEPTH} * \text{DENSITY} \\
&\quad * (1. - \text{POROSIT}) * \text{REXTSD} * \text{DFEXT}(I,1,J) * \text{DPOP}
\end{aligned}
\tag{3.33}$$

and

$$\begin{aligned}
\text{EXSDHE}(I,J) &= [\text{DCOEF}(I) * \text{TD}(I) * \text{DEPTH} * \text{DENSITY} \\
&\quad * (1. - \text{POROSIT}) / \text{F} * \text{T}] * [\text{REXTSD} * \text{DFEXT}(I,1,J) \\
&\quad * 70.] * \text{RISK}(J) * [\text{DPOP} * \text{F} * \text{T} / 70.] \\
&= \text{DCOEF}(I) * \text{TD}(I) * \text{DEPTH} * \text{DENSITY} * (1. - \text{POROSIT}) \\
&\quad * \text{REXTSD} * \text{DFEXT}(I,1,J) * \text{RISK}(J) * \text{DPOP} .
\end{aligned}
\tag{3.34}$$

Thus, the total cancers from radionuclide I are given by

$$\text{EXSDHET}(I) = \sum_J \text{EXSDHE}(I,J) .
\tag{3.35}$$

### 3.7 Exposure From Suspended Sediment

The population exposures and resultant health effects are now calculated for external exposure from suspended sediment. The external exposure (units: rem/ind) to the organ associated with cancer J due to radionuclide I and the resultant cancer risk (units: cancer/ind) are given by

$$\begin{aligned}
& \text{CSED}(I) * \text{AIRCON} * \text{REXARSD} * \text{DFEXT}(I, 3, J) * 70. \\
& = [\text{DCOEF}(I) * \text{TD}(I) * \text{AIRCON} * \text{REXARSD} * \text{DFEXT}(I, 3, J) * 70.] \\
& \quad / [\text{F} * \text{T}] \qquad \qquad \qquad (3.36) \\
& \qquad [\text{From (3.18)}]
\end{aligned}$$

and

$$\begin{aligned}
& [\text{DCOEF}(I) * \text{TD}(I) * \text{AIRCON} * \text{REXARSD} * \text{DFEXT}(I, 3, J) * 70. * \text{RISK}(J)] \\
& \quad / [\text{F} * \text{T}] , \qquad \qquad \qquad (3.37)
\end{aligned}$$

respectively, where

REXARSD = exposure rate to suspended sediment (units: hr/yr),

70. = average life expectancy (units: yr/ind).

Population exposure and risk now follow from the expressions in (3.36) and (3.37). Specifically, with use of the relation in (3.4),

$$\begin{aligned}
\text{EXARSDD}(I, J) & = \left\{ [\text{DCOEF}(I) * \text{TD}(I) * \text{AIRCON} * \text{REXARSD} \right. \\
& \quad \left. * \text{DFEXT}(I, 3, J) * 70.] / [\text{F} * \text{T}] \right\} * \left\{ \text{DPOP} * \text{F} * \text{T} / 70. \right\} \\
& = \text{DCOEF}(I) * \text{TD}(I) * \text{AIRCON} * \text{REXARSD} \\
& \quad * \text{DFEXT}(I, 3, J) * \text{DPOP} \qquad \qquad \qquad (3.38)
\end{aligned}$$

and

$$\begin{aligned}
\text{EXARSDH}(I,J) &= \left\{ [\text{DCOEF}(I) * \text{TD}(I) * \text{AIRCON} * \text{REXARSD} \right. \\
&\quad * \text{DFEXT}(I,3,J) * 70. * \text{RISK}(J)] \\
&\quad \left. / [F * T] \right\} * \left\{ \text{DPOP} * F * T / 70. \right\} \\
&= \text{DCOEF}(I) * \text{TD}(I) * \text{AIRCON} * \text{REXARSD} \\
&\quad * \text{DFEXT}(I,3,J) * \text{DPOP} * \text{RISK}(J) . \qquad (3.39)
\end{aligned}$$

Thus, the total cancers from radionuclide I are given by

$$\text{EXARSDT}(I) = \sum_J \text{EXARSDH}(I,J) . \qquad (3.40)$$

## 4. Release to Soil

### 4.1 Preliminary Comments

Population exposures and resultant health effects are now calculated for radionuclide release to soil. In particular,  $PLDS(I,J)$ ,  $PLHE(I,J)$  and  $PLHETOT(I)$  are determined for exposure from plant consumption, where

$PLDS(I,J)$  = population dose (units: rems) to organ associated with cancer J from radionuclide I,

$PLHE(I,J)$  = number of occurrences of cancer J in population due to radionuclide I,

$PLHETOT(I)$  = total number of cancers in population due to radionuclide I.

Similarly,  $MKDS(I,J)$ ,  $MKHE(I,J)$  and  $MKHETOT(I)$  are determined for milk consumption;  $MTDS(I,J)$ ,  $MTHE(I,J)$  and  $MTHETOT(I)$  are determined for meat consumption;  $INSLDS(I,J)$ ,  $INSLHE(I,J)$  and  $INSLTOT(I)$  are determined for inhalation of suspended soil;  $EXSLDS(I,J)$ ,  $EXSLHE(I,J)$  and  $EXSLTOT(I)$  are determined for external exposure from soil; and  $EXARSLD(I,J)$ ,  $EXARSLH(I,J)$  and  $EXARSLT(I)$  are determined for external exposure from suspended soil. The preceding quantities are determined in a manner similar to that used in Chapter 3.

It is assumed that the region under consideration can be represented as a single uniformly-mixed cell as described by the differential equation appearing in (2.21). A specific form of this equation is now derived for use in this chapter. The following symbols are introduced for use in this derivation:

$X(I)$  = amount of radionuclide I in soil (units: Ci),

$XS(I)$  = amount of radionuclide I in soil sorbed to solid material (units: Ci),

$XW(I)$  = amount of radionuclide I in soil dissolved in water (units: Ci),

$DP$  = depth of soil (units: m),

$AR$  = area of soil (units:  $m^2$ ),

ER = erosion rate per unit area (units: kg/m<sup>2</sup> per yr),

RO = runoff rate per unit area (units: L/m<sup>2</sup> per yr),

DCOEF(I) = distribution coefficient for radionuclide I (units: Ci/kg per Ci/L),

MS = mass of solid material in soil (units: kg),

VW = volume of water in soil (units: L),

PO = porosity of soil (units: unitless),

DE = mean particle density of soil material (units: kg/m<sup>3</sup>),

SA = percent saturation of pore space in soil (units: unitless).

Radionuclide partitioning is considered first. The solid mass MS and the water volume VW in the soil are given by

$$MS = AR*DP*(1. - PO)*DE \quad (4.1)$$

and

$$VW = AR*DP*PO*SA*1000 \quad (4.2)$$

Thus, the factor S(I) used in the determination of radionuclide partitioning between the liquid and solid phases of a system is given by

$$\begin{aligned} S(I) &= \frac{DCOEF(I)*MS}{DCOEF(I)*MS + VW} && \text{[From (2.20)]} \\ &= \frac{DCOEF(I)*AR*DP*(1. - PO)*DE}{DCOEF(I)*AR*DP*(1. - PO)*DE + AR*DP*PO*SA*1000} \\ &= \frac{DCOEF(I)*(1. - PO)*DE}{DCOEF(I)*(1. - PO)*DE + PO*SA*1000} && (4.3) \end{aligned}$$

Hence, it follows from (2.16) and (2.17) that the partitioning of radionuclide I between the liquid and solid phases of the system is given by

$$XS(I) = S(I)*X(I) \quad \text{and} \quad XW(I) = [1. - S(I)]*X(I) . \quad (4.4)$$

The desired equation can now be constructed. In particular, it follows from (2.21) that

$$\begin{aligned} dX(I)/dt &= R(I) - [XS(I)/MS]*AR*ER \\ &\quad - [XW(I)/VW]*AR*RO - \lambda*X(I) \\ &= R(I) - \left\{ \frac{S(I)*X(I)}{AR*DP*(1. - PO)*DE} \right\} *AR*ER \\ &\quad - \left\{ \frac{[1. - S(I)]*X(I)}{AR*DP*PO*SA*1000} \right\} *AR*RO - \lambda*X(I) \end{aligned}$$

[From (4.1), (4.2), (4.4)]

$$= R(I) - A(I)*X(I) , \quad (4.5)$$

where

$$A(I) = \frac{S(I)*ER}{DP*(1. - PO)*DE} + \frac{[1. - S(I)]*RO}{DP*PO*SA*1000} + \lambda . \quad (4.6)$$

For radionuclide I, the decay constant  $\lambda$  is given by

$$\lambda = \text{ALOG}(2.)/\text{HLIFE}(I) , \quad (4.7)$$

where

HLIFE(I) = half-life of radionuclide I (units: yr).

As indicated in (2.9), the asymptotic solution to the equation in (4.5) is given by

$$R/A(I) = TD(I)/T*A(I) , \quad (4.8)$$

where the second part of the preceding equality follows from the assumption that the annual discharge (units: Ci/yr) for radionuclide I is given by  $TD(I)/T$ . Thus, for each radionuclide, the asymptotic concentration (units: Ci/kg) in the soil is given by

$$\begin{aligned} CSL(I) &= [TD(I)/T*A(I)]/MS \\ &= [TD(I)]/[T*A(I)*AR*DP*(1. - PO)*DE] \\ &\quad [From (4.1)] \\ &= TD(I)*FAC(I)/T*AR , \end{aligned} \quad (4.9)$$

where the factor  $FAC(I)$  is introduced for notational convenience and is defined by

$$FAC(I) = [A(I)*DP*(1. - PO)*DE]^{-1} . \quad (4.10)$$

It is noted that  $FAC(I)$  contains no term which depends on the area  $AR$  of the soil region under consideration or the length  $T$  of the time period under consideration.

In similarity to the Environmental Protection Agency analysis, the following parameters are assumed to be known for the region under consideration:

- FPLT = fraction of land used to grow plants for human consumption (units: unitless),
- FMLK = fraction of land used for milk production (units: unitless),
- FMT = fraction of land used for meat production (units: unitless),

DPLT = number of people supported per m<sup>2</sup> by plant production (units: ind/m<sup>2</sup>),

DMLK = number of people supported per m<sup>2</sup> by milk production (units: ind/m<sup>2</sup>),

DMT = number of people supported per m<sup>2</sup> by meat production (units: ind/m<sup>2</sup>)

DSL = population density for inhalation and external exposure calculations (units: ind/m<sup>2</sup>).

The preceding variables lead to the following populations for use in later exposure calculations:

$$TPPLT = AR * FPLT * DPLT * T / 70. \quad (4.11)$$

$$TPMLK = AR * FMLK * DMLK * T / 70. \quad (4.12)$$

$$TPMT = AR * FMT * DMT * T / 70. \quad (4.13)$$

$$TPSL = AR * DSL * T / 70. \quad (4.14)$$

where

TPPLT = total population exposed to plant ingestion (units: ind),

TPMLK = total population exposed to milk consumption (units: ind),

TPMT = total population exposed to meat consumption (units: ind),

TPSL = total population for inhalation and external exposure calculations (units: ind),

70. = average life expectancy (units: yr).

#### 4.2 Exposure From Plant Consumption

The population exposures and resultant health effects are now calculated for plant ingestion. It follows from (4.9) that the amount of radionuclide I ingested by an individual (units: Ci/yr) is given by

$$\text{CPLT} * \text{CSL}(\text{I}) * \text{CRSP}(\text{I})$$

$$= \text{CPLT} * \text{TD}(\text{I}) * \text{FAC}(\text{I}) * \text{CRSP}(\text{I}) / \text{T} * \text{AR} , \quad (4.15)$$

where

CPLT = individual plant consumption (units: kg/yr),

CRSP(I) = concentration ratio from soil to plant for radionuclide I (units: Ci/kg per Ci/kg).

Thus, the dose (units: rem/ind) to the organ associated with cancer J due to radionuclide I and the resultant cancer risk (units: cancer/ind) are given by

$$\text{CPLT} * \text{TD}(\text{I}) * \text{FAC}(\text{I}) * \text{CRSP}(\text{I}) * \text{DFING}(\text{I}, \text{J}) / \text{T} * \text{AR} \quad (4.16)$$

and

$$\text{CPLT} * \text{TD}(\text{I}) * \text{FAC}(\text{I}) * \text{CRSP}(\text{I}) * \text{DFING}(\text{I}, \text{J}) * \text{RISK}(\text{J}) / \text{T} * \text{AR} , \quad (4.17)$$

respectively.

Population exposure and risk now follow from the expressions in (4.16) and (4.17). Specifically, with use of the relation in (4.11),

$$\text{PLDS}(\text{I}, \text{J}) = [\text{CPLT} * \text{TD}(\text{I}) * \text{FAC}(\text{I}) * \text{CRSP}(\text{I}) * \text{DFING}(\text{I}, \text{J}) / \text{T} * \text{AR}]$$

$$* [\text{AR} * \text{FPLT} * \text{DPLT} * \text{T} / 70.]$$

$$= \text{CPLT} * \text{TD}(\text{I}) * \text{FAC}(\text{I}) * \text{CRSP}(\text{I}) * \text{DFING}(\text{I}, \text{J}) * \text{FPLT}$$

$$* \text{DPLT} / 70.$$

$$(4.18)$$

and

$$\begin{aligned}
\text{PLHE}(I,J) &= [\text{CPLT} \cdot \text{TD}(I) \cdot \text{FAC}(I) \cdot \text{CRSP}(I) \cdot \text{DFING}(I,J) \\
&\quad \cdot \text{RISK}(J) / \text{T} \cdot \text{AR}] \cdot [\text{AR} \cdot \text{FPLT} \cdot \text{DPLT} \cdot \text{T} / 70.] \\
&= [\text{CPLT} \cdot \text{TD}(I) \cdot \text{FAC}(I) \cdot \text{CRSP}(I) \cdot \text{DFING}(I,J) \\
&\quad \cdot \text{RISK}(J) \cdot \text{FPLT} \cdot \text{DPLT}] / 70.
\end{aligned}
\tag{4.19}$$

Thus, the total cancers from radionuclide I are given by

$$\text{PLHETOT}(I) = \sum_J \text{PLHE}(I,J) .
\tag{4.20}$$

#### 4.3 Exposure From Milk Consumption

The population exposures and resultant health effects are now calculated for milk ingestion. It follows from (4.9) that the amount of radionuclide I ingested by an individual (units: Ci/yr) is given by

$$\begin{aligned}
&\text{CSL}(I) \cdot \text{CRSP}(I) \cdot \text{PMLK} \cdot \text{CRDM}(I) \cdot \text{CMLK} \\
&= \text{TD}(I) \cdot \text{FAC}(I) \cdot \text{CRSP}(I) \cdot \text{PMLK} \cdot \text{CRDM}(I) \cdot \text{CMLK} / \text{T} \cdot \text{AR} ,
\end{aligned}
\tag{4.21}$$

where

PMLK = plant consumption by dairy cattle (units: kg/day),

CRDM(I) = concentration ratio from diet to milk for radionuclide I (units: Ci/L per Ci/day),

CMLK = individual milk consumption (units: L/yr).

Thus, the dose (units: rem/ind) to the organ associated with cancer J due to radionuclide I and the resultant cancer risk (units: cancer/ind) are given by

$$TD(I)*FAC(I)*CRSP(I)*PMLK*CRDM(I)*CMLK*DFING(I,J)/T*AR \quad (4.22)$$

and

$$\begin{aligned} & [TD(I)*FAC(I)*CRSP(I)*PMLK*CRDM(I)*CMLK*DFING(I,J) \\ & *RISK(J)]/[T*AR] , \quad (4.23) \end{aligned}$$

respectively.

Population exposure and risk now follow from the expressions in (4.22) and (4.23). Specifically, with use of the relation in (4.12),

$$\begin{aligned} MKDS(I,J) &= \{ [TD(I)*FAC(I)*CRSP(I)*PMLK*CRDM(I)*CMLK \\ & *DFING(I,J)]/[T*AR] \} * \{ AR*FMLK*DMLK*T/70. \} \\ &= [TD(I)*FAC(I)*CRSP(I)*PMLK*CRDM(I)*CMLK \\ & *DFING(I,J)*FMLK*DMLK]/70. \quad (4.24) \end{aligned}$$

and

$$\begin{aligned} MKHE(I,J) &= \{ [TD(I)*FAC(I)*CRSP(I)*PMLK*CRDM(I)*CMLK \\ & *DFING(I,J)*RISK(J)]/[T*AR] \} * \{ AR*FMLK*DMLK \\ & *T/70. \} \\ &= [TD(I)*FAC(I)*CRSP(I)*PMLK*CRDM(I)*CMLK \\ & *DFING(I,J)*RISK(J)*FMLK*DMLK]/70. \quad (4.25) \end{aligned}$$

Thus, the total cancers from radionuclide I are given by

$$MKHETOT(I) = \sum_J MKHE(I,J) . \quad (4.26)$$

#### 4.4 Exposure From Meat Consumption

The population exposures and resultant health effects for meat consumption are determined the same as those for milk consumption with the exceptions that PMT, CRDMT(I), CMT, FMT and DMT are used instead of PMLK, CRDM(I), CMLK, FMLK and DMLK, respectively, where

PMT = plant consumption by beef cattle (units: kg/day),

CRDMT(I) = concentration ratio from diet to meat for radionuclide I (units: Ci/kg per Ci/day),

CMT = individual meat consumption (units: kg/yr)

and the remaining two variables are defined after (4.14). Thus,

$$MTDS(I,J) = [TD(I)*FAC(I)*CRSP(I)*PMT*CRDMT(I)*CMT *DFING(I,J)*FMT*DMT]/70. , \quad (4.27)$$

$$MTHE(I,J) = [TD(I)*FAC(I)*CRSP(I)*PMT*CRDMT(I)*CMT *DFING(I,J)*RISK(J)*FMT*DMT]/70. \quad (4.28)$$

and

$$MTHETOT(I) = \sum_J MTHE(I,J) . \quad (4.29)$$

#### 4.5 Exposure From Inhalation of Suspended Soil

The population exposures and resultant health effects for inhalation of suspended soil are determined in the same manner as those for inhalation of suspended sediment with the exceptions that CSL(I), TPSL and TMINSL are used instead of CSED(I), TP and TMINSD, respectively, where

TMINSL = fraction of year that individual is exposed to suspended soil (units: unitless).

Specifically, the amount of radionuclide inhaled by an individual (units: Ci/yr) is given by

$$CSL(I)*AIRCON*RINHAIR*TMINSL \quad (4.30)$$

$$= TD(I)*FAC(I)*AIRCON*RINHAIR*TMINSL/T*AR .$$

Thus, the dose (units: rem/ind) to the organ associated with cancer J due to radionuclide I and the resultant cancer risk (units: cancer/ind) are given by

$$TD(I)*FAC(I)*AIRCON*RINHAIR*TMINSL*DFINH(I,J)/T*AR \quad (4.31)$$

and

$$\frac{[TD(I)*FAC(I)*AIRCON*RINHAIR*TMINSL*DFINH(I,J)*RISK(J)]}{[T*AR]} , \quad (4.32)$$

respectively.

Population exposure and risk now follow from the expressions in (4.31) and (4.32). Specifically, with use of the relation in (4.14),

$$\begin{aligned} INSLDS(I,J) &= \{ [TD(I)*FAC(I)*AIRCON*RINHAIR*TMINSL \\ &\quad *DFINH(I,J)]/[T*AR] \} * \{ AR*DSL*T/70. \} \\ &= TD(I)*FAC(I)*AIRCON*RINHAIR*TMINSL \\ &\quad *DFINH(I,J)*DSL/70. \end{aligned} \quad (4.33)$$

and

$$\begin{aligned}
 \text{INSLHE}(I,J) &= \{[\text{TD}(I)*\text{FAC}(I)*\text{AIRCON}*\text{RINHAI}R*\text{TMINSL} \\
 &\quad * \text{DFINH}(I,J)*\text{RISK}(J)]/[\text{T}*AR]\} * \{AR*\text{DSL}*T/70\}. \\
 &= [\text{TD}(I)*\text{FAC}(I)*\text{AIRCON}*\text{RINHAI}R*\text{TMINSL} \\
 &\quad * \text{DFINH}(I,J)*\text{RISK}(J)*\text{DSL}]/70. \tag{4.34}
 \end{aligned}$$

Thus, the total cancers from radionuclide I are given by

$$\text{INSLTOT}(I) = \sum_J \text{INSLHE}(I,J) . \tag{4.35}$$

#### 4.6 Exposure From Soil

The population exposures and resultant health effects for external exposure from soil are determined in the same manner as those for external exposure from sediment with the exceptions that CSL(I), TPSL and REXTSL are used instead of CSED(I), TP and REXTSED, respectively, where

REXTSL = exposure rate to soil (units: hr/yr).

First, as was done in (3.30), it is necessary to convert the soil concentration CSL(I) (units: Ci/kg) to a surface concentration CSURF(I) (units: Ci/m<sup>2</sup>), where

$$\begin{aligned}
 \text{CSURF}(I) &= \text{CSL}(I)*\text{DEPTH}*DENSITY*(1. - \text{POROSIT}) \\
 &= \text{TD}(I)*\text{FAC}(I)*\text{DEPTH}*DENSITY*(1. - \text{POROSIT})/T*AR \\
 &\tag{4.36}
 \end{aligned}$$

Hence, the external exposure (units: rem/ind) to the organ associated with cancer J due to radionuclide I and the resultant cancer risk (units: cancer/ind) are given by

$$CSURF(I) * REXTSL * DFEXT(I, 1, J) * 70.$$

$$= [TD(I) * FAC(I) * DEPTH * DENSITY * (1. - POROSIT) / T * AR] \\ * [REXTSL * DFEXT(I, 1, J) * 70.] \quad (4.37)$$

and

$$[TD(I) * FAC(I) * DEPTH * DENSITY * (1. - POROSIT) / T * AR] \\ * [REXTSL * DFEXT(I, 1, J) * 70.] * RISK(J) \quad (4.38)$$

respectively.

Population exposure and risk now follow from the expressions in (4.37) and (4.38). Specifically, with use of the relation in (4.14),

$$EXSLDS(I, J) = [TD(I) * FAC(I) * DEPTH * DENSITY * (1. - POROSIT) \\ / T * AR] * [REXTSL * DFEXT(I, 1, J) * 70.] \\ * [AR * DSL * T / 70.] \\ = TD(I) * FAC(I) * DEPTH * DENSITY * (1. - POROSIT) \\ * REXTSL * DFEXT(I, 1, J) * DSL \quad (4.39)$$

and

$$\begin{aligned}
\text{EXSLHE}(I,J) &= [\text{TD}(I)*\text{FAC}(I)*\text{DEPTH}* \text{DENSITY}*(1. - \text{POROSIT}) \\
&\quad / \text{T}*\text{AR}] * [\text{REXTSL}*\text{DFEXT}(I,1,J)*70.] * \text{RISK}(J) \\
&\quad * [\text{AR}*\text{DSL}*\text{T}/70.] \\
&= \text{TD}(I)*\text{FAC}(I)*\text{DEPTH}* \text{DENSITY}*(1. - \text{POROSIT}) \\
&\quad * \text{REXTSL}*\text{DFEXT}(I,1,J)*\text{RISK}(J)*\text{DSL} . \quad (4.40)
\end{aligned}$$

Thus, the total cancers from radionuclide I are given by

$$\text{EXSLTOT}(I) = \sum_J \text{EXSLHE}(I,J). \quad (4.41)$$

#### 4.7 Exposure From Suspended Soil

The population exposures and resultant health effects for external exposure from suspended soil are determined in the same manner as those for external exposure from suspended sediment with the exceptions that CSL(I), and REXARSL are used instead of CSED(I) and REXARSD, respectively, where

REXARSL = exposure rate to suspended soil (units: hr/yr).

The external exposure (units: rem/ind) to the organ associated with cancer J due to radionuclide I and the resultant cancer risk (units: cancer/ind) are given by

$$\begin{aligned}
&\text{CSL}(I)*\text{AIRCON}*\text{REXARSL}*\text{DFEXT}(I,3,J)*70. \\
&= [\text{TD}(I)*\text{FAC}(I)*\text{AIRCON}*\text{REXARSL}*\text{DFEXT}(I,3,J)*70.] \\
&\quad / [\text{T}*\text{AR}] \quad (4.42)
\end{aligned}$$

and

$$\frac{[TD(I)*FAC(I)*AIRCON*REXARSL*DFEXT(I,3,J)*70.*RISK(J)]}{[T*AR]} , \quad (4.43)$$

respectively.

Population exposure and risk now follow from the expressions in (4.42) and (4.43). Specifically, with use of the relation in (4.14),

$$\begin{aligned} EXARSLD(I,J) &= \{ [TD(I)*FAC(I)*AIRCON*REXARSL*DFEXT(I,3,J) \\ &\quad *70.]/[T*AR] \} * \{ AR*DSL*T/70. \} \\ &= TD(I)*FAC(I)*AIRCON*REXARSL*DFEXT(I,3,J)*DSL \end{aligned} \quad (4.44)$$

and

$$\begin{aligned} EXARSLH(I,J) &= \{ [TD(I)*FAC(I)*AIRCON*REXARSL*DFEXT(I,3,J) \\ &\quad *70.*RISK(J)]/[T*AR] \} * \{ AR*DSL*T/70. \} \\ &= TD(I)*FAC(I)*AIRCON*REXARSL*DFEXT(I,3,J) \\ &\quad *RISK(J)*DSL . \end{aligned} \quad (4.45)$$

Thus, the total cancers from radionuclide I are given by

$$EXARSLT(I) = \sum_J EXARSLH(I,J) . \quad (4.46)$$

## 5. Irrigation After Release to Surface Water

### 5.1 Preliminary Comments

Population exposures and resultant health effects are now calculated for irrigation after a radionuclide release to a surface-water body. Similar calculations are considered in Chapter 4. However, there the only uptake mode considered is direct uptake from soil to plant. In this chapter the additional uptake modes resulting from radionuclides retained on plants due to sprinkler irrigation and from radionuclides in drinking water for milk and beef cattle are considered. In particular, IPLRDS(I,J), IPLRHE(I,J) and IPLRHET(I) are determined for exposure resulting from human ingestion of plants containing radionuclides deposited by sprinkler irrigation, where

IPLRDS(I,J) = population dose (units: rems) to organ associated with cancer J due to radionuclide I,

IPLRHE(I,J) = number of occurrences of cancer J in population due to radionuclide I,

IPLRHET(I) = total number of cancers in population due to radionuclide I.

Further, IMKRDS(I,J), IMKRHE(I,J) and IMKRHET(I) are determined for that part of the dose from milk ingestion which results from milk cattle ingesting radionuclides deposited on feed due to sprinkler irrigation, where

IMKRDS(I,J) = population dose (units: rems) to organ associated with cancer J due to radionuclide I,

IMKRHE(I,J) = number of occurrences of cancer J in population due to radionuclide I,

IMKRHET(I) = total number of cancers in population due to radionuclide I.

Similarly, IMKWDS(I,J), IMKWHE(I,J) and IMKWHET(I) are determined for that part of the dose from milk ingestion which results from milk cattle ingesting radionuclides in their drinking water. In like manner, IMTRDS(I,J), IMTRHE(I,J), IMTRHET(I), IMTWDS(I,J), IMTWHE(I,J) and IMTWHET(I) are determined for human ingestion of beef.

The preceding quantities are determined in a manner similar to that used in Chapter 4.

As already indicated, this section considers foliar deposition due to sprinkler irrigation. The concentration of radionuclide retained on, or in a plant, as the result of sprinkler irrigation is determined by solving a differential equation which represents the change in this concentration as the difference between the rate at which the radionuclide is contaminating the plant and the rate at which the radionuclide is being removed by weathering. This equation is

$$dC(t)/dt = D(t) - \lambda_w(t) \quad (5.1)$$

where

$C(t)$  = concentration of radionuclide on plant material (in Ci/kg),

$D(t)$  = rate of radionuclide deposition (in Ci/kg/yr), and

$\lambda_w$  = rate constant for removal by weathering (in  $\text{yr}^{-1}$ ).

With the initial condition  $C(0) = 0$  and the assumption that  $D(t)$  has a constant value  $D$ , the preceding equation has the solution

$$C(t) = (D/\lambda_w) (1 - e^{-t}), \quad (5.2)$$

which provides the concentration due to foliar deposition.

The weathering half-life is often taken to be 14 days. This yields a value for  $\lambda_w$  of  $18.1 \text{ yr}^{-1}$ . It is pointed out that  $1 - e^{-\lambda_w t}$  approaches 1 rapidly. With  $t = 0.17 \text{ yr}$ , the value is 0.95, and with  $t = 0.25 \text{ yr}$ , the value is 0.99. Thus, the length of time for irrigation is probably not critical. The deposition rate  $D$  is given by

$$D = \text{FRET} * \text{CWAT} * \text{IRAT} / \text{PDEN} , \quad (5.3)$$

where

FRET = fraction of deposited radionuclides retained on crops, often taken to be 0.25 (dimensionless),

CWAT = concentration of radionuclide in irrigation water (in Ci/L),

IRAT = irrigation rate (in L/m<sup>2</sup>/yr), and

PDEN = standing crop (in kg/m<sup>2</sup>).

The values indicated for  $\lambda_w$  and FRET are widely used and appear to come from a study by Milbourn and Taylor [Mi65].

The manner in which the relations in (5.2) and (5.3) will be used is now indicated. First, for simplicity, the asymptotic value for C(t) will be used. That is, the concentration C (units: Ci/kg) due to foliar deposition as a result of sprinkler irrigation is taken as

$$C = D/\lambda_w = \text{FRET} \cdot \text{CWAT} \cdot \text{IRAT} / \lambda_w \cdot \text{PDEN} . \quad (5.4)$$

Values for the variables in (5.4) are now obtained for radionuclide I in the context of the situation under consideration. From (3.1),

$$\text{CWAT}(I) = \text{TD}(I) / \text{F} \cdot \text{T} . \quad (5.5)$$

Further,

$$\text{IRAT} = \text{FRIV} \cdot \text{F} / \text{AR} , \quad (5.6)$$

where

FRIV = fraction of river used for sprinkler irrigation (units: unitless).

Also,

$$\lambda_w = \text{ALOG}(2.) / \text{WHRHL} , \quad (5.7)$$

where

WHRHL = weathering half-life for radionuclides deposited by sprinkler irrigation (units: yrs).

Thus, the concentration C(I) (units: Ci/kg) of radionuclide I on plants due to sprinkler irrigation is given by

$$C(I) = \frac{[FRET*TD(I)*FRIV*WHRHL]}{[T*AR*PDEN*ALOG(2.)]} \quad (5.8)$$

## 5.2 Exposure From Plant Consumption

The population exposures and resultant health effects are now determined for human ingestion of plants containing radionuclides deposited by sprinkler irrigation. It follows from (5.8) that the amount of radionuclide I ingested by an individual (units: Ci/yr) is given by

$$C(I)*CPLT = \frac{[FRET*TD(I)*FRIV*WHRHL*CPLT]}{[T*AR*PDEN*ALOG(2.)]} \quad (5.9)$$

Thus, the dose (units: rem/ind) to the organ associated with cancer J due to radionuclide I and the resultant cancer risk (units: cancer/ind) are given by

$$\frac{[FRET*TD(I)*FRIV*WHRHL*CPLT*DFING(I,J)]}{[T*AR*PDEN*ALOG(2.)]} \quad (5.10)$$

and

$$\frac{[FRET*TD(I)*FRIV*WHRHL*CPLT*DFING(I,J)*RISK(J)]}{[T*AR*PDEN*ALOG(2.)]} \quad (5.11)$$

respectively.

Population exposure and risk now follow from the expressions in (5.10) and (5.11). Specifically, with use of the relation in (4.11) for total population available for plant consumption,

$$\begin{aligned}
 \text{IPLRDS}(I,J) &= \{[\text{FRET} \cdot \text{TD}(I) \cdot \text{FRIV} \cdot \text{WHRHL} \cdot \text{CPLT} \cdot \text{DFING}(I,J)] \\
 &\quad / [\text{T} \cdot \text{AR} \cdot \text{PDEN} \cdot \text{ALOG}(2.)]\} \cdot \{\text{AR} \cdot \text{FPLT} \cdot \text{DPLT} \cdot \text{T} / 70.\} \\
 &= [\text{FRET} \cdot \text{TD}(I) \cdot \text{FRIV} \cdot \text{WHRHL} \cdot \text{CPLT} \cdot \text{DFING}(I,J) \\
 &\quad \cdot \text{FPLT} \cdot \text{DPLT}] / [\text{PDEN} \cdot \text{ALOG}(2.) \cdot 70.] \quad (5.12)
 \end{aligned}$$

and

$$\begin{aligned}
 \text{IPLRHE}(I,J) &= \{[\text{FRET} \cdot \text{TD}(I) \cdot \text{FRIV} \cdot \text{WHRHL} \cdot \text{CPLT} \cdot \text{DFING}(I,J) \\
 &\quad \cdot \text{RISK}(J)] / [\text{T} \cdot \text{AR} \cdot \text{PDEN} \cdot \text{ALOG}(2.)]\} \\
 &\quad \cdot \{\text{AR} \cdot \text{FPLT} \cdot \text{DPLT} \cdot \text{T} / 70.\} \\
 &= [\text{FRET} \cdot \text{TD}(I) \cdot \text{FRIV} \cdot \text{WHRHL} \cdot \text{CPLT} \cdot \text{DFING}(I,J) \\
 &\quad \cdot \text{RISK}(J) \cdot \text{FPLT} \cdot \text{DPLT}] / [\text{PDEN} \cdot \text{ALOG}(2.) \cdot 70.] \\
 &\quad (5.13)
 \end{aligned}$$

Thus, the total cancers from radionuclide I are given by

$$\text{IPLRHET}(I) = \sum_J \text{IPLRHE}(I,J) \quad (5.14)$$

### 5.3 Exposure From Milk Consumption

The population exposures and resultant health effects are now determined for milk ingestion. Two sets of determinations are made. The first is for that part of exposure and health effects which results from foliar deposition of radionuclides due to sprinkler irrigation. The second is

for that part of exposure and health effects which results from radionuclides in water given to livestock.

It follows from (5.8) that the amount of radionuclide I ingested by an individual (units: Ci/yr) due to foliar deposition and subsequent plant use in milk production is given by

$$\begin{aligned}
 & C(I) * PMLK * CRDM(I) * CMLK \\
 &= \left\{ [FRET * TD(I) * FRIV * WHRHL] / [T * AR * PDEN * ALOG(2.)] \right\} \\
 & \quad * \left\{ PMLK * CRDM(I) * CMLK \right\} \\
 &= [FRET * TD(I) * FRIV * WHRHL * PMLK * CRDM(I) * CMLK] \\
 & \quad / [T * AR * PDEN * ALOG(2.)] . \qquad (5.15)
 \end{aligned}$$

Thus, the dose (units: rem/ind) to the organ associated with cancer J due to radionuclide I and the resultant cancer risk (units: cancer/ind) are given by

$$\begin{aligned}
 & [FRET * TD(I) * FRIV * WHRHL * PMLK * CRDM(I) * CMLK \\
 & \quad * DFING(I, J)] / [T * AR * PDEN * ALOG(2.)] \qquad (5.16)
 \end{aligned}$$

and

$$\begin{aligned}
 & [FRET * TD(I) * FRIV * WHRHL * PMLK * CRDM(I) * CMLK \\
 & \quad * DFING(I, J) * RISK(J)] / [T * AR * PDEN * ALOG(2.)] , \qquad (5.17)
 \end{aligned}$$

respectively.

Population exposure and risk now follow from the expressions in (5.16) and (5.17). Specifically, with use of the relation in (4.12) for total population available for milk consumption,

$$\begin{aligned}
\text{IMKRDS}(I,J) &= \left\{ [\text{FRET} \cdot \text{TD}(I) \cdot \text{FRIV} \cdot \text{WHRHL} \cdot \text{PMLK} \cdot \text{CRDM}(I) \right. \\
&\quad \left. \cdot \text{CMLK} \cdot \text{DFING}(I,J)] / [\text{T} \cdot \text{AR} \cdot \text{PDEN} \cdot \text{ALOG}(2.)] \right\} \\
&\quad \cdot \left\{ \text{AR} \cdot \text{FMLK} \cdot \text{DMLK} \cdot \text{T} / 70 \right\}. \\
&= [\text{FRET} \cdot \text{TD}(I) \cdot \text{FRIV} \cdot \text{WHRHL} \cdot \text{PMLK} \cdot \text{CRDM}(I) \cdot \text{CMLK} \\
&\quad \cdot \text{DFING}(I,J) \cdot \text{FMLK} \cdot \text{DMLK}] / [\text{PDEN} \cdot \text{ALOG}(2.) \cdot 70.] \\
&\hspace{20em} (5.18)
\end{aligned}$$

and

$$\begin{aligned}
\text{IMKRHE}(I,J) &= \left\{ [\text{FRET} \cdot \text{TD}(I) \cdot \text{FRIV} \cdot \text{WHRHL} \cdot \text{PMLK} \cdot \text{CRDM}(I) \right. \\
&\quad \left. \cdot \text{CMLK} \cdot \text{DFING}(I,J) \cdot \text{RISK}(J)] / [\text{T} \cdot \text{AR} \cdot \text{PDEN} \right. \\
&\quad \left. \cdot \text{ALOG}(2.)] \right\} \cdot \left\{ \text{AR} \cdot \text{FMLK} \cdot \text{DMLK} \cdot \text{T} / 70 \right\}. \\
&= [\text{FRET} \cdot \text{TD}(I) \cdot \text{FRIV} \cdot \text{WHRHL} \cdot \text{PMLK} \cdot \text{CRDM}(I) \cdot \text{CMLK} \\
&\quad \cdot \text{DFING}(I,J) \cdot \text{RISK}(J) \cdot \text{FMLK} \cdot \text{DMLK}] \\
&\quad / [\text{PDEN} \cdot \text{ALOG}(2.) \cdot 70.] . \\
&\hspace{20em} (5.19)
\end{aligned}$$

Thus, the total cancers from radionuclide I are given by

$$\text{IMKRHET}(I) = \sum_J \text{IMKRHE}(I,J) . \hspace{10em} (5.20)$$

It follows from (3.1) that the amount of radionuclide I ingested by an individual (units: Ci/yr) due to water used for milk cattle is given by

$$\text{CW}(I) \cdot \text{WMLK} \cdot \text{CRDM}(I) \cdot \text{CMLK} = \text{TD}(I) \cdot \text{WMLK} \cdot \text{CRDM}(I) \cdot \text{CMLK} / \text{F} \cdot \text{T}, \hspace{2em} (5.21)$$

where

WMLK = water consumption by dairy cattle (units:  
L/day).

Thus, the dose (units: rem/ind) to the organ associated with cancer J due to radionuclide I and the resultant cancer risk (units: cancer/ind) are given by

$$TD(I) * WMLK * CRDM(I) * CMLK * DFING(I, J) / F * T \quad (5.22)$$

and

$$TD(I) * WMLK * CRDM(I) * CMLK * DFING(I, J) * RISK(J) / F * T, \quad (5.23)$$

respectively.

Population exposure and risk now follow from the expressions in (5.22) and (5.23). Specifically, with use of the relation in (4.12) for total population available for milk consumption,

$$\begin{aligned} IMKWDS(I, J) &= [TD(I) * WMLK * CRDM(I) * CMLK * DFING(I, J) / F * T] \\ &\quad * [AR * FMLK * DMLK * T / 70.] \\ &= [TD(I) * WMLK * CRDM(I) * CMLK * DFING(I, J) * AR \\ &\quad * FMLK * DMLK] / [F * 70.] \end{aligned} \quad (5.24)$$

and

$$\begin{aligned} IMKWHE(I, J) &= [TD(I) * WMLK * CRDM(I) * CMLK * DFING(I, J) * RISK(J) \\ &\quad / F * T] * [AR * FMLK * DMLK * T / 70.] \\ &= [TD(I) * WMLK * CRDM(I) * CMLK * DFING(I, J) * RISK(J) \\ &\quad * AR * FMLK * DMLK] / [F * 70.] \end{aligned} \quad (5.25)$$

Thus, the total cancers from radionuclide I are given by

$$IMKWHET(I,J) = \sum_J IMKWHE(I,J) . \quad (5.26)$$

Unlike all earlier calculations for population effects, the variables F and AR did not drop out of the expressions in (5.24) and (5.25). However, if one assumes that the irrigation rate IRAT (units: L/m<sup>2</sup> per yr) is known, it is possible to remove F and AR. Specifically,

$$F*FRIV = AR*IRAT \quad (5.27)$$

and so

$$AR/F = FRIV/IRAT . \quad (5.28)$$

Now, with use of the relation in (5.28), the equalities in (5.24) and (5.25) can be rewritten as

$$IMKWDS(I,J) = [TD(I)*WMLK*CRDM(I)*CMLK*DFING(I,J)*FRIV \\ *FMLK*DMLK]/[IRAT*70.] \quad (5.29)$$

and

$$IMKWHE(I,J) = [TD(I)*WMLK*CRDM(I)*CMLK*DFING(I,J)*RISK(J) \\ *FRIV*FMLK*DMLK]/[IRAT*70.] . \quad (5.30)$$

#### 5.4 Exposure From Meat Consumption

The population exposures and resultant health effects for meat consumption are determined in the same manner as those for milk consumption with the exceptions that PMT, CRDMT(I), CMT, FMT, DMT and WMT are used instead of PMLK, CRDM(I), CMLK, FMLK, DMLK and WMLK, respectively.

Thus,

$$\begin{aligned} \text{IMTRDS}(I,J) &= [\text{FRET}*\text{TD}(I)*\text{FRIV}*\text{WHRHL}*\text{PMT}*\text{CRDMT}(I)*\text{CMT} \\ &\quad * \text{DFING}(I,J)*\text{FMT}*\text{DMT}]/[\text{PDEN}*\text{ALOG}(2.)*70.] , \\ & \hspace{15em} (5.31) \end{aligned}$$

$$\begin{aligned} \text{IMTRHE}(I,J) &= [\text{FRET}*\text{TD}(I)*\text{FRIV}*\text{WHRHL}*\text{PMT}*\text{CRDMT}(I)*\text{CMT} \\ &\quad * \text{DFING}(I,J)*\text{RISK}(J)*\text{FMT}*\text{DMT}] \\ &\quad /[\text{PDEN}*\text{ALOG}(2.)*70.] \hspace{15em} (5.32) \end{aligned}$$

$$\begin{aligned} \text{IMTWDS}(I,J) &= [\text{TD}(I)*\text{WMT}*\text{CRDMT}(I)*\text{CMT}*\text{DFING}(I,J)*\text{AR} \\ &\quad * \text{FMT}*\text{DMT}]/[\text{F}*70.] \\ &= [\text{TD}(I)*\text{WMT}*\text{CRDMT}(I)*\text{CMT}*\text{DFING}(I,J)*\text{FRIV} \\ &\quad * \text{FMT}*\text{DMT}]/[\text{IRAT}*70.] \hspace{15em} (5.33) \end{aligned}$$

and

$$\begin{aligned} \text{IMTWHE}(I,J) &= [\text{TD}(I)*\text{WMT}*\text{CRDMT}(I)*\text{CMT}*\text{DFING}(I,J)*\text{RISK}(J) \\ &\quad * \text{AR}*\text{FMT}*\text{DMT}]/[\text{F}*70.] \\ &= [\text{TD}(I)*\text{WMT}*\text{CRDMT}(I)*\text{CMT}*\text{DFING}(I,J)*\text{RISK}(J) \\ &\quad * \text{FRIV}*\text{FMT}*\text{DMT}]/[\text{IRAT}*70.] \hspace{15em} (5.34) \end{aligned}$$

The total cancers from radionuclide I are given by

$$\text{IMTRHET} = \sum_{\text{J}} \text{IMTRHE}(\text{I}, \text{J}) \quad (5.35)$$

and

$$\text{IMTWHET} = \sum_{\text{J}} \text{IMTWHE}(\text{I}, \text{J}). \quad (5.36)$$

## References

- Bon73 Bond, R. G. and C. P. Straud (Eds.), 1973, Handbook of Environmental Control, Vol. 1, CRC Press, Cleveland, OH.
- Boo81 Boone, F. W., Y. C. Ng, and J. M. Palms, 1981 "Terrestrial Pathways of Radionuclide Particulates," Health Physics 41, 735-747.
- Cu73 Cummins, A. B. and I. A. Given (Eds.), 1973, SME Mining Engineering Handbook, Society of Mining Engineers, Littleton, CO.
- En80 Environmental Protection Agency, 1980, Environmental Radiation Protection Standards for Management and Disposal of Spent Nuclear Fuel, High-Level and Transuranic Radioactive Wastes, 40CFR191 (Working Draft No. 16, October 21, 1980).
- Im78 Iman, R. L., J. C. Helton, and J. E. Campbell, 1978, Risk Methodology for Geologic Disposal of Radioactive Waste: Sensitivity Analysis Techniques, SAND78-0912, Sandia Laboratories, Albuquerque, NM.
- He82 Helton, J. C. and N. C. Finley, 1982, PATH1 Self-Teaching Curriculum: Example Problems for Pathways-To-Man Model, SAND81-2377, Sandia National Laboratories, Albuquerque, NM.
- Mi65 Milbourn, G. M. and R. Taylor, 1965, "The Contamination of Grasslands With Radioactive Strontium: I, Initial Retention and Loss," Radiation Botany 5, 337-347.
- Nu76 Nuclear Regulatory Commission, 1976, Calculation of Annual Doses to Man From Routine Releases of Reactor Effluents for the Purpose of Evaluating Compliance With 10CFR Part 50, Appendix I, Regulatory Guide 1.109, U.S. Nuclear Regulatory Commission, Washington, DC.
- Ru81 Runkle, G. E., R. M. Cranwell, and J. D. Johnson, 1981, Risk Methodology for Geologic Disposal of Radioactive Waste: Dosimetry and Health Effects, SAND80-1372, Sandia National Laboratories, Albuquerque, NM.

- Sm81 Smith, J. M., T. W. Fowler, and A. S. Goldin, 1981, Environmental Pathway Models for Estimating Population Health Effects From Disposal of High-Level Radioactive Waste in Geologic Repositories, EPA520/5-80-002 (Draft June 8, 1981), Environmental Protection Agency, Washington, DC.
- To70 Todd, D. K. (Ed.), 1970, The Water Encyclopedia, Water Information Center, Huntington, NY.
- We74 Weast, W. E., 1974, Handbook of Chemistry and Physics (55th edition), CRC Press, Cleveland, OH.

**Volume 6**

**Calculation of Health Effects per Curie Release  
for Comparison with the EPA Standard**



NUREG/CR-3235  
SAND82-1557  
WH

TECHNICAL ASSISTANCE FOR REGULATORY DEVELOPMENT:  
REVIEW AND EVALUATION OF THE DRAFT EPA STANDARD 40CFR191  
FOR DISPOSAL OF HIGH-LEVEL WASTE

VOL. 6

CALCULATION OF HEALTH EFFECTS PER  
CURIE RELEASE FOR COMPARISON WITH  
THE EPA STANDARD

GENE E. RUNKLE\*

Manuscript Completed: April 1983  
Date Published: April 1983

Sandia National Laboratories  
Albuquerque, New Mexico 87185  
operated by  
Sandia Corporation  
for the  
U. S. Department of Energy

Prepared for  
Division of Waste Management  
Office of Nuclear Material Safety and Safeguards  
Washington, D.C. 20555

NRC FIN. No. A-1165

\*Raytheon Service Company

## ABSTRACT

The Environmental Protection Agency (EPA) is developing a standard for geologic disposal of high-level radioactive wastes (40CFR191) based on radioactive releases (expressed in curies) that may result in 1,000 health effects (i.e., latent cancer fatalities) over a 10,000 year period. Health effects calculations were used by EPA to establish the curie release limits. The Fuel Cycle Risk Analysis Division of Sandia National Laboratories was requested by the Nuclear Regulatory Commission (NRC) High-Level Waste Licensing Management Branch to perform calculations, using the methodology developed under the Risk Assessment Methodology Program, to compare with the results from the EPA analysis. The intent was to provide some insights into the degree of conservatism in the health effects per curie values presented by the EPA standard. No attempt was made to encompass all the uncertainty in the input parameters used in the calculations and some of the modeling assumptions used in this analysis are different from those of the EPA. Three sets of calculations of health effects (cancer deaths) per curie release were performed in this analysis. The calculational methods, the results of the analysis, and the potential implication of these results upon the curie release limits of the EPA are discussed in this report.

TABLE OF CONTENTS

	<u>PAGE</u>
1.0 Introduction.....	1
2.0 Description of the EPA/SANDIA Analysis.....	3
2.1 Ingestion.....	9
2.1.1 Dose Factors and Health Effects Estimates.....	9
2.1.2 Population at Risk.....	9
2.1.3 Quantity Intake of Radionuclides.....	13
2.1.3.1 Drinking Water.....	17
2.1.3.2 Fish.....	17
2.1.3.3 Crops.....	17
2.1.3.4 Milk.....	17
2.1.3.5 Beef.....	18
2.2 Inhalation.....	19
2.2.1 Dose Factors and Health Effects Estimates.....	19
2.2.2 Population at Risk.....	19
2.2.3 Quantity Intake of Radionuclides.....	20
2.3 External Exposure.....	20
2.3.1 Dose Factors and Health Effects Estimates.....	20
2.3.2 Population at Risk.....	20
2.3.3 Exposure Level.....	20
2.3.3.1 Contaminated Soil.....	20
2.3.3.2 Contaminated Air.....	21
3.0 Description of the SANDIA Analysis.....	21

TABLE OF CONTENTS (Cont'd)

	<u>PAGE</u>
4.0 Description of SAMPLED SANDIA Analysis.....	31
5.0 Results and Discussion.....	34
References.....	43

FIGURES

	<u>PAGE</u>
5.1 Deaths Per Curie Calculated with Sampled Kd Ranges and No Adsorption onto Solid Phase of the Surface Water for Pathways 1-5.....	38
5.2 Deaths Per Curie Calculated with Sampled Kd Ranges and No Adsorption onto Solid Phase of the Surface Water for Pathways 6-8.....	39
5.3 Deaths Per Curie Calculated with Sampled Kd Ranges and Adsorption onto Solid Phase of the Surface Water for Pathways 1-5.....	41
5.4 Deaths Per Curie Calculated with Sampled Kd Ranges and Adsorption onto Solid Phase of the Surface Water for Pathways 6-8.....	42

TABLES

		<u>PAGE</u>
2.1	Environmental Transport Input Parameters.....	5
2.2	Distribution Coefficients (Kd) Assumed by EPA.....	7
2.3	Radionuclide Concentrations in the Surface Water and Soil From the Pathways Analysis.....	8
2.4	Health Effects Conversion Factors (EPA).....	10
2.5	Ingestion, Inhalation and External Exposure Rates Assumed by EPA.....	14
2.6	Crop and Animal Parameters Assumed by EPA.....	15
2.7	Concentration Ratios Assumed by EPA.....	16
3.1	Basic Equations for Calculating Radionuclide Concentrations for Various Pathways.....	22
3.2	Concentration Ratios for Human and Animal Food Sources (Used in Reference Site Analysis).....	24
3.3	Ingestion, Inhalation and External Exposure Rates for an Average Individual (Used in Sandia Reference Site Analysis).....	25
3.4	Crop and Animal Parameters (Used in Sandia Reference Site Analysis).....	26
3.5	Dose Conversion Factors - Ingestion (rem/Ci).....	27
3.6	Dose Conversion Factors - Inhalation (rem/Ci).....	28
3.7	Dose Conversion Factors - External.....	29
3.8	Cancer Risk Estimates Used in the SANDIA Analysis.	30

TABLES (Cont'd)

	<u>PAGE</u>
4.1 Latin Hypercube Sample.....	32
4.2 Variables Which Affect the Physical Description of the Surface Environment.....	33
5.1 Individual Pathways and Dosimetry and Health Effects Comparison Table Expressed as Deaths Per Curie.....	35
5.2 Pathways and Dosimetry and Health Effects Comparison Table.....	37

## 1.0 Introduction

The Environmental Protection Agency (EPA) is developing a standard for geologic disposal of high-level radioactive wastes that would limit the curie releases to the accessible environment of the various radionuclides found in high-level waste. The EPA guidance establishes that the releases of radionuclides to the accessible environment from the wastes from 100,000 Metric Ton of Heavy Metal (MTHM) should not result in excess of 1,000 health effects (i.e., latent cancer fatalities) over a 10,000 year period. The process by which EPA established the release limits consisted of two steps. In the first step, the projected releases of radioactivity from a generic geologic repository in various geologic media (bedded salt, domed salt, granite, basalt and shale) were calculated and in the second step, the potential excess cancer deaths from the releases were estimated. A set of calculated health effects per curie released into the environment for all the radionuclides considered in the EPA analysis was established to estimate the potential health hazard. The EPA analyses of the various media were used to select the limit of 1,000 health effects over 10,000 years for a 100,000 MTHM repository. The 1,000 health effects criteria was then used to establish the release limits for individual radionuclides. The Nuclear Regulatory Commission (NRC) requested the Fuel Cycle Risk Analysis Division of Sandia National Laboratories (SNL) to perform an evaluation using the methodology developed under the Risk Assessment Methodology Program (FIN:A-1192) to calculate the health effects that may result from the release of one curie of each of various radionuclides to the biosphere. The intent of this two week effort was to provide some insights into the degree of conservatism in the health effects per curie values calculated by the EPA. The intent was not to present values to replace the EPA curie values, but rather to perform calculations similar to the EPA analysis that would provide some perspective on the EPA release limits. No attempt was made to bound all of the uncertainty in the input parameters in the pathway modeling effort, to encompass all the possibilities of release or to address the uncertainties in the dose conversion factors and health effects estimates. The calculations presented in this report were designed to flag potential problems with the EPA release limits that may warrant further analysis.

Three sets of calculations were performed in this work. The first set of calculations (EPA/SANDIA Analysis) used the Pathways Model developed at Sandia (Helton and Kaestner, 1981) and the input parameters (e.g., distribution coefficients (Kd), concentration ratios, dose conversion factors, risk estimates, etc.) and the health effects calculational methods from the EPA. A second set of calculations (SANDIA Analysis) was made using the Pathways Model (Helton and Kaestner, 1981) and the

Dosimetry and Health Effects Model (Runkle, et al., 1981). In these calculations the input parameters to the Pathways Model were selected from those used in demonstrating the Risk Assessment Methodology (described in Cranwell, et al., 1982). The reference site used in this demonstration was based on a hypothetical site and generic parameters representing several sites throughout the United States. The EPA point value for the distribution coefficients (Kd) for the various radionuclides were used in the analysis. The third set of calculations (SAMPLED SANDIA Analysis) were performed using a statistical technique to sample an assigned range of values for some of the input parameters to the Pathways Model. A distribution was assigned to each range of values. This approach can be used to represent some of the uncertainty in the calculated results due to input data uncertainties. Many other uncertainties have not been addressed in this analysis and include uncertainties in the concentration ratios, the dose conversion factors, and the risk estimators of health effects, to name only a few.

There are several differences in the modeling approaches used in this analysis that may affect the results and are therefore detailed below. First, for calculating the health effects per curie release for the water based pathway, the EPA input a unit curie source over 10,000 years (i.e.,  $10^{-4}$  Ci/yr) into the surface (river) water to calculate the drinking water and fish intakes. For the land based pathways (which include ingestion of crops, beef and milk), EPA input a 0.5 curie source into the soil compartment over 10,000 years (i.e.,  $5 \times 10^{-5}$  Ci/yr) to estimate the soil concentrations, and further assumed that 50% of the contaminated land was used for crop production for direct human consumption, 25% for milk production and 25% for beef production.

In the analyses (EPA/SANDIA, SANDIA, SAMPLED SANDIA) presented in this report, a unit curie source was input to the liquid phase of the surface water over 10,000 years (i.e.,  $10^{-4}$  Ci/yr) and the interchange between the surface water and the soil compartments of the Pathways Model determined the soil concentration. The calculations performed by the Pathways Model resulted in an input of  $2.3E-3$  Ci to the soil over the 10,000 year period. In addition, the fractional partitioning of land use (assumed by EPA) was not incorporated in this analysis.

Second, the EPA analysis considered a population detriment that was based on a linear relationship of population to the flow rate in a river for the water based pathways and was linearly proportional to the area of land for the land based pathways. In the approach used by EPA, it is important to note

that the area (A) canceled out of the equation for the land based ingestion calculation, which eliminated the linear relationship between area and population.

The Risk Assessment Methodology used for this analysis was based on the risk to an average individual and was converted to a population risk by relating the river flow rate to the population density (persons/ℓ) assumed by EPA to estimate the population for the water based pathways. For the land based pathways the density (persons/m<sup>2</sup>) defined by EPA was multiplied by the area considered in the reference site analysis (Cranwell et al., 1982). The land area was defined as 40 km x 2 km on both sides of a river (160 km<sup>2</sup>), that was assumed to fall within the flood plain of the river and to provide food (crops, beef and milk) for the population. With this approach, the population is a linear function of the assumed area and doubling the area will result in a doubling of the population.

The three calculational methods for the EPA/SANDIA, SANDIA and SAMPLED SANDIA Analyses are detailed in Chapters 2-4, respectively. Chapter 5 is a summary of the results calculated in this analysis.

## 2.0 Description of the EPA/SANDIA Analysis

The EPA/SANDIA Analysis used the Environmental Pathways Model developed at Sandia (Helton and Kaestner, 1981) and the input parameters used by EPA in their analysis. The input parameters included concentration ratios, human and animal consumption rates, dose conversion factors and risk estimates. These calculations were designed to estimate the health effects per curie release by employing the Risk Assessment Methodology developed at SNL and the EPA input parameters.

The Pathways Model (Helton and Kaestner, 1981) was used to estimate the radionuclide concentrations in the surface water and soil compartments following a 10<sup>-4</sup> curie/year release into the surface water for a 10,000 year period. For the simplified analysis presented in this report, a system consisting of two compartments, soil and surface water, was used. For this situation, the mathematical formulation for each radionuclide considered is a system of two differential equations of the following form:

$$\begin{aligned} dx_1/dt &= h_1 - (\lambda + k_{21}) x_1 + k_{12} x_2 \\ dx_2/dt &= h_2 + k_{21} x_1 - (\lambda + k_{02} + k_{12}) x_2 \end{aligned} \quad (1)$$

where  $x_i$  is the amount (units: Ci) of radionuclide in compartment  $i$  (1 ~ soil, 2 ~ surface water),  $h_i$  is the rate of radionuclide input (units: Ci/yr) to compartment  $i$ , and  $\lambda$

is the decay constant (units: yr<sup>-1</sup>) for the radionuclide under consideration. The  $k_{ij}$  is the rate constant for movement from compartment  $j$  to compartment  $i$ , where  $i = 0$  denotes a flow from compartment  $j$  to an area outside the modeled system. Each coefficient,  $k_{ij}$ , is of the following form:

$$k_{ij} = \frac{(1 - S_j)RW_{ij}}{VW_j} + \frac{S_j RS_{ij}}{MS_j} \quad (2)$$

where  $VW_j$  denotes the volume of water in compartment  $j$  (units:  $\ell$ ),  $MS_j$  denotes the mass of solids in compartment  $j$  (units: kg),  $RW_{ij}$  denotes the rate at which water flows from compartment  $j$  to compartment  $i$  (units:  $\ell/\text{yr}$ ), and  $RS_{ij}$  denotes the rate at which solid material flows from compartment  $j$  to compartment  $i$  (units: kg/yr). Further, the unitless quantity  $S_j$  represents the effects of radionuclides partitioning in compartment  $j$  and is defined by

$$S_j = \frac{Kd_j MS_j}{Kd_j MS_j + VW_j} \quad (3)$$

where  $Kd_j$  is the distribution coefficient in compartment  $j$  for the radionuclide under consideration (units:  $\ell/\text{kg}$ ). The nonzero values for the  $VW_j$ ,  $MS_j$ ,  $RW_{ij}$  and  $RS_{ij}$  for the site described in this section are given in Table 2.1.

The system of equations in (1) can be reformulated in matrix notation as

$$dx/dt = h + Kx, \quad (4)$$

where

$$x = \begin{bmatrix} x_1 \\ x_2 \end{bmatrix}, \quad h = \begin{bmatrix} h_1 \\ h_2 \end{bmatrix} \quad \text{and} \quad K = \begin{bmatrix} -(\lambda + k_{21}) & k_{12} \\ k_{21} & -(\lambda + k_{02} + k_{12}) \end{bmatrix} \quad (5)$$

For this analysis  $h_1$  was assumed to be  $10^{-4}$  curies/yr and  $h_2$  was assumed to be 0. As the system under consideration is completely open, the equations represented in (1) and (2) have a unique asymptotic solution,  $sx$ , where

$$sx = -K^{-1} h. \quad (6)$$

For the analysis presented in this report, the asymptotic solutions indicated in (6) were used instead of time-dependent solutions. Variables  $R_1$  to  $R_4$  were used to introduce variance in the exchange rate between subzones and may be sampled from a user-specified range. For this analysis, a mid-point value (see Table 2.1) was assumed.

Table 2.1

Environmental Transport Input Parameters  
(Helton and Kaestner, 1981)

Surface Water:

VW <sub>2</sub> = Volume of Water	2.2x10 <sup>10</sup> ℓ
MS <sub>2</sub> = Mass of Solid	6.8x10 <sup>5</sup> $\left(\frac{R_4}{R_1}\right)$ kg
RS <sub>12</sub> = Rate of mass outflow to soil subzone	1.1x10 <sup>11</sup> (R <sub>3</sub> ) kg/y
RW <sub>02</sub> = Rate of water outflow to surface water in next zone	1.9x10 <sup>13</sup> (R <sub>1</sub> ) ℓ/y
RS <sub>02</sub> = Rate of solid outflow to surface in next zone	5.9x10 <sup>8</sup> (R <sub>4</sub> ) kg/y
RW <sub>12</sub> = Rate of water outflow to soil subzone	4.0x10 <sup>10</sup> (R <sub>2</sub> ) ℓ/y

Soil:

VW <sub>1</sub> = Volume of water	2.0x10 <sup>10</sup> ℓ
MS <sub>1</sub> = Mass of solid	1.1x10 <sup>11</sup> kg
RW <sub>21</sub> = Rate of water outflow to surface water	4.0x10 <sup>10</sup> (R <sub>2</sub> ) ℓ/y
RS <sub>21</sub> = Rate of mass outflow to surface water	0.0 (kg/y)

Assumed Values:

R <sub>1</sub> = 1.0	} Variables to introduce variation in the subzones indicated above. Variations were not considered in the EPA/SANDIA or the SANDIA analyses, therefore these variables were assigned the point values given in this table.
R <sub>2</sub> = 1.0	
R <sub>3</sub> = 10 <sup>-3</sup>	
R <sub>4</sub> = 9.0	

Also for this analysis, the radionuclides were assumed to be released to the liquid phase of the surface water. Further, no adsorption onto the solid particulate phase of the surface water was considered. This would represent a situation where there are no Kd effects in the water. In an alternative scenario that considers river flooding, particulates are carried onto the surrounding land mass and contribute a large radionuclide burden to the soil. This analysis placed the radionuclide solely in the liquid phase of the surface water, as assumed by the EPA. However, the distribution coefficient, Kd, was taken into account in the radionuclide concentration in the soil subzone. The point values for the Kd values for the radionuclides that were used in this analysis and also by the EPA are given in Table 2.2. The EPA data (unless otherwise specified) were obtained from personal communication with J. M. Smith, EPA, Montgomery, Alabama. Since the initial work in 1981, these EPA parameters and the environmental calculations have been published in Smith, et al., 1982.

In the analysis presented in this section, a unit curie source was input to the liquid phase of the water over 10,000 years and the interchanges between the surface water and the soil compartments of the Pathways Model determined the soil concentration. The results of the Pathways analysis are given in Table 2.3 for the surface water and soil compartments. These radionuclide concentrations were used to calculate the health effects (cancer deaths) per curie release. The calculations of the cumulative health effects over time, T, may be summarized by the following general equation

$$RSK_{ij} = Q_{ij} * \left( \sum_k DF_{ijk} * HE_{jk} \right) * POP_j * T \quad (7)$$

where

$RSK_{ij}$  = health effects (cancer deaths) per curie release of radionuclide i via pathway j (ingestion, inhalation or external)

$Q_{ij}$  = quantity intake per year (via ingestion or inhalation) or exposure (external) to radionuclide i via pathway j (Ci/y)

$DF_{ijk}$  = dose conversion factor to calculate the dose commitment to organ k from radionuclide i via pathway j (rem/Ci)

Table 2.2  
 Distribution Coefficients (Kd)  
 Assumed by EPA

<u>Radionuclide</u>	<u>Kd Value (cm<sup>3</sup> / gm)</u>
Am241	2000
Am243	2000
Cs135	200
Cs137	200
I129	0
Np239	15
Pu239	2000
Pu240	2000
Pu242	2000
Sr90	20
Tc99	0
Sn126	250

Table 2.3

Radionuclide Concentrations in the Surface Water and  
Soil From the Pathways Analysis

<u>Radionuclide</u>	<u>Surface Water</u> (Ci/l)	<u>Soil</u> (Ci/kg)
Am241	5.26E-18	1.13E-15
Am243	5.26E-18	7.02E-15
Cs135	5.26E-18	1.05E-15
Cs137	5.26E-18	7.66E-17
I129	5.26E-18	9.57E-19
NP237	5.26E-18	7.99E-17
PU239	5.26E-18	9.10E-15
PU240	5.26E-18	6.54E-15
PU242	5.26E-18	1.04E-14
SR90	5.26E-18	4.56E-17
TC99	5.26E-18	9.57E-19
SN126	5.26E-18	1.31E-15

- HE<sub>jk</sub> = health effects conversion factor to estimate the potential fatal cancers from the dose commitment to organ k via pathway j  $\left( \frac{\text{health effects}}{\text{rem}} \right)$
- POP<sub>j</sub> = population exposed to the dose commitment from pathway j (persons)
- T = time interval of the calculation. For this analysis (and EPA) the time interval was assumed to be 10,000 years.

The three pathways included in this analysis were the ingestion (includes several subpathways), inhalation and external exposure. The calculations of health effects per curie release for each of these pathways are detailed in subsections 2.1, 2.2 and 2.3, respectively.

## 2.1 Ingestion

The ingestion pathway consists of intake of radionuclides from various subpathways including drinking water, fish, plants, milk and meat. The calculations for these subpathways used the following components: (1) dose factors and health estimates (2) population at risk and (3) quantity intake. Each component is discussed below with reference to the various subpathways.

### 2.1.1 Dose Factors and Health Effects Estimates

The dose conversion factors and the health effects estimates per rem of exposure were taken from Table 2.4. For each radionuclide, the product of the ingestion dose commitment factors and health effects conversion factors were summed over all organs. The summation was used to calculate the health effects from all of the subpathways. The dose conversion factors used by EPA represent a 50-year dose commitment (rem) to an individual which results from the initial intake of one curie of the radionuclide.

### 2.1.2 Population at Risk

EPA used the flow rate of the world's rivers and the world population to estimate the population that can be supported by a given river flow rate. This ratio, of the flow rate to the world population, was applied to the flow rate of the river considered in this analysis (1.9E13 l/yr) to define the population for the drinking water. A resulting population of 6.3E6 persons was used for the EPA/SANDIA calculations. EPA also related the world's average fish consumption rate (10<sup>10</sup> kg/yr) to the world's river flow rate (3E16 l/yr) to estimate the

Table 2.4

HEALTH EFFECTS CONVERSION FACTORS, HEALTH EFFECTS/MAN REM  
(FATAL CANCERS FOR ALL ORGANS EXCEPT OVARIES AND TESTES. GENETIC EFFECTS TO FIRST GENERATION FOR OVARIES AND TESTES)

NUCLIDE	BONE	RED MARROW	LUNGS	LIVER	GI-LLI WALL	THYROID	KIDNEYS	OTHER ORGAN	OVARIES	TESTES
	1.000E-05	4.000E-05	4.000E-05	1.000E-05	2.000E-05	1.000E-06	1.000E-05	7.000E-05	2.000E-05	2.000E-05

NUCLIDE DEPENDENT INPUT DATA

NUCLIDE	PATHWAY (INHALATION AND INGESTION=REM/CI INTAKE)	DOSE COMMITMENT FACTORS AIR SUBMERSION=REM/Y PER CI/M**3 GROUND CONTAMINATION=REM/Y PER CI/M**2)									
		BONE	RED MARROW	LUNGS	LIVER	GI-LLI WALL	THYROID	KIDNEYS	OTHER ORGAN	OVARIES	TESTES
C-14	INHAL1	8.460E+00	2.420E+01	6.180E+00	8.880E+00	7.220E+00	6.480E+00	7.920E+00	1.410E+01	5.290E+00	5.420E+00
	INHAL2	8.460E+00	2.420E+01	6.180E+00	8.880E+00	7.220E+00	6.480E+00	7.920E+00	1.410E+01	5.290E+00	5.420E+00
	INGEST	1.170E+03	3.380E+03	8.490E+02	1.230E+03	1.460E+03	8.890E+02	1.060E+03	1.920E+03	7.360E+02	7.230E+02
	EXT AIR	0.0	0.0	0.0	0.0	0.0	0.0	0.0	0.0	0.0	0.0
	EXT GND	0.0	0.0	0.0	0.0	0.0	0.0	0.0	0.0	0.0	0.0
NI-59	INHAL1	1.290E+04	2.150E+03	8.470E+03	4.983E+03	7.120E+02	2.150E+03	2.150E+03	2.150E+03	2.150E+03	2.150E+03
	INHAL2	1.290E+04	2.150E+03	8.470E+03	4.980E+03	3.560E+02	2.150E+03	2.150E+03	2.150E+03	2.150E+03	2.150E+03
	INGEST	9.670E+03	1.610E+03	1.610E+03	3.320E+03	9.700E+02	1.610E+03	1.610E+03	1.610E+03	1.610E+03	1.610E+03
	EXT AIR	0.0	0.0	0.0	0.0	0.0	0.0	0.0	0.0	0.0	0.0
	EXT GND	0.0	0.0	0.0	0.0	0.0	0.0	0.0	0.0	0.0	0.0
SR-90	INHAL1	3.210E+05	1.210E+05	8.540E+06	1.930E+04	9.310E+05	3.740E+03	3.740E+03	1.510E+05	3.740E+03	3.730E+03
	INHAL2	3.000E+06	1.100E+06	4.920E+04	1.490E+04	5.500E+04	1.540E+04	1.540E+04	2.410E+05	1.540E+04	1.540E+04
	INGEST	1.200E+06	4.300E+05	1.570E-02	5.710E+03	1.980E+05	5.990E+03	5.990E+03	9.500E+04	5.990E+03	5.990E+03
	EXT AIR	0.0	0.0	0.0	0.0	0.0	0.0	0.0	0.0	0.0	0.0
	EXT GND	0.0	0.0	0.0	0.0	0.0	0.0	0.0	0.0	0.0	0.0
ZR-93	INHAL1	1.470E+03	1.750E+03	5.850E+04	2.930E+03	7.160E+03	1.600E+03	1.360E+03	2.500E+03	1.040E+03	1.470E+02
	INHAL2	4.120E+03	2.460E+03	3.080E+04	2.110E+03	6.980E+03	1.320E+03	1.320E+03	2.130E+03	1.460E+03	4.950E+02
	INGEST	1.970E+02	3.340E+02	3.900E+01	1.430E+02	1.750E+04	1.690E+01	1.990E+02	2.470E+02	1.360E+03	1.340E+02
	EXT AIR	0.0	0.0	0.0	0.0	0.0	0.0	0.0	0.0	0.0	0.0
	EXT GND	1.780E+04	1.780E+04	1.780E+04	1.780E+04	1.780E+04	1.780E+04	1.780E+04	1.780E+04	1.780E+04	1.780E+04
TC-99	INHAL1	2.420E+02	2.150E+02	5.220E+04	4.210E+02	1.660E+03	9.460E+03	3.070E+02	8.870E+02	2.120E+02	2.120E+02
	INHAL2	2.420E+02	2.150E+02	5.220E+04	4.210E+02	1.660E+03	9.460E+03	3.070E+02	8.870E+02	2.120E+02	2.120E+02
	INGEST	3.610E+02	3.220E+02	0.0	6.280E+02	3.200E+03	1.410E+04	4.580E+02	2.140E+02	3.170E+02	3.170E+02
	EXT AIR	0.0	0.0	0.0	0.0	0.0	0.0	0.0	0.0	0.0	0.0
	EXT GND	0.0	0.0	0.0	0.0	0.0	0.0	0.0	0.0	0.0	0.0

Taken from Smith, et al., 1982

Table 2.4 (continued)

		ORGAN									
		BONE	RED MARROW	LUNGS	LIVER	GI-LLI WALL	THYROID	KIDNEYS	OTHER ORGAN	OVARIES	TESTES
SN-126	INHAL1	1.580E+05	1.580E+05	1.270E+06	4.190E+03	7.600E+04	1.230E+03	6.160E+03	6.160E+03	6.160E+03	6.160E+03
	INHAL2	1.580E+05	1.580E+05	1.270E+06	4.190E+03	7.600E+04	1.230E+03	6.160E+03	6.160E+03	6.160E+03	6.160E+03
	INGEST	8.570E+04	8.570E+04	3.110E+03	1.690E+03	1.190E+05	4.990E+02	2.830E+03	2.820E+03	2.820E+03	2.820E+03
	EXT AIR	1.150E+07	1.150E+07	1.150E+07	1.150E+07	1.150E+07	1.150E+07	1.150E+07	1.150E+07	1.150E+07	1.150E+07
	EXT GND	2.090E+05	2.090E+05	2.090E+05	2.090E+05	2.090E+05	2.090E+05	2.090E+05	2.090E+05	2.090E+05	2.090E+05
I-129	INHAL1	5.790E+02	6.050E+02	7.880E+02	4.660E+02	4.280E+01	5.000E+06	4.490E+02	2.050E+03	3.780E+02	3.570E+02
	INHAL2	5.790E+02	6.050E+02	7.880E+02	4.660E+02	4.280E+01	5.000E+06	4.490E+02	2.050E+03	3.780E+02	3.570E+02
	INGEST	9.020E+02	9.420E+02	1.790E+02	7.240E+02	6.700E+01	7.800E+06	7.020E+02	3.180E+03	5.920E+02	5.530E+02
	EXT AIR	1.450E+05	1.310E+05	4.850E+04	3.600E+04	1.150E+04	1.010E+05	5.380E+04	9.540E+04	3.400E+04	1.310E+05
	EXT GND	8.730E+03	7.870E+03	2.910E+03	2.160E+03	6.900E+02	6.040E+03	3.230E+03	5.730E+03	2.040E+03	7.880E+03
CS-135	INHAL1	7.470E+03	7.470E+03	6.400E+02	7.470E+03	8.510E+01	7.480E+03	7.470E+03	4.400E+03	7.470E+03	7.470E+03
	INHAL2	7.470E+03	7.470E+03	6.400E+02	7.470E+03	8.510E+01	7.480E+03	7.470E+03	4.400E+03	7.470E+03	7.470E+03
	INGEST	1.120E+04	1.120E+04	0.0	1.120E+04	5.350E+02	1.130E+04	1.120E+04	6.610E+03	1.120E+04	1.120E+04
	EXT AIR	0.0	0.0	0.0	0.0	0.0	0.0	0.0	0.0	0.0	0.0
	EXT GND	0.0	0.0	0.0	0.0	0.0	0.0	0.0	0.0	0.0	0.0
CS-137	INHAL1	4.540E+04	4.910E+04	1.620E+04	5.230E+04	1.600E+04	4.470E+04	5.130E+04	3.260E+04	5.000E+04	4.440E+04
	INHAL2	4.540E+04	4.910E+04	1.620E+04	5.230E+04	1.600E+04	4.470E+04	5.130E+04	3.260E+04	5.000E+04	4.440E+04
	INGEST	6.820E+04	7.380E+04	1.990E+04	7.870E+04	2.590E+04	6.720E+04	7.730E+04	4.910E+04	7.540E+04	6.680E+04
	EXT AIR	4.660E+06	4.450E+06	3.600E+06	3.180E+06	2.750E+06	4.020E+06	3.380E+06	3.810E+06	1.390E+06	4.240E+06
	EXT GND	8.290E+04	7.920E+04	6.400E+04	5.650E+04	4.900E+04	7.150E+04	6.030E+04	6.790E+04	2.490E+04	7.550E+04
SM-151	INHAL1	5.100E+02	2.090E+02	6.780E+04	1.900E+03	3.040E+03	1.920E+01	5.540E+02	1.090E+03	1.470E+01	1.070E+01
	INHAL2	4.910E+03	1.940E+03	1.590E+04	1.890E+04	2.810E+03	1.040E+02	5.380E+03	1.190E+03	1.090E+02	1.030E+02
	INGEST	4.910E+00	3.200E+00	1.050E-01	1.730E+01	5.850E+03	1.030E-01	5.520E+00	2.340E+01	5.660E+00	5.360E-01
	EXT AIR	2.440E+01	2.130E+01	4.240E+00	2.350E+00	2.920E+00	9.060E+00	7.020E+00	3.070E+01	3.920E+00	3.860E+01
	EXT GND	4.590E+00	4.000E+00	7.960E-01	4.410E-01	5.480E-01	1.700E+00	1.320E+00	5.780E+00	7.360E-01	7.300E+00
RA-226	INHAL1	1.100E+07	9.800E+05	2.810E+07	3.400E+05	1.000E+05	3.400E+05	3.490E+05	4.600E+06	3.400E+05	3.400E+05
	INHAL2	1.100E+07	9.800E+05	2.810E+07	3.400E+05	1.000E+05	3.400E+05	3.490E+05	4.600E+06	3.400E+05	3.400E+05
	INGEST	6.320E+07	2.140E+06	2.710E+02	1.870E+06	8.160E+05	8.010E+05	5.790E+06	7.790E+06	8.060E+05	8.010E+05
	EXT AIR	1.500E+07	1.390E+07	1.270E+07	1.120E+07	1.030E+07	1.280E+07	1.060E+07	1.180E+07	9.900E+06	1.130E+07
	EXT GND	2.520E+05	2.340E+05	2.070E+05	1.850E+05	1.690E+05	2.120E+05	1.750E+05	2.210E+05	1.630E+05	1.890E+05
U-234	INHAL1	2.000E+07	8.100E+05	2.730E+08	5.900E+05	5.480E+04	5.900E+05	8.700E+05	9.800E+06	5.900E+05	5.900E+05
	INHAL2	5.900E+07	2.400E+06	2.800E+07	1.700E+06	4.790E+04	1.700E+06	2.500E+06	5.500E+06	1.700E+06	1.700E+06
	INGEST	2.000E+07	8.000E+05	8.230E+02	5.800E+05	8.860E+04	5.800E+05	8.500E+05	1.700E+06	5.800E+05	5.800E+05
	EXT AIR	2.940E+03	2.640E+03	1.030E+03	7.640E+02	8.560E+02	1.280E+03	8.130E+02	2.490E+03	6.640E+02	2.090E+03
	EXT GND	5.630E+02	5.050E+02	1.970E+02	1.460E+02	1.640E+02	2.460E+02	1.560E+02	4.780E+02	1.270E+02	4.000E+02
NP-237	INHAL1	9.040E+08	3.010E+08	2.900E+08	4.020E+08	1.380E+05	3.000E+06	5.200E+07	8.500E+07	1.800E+06	5.800E+06
	INHAL2	2.240E+09	7.470E+08	3.000E+07	9.910E+08	1.260E+05	7.400E+06	1.280E+08	1.900E+08	4.600E+06	1.400E+07
	INGEST	1.900E+07	6.200E+06	8.870E+02	8.200E+06	1.460E+05	6.080E+04	1.100E+06	1.600E+06	3.900E+04	1.200E+05
	EXT AIR	3.270E+06	3.030E+06	1.790E+06	1.560E+06	1.130E+06	2.150E+06	1.500E+06	2.050E+06	1.020E+06	2.410E+06
	EXT GND	7.250E+04	6.720E+04	3.970E+04	3.460E+04	2.500E+04	4.470E+04	3.340E+04	4.570E+04	2.270E+04	5.350E+04

Table 2.4 (continued)

		ORGAN									
		BONE	RED MARROW	LUNGS	LIVER	GI-LLI HALL	THYROID	KIDNEYS	OTHERORGAN	OVARIES	TESTES
PU-238	INHAL1	7.910E+08	2.640E+08	3.090E+08	3.550E+08	6.200E+04	2.600E+06	4.600E+07	7.600E+07	1.600E+06	5.000E+06
	INHAL2	2.030E+09	6.770E+08	3.200E+07	9.070E+08	5.510E+04	6.600E+06	1.170E+08	1.730E+08	4.100E+06	1.300E+07
	INGEST	5.000E+05	1.700E+05	7.890E-02	2.200E+05	1.100E+05	1.640E+03	2.910E+04	4.320E+04	1.030E+03	3.200E+03
	EXT AIR	1.260E+03	1.090E+03	3.020E+02	1.330E+02	4.450E+02	2.460E+02	1.770E+02	1.660E+03	1.860E+02	1.320E+03
	EXT GND	2.470E+02	2.140E+02	5.920E+01	2.600E+01	8.710E+01	4.810E+01	3.460E+01	3.250E+02	3.640E+01	2.580E+02
PU-239	INHAL1	9.120E+08	3.040E+08	2.940E+08	4.040E+08	5.780E+04	3.000E+06	5.200E+07	8.600E+07	1.800E+06	5.800E+06
	INHAL2	2.280E+09	7.610E+08	3.000E+07	1.000E+09	5.130E+04	7.400E+06	1.300E+08	1.920E+08	4.600E+06	1.500E+07
	INGEST	5.700E+05	1.900E+05	6.090E-02	2.500E+05	9.850E+04	1.850E+03	3.220E+04	4.820E+04	1.150E+03	3.600E+03
	EXT AIR	6.410E+02	5.610E+02	1.710E+02	9.380E+01	1.900E+02	1.890E+02	1.230E+02	7.220E+02	1.170E+02	6.110E+02
	EXT GND	1.220E+02	1.070E+02	3.240E+01	1.780E+01	3.600E+01	3.590E+01	2.330E+01	1.370E+02	2.210E+01	1.160E+02
PU-240	INHAL1	9.130E+08	3.040E+08	2.950E+08	4.050E+08	5.820E+04	3.000E+06	5.200E+07	8.600E+07	1.800E+06	5.800E+06
	INHAL2	2.280E+09	7.600E+08	3.100E+07	1.010E+09	5.170E+04	7.400E+06	1.300E+08	1.940E+08	4.600E+06	1.500E+07
	INGEST	5.700E+05	1.900E+05	8.320E-02	2.500E+05	9.930E+04	1.840E+03	3.220E+04	4.830E+04	1.150E+03	3.600E+03
	EXT AIR	1.160E+03	1.000E+03	2.890E+02	1.400E+02	3.990E+02	2.530E+02	1.780E+02	1.460E+03	1.600E+02	1.170E+03
	EXT GND	2.250E+02	1.960E+02	5.640E+01	2.720E+01	7.790E+01	4.930E+01	3.470E+01	2.850E+02	3.520E+01	2.280E+02
AM-241	INHAL1	9.430E+08	3.140E+08	3.130E+08	4.190E+08	6.520E+04	3.100E+06	5.400E+07	8.900E+07	1.900E+06	6.000E+06
	INHAL2	2.350E+09	7.830E+08	3.200E+07	1.040E+09	6.110E+04	7.700E+06	1.340E+08	1.990E+08	4.800E+06	1.500E+07
	INGEST	1.900E+07	6.400E+06	1.270E+02	8.500E+06	1.100E+05	6.320E+04	1.100E+06	1.600E+06	3.940E+04	1.200E+05
	EXT AIR	2.720E+05	2.480E+05	1.010E+05	8.300E+04	5.680E+04	1.380E+05	8.800E+04	1.440E+05	8.510E+04	1.250E+05
	EXT GND	1.420E+04	1.300E+04	5.300E+03	4.330E+03	2.960E+03	7.210E+03	4.590E+03	7.500E+03	4.440E+03	6.570E+03
PU-242	INHAL1	8.690E+08	2.890E+08	2.800E+08	3.850E+08	5.510E+04	2.800E+06	5.000E+07	8.200E+07	1.800E+06	5.500E+06
	INHAL2	2.170E+09	7.220E+08	2.900E+07	9.560E+08	4.900E+04	7.100E+06	1.230E+08	1.840E+08	4.400E+06	1.400E+07
	INGEST	5.400E+05	1.800E+05	1.600E-01	2.400E+05	9.400E+04	1.760E+03	3.060E+04	4.600E+04	1.090E+03	3.420E+03
	EXT AIR	1.040E+03	8.930E+02	2.360E+02	9.370E+01	3.650E+02	1.770E+02	1.320E+02	1.390E+03	1.510E+02	1.100E+03
	EXT GND	2.030E+02	1.750E+02	4.630E+01	1.840E+01	7.160E+01	3.470E+01	2.590E+01	2.720E+02	2.970E+01	2.170E+02
AM-243	INHAL1	9.430E+08	1.560E+09	3.030E+08	4.210E+08	3.220E+05	3.100E+06	5.400E+07	8.900E+07	1.900E+06	6.000E+06
	INHAL2	2.340E+09	3.870E+09	3.100E+07	1.040E+09	1.500E+05	7.700E+06	1.340E+08	1.990E+08	4.800E+06	1.500E+07
	INGEST	1.900E+07	3.200E+07	9.640E+02	8.500E+06	1.490E+05	6.340E+04	1.100E+05	1.600E+06	4.070E+04	1.200E+05
	EXT AIR	2.170E+06	2.010E+06	1.060E+06	9.140E+05	6.490E+05	1.330E+06	8.970E+05	1.290E+06	6.760E+05	1.410E+06
	EXT GND	5.290E+04	4.880E+04	2.630E+04	2.260E+04	1.610E+04	3.260E+04	2.210E+04	3.150E+04	1.650E+04	3.480E+04

population intake of fish ( $3.3E-7$  kg per person/l). The EPA estimate of  $3.3E-7$  kg per person/l is the same as assuming a 1 kg/yr fish intake. Therefore, for the EPA/SANDIA calculations a 1 kg/yr consumption of fish and the same population used for the drinking water calculations ( $6.3E6$  persons) were assumed.

The population for the land-based ingestion intakes was calculated by multiplying the density (persons/ $m^2$ ) provided by EPA for the three subpathways by the area considered in the hypothetical reference site analysis ( $160 km^2$ ) (Cranwell, et al., 1982). The populations used in these subpathway calculations were

CROP

$$160 km^2 * 1.0E-3 \frac{\text{person}}{m^2} = 1.6E5 \text{ persons}$$

MILK

$$160 km^2 * 1.5E-3 \frac{\text{person}}{m^2} = 2.4E5 \text{ persons}$$

BEEF

$$160 km^2 * 2.1E-4 \frac{\text{person}}{m^2} = 3.4E4 \text{ persons}$$

### 2.1.3 Quantity Intake of Radionuclides

The quantity intake of a radionuclide is dependent upon the concentration of the radionuclide in the food source and the rate of intake or consumption. The EPA/SANDIA calculations utilized the equations for each subpathway available in the Pathways Model and substituted the appropriate EPA parameter values. In some cases, the modeling approaches differed between EPA and the Pathways Model, and in these cases, the input parameters were selected from those used in the reference site analysis (Cranwell, et al., 1982). The EPA point values used in the analysis are given with each equation and are summarized in Tables 2.5 and 2.6. The radionuclide dependent concentration ratios were taken from a computer output provided by J. M. Smith, EPA, and are given in Table 2.7 (recently published in Smith, et al., 1982). The equations for the various ingestion subpathways are defined in Sections 2.1.3.1 to 2.1.3.5.

Table 2.5

Ingestion, Inhalation and External Exposure Rates  
Assumed by EPA

Ingestion Rates

Water Consumption by Humans	6.03E02 l/yr
Plant Consumption by Humans	1.94E02 kg/yr
Milk Consumption by Humans	1.12E02 l/yr
Beef Consumption by Humans	8.5E01 kg/yr
Fish Consumption by Humans	1.0E00 kg/yr

Inhalation Rate

Average Air Consumption by Humans	8.40E03m <sup>3</sup> /y
-----------------------------------	--------------------------

Annual External Exposure

Submersion in Air	1/3 year
Groundshine from Soil*	1/3 year

\*An effective depth of 0.15m was assumed for soil by EPA.

Table 2.6  
Crop and Animal Parameters  
Assumed by EPA

<u>Animal Consumption Rates</u>	
Plant Consumption by Dairy Cows	5.0E01 kg/day
Plant Consumption by Beef Cows	5.0E01 kg/day
<u>Sprinkler Irrigation for Crops</u>	
Irrigation Rate	3.0E02 l/m <sup>2</sup> /y*
Retention Fraction	2.5E-01*
Standing Crop	7.16E-01 kg/m <sup>2</sup>
Rate Constant for Weathering ( $\lambda_w$ )	1.8E01y <sup>-1</sup> (13.75 day half-life)
Irrigation Time ( $\tau$ )	1.7E-1 y
$e^{-\lambda_w\tau}$	4.65E-2
<u>Sprinkler Irrigation for Pasture</u>	
Irrigation Rate	3.0E02 l/m <sup>2</sup> /y*
Retention Fraction	2.5E-01*
Standing Crop	2.8E-01 kg/m <sup>2</sup>
Rate Constant for Weathering ( $\lambda_w$ )	1.8E01 y <sup>-1</sup> (13.75 day half-life)
Irrigation Time ( $\tau$ )	1.7E-1 y
$e^{-\lambda_w\tau}$	4.65E-2

\*These parameters were not defined in the EPA Analysis; therefore the values used in reference site analysis to demonstrate the SNL Risk Assessment Methodology were substituted for the calculation.

Table 2.7

## Concentration Ratios Assumed by EPA

	FISH/WATER (Ci/kg per Ci/l)	CROP/SOIL (dimensionless)	PASTURE (FEED)/SOIL (dimensionless)	MILK/FEED (day • kg) (kg • l)	BEEF/FEED (day • kg) (kg • kg)
Am241	2.5E1	0.11E-2	0.74E-2	0.36E-4	0.16E-5
Am243	2.5E1	0.22E-3	0.15E-2	0.36E-4	0.16E-5
CS135	4.0E2	0.10E-5	0.17E-4	0.56E-2	0.14E-1
CS137	4.0E2	0.85E-2	0.14E0	0.56E-2	0.14E-1
I129	1.5E1	0.19E-7	0.68E-7	0.99E-2	0.70E-2
NP237	1.0E1	0.16E-7	0.65E-7	0.50E-5	0.20E-3
Pu239	3.5E2	0.59E-4	0.36E-3	0.53E-7	0.19E-7
Pu240	3.5E2	0.19E-3	0.12E-2	0.53E-7	0.19E-7
Pu242	3.5E2	0.40E-5	0.24E-4	0.45E-7	0.41E-6
SR90	5.0E0	0.21E0	0.86E0	0.24E-2	0.30E-3
TC99	1.5E1	0.14E-5	0.28E-3	0.99E-2	0.87E-2
SN126	3.0E3	0.77E-5	0.31E-4	0.12E-2	0.80E-1

2.1.3.1 Drinking Water

$$\text{amt of nuclide intake per year} = \left( \begin{array}{c} \text{nuclide conc} \\ \text{in surface water} \end{array} \right) * \left( \begin{array}{c} \text{rate of water} \\ \text{ingestion} \end{array} \right)$$

$$C_i/y = (C_i/l) * (603l/y)$$

2.1.3.2 Fish

$$\text{amt of nuclide intake per year} = \left( \begin{array}{c} \text{nuclide conc in} \\ \text{surface water} \end{array} \right) * \left( \begin{array}{c} \text{conc} \\ \text{ratio} \end{array} \right) * \left( \begin{array}{c} \text{rate of fish} \\ \text{ingestion} \end{array} \right)$$

$$C_i/y = (C_i/l) * (l/kg) * (1.0 \text{ kg/y})$$

where

$$\text{conc ratio} = \frac{\text{conc of nuclide in fish}}{\text{conc of nuclide in water}}$$

2.1.3.3 Crops

$$\text{amt of nuclide intake per year} = \left( \begin{array}{c} \text{nuclide conc} \\ \text{in crops} \end{array} \right) * \left( \begin{array}{c} \text{rate of crop} \\ \text{ingestion} \end{array} \right)$$

$$C_i/y = (C_i/kg) * (194 \text{ kg/y})$$

$$\text{nuclide conc in crops} = \left( \begin{array}{c} \text{nuclide conc} \\ \text{in soil} \end{array} \right) * \left( \begin{array}{c} \text{conc} \\ \text{ratio} \end{array} \right) + \left( \begin{array}{c} \text{conc due to} \\ \text{sprinkler irrigation} \end{array} \right)$$

$$C_i/kg = (C_i/kg) * (\text{dimensionless}) + (C_i/kg)$$

where

$$\text{conc ratio} = \frac{\text{conc of nuclide in crops}}{\text{conc of nuclide in soil}}$$

$$\text{nuclide conc due to sprinkler irrigation} = \frac{1}{\text{rate constant for weathering}} \left( \frac{\text{retention fraction} * \text{nuclide conc in surface water} * \text{irrigation rate}}{\text{standing crop}} \right) (1 - e^{-\lambda_{\omega}t})$$

$$C_i/kg = \left( \frac{1}{18.05 \text{ y}^{-1}} \right) \left( \frac{0.25 * (C_i/l) * 300 \text{ l/m}^2/\text{y}}{0.716 \text{ kg/m}^2} \right) (0.9535)$$

2.1.3.4 Milk

$$\text{amt of nuclide intake per year} = \left( \begin{array}{c} \text{nuclide conc} \\ \text{in milk} \end{array} \right) * \left( \begin{array}{c} \text{rate of milk} \\ \text{ingestion} \end{array} \right)$$

$$C_i/y = (C_i/l) * (112l/y)$$

$$\text{nuclide conc in milk} = \left( \begin{array}{l} \text{nuclide conc} \\ \text{in dairy feed} \end{array} \right) * \left( \begin{array}{l} \text{conc} \\ \text{ratio} \end{array} \right) * \left( \begin{array}{l} \text{consumption rate} \\ \text{of contaminated feed} \end{array} \right)$$

$$C_i/l = (C_i/kg) * \left( \frac{\text{day} * \text{kg}}{\text{kg} * \text{l}} \right) * \left( 50 \frac{\text{kg}}{\text{day}} \right)$$

where

$$\text{conc ratio} = \frac{\text{conc of nuclide in milk}}{\text{intake of nuclide per day}}$$

$$\text{nuclide conc in dairy and beef feed} = \left( \begin{array}{l} \text{nuclide conc} \\ \text{in soil} \end{array} \right) * \left( \begin{array}{l} \text{conc} \\ \text{ratio} \end{array} \right) + \left( \begin{array}{l} \text{nuclide} \\ \text{conc due to} \\ \text{sprinkling} \\ \text{pasture} \end{array} \right)$$

$$\frac{C_i}{\text{kg}} = (C_i/kg) * (\text{dimensionless}) + (C_i/kg)$$

where

$$\text{conc ratio} = \frac{\text{conc of nuclide in pasture}}{\text{conc of nuclide in soil}}$$

$$\text{nuclide conc due to sprinkling pasture} = \frac{1}{\text{rate constant for weathering}} \left( \frac{\text{retention fraction} * \text{nuclide conc in surface water} * \text{irrigation rate}}{\text{standing crop}} \right) (1 - e^{-\lambda_{\omega} t})$$

$$C_i/kg = \left( \frac{1}{18.05 \text{ y}^{-1}} \right) \left( \frac{0.25 * (C_i/l) * 300 \text{ l/m}^2/\text{y}}{0.28 \text{ kg/m}^2} \right) (0.9535)$$

#### 2.1.3.5 Beef

$$\text{amt of nuclide intake per year} = \left( \begin{array}{l} \text{nuclide conc} \\ \text{in beef} \end{array} \right) * \left( \begin{array}{l} \text{rate of beef} \\ \text{ingestion} \end{array} \right)$$

$$C_i/y = (C_i/kg) * (85 \text{ kg/y})$$

$$\text{nuclide conc in beef} = \left( \begin{array}{l} \text{nuclide conc} \\ \text{in beef feed} \end{array} \right) * \left( \begin{array}{l} \text{conc} \\ \text{ratio} \end{array} \right) * \left( \begin{array}{l} \text{consumption} \\ \text{rate of} \\ \text{contaminated} \\ \text{feed} \end{array} \right)$$

$$Ci/kg = \left( \frac{Ci}{kg} \right) * \left( \frac{day \cdot kg}{kg \cdot kg} \right) * (50 \text{ kg/day})$$

where

$$\text{conc ratio} = \frac{\text{conc of nuclide in beef}}{\text{intake of nuclide per day}}$$

nuclide conc in beef feed = calculated the same as dairy feed  
(See 2.1.3.4)

## 2.2 Inhalation

The inhalation pathway considers inhaled radionuclides that are resuspended from the soil. The EPA obtained suspended radionuclide concentrations through multiplication of surface radionuclides concentration (expressed in Ci/m<sup>2</sup>) by a resuspension factor of 10<sup>-9</sup>m<sup>-1</sup> (Smith, et al., 1982). In contrast, in this analysis the suspended radionuclide concentration was obtained by multiplying the soil concentration (Ci/kg) by an assumed concentration of suspended material in air of 3.5E-9 kg/m<sup>3</sup>. The latter concentration of suspended material was taken from the listing of various soil types in the CRC Handbook of Environmental Control, Volume 1 (Bond and Straud, 1973).

### 2.2.1 Dose Factors and Health Effects Estimates

The dose conversion factors (rem/Ci) for the inhalation pathway were taken from Table 2.4 and were multiplied by the appropriate health effects estimates for the organs considered. INHAL1 dose factors are for insoluble (Y class) material retained in the lung for long biological half-times, while INHAL2 dose factors are for more soluble (W class) inhaled material and result in more dose to the other body organs. For this comparative calculation, the INHAL2 dose commitment factors were multiplied by the health effects estimators and summed over all organs for each radionuclide considered.

### 2.2.2 Population at Risk

The population at risk for the inhalation pathway was calculated by multiplying the population density (6.7E-5 persons/m<sup>2</sup>) provided by EPA and the area considered in the reference site analysis (160 km<sup>2</sup>). The area dependent population of 1.1E4 persons was used for these calculations.

### 2.2.3 Quantity Intake of Radionuclides

$$\text{amt of nuclide intake per year} = \left( \begin{array}{c} \text{nuclide conc} \\ \text{in soil} \end{array} \right) * \left( \begin{array}{c} \text{conc of} \\ \text{suspended} \\ \text{material} \\ \text{in air} \end{array} \right) * \left( \begin{array}{c} \text{average} \\ \text{breathing} \\ \text{rate} \end{array} \right)$$

$$Ci/y = (Ci/kg) * (3.5E-9 \text{ kg/m}^3) * (8400\text{m}^3/y).$$

### 2.3 External Exposure

EPA considered external exposure from contaminated soil and air in their analysis. The soil concentrations calculated by the Pathways Model (see Table 2.3) were used to estimate the external exposure for this comparison analysis. The approach detailed in Subsection 2.2 for calculating the radionuclide concentration in the air was used to estimate the air concentrations for the air submersion exposure calculations. An assumed exposure time of 1/3 year was multiplied by the soil concentration and the air concentration to estimate the exposure level.

#### 2.3.1 Dose Factors and Health Effects Estimates

The dose conversion factors for the air exposure pathway and for the soil exposure pathway were multiplied by the appropriate health effects estimates (Table 2.4) and were summed over all organs for each radionuclide.

#### 2.3.2 Population at Risk

The population density of ( $6.7E-5$  persons/ $\text{m}^2$ ) provided by EPA was multiplied by the area of  $160 \text{ km}^2$  considered in the reference site analysis. Again, the area dependent population of  $1.1E4$  persons was used for the calculation of air and soil exposure.

#### 2.3.3 Exposure Level

##### 2.3.3.1 Contaminated Soil

$$\text{Exposure Level} = \left( \begin{array}{c} \text{nuclide conc} \\ \text{in soil} \end{array} \right) * \left( \begin{array}{c} \text{soil} \\ \text{density} \end{array} \right) * \left( \begin{array}{c} \text{effective} \\ \text{depth} \end{array} \right) * \left( \begin{array}{c} \text{exposure} \\ \text{time} \end{array} \right)$$

$$\left( \begin{array}{c} Ci \cdot y \\ m^2 \end{array} \right) = \left( \frac{Ci}{kg} \right) * \left( \frac{2.8E3 \text{ kg}}{m^3} \right) * (.15\text{m}) * \left( \frac{1}{3} y \right)$$

### 2.3.3.2 Contaminated Air

$$\text{Exposure Level} = \left( \begin{array}{c} \text{nuclide conc} \\ \text{in soil} \end{array} \right) * \left( \begin{array}{c} \text{conc of} \\ \text{suspended} \\ \text{material} \\ \text{in air} \end{array} \right) * \left( \begin{array}{c} \text{exposure} \\ \text{time} \end{array} \right)$$

$$\left( \frac{\text{Ci} \cdot \text{y}}{\text{m}^3} \right) = \left( \frac{\text{Ci}}{\text{kg}} \right) * \left( \frac{3.5\text{E}-9\text{kg}}{\text{m}^3} \right) * \left( \frac{1}{3} \text{y} \right)$$

### 3.0 Description of the SANDIA Analysis

The SANDIA health effects per curie release values were calculated using the modeling approaches and input parameters presented in the Pathways Model (Helton and Kaestner, 1981) and the Dosimetry and Health Effects Model (Runkle, et al., 1981). The two compartment system of the Pathways Model, described in Chapter 2, was used in this analysis. The input parameters (distribution coefficients (Kd) and variables to vary flow between subzones) to the Pathways Model were assumed to be the point values presented in Table 2.1. The dose conversion factors (70 year intake/70 year dose commitment), concentration ratios, environmental parameters and health effects estimates from the Risk Assessment Methodology (Cranwell, et al., 1982) were used to calculate the SANDIA health effects per curie values. The average individual risk estimates were converted to population risk by multiplying the density values assumed by EPA (in persons/m<sup>2</sup>) and the area considered in the reference site analysis for the land-based pathways. The population estimates for drinking water and fish intake were based on a linear relationship of world population to the river flow rate of the world's rivers and the flow rate of the river considered in the reference site analysis. The equations used in the calculations for the ingestion, inhalation and external exposures are given in Table 3.1. The input parameters that were used in the calculations are given in Tables 3.2-3.8. The dose conversion factors used in the Risk Assessment Methodology consider a 70 year chronic intake and estimate a 70 year dose commitment. The 70 year dose commitment is essentially equivalent to the 50 year dose commitment (considered by EPA), however, the 70 year chronic intake must be adjusted to account for the ~143 generation that can occur in 10,000 years. Therefore, the health effects estimates were divided by a factor of 70 for estimating the health effects per curie release values.

Many of the parameters used in the SANDIA Analysis are different from those presented in the EPA analysis and may be the source of some of the differences between the SANDIA and EPA health effects per curie values. For example, in the

Table 3.1

Basic Equations for Calculating Radionuclide Concentrations for Various Pathways

WATER BASED

- (1) Drinking Water Intake (Ci/yr) = Water Consumption (370 l/yr)  
\* Water Treatment Factor (1.0) \* Water Conc. (Ci/l)
- (2) Fish (kg/yr) = Fish Consumption (6.9 kg/yr)  
\* Water/Fish Conc. Factor (CF)<sup>a</sup> \* Water Conc. (Ci/l)

LAND WITHOUT IRRIGATION

- (3) Plant Conc. (Ci/kg) = Soil/Plant CF<sup>a</sup> \* Soil Conc. (Ci/kg)
- (4) Plant Intake (Ci/yr) = Plant Consumption (190.0 kg/yr)  
\* Plant Conc. (Ci/kg)
- (5) Milk Intake (Ci/yr) = [Dairy Cow Consumption of Plants (50 kg/day) \* Plant Conc. (Ci/kg)  
+ Dairy Cow Drinking Rate Per Day (60.0 l/day)  
\* Water Conc. (Ci/l)] \* Milk/Diet CF<sup>a</sup>  
\* Milk Consumption Rate (110.0 l/yr)
- (6) Meat Intake (Ci/yr) = [Beef Cattle Consumption of Plants (50 kg/day) \* Plant Conc. (Ci/kg)  
+ Beef Cattle Drinking Rate Per Day (500 l/day)  
\* Water Conc. (Ci/l)] \* Beef/Diet CF<sup>a</sup>  
\* Meat Consumption Rate (95.0 kg/yr)

LAND WITH IRRIGATION

- (7) Deposition Rate (Ci/kg-yr) = Retained Fraction on Plant (.25)  
\* Water Conc. (Ci/l)  
\* [Rate Irrigation (300 l/m<sup>2</sup>-yr)/Plant Density (5.2 kg/m<sup>2</sup>)]
- (8) Rate Constant for Weathering (yr<sup>-1</sup>) = ln2/.0384 yr (14 Day Half Life)
- (9) Plant Conc. (Ci/kg) = [Soil/Plant CF<sup>a</sup> \* Soil Conc. (Ci/kg)]  
+ [(Deposition Rate (Ci/kg)/Weathering Rate (yr<sup>-1</sup>)]  
\* {1 - [Exp -ln2/.0384 \* Irrigation Time (.17 yr)]}

Plant, Beef, Milk Consumptions with Irrigation are Calculated Using Formulas 4-6 and the Plant Conc. (9).

<sup>a</sup>See Table 3.2 These concentration factors are radionuclide dependent.

Table 3.1 (Continued)

INHALATION

(10) Air Conc. (Ci/m<sup>3</sup>) = Soil Conc. (Ci/kg)  
\* Concentration of Suspended Material in the Air  
(3.5E-9 kg/m<sup>3</sup>)

(11) Inhalation (Ci/yr) = Air Conc. (Ci/m<sup>3</sup>)

\* Breathing Rate (8000 m<sup>3</sup>/yr)

EXTERNAL

(12) Air Submersion = (6.13E5 hrs (Lifetime Exposure))  
\* Air Conc. (Ci/m<sup>3</sup>)

(13) Soil Exposure = [2.04E5 hrs (1/3 year Exposure for 70 years)

\* Soil Conc. (Ci/kg) \* Soil Density (2.8E3 kg/m<sup>3</sup>)

\* Soil Depth (.025m)]

(14) Sediment Exposure = [1.05E3 hrs (15 hrs/yr for 70 years)

\* Sediment Conc. (Ci/kg) \* Sediment Density (2.6E3kg/m<sup>3</sup>)

\* Sediment Depth (.025m)]

(15) Water Immersion = (1.06E3 hrs (15 hrs/yr for 70 years)

\* Water Conc. (Ci/l) \* 1000 l/m<sup>3</sup>)

Table 3.2  
 Concentration Ratios for Human and Animal Food Sources  
 (Used in Reference Site Analysis)

<u>Radionuclide</u>	<u>FISH/WATER</u> (Ci/kg per Ci/l)	<u>CROP/SOIL</u> <u>PASTURE/SOIL</u> (dimensionless)	<u>MILK/FEED</u> (day • kg/kg • l)	<u>BEEF/FEED</u> (day • kg/kg • kg)
AM	2.5E01	2.5E-04	5.0E-06	2.0E-04
CS	2.0E03	1.0E-02	1.2E-02	4.0E-03
I	1.5E01	2.0E-02	6.0E-03	2.9E-03
NP	1.0E01	2.5E-03	5.0E-06	2.0E-04
Pu	3.5E00	2.5E-04	2.0E-06	1.4E-05
SR	3.0E01	1.7E-02	8.0E-04	6.0E-04
TC	1.5E01	2.5E-01	2.5E-02	4.0E-01
SN	3.0E03	2.5E-03	2.5E-03	8.0E-02

\*Taken from USNRC (1977)

Table 3.3

Ingestion, Inhalation and External Exposure Rates  
for an Average Individual  
(Used in Sandia Reference Site Analysis)

Ingestion Rates

Water Consumption by Humans	3.7 EO2 l/yr
Plant Consumption by Humans	1.9 EO2 kg/yr
Milk Consumption by Humans	1.1 EO2 l/yr
Beef Consumption by Humans	9.5 EO1 kg/yr
Fish Consumption by Humans	6.9 EO0 kg/yr

Inhalation Rate

Average Air Consumption by Humans	8.0 EO3 m <sup>3</sup> /yr
-----------------------------------	----------------------------

External Exposure Rates

Submersion in Air	8.7 EO3 hr/yr
Groundshine from Soil	2.9 EO3 hr/yr*

---

\*An effective depth of 0.025 m was assumed for soil and sediment.

Table 3.4

Crop and Animal Parameters  
(Used in Sandia Reference Site Analysis)

<u>Animal Consumption Rates</u>	
Plant Consumption by Dairy Cows	5.0E01 kg/day
Water Consumption by Dairy Cows	6.0E01 l/day
Plant Consumption by Beef Cows	5.0E01 kg/day
Water Consumption by Beef Cows	5.0E01 l/day
<u>Sprinkler Irrigation of Crops and Pasture</u>	
Irrigation Rate	3.0E02 l/m <sup>2</sup>
Retention Fraction	2.5E-01
Standing Crop (Plant Density)	5.2E00 kg/m <sup>2</sup>
Constant Rate of Weathering ( $\lambda_w$ )	1.8E01 yr <sup>-1</sup> (14 day half life)
Irrigation Time ( $\tau$ )	1.7E-01 yr
$e^{-\lambda_w \tau}$	4.65E-02

Table 3.5

Dose Conversion Factors - Ingestion  
(rem/Ci)

(70-year intake/70-year dose commitment)

	<u>TOTAL BODY</u>	<u>BONE</u>	<u>LUNG</u>	<u>GI TRACT</u>
SR90	1.01E8	4.07E8	0.0	1.53E7
TC99	3.51E3	8.76E3	1.11E3	2.89E4
SN126	1.68E5	5.88E6	0.0	1.70E6
I129	6.41E5	2.29E5	0.0	3.11E4
CS135	5.55E5	1.35E6	1.42E5	2.95E4
CS137	4.96E6	5.53E6	8.51E5	1.48E5
NP237	2.77E6	6.80E7	0.0	5.56E6
Pu239	9.51E5	3.91E7	0.0	4.66E6
Pu240	9.50E5	3.91E7	0.0	4.75E6
Pu242	9.16E5	3.63E7	0.0	4.57E6
AM241	2.75E6	4.08E7	0.0	5.19E6
AM243	2.68E6	4.07E7	0.0	6.09E6

---

Taken from Runkle, et al., 1981.

Table 3.6

Dose Conversion Factors - Inhalation  
(rem/Ci)

(70-year intake/70-year dose commitment)

	<u>TOTAL BODY</u>	<u>BONE</u>	<u>LUNG</u>	<u>GI TRACT</u>
SR90	1.35E8	2.17E9	8.67E7	6.31E6
TC99	3.51E3	8.76E3	7.32E6	5.28E5
SN126	9.39E5	2.35E7	8.47E7	1.11E6
I129	4.80E5	1.73E5	0.0	1.55E4
CS135	4.17E5	1.01E6	5.91E6	1.48E4
CS137	3.72E6	4.15E6	3.55E7	7.35E4
NP237	6.93E9	1.66E11	3.78E9	3.44E6
Pu239	7.93E9	3.26E11	1.22E10	2.89E6
Pu240	7.91E9	3.26E11	1.22E10	2.95E6
Pu242	7.63E9	3.02E11	1.18E10	2.83E6
AM241	6.86E9	1.03E11	4.39E9	3.22E6
AM243	6.70E9	1.03E11	4.16E9	3.78E6

---

Taken from Runkle, et al., 1981.

Table 3.7

## Dose Conversion Factors - External

	TOTAL BODY	
	SOIL (rem/hr/Ci/m <sup>2</sup> )	AIR (rem/hr/Ci/m <sup>3</sup> )
SR90	0.0	2.40E-1
TC99	0.0	5.80E-2
SN126	9.00E0	1.32E4
I129	4.50E-1	1.80E1
CS135	0.0	2.80E-2
CS137	4.20E0	4.70E2
NP237	1.40E0	1.45E2
Pu239	7.90E-4	5.60E-2
Pu240	1.30E-3	6.50E-2
Pu242	1.10E-3	5.10E-2
AM241	1.80E-1	1.80E-1
AM243	1.30E0	1.40E2

---

Taken from Runkle, et al., 1981.

Table 3.8

Cancer Risk Estimates Used in the SANDIA Analysis

<u>Type of Cancer</u>	<u>Individual Risk per rem*</u>	<u>Organ Dose Commitment Associated With This Cancer Type</u>
Leukemia	2.9E-05	Bone
Lung	2.5E-05	Lung
GI Tract	1.9E-05	GI Tract
Breast	2.9E-05	Total Body
Bone	9.8E-06	Bone
All Other	3.6E-05	Total Body

---

\*Based on a lifetime plateau period for the solid tumor cancers.

---

Taken from Runkle et al., 1981.

ingestion calculations for land-based food sources, the contributions from crop irrigation were taken into account in the SANDIA Analysis. Also, the intake of contaminated drinking water by the animals that provide milk and beef was considered. In contrast, the EPA considered only the intake of contaminated forage by the milk and beef producing animals.

#### 4.0 Description of SAMPLED SANDIA Analysis

This set of calculations was performed to consider some of the uncertainty that results from variability in the input parameters. However, only a few of the parameters were varied and the uncertainties in many other aspects of the modeling effort were not addressed. In this analysis, the Pathways Model utilized a set of sampled input parameters selected by the Latin Hypercube sampling technique (Iman, et al., 1980). The distribution coefficients ( $K_d$ ) and variables to adjust the flow rates between various subzones were sampled and the range, description and assigned distribution of each input parameter are defined in Table 4.1. The results of the analysis represent a  $3\sigma$  variation in the input data for those variables with a log-normal or normal distribution assigned to their ranges. Those variables with a uniform or log-uniform distribution assigned were sampled over the entire range. Variables 1 to 4, that adjust the flow rates, are further described in Table 4.2. Fifteen runs of the computer code were made, each with a different sampled set of input variables. The output of each computer run (in the form of radionuclide concentration in the soil and surface water) was processed by the Dosimetry and Health Effects Computer Code, and health effects (cancer deaths) per curie release were calculated. The concentration ratios, dose conversion factors and risk estimates used in this analysis are described in Chapter 3.

The population for the water based pathways was based on the linear relationship between river flow rate and population described above. To estimate the population at risk for this calculation, the flow rate of the river was varied by the sampled variable ( $R_1$ ) and the population was adjusted for each of the fifteen computer runs. The population for the land based and external pathways was based on the density defined by EPA and the area of the reference site of  $160 \text{ km}^2$ . These populations, which are area dependent, were kept constant for the fifteen computer runs for land based and external pathways.

As discussed in Chapter 3, the health effects per curie release were divided by 70 to account for the ~ 143 generations that can occur in a 10,000 year period.

Two types of calculations were performed depending on whether or not adsorption was allowed to influence the solid phase (particulates) of the surface water. For the first set

Table 4.1  
Latin Hypercube Sample

TITLE-LHS PATH EPA

RANDOM SEED = 5114652675042517

NUMBER OF VARIABLES = 12 SAMPLE SIZE = 15

DISTRIBUTION AND RANGE ASSUMED FOR EACH VARIABLE

Variable	Distribution Assumed	Range	
1	Uniform	.250 to 2.00	Scale Factor Rivr Dischrg
2	Log Uniform	1.000E-02 to 1.00	Scale Factor Water Xchng
3	Log Uniform	1.000E-04 to 1.000E-02	Scale Factor Solid Xchng
4	Uniform	3.00 to 15.0	Regional Erosion Rate
5	Log Normal	1.000E-02 to 2.500E+05	KD for CM(AM)
6	Log Normal	1.000E-02 to 1.000E+04	KD for Pu
7	Log Normal	1.000E-02 to 50.0	KD for NP
8	Log Normal	1.000E-02 to 1.000E+03	KD for TC
9	Log Normal	1.000E-02 to 3.000E+03	KD for SR
10	Log Normal	1.000E-02 to 1.000E+04	KD for CS
11	Log Normal	1.000E-02 to 1.000E+03	KD for I
12	Log Normal	1.000E-02 to 1.000E+03	KD for SN

Table 4.2

Variables Which Affect the Physical Description  
of the Surface Environment

- 
- R<sub>1</sub>: scale factor used to introduce variation in hydrologic properties. New values for water flow from the soil compartment to the ground-water compartment are obtained by multiplication with this factor. As the reference site was defined with an annual rainfall of 1 m, use of R<sub>1</sub> amounts, in a crude way, to varying the rainfall from .25 m to 2 m. This is only approximate, as the indicated rates do not move in a strictly linear manner with rainfall; however, it is felt that this provides a way of varying between wet and dry conditions. (Units: Unitless; Range: .25, 2.; Sampling Dist.: Uniform.)
- 
- R<sub>2</sub>: scale factor used to introduce variation in water movement between the soil compartment and the surface water compartment. New values for such movements are obtained by multiplication of the pore volume of the soil compartment by R<sub>2</sub>. This variable is introduced to allow for variation in water movements which might result from runoff, irrigation or overbank flooding. (Units: yr<sup>-1</sup>; Range: 10<sup>-2</sup>, 10<sup>0</sup>; Sampling Dist.: Log Uniform.)
- 
- R<sub>3</sub>: scale factor used to introduce variation in solid movement between the soil compartment and the surface water compartment. New values for such movements are obtained by multiplication of the mass of solids contained in a soil compartment by R<sub>3</sub>. This variable is introduced to allow for variation in solid movements which might result from runoff, irrigation or overbank flooding. (Units: yr<sup>-1</sup>; Range: 10<sup>-4</sup>, 10<sup>-2</sup>; Sampling Dist.: Log Uniform.)
- 
- R<sub>4</sub>: regional erosion rate. (Units: cm/1000 yr; Range: 3., 15.; Sampling Dist.: Uniform.)
-

of calculations, the radionuclides were input into the surface water with no adsorption onto the solid phase (particulates) of the water (i.e.,  $K_d = 0$  for all radionuclides in the water). However, the  $K_d$  influence in the soil compartment was considered. This technique is similar to the procedures used by EPA in their analysis and in the EPA/SANDIA and SANDIA calculations.

When flooding of a river occurs, the particulates suspended in the surface water may carry the adsorbed radionuclides onto the surrounding land mass. If adsorption of radionuclides onto solid phase of the surface water is ignored, there is a much smaller quantity of a radionuclide carried to the soil compartment by the surface water. In the second set of calculations, the radionuclides were allowed to adsorb onto the solid phase of the surface water as well as the liquid phase. The exchange to the soil compartment was influenced by the particulates suspended in the water, and the distribution coefficients ( $K_d$ ) determined the partition of a radionuclide between the solid and liquid phases. The results of this analysis may simulate exchange that could occur with flooding and erosion or with irrigation and erosion.

## 5.0 Results and Discussion

The health effects per curie release for the individual pathways are given in Table 5.1. The EPA values were taken from the Health Effects per Curie Release Model and Subpathway Table provided to the author by the EPA. A slightly revised version of this table was published in Smith, et al., 1982. These values represent the health effects (deaths) per curie release. The EPA/SANDIA values were calculated using the procedures outlined in Chapter 2. This procedure utilized the Pathways Model and point  $K_d$  values provided by EPA to calculate the radionuclide concentrations in the soil and surface water. Other parameters (e.g., dose conversion factors, health effects estimates, etc.) from EPA were also used. The SANDIA values were calculated with Pathways Model and Dosimetry and Health Effects Model using the 70-year intake/ 70-year dose commitment factors, environmental parameters and risk estimates used in the reference site analysis. However, the same point  $K_d$  values from EPA (and used in the EPA/SANDIA calculations) were used in the analysis.

There is good agreement between the EPA and the EPA/SANDIA results for the drinking water and the fish pathways for most of the radionuclides. Marked differences are noted for the crop, milk and meat subpathways. EPA assumed that 0.5 curies were released to the soil over the 10,000-year interval and further assumed that 50% of the contaminated land was used for crop production for direct human consumption, 25% for milk

Table 5.1

Individual Pathways and Dosimetry and Health Effects Comparison Table  
Expressed as Deaths Per Curie

		<u>Drinking Water</u>	<u>Fish</u>	<u>Crop</u>	<u>Milk</u>	<u>Meat</u>	<u>Inhala- tion</u>	<u>External Soil</u>	<u>External Air</u>
Am241	EPA	1.29E-1	3.7E-3	5.5E-1	8.2E-4	2.7E-6	2.2E-5	1.4E-5	2.9E-13
	EPA/Sandia	1.32E-1	5.45E-3	6.18E-3	2.62E-5	1.24E-7	3.03E-7	2.72E-5	4.34E-15
	Sandia	3.23E-3	1.51E-3	3.42E-5	1.84E-8	8.00E-8	2.27E-7	6.84E-7	1.02E-14
Am243	EPA	3.4E-1	1.2E-2	2.1E0	3.2E-3	1.5E-5	5.7E-5	7.3E-5	3.0E-12
	EPA/Sandia	1.06E-1	4.4E-3	5.03E-3	2.17E-5	1.03E-7	4.74E-6	7.01E-4	2.43E-13
	Sandia	3.25E-3	1.52E-3	4.62E-5	2.10E-8	9.28E-8	1.40E-6	3.08E-5	4.97E-13
Cs135	EPA	2.6E-4	1.7E-4	2.1E-3	9.9E-4	2.6E-4	2.4E-10	0	0
	EPA/Sandia	1.83E-4	1.21E-4	8.24E-6	5.11E-6	1.3E-6	3.01E-12	0.0	0.0
	Sandia	1.62E-4	6.02E-3	5.79E-6	4.33E-6	1.66E-7	1.01E-11	0.0	1.49E-17
Cs137	EPA	2.1E-3	1.3E-3	7.8E-3	2.1E-3	5.5E-4	1.9E-9	1.5E-4	8.4E-12
	EPA/Sandia	2.0E-3	1.33E-3	9.25E-5	6.42E-5	1.71E-5	1.71E-12	1.6E-5	7.53E-15
	Sandia	9.79E-4	3.65E-2	1.15E-5	1.40E-5	5.09E-7	4.42E-12	1.09E-6	1.82E-14
I129	EPA	1.6E-3	4.0E-5	6.4E-3	2.4E-3	1.8E-4	1.5E-9	1.1E-5	1.8E-13
	EPA/Sandia	1.63E-3	4.04E-5	7.32E-5	8.02E-5	6.03E-6	1.64E-14	1.48E-8	2.05E-18
	Sandia	8.95E-5	2.50E-5	8.89E-7	5.95E-7	3.12E-8	1.63E-15	1.45E-9	8.70E-18
Np237	EPA	1.3E-1	2.2E-3	4.6E-1	9.2E-5	3.9E-4	2.2E-5	1.0E-4	4.7E-12
	EPA/Sandia	1.3E-1	2.15E-3	5.84E-3	3.23E-6	1.38E-5	1.87E-8	3.76E-8	2.03E-8
	Sandia	5.08E-3	9.48E-4	5.28E-5	2.86E-8	1.25E-7	2.47E-8	3.77E-7	5.85E-15
Pu239	EPA	4.3E-3	2.5E-3	2.5E-2	5.4E-8	2.1E-9	3.1E-2	1.9E-7	1.0E-15
	EPA/Sandia	4.31E-3	2.5E-3	1.97E-4	1.19E-9	4.52E-11	2.37E-6	2.47E-6	1.09E-16
	Sandia	2.90E-3	1.89E-4	4.50E-5	7.83E-9	6.07E-9	5.42E-6	2.43E-8	2.58E-16
Pu240	EPA	4.3E-3	2.5E-3	2.4E-2	5.2E-8	2.0E-9	2.2E-5	3.8E-7	2.0E-15
	EPA/Sandia	3.31E-3	1.92E-3	1.55E-4	9.67E-10	3.70E-11	1.71E-6	3.48E-6	1.48E-16
	Sandia	2.90E-3	1.89E-4	4.03E-5	7.42E-9	5.73E-9	3.89E-6	2.87E-8	2.15E-16
Pu242	EPA	4.1E-3	2.4E-3	2.4E-2	4.4E-8	4.3E-8	2.1E-5	3.5E-7	1.8E-15
	EPA/Sandia	4.10E-3	2.38E-3	1.85E-4	9.22E-10	8.92E-10	2.58E-6	5.17E-6	2.18E-16
	Sandia	2.70E-3	1.76E-4	4.41E-5	7.48E-9	5.81E-9	5.76E-6	3.87E-8	2.69E-16
Sr90	EPA	8.0E-3	6.0E-5	1.0E-1	7.8E-3	1.0E-4	2.6E-8	0	0
	EPA/Sandia	7.99E-3	6.63E-5	4.78E-4	1.46E-4	1.95E-6	1.42E-11	0.0	0.0
	Sandia	3.94E-2	2.20E-2	4.65E-4	3.74E-5	3.07E-6	1.92E-10	0.0	5.53E-18
Tc99	EPA	2.4E-5	6.0E-7	1.9E-4	6.3E-5	5.8E-6	6.2E-10	0	0
	EPA/Sandia	2.39E-5	5.95E-7	1.08E-6	1.18E-6	1.10E-7	6.96E-15	0.0	0.0
	Sandia	2.02E-6	5.64E-7	2.11E-8	5.70E-8	9.93E-8	8.30E-15	0.0	2.80E-20
Sn126	EPA	1.4E-3	7.0E-3	6.7E-3	2.9E-4	2.1E-3	1.7E-8	4.6E-4	2.6E-11
	EPA/Sandia	1.38E-3	6.83E-3	6.19E-5	8.22E-6	5.82E-5	2.62E-10	8.54E-4	3.91E-13
	Sandia	4.72E-4	2.64E-2	8.49E-6	1.72E-6	6.14E-6	1.82E-10	3.98E-5	8.74E-12

production and 25% for beef production. The soil concentrations calculated by the Pathways Model used an asymptotic solution, dependent upon the flow rates between the soil and surface water subzones, and were based on a different input rate than the EPA analysis. The calculations performed by the Pathways Model resulted in an input of  $2.3E-3$  Ci to the soil over the 10,000 year period. Another contributor to the difference between the EPA and EPA/ SANDIA values is the different rate of input to the plants via sprinkler irrigation. For the calculations presented in this report, the input to plants by irrigation was  $2.5E-7$  Ci/yr, while EPA assumed a value of  $5.0E-5$  Ci/yr. This difference of greater than two orders of magnitude in the input rate is reflected in the results.

Generally, the SANDIA health effects per curie values are smaller than the EPA values for most of the paths and this difference appears to be due to differences in the input rates, concentration factors, dose conversion factors and exposure times used in the calculations. Again, the land based pathways are affected by differences in the input rates.

When the health effects per curie values from EPA and SANDIA are summed over subpathways 1-5 (includes drinking water, fish, crop, milk and meat) and 6-8 (includes inhalation, external soil and external air) the SANDIA values are lower in all cases (Table 5.2). Some values differ by factors of greater than  $10^2$ ; however, pathways 1-5 do not show as much variation as pathways 6-8. The risk of adverse health effects from pathways 6-8 is lower than the risk from pathways 1-5; therefore, the difference noted in pathways 6-8 is less significant. We have not attempted to account for all the differences; but the input rates, dose factors, and concentration ratios used in the two analyses appear to account for the major differences.

The results of the SANDIA SAMPLED calculations (described in Chapter 4) are presented graphically in Figures 5.1 to 5.4. The  $K_d$  ranges and the  $R_1$  to  $R_4$  variables were sampled using the Latin Hypercube Sampling technique for this analysis. The populations for the various subpathways, defined in Sections 2.1.2; 2.2.2; and 2.3.2, were used in this analysis. The population for the drinking water and fish intakes were adjusted by the sampled variable,  $R_1$ , to account for changes in the river flow. The population for land based pathways was held constant for all 15 calculations.

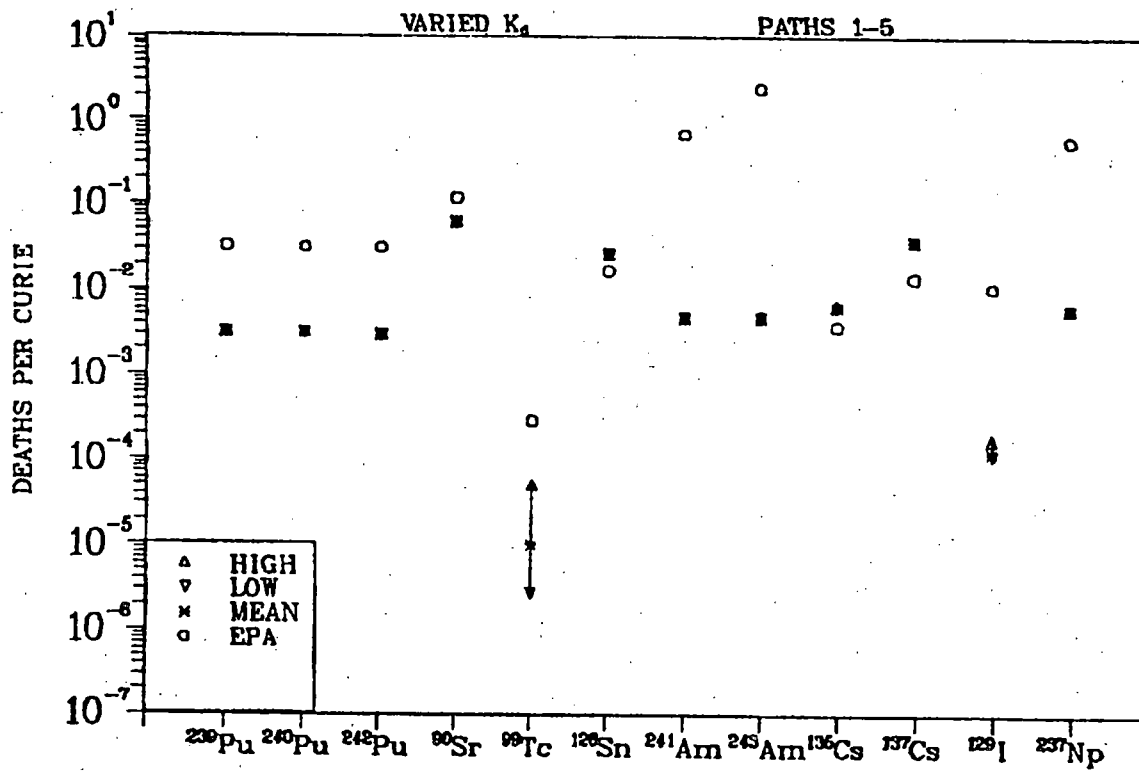
In Figures 5.1 and 5.2 the results are given for the case when there was no adsorption of the radionuclide onto the solid phase of the surface water. The subpathways 1 to 5 (Figure 5.1) and 6 to 8 (Figure 5.2) were summed and the mean, maximum and minimum values of the fifteen computer runs are presented

Table 5.2

Pathway and Dosimetry and Health Effects  
Comparison Table

Health Effects Per Curie

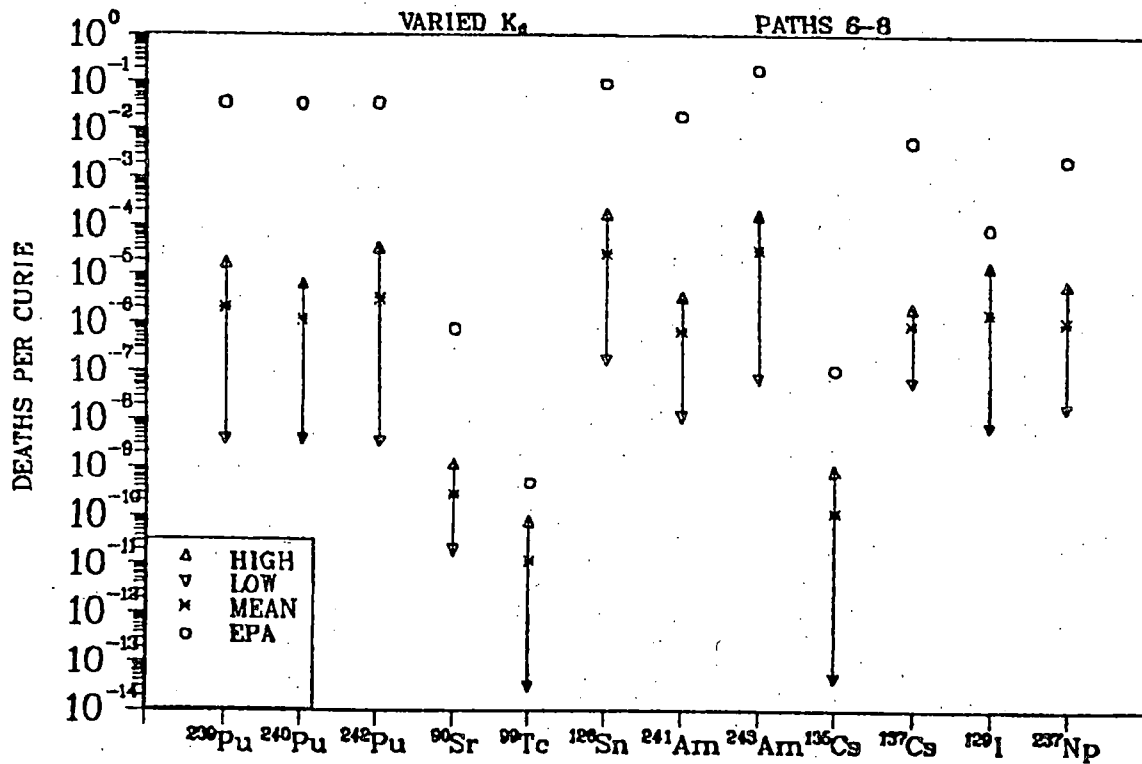
<u>Radionuclide</u>		<u>EPA Pathways 1-5</u>	<u>EPA Pathways 6-8</u>
Am241	EPA	7.0E-1	2.0E-2
	Sandia	4.8E-3	9.1E-7
Am243	EPA	2.5E00	2.0E-1
	Sandia	4.8E-3	3.2E-5
Cs135	EPA	3.8E-3	1.1E-7
	Sandia	6.2E-3	1.0E-11
Cs137	EPA	1.4E-2	6.0E-3
	Sandia	3.8E-2	1.1E-6
I129	EPA	1.1E-2	9.2E-5
	Sandia	1.2E-4	1.5E-9
Np237	EPA	5.9E-1	2.5E-3
	Sandia	6.1E-3	4.0E-7
Pu239	EPA	3.2E-2	3.7E-2
	Sandia	3.1E-3	5.4E-6
Pu240	EPA	3.1E-2	3.5E-2
	Sandia	3.1E-3	3.9E-6
Pu242	EPA	3.1E-2	3.7E-2
	Sandia	2.9E-3	5.8E-6
Sr90	EPA	1.2E-1	7.9E-7
	Sandia	6.2E-2	1.9E-10
Tc99	EPA	2.9E-4	4.9E-10
	Sandia	2.8E-6	8.3E-15
Sn126	EPA	1.7E-2	1.0E-1
	Sandia	2.7E-2	4.0E-5



- (1) VARIED  $K_d$  RANGES (LATIN HYPERCUBE SAMPLE)
- (2) INPUT OF RADIONUCLIDE TO LIQUID PHASE OF SURFACE WATER.

Figure 5.1.

Deaths per curie calculated with sampled  $K_d$  ranges and no adsorption onto solid phase of the surface water for Pathways 1-5.



(1) VARIED  $K_d$  RANGES (LATIN HYPERCUBE SAMPLE)

(2) INPUT OF RADIONUCLIDE TO LIQUID PHASE OF SURFACE WATER.

Figure 5.2.

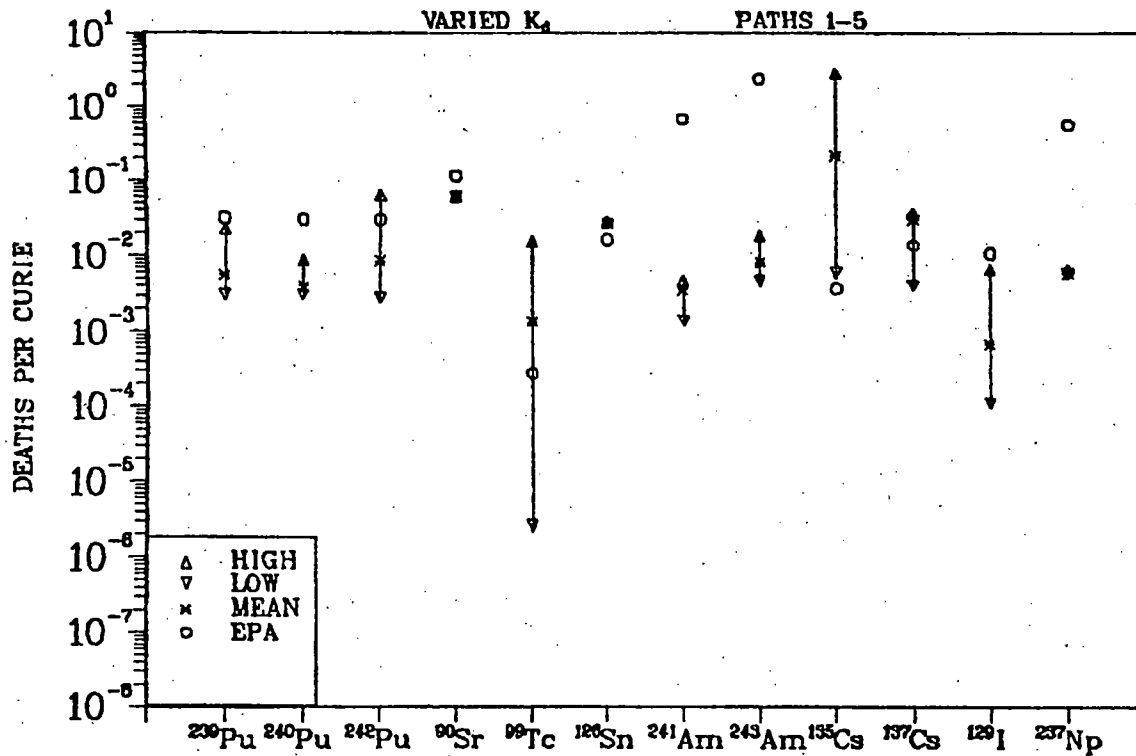
Deaths per curie calculated with sampled  $K_d$  ranges and no adsorption onto solid phase of the surface water for Pathways 6-8.

along with the point values from EPA. In general, the EPA values for pathways 1-5 are higher than the results calculated with the sampled values. The exceptions are  $^{126}\text{Sn}$ ,  $^{135}\text{Cs}$  and  $^{137}\text{Cs}$ . The sum of pathways 1-5 is dominated by the water based pathways and, since the populations are adjusted by the sampled variable R1, the results are clustered. If a constant population were assumed for the calculation and the flow rate were varied, the results would vary in an approximately linear fashion. That is, a one order of magnitude variation in the flow rate would result in a one order variation in the response. In pathways 6-8, there is more variability than in Paths 1-5; however the EPA values are always higher than the deaths per curie values calculated by the sampled values.

In Figures 5.3 and 5.4 the results are presented for the case when adsorption of the radionuclide onto the solid phase was assumed. The partitioning was determined by the distribution coefficients (Kd). This approach significantly affects the soil concentration and the resulting risk to the human population. For the analysis that considers adsorption, the EPA values for both the 1-5 and 6-8 pathways are generally within the range or only slightly higher than the results using the sampled ranges, for most radionuclides.

Of note are the EPA values for  $^{241}\text{Am}$ ,  $^{243}\text{Am}$  and  $^{237}\text{Np}$  for pathways 1-5 (Figure 5.3). The results of this analysis for  $^{241}\text{Am}$  and  $^{243}\text{Am}$  indicate that the release limits for these radionuclides may be overly conservative and may warrant a reexamination by the EPA. Also, the EPA release limit for  $^{135}\text{Cs}$  would appear not to be restrictive enough from the results of this analysis and again may warrant some reconsideration.

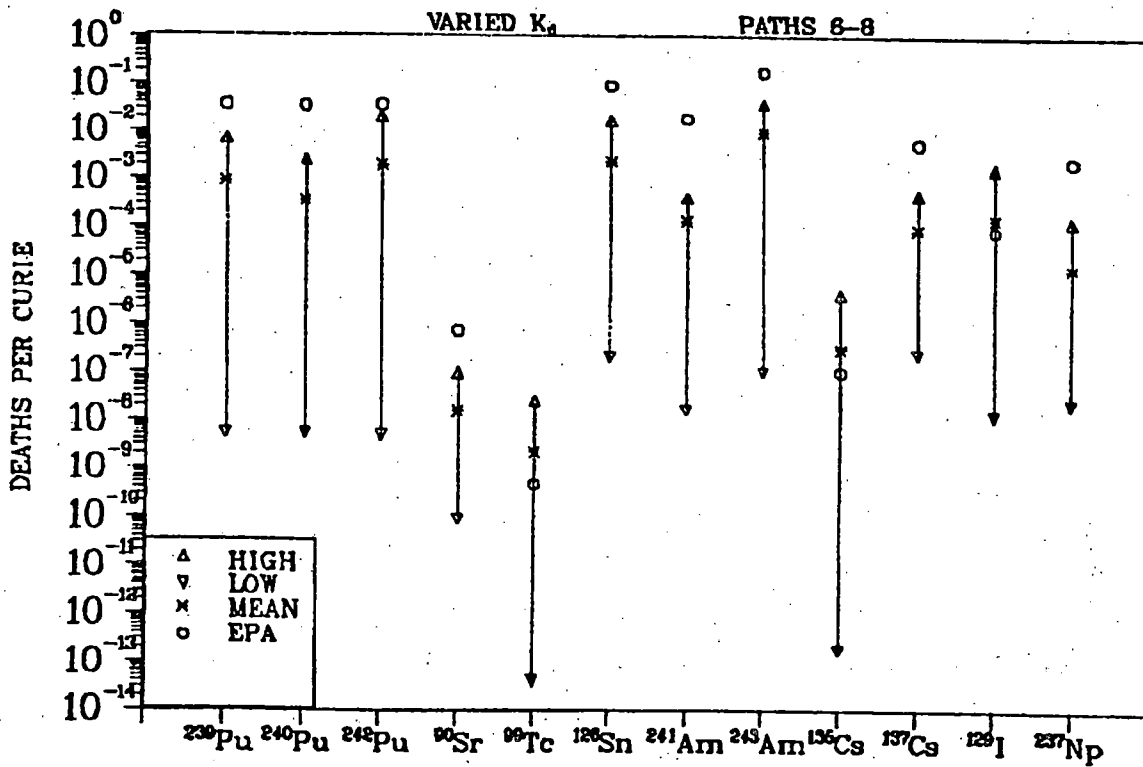
Although these results certainly do not establish that the EPA release limits proposed in the Standard are overly conservative, generally they do suggest that the allowed release limits might be higher if the health effects per curie calculated in this analysis were used.



- (1) VARIED  $K_d$  RANGES (LATIN HYPERCUBE SAMPLE)
- (2) INPUT OF RADIONUCLIDE TO LIQUID AND SOLID PHASE OF SURFACE WATER.

Figure 5.3.

Deaths per curie calculated with sampled  $K_d$  ranges and adsorption onto solid phase of the surface water for Pathways 1-5.



- (1) VARIED  $K_d$  RANGES (LATIN HYPERCUBE SAMPLE)
- (2) INPUT OF RADIONUCLIDE TO LIQUID AND SOLID PHASE OF SURFACE WATER.

Figure 5.4.

Deaths per curie calculated with sampled  $K_d$  ranges and adsorption onto solid phase of the surface water for Pathways 6-8.

## References

Bond, R. G., and C. P. Stroud (Eds.), CRC Press, Handbook of Environmental Control, Volume 1, 1973.

Cranwell, R. M., J. E. Campbell, J. C. Helton, R. L. Iman, D. E. Longsine, N. R. Ortiz, G. E. Runkle, and M. J. Shortencarier, Sandia National Laboratories, "Risk Methodology for Geologic Disposal of Radioactive Waste: Final Report," SAND81-2573, NUREG/CR-2452, 1982.

Helton, J. C., and P. C. Kaestner, Sandia National Laboratories, "Risk Methodology for Geologic Disposal of Radioactive Waste: User's Manual Pathways Model," SAND78-1711, NUREG/CR-1636, 1981.

Iman, R. L., J. M. Davenport, and D. K. Leigler, Sandia National Laboratories, "Latin Hypercube Sampling Program User's Guide," SAND79-1473, January 1980.

Runkle, G. E., R. M. Cranwell, and J. D. Johnson, Sandia National Laboratories, "Risk Methodology for Geologic Disposal of Radioactive Waste: Dosimetry and Health Effects," SAND80-1372, NUREG/CR-2166, 1981.

Smith, J. M., T. W. Fowler, and A. S. Goldin, U.S. Environmental Protection Agency, Montgomery, Alabama, "Draft -- Environmental Pathway Models for Estimating Population Health Effects From Disposal of High-Level Radioactive Waste in Geologic Repositories," EPA 520/5-80-002, July 1981.

Smith, J. M., T. W. Fowler and A. S. Goldin, U.S. Environmental Protection Agency, Montgomery, Alabama, "Environmental Pathways Model for Estimating Population Health Effects from Disposal of High-Level Radioactive Waste in Geologic Repositories," EPA 520/5-80-002, December 1982).

U.S. DOE (U.S. Department of Energy), Office of Nuclear Waste Management, Washington, DC, "Environmental Aspects of Commercial Radioactive Waste Management," DOE/ET-0029, UC-70, 1979.

U.S. NRC (U.S. Nuclear Regulatory Commission), Office of Standards Development, "Calculations of Annual Doses to Man From Routine Releases of Reactor Effluents for the Purpose of Evaluating Compliance With 10 CFR, Part 50, Appendix I," Regulatory Guide 1.109, 1977.

<b>NRC FORM 335</b> (11-81)		<b>U.S. NUCLEAR REGULATORY COMMISSION</b> <b>BIBLIOGRAPHIC DATA SHEET</b>		<b>1. REPORT NUMBER (Assigned by DDC)</b> NUREG/CR-3235, Vols. 5 and 6 SAND82-1557	
<b>4. TITLE AND SUBTITLE (Add Volume No., if appropriate)</b> Technical Assistance for Regulatory Development: Review and Evaluation of the Draft EPA Standard 40CFR191 for Disposal of High-Level Waste		<b>2. (Leave blank)</b>		<b>3. RECIPIENT'S ACCESSION NO.</b>	
<b>7. AUTHOR(S)</b> Fuel Cycle Risk Analysis Division		<b>5. DATE REPORT COMPLETED</b> MONTH: April   YEAR: 1983		<b>6. (Leave blank)</b>	
<b>9. PERFORMING ORGANIZATION NAME AND MAILING ADDRESS (Include Zip Code)</b> Sandia National Laboratories Fuel Cycle Risk Analysis Division 9413 Albuquerque, NM 87185		<b>DATE REPORT ISSUED</b> MONTH: April   YEAR: 1983		<b>8. (Leave blank)</b>	
<b>12. SPONSORING ORGANIZATION NAME AND MAILING ADDRESS (Include Zip Code)</b> Division of Waste Management Office of Nuclear Material Safety and Safeguards U.S. Nuclear Regulatory Commission Washington, DC 20555		<b>10. PROJECT/TASK/WORK UNIT NO.</b>		<b>11. FIN NO.</b> A1165 Task 3	
<b>13. TYPE OF REPORT</b> Formal Report		<b>PERIOD COVERED (Inclusive dates)</b> July 1981 - April 1983			
<b>15. SUPPLEMENTARY NOTES</b>		<b>14. (Leave blank)</b>			
<b>16. ABSTRACT (200 words or less)</b> Simple models are presented for the estimation of individual and population health effects for long-term radionuclide releases to the surface environment. In volume 5, models based on the use of asymptotic solutions to mixed cell models in conjunction with appropriate usage rates, dose factors, risk factors, and population estimates are demonstrated. These simple models may be useful in evaluating topics such as the potential importance of individual radionuclides, different release patterns or exposure pathways, and the relationship between individual and population exposures. Illustrative model calculations are compared with the calculated population exposures on which the Draft (#19) EPA Standard 40CFR191 is based. In Volume 6, simple models are employed to provide insights into the degree of conservatism in the health effects per curie value presented by the draft standard. No attempt is made to encompass all uncertainty in the input parameters use in the calculations, and some of the modeling assumptions used in this analysis are different from those of the EPA. Three sets of calculations of health effects (cancer deaths) per curie release are presented and discussed in terms of their potential implications upon the curie release limits of the EPA draft standard.					
<b>17. KEY WORDS AND DOCUMENT ANALYSIS</b>			<b>17a. DESCRIPTORS</b>		
<b>17b. IDENTIFIERS/OPEN-ENDED TERMS</b>					
<b>18. AVAILABILITY STATEMENT</b> Unlimited		<b>19. SECURITY CLASS (This report)</b> Unclassified		<b>21. NO. OF PAGES</b>	
		<b>20. SECURITY CLASS (This page)</b> Unclassified		<b>22. PRICE</b> S	